⬩EPA

Proceedings: Second Conference on Waste Heat Management and Utilization (December 1978, Miami Beach, FL) Volume 1

EPRI

FPL
FLORIDA POWER & LIGHT COMPANY

RESEARCH REPORTING SERIES

Research reports of the Office of Research and Development, U.S. Environmental Protection Agency, have been grouped into nine series. These nine broad categories were established to facilitate further development and application of environmental technology. Elimination of traditional grouping was consciously planned to foster technology transfer and a maximum interface in related fields. The nine series are:

1. Environmental Health Effects Research

2. Environmental Protection Technology

3. Ecological Research

4. Environmental Monitoring

5. Socioeconomic Environmental Studies

6. Scientific and Technical Assessment Reports (STAR)

7. Interagency Energy-Environment Research and Development

8. "Special" Reports

9. Miscellaneous Reports

This report has been assigned to the MISCELLANEOUS REPORTS series. This series is reserved for reports whose content does not fit into one of the other specific series. Conference proceedings, annual reports, and bibliographies are examples of miscellaneous reports.

EPA REVIEW NOTICE

Proceedings: Second Conference on Waste Heat Management and Utilization
(December 1978, Miami Beach, FL)
Volume 1

S.S. Lee and Subrata Sengupta, Compilers

Mechanical Engineering Department
University of Miami
Coral Gables, Florida 33124

ACKNOWLEDGEMENTS

FOREWORD

The first conference on Waste Heat Management and Utilization held in
Miami during May 9-12, 1977 was a success in terms of participation,
comprehensive technical representation and quality. A questionnaire
submitted to the sponsors and participants at the meeting indicated a
strong interest in an annual or biannual meeting. In response to this
the second comprehensive conference in the subject area is being held during
December 4-6, 1978. This will estabish a biannual frequency and allow
significant progress during meetings.

A perusal of the table of contents will indicate that causes, effects,
prediction, monitoring, utilization and abatement of thermal discharges are
represented. Utilization has become of prime importance owing to increased
awareness, that waste heat is a valuable resource. Sessions on Co-generation
and Recovery Systems have been added to reflect this emphasis.

This second conference has working sessions covering important topics
in the subject area. This provides an interactive forum resulting in
relevant recommendations regarding research directions.

A well balanced Organizing Committee with an Advisory Board with
international composition has brought this conference to fruition. The
sponsoring organizations include governmental and private organizations
who are active in waste heat research and development.

Samuel S. Lee
Subrata Sengupta

iv

CONTENTS

WASTE HEAT MANAGEMENT AND UTILIZATION CONFERENCE

ECOLOGICAL EFFECTS I

COOLING TOWER PLUMES

ECOLOGICAL EFFECTS II

COOLING TOWERS I

COGENERATION

KEYNOTE ADDRESS

Eric H. Willis

IT IS COMMONLY SUPPOSED, AND SOMETIMES QUITE APPROPRIATELY,
THAT THE GOVERNMENT COLLECTS MONEY BY TAXING THE DAYLIGHTS
OUT OF ITS CITIZENS, AND THEN PROCEEDS TO SPEND IT -- PERIOD.
IT IS THE SPENDING PART WHICH I WANT TO ADDRESS THIS MORNING,
PARTICULARLY AS IT PERTAINS TO RESEARCH AND DEVELOPMENT IN
ENERGY SUPPLY TECHNOLOGIES, AND THE BALANCE AND EMPHASIS THAT
HAS TO BE PLACED UPON USING THOSE NEW, AND EXPENSIVE, SUPPLY
SOURCES SO THAT EVERY B.T.U. IS MADE TO COUNT. HOW, AS IT
WERE, TO GET EVERY OUNCE OF JUICE OUT OF THE ORANGE. OUR
BUDGET IN THIS AREA FOR THE FISCAL YEAR JUST STARTED IS
$2.77B. THIS IS A LOT OF MONEY -- IT'S THE TAXPAYERS DOLLAR,
YOURS AND MINE, AND DESERVES BETTER THAN TO BE MERELY SPENT --
IT SHOULD BE PRUDENTLY INVESTED, JUST AS IN ANY OTHER BUSINESS
VENTURE. THE SIMPLE QUESTION THEN IS, "HOW CAN WE BEST
INVEST THE TAXPAYERS DOLLAR SO THAT IT EXERTS THE GREATEST
LEVERAGE AND THE GREATEST RETURN IN TERMS OF ASSURING THIS
NATION OF ALTERNATIVE AND RELIABLE ENERGY SUPPLIES, AND USING
THOSE SUPPLIES EFFICIENTLY."

CLEARLY ONE MUST, AS IN ANY ENTERPRISE, HAVE AN
INVESTMENT STRATEGY IF ONE IS TO CIRCUMVENT THE ALL TOO
MANY RATHOLES THAT ARE WILLING RECIPIENTS OF MISDIRECTED
CASH.

SINCE A STRATEGY IS IN A SENSE A ROAD MAP OF HOW YOU GET THERE FROM HERE, ONE HAS TO BE ABLE TO PREDICT WITH SOME DEGREE OF CONFIDENCE WHAT THE "THERE" LOOKS LIKE -- IT DEFINES THE GOAL. WITHOUT A GOAL, A STRATEGY IS A ROAD MAP TO NOWHERE.

I RATHER LIKE THE STORY OF THE COUPLE OF FELLOWS GOING TO THE COUNTRY FAIR. ONE WAS A BIG BURLY GUY AND THE OTHER A WIZENED LITTLE SOUL WITH GLASSES LIKE THE BOTTOMS OF COKE BOTTLES. THEY WENT INTO THE FAIR AND CAME UPON A SHOOTING BOOTH. IN THE SHOOTING BOOTH WAS A PIPE, AND THE PIPE HAD FIVE LITTLE HOLES IN IT, AND OUT OF THE FIVE LITTLE HOLES CAME FIVE JETS OF WATER. ON THE FIVE JETS OF WATER DANCED FIVE COLORED PING PONG BALLS. WITH FIVE SHOTS FOR 50 CENTS, THE BIG GUY WENT UP FIRST. HE HAD HIS FIVE SHOTS, AND DOWN CAME THREE PING PONG BALLS. THE LITTLE GUY STANDING BESIDE HIM THEN TOOK THE GUN, AND THE BIG GUY, LOOKING AT HIM WITH A GRIN, SAID "SEE WHAT YOU CAN DO." SO THE LITTLE GUY TOOK AIM, THE GUN WENT BANG, AND LO AND BEHOLD ALL FIVE BALLS FELL DOWN. THE BIG GUY WAS FLABBERGASTED, AND SAID, "MY GOD, HOW DID YOU DO IT?" HE SAID, "IT WAS EASY. I JUST SHOT THE GUY WHO PUMPS THE WATER." THE MORAL OF THE STORY IS THAT YOU HAVE TO GO AFTER THE KEY ISSUES THAT DRIVE THE SYSTEM.

SO WHAT DRIVES THE SYSTEM? CLEARLY AT THE MOMENT IT IS
DOMINATED BY THE WORLD PRICE OF OIL, ALTHOUGH IT COULD AS
WELL BE DRIVEN BY AN INTERRUPTION IN SUPPLIES SUCH AS WE
EXPERIENCED IN '73. WHILE WE MAY LAY ASIDE THIS DISCONTINUITY
FOR A MOMENT, WE CANNOT IGNORE IT. THE RECENT IRANIAN OIL
WORKERS STRIKE COULD HAVE HAD WORLD WIDE REPERCUSSIONS.
SUPPOSING THERE IS NO SUCH DISCONTINUITY, IF WE LOOK INTO THE
CRYSTAL BALL TO SEE WHAT THE PRICE OF OIL IS LIKELY TO BE
IN THE FUTURE, WE AT ONCE HAVE A SENSE OF FRUSTRATION. TWO,
AT LEAST TWO, SCENARIOS TEND TO EMERGE. ONE SCENARIO SAYS
THAT ALTHOUGH THERE IS PRESENTLY A WORLD GLUT OF OIL TENDING
TO HOLD DOWN PRICES, THIS COULD GIVE WAY TO AN EXCESS OF
DEMAND IN THE '83-'85 TIME FRAME, RESULTING IN SIGNIFICANTLY
HIGHER PRICES. IF THE SOVIET UNION BECAME A NET IMPORTER
OF OIL IN THIS TIME FRAME, PARTICULARLY FROM THE MIDDLE EAST,
THE POSITION COULD SIGNIFICANTLY DETERIORATE.

A MORE OPTIMISTIC SCENARIO CONTINUES THIS SURPLUS OF
SUPPLY OVER DEMAND MUCH FURTHER THAN '85 WITH ONLY MODERATE
INCREASES IN PRICES. THE MEXICAN OIL RESOURCE PROSPECT
REINFORCES THIS. THERE IS TROUBLE EITHER WAY, FOR OIL
RICHES IN OTHER PEOPLE'S LANDS DO NOT ENDOW US WITH TITLE
TO THEM. THEY HAVE TO BE PAID FOR -- WE ALREADY HAVE ABOUT
25% OF ALL THE OIL MOVING IN INTERNATIONAL TRADE, WHICH TURNS
OUT TO BE HALF OUR REQUIREMENTS, AND THE CONSEQUENCES ARE

CLEAR TO ALL WHO READ NEWSPAPERS OR EVEN CARTOONS. THE

U.S. IS NOT IMMUNE TO THE CONSEQUENCES OF UNPAID DEBTS.

TO EXACERBATE THE PROBLEM, OUR DOMESTIC SUPPLIES OF OIL

PRESENTLY AT 8M B/D ARE DECLINING. EVEN WITH KNOWN FIELDS

AND CONVENTIONAL TECHNOLOGIES, AND INCLUDING ALASKA, 1990 MAY

SEE THIS AMOUNT HALVED. ADDITIONAL DISCOVERIES MAY ONLY

ADD ANOTHER 3M B/D, MAKING 7M B/D IN ALL. BY PAYING WORLD

OIL PRICE, AND EXPANDED R&D, ENHANCED RECOVERY TECHNOLOGIES

MIGHT ADD AN EXTRA 3.3M B/D TO THIS. CLEARLY, NO SIGNIFICANT

INCREMENTAL DOMESTIC CONTRIBUTION TO OUR OIL REQUIREMENTS BY

1990 IS IN THE CRYSTAL BALL. ALSO CLEARLY, OUR TRANSPORTATION

SECTOR WILL STILL BE HEAVILY RELIANT UPON LIQUID FUELS --

ELECTRIC VEHICLES WILL ONLY PENETRATE THE MARKET WHEN THE

CHARGE DENSITY, WEIGHT AND DISCHARGE/RECHARGE RATES OF

BATTERIES ARE IMPROVED DRAMATICALLY.

LET US FOR A MOMENT EXAMINE OUR OPTIONS IN TERMS OF THE

CONSTRAINTS WHICH WE, AS SOCIETY HAVE PLACED UPON THOSE

OPTIONS. I WANT TO DEAL WITH THREE SUPPLY AREAS, FOSSIL

FUELS, NUCLEAR AND SOLAR, IN PARTICULAR. WHILE WE HAVE THE

PRIVILEGE OF LIVING IN A DEMOCRACY, WE ALSO HAVE THE

FRUSTRATIONS OF SPEAKING IN CONTRADICTIONS IN OUR DIFFERENT

ROLES AS CITIZENS. OUR FRIENDLY CITIZEN STARES WITH DISBELIEF

AT HIS ASTRONOMIC PUBLIC UTILITY BILL, CURSES THEM FOR WASTE

AND RIP-OFF, TURNS HIS THERMOSTAT DOWN TO A MERE 70°, GETS

IN HIS ONE-DRIVER CAR, COMPLAINS OF THE AIR POLLUTION AND

THE EXCRESIENCES OF SMOKE STACKS, MENTALLY WRITES A STINGING LETTER TO HIS CONGRESSMAN DEMANDING THAT THE GOVERNMENT DO SOMETHING TO CLEAR IT ALL UP, AND FINALLY ENTERS THE QUIET OF HIS OFFICE WHERE HE DASHES OFF YET ANOTHER IRATE LETTER COMPLAINING ABOUT THE VICISSITUDES OF GOVERNMENT REGULATION AND THE COST OF ENVIRONMENTAL COMPLIANCE.

IT IS IN THIS CLIMATE THAT WE SEEK TO DEVELOP OUR NATIONS GREATEST RESOURCE -- COAL.

THE REPLACEMENT OF OIL AND GAS BURNING FOR COAL IN UTILITY AND INDUSTRIAL PLANTS IS AN IMPERATIVE. THIS WOULD ALLOW OIL TO BE AVAILABLE FOR THE TRANSPORTATION SECTOR AND GAS FOR THE MORE VULNERABLE DOMESTIC MARKET. THE DIRECT COMBUSTION OF COAL IN AN ENVIRONMENTALLY ACCEPTABLE MANNER POSES TODAY'S DILEMMA. THE NEW SOURCE PERFORMANCE STANDARDS MAKE STRINGENT DEMANDS ON THE PERCENTAGE REDUCTION IN SULPHUR DIOXIDE, NITROGEN OXIDES AND PARTICULATES, IRRESPECTIVE OF WHETHER THE COAL IS HIGH-HEAT CONTENT, HIGH SULPHUR COALS OR LOWER-HEAT CONTENT LOWER SULPHUR COALS. SIMILARLY, THERMAL POLLUTION IS GENERATING INCREASING AWARENESS -- SOME ILL INFORMED. THE PHENOMENA INVOLVED HAVE TO BE BETTER UNDERSTOOD AND THE ABATEMENT OF THERMAL DISCHARGES FULLY PERSUED. I NOTE THE WELL MATCHED EMPHASES ON MODELLING, ECOLOGY AND CONTROL TECHNOLOGY IN THE CONFERENCE PROGRAM.

THE EXACTING STANDARDS THAT SOCIETY DEMANDS CAN BE MET --
AT A PRICE. THE DAY OF RECKONING COMES WHEN THE PERCEIVED
BENEFITS ARE INSUFFICIENT TO JUSTIFY ADDITIONAL COSTS -- WE
ARE NOT YET AT THAT POINT, BUT MAY BE QUITE CLOSE.

HOW SHOULD WE APPROACH OUR R&D INVESTMENTS INTO COAL
UTILIZATION? POLLUTANTS CAN BE TAKEN OUT AT THREE STAGES --
BEFORE, DURING AND AFTER COMBUSTION. PRIOR TO COMBUSTION
WE MAY CLEAN UP THE COAL (COAL BENEFICIATION) OR CONVERT IT
INTO A LOW-SULPHUR SOLID, SUCH AS THE SOLVENT REFINED COAL-I
PROCESS, WHICH MAKES A DEASHED AND DESULPHURIZED BOILER FUEL.
ALTERNATIVELY, COAL LIQUEFACTION PROCESSES CAN PROVIDE
DESULPHURIZED LIQUIDS FOR BOILER FUEL AND PROSPECTIVELY AS A
REFINERY FEED STOCK AS A SYNTHETIC SUCCESSOR TO CONVENTIONAL
OIL. REMOVAL OF MOST POLLUTANTS DURING COMBUSTION CAN BE
ACHIEVED IN THE ATMOSPHERIC FLUIDIZED BED PROCESS AND AFTER
COMBUSTION BY FLUE GAS DESULPHURIZATION IN SCRUBBERS AND
BAG HOUSES.

COAL GASIFICATION IS ALSO POTENTIALLY ATTRACTIVE,
PARTICULARLY HIGH BTU GAS WHICH PROMISES TO BE A SYNTHETIC
SUBSTITUTE FOR NATURAL GAS AND THUS A METHOD OF SUPPLEMENTING
DWINDLING SUPPLIES OF THAT PRECIOUS FUEL TO FILL THE ALREADY
EXISTING PIPE LINE SYSTEM AND DISTRIBUTION INFRASTRUCTURE
WHICH REPRESENT A LARGE CAPITAL INVESTMENT.

AT THE MOMENT HOWEVER, NEITHER SYNTHETIC OIL OR GAS FROM COAL COME CHEAP -- OIL FROM THIS SOURCE IS PROJECTED AT AROUND $25-30 PER BBL. AND $5.00 PER MILLION BTU COMPARED WITH THE PRESENT AVERAGE WORLD OIL PRICE OF $L3.50 PER BBL. AND ITS GAS EQUIVALENT OF ABOUT $2.30 PER MILLION BTU. CLEARLY UNDER THESE CIRCUMSTANCES, THE GOVERNMENT HAS A CLEAR ROLE TO PLAY. COAL GASIFICATION PLANTS ARE NOW IN THE BILLION TO THE BILLION AND A HALF DOLLAR RANGE AND ACTUALLY APPROACH THE TOTAL EQUITY OF MANY POTENTIAL PRODUCER COMPANIES. PRIVATE CAPITAL IS UNLIKELY TO FLOW TO SUCH ENTERPRISES WHOSE PRODUCT COST IS HIGH BY TODAY'S STANDARDS AND ITS TECHNOLOGY, RELIABILITY AND ECONOMICS ARE UNPROVEN. I AM REMINDED BY MY BANKING FRIENDS THAT BANKS RENT MONEY -- THEY DO NOT TAKE RISKS. THE GOVERNMENT ROLE HERE SEEMS BETTER DEFINED.

HOWEVER, THERE ARE SOME CASES, PARTICULARLY IN THE RECOVERY OF OIL SHALE AND ENHANCED OIL RECOVERY IN EXISTING FIELDS BY TERTIARY RECOVERY PROCESSES WHERE THE COST OF THE PRODUCT IS NOT SO FAR ABOVE PRESENT WORLD OIL PRICE AS TO PROVIDE FOR OTHER FORMS OF INCENTIVES OTHER THAN DIRECT GOVERNMENT R&D FUNDING. IN THE CASE OF OIL SHALE FOR INSTANCE, A TANTALIZINGLY LARGE, BUT LOGISTICALLY DIFFICULT RESOURCE, THE PRICE IS PROJECTED AROUND $20 PER BBL. THE DIFFERENCE BETWEEN THE WORLD OIL PRICE AND THIS PRODUCT COST IS BRIDGEABLE WITHIN LIMITS BY TAX INCENTIVES, AND IT IS THE ADMINISTRATION'S POLICY, DESPITE ITS FAILURE TO SURVIVE THE

LAST FRANTIC MOMENTS OF THE 95TH CONGRESS, TO OBTAIN A $3 PER
BBL. TAX CREDIT FOR PLANTS UP TO 10,000 BBL. PER DAY. FOR
ENCHANCED OIL RECOVERY, PRICE INCENTIVE ALSO SEEMS THE MOST
PRUDENT APPROACH. HERE IS AN INDUSTRY, VERY DIVERSE, A LARGE
NUMBER OF INDEPENDENTS, WITH A TREMENDOUS TRADITION OF
RESOURCEFULNESS, GOOD BUSINESS JUDGMENT, AND TECHNICAL KNOWHOW.
MY EXPERIENCE OF BUREAUCRATIC WASHINGTON MAKES ME SHUDDER AT
TELLING THIS COMMUNITY HOW TO DO ITS JOB. IT IS A COMMUNITY
USED TO RISKS AND REWARDS -- WITH THE APPROPRIATE REWARDS,
RISKS WILL BE ACCEPTED. I MENTION THIS BECAUSE I BELIEVE
THERE ARE AREAS WHERE DIRECT GOVERNMENT INVOLVEMENT IS A
NECESSARY CONDITION FOR SUCCESS, AND OTHERS WHERE PRICE
INCENTIVES WILL INDUCE THE PRIVATE SECTOR TO MAKE THE FRONT
RUNNING. THE NATURE OF THE MIX IS VERY MUCH INVOLVED IN
DECIDING OUR R&D INVESTMENT STRATEGY -- OUR RESOURCES ARE
NOT INFINITE, AND HARD CHOICES WILL HAVE TO BE MADE BETWEEN
COMPETING TECHNOLOGIES. IN THE PRESENT FISCAL YEAR, CONGRESS
HAS APPROPRIATED ABOUT $803 MILLION FOR FOSSIL FUEL TECHNOLOGY
DEVELOPMENT.

CLEARLY, WITH THE COST OF PRIME ENERGY RISING AS IT WILL,
WHATEVER THE PRECISE TIME SCHEDULE, THE COST PER USABLE ENERGY
UNIT, I.E., WATT OR BTU HAS TO BE KEPT AS LOW AS POSSIBLE.
THIS SETS A PREMIUM UPON MORE EFFICIENT ENERGY CONVERSION
PROCESSES, BE THEY ENGINES OR COMBUSTION TECHNOLOGIES, AND
ALSO FULLY UTILIZING THE HEAT LEFT OVER AFTER THOSE PROCESSES.

8

THE THRUST OF PART OF THIS CONFERENCE THUS, COMES INTO PERSPECTIVE -- IT IS UNCONSCIONABLE TO SQUANDER THOSE HARD WON ENERGY SUPPLIES IN THE WAY WE DID WHEN WE ASSUMED, INCORRECTLY OF COURSE, THAT ENERGY CAME FREE. OUR ECONOMY WILL JUST NOT ACCOMODATE SUCH PRODIGAL ATTITUDES. THE MORAL EQUIVALENT OF WAR MAY BE APPROPRIATE, BUT IT IS IN THE POCKET BOOK AND IN OUR STANDARD OF LIVING THAT THE IMPACT WILL BE FELT. I AM THUS GREATLY ENCOURAGED TO SEE SUCH EMPHASIS ON COGENERATION AND RECOVERY SYSTEMS ON THE CONFERENCE PROGRAM.

IN THE NUCLEAR ARENA, WE HAVE A DIFFERENT SET OF CIRCUMSTANCES. THE CONSTRAINTS, ALTHOUGH HAVING A MAJOR ENVIRONMENTAL COMPONENT, ARE HEAVILY SOCIETAL AND INSTITUTIONAL IN NATURE. THE SEASONED PRACTITIONERS OF THIS TECHNOLOGY, HAVING SPENT THEIR LIVES ON A NEW FRONTIER AND FOR A BRAVE NEW WORLD, FIND THEMSELVES CHARACTERIZED AS THE ARCH APOSTLES OF THE DEVIL HIMSELF. THIS WAS A TECHNOLOGY WHOSE DEVELOPMENT WAS ALMOST ENTIRELY FINANCED BY AND CONDUCTED BY THE GOVERNMENT ITSELF. BY DEFINITION IT WAS "GOOD" BECAUSE THE END PRODUCT -- CHEAP, RELIABLE AND ABUNDANT ELECTRICITY -- WAS "GOOD." IT IS NOT TRUE TO SAY THAT POSSIBLE DETRIMENTAL ISSUES WERE IGNORED, BUT THEIR EMPHASES WERE NOT THOSE OF TODAY. CONSTRAINTS ON NUCLEAR POWER DEVELOPMENT TODAY CENTER ON THREE ISSUES. THE PROLIFERATION POTENTIAL OF THE POSSIBLE

DIVERSION OF PLUTONIUM FROM REPROCESSING PLANTS, REACTOR

SAFETY AND SITING, AND THE THORNY QUESTION OF WHAT TO DO WITH

THE NUCLEAR WASTE, OR, UNTIL WE GET A GOOD SOLUTION TO THE

REPROCESSING PROBLEM, THE STORAGE OF SPENT FUEL RODS. THIS

LATTER PROBLEM, WHETHER ANOTHER NUCLEAR POWER STATION IS

ORDERED BY A UTILITY OR NOT, HAS TO BE SOLVED MERELY TO TAKE

CARE OF THE RESIDUES FROM THOSE POWER STATIONS IN OPERATION

OR BEING BUILT.

ON THE NUCLEAR TECHNOLOGY SIDE, OUR THRUST IS DIRECTED

TO EXTENDING THE FUEL LIFE OF THE EXISTING LIGHT WATER

REACOTRS AND CONDUCTING PRELIMINARY RESEARCH INTO PROLIFERATION

RESISTANT BREEDER TECHNOLOGIES. THIS IS A LONG RANGE, HIGH

RISK, HIGH PAY OFF VENTURE WHOSE COMMERCIALIZATION AT THE

EARLIEST WILL NOT BE BEFORE THE TURN OF THE CENTURY, AS IS

ALSO THE CASE WITH FUSION POWER.

SOLAR ENERGY IS CURRENTLY EVERYONES DARLING, AND IS IN

DANGER OF BEING THOROUGHLY SPOILED IF ITS DIRECTION BOWS TO

EVERY WHIM OF THE DAY. THE PRESIDENT IS JUST ABOUT TO RECEIVE

A DOMESTIC POLICY REVIEW ON SOLAR ENERGY WHICH WE HOPE WILL

PROVIDE A MUCH FIRMER BASE FOR PLANNING THAN WE HAVE HAD IN

RFCENT YEARS. THE PROBLEM AT THE MOMENT IS THAT WHILE THE

SUNSHINE COMES FREE, THE HARDWARE TO HARNESS IT DOES NOT.

ALSO THE GOOD LORD RATIONS IT ABOUT 2 TO 5 KW HOURS PER

SQUARE METER PER DAY.

LET US TAKE PHOTOVOLTAICS FOR EXAMPLE, MAKING ELECTRICITY
DIRECTLY FROM SUNLIGHT WITH ABOUT 10% EFFICIENCY. TO REPLACE
A 1000 MWE CENTRAL POWER STATION WITH THE EQUIVALENT OUTPUT
FROM PHOTOVOLTAIC CELLS REQUIRES A COLLECTING AREA OF SOME
TWENTY SQUARE MILES. WITH SOLAR PONDS AT 2% EFFICIENCY, ONE
WOULD NEED 200 SQUARE MILES!

AT PRESENT A PRICE OF 4 TO 6 CENTS PER KILOWATT HOUR OF
ELECTRICITY IS ABOUT THE UTILITY INDUSTRY NORM AND PHOTOVOLTAICS
AT THIS COST WOULD BE COMPETITIVE. TODAY'S COST OF PHOTOVOLTAIC
ELECTRICITY RANGES FROM 50 CENTS FOR THE MOST BASIC DC SYSTEM
TO $2 PER KWH FOR AN ON-THE-GRID RESIDENTIAL DESIGN. IF
PRESENT TRENDS CONTINUE WE EXPECT THIS WILL DROP TO THE RANGE
OF 10 TO 50 CENTS BY 1982. THIS 1982 PRICE DEPENDS ON ARRAY
COSTS OF ABOUT $2 PER PEAK WATT. WE HAVE DESIGNED OUR PROGRAM
WITH THE GOAL OF BRINGING THIS COST DOWN BY AS EARLY AS 1986
TO THE RANGE OF 6-12 CENTS IN 1978 DOLLARS FOR POWER GENERATED
ON SITE AND USED BY CONSUMERS WITHOUT ON-SITE STORAGE.

HOWEVER, THERE IS A SIDE BENEFIT HERE WHICH COULD
SUBSTANTIALLY ALTER THESE ECONOMICS. SINCE, AS WE HAVE SEEN,
PHOTOVOLTAIC CELLS ARE ONLY 10-12% EFFICIENT AT THE MOMENT
IT FOLLOWS THAT 90% OF THE INCIDENT RADIATION IS NOT UTILIZED.
HERE SURELY IS A GREAT OPPORTUNITY FOR THE RECOVERY AND
UTILIZATION OF WHAT IS ESSENTIALLY WASTE HEAT. WE GRACE IT
WITH FANCY NAMES LIKE TOTAL ENERGY SYSTEMS, BUT THE ABILITY

TO GET THE MOST ENERGY, ELECTRIC AND THERMAL OUT OF SOLAR
INSTALLATIONS IS GOING TO HAVE A MAJOR IMPACT ON THE MARKET
PENETRATION OF SOLAR ENERGY. SOMEWHERE ALONG THE LINE, THIS
TOPIC MIGHT BE APPROPRIATE FOR DISCUSSION IN A CONFERENCE
SUCH AS THIS.

THUS, THE WHOLE THRUST OF OUR SOLAR ENERGY INVESTMENT IS
COST REDUCTION. TO GET THIS TECHNOLOGY ACCEPTED INTO THE
MARKETPLACE AND MAKE THE CONTRIBUTION WE HOPE WILL REQUIRE A
VERY DEFINITE CHANGE IN LIFE STYLES. IT WILL ONLY DO SO
WITH A MULTITUDE OF CHEAP, SOCIALLY ACCEPTABLE, DISPERSED
SYSTEMS. ONE HAS ONLY TO DRIVE THROUGH THE TOWNS AND VILLAGES
OF ISRAEL TO SEE THOUSANDS OF PRACTICAL DEMONSTRATIONS. THE
INVESTMENT FOR THIS WILL LARGELY BE PRIVATE CAPITAL, AND WAYS
HAVE TO BE FOUND OF FINANCING SOLAR APPLICATIONS.

IN CONCLUSION THEN, WE HAVE TO WALK BOTH SIDES OF THE
STREET -- ENSURING RELIABLE ENERGY SUPPLIES IN ENVIRONMENTALLY
ACCEPTABLE WAYS, AND USING THOSE SUPPLIES IN THE MOST PRUDENT
MANNER. I CONGRATULATE THE ORGANIZERS OF THIS CONFERENCE
ON AN EXCELLENT PROGRAM ADDRESSING THOSE ISSUES, AND WISH
YOU ALL WELL IN YOUR DISCUSSIONS OF THE NEXT THREE DAYS.

A WASTE HEAT UTILIZATION PROGRAM

J. Neal
Division of Fossil Fuel Utilization
Department of Energy
Washington, D.C.

W.F. Adolfson
Senior Scientist
Booz·Allen & Hamilton Inc.
Bethesda, Maryland

ABSTRACT

The cornerstone of the National Energy Plan is conservation. While "housekeeping" and modifications to existing equipment can result in modest energy savings, major changes could result in substantial energy savings.

New technologies which would utilize waste heat are one way of reducing national energy needs, conserving valuable oil and natural gas, and mitigating the severity of the impact of shifting to coal and coal-derived fuels on a national scale. The recoverable energy amounts to 20 to 30 percent of the forecast national energy consumption.

This paper describes the potential for waste heat utilization in the four market sectors: industry, residential/commercial, transportation and utilities. There are, however, barriers to using new waste heat recovery technologies. The Department of Energy technological program, which is briefly described, is one part of a Federal strategy to overcome some of these barriers.

*   *   *   *   *

INTRODUCTION

The Arab oil embargo of 1973-74 and the subsequent qua-
drupling of oil prices made our nation acutely aware of
its dependence on fuels in critically short supply—oil
and natural gas, which currently account for about 75
percent of domestic consumption. Moreover, over 25 percent
of this usage is supplied by imports and the supply shortfall
could increase by 50 percent by the year 2000, according
to statistics compiled by the Department of Energy. To
continue a dependence on such heavily used, fast diminishing,
and increasingly expensive energy resources could jeopardize
our national security, and risk economic, social, and poli-
tical dislocations in the relatively near future. To deal
with these risks the Administration and Congress are developing
a national energy policy with four major features: to enhance
conservation and lower the rate of growth of total U.S.
energy demand; to shift industrial and utility consumption
of natural gas and oil to other abundant resources; to
develop synthetic substitutes for oil and gas; and to re-
duce dependence on oil imports and vulnerability to inter-
ruptions of foreign oil supply.

The magnitude of effort required to induce industry and
utilities to convert from oil and natural gas, our favorite
fuels, to coal and other abundant fuels and to curb the
growth in energy demand is enormous, and the U.S. will
probably remain dependent on oil and natural gas for the
foreseeable future. Thus, conservation and fuel efficiency
become an essential step in the transition strategy.
Neither a complete solution nor a substitute for developing
new resources, conservation of existing supplies is often
cheaper than production of new resources, effectively
protects the environment, and moderates the impact of
rising prices.

Industry has in the past and probably will continue to
conserve energy as is economic, without Federal participation.
While "housekeeping" and modifications of existing equipment
can result in modest energy savings (10 to 15 percent),
major process changes and capital expenditures would be
needed for more significant savings (20 to 90 percent).

One way of actively pursuing a conservation strategy is to
develop the technology to recover waste heat from industrial
processes or electrical generation. Utilizing heat rejected
from a process at a temperature high enough about the lower
reservoir temperature (commonly ambient temperature) so that
additional work can be extracted from it can make a

substantial contribution to reducing national energy consumption. Opportunity exists in all four market sectors—industry, residential/commercial, utility and transportation—to employ waste heat recovery technologies.

However, there are many barriers hindering adoption of heat recovery technologies, and the Department of Energy (DOE) program is designed to mitigate the effects of some of these impediments.

POTENTIAL FOR WASTE HEAT UTILIZATION

Studies have estimated that the overall economy of the U.S. is less than ten percent energy efficient, which is based on the second-law efficiencies of various energy consuming activities (Figure 1). The potential for energy savings is enormous. A modest improvement in efficiency would represent a substantial savings in oil and natural gas usage. Recent analysis has concluded that the U.S. could expend between 20 and 50 percent less energy and still maintain overall economic growth into the 1990's. The National Energy Plan is based on the calculation that enough waste energy exists to allow the U.S. to cut the growth of its total energy use to two percent or less per year, as compared to 4.8 percent in 1976.

Many estimates have been made for the potential energy savings which might accrue from successful commercialization of advanced heat recovery technology. Bearing in mind the difficulties in separating potential energy savings due to component improvements and recovering waste heat, it is estimated that about 30 percent of the forecast national energy consumption could be recovered from fuel utilization of waste heat recovery programs and concepts (Figure 2). In the industrial sector, increased use of recuperators, heat pumps, and cogeneration could significantly reduce energy consumption. Space heating in residential/commercial applications could be supplied by incorporating total energy or integrated energy systems. By bottoming diesel and gas turbine engines in the transportation sector, waste thermal energy could be converted into additional mechanical energy (Figure 3).

The successful commercialization of ongoing waste heat recovery programs have the potential for reducing our annual expenditures for imported oil by $15 billion in 1985 and by $48 billion in the year 2000. Full utilization of all recoverable waste heat energy could reduce expenditures by

15

$57 billion in 1985 and by $68 billion in the year 2000 (Figure 4). These savings would have a tremendous beneficial impact on our balance of payments posture. In addition, waste heat recovery maximizes desired output per unit of fuel. This will tend to reduce energy costs to American industry and the American public. It will also alleviate the situation that occured in the winter of 1976-1977, when plants were shut down because of fuel curtailments, resulting in production disruptions and worker layoffs.

Waste heat recovery has a beneficial environmental impact. Thermal pollution of atmosphere and waterways is reduced when rejected heat is harnessed and used. Waste heat recovery also reduces the quantity of fossil fuel that must be burned to achieve a given performance level, with a consequent reduction in air pollution.

FEDERAL STRATEGY

Industry is affected uniquely by the various barriers to employing new waste heat recovery technology. These constraints are technological, financial and institutional (Figure 5).

There are several Federal programs—technological programs, incentives, regulations—that can help overcome these barriers (Figure 6). To illustrate the DOE approach to solving the technological problems, a strategy was formulated to develop heat recovery technology as an alternative source of energy by developing the necessary technology base for recovering and using waste heat and by demonstrating the technical and economic feasibility of the technological components. These goals are being accomplished by focusing on three activities: low grade heat recovery; high grade heat recovery; and heat exchanger technology.

LOW GRADE HEAT RECOVERY

Temperatures below 200°F are categorized as low-grade heat. Although there are large quantities of this source, much can be recovered only at great energy costs. This low quality heat can be best used for space heating and agricultural applications, where it does not have to be pumped very far.

The low grade heat recovery activity has three objectives: to reduce energy consumption by eliminating available energy losses, to improve the efficiency of energy converters, and to develop low-grade heat recovery technologies as alternative sources of energy. Effort in this activity is directed at development of low-temperature technology by evaluating conceptual designs of selected novel heat engines and recovery devices (e.g., elastomer heat engines, nitinol and other shape memory alloy heat engines, and advanced industrial size heat pumps) and by improving performance of low-temperature heat exchangers and is directed at making use of rejected heat from Federal facilities.

HIGH-GRADE HEAT RECOVERY

Temperatures above 200°F are classed as high grade heat. The use of waste heat in this range offers the highest potential for immediate benefit, since high grade heat is suitable for various bottoming and topping cycles. Bottoming cycles can increase the efficiency of a powerplant from about 35 percent to 50 percent, thereby saving 20 to 30 percent of the fuel for a given power output. Topping cycles can achieve slightly better fuel efficiencies.

The high grade heat recovery activity has two objectives: To develop a technology base for the recovery and reuse of waste heat at temperatures exceeding 200°F and to develop and demonstrate thermionic conversion technology. Associated with these objectives are two activities. First, the bottoming-cycle systems programs is aimed at developing heat recovery systems for applications in the 200 - 1000°F range. Four unique concepts in organic Rankine Cycle (ORC) systems technology are underway, which employ binary, toluene, fluorinol, and two-phase approaches. Secondly, the topping-cycle systems program is developing thermionic energy conversion technology, which converts high temperature heat from any source to electricity without using high pressures or moving parts.

HEAT EXCHANGER TECHNOLOGY

Heat exchangers have been used by industry for many years. The thrust of DOE's R&D program is to reduce the cost of heat exchangers by increasing their efficiency, reliability and durability and to extend the capability of heat exchangers for operation at temperatures above 2000°F. Specific efforts of this activity include: development of a data base on

vibration, fouling and corrosion, investigation of ceramic materials including developing ceramic materials and non-destructive tests for heat exchangers and components and developing the ceramic heat pipe; development of a heat exchanger for low-grade heat applications; and development of fluidized bed heat exchangers for applications to diesel bottoming cycle boilers and residential heat pumps.

In summary, these efforts and related applications studies in areas of cogeneration, district heating, total energy systems, integrated energy systems, high temperature re-cuperation and industrial heat pumps reflect an essential step in the national energy strategy to transition to coal and alternative energy sources. The Government is developing and demonstrating new technologies that give industry the opportunity to adopt equipment which could make substantial improvements in energy savings.

Second Law Efficiencies

Energy Consuming Activity (Current Technology)	Second Law Efficiency (Percent
Industrial Sector	
Process Steam Production	33.0
Steel Production	23.0
Aluminum Production	13.0
Residential/Commercial Sector	
Fossil Fuel-Fired Furnace	5.0
Electric Resistive Furnace	2.5
Air Conditioning	4.5
Gas Water Heating	3.0
Electric Water Heating	1.5
Refrigeration	4.0
Transportation	
Automobile	9.0
Electric Power Generation	33.0

Source: John A. Belding, "Alternatives to Oil and Gas Through Energy Management," (AIAA/EEI/IEEE 77-1006) 7

78 5871 32-32

Figure 1

Recoverable Energy from Full Utilization of Waste Heat Recovery Programs

Energy Consuming Sector
- [ ] Industry
- [ ] Residential/Commercial
- [■] Transportation
- [▦] Electric Power Generation

Year: 1985

Year: 2000

/8 58/1 19·32
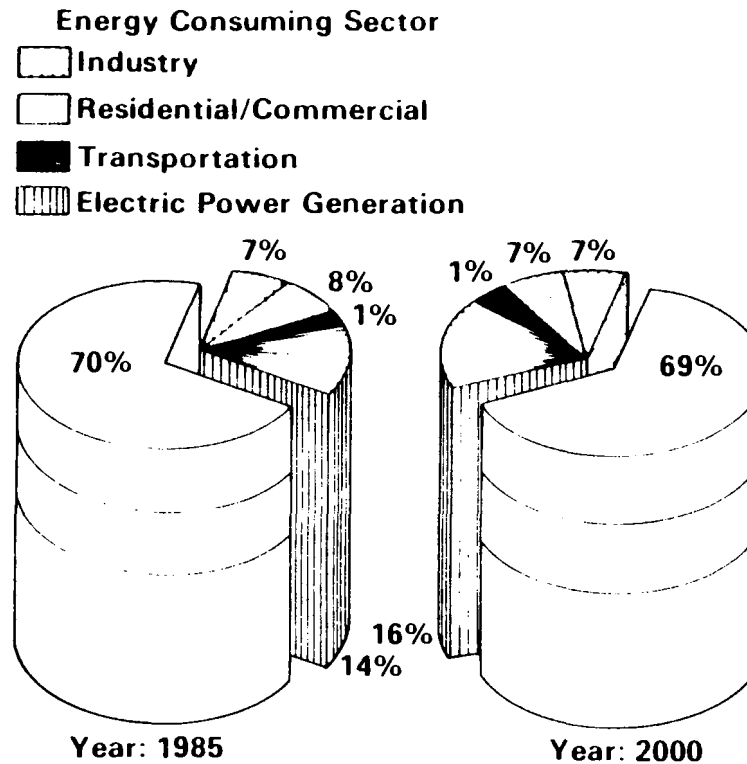
Figure 2

Total Waste Heat Recovery Summary

Sector	1985		2000	
	MBDOE	QUADS	MBDOE	QUADS
Industrial				
• Ongoing Projects	1.1	2.2	3.2	6.3
• Total	3.4	6.8	4.5	9.0
Residential/Commercial				
• Ongoing Projects	1.0	2.1	3.1	6.1
• Total	3.8	7.7	4.8	9.6
Transportation				
• Ongoing Projects	0.1	0.2	0.4	0.7
• Total	0.6	1.2	0.8	1.6
Electric Power Generation				
• Ongoing Projects	0.5	1.0	2.1	4.2
• Total	6.8	13.5	10.8	21.7
Four Sector Total				
• Ongoing Total	2.7	5.5	8.8	17.3
• Total	14.6	29.2	20.9	41.9

78 - 5871 30-32

21

Figure 3

Potential Savings in Oil Imports

Category	Estimated Energy Savings			
	Ongoing Projects		Total Recoverable Energy	
	1985	2000	1985	2000
Total Savings of Oil (MBDOE)	2.7	8.7	10.4	12.5
Total Savings of Oil (Quads)	5.4	17.4	20.8	25.0
% Reduction in Oil Imports	23	76	66	79
$/Yr. Savings on Oil Imports*	14.8B	47.6B	56.9B	68.4B

*Based on an estimated value of $15 per barrel, which appears quite conservative for the 1985–2000 time frame.

78 - 5871 31-32

Figure 4

TECHNOLOGICAL CONSTRAINTS

- New, Unproven Technology
- Technical and Economic Risks to the Production Process
- Concentration of R&D Funds Within a Few Companies

FINANCIAL CONSTRAINTS

- Shortage of Capital
- Shortage of Discretionary Capital for Energy Conservation

INSTITUTIONAL CONSTRAINTS

- Energy Cost is Low Percent of Total Cost of Sales
- Security of Energy Supply More Important Than Price
- Uncertainty Regarding Future Prices
- Low Turnover Rate of Plant and Equipment
- Resistance to Changes in Production Processes

Figure 5

MAJOR CONSTRAINTS TO ENHANCED ENERGY CONSERVATION

KEY:

● = STRONG IMPACT ON OVERCOMING CONSTRAINT
○ = MODERATE IMPACT ON OVERCOMING CONSTRAINT
BLANK = LITTLE IMPACT ON OVERCOMING CONSTRAINT

MAJOR STRATEGIC OPTIONS	TECHNICAL			FINANCIAL		INSTITUTIONAL & OTHER				
	Lack of unproven technology concepts	Lack of proven technology options	Lack of industry wide R&D funds	Shortage of capital funds	Shortage of discretionary capital	Energy cost is a low percent of total costs	Supply security is more critical than price	Fuel price uncertainties defer investment action	Low asset turnover	Risk to production process from retrofit
TECHNOLOGY PROGRAMS										
R&D	●	○	●							
DEMONSTRATION	○	●	●	○					○	●
INFORMATION	○	○	○	○					○	○
INCENTIVES										
FUEL USE TAX						○	●	○	○	
TAX DEDUCTIONS			○						○	
INVESTMENT CREDITS			○	●	●				○	
FAVORABLE LOANS				○	○				○	
SUBSIDIES				○	○					
REGULATIONS										
FUEL CONVERSION				○		●	●		●	○
FUEL PRICING				○		○	○	●	○	
EFFICIENCY TARGETS				○		●	●	○	●	
DATA REPORTING				○	○					

Figure 6

EPA PROGRAMS IN WASTE HEAT UTILIZATION

by

Theodore G. Brna

U.S. Environmental Protection Agency
Office of Research and Development
Office of Energy, Minerals and Industry
Industrial Environmental Research Laboratory
Research Triangle Park, North Carolina

To be presented at:

The Second Conference
on
Waste Heat Management and Utilization
Miami Beach, Florida
December 4-6, 1978

ABSTRACT

Waste heat utilization which supports the Environmental Protection Agency's thermal pollution control activities is discussed. Waste heat utilization/reduction is classed into three options--utilization of waste heat, in-plant electrical generation, and integrated energy production/use facilities. Current projects with promising environmental benefits are presented with particular emphasis on applications in agriculture.

INTRODUCTION

Waste heat has been defined as heat rejected by a process at a temperature enough above the ambient temperature so that additional value may be extracted from this heat (1). In addition, the sources of the waste heat are placed in the high temperature range if above 698°C (1200°F) and in the low temperature range if below 282°C (450°F).

The heat rejected by power plant cooling systems is often called waste heat and would be placed in the low temperature range using the given criterion. However, steam-electric power plant cooling systems usually reject heat at temperatures between 5.5 and 22°C (10 and 40°F) above intake water temperatures; consequently, this heat, which will receive particular attention here, has a limited potential for beneficial use. In fact, many power plant engineers would term "waste heat" an unfortunate choice of name for this rejected heat as it is a consequence of the second law of thermodynamics and is held to the lowest practical value in steam-electric power production.

Natural and man-made factors impact the magnitude and quality (as indicated by temperature above ambient temperature) of waste heat from power plants. Increasing demands for electrical energy without corresponding gains in the efficiency of electrical energy generation effect greater quantities of rejected or waste heat. Measures to limit adverse environmental impacts through requiring off-stream or closed cycle cooling in lieu of on-stream or open cycle cooling at steam-electric generating stations lead to slightly higher temperatures and heat rates and correspondingly higher heat rejection rates. This higher quality waste heat, plus the Nation's commitment to greater energy conservation, provides added impetus for seeking economical methods for using waste heat beneficially.

The amendments to the Federal Water Pollution Control Act in 1972 established zero discharge of pollutants for 1985 as a national goal and required technology-based effluent limitations to be considered prior to granting water discharge permits. Subsequent effluent guidelines, issued by EPA in 1974 and based on the use of best available technology for dissipating the heat rejected by steam-electric generating stations, resulted in increased use of closed cycle cooling systems, particularly evaporative cooling towers. In addition to compliance with these guidelines, encompassing both thermal and chemical

effluents from power plants, cooling water shortages in some areas of the United States are an additional factor for heat rejection at temperatures above those characteristic of once-through or open cycle cooling. Currently, these guidelines are being updated and are expected to lead to further progress toward achieving the zero discharge goal. These guidelines will also address the "best conventional pollutant control technology" (BCT) which is to be implemented by July 1, 1984 according to the provisions of the Clean Water Act of 1977, another amendment to the Federal Water Pollution Control Act.

In addition to the act cited, Congress has passed other legislation which may limit effluent discharges from power plants. Table 1 shows EPA's legislative mandates and lists the Safe Drinking Water Act, the Toxic Substances Control Act and the Resource Conservation and Recovery Act. Future guidelines for implementing these acts could impact power plant cooling system choices, practices, and heat rejection rates and temperatures. For example, limitations on discharges from evaporative or wet cooling towers could lead to the use of wet/dry or dry cooling towers, which would generally reject heat at higher temperatures and rates than wet towers. Such guidelines could make the benefits of utilizing waste heat from power plants more attractive.

WASTE HEAT UTILIZATION

The EPA program in waste heat utilization supports the reduction of adverse environmental impacts. Environmental benefits enhanced by waste heat utilization include (2):

1. Reduction of pollutant generation and release for a given useful energy requirement

2. Cost savings for pollution abatement equipment

3. Conservation of energy

4. Potential generation of revenue to offset costs of pollution abatement

5. Elimination of adverse environmental impacts related to obtaining, processing, and supplying the energy equivalent to the beneficially-used waste heat

Funding for beneficial uses of waste heat is provided through EPA's Office of Research and Development (ORD), which received its first separate budget during Fiscal Year 1977. Table 2 gives ORD funding for 17 functions or programs, the program receiving the greatest funding being Energy Conversion, Use and Assessment for both FY 77 and FY 78 (3). Table 3 shows ORD funding for 10 media, with Energy receiving around 40 percent for these fiscal years (3). Percentage of ORD support via four funding mechanisms is shown in Table 4 (3). Various ORD laboratories and functional elements support programs in waste heat utilization, and consequently, the total level of this support is not provided here. With regard to funding mechanism, the projects shown in Table 5 were supported via grants and interagency transfers.

27

Numerous approaches to waste heat utilization are available, with waste heat from power plant cooling systems being considered mainly for agricultural and aquacultural applications. Projects supported through the Industrial Environmental Research Laboratory-Research Triangle Park (IERL-RTP) have focused on agricultural uses of waste heat as these applications reduce thermal discharges to water bodies, while many aquacultural applications involve natural water bodies heated by thermal discharges. Consequently, the latter applications do not reduce thermal pollution although they make beneficial use of heated waters. It is also noted that guidelines have been issued for the discharge of specific pollutants, including waste heat, in a controlled manner from a point source to an aquacultural project as a consequence of the 1972 and 1977 amendments to the Federal Water Pollution Control Act.

The EPA program for waste heat utilization/reduction has emphasized three options because of their high potential application in supporting the Agency's environmental mandates. These options are (4):

1. Utilization of waste heat discharged from industrial and utility plants for agriculture and aquaculture

2. Generation of electricity in industrial plants

3. Development of integrated energy production/use facilities which are more energy-efficient

The first option uses heat after its discharge from a process or facility, while the others serve to reduce waste heat through optimized design and management. The projects listed in Table 5 concern the first option and will be emphasized here. Option 2, which refers to cogeneration, is a responsibility of the Industrial Environmental Research Laboratory-Cincinnati (IERL-Ci), and several studies supported by this Laboratory will be discussed in a later session of this conference. The last option has received limited attention from the waste heat utilization viewpoint.

Agricultural and Aquacultural Uses of Waste Heat

Most waste heat applications supported by EPA have concerned agriculture as this option was believed to have the greatest potential for near-term energy savings (through 1985) while reducing thermal discharges to water bodies or air. This waste heat, appropriate generally to electric utility cooling system sources, was at low temperatures and represented a very small fraction of what would be available from a modern steam-electric generating station and had seasonal use limitations.

Since previously completed studies concerning agricultural uses of waste heat and supported by EPA have been reported elsewhere (2), the projects discussed here will be those currently underway or completed very recently. Most of the active projects pertain to greenhouse applications, which appear to be economically attractive when selected flowers and vegetables are involved.

28

A demonstration grant partially funded the greenhouse study at Northern
States Power Company's Sherburne County (Sherco) Power Plant in Becker, Minne-
sota. Warm condenser cooling water from the first 680-MWe unit is supplied
from the cooling tower main to the 0.2 hectare (0.5 acre) greenhouse. The
water, nominally at 29.5°C (85°F), provides both soil and air heating through
buried pipes and surface heat exchangers. The first 2 years of the demonstra-
tion, which was completed in May 1977, was successful and led to two commercial
greenhouses being constructed on the plant site. A third year of performance
data was funded with grant-derived income that was generated from the sale of
flowers and vegetables grown during the demonstration. The grant period was
recently extended to May 1980, and a study was begun to assess the feasibility
of using a waste heat greenhouse for fish hatchery operations. Currently,
three commercial firms are using waste heat at this plant site to heat about
0.7 hectare (1.7 acres) of greenhouse area. Further details on the economic
advantages and operating aspects of the greenhouse complexes at the Sherco
Plant will be presented by Ashley et al. (5) later during this conference.

Since fiscal year 1975, the Office of Energy, Minerals, and Industry in
EPA's Office of Research and Development has coordinated a Federal Energy/Environ-
ment Research and Development program that is conducted by 17 government
agencies. Under this program EPA and TVA have jointly supported studies by
TVA at its National Fertilizer Development Center in Muscle Shoals, Alabama.
Two major tasks are being addressed in these studies, both slated for completion
by the end of next year.

Soil heating to extend the growing season of field crops is being studied
using simulated condenser cooling water temperatures from two TVA plants. The
water is supplied to plastic pipes at various row spacings and depths beneath
the surface of the soil. Using several pipe arrangements as determined from
preliminary tests, soil heating was found to increase maturation and yields of
the crops studied (bush beans, cantaloupe, corn, okra, peanuts, squash, and
watermelon) during the spring months (up to mid-June) and to not change or
slightly decrease yields (squash and watermelon) during the summer. Although
spring-grown crops were available for the market a week or so earlier, more
data are needed to determine if soil heating is economically attractive in
this southern area. Preliminary indications are that soil heating is not now
economical for this area.

The other project with TVA treats the biological recycling of nutrients
in livestock wastes through use of waste heat. Currently, fish (tilapia and
silver and bighead carp) are being grown in tanks containing three different
concentrations of swine manure for growing algae at different water temperatures.
At different frequencies equivalent to water retention times of 5, 10, and 15
days, waste slurries from these tanks are supplied daily to Chinese water
chestnuts planted in sand beds. Tilapia weight increases from 50 to over
500 grams in 6 months have been obtained, while preliminary tests showed the
harvested water chestnuts and foliage to be of excellent quality for ruminant
forage. The water from these sand beds has been low in nutrients (nitrogen
and potassium) and has a greatly improved biological quality. Studies to

optimize fish production are continuing as are greenhouse studies to optimize duckweed and algae production in swine manure slurries warmed with simulated waste heat. Future efforts to complement this nutrient recycling will include biogas production from swine manure. Biogas generation does not remove major plant nutrients (nitrogen, phosphorous and potassium), but can significantly reduce the biological oxygen demand of the manure and the risk of oxygen depletion in aquatic systems fertilized with digester effluent.

The use of waste heat from a nuclear plant for greenhouse agriculture has caused some apprehension because of the possibility of radioactive contamination. The potential impact of the Delaney Amendment to the Food, Drug and Cosmetic Act on greenhouse food production using waste heat from the Vermont Yankee Nuclear Plant was assessed, and a model for the New England marketing of greenhouse-grown products at this site was developed. It was concluded that the use of surface heat exchangers between the plant's condenser cooling water and the greenhouse heating medium would essentially preclude potential radioactive contamination of greenhouse products. It was also concluded that the low temperature of the condenser water (23°C or 70°F) was too low to maintain the required greenhouse temperature. Consequently, it was proposed to use a biogas generation facility at a dairy farm near the plant so that waste heat from the plant could enhance biogas generation and some of the gas generated could serve for supplemental heating of the greenhouse.

The grant to Fort Valley State College supports comparison of foliage plants, cut flowers, and bedding plants in a conventionally heated greenhouse with one heated with waste heat and using an evaporative system which leads to high humidity in the greenhouse. These greenhouses became operational last September. The performance evaluation of the environmental control system in the research greenhouse, techniques for controlling diseases related to high humidity operation, and assessment of plant quality in the two greenhouses are presently underway.

Efforts to identify, develop and demonstrate heat recovery within industries emitting thermal discharges to water and air streams are also being made. Some applications have been identified and selected for demonstration under the industrial energy conservation program and will be discussed by Latour and Lee (6) during the "Utilization IV" session of this conference on Wednesday. Also, during this session some environmental aspects of effective energy utilization by industry will be presented by Mornighan and Heim (7).

Electrical Generation by Industry

Electrical generation by industry appears to have a high potential for reducing waste heat for the period 1985-2000 (2). The use of the more efficient field-erected boilers in lieu of currently used package boilers seems economically conducive to cogeneration applications encompassing both process steam generation and electrical generation for in-plant uses. Other approaches to promising cogeneration approaches will be discussed during this conference.

Electrical generation by industry can reduce thermal and air pollutants through fuel conservation, reduce the capital required for a given electrical demand, and lower the cost of producing electrical power and processing steam. These advantages become apparent when it is noted that process steam requires about 20 percent of this Nation's primary fuel with less than a third of this amount being used to generate electricity prior to its process use.

Integrated Energy Production/Use Facilities

This option appears attractive for waste heat utilization/reduction over the long-term (beyond 2000) (2). This application would have facilities which are operationally compatible in terms of energy form, load characteristics, and equipment lifetime. An increase in energy utilization of 10 percent or more would be expected through joint utility-industry ventures.

Integrated energy facilities in the United States are inhibited by various institutional problems, the incompatibility of production and user systems, financial risk, lack of capital, and inappropriate planning. Candidates for integrated energy facilities include district heating, power park complexes with process heating and electrical power from the same source, surplus electrical power from industries to electrical utilities, off-peak storage and on-peak use of energy, and selected combinations from these candidates.

Although integrated energy facilities would serve to enhance environmental quality and energy conservation, these factors have not yet spurred development of such facilities in the United States. Hopefully, the recent passage of the National Energy Act will stimulate industry, utilities, and government to concerted action in the development of integrated energy facilities. Increasing fuel costs and energy resource limitations may also hasten the day of integrated energy facilities as the public becomes more convinced of the need for more efficient utilization of energy.

SUMMARY

The effective utilization of rejected or waste heat contributes to improved environmental quality and energy conservation. Consequently, the beneficial use of waste heat supports several objectives of the Environmental Protection Agency. Most EPA-sponsored projects have involved agricultural applications, but the Agency is also supporting research and development in other promising areas. Joint programs are a major mechanism for implementing ongoing agricultural waste heat utilization projects. Integrated energy production/use facilities have the potential for a major impact for the long-term utilization of waste heat, and will require the cooperation of the private, public, and governmental sectors if such facilities are to be viable.

31

REFERENCES

1. Rohrer, W. M., Jr. and K. G. Krieder, "Sources and Uses of Waste Heat," In Waste Heat Management Guidebook, NBS Handbook 121, U.S. Department of Commerce, Washington, D.C. February 1977.

2. Graham, D. J., "EPA Views on Waste Heat Management and Utilization," In Proceedings of the Conference on Waste Heat Management and Utilization, Miami Beach, FL, May 9-11, 1977, Volume I (University of Miami, Florida).

3. U.S. Environmental Protection Agency, "Research Highlights 1977," EPA-600/9-77-044 (NTIS No. PB 281305), Office of Research and Development, Washington, D.C., December 1977.

4. Christianson, A. G., "Waste Heat Utilization/Reduction," In Proceedings of the National Conference on Health, Environmental Effects, and Control Technology of Energy Use, EPA-600/7-76-002 (NTIS No. PB 256845), U.S. Environmental Protection Agency, Washington, D.C., February 1976.

5. Ashley, G. C., J. S. Hietala and R. V. Stansfield, "The Sherco Experience: From Demonstration to Commercial Use of Condenser Waste Heat," to be presented at the Second Conference on Waste Heat Management and Utilization, Miami Beach, FL, December 4-6, 1978.

6. Latour, S. R. and C. C. Lee, "Waste Heat Recovery Potential for Environmental Benefit in Selected Industries," to be presented at the Second Conference on Waste Heat Management and Utilization, Miami Beach, FL, December 4-6, 1978.

7. Mornighan, R. E. and W. G. Heim, "Environmental Aspects of Effective Energy Utilization in Industry," to be presented at the Second Conference on Waste Heat Management and Utilization, Miami Beach, FL, December 4-6, 1978.

TABLE 1. EPA LEGISLATIVE MANDATES

Public Law No.	Title	Year Passed
1. 78-410	Public Health Service Act	1944
2. 89-272	Solid Waste Disposal Act	1965
3. 91-190	National Environmental Policy Act	1969
4. 91-604	Clean Air Act Amendments	1970
5. 92-500	Federal Water Pollution Control Act Amendments	1972
6. 92-532	Marine Protection, Research and Sanctuaries Act	1972
7. 92-574	Noise Control Act	1972
8. 92-583	Federal Insecticide, Fungicide and Rodenticide Act Amendments	1972
9. 93-523	Safe Drinking Water Act	1974
10. 94-469	Toxic Substances Control Act	1976
11. 94-580	Resource Conservation and Recovery Act	1976
12. 95-95	Clean Air Act Amendments of 1977	1977
13. 95-217	Clean Water Act	1977

TABLE 2. ORD FUNDING BY FUNCTION OR PROGRAMMATIC CATEGORY

Function or Program	Funding (millions of dollars) Fiscal Year	1977	1978
Health Effects		28.2	35.4
Ecological Processes & Effects		17.9	21.3
Transport & Fate of Pollutants		13.3	13.5
Stratospheric Modification		2.5	
Minerals Processing & Manufacturing		13.1	12.5
Renewable Resources		6.2	5.6
Waste Management		14.2	28.1
Water Supply		13.8	16.3
Environmental Management		1.4	1.6
Measurement Techniques & Equipment		4.0	3.8
Characterization/Measurement Methods		8.1	6.9
Quality Assurance		4.8	5.4
Technical Support		11.3	11.9
Energy Extraction & Processing		25.4	27.6
Energy Conversion, Use & Assessment		33.4	63.9
Energy-Environmental Effects		33.1	37.2
Other		7.0	7.4
TOTAL		237.7	298.4

TABLE 3. ORD FUNDING BY MEDIA

Medium	Funding (millions of dollars)		
	Fiscal Year	1977	1978
Air		45.0	42.3
Water Quality		42.6	56.8
Water Supply		13.8	16.3
Solid Waste		4.1	7.6
Pesticides		8.1	9.5
Radiation		0.8	0.8
Interdisciplinary		21.1	23.2
Toxics		1.4	3.5
Energy		93.8	131.0
Program Management		7.0	7.4
		237.7	298.4

TABLE 4.   ORD FUNDING MECHANISMS

Mechanism	Funding (Percentage of Total)		
	Fiscal Year	1977	1978
Contracts		33	38
Grants		20	21
Interagency Transfers		15	13
In-House Programs		32	28

TABLE 5. ORD PROJECTS IN WASTE HEAT UTILIZATION
(Industrial Environmental Research Laboratory-Research Triangle Park)

Project Title	Grantee/Agency
1. Beneficial Uses of Warm Water from Condensers of Electric Generating Plants	Northern States Power Company
2. Soil Heating to ᵛᵛtend Crop Growing Season	Tennessee Valley Authority
3. Optimization of Biological Recycling of Nutrients in Livestock Wastes via Utilizing Waste Heat	Tennessee Valley Authority
4. Horticulture Economic and Quality Control Study	Vermont Yankee Nuclear Power Corporation
5. Potential Beneficial Use of Industrial Waste Heat for Greenhouse Production of Bedding Plants, Cut Flowers, and Foliage Plants	Fort Valley State College

REVIEW OF EPRI PROGRAM*

Q. Looney, J. Maulbetsch,
Electric Power Research Institute,
Palo Alto, California

*This paper was not presented.

THE ENERGY SHORTAGE AND INDUSTRIAL ENERGY CONSERVATION

E. H. Mergens, Manager Energy Conservation
Shell Oil Company
Houston, Texas U.S.A.

ABSTRACT

The industrial sector of the United States economy has been the mainstay of the nation's energy conservation program. Two industries, Petroleum Refining and Chemical and Allied Products, have made large contributions to the reduction of waste heat and lower energy consumption. The performance of these two industries are compared to targeted goals for energy conservation. Specific areas of waste heat recovery are discussed and examples of several actual industrial installations are presented.

INTRODUCTION

Good Afternoon ladies and gentlemen, it is my pleasure to come here and join in a discussion of energy conservation in United States industry, particularly in the petroleum and chemical industries.

The petroleum refining and the chemical industry are two of the largest energy users in the country each using about (3) quadrillion BTU's of energy, sometimes called energy quads. In total, industry uses about 37 percent of the nation's energy.

Energy conservation is not a new activity in industry. Indeed much of the technological innovation in industry has been directed at using the BTU of energy as many times as possible in the manufacturing process.

Analysis of Past Trends

In economic analysis of this trend toward increased energy utilization, one of the commonly used indicators is the ratio of energy used to the gross national product (Slide 1). The general slope in the last 25 to 30 years has been around (5) to (7) tenths of a percent per year reduction in energy per constant dollar of gross national product. In using historical GNP as a measure, care must be taken, however, to recognize that the character of GNP has changed over the years. Government spending, in the form of transfer payments, and a general increase in services activity have distorted some of the real changes which have taken place.

We believe it is better to analyze some individual components of the economy to get a better picture of what is actually happening. The next series of slides shown statistical data for various segments of the economy. The years selected for comparison were 1968, 1972 and 1977.

Activity indicators such as population, commercial employment, vehicle registrations and industrial production (as measured by the Federal Reserve Board Index), all increased over the period. (Slide 2) Energy use also grew as shown in the next slide (3) increasing from 63 quads to 76 quads. The growth was in residential, commercial and transportation sectors, while industrial use stayed relatively constant.

Comparing the percentage change of both the demographic items and the energy consumption figures in the next two slides, reveals the pattern of what is happening in the economy. Over the whole period, (Slide 4) residential energy consumption rose four times as fast as the activity indicators did, while commercial and transportation consumption nearly matched activity increases. During the same period, industrial energy consumption rose only one fifteenth as fast as production increased.

Even after the Arab Embargo, (Slide 5) the residential energy used increased 1.5 times the rate of the activity indicator, commercial matched increases and transportation's rate of increase slowed considerably, while industry produced more goods using less energy.

The reasons for these patterns are not hard to imagine. Industry is price sensitive. In a competitive economy, the effect of the Arab actions on crede oil price and, the effect of declining gas supplies on the intrastate market price, have accelerated the activity of industry's cost managers to accomplish energy conservation. Transportation energy consumption responds more slowly as equipment modifications and change-out are only part of the picture. Lower speed limits, where enforced, have some effect, as does car-pooling, etc., but by and large American driving habits aren't changing rapidly. Finally, in the residential and commercial area, the consumer is not as rigorous a cost manager. Moreover, this sector of the economy has been buffered by price control mechanisms such as those on interstate natural gas or petroleum products. Until this consumer gets the right price signals we can expect a continued disproportional growth in energy consumption.

Current Performance of Industry

From the foregoing, it is evident that industrial energy conservation is a significant factor in the economy's improved energy utilization, averaging about one percent per year since 1968 and 2.8 percent per year in the post-Arab Embargo period.

The Federal Government has also reacted since the Arab Embargo in the area of industrial energy conservation. The Energy Policy and Conservation Act of 1975 required establishing voluntary goals for the ten most energy intensive industries in the United States. The goal for petroleum refining was set at 20 percent reduction, in energy per barrel intake, using 1972 as a base year and to be accomplished by January 1, 1980. The chemical industrial goal was a 14 percent reduction in energy per pound of product over the same time frame.

Progress toward the goal has been steady over the last five years. The petroleum industry is processing now nearly 20 percent more crude while using about the same fuel as in 1972. (Slide 6A) After making suitable corrections to today's operations versus 1972 there is a net savings of 16.5 percent as reported by the American Petroleum Institute. The chemical industry progress was equally impressive producing over .3 trillion more pounds at comparable fuel usage. Compared to 1972 the conservation reported by the Manufacturing Chemists Association is 14.3%. (Slide 6B)

The goal for petroleum industry was established for the government by the consulting firm, Gordian and Associates based in New York City. The components for the target are shown in the next slide (7A). For simplicity, the 19.4 percent was rounded up to 20 percent by the government in setting the goal. The items enumerated are typical areas for investment in improved energy efficiency.

The API recently conducted a survey of members, which got a partial response, but gave us some insight into how the industry is actually achieving their savings. Next slide (7B). It is interesting to compare the actual with the predictions of the consultants in this slide. Comparing with the Gordian estimate, we find that a fair amount of activity occurred in all areas. Industry found more insulating projects and waste heat/power recovery projects than predicted. However, it looks like industry may find less potential in heater and heat exchange investment than the consultant predicted.

41

The industry is also responding to the change in fuel supply, particularly the decline in natural gas availability. The next slide (8A) compares the average refinery fuel composition in 1972 and in 1977 as reported to the API. Note how distillate, residual, refinery gas, and electricity have all increased to make up for the short fall in natural gas. A similar trend is shown in the chemical industry slide (8B).

Shell Oil Program

Shell Oil Company participates in this voluntary reporting program for manufacturing industries and reports its results through the industry trade associations. (API in the case of refining and MCA for chemical). Our company's program encompases more than just manufacturing, however. The next slide (9) shows the organization of our company energy conservation team of which I am chairman.

Through the efforts of functions represented on this team more than 11 million barrels per year fuel oil equivalent are being saved in Shell operations by actions taken since 1972. Last year, over 17 million dollars were invested in energy conservation projects, and we continue to find additional opportunities for savings. As of the end of 1977, savings by the major sectors of the company amounted to: 12 percent in the oil and chemical manufacturing operations; 15 percent in transportation and distribution of the product; and 16 percent in our exploration and production activities. Manufacturing plants and refineries play a significant role in these savings as they use over 70 percent of the corporate energy, but contributions have been made by each of the functions represented on this chart. Employee carpools, heating and lighting reductions, more efficient product transportation systems, and computer control in many areas.

In the final minutes of this talk, I'd like to show a few specific examples of things we are doing in our manufacturing plants. First, in several locations we carry out both oil and chemical processing at the same site. One of the characteristics of oil processing compared to chemical processing is shown in the next slide (10).

Oil operations are typically process heat related where we heat oil to relatively high temperatures, while chemical operations are steam heat related-distilling at lower temperatures. This allowed us to do the following at our Norco Louisiana Manufacturing Complex. This slide (11) shows a heat medium circulating loop. It takes waste heat from oil operations - coker, distiller, hydrocracker and cat cracker and uses it to heat steam boiler feed water and operate a chemical distilling column. This single project saves nearly a half million barrels of fuel per year, and the loop spans more than two miles as it loops around the processing complex.

42

This is an example of the way high level heat can be cascaded down to low level heat users. It is a demonstration of the 2nd Law of Thermodynamics efficiency at work in a practical manner. The 2nd Law consideration has been touted by theorists as a means of greatly increasing our conservation progress. But as demonstrated here it takes the right set of circumstances to make it practical. Other physical limitations have to be met as well. The chemistry, metallurgy, reaction kinetics, and even the geography involved, can influence how closely we can come to a theoretical goal.

A similar caution should be expressed here concerning many of the recent studies and the National Energy Plan approach to cogeneration. The potential for cogeneration may have been greatly oversold as an conservation tool. The potential for large amounts of byproduct electricity while supplying industrial heat demand is not likely. In the first place, there are few areas where large industry heat demands are concentrated into the required geographical area. Secondly, the estimators of this potential greatly underestimate the amount of mechanical horsepower most large industrial complexes generated from the steam raised. A recent survey indicates from two to four times as much energy is used as mechanical horsepower rather than electrical power from the steam generated in industry. Thus, most cogeneration projects under consideration now by industry, while large in steam generation capacity. provide only modest electbical generation (say 30 to 80 MW) which is mostly used up within the industry's own plant.

Finally in many industrial complexes, the installed capital and existing plant utility balances preclude a radical change over to cogeneration with current economics.

A conservation technique which can be applied in our operations, is the use of a heat pump to help heat distillation columns. If the right circumstances are available the heat pump to help boil the liquids in a distillation column. The heat pump can reduce the amount of energy required to boil the liquid by 15 to 30%. The next slide (12) shows how an existing or new distilling column can be equipped with this system. The main variables are the temperature difference between the top and the bottom of the column, the pressure level of the column, the size of the heat requirement, and finally the temperature difference in the reboiler and the cost of the horsepower needed to provide that temperature difference. The major considerations to make the system economic, are the column temperature difference and the size of the heat load. As can be seen (Slide 13) this type of heat savings can be very attractive at today's fuel costs. Shell has five such installations operating or under construction now.

As shown in a previous slide (10), a large portion of our fuel is consumed to produce process heat by firing various furnaces. Today we are fitting out many of these heaters with equipment which preheats the combustion air making the fuel firing process much more efficient. The schematic on the next slide (14) shows a before and after case, which will save about 35,000 barrels per year of fuel while doing the same processing job.

Another slide (15) shows a real example of such a combustion air preheater on our crude oil heater furnace in our Martinez, California Manufacturing Complex. This slide shows the elaborate duct work needed to take hot stack gases out of the top of the heater and pass it by fresh cold air coming into the heater with the fuel. This project increases the firing efficiency from about 80 percent up to 91 percent and saves nearly 60,000 barrels of fuel per year. All told we now have 8 recently completed air preheaters and several in design which will save 450,000 barrels per year of fuel. This type of installation, while common on most boilers has great promise in the process heater application.

Finally, not to overlook the simplest way to conserve, we have even put insulating covers over the clean out flanges of our hot oil heat exchanges to save several thousand barrels per year of fuel. The slide (16) depicts such an installation. A unique engineering problem here had to do with the bolts which hold on the covers. When insulated, the bolts got hotter and tended to elongate and this loosened the cover and caused leaks. One of our engineers solved that problem by using washers which were dish-shaped. The washers flattened out when tightened. Then as the bolt lengthened with heat, the washer flexed and kept the cover tight. So now we have heat recovery without leaks. Of course, there are many additional items which comprise the total company program and these are only a few examples.

Summary

In summary I'd like to reiterate several points. We have seen that free market forces in the industrial area have been effective in causing conservation. Industry and in particular the oil and chemical industry have and will continue, to respond to the need to conserve increasingly scarce fossil fuels. Considerable progress has been made toward the 1980 goal and we expect to continue beyond that. As we have in the past, we will operate our facilities as efficiently as we know how applying theory where practical and using the technical innovations that have characterized these industries since their start.

Thank you for your attention and I'd be pleased to answer any questions if I can.

REFERENCES

American Petroleum Institute - Semi-Annual Energy Conservation Report to Department of Energy - April 28, 1978

Battelle Columbus Laboratories - Draft Target and Support Document on Developing an Maximum Energy Efficiency Improvement Target - SIC 28 Chemical and Allied Products - Washington, D.C. Federal Energy Administration - July 1, 1976

Department of Energy - Voluntary Business Energy Conservation Program - Progress Report No. 6 Department of Energy - Assistant Secretary for Conservation and Solar Applications - Office of Business Assistance Programs - April 1978

Department of Commerce - Volume Business Energy Conservation Program - Progress Report 4 Office of Energy Programs - Federal Energy Administration Office of National Energy Conservation Programs - November 1976

Gordian Associates, Inc. - An Energy Conservation Target for Industry SIC-29 Washington, D.C. Federal Energy Administration - June 25, 1976

Gordian Associates, Inc. - The Data Base: Potential for Energy Conservation in Nine Selected Industries. Volume 2: Petroleum Refining Conservation Paper 10 Washington, D.C. Federal Energy Administration - June 1974

Grace, E. C., Born, Inc., Fidoe, H. L., Shell Oil - U. S. Refineries Conserve Energy - Hydrocarbon Processing - May 1976, pp 120-121

Manufacturing Chemists Association - Semi-Annual Energy Conservation Report by Department of Energy - May 1, 1978

Mergens, E. H., Shell Oil - How Shell Conserves Energy - Hydrocarbon Processing - July 1977, pp 120-123

Pringle, W. H., Jr., Potential for Energy Conservation in Industrial Operations in Texas Report NSF-RANN 74-231 NTIS Springfield, VA - November, 1974

Sittig, Marshall - Practical Techniques for Saving Energy in Chemical, Petroleum and Metals Industries - Noyes Data Corp., Park Ridge, NJ Lib. Cong. No. 77-71855 - 1977

U.S. ENERGY — GNP RATIO (1972$)

BEB
1.5/78
CP/EE
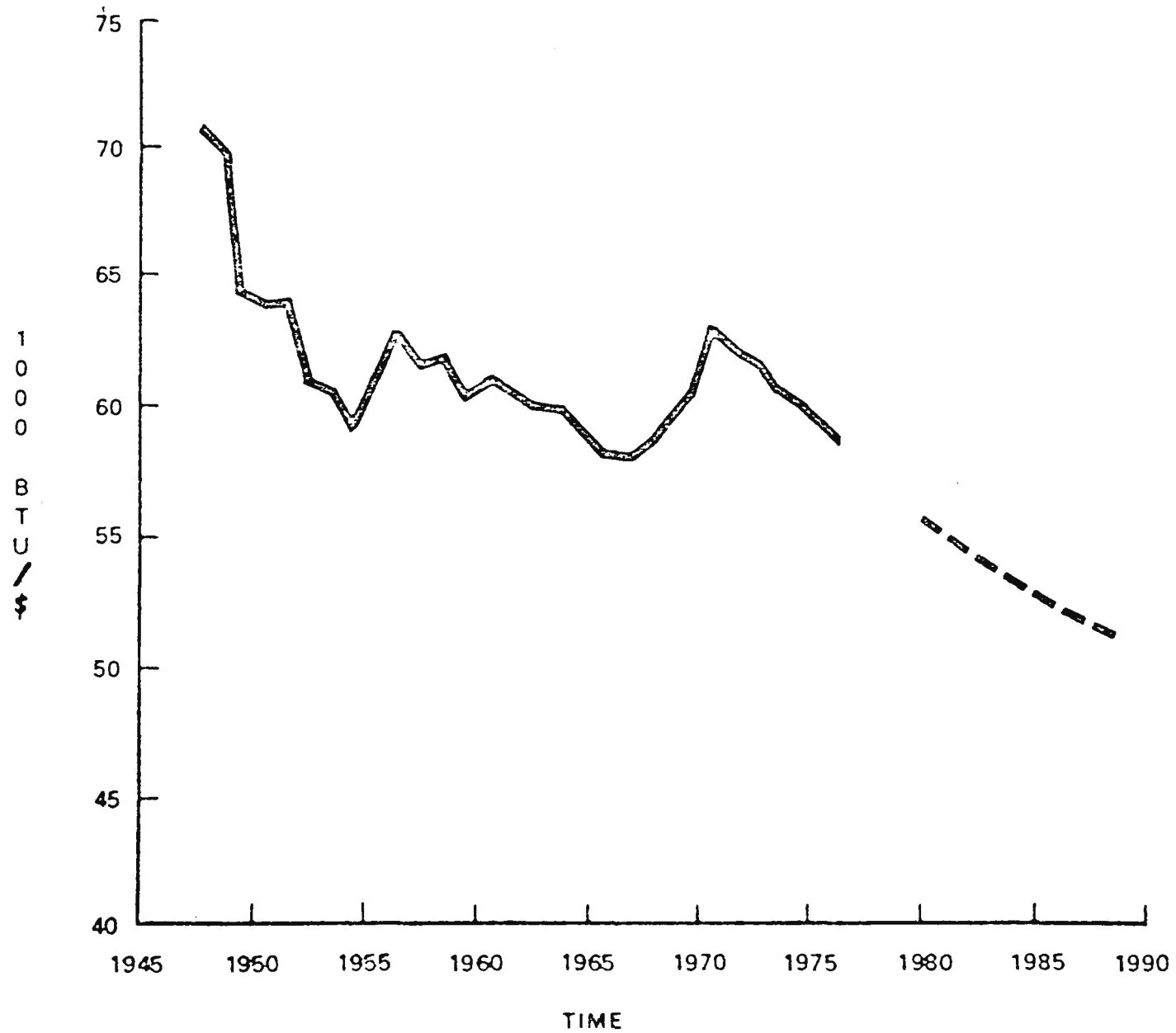
UNITED STATES

ACTIVITY INDICATORS

YEAR	1968	1972	1977
POPULATION, MILLIONS	200.7	208.8	216.9
COMMERCIAL EMPLOYMENT, MILLIONS	39.9	45.7	53.3
VEHICLE REGISTRATIONS, MILLIONS	101.0	118.5	143.0
INDUSTRIAL PRODUCTION, FRB INDEX	1.063	1.197	1.371

UNITED STATES

QUADS [1]

YEAR	1968	1972	1977
RESIDENTIAL	12.8	15.4	17.3
COMMERCIAL	8.2	9.0	10.7
TRANSPORTATION	14.7	17.3	20.0
INDUSTRIAL	27.4	29.5	28.0
TOTAL	63.1	71.2	76.0

1) QUADRILLION BTU'S (10^{15})

UNITED STATES
CHANGES
1968 vs 1977

	ACTIVITY INCREASE	ENERGY INCREASE
RESIDENTIAL	8%	36%
COMMERCIAL	33%	29%
TRANSPORTATION	41%	36%
INDUSTRIAL	29%	2%

UNITED STATES

CHANGES

1972 vs 1977

	ACTIVITY INCREASE	ENERGY INCREASE
RESIDENTIAL	8%	13%
COMMERCIAL	17%	18%
TRANSPORTATION	21%	16%
INDUSTRIAL	15%	-5%

REFINING INDUSTRY

OPERATING STATISTICS

	1972	1977
REFINERY INTAKE, MMB/D	12.6	15.1
ENERGY USE, QUADS[1]	3.0	3.0
WEIGHTED AVG. MBTU/BBL	650	546

[1] QUAD = BTU X 10^{15}

SOURCE: API

CHEMICAL INDUSTRY
OPERATING STATISTICS

	1972	1977
PRODUCTION, POUNDS X 10^9	400	650
ENERGY USE, QUADS[1]	3.4	3.3
WEIGHTED AVERAGE, 1972 MBTU/LB	8.3	7.1

1] QUAD = BTU X 10^{15}

SOURCE: MCA

GORDIAN ASSOCIATES
ENERGY CONSERVATION MEASURES
SIC 2911

CATEGORY	% OF ENERGY SAVINGS 1980 VS 1972
PROCESS HEATERS	3.0
BOILERS	1.2
INSULATION	1.0
HEAT EXCHANGE	3.9
PROCESS CONTROL/REVISIONS	0.8
WASTE. HEAT/POWER RECY	0.8
LOSS CONTROL	1.0
HOUSEKEEPING	7.1
OTHER	0.6
	19.4

REPORTED ENERGY CONSERVATION
MEASURES
SIC 2911.

CATEGORY	% OF ENERGY SAVINGS 1977 VS 1972
PROCESS HEATERS } BOILERS	2.9
INSULATION	1.5
HEAT EXCHANGE	1.3
PROCESS CONTROL/INSTRUMENTS	0.9
WASTE HEAT/POWER RECY	2.3
HOUSEKEEPING	6.6
OTHER	1.1
	16.5

SOURCE: PARTIAL SURVEY OF
API REPORTING CO'S. 54

GORDIAN
PRORATED

3.6

0.9

3.3

0.7

1.5

6.0

0.5
=====
16.5

REFINING INDUSTRY

FUEL COMPOSITION

PERCENT

	1972	1977
CRUDE	0.1	0.1
DISTILLATE	0.5	0.9
RESIDUAL	8.6	10.1
LPG	1.4	0.9
NATURAL GAS	31.4	24.9
REFY GAS	35.5	39.7
COKE	14.6	14.2
COAL	0.1	0.1
PURCHASED STEAM	1.1	1.3
PURCHASED ELECTRICITY	6.7	7.8

SOURCE: API

CHEMICAL INDUSTRY

FUEL COMPOSITION
PERCENT

	1972	1977
DISTILLATE	0.8	2.3
RESIDUAL	5.6	7.3
LPG	0.6	0.4
NATURAL GAS	47.3	39.5
PROCESS GAS	8.6	8.7
PROCESS LIQUID	1.7	3.5
PROCESS SOLIDS	0.4	0.2
COKE	0.2	0.2
COAL	9.4	8.7
PURCHASED STEAM	3.9	3.6
PURCHASED ELECTRICITY	21.5	25.6

SOURCE: MCA

SHELL OIL COMPANY
CORPORATE ENERGY TEAM

EXPLORATION
AND
PRODUCTION

MANUFACTURING
OIL AND CHEMICALS

RESEARCH

EMPLOYEE
RELATIONS

INFORMATION
AND
COMPUTER SERVICES

CORPORATE
ENERGY
CONSERVATION
TEAM

PUBLIC
AFFAIRS

PURCHASING
AND
GENERAL SERVICES

FINANCIAL   LEGAL

REPORTS
TO

TRANSPORTATION
AND
DISTRIBUTION

MARKETING

GENERAL EXECUTIVE
COMMITTEE

58
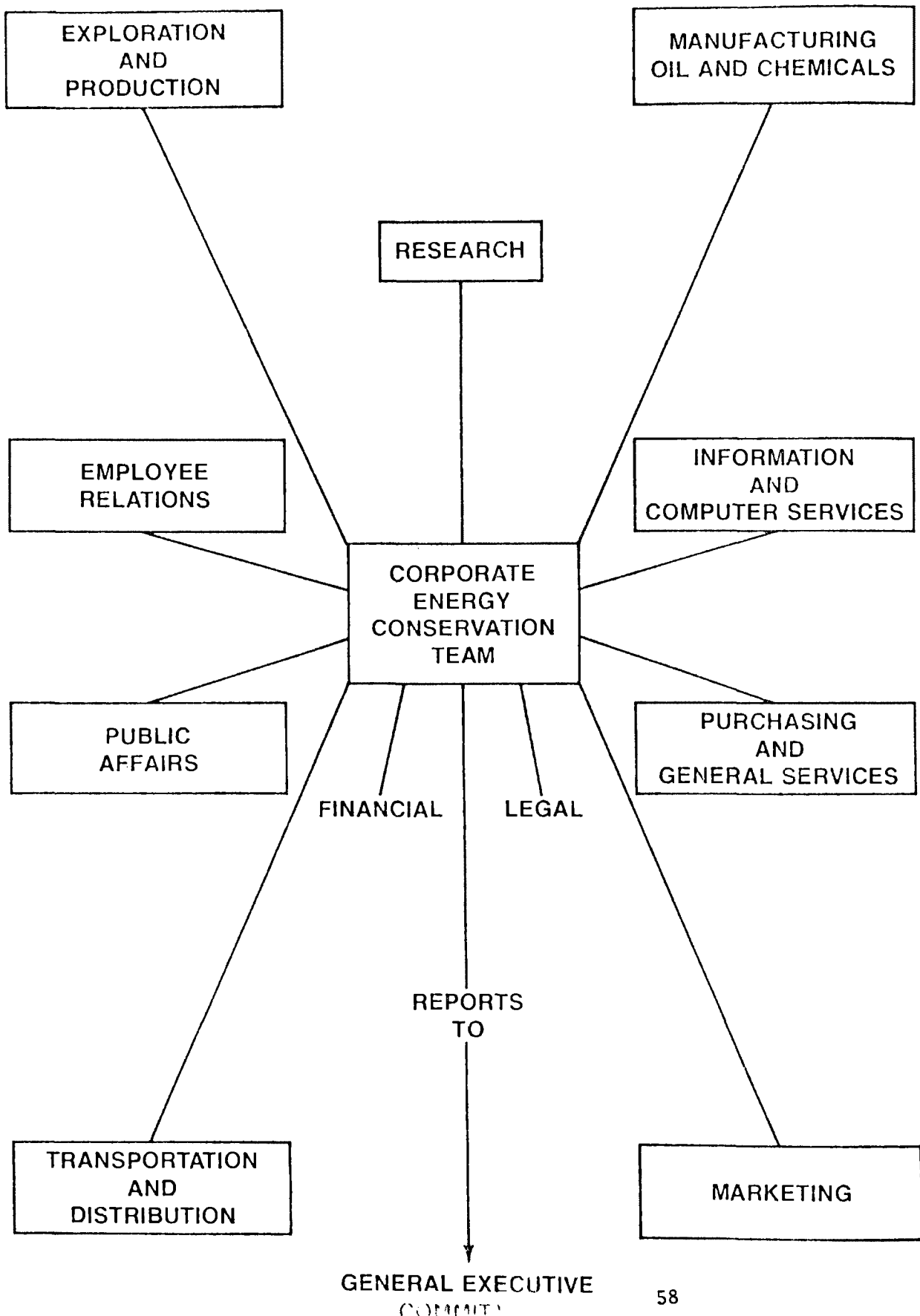
REFINERY/CHEMICAL ENERGY CONSUMPTION-
PROCESS HEAT, STEAM GENERATION,
AND PURCHASED ELECTRICITY
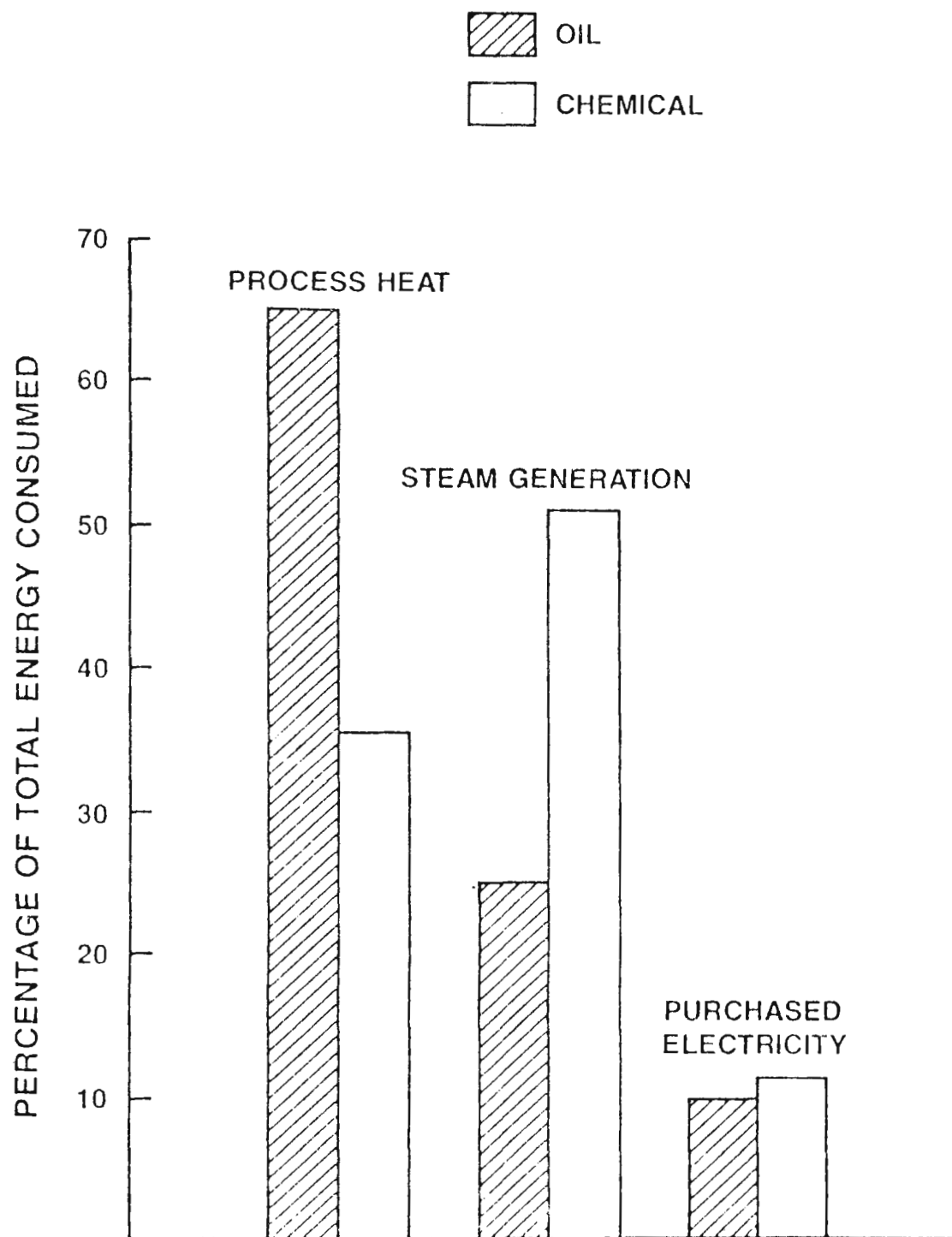
HEAT TRANSFER LOOP
EXAMPLE OF MULTIPLE UNIT HEAT INTEGRATION

HEAT PICKUP

350°F   200°F

+35 MMBTU/HR

COKER PRODUCTS

330°F   200°F

+53 MMBTU/HR

CRUDE DISTILLATION PRODUCTS
AND REFLUX

330°F   200°F

+32 MMBTU/HR

HYDROCRACKER REFLUX

+82 MMBTU/HR

CO HEATER STACK GASES

CHEMICAL
PLANT
BOILER FEED   FRACTIONATOR
WATER

420°F   290 F

HEAT RETURN   129 MMBTU/HR   74 MMBTU/HR

60

HEAT PUMP REBOILING

EXISTING CONDENSER

TOPS ACCUM

COLUMN

TOP PRODUCT

FEED

EXISTING REBOILER

BTM PRODUCT

PREHEATER CONDENSER

COMPRESSER

MOTOR

M

REBOILER CONDENSER

—— NEW
EXISTING

ECONOMIC RETURN
ON
REBOIL HEAT PUMPS

RATE OF RETURN ON INVESTMENT, %

100MM BTU/HR

50MM BTU/HR

COLUMN TEMPERATURE DIFFERENCE, °F

COMBUSTION
AIR PRE-HEAT

↑ 600° F

OIL
100° F

1000° F

OIL
600° F

AIR 70° F

FUEL
1000 BARRELS PER DAY

350° F

AIR 70° F

OIL
100° F

1050° F

OIL
600° F

AIR 500° F

FUEL
900 BARRELS PER DAY
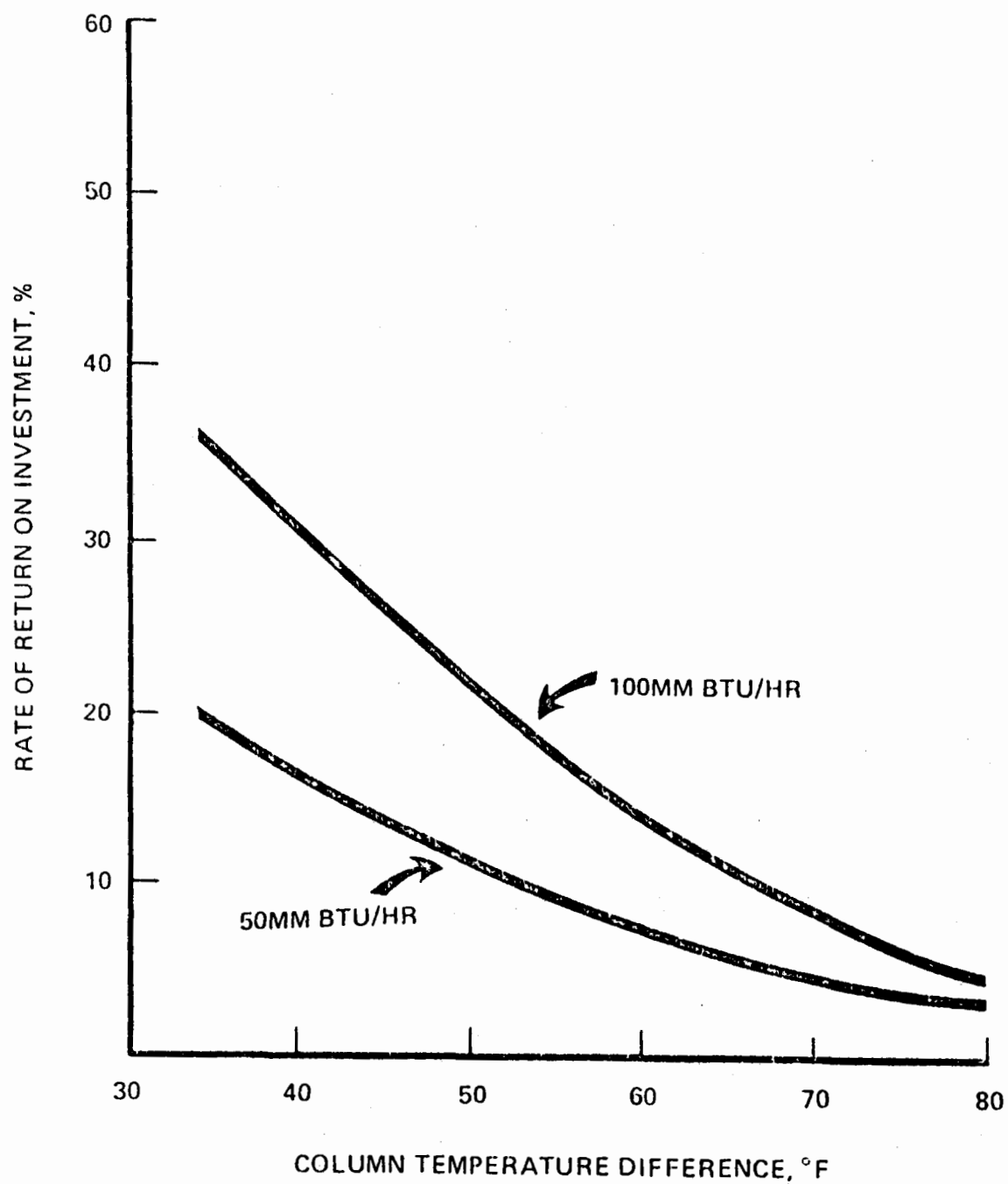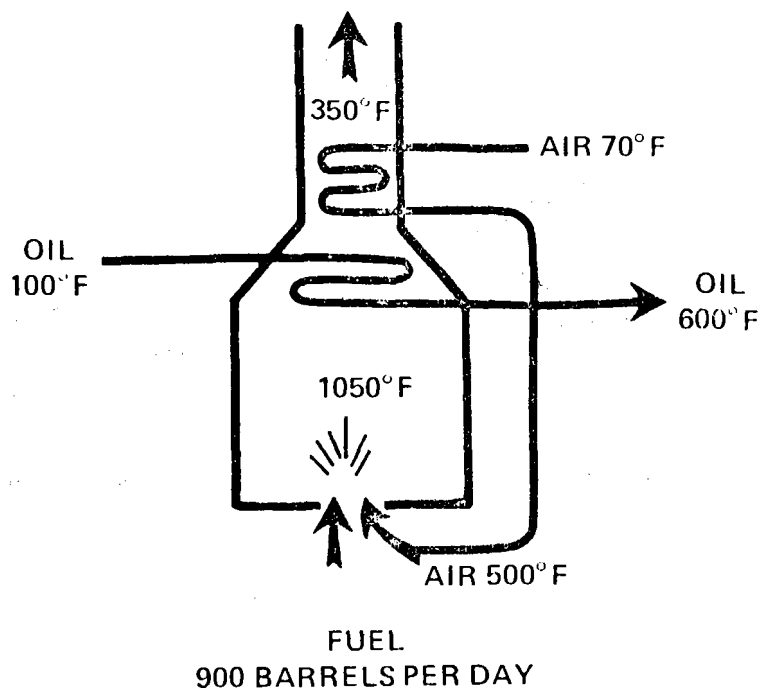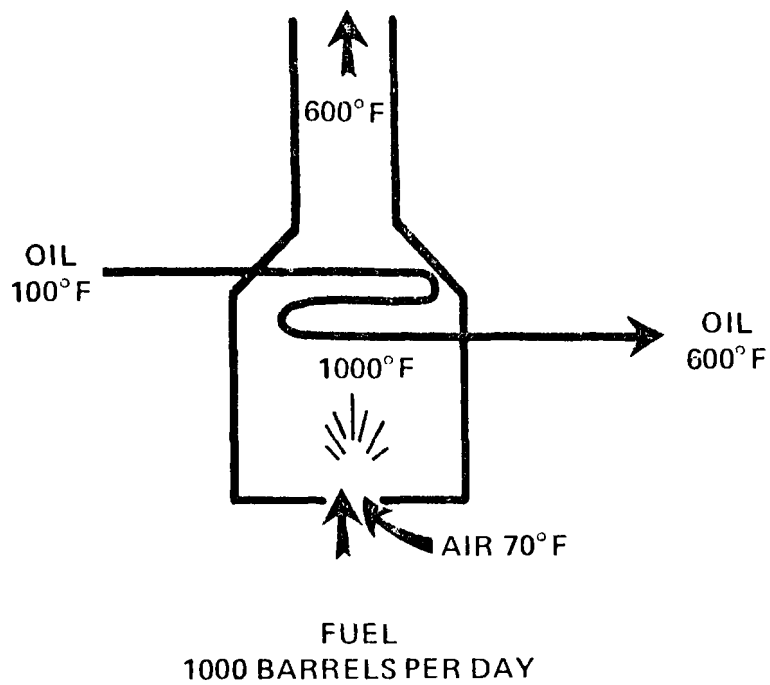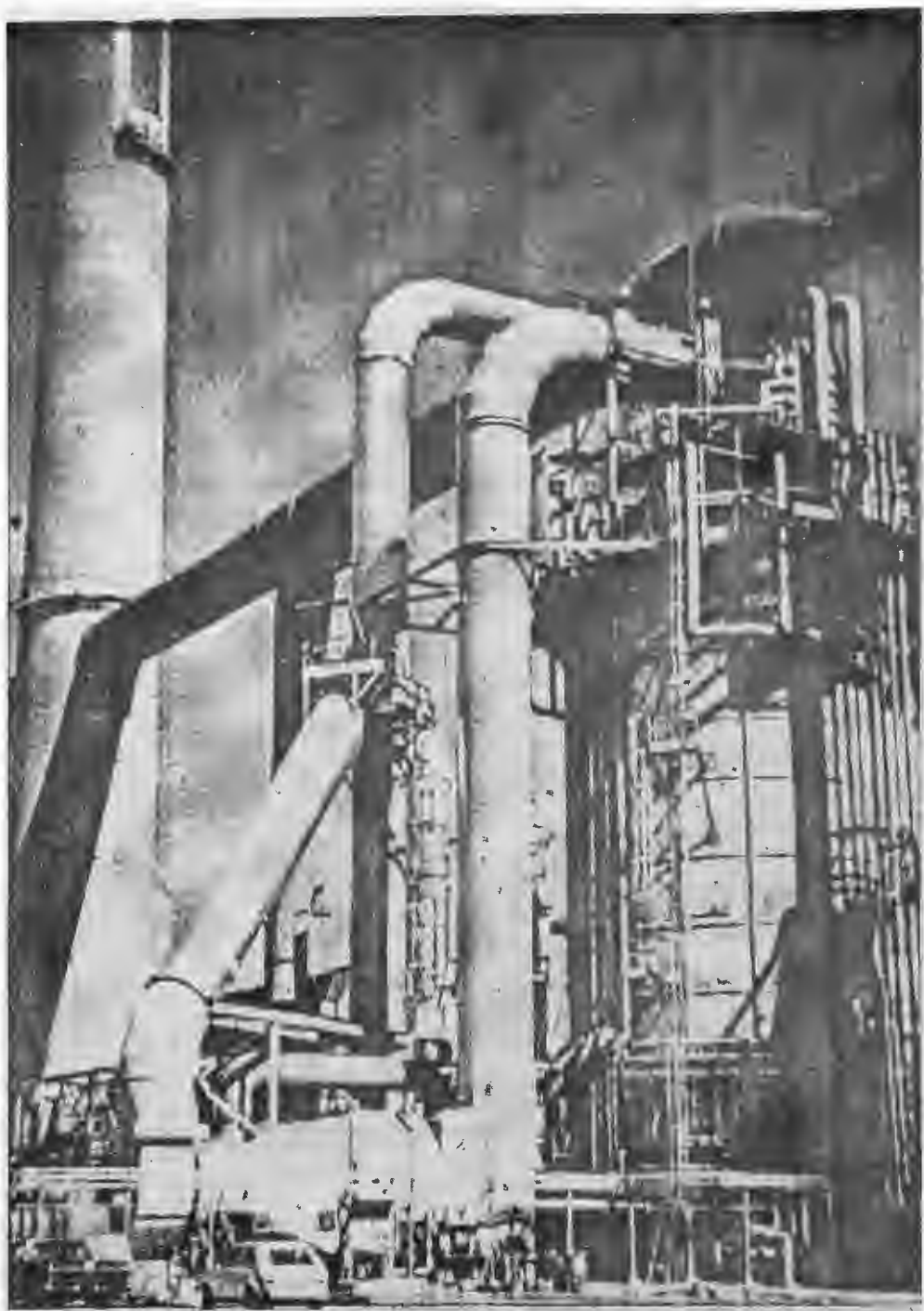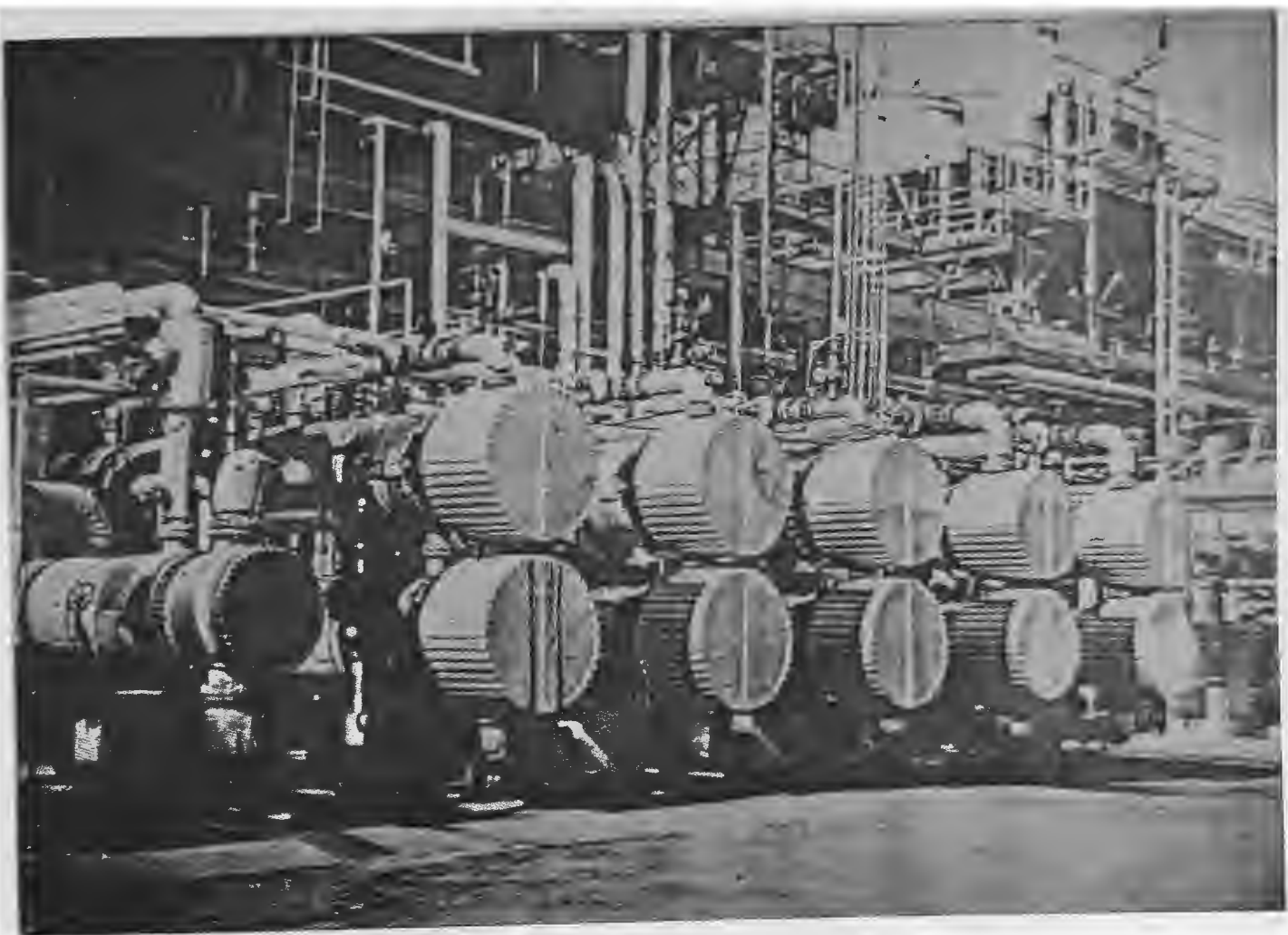
Use of Soil Warming and Waste Water Irrigation

for Forest Biomass Production

by

D. R. DeWalle and W. E. Sopper

School of Forest Resources
and
Institute for Research on Land and Water Resources
The Pennsylvania State University
University Park, PA, 16802, U.S.A.

ABSTRACT

   The opportunities for increasing biomass production from hybrid poplar plantations through the use of soil warming and waste water irrigation were studied in central Pennsylvania. Plots were established to determine the growth and development of hybrid poplar at three planting densities and three treatments: (1) soil warming plus waste water irrigation, (2) waste water irrigation only, and (3) no heat or irrigation. Soil heat was supplied to the soil from a buried hot-water pipe network. Spray irrigation of treated municipal waste water was conducted at a rate of 5 cm per week. In each of the three treatments the growth and development of sycamore, sweetgum, yellow-poplar and cottonwood were also evaluated at the intermediate tree density. Biomass production of hybrid poplar was doubled during the first growing season by waste water irrigation. Sycamore and sweetgum showed a positive height growth response to soil warming.

INTRODUCTION

Soil warming by circulation of condenser cooling water through pipe networks buried in the soil has been proposed as a method for utilization and dissipation of waste heat (DeWalle and Chapura, 1978; DeWalle, 1977). Considering the tremendous quantities of waste heat produced in power generation, large acreages of land could be artifically heated in this manner. Although yields of various vegetable and forage crops have been shown to increase in response to soil warming, virtually no information exists on the response of woody vegetation. Because of the potential usefulness of forest biomass as an alternate, low-sulfur fuel source in electric power production, the feasibility of using soil warming to stimulate the growth of forest biomass was investigated.

Treated municipal waste water is another by-product of our modern society which has proven useful in stimulating the growth of woody plants (Sopper, 1975). Spray irrigation of treated municipal waste water permits the natural recycling of nutrients through uptake by the biological system and the recharge of potable water. If used in conjunction with soil warming waste water irrigation could help to prevent excessive soil drying and provides nutrients for accelerated plant growth. A moist soil also has a higher thermal conductivity for more efficient heat dissipation from the buried pipes.

Intensively-managed, short rotation, forest plantations can supply significant amounts of biomass for fuel. Blankenhorn, et al. (1977) have estimated that forest land within a 56.3 km radius of Renovo, Pennsylvania could provide enough fuel to easily sustain a 100 MW electric generating facility. Intensive management of this forest land could increase the supply of biomass considerably. Bowersox and Ward (1976) have shown that two harvests of hybrid poplar trees in seven years (poplar trees sprout when cut) are capable of producing an average yield of 11.2 ovendry metric tons of wood and bark per hectare per year in Pennsylvania. Even greater yields of woody biomass are desirable to improve opportunities for fuel production.

The results of a study of the effects of soil warming and waste water irrigation on forest biomass production after the first growing season are reported in this paper. Plots were established to determine growth and development of hybrid poplar trees at three densities with 1) soil heat plus waste water irrigation, 2) waste water irrigation only and 3) no heat or irrigation. In addition, the effects of each treatment on sycamore, cottonwood, tulip poplar and sweetgum trees were also evaluated at one planting density.

STUDY AREA

The study was conducted 4 km north of The Pennsylvania State University campus at State College in Centre County at the site of the soil warming research facility. The site is located in the bottom of a small valley where the soil is classified as a Chagrin gravelly, sandy loam. The climate

of State College is a composite of a dry midwestern continental climate and the more humid eastern coastal climate. Mean annual air temperature is 10.0°C with a monthly average of -1.8°C in January and 22.2°C in July. Average dates of the first and last freezing temperatures are 12 October and 29 April, respectively. Annual precipitation averages 100 cm and is evenly distributed throughout the year.

METHODS

Soil was artificially heated by continuously circulating hot water through 5-cm diameter polyethylene plastic pipes buried at 26-cm depth and 61-cm spacing. Circulating inlet water temperatures were 38°C in June-August, 32°C in September-November and March-May and 27°C in December-February. Average soil temperatures in each treatment at the 30.5- and 15.2-cm depths during the first growing season are shown in Figure 1. Soil warming with waste water irrigation increased soil temperatures, while waste water irrigation alone reduced soil temperatures relative to the control area at both depths. Details of the soil warming and spray irrigation facilities have been previously described (DeWalle, 1977).

Waste Water Irrigation

Municipal waste water from State College, Pa. was sprayed above the trees at a design rate of 5 cm per week with two applications per week. A total of 86 cm of waste water was applied during the growing season from 7 June to 27 October, 1978. Irrigation was terminated on 27 October until spring. Precipitation during this same period was 43 cm. Average concentrations of dissolved solid in the waste water for the growing season are given in Table 1. Average pH of the waste water was 8.4. Based on the amount of effluent applied and the average concentrations in Table 1, the irrigation was equivalent to 144 kg/ha of nitrogen and 60 kg/ha of phosphorus as P_2O_5.

TABLE 1

AVERAGE CHEMICAL COMPOSITION OF MUNICIPAL WASTE WATER
APPLIED DURING FIRST GROWING SEASON

Constituent	Concentration (mg/ℓ)	Constituent	Concentration (mg/ℓ)
Ortho-P	3.27	Hg	0.6
Total-P	3.14	Cu	0.07
NO_3-N	7.3	Zn	0.13
NH_4-N	9.27	Cr	0.02
Org-N	0.64	Pb	0.06
Total N	17.21	Co	0.01
K	0.01	Cd	0.001
Cl	57.1	Ni	0.03
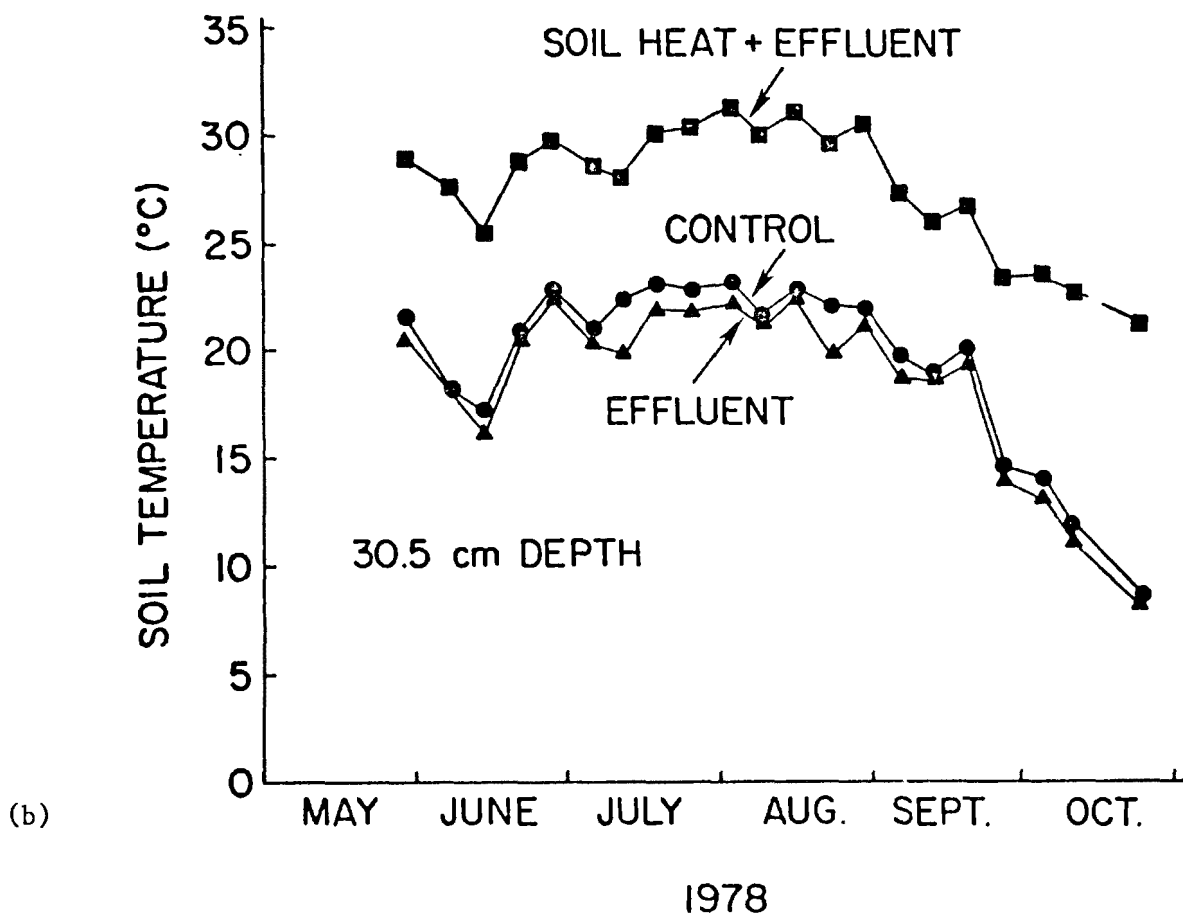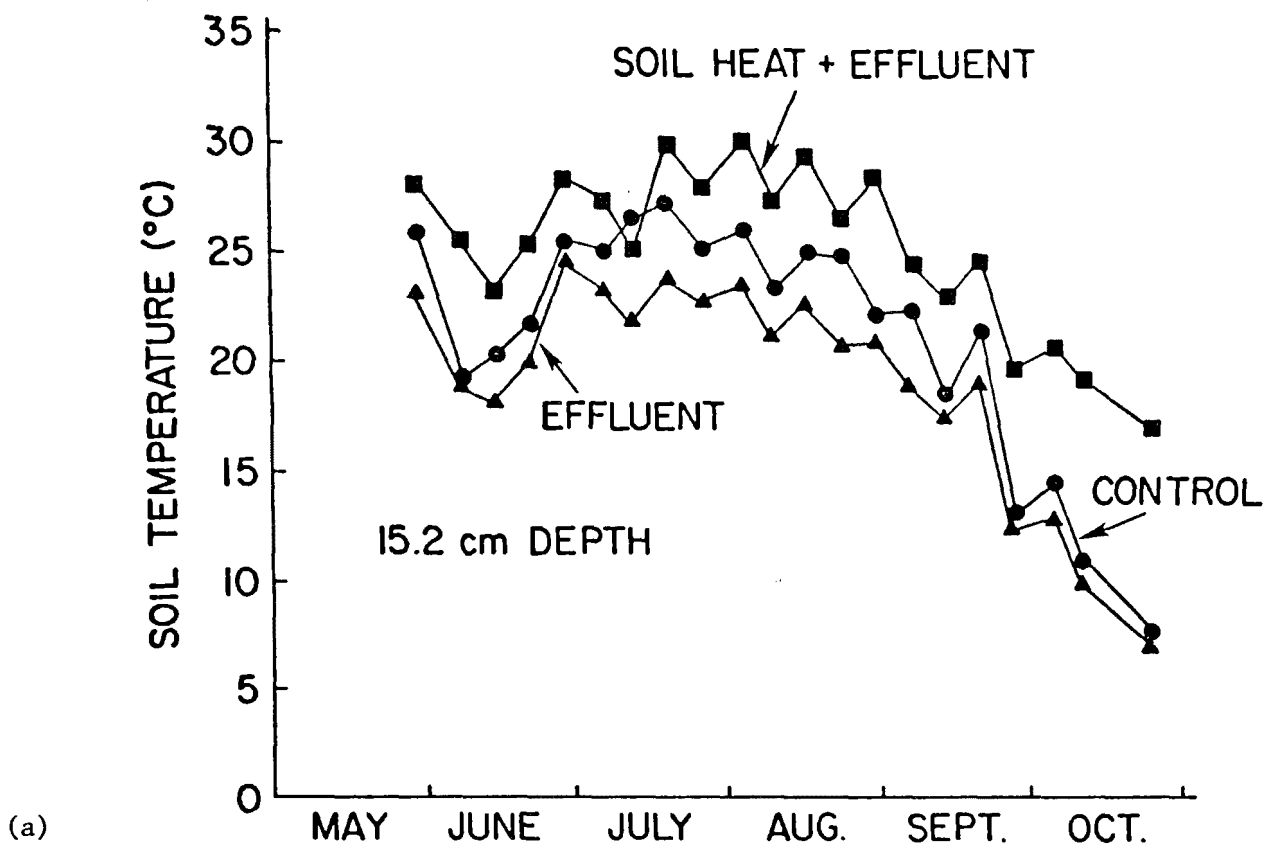
Figure 1.   Comparison of soil temperatures among treatments at the
a) 15.2- and b) 30.5-cm depths.

Soil moisture contents were increased substantially by the waste water irrigation. Moisture contents at 15.2-cm and 30.5-cm depths were gravimetrically determined on the day prior to irrigation at 14 locations in each treatment (Table 2). Moisture contents on the irrigated plots

TABLE 2

AVERAGE SOIL MOISTURE CONTENT ON 28 SEPTEMBER, 1978
AT TWO DEPTHS FOR EACH TREATMENT

Treatment	Soil Moisture Content (% wt.)	
	15.2-cm depth	30.5-cm depth
Soil heat and waste water	13.1	12.8
Waste water only	10.9	15.2
Control	8.0	8.2

were from 2.9 to 5.1% by weight greater at the 15.2-cm depth and from 4.6 to 7.0% by weight greater at the 30.5-cm depth than on the control area. The heated area was drier at the 30.5-cm depth than the area receiving effluent only due to the drying influence of the heated pipes. At the 15.2-cm depth trend was reversed with the effluent-only having drier soil.

Plantation Establishment

Hybrid poplar plantations (Populus spp.) were established in 3 m square subplots with 61 cm betw   rows and either 12, 24 or 48 cm spacing between plants in a row. These sp   gs gave 0.09, 0.18 and 0.36 m^2 of growing space per tree. Three replicate su   lots of each spacing were randomly located in each treatment area. Hybrid poplar cuttings were planted during the period 11-16 May, 1978. Cuttings were obtained from a Pennsylvania state tree nusery and were a mixture of clones.

At the same time, single subplots were established in each treatment area with cottonwood (Populus deltoides, Bartr.), yellow-poplar (Liriodendron tulipifera L.), sweetgum (Liquidamber styraciflua L.) and sycamore (Platanus occidentalis, L.) trees at the 24-cm spacing. Cottonwood was established from cuttings obtained locally, but the sycamore, sweetgum and yellow-poplar were planted as seedlings. Sycamore and tulip-poplar seedlings were purchased from a Pennsylvania state nursery, while sweetgum seedlings were purchased from a commercial nursery in Tennessee.

Competition from weeds was controlled by mowing between rows and hand cultivation within rows. Sycamore subplots were sprayed with SEVIN

70

to control a minor infestation by Japanese beetles.

RESULTS

Survival

Survival of the planted cuttings and seedlings as of 14 September 1978 was quite good, except for cottonwood (Table 3). Hybrid poplar survival averaged 96% or higher on all subplots with no major trend due to spacing or treatment apparent. Sycamore seedling survival was also quite high (>97%) with the highest survival in the waste water only area. A tendency for survival to be higher on the areas receiving waste water only was even more noticeable with yellow-poplar and sweetgum. Poor survival was only experienced with cottonwood due to the poor condition of cuttings at planting.

TABLE 3

AVERAGE TREE SURVIVAL AT END OF FIRST GROWING SEASON
(14 September 1978)

Species	Survival (%)		
	Control	Waste Water Only	Soil Heat and Waste Water
Hybrid poplar			
12 cm plant spacing	97	97	99
24 cm plant spacing	97	98	96
48 cm plant spacing	98	98	98
Yellow-poplar	71	88	86
Sycamore	98	100	97
Sweetgum	71	89	80
Cottonwood	49	35	49

Growth and Development

At the end of the first growing season, average stem height, mean basal diameter and biomass production were all greater on the areas receiving waste water only (Table 4). Areas receiving a combination of soil heat and waste water irrigation were less effective in promoting growth of hybrid poplar. The control areas receiving no waste water and no supplemental soil heat had the lowest mean heights, basal diameters and biomass production.

Planting density did not show any consistent relationship to growth among the treatments. In areas receiving heat and waste water the greater mean height occurred at the 12 cm spacing; however, the 48 cm spacing was associated with greater mean stem heights in the other treatments. Mean basal diameters were greater with the 24 cm in-row spacing in the heat plus waste water treatment, but in other treatments greater basal diameters occurred with the 48 cm spacing. The explanation of this inconsistency may be in the fact that the soil warming produced more small sprouts per cutting, especially with the 48-cm spacing. Numbers of stems on the areas receiving heat and waste water irrigation were 20% and 10% greater than on the waste water only and control areas, respectively.

TABLE 4

MEAN HEIGHT, MEAN BASAL DIAMETER, AND TOTAL BIOMASS PRODUCTION
FOR ALL HYBRID POPLAR STEMS AFTER FIRST GROWING SEASON

Treatment	Stems[1]	Mean Height (cm)	Mean Basal[2] Diameter (cm)	Estimated[3] Total Biomass (metric tons/ha)
Soil heat and waste water				
12 cm in-row spacing	643	96	0.78	
24 cm in-row spacing	365	91	0.80	
48 cm in-row spacing	204	84	0.74	
all spacings	1,212	92	0.78	1.42
Waste water only				
12 cm in-row spacing	638	111	0.89	
24 cm in-row spacing	353	108	0.93	
48 cm in-row spacing	170	115	0.97	
all spacings	1,161	111	0.91	2.14
Control				
12 cm in-row spacing	622	82	0.67	
24 cm in-row spacing	346	82	0.68	
48 cm in-row spacing	186	85	0.76	
all spacings	1,154	82	0.69	0.98

[1] Includes all multiple stems >30 cm height growing from cutting.

[2] Outside bark.

[3] Based upon average stem diameter, height and number; tentative.

72

Growth of hybrid poplar on the heated areas in June was similar to growth on areas getting waste water only; however, after July 1 differences in growth became apparent (Figure 2)   Excessively high soil temperatures, which exceeded 30°C at 15.2 cm during July and August (Figure 1), probably caused reduced height growth on the heated areas.   Height growth was essentially complete by early to mid-September when soil temperatures began to decline to more optimal levels.
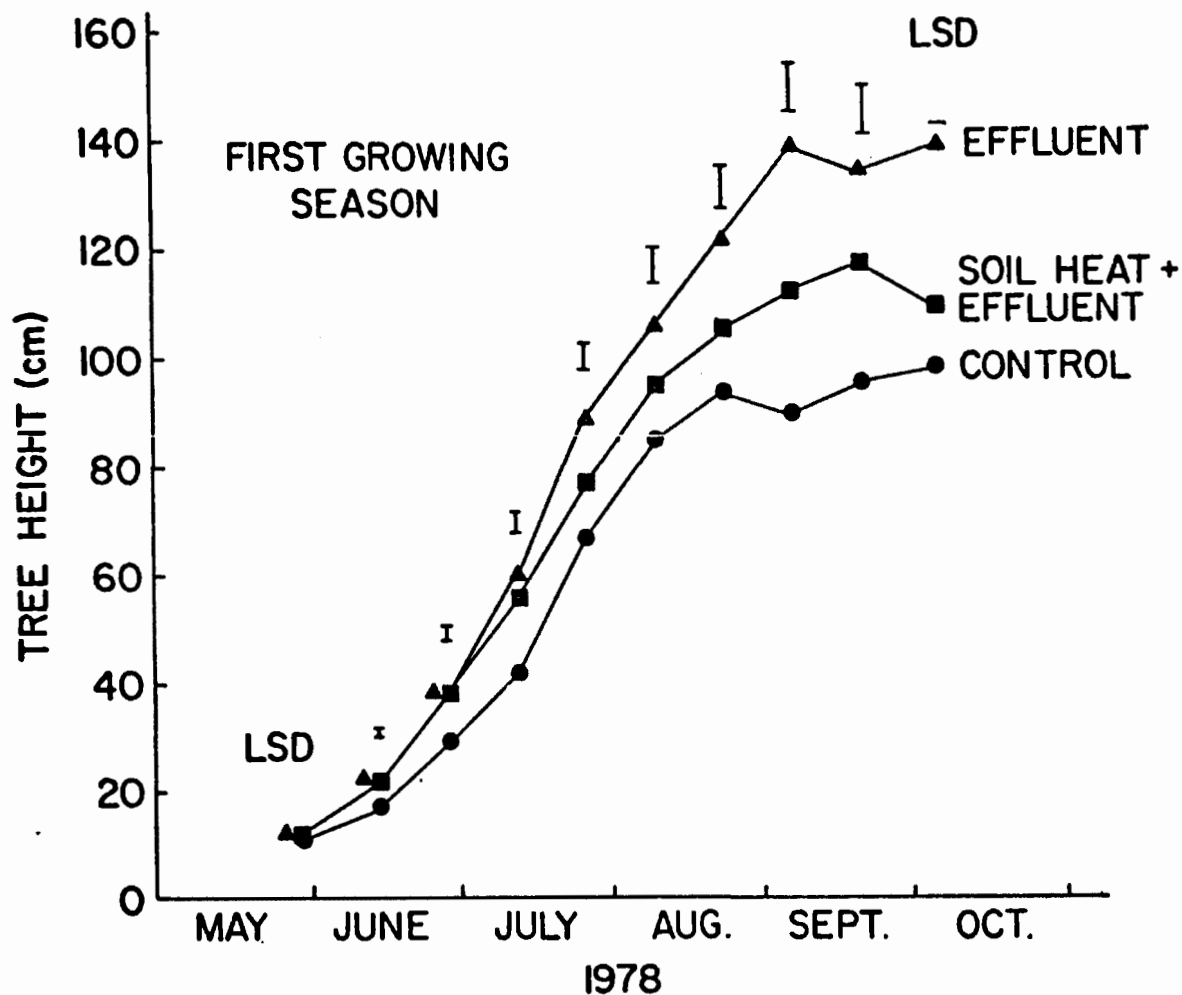
Figure 2.   Average height of hybrid poplar sprouts during first growing season for each treatment.   Each point represents the average of 90 randomly selected trees.

Height growth of other tree species tested showed variable response to irrigation and soil warming (Table 5). Yellow-poplar and cottonwood exhibited the greater mean height in areas receiving effluent irrigation only, as did the hybrid poplar. However, both sycamore and sweetgum had greater height growth in areas receiving a combination of soil warming and waste water irrigation than in areas which were only irrigated or held as controls.

TABLE 5

MEAN HEIGHT GROWTH OF SELECTED TREE SPECIES
AFTER FIRST GROWING SEASON

Species	Height Growth (cm)		
	Control	Waste Water Only	Soil Heat and Waste Water
Hybrid poplar (24 cm spacing)	82	108	91
Yellow-poplar	45	64	60
Sycamore	65	122	126
Sweetgum	25	38	47
Cottonwood	45	73	62

CONCLUSIONS

During the first growing season, hybrid poplar with a combination of soil warming and waste water irrigation grew less than with waste water irrigation alone. High soil temperatures during July and August on the heated plot may have caused stress in the young trees. Earlier planting to stimulate earlier initial growth in the first growing season is recommended for heated soils to compensate for any reduced growth in mid-summer. Effects of soil warming on spring growth initiation will be observed during the second growing season.

Height growth of both sycamore and sweetgum was enhanced by a combination of soil warming and waste water irrigation during the first growing season. A more intensive study of these species will be conducted during the second growing season.

Waste water irrigation alone at rates of 5 cm per week doubled the biomass production of hybrid poplar during the first growing season relative to the control area. Waste water irrigation increased soil moisture contents, increased available nutrients and reduced soil temperatures. Waste water irrigation plus soil warming increased hybrid poplar biomass production by 45% in the first growing season relative to the control.

ACKNOWLEDGMENT

LITERATURE CITED

Blankenhorn, P. R., T. W. Bowersox; J. Hillebrand and W. K. Murphey. 1977. Forest biomass evaluation procedure for consideration as a fuel source for a 100 megawatt electric generating facility. Pa. Science and Engin. Foundation, Final Report PSEF Grant 310, 63 pp.

Bowersox, T. W. and W. W. Ward. 1976. Growth and yield of close-spaced young hybrid poplars. Forest Science 22(4):449-453.

DeWalle, D. R. 1977. Utilization and dissipation of waste heat by soil warming. Univ. Miami, Dept. of Mech. Engin.; Proc., Conf. Waste Heat Management and Utilization, Session VII A, 73-86.

DeWalle, D. R. and A. M. Chapura, Jr. 1978. Soil warming for utilization and dissipation of waste heat in Pennsylvania. Nuclear Technology 38(1):83-89.

Sopper, W. E. 1975. Wastewater recyclcing on forest lands. in Forest Soils and Forest Land Management, edited by B. Bernier and C. H. Winget, Laval Univ. Press, pp. 227-243.

POWER PLANT LAND AVAILABILITY CONSTRAINTS
ON WASTE HEAT UTILIZATION*

M. Olszewski and H. R. Bigelow
Engineering Technology Division
Oak Ridge National Laboratory
Oak Ridge, Tennessee U.S.A.

ABSTRACT

An assessment of land available at nuclear power stations was performed in
an effort to determine the limitations land availability would impose on the
implementation of reject heat utilization systems. A waste heat utilization
factor was defined for all operating and planned nuclear power stations for
which a Preliminary Safety Analysis Report has been filed. This factor is
the percentage of the station's reject heat that could be utilized on the
land available for such use at the site.

The results indicate that reject heat from 115,000 MW(e) of generating
capacity could be utilized on the land which is available. The results
further indicate that about half of this potential implementation is at
stations that have enough land to accommodate waste heat utilization systems
sized to use all of the stations's reject heat. Utilization of the remain-
ing 50% is about equally distributed among sites capable of using between
10 and 90% of their reject heat. Further, it seems reasonable that for many
applications an integrated waste heat complex, using several waste heat
technologies, will be required to avoid marketing problems. It also appears
that single application systems will be important for the sites that can
use only a small fraction of their total reject heat.

INTRODUCTION

Recent utility statistics [1] indicate that thermal power stations generated
about 1.6×10^{12} MW(e)-hr of electrical power during 1975. Because of the
second law of thermodynamics, this resulted in about 11.0×10^{9} GJ
(11×10^{15} Btu) of low temperature heat being rejected to the atmosphere.
This low grade energy is equivalent to 4.4×10^{8} m^3 (2.8×10^{9} bbl) of oil
per year. Thus, if uses for this low grade heat could be identified and
implemented, a significant energy source could be added to the nation's
energy resources.

Various techniques have been proposed and studied to utilize this reject
heat, which is contained in power plant condenser cooling streams. These

76

applications have focused primarily on agricultural (greenhouse and live-stock facility heating, open field undersoil heating and spray irrigation) and aquacultural applications. Most of the efforts in these areas have been directed at developing the individual applications.

To date, however, there has been little information available concerning possible implementation levels for these systems on a national scale. As mentioned above the potential energy resource is large. However, since the major uses for this heat appear to be in the agriculture and aqua-culture areas, product marketing constraints may limit the use of reject heat to only a small fraction of the available resource. A second con-straint that may limit waste heat implementation is lack of available land surrounding power stations. Since it is generally uneconomical to transport the low grade reject heat any significant distance from the station, the waste heat applications must be sited in close proximity to the power station.

Information concerning the potential impact waste heat utilization can make in the power industry would be important to power companies and research organizations in determining research priorities in this area. If the poten-tial exists to utilize a significant fraction of reject heat in the power industry, then research efforts for the applications should receive priority and demonstrations and commercial applications be developed as quickly as possible. If, however, technical barriers to large-scale implementation are identified, research can be redirected to remove these obstacles.

A recent Oak Ridge National Laboratory (ORNL) study [2] attempted to define national implementation level for various waste heat utilization techniques by examining economic and marketing constraints from the waste heat user's perspective. The results of this study indicate that about 45% of the reject heat from thermal power stations could be utilized. This study, how-ever, did not account for land availability constraints associated with the power plant sites. Since most of the reject heat uses currently being examined require relatively large [on the order of 400 ha for a 1000-MW(e) plant] land areas to utilize a significant portion of the station's reject heat, land availability at the power station may limit wide-scale implementa-tion of such systems in the power industry.

The present study was initiated in an effort to determine if the implementa-tion levels reported in the previous study would be achievable when power plant site considerations were included in the analysis. The assessment was performed by analyzing site sizes for operating and planned nuclear sta-tions to determine the constraints land availability around these stations could impose on implementation of waste heat use systems. Because relevant site information was readily available for nuclear power stations, the study was confined to this segment of the power industry.

ANALYSIS TECHNIQUE

Information concerning the power plant sites was taken from Refs. 3, 4, 5 and 6. Since these sources used Preliminary Safety Analyis Reports (PSAR's)

as their source, the sites under consideration were confined to existing or planned nuclear power stations. Pertinent data concerning electrical output, site size, exclusion distance, and utility ownership are detailed in a recent ORNL report [7] for each station included in the study and will not be repeated here.

The portion of the power plant site, available for waste heat utilization facilities was estimated at 75% of the total site size. Initially, this area was computed using the exclusion distance and the total site size. In this scheme, the exclusion distance radius was used to calculate a circular exclusion area. This exclusion area was then subtracted from the site size to give the area that could be used for waste heat utilization facilities. However, for some sites this method yielded exclusion areas that were greater than the total site area. This was typically true for less than 10% of the sites, namely those that were located near bodies of water. When these sites were excluded, it was found that the exclusion area generally occupied 25% of the total site. Therefore, it was decided to uniformly use 75% of the total site area as the area available for reject heat facilities.

The area available for waste heat utilization systems was then used to determine what fraction of reject heat from the station could be utilized. To perform this analysis, however, it was necessary to estimate the area required by waste heat utilization systems to dissipate all of the reject heat from the power station. This area is a function of the waste heat utilization system being used and the site ambient weather conditions during the summer (high ambient temperatures during the summer result in minimum heat dissipation, hence, maximum system size). Such a detailed analysis, however, was beyond the scope of this study. Therefore, an average required waste heat utilization system size was used for the analysis.

This average system size was estimated using the results of a previous study [2] comparing various reject heat use alternatives. This study included greenhouse, animal shelter, and aquaculture applications and, thus, included the major waste heat use applications currently being examined. These systems were designed to accommodate, if possible, the yearly cooling needs of a 1000-MW(e) power station in Portland, Oregon. The results of the study indicated that an average area of 400 ha is required to utilize all of the reject heat from a 1000-MW(e) power station. Thus, for the purposes of this study, it was assumed that 0.4 ha/MW(e) of installed capacity was required to utilize all the reject heat from a power plant.

The area available at nuclear power stations and the average area required to utilize all of the reject heat from the station were then used to calculate a waste heat utilization factor (WHUF). The WHUF was calculated by dividing the area available for reject heat utilization by the area required to utilize all of the station's reject heat. The latter figure was obtained by multiplying the average area requirement of 0.4 ha/MW(e) by the total installed capacity of the station.

The WHUF thus indicates the percentage of the total reject heat of the station that can be utilized if all of the unused area at the station

78

was dedicated to a waste heat utilization system. (This system could consist of a single application, such as greenhouses, or include a number of applications.) A site having a WHUF of 100%, or greater, has enough land available to utilize all of its reject heat. Thus land availability will not constrain implementation of waste heat utilization systems at these sites. Sites having a WHUF less than 100% have only enough land to utilize a portion of their reject heat. Thus, for these sites, land availability will restrict the use of reject heat.

The WHUF data were then used to obtain the distribution of stations, with respect to their ability to use reject heat, by summing the number of stations in each 10% range (0–9, 10–19, etc.) and plotting them in Fig. 1. To obtain a better understanding of the relative importance of each WHUF range, the total installed capacity distribution, corresponding to the site distribution in Fig. 1, was plotted in Fig. 2.

The primary intent of this study was to determine the nuclear generating capacity from which waste heat could be utilized. The distribution of this capacity among the WHUF ranges is given in Fig. 3. These results were obtained by multiplying the installed capacity values in Fig. 2 by the mid-point WHUF for the range. The results in Fig. 3 thus indicate the generating capacity whose waste heat could be utilized for the various WHUF ranges. For example, at sites that can utilize 70 to 79% of their reject heat land availability considerations would allow reject heat from 8500 MW(e) of installed capacity to be utilized [this is in contrast to the total installed capacity of 11,500 MW(e) for this range from Fig. 2].

The results in Fig. 3 were then used to develop cumulative plots with respect to the installed capacity from which reject heat could be utilized (Fig. 4) and on a percentage basis (Fig. 5).

DISCUSSION OF RESULTS

The results illustrated in Figs. 1 and 2 indicate that, in terms of both number of stations and generating capacity, sites that have enough land available to utilize all of their reject heat (WHUF ≥ 100%) provide the greatest potential for implementing reject heat use systems. These sites comprised 32% of the stations and 28% of the total generating capacity included in the study and thus represented a large fraction of the nuclear power generating capability.

The relative importance of these sites is further illustrated by considering the amount of generating capacity from which reject heat can be utilized (see Figs. 3–5). The results in Fig. 3 indicate that the waste heat from 53,000 MW(e) of generating capacity can be utilized at sites having a WHUF of 100% or greater. The cumulative results plotted in Figs. 4 and 5 indicate that these sites comprise about 50% of the total capacity that could utilize reject heat. Thus, if reject heat utilization is to be implemented at significant levels, much of this potential will have to be exploited.

From Fig. 2 it would seem that the next most important group would be those stations that have a WHUF in the range of 20–29% (i.e., could utilize between 20 and 29% of their reject heat). However, the results in Fig. 3 indicate that most of the remaining WHUF ranges are of about equal importance in terms of capacity from which reject heat could be utilized. This is due to the fact that, although the installed capacity represented by the power stations in the lower WHUF ranges is greater than those in the higher ranges, the fraction of this capacity which could utilize its reject heat is decreasing. Thus, the two trends offset each other and the capacity for which reject heat could be utilized remains about constant. Therefore, the results in Fig. 3 indicate that the sites in the WHUF ranges less than 100% are of about equal importance in terms of implementation significance.

The relative importance of the various WHUF ranges is important when considering the type of waste heat utilization complex that would probably be required to utilize the reject heat. Since the sites whose WHUF is 100% or greater are about as important, in terms of implementation potential, as those having a WHUF less than 100%, discussion of the makeup of the reject heat complex will focus on these two applications. From Figs. 1 and 2 it is apparent that the stations in the 100% or over WHUF groups are fairly large stations. Dividing the total capacity [56,200 MW(e)] by the total number of stations (36) yields an average station size of 1560 MW(e). A waste heat utilization complex sized to utilize all the reject heat from a station of this size would require about 600 ha. Since it is unlikely that local conditions would permit the marketing of only one type of product, the waste heat utilization system would be required to produce a number of products. The required diversity of production could be accomplished in one of two ways. One method could have the entire complex comprised of a single application, which would market a number of products. For example, the waste heat utilization system could be a large greenhouse complex producing tomatoes, cucumbers, lettuce, and various floral crops. A second, and more realistic, alternative would be an integrated system consisting of a variety of applications. For example, the complex could include greenhouses, animal shelter heating, aquaculture, and undersoil heating applications. Since each of these applications markets a different product, this type of system would offer greater design flexibility in sizing each individual application to meet local marketing constraints.

For sites that utilize only a fraction of their reject heat, design of the waste heat utilization system will depend upon specific site conditions. Since most of the WHUF ranges are of about equal importance, some of the systems will be large (for sites in the higher WHUF ranges) while others will be smaller. The larger systems will face the same marketing constraints mentioned above and will probably include several applications. The smaller systems, however, are not likely to face these constraints and could include only one application.

Therefore, it appears that if reject heat utilization is to be implemented at a significant level, integrated systems, involving several waste heat technologies, will play an important role. It further appears that systems comprised of only one application will also be utilized to a significant degree.

The results in Fig. 4, showing the cumulative capacity from which waste heat could be utilized indicate that waste heat utilization systems could utilize all the reject heat from 111,500 MW(e) of generating capacity, if land availability at nuclear stations were the only criterion. Previous analysis [2] of economic and marketing constraints showed that all the reject heat from 180,000 MW(e) of generating capacity could be used if only economic and marketing constraints were considered. Therefore, if the maximum indicated potential of these systems at nuclear stations was achieved, about 60% of the projected maximum industry-wide implementation could be achieved. Since nuclear power stations comprise only about 8% of the total thermal generating capacity in this country, it is reasonable to expect that the implementation levels based on economic and marketing constraints would not be further limited by power plants site size considerations.

CONCLUSIONS

Analysis of power plant site size barriers to waste heat utilization has indicated that enough land is available at nuclear stations to utilize the reject heat from 111,500 MW(e) of generating capacity.

The results further indicated that sites that can utilize all of their reject heat make up approximately 50% of this capacity. The remaining capacity is distributed fairly uniformly among the WHUF ranges below 100%. This result indicates that integrated systems involving several waste heat utilization technologies will be important for over 50% of the possible implementation, while single application systems could be used for the sites that are constrained to use smaller systems.

The results also indicate that economic and marketing criteria constrain waste heat utilization implementation more severely than power plant land availability considerations.

REFERENCES

1. Edison Electric Institute, *Statistical Yearbook of the Electric Utility Industry*, Publications No. 75-39 (November 1975).

2. M. Olszewski, *Power Plant Reject Heat Utilization: An Assessment of the Potential for Wide-Scale Implementation*, ORNL/TM-5841 (December 1977).

3. F. A. Heddleson, *Design Data and Safety Features of Commercial Nuclear Power Plants*, ORNL/NSIC-55, Vol. 1-4 (1973-1976).

4. F. A. Heddleson, *Design Data and Safety Features of Commercial Nuclear Power Plants*, ORNL/NSIC-96 (June 1976).

5. F. A. Heddleson, *Design Data and Safety Features of Commercial Nuclear Power Plants*, ORNL/NUREG/NSIC-136 (June 1977).

6. D. F. Cope and H. F. Bauman, *Expansion Potential for Existing Nuclear Power Station Sites*, ORNL/TM-5927 (November 1977).

7. M. Olszewski and H. R. Bigelow, *Analysis of Potential Implementation Levels for Waste Heat Utilization in the Nuclear Power Industry*, ORNL/TM-6312 (to be published).
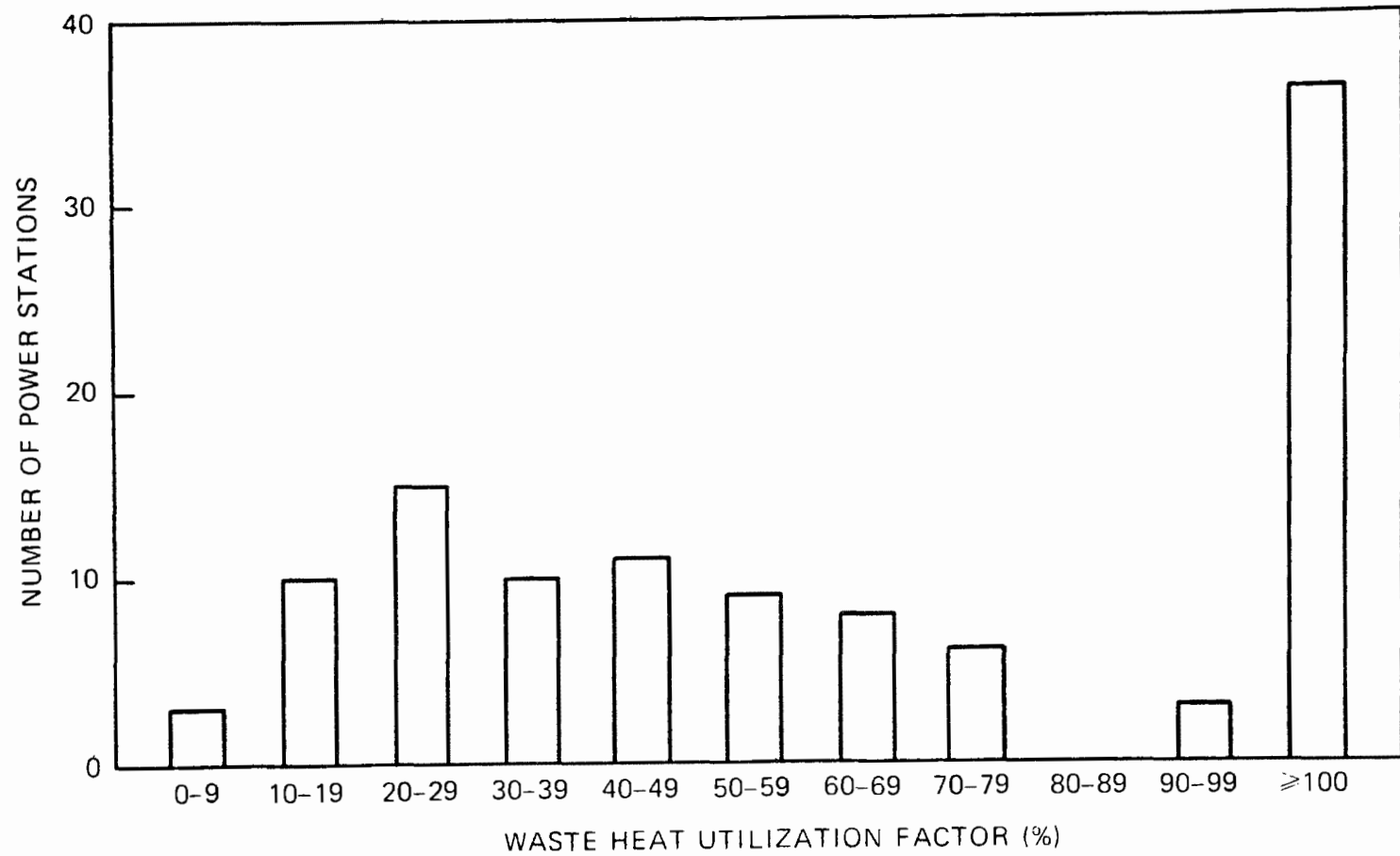
Fig. 1.   Number of Power Stations that Can Utilize a Given Fraction of Their Waste Heat.
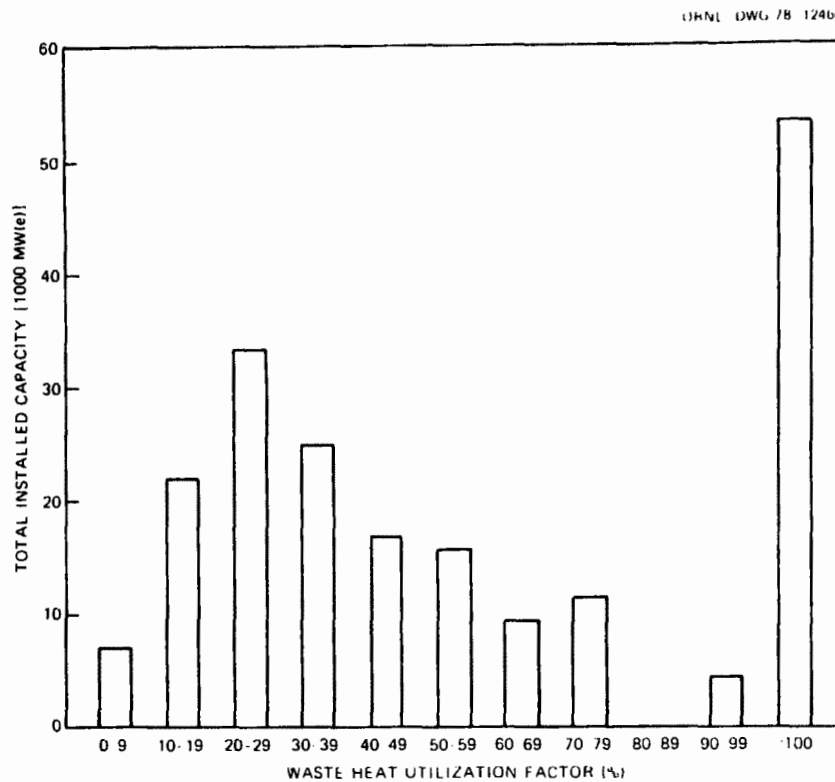
Fig. 2. Total Installed Capacity of Stations that Can Utilize a Given
Fraction of Their Waste Heat.
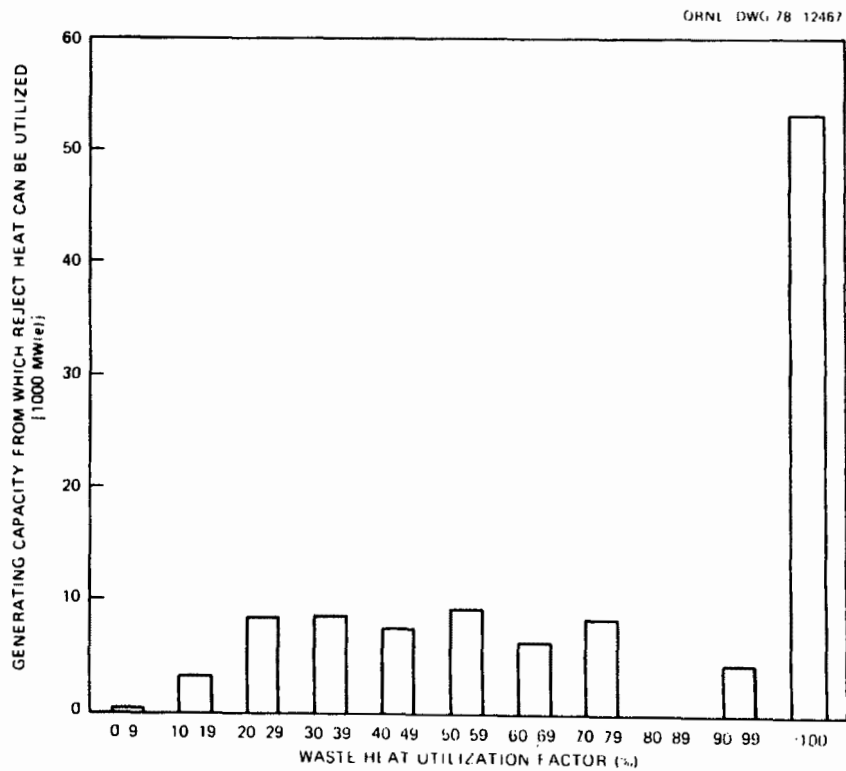
Fig. 3. Installed Capacity for Which Reject Heat is Utilized.
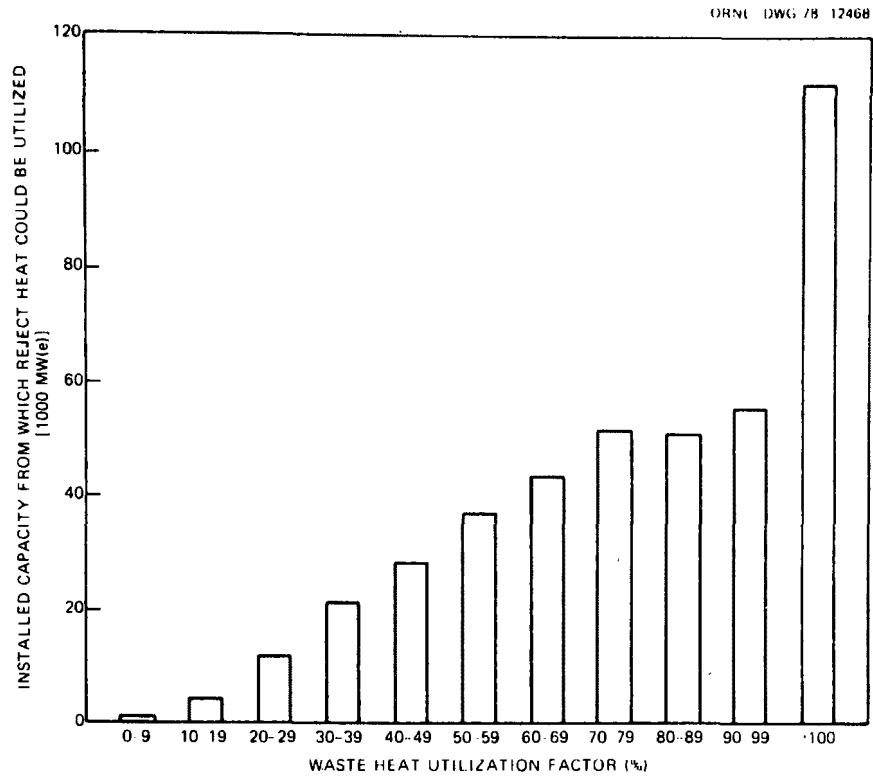
Fig. 4. Cumulative Installed Capacity Utilizing Waste Heat Utilization.
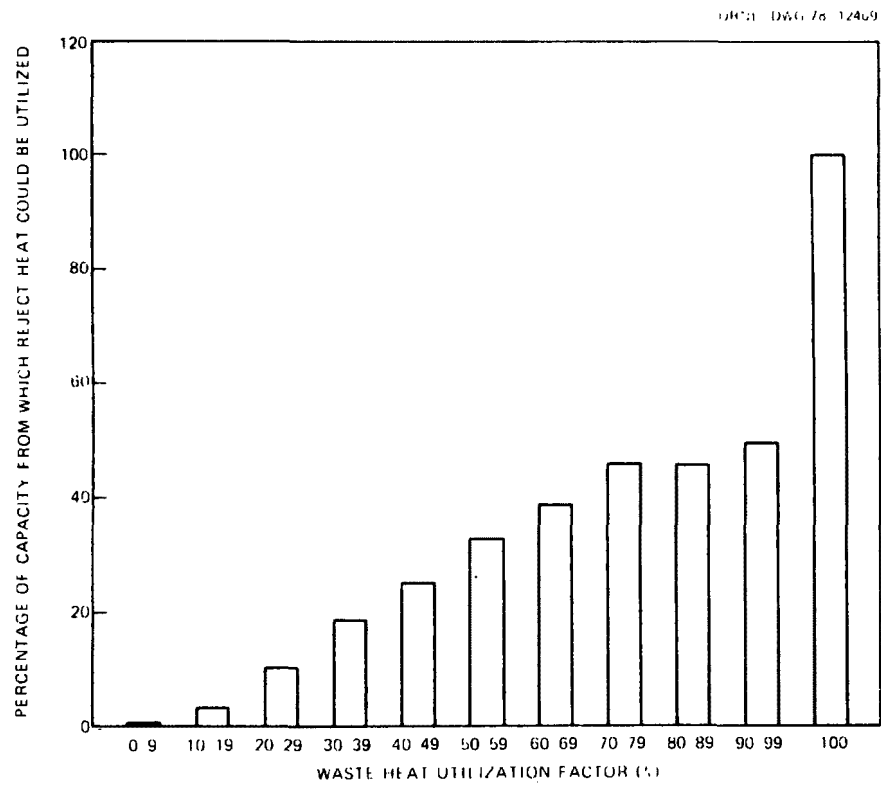
Fig. 5. Cumulative Percentage of Capacity Utilizing Reject Heat.

COOLING PONDS AS RECREATIONAL FISHERIES
A READY MADE RESOURCE

J. H. Hughes
Commonwealth Edison Company
Chicago, Illinois U.S.A.

ABSTRACT

The 1275 acre perched cooling pond constructed to enable the
thermal discharge from Dresden Nuclear Station to meet State
Water Quality Standards shows potential as being a recrea-
tional fishery and Illinois River hatchery.

This resource can be used in either or both of two ways.
The pond itself might be developed as a recreational fishery
by opening it to the public. The use of the cooling pond as
a hatchery to supply the Illinois River is also a possibil-
ity.

Recently while analysing data collected to support our
§316(b) demonstration at Dresden Station we came to an
interesting conclusion: The perched cooling pond used for
condenser cooling has a large fish population.

Dresden is a nuclear generating station consisting of three
boiling water reactor units with a net capacity of 1795 mw_e
Unit 1, a 207 mw_e unit, began commercial service in 1960.
It uses a once-through condenser cooling water system which
is separate from units 2 and 3. Units 2 and 3 each have a
capacity of 794 mw_e and were placed in service in 1970 and
1971. These two large units have a spray canal, cooling
pond system which can be operated as a closed cycle cooling
facility or as a condenser cooling water trimming facility
wherein all of the cooling water flows through the pond then
is discharged to the river. Any discharge flow in between
these extremes can also be obtained. See Figures 1 - 4.

All three units withdraw water from the Kankakee and Des
Plaines Rivers at their point of confluence. The cooling
water is discharged to the Illinois River which is formed by

86

the combination of the two previously named rivers. The temperature rise through the unit 2 and 3 condensers is 24°F maximum.

Open cycle operation of units 2 and 3 occurred for the first year after unit 3 was placed in service while the cooling pond was constructed. The cooling pond was an add-on feature of the plant made necessary because of a reduction in thermal standards of the Illinois River by the Illinois Pollution Control Board. For the next three years the four mile long spray canal and 1275 acre pond were operated in the once-through mode.

Starting in 1977 a modified closed cycle operation has been employed to avoid a severe megawatt derating of the station due to high temperature of the water returning to the condensers. Under this plan the blowdown from the pond is adjusted on a daily basis to obtain a condenser inlet temperature no greater than 91.5°F. Blowdown rates vary from 50,000 gpm to 500,000 gpm under this mode.

While collecting impingement data for the unit 2-3 intake structure we found that a considerable number of fish were impinged. This prompted U.S. EPA to make a preliminary determination that the intake structure did not confrom to BAT criteria Note however that the water returning from the pond in the closed cycle mode of operating also passes through the intake. A close examination of the data coupled with verification in the form of studies of fish passing over the pond discharge spillway confirmed that most of the fish impinged originated in the cooling pond, not in the Kankakee River. Electroshocking studies of the pond have shown that there is a large population of carp and gizzard shad present with a small but significant number of small mouth bass, bluegill, greensunfish and largemouth bass. We also know from the spillway studies mentioned above that large numbers of freshwater drum and channel catfish exist in the pond.

The question arises, what conditions exist in the pond to support these fish and how did they get there? Before the cooling pond was constructed the underlying land contained virtually no surface waters. All fish now present entered by passing through the intake, circulating water pumps, con-

densers and lift pumps either in the egg or larval stage. Sufficient numbers survived to populate the pond. No intentional stocking has ever occurred.

The water quality of the cooling pond has been found to be superior to either of the two rivers which provide make-up water. This is not an unexpected phenomenon, ponds have played an important role in water treatment for years, providing an enhanced settling and oxidation environment for pollutants. In addition the combined "heat treatment" of the condensers, followed by aeration in the spray canals and spillway improve the quality of the water beyond what would be expected in a quiescent settling pond.

For years the belief that fish would not do well in an environment heated to the extent of Dresden pond has been widely accepted. However, the fish in the Dresden cooling pond live in an environment that varies from about 113°F to 95°F. We have found that during the summer when the cooling pond temperatures are highest that the fish avoid the warmest part of the pond, but seem to have little trouble surviving in the cooler pools which still exceed 90 F. This conclusion is born out by extensive studies performed at our Lake Sangchris which is an impounded lake constructed to provide condenser heat dissipation at a coal fired generating station in Central Illinois. Lake Sangchris is a productive lake for bass and is quite popular with fishermen in water deficient central Illinois.

Table 1 indicates numbers of some of the species that left Dresden Pond in the interval May through August 1978. As expected the majority of the fish exited in July and August when temperatures in the lake are warmest and this can be attributed to avoidance of warmer temperatures in the lake by these species. We believe that it is remarkable that such large numbers can even exist in the lake in light of past thinking about heat, entrainment, and impingement.

These data suggest that more thought should be given by regulators and fisheries management personnel to considering cooling lakes as nursery areas for receiving wate . These ponds would be operated in the closed cycle mode i ut of the year and in the indirect open cycle mode in the summer. This would maximize fish production in that optimal tem-

peratures would exist in some portion of the pond throughout the year. It would also minimize entrainment effects (if any) in the makeup and receiving water since most fish eggs and larvae are present in the spring and early summer.

You may recall from Table 1 that most of the fish that left Dresden Pond were of a forage variety and few are sport fish. Large numbers of sport species do not exist in Dresden Pond and this has been attributed to a lack of suitable spawning habitat. Dresden Pond is bermed with a shoreline consisting almost entirely of rip rap with a 3-1 slope. No extreme shallow areas for nest builders exist. However this deficiency could have been corrected had it been considered before the lake was constructed.

There are a number of other methods available for making cooling ponds suitable for spawning areas. Addition of long canals provide spawning habitat for white bass as is evidenced by large populations of this species in Lake Sangchris and in another Commonwealth Edison cooling pond, Collins pond. Also the presence of large areas of rooted macrophytes and bushy shoreline areas results in good year classes of crappies at Lake Sangchris and Collins. Pond levels can also be designed so that they can be manipulated for drawdown in the summer to provide areas for establishment of terrestrial vegetation and flooded again the following spring. This provision will also provide additional spawning habitat, and it may be that species such as the northern pike will reproduce successfully under these conditions. Collins Pond has a reasonably large population of northern pike despite relatively high temperatures for this cool water species. However, there has not been any successful reproduction in this cooling pond.

Sport fish enhancement could also be undertaken by means of small hatcheries. In this case desirable sport species would be stocked as fry in small ponds adjacent to the cooling ponds and allowed to grow through the summer. These fingerlings in turn would be allowed to enter the lake by simply pulling a standpipe and allowing the hatchery pond water and fish to enter the cooling pond where abundant forage exists. The forage and sport fish will concentrate in the warmer water as winter approaches. We consider threadfin shad as the forage base for the stocked predators.

This scheme will require very little effort since once stocked in the hatchery ponds, no additional effort is needed until fall. At that time the only effort needed is in removing the hatchery pond standpipes.

In summary, data from Dresden Pond and other cooling ponds and lakes leads us to believe that heat, entrainment and impingement effects so vigorously pursued by regulatory agencies are largely nonexistent. Compensation or the ability to adjust to various population impacts is far greater than has been considered in the past. This is not to say that power plants should be sited just anywhere and no impacts are occurring.

Furthermore, it is appropriate that the beneficial aspects of waste heat should be considered in designing closed cycle or partial closed cycle cooling systems. Cooling ponds and lakes frequently offer substantial recreational benefits over cooling towers and this alternative should be seriously considered by regulatory agencies when it is available. Also, the concept of cooling ponds as nursery areas for receiving waters should be addressed with detailed studies in the near future.

The major advantage of using the warm cooling pond water in this way is that little additional capital expenditure is required. In addition, this use fills an important need for the metropolitan Chicago area. There is a need for additional recreational fishing areas in this area, especially geared to the desires of the casual fisherman who wishes to have a resource nearby that he can visit for a short time and be reasonably sure of a satisfying catch.

TABLE 1 ESTIMATED NUMBERS OF SOME FISH SPECIES LOST
AT THE DRESDEN COOLING POND SPILLWAY,
MAY THROUGH AUGUST, 1978

Month

Species	May	June	July	August	Totals
Gizzard shad	48,371	224,423	188,271	329,734	790,799
Bluegill	365	1,227	1,040	620	3,252
Channel Catfish	715	1,296	1,461	1,069	4,542
Fresh ter Drum	1,100	1,390	1,462	979	4,931
Green Sunfish	81	1,017	342	313	1,753
Smallmouth bass	20	29	67	78	194
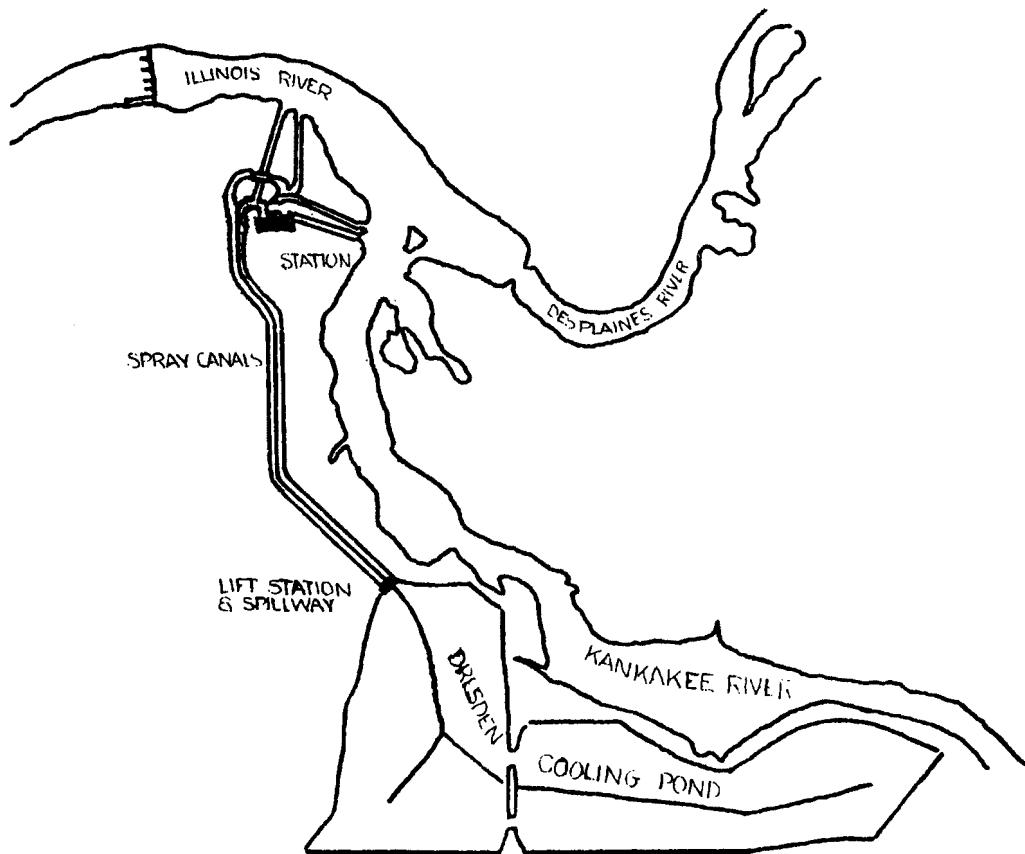
Fig. 1 Dresden Station and Cooling System
General Arrangement
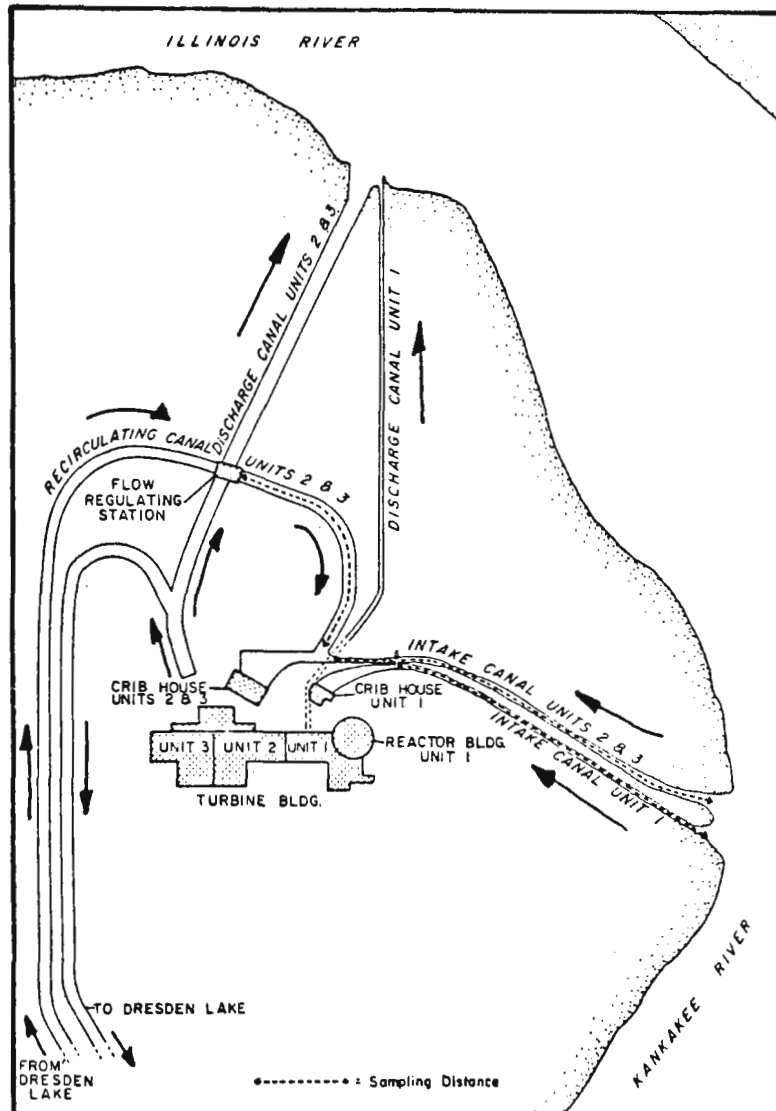
Fig. 2   Dresden Station Detail

Fig. 3   Dresden Cooling Pond

94

Fig. 4 Dresden Station and Spray Canals

HEAT RECOVERY AND UTILIZATION FOR GREEN BAY'S WASTE WATER TREATMENT FACILITY

R. W. Lanz
University of Wisconsin - Green Bay
Green Bay, Wisconsin U. S. A.

ABSTRACT

A feasibility study to identify and evaluate commercially available heat recovery systems for cost effective use in the three year old energy intensive Green Bay Metropolitan Sewage Treatment Plant has been completed. After studying all the systems at the facility, it was found that the liquid system showed the most potential for energy recovery and the fuel oil fired hydronic heating system showed the greatest potential for energy savings. It was determined that heat recovered from the liquid system should be utilized in the heating system and that heat pumps would be the most applicable equipment for this heat recovery and utilization scheme. Energy cost savings using heat pumps rather than the exclusive use of fuel oil boilers to heat the facility should be $101,000 per year with a capital equipment investment of about $425,000. The total annual savings including maintenance and equipment amoritization cost should be $58,000.

INTRODUCTION

A proposal was approved by the Commissioners of the Green Bay Metropolitan Sewage District to have this investigator conduct a feasibility study to identify and evaluate alternate energy sources or systems for cost effective use in the three year old Green Bay Metropolitan Sewage Treatment Plant.

A first step in the study required a knowledge of the systems at the facility and the interrelationships between these systems. This knowledge was gained by studying system schematics, conferring with plant personnel who were involved with these systems and studying system components during operating conditions.

Knowledge of the current energy consumption of particular systems at the facility was also required before recommendations concerning conservation of energy or alternate energy systems could be made. However, because most systems were not monitored for energy consumption, the precise division of the total energy consumption at the facility among its particular systems was unknown. Therefore this division was determined by thermodynamic calculations on these systems.

As a result of these calculations, it became obvious that recovering waste

heat at the facility should take precedence over considerations of the generation of more heat. Therefore this study was expanded to include applicability of commercially available heat recovery systems to the facility. It is this aspect of the study which is presented in this paper.

EXISTING SYSTEMS AND THEIR ENERGY POTENTIAL

The systems at the facility were divided into two major catagories. The first catagory, called the main systems, includes both the major energy users and major energy transfer systems while the second catagory, called minor systems, includes the minor energy users or energy transfer systems. The main systems are the liquid system, solid system, process air system, process boiler system, electric power system and hydronic heating system. The minor systems are the control air system, cooling water system and the chemical addition system.

The liquid system handles 18 to 20 million gallons per day of waste from metropolitan Green Bay in addition to 16 to 18 million gallons per day of waste from several paper mills in the Green Bay area. The energy consumed by this system is used for the numerous electric motor driven pumps to lift the waste from the intercepters for treatment and electric motor driven a-rators to treat the waste in the contact basins. The mixture of metropolitan and mill waste handled by the facility varies in temperature from a minimum of 18 C (64 F) in January to a maximum of 31 C (88 F) in July. The obvious resource in this system is the heat contained in 34 to 38 million gallons of liquid at these temperatures. Possibilities were immediately visualized for extracting some of this heat, keeping in mind that lowering the temperature of the liquid in the contact basins may impair efficient sewage treatment.

The solids system transports the solids from various basins to the solids handling building for the heat treatment and incineration process. Energy consumed by this system is used for the electric motor driven pumps to transport the solids. Little opportunity for energy recovery or utilization was seen for this system.

The process air system provides compressed air for the aeration contact basins used in the treatment process. Four air compressors, each driven by a 2500 H. P. electric motor are the heart of the system. There have been efforts by plant personnel to reduce the energy consumption of this system by operating at a minimum air flow while maintaining adequate treatment in the contact basins. As with the solids system, little opportunity for energy recovery or utilization was seen for this system.

The process boiler system supplies steam at 500 psi for the purpose of heat treating the sewage sludge. The steam used in this process cannot be recondensed for boiler feed water because of the type of heat treatment used. Therefore 100 percent boiler makeup water is required.

Because of this characteristic, energy recovery from this system was not evident.

The electric power system is the most nebulous of any system in the facility. It runs throughout the facility and is of utmost importance in the operation of the plant. It provides energy for the hundreds of electric motors needed to drive pumps, fans, compressor, agitators, and aerators and for lighting, maintenance and control. Plant personnel have been reducing the energy requirements of this system by using the most prudent use of electric power in operating the plant.

The hydronic heating system for the facility uses a pair of fuel oil fired hot water boilers located at one end of the facility. The heated water is pumped through a 14 inch diameter pipe located in a tunnel system in a circumferential path around the facility. Secondary heating loops supplied by the 14 inch line heat the seven individual buildings at the facility. The water temperature at the cold end of the heating loop is controlled at 82 C (180 F) which produces temperatures at the hot end of about 91 C (196 F).

Since the facility is located in an extreme northern climate, it seemed reasonable that heat recovered from the final effluent could be utilized most of the time of the year in the heating system. However, the problem of raising the temperature of large quantities of heat at a minimum effluent temperature of 18 C (64 F) to a temperature adequate for the heating system had to be solved.

CURRENT ENERGY USE

The major forms of energy used at the plant are purchased electric power and fuel oil. Although there is the capability of using natural gas,consumption of this fuel will probably remain minor. Electric power consumption at the facility, although of major importance, was not addressed in this investigation. Fuel oil is burned for incineration, process steam and space heating. Oil consumption is approximately 6500 gal/mo. for incineration and 33,000 gal/mo. for process steam. Since the sewage treatment process is essentially independent of the time of year, these values are relatively constant throughout the year. The fuel oil consumption for heating varies throughout the year.

The heating demand for the facility during the 1976-77 heating season is shown in Table 1. As seen by the table, the peak heating load occurred in January when 21.5 MM Btuh were needed, the minimum load occurred in September when 4.2 MM Btuh were needed. The average heat rate throughout the season was 12.2 MM Btuh.

HEAT RECOVERY SYSTEM

The nominal size of the heat recovery equipment for the facility was assumed to have a capacity between 10 and 15 MM Btuh. Equipment smaller than 10 MM Btuh would not produce energy savings that would justify the investment in equipment. Equipment greater than 15 MM Btuh would tie up heat recovery equipment that would not be used most of the year and greatly reduce the use of the facility's relatively new fuel oil boiler equipment.

Five types of commercially available heat recovery systems were considered for the facility. They were: heat pipes, liquid sorbent enthalpy exchange systems, total and sensible heat recovery wheels, coil energy recovery loops and heat pumps. Considering the magnitude of energy to be recovered and considering that a liquid to liquid heat transfer device would be used, it was determined that heat pump equipment would be the best choice for this application.

HEAT PUMP CHARACTERISTICS

Heat pumps have been used for several years for air conditioning and home heating in moderate climates. Their use in northern climates has not been popular because of their high cost of operation. However, increasing energy costs are precipitating an increase in heat pumps for heat recovery applications even in northern climates.

Heat pumps employ a refrigeration cycle in their operation. The four main components of a heat pump are the compressor, which compresses the refrigerant; a condenser which rejects heat from the refrigerant; an expansion device which expands the refrigerant to low temperature and pressure; and an evaporator which receives heat from some medium and thereby heats the refrigerant before it enters the compressor for re-compression. The sum of all energy into the system must equal the sum of all energy out of the system. Hence the rate of heat being rejected by the condenser is numerically greater than the rate at which work is delivered to drive the compressor because of the addition of heat into the evaporator.

The useful effect desired from a heat pump is a maximum rate of heat rejection from the condenser for a minimum energy flow into the system to drive the compressor. The ratio of heat rejected to the work input to the system both expressed in the same thermodynamic units, is called the coefficient of performance or COP. The numerical value of this ratio is always greater than or equal to one since the heat rejected is the sum of the heat input to the system plus the work into the system. A COP as large as possible is desired so that the multiplicative effect on the work input by the heat pump gives the largest possible heat rejection to the condenser.

The COP is influenced in relatively minor ways by details of the heat pump cycle design, the efficiency of the compressor, the design and sizing of the evaporator and condenser, the choice of refrigerant, and even the sizing of the refrigerant lines which interconnect all the components. However, the most important factors which influence the COP are the temperatures between which the heat pump must operate. The COP is maximized by using the highest possible heat source temperature and the lowest possible temperature at which heat is rejected. More specifically, the greatest COP is obtained when the evaporator temperature is as high as possible and the condenser temperature is as low as possible.

Because of the characteristics of the pressure enthalpy diagram for normal refrigerants, the COP is more sensitive to evaporator temperatures than to condenser temperatures. Therefore the primary consideration in increasing the COP is to have the evaporato operating at as high a temperature as possible.

The cost of operation of the heat pump depends upon the COP and the cost of electric power. The greater the COP and the lower the cost of electric power, the cheaper the energy produced by the heat pump. If a heat source at a relatively high temperature can be utilized by the heat pump thereby assuring a reasonable COP along with a modest electric power rate, then the heat pump compares favorably to fuel oil fired equipment.

HEAT PUMP APPLICATION TO THE FACILITY

Table 2 illustrates the application of a 10 MM Btuh heat pump to the facility. As seen by the table, this heat pump would meet the heating load for the facility for the months of September, October, April and May. For the remaining months of the heating season, the heating boiler would provide the additional heat needed. The totals in the table show that the heat pump would provide approximately 69 percent of the heat required by the facility.

Table 3 shows the application of a 15 MM Btuh heat pump to the facility. As seen in the table, the heat pump would meet the total heating load for the facility except for the months of December, January and February. The totals show that the heat pump would provide 87 percent of the heating load for the season.

Two industrial heat pump manufacturers in the United States claimed that they could manufacture equipment to meet this load. One manufacturer limits the size of their heat pumps to 5 MM Btuh, therefore two or three of these machines would have to be used in series. The other manufacturer is capable of building one machine to handle any load required by the facility.

Three commercially available machines with the following characteristics were considered. 1) A 10 MM Btuh machine with a COP of three receiving

31,028 gpm of final effluent at 13 C (55 F) and discharging 2,300 gpm of heating water at 71 C (160 F) with a capital cost of $300,000. 2) A 15 MM Btuh machine with a COP of three receiving 4,000 gpm of final effluent at 13 C (55 F) and discharging 3,000 gpm of heating water at 71 C (160 F) with a capital cost of $425,000. 3) A 15 MM Btuh machine with a COP of two receiving 4,000 gpm of final effluent at 13 C (55 F) and discharging 1,650 gpm of heating water at 85 C (185 F) with a capital cost of $300,000.

These choices represent equipment obtaining a maximum COP under the operating temperature specifications. The machine with the lower COP would produce heating water near the temperature previously used at the facility. However, experimentation on the heating system during the past winter showed that the facility could be adequately heated with water temperatures as low as 71 C (160 F) thereby allowing the use of a heat pump with a COP of three.

ECONOMIC ANALYSIS

Table 4 shows the energy costs for the existing heating system and the three heat pumps described above. These values were calculated by using the amount of heat produced by each type of equipment, shown in Tables 2 and 3, the current fuel oil price and electric power rate paid by the district, the stated COP of each machine and a fuel oil boiler efficiency of 70 percent. As shown by the table, maximum annual energy savings of $101,450 would be realized by using the 15 MM Btuh machine with a COP of three.

Total annual cost of each alternative was calculated by including maintenance, replacement and energy costs. Preventive maintenance cost was quoted to be $750. per year by one of the major heat pump manufacturers. Unscheduled maintenance was not estimated. The replacement cost was calculated assuming a 20 year equipment life and an 8 percent return on capital. These costs were found to be $30,570 per year for the $300,000 heat pump and $43,300 per year for the $425,000 heat pump. The installation cost for the equipment was not available at the time this paper was written therefore the economic analysis does not include these costs.

Table 5 shows the total cost of the four alternatives and the savings over the present system. As shown by the table, a maximum savings of $58,000 per year is realized with the 15 MM Btuh heat pump with a COP of three. It is shown that there is a net loss of $27,400 per year by using the large heat pump with the low COP. The smaller heat pump shows a savings of $49,230 per year which is less than the savings from the larger heat pump with the same COP.

It should be noted that replacement and maintenance costs are not included in the analysis for the fuel oil equipment currently being used.

101

The reason is that the heat pump equipment would be installed in addition to and used in conjunction with the present system. Therefore the heat pump replacement and maintenance costs are added costs that would not exist if the heat pump was not added to the facility.

If the heat pump equipment was being installed in a new facility then the savings over fuel oil equipment would be closer to the energy cost savings shown in Table 4 rather than the savings shown in Table 5. This is because replacement costs would have to be included for the fuel oil equipment as well as with the heat pump equipment.

CONCLUSIONS

This analysis has shown that sewage treatment plants offer a unique opportunity for economically recovering and utilizing waste heat with heat pumps. All sewage treatment plants have an inexhaustible heat source in relatively warm, clean final effluent. Unless the treatment facility is located in a tropical climate, these treatment facilities could use some portion of the heat for space heating. Therefore, if the economic incentive were presented, large savings to the taxpayers could be realized in the utilization and recovery of waste heat at these facilities.

TABLE 1
HEATING LOAD FOR THE FACILITY
DURING THE 1976-77 HEATING SEASON

Month	Oil Consumption (Gals.)	Heating Btu X 10^{-9}	Boiler Output MM Btuh
Sept. 1976	31,000	3.05	4.24
Oct. 1976	72,800	7.13	9.58
Nov. 1976	96,600	9.47	13.15
Dec. 1976	150,200	14.72	19.78
Jan. 1977	163,700	16.04	21.56
Feb. 1977	121,400	11.90	17.71
Mar. 1977	86,000	8.43	11.33
Apr. 1977	56,300	5.52	7.67
May 1977	18,100	1.77	4.92
TOTAL		78.00	

TABLE 2
APPLICATION OF 10 MM Btuh HEAT PUMP

Month	Heat Pump (Btu X 10^{-9})	(MM Btuh)	Heating Boiler (Btu X 10^{-9})	(MM Btuh)
Sept.	3.05	4.24	---	---
Oct.	7.13	9.58	---	---
Nov.	7.20	10.0	2.27	3.2
Dec.	7.44	10.0	7.26	9.8
Jan.	7.44	10.0	8.63	11.6
Feb.	6.72	10.0	5.18	7.7
Mar.	7.44	10.0	.96	1.3
Apr.	5.50	7.67	---	---
May	1.80	4.92	---	---
TOTALS	53.72		24.3	

TABLE 3

APPLICATION OF 15 MM Btuh HEAT PUMP

Month	Heat Pump $(Btu \times 10^{-9})$	(MM Btuh)	Heating Boiler $(Btu \times 10^{-9})$	(MM Btuh)
Sept.	3.05	4.24	---	---
Oct.	7.13	9.58	---	---
Nov.	9.47	13.2	---	---
Dec.	11.2	15.0	3.57	4.8
Jan.	11.2	15.0	4.80	6.6
Feb.	10.1	15.0	1.81	2.7
Mar.	8.4	11.3	---	---
Apr.	5.5	7.67	---	---
May	1.8	4.92	---	---
TOTALS	67.8		10.2	

TABLE 4
ANNUAL ENERGY COST ALTERNATIVES FOR HEATING
THE FACILITY

Alternative	Fuel Oil Cost	Electric Power Cost	Total Energy Cost	Energy Cost Savings Over Present System
Current heating system	$312,000	---	312,000	---
10 MM Btuh heat pump COP of 3	$ 97,200	$134,300	231,500	80,500
15 MM Btuh heat pump COP of 3	$ 40,800	$169,750	210,550	101,450
15 MM Btuh heat pump COP of 2	$40,800	$254,625	295,425	16,575

TABLE 5
TOTAL ANNUAL COST OF EACH ALTERNATIVE

Alternative	Energy Cost	Maintenance Cost	Replacement Cost	Total Cost	Savings Over Present System
No heat pump	312,000	---	---	312,000	---
10 MM Btuh heat pump COP of 3	231,500	700	30,570	262,770	49,230
15 MM Btuh heat pump COP of 3	210,000	700	43,300	254,000	58,000
15 MM Btuh heat pump COP of 2	295,400	700	43,300	339,400	-27,400

WHY FROUDE NUMBER REPLICATION DOES NOT NECESSARILY ENSURE MODELING SIMILARITY

W. E. Frick[*] and L. D. Winiarski
Corvallis Environmental Research Laboratory
U.S. Environmental Protection Agency

ABSTRACT

It is commonly assumed that Froude number replication ensures similarity between fluid phenomena prototypes and their fluid models. The densimetric Froude number typical in plume modeling is:

$$Fr = \frac{V}{\sqrt{\frac{\rho_a - \rho}{\rho} Dg}}$$

Where V is a characteristic velocity, ρ_a and ρ are the ambient and plume densities respectively, D is a characteristic dimension and g is the acceleration of gravity. It is generally assumed that equivalent predictions will result when equal Froude numbers and dimensionless coordinates are used. However, the nonlinear density behavior of many fluids as functions of temperature, salinity or water vapor proves this assumption to be false, and the discrepancy is not trivial. A buoyant plume in water may not behave the same as a buoyant plume in air even if both have the same Froude number as defined above. There can be a noticeable difference between plumes in the same medium with the same Froude number but at different temperature conditions. For example, a horizontal water plume at 40°C in stagnant water of 0°C rises only briefly before sinking, while another water plume at 40°C in ambient water of 20°C with the same Froude number rises monotonically. The implications for various plumes and outfalls are numerous. The explanation for this behavior is the subject of this paper.

INTRODUCTION

The most commonly accepted parameters in buoyant plume modeling are the initial densimetric Froude number and the initial velocity ratio. Sometimes the Reynolds number is also considered. Generally these are considered sufficient for characterizing the plume in neutrally stable environments such as water with zero vertical density gradient or air with an adiabatic temperature gradient. Otherwise a parameter reflecting the stability of the ambient must be used (1,2). The reason the densimetric Froude number works as well as it does as a similarity parameter in buoyant plume modeling is that the term relates directly to the initial net buoyant force per unit mass of plume material (i.e. the vertical acceleration). As long as the behavior of the vertical acceleration throughout

---

[*] Now affiliated with the Oregon Dept. of Transportation, Salem, Oregon

the plume trajectory can be uniquely characterized by initial values, the densimetric Froude number appears to be a useful similarity parameter. Unfortunately this appears to be true only if we are dealing with a medium that is neutrally stable and has a linear equation of state. Apparently there appears to be an implicit assumption that nonlinear density effects are insignificant in comparison to other effects. We will show that this is frequently not the case.

A CATASTROPHIC EXAMPLE

As indicated, the equation of state is important in determining the value of the buoyant acceleration. What can happen when two plumes have the same densimetric Froude number but have different ambient and initial plume temperatures? An extreme example is shown in Figure 1. The curves are the trajectories of two horizontally discharged plumes in quiescent, neutrally stabl⌐ ambient, however, they are not similar even though they have the same ⌐ nsimetric Froude number. One plume rises briefly before sinking; its initial conditions are described in the lower right corner of the figure. The other plume rises monotonically. The behavior of the sinking plume can be understood when it is realized that the initial plume temperature is 40°C and the ambient temperature is 0°C. Water happens to have its maximum density at about 4°C. Figure 2 shows this graphically: anywhere between 7.5°C and 0°C the density of water is greater than it is at 0°C. Thus, when the plume temperature falls below 7.5°C, as it would from mixing in the ambient water, the plume density becomes greater than the ambient density and the plume becomes negatively buoyant.

IMPLICATIONS ON PHYSICAL MODELING

Another example will illustrate the problem of trying to simulate buoyant air plumes in air with buoyant water plumes in water at the same densimetric Froude number. This is a common practice that needs to be critically examined. Figure 3 makes such a comparison using a linear equation of state instead of the ideal gas law. The ideal gas law:

$$\rho = p/(RT)$$

is, relatively speaking, considerably more linear at room temperature than the corresponding case for water. However, its curvature is opposite to that of water (see Figure 4).

Returning to Figure 3, it shows four plume trajectories, two with a densimetric Froude number of 6 and two with 20. The plumes have an initial temperature of 40°C and diameter of 2 meters. All are discharged horizontally into quiescent fluid at 20°C with the velocities shown in the figure. Those trajectories labelled LES are using a fluid with a linear equation of state, the others are water. It can be seen that the predictions are substantially different even though the same conditions exist. A study of Figure 2 reveals why the trajectories are so different. The densimetric Froude number only takes into account the initial buoyant acceleration and says nothing of how the density behaves between the

initial and the ambient temperatures. Suppose the plume at a particular location has effectively mixed an equal amount of ambient into itself. The average temperature is then 30°C at that point. The plume buoyancy at that temperature using the equation of state for water can be seen to be somewhat less than the plume buoyancy at the same temperature using the linear equation of state. (To emphasize our point further, it is the difference in density that is being discussed.) Thus the plume governed by the linear equation of state always is more buoyant than the corresponding water plume. At 22.5°C the ratio of buoyant accelerations (defined in the figure) drops all the way to 0.74.

As can be seen from Figure 4, the ideal gas law is considerably more linear than the equation of state for water at the same temperatures. However, had the ideal gas law been used instead of the linear equation of state the difference in trajectories would have been even greater.

THE RELATIONSHIP BETWEEN PLUME PROFILES AND BUOYANCY

So far we have not considered temperature or density distributions in speaking about plumes. Many numerical models, including the one used in this paper (3,4) make use of the "top hat" assumption. In such a model the average temperature is often used to define the magnitude of the buoyant acceleration. However, real plumes will exhibit temperature and density profiles. This characteristic affects the overall buoyancy. Using a water plume as an example (and assuming its temperature ranges from 20 to 40°C across the plume section), the warmer portion of the plume has more influence (making the plume less dense) than does the cooler portion. Thus the plume is actually more buoyant than the "top hat" model indicates. Using the linear equation of state in modeling will tend to reduce the error that would otherwise occur by using the "top hat" assumption but with a better equation of state. However, preliminary integration shows that the magnitude of this effect is small in comparison.

CONCLUSION AND RECOMMENDATIONS

The densimetric Froude number is sometimes deficient as a similarity parameter and must be augmented by knowledge of the equation of state. This deficiency may impact the conduct of physical modeling, and the modeling results may require critical examination for invalid applications. Also, it follows that accurate equations of state should be used in computer models. Application of these recommendations in modeling will improve research on plume phenomena by removing an otherwise misleading source of error.

REFERENCES

1. Shirazi, M.A. and Davis, L.R.   Workbook of Thermal Plume Prediction: Volume 1: Submerged Discharge, USEPA Environmental Protection Technology Series, EPA-R2-72-005a, August 1972.

2. Winiarski, L.D. and Frick, W.E.   Atmospheric Plume Nomographs with Computer Model for Cooling Tower Plumes, USEPA Interagency Energy-Environment Research and Development Series, manuscript.

3. Winiarski, L.D. and Frick, W.E.   Cooling Tower Plume Model, USEPA Ecological Research Series, EPA-600/3-76-100, September 1976.

4. Winiarski, L.D. and Frick, W.E.   "Methods of Improving Plume Models," Cooling Tower Environment--1978 Proceedings, University of Maryland, May 1978.
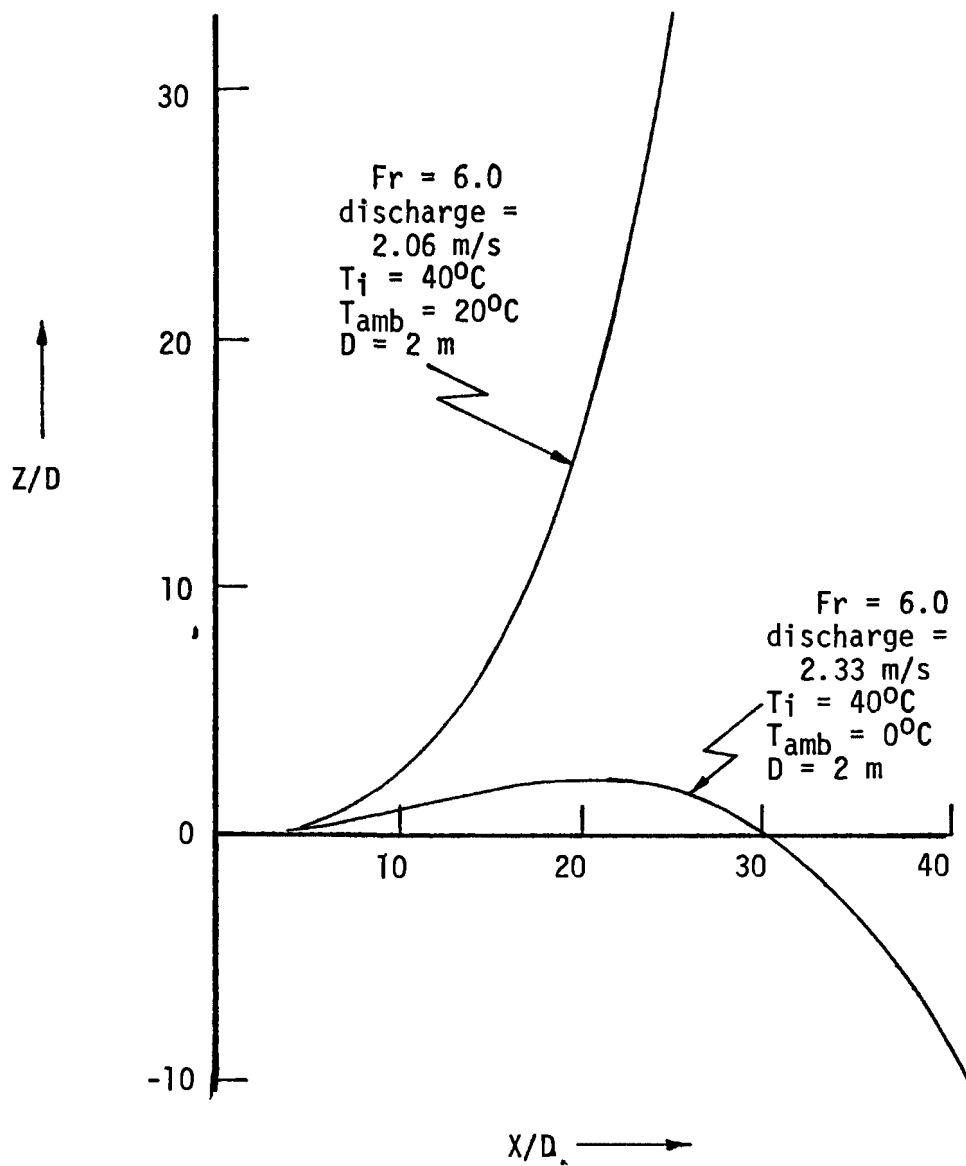
Figure 1. Plume trajectories in quiescent ambient showing complet-
ely different behavior for two plumes in water with the
same Densimetric Froude Number.

110
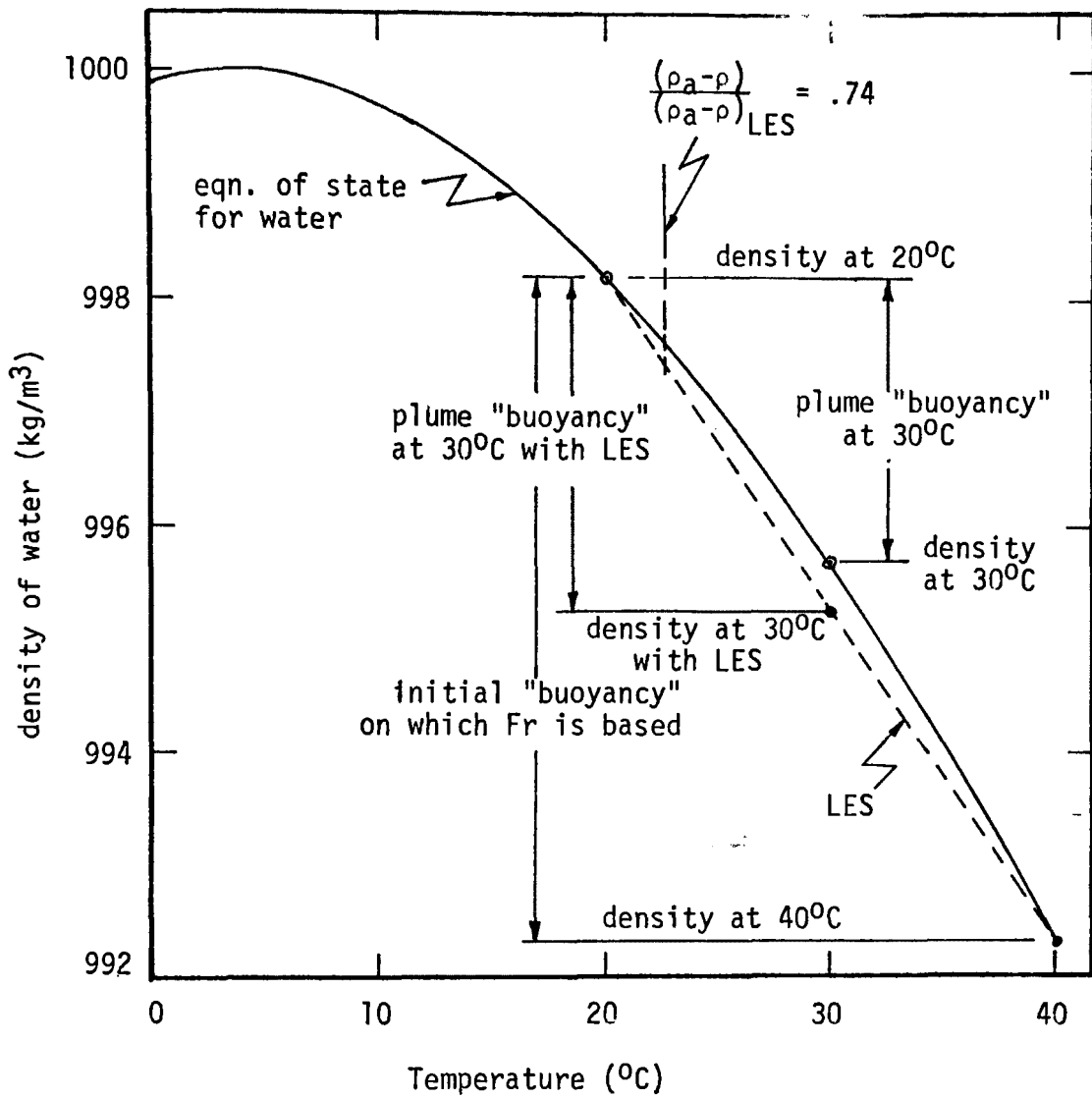
Figure 2. Comparison of plume buoyancy in water using different equation of state assumptions.

111
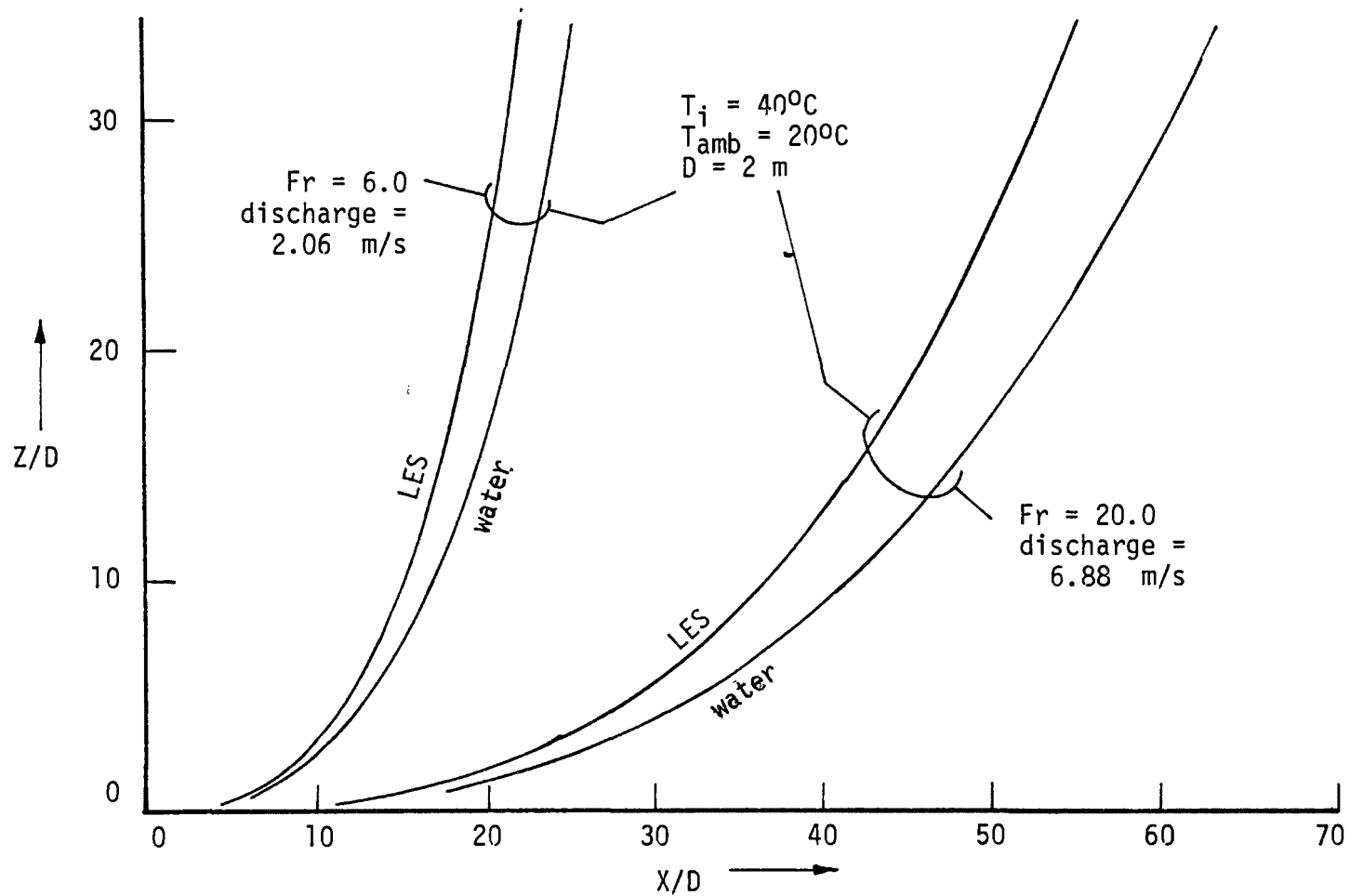
Figure 3. Plume trajectories in quiescent ambient showing the differences between the LES assumption and the actual equation of state for water.
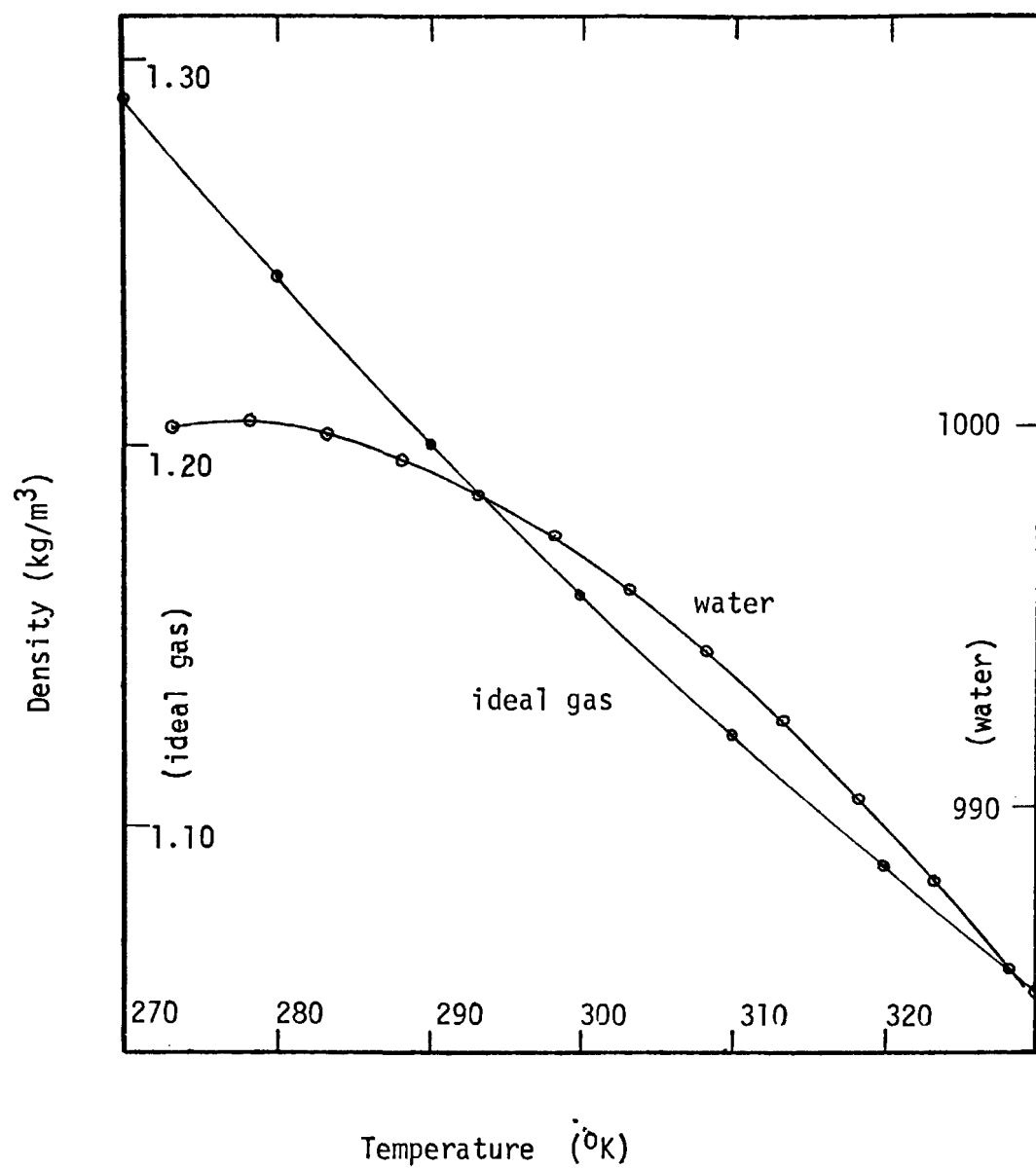
Figure 4. A relative comparison between the ideal gas equation and the equation of state for water under an atmosphere of pressure.

113

A CALIBRATED AND VERIFIED THERMAL PLUME MODEL
FOR SHALLOW COASTAL SEAS AND EMBAYMENTS

S. L. Palmer[1]
Florida Department of Environmental Regulation
Tallahassee, Florida U.S.A.

ABSTRACT

A numerical thermal dispersion model has been developed and linked to a tidally driven, barotropic, hydraulic model of shallow coastal embayments. The solution algorithm is multi-operational with the advective terms treated implicitly and the diffusive terms treated explicitly. Analysis of the computational dispersive and dissipative effects shows the model to be similar in behavior to multi-operational implicit models. However, the magnitudes of the amplitude and phase errors are smaller than for either a purely implicit or explicit algorithm.

The model has been employed to predict the distribution of temperature resulting from a once-through, seawater-cooled power generation facility near Crystal River, Florida. Calibration was achieved by experimentally determining the model parameters and coefficients for the impacted basin. The model was then verified by comparing the position and shape of the simulated plume to those of the observed plume. After simulation of five real-time days (6/15/75 to 6/19/75) the simulated plume area was within 15% of the observed plume area and the simulated mean plume temperature differed from the observed value by only 0.05°C.

INTRODUCTION

Recent concern about the ecological future of "natural" environments has precipitated a need for accurate and efficient methods of predicting the impact of "man-made" stresses on environmental systems. Due to the widespread use of natural water bodies as receiving basins for waste products, it is of special importance that methods be developed for predicting the effects of waste products on water quality.

A natural body of water may be described by a mathematical system composed of interacting subsystems. The system is influenced by a variety of phenomena such as wind, rainfall, solar radiation and runoff. The geometric configuration and geomorphic composition of the basin will also have a significant influence on the system. The response of the system to these influences determines the spatial and temporal distribution of concentrations of various substances which affect water quality.

---

[1] The work on which this paper is based was done while the author was at the Department of Marine Science, University of South Florida, and was supported by a grant from the Office of Water Research and Technology, U. S. Department of the Interior.

GENERAL MATHEMATICAL MODEL

Fundamental to the mathematical modeling of water quality is the concept of constituent mass balance which embodies a relationship among the material change of the constituents, the diffusive flux and any local sources and sinks. The general mass balance equation for a dissolved constituent in an incompressible fluid is

$$\frac{DC}{Dt} = \nabla \cdot (K_c \nabla C) + r_1 C + r_2, \tag{1}$$

where the material derivative (D/Dt) implies dependence upon the velocity field. Under general conditions, a determination of the velocity field involves the solution of a large set of complicated equations that define the relationships between mass, momentum, thermodynamic state, salt, internal energy and entropy. However, several simplifying assumptions can be made that are applicable to many coastal environments.

Although the velocity field is three-dimensional, the fluid flow in a shallow body of water is primarily horizontal. If it is assumed that in shallow water bodies turbulence caused by frictional stress and vertical eddy transfer uniformly mixes the fluid mass, the water quality model can be reduced to a vertically independent, two-dimensional system by integration from the bottom to the sea surface. Assuming that the pressures are hydrostatic, that the mass densities of the substances transported in the estuary are small compared with the density of the water, that only shear stresses from horizontal components are important and that the effects of small-scale velocity fluctuations are aggregated into shear stress terms, the vertically averaged conservation of mass and momentum of the fluid can be expressed as follows:

$$\frac{\partial \eta}{\partial t} + \frac{\partial U}{\partial x} + \frac{\partial V}{\partial y} = Q, \tag{2}$$

$$\frac{DU}{Dt} - fV + g\frac{H\partial \eta}{\partial x} + \frac{1}{\rho}\left(\tau_x^b - \tau_x^s\right) = 0, \tag{3}$$

and

$$\frac{DV}{Dt} + fU + g\frac{H\partial \eta}{\partial y} + \frac{1}{\rho}\left(\tau_y^b - \tau_y^s\right) = 0, \tag{4}$$

Under these assumptions the constituent mass balance equation becomes

$$\frac{D(HC)}{Dt} = \frac{\partial}{\partial x}\left(HK_x\frac{\partial C}{\partial x}\right) + \frac{\partial}{\partial y}\left(HK_y\frac{\partial C}{\partial y}\right) + \left(R_1 C + R_2\right)H. \tag{5}$$

This model, although greatly simplified, still does not lend itself readily to analytic solution. The problem is further complicated when the boundary and initial conditions are made to conform to estuaries with irregular geometry and are driven by forces that are temporally and spacially varying. The solution, however can be approximated by the numerical technique of finite differences.

In the finite-difference approximations of equations 2 through 5, the discrete values of the variables were described on a space-staggered grid as shown in Fig. 1. The water level η, the constituent concentration C, and mean sea level depth h were computed at integer values of j and k. The mass transports U were computed at half-integer values of j and integer values of k, while the mass transports V were computed at half-integer values of k and integer values of j.

Solution of the momentum equations yields the velocity components required for solution of the constituent balance equation. The finite-difference approximations to the momentum equations were explicit in form and with the exception of the Coriolis terms were the same as those used by Reid and Bodine [1]. In his comparison of several finite-difference schemes, Sobey [2] found that, within the range of numerical stability, Reid and Bodine's algorithm held an advantage over the others in that their scheme had the smallest numerical dispersion errors.

The finite-difference approximation of the constituent balance equation was a space-centered, multi-operational system that treated the advective terms implicitly and the dispersive terms explicitly. Computational errors resulting from the finite-difference approximation to the continuum equation can be classified as dissipative and dispersive. Numerical dissipation results in a decrease in the amplitude of the solution wave components without physical reason. Numerical dispersion causes the components of the numerical solution (computed wave) to propagate at a different speed than the components of the analytic solution (physical wave).

The ratio of the computed wave in amplitude and phase to the physical wave after the time required for the physical wave to propagate over its wave length provides a measure of the dissipation and dispersion associated with the computational procedure [3]. Analysis of the numerical behavior of the model algorithm showed that the computational scheme tended to be somewhat dissipative and highly dispersive whenever there were fewer than ten finite-differences per wave length. However, as the grid size became smaller the computational solution converged to the physical solution in both amplitude and phase. The magnitude of the dissipation and dispersion associated with this scheme was smaller than for either a purely implicit or explicit scheme.

CRYSTAL RIVER MODEL

The water quality model has been applied to the estuary (Crystal River Estuary; Fig. 2) adjacent to the Crystal River electric power generating facility of the Florida Power Corporation (FPC) for the prediction of thermal enrichment by heated effluent. The estuary is a gulf coastal region of North-central Florida encompassing the area in which the Cross Florida Barge Canal encounters the Gulf of Mexico as well as the area in which the generating facility discharges heated effluent. The estuary is bounded on the north and south by dredging spoils, on the east by a salt

marsh, and is open to the Gulf of Mexico on the west. The estuary itself is criss-crossed by several irregular strings of oyster bars which form barriers to water flow, resulting in a basin with very complex bathymetric features.

For the purpose of determining the dispersion of heated effluents in the estuary, the estuary was modeled by a mesh compatible with the finite-difference definitions of the previous section. A field measurement program was then initiated for gathering data necessary for calculation of bottom friction coefficients, eddy diffusion coefficients and metero-logical exchange parameters.

MODEL CALIBRATION

Friction Coefficients

In shallow estuaries, energy losses due to dissipative forces cause significant sea surface slopes. The energy dissipation is brought about by a combination of phenomena for which the individual components would be almost impossible to determine. Thus for computational purposes all of the losses were merged into one "frictional" resistance force which was assumed to be uniformly distributed throughout the region under investigation.

The exact nature of frictional resistance in free surface flow is not known. However, the phenomenon has been studied for channel flow by Chezy and Manning [4] and was empirically found to be proportional to the square of the flow velocity vector. An extension to two-dimensional flow can be made by considering the components of the associated mass transport vector.

Determination of friction coefficients for shallow estuaries from field measurements can be extremely complicated. Dronkers [5] suggested a method of calculating Chezy (friction) coefficients for a river section using measurements of the vertical tide at both ends of the section and the volume discharge through a cross-section as a function of time. A relationship for two-dimensional flow that is analogous to Dronkers' unidirectional formulation is

$$C = H|V^*|/\sqrt{\partial\eta/\partial x^*},\tag{6}$$

where V^* is the vertically integrated water velocity and x^* is a coordinate axis in the direction of V^*.

Since a resolution of the sea surface slope over a short distance is difficult to ascertain even with intercalibrated tide gauges, a method for determining the surface slope in terms of a measurable quantity was devised. Several attempts were made to gather the necessary data to impliment the technique proposed by Palmer et al. [6]; however, repeated equipment malfunction prevented any degree of success.

117

The sea surface slope is, however, a necessary factor in determining the Chezy coefficients. A limiting slope for the sea surface was calculated from Airy wave theory as

$$\frac{\partial \eta}{\partial x^*} = \frac{1}{Cg} \frac{\partial \eta}{\partial t}.$$
(7)

To provide a means of classifing frictional influences due to different bottom types, the bottom composition of the estuary was surveyed. Each grid in the estuary was then assigned one of eight bottom types: mud, shell, limestone, grass, algae, sponge, patchy grass or sand.

In the "friction surveys", vertical velocity profiles were measured and mean velocities were calculated for each of the bottom types. The velocity profiles were measured at maximum ebb flow or maximum flood flow so that the full effect of the friction was measured. Values of the Chezy coefficients were then calculated, converted and compared to the literature values of the Manning number for each bottom type. As seen in Table 1 the values for channel flow were in good agreement with the values calculated for the two-dimensional flow.

Dispersion Coefficients

Any dissolved constituent released into an estuary will undergo dispersion due to advection by currents and large-scale turbulence and due to diffusion by small-scale turbulence and molecular dynamics. However, the molecular diffusion is small compared to the advective and large-scale turbulent dispersion and is considered negligible.

A neutrally bouyant constituent released on the water surface should in theory disperse such that isolines on the surface form a radially symmetric patch about the center of mass. This center of mass, which is the point of peak concentration within the patch, should coincide with the point of injection. In fact such patches are rarely symmetric. However, pertubations are random and on the average a radially symmetric patch describes the spread by dispersion. Advection will then translate the patch downstream and shear will cause the transport to be differential, deforming the patch somewhat.

Kolmogorov [7] states that for vertically well mixed water bodies and for scales of small magnitude, horizontal diffusion can be assumed isotropic, thereby forming the radially symmetric patch. Thus, in a frame of reference moving with the current, the dispersion of heat along the surface can be described by an equation written in polar coordinates with one coefficient D_r which is in the form

$$D_r = \delta_r{}^q,$$
(8)

where δ and q are empirically determined coefficients. The dispersion equation becomes

$$\frac{\partial C}{\partial t} = \frac{1}{r}\frac{\partial}{\partial r}\left(r\, D_r\, \frac{\partial C}{\partial r}\right).$$

(9)

Various values of q found by experimentors yield special cases of the equation. For a diffusion coefficient constant with position within the patch, $q=0$, $D_r=\delta$, and

$$C = \frac{C_0}{4\pi\delta t}\exp\left(-\frac{r^2}{4\delta t}\right).$$

(10)

A diffusion coefficient varying directly with r, as reported by Joseph and Sendner [8] requires that $q=1$, $D_r=r\delta$, and

$$C = \frac{C_0}{2\pi\delta^2 t^2}\exp\left(-\frac{r^2}{\delta t}\right).$$

(11)

Ozmidov [9] found that D_r varied with $r^{4/3}$ so that $q=\,^{4/3}$, $D_r=r^{3/4}\delta$, and

$$C = \frac{243 C_0}{\partial\pi t^3}\exp\left(-\frac{9r^{2/3}}{4\delta t}\right).$$

(12)

An experiment was set up to see which of the above cases (if any) approximated dispersion in the Crystal River estuary. Instantaneous Rhodamine B dye releases were made in an area of the estuary especially shallow (approximately 1 meter) and vertically well-mixed. This region was chosen since it was in the high temperature gradient region near the outfall where dispersion is most critical. To justify the use of the radially symmetric patch model, the dye concentrations were measured at short time intervals at points on a grid small enough to ensure horizontal isotropy. Deformation was disregarded with the assumption of a horizontally uniform advection field.

The dye concentrations were measured at points along perpendicular transects of the patch. The associated shift in the maximum concentrations with time were attributed to advection of the center of mass of the patch. This shift was determined from time-series plots of the transects to yield advection rates. The average advection rates, $dx/dt = .18$ m/sec and $dy/dt = .015$ m/sec, agreed with visual estimates. These velocities were then used to compute the position of the center of mass r_0. With r_0 known at any time t, the location r_i of concentration C_i were determined.

Four experimental replicates were performed with observation taken at six time steps. The resulting cross-sectional plots were neither perfectly symmetric nor consistent in their skewness, which agrees with the known behavior of such patches. Therefore, the most symmetric cross-section, and subsequently the 'average', was selected for comparison with the dispersion equation solutions.

The cross-section chosen had four concentrations C_i, each with an associated r_i. These four points yielded six C_j, C_k pairs, and so $\ln(C_j/C_k)$ was plotted against the quantities (r_k-r_j), $(r_k^2-r_j^2)$ and $(r_k^{2/3}-r_j^{2/3})$.

which, according to the solutions, vary linearly with $\Delta(r)$, $\Delta(r^2)$, $\Delta(r^{2/3})$, respectively. The results are shown in Fig. 3. Clearly, only the first order pairing approximated a linear relationship. Here $t=129$ seconds, and the slope was .053/ft. The slope equals $1/\delta t$, and so $q=1$ and $\delta=.045$ m/sec.

Since heat can be expected to diffuse in the same manner as the dye in a vertically well mixed region, the results of the above experiment were used to determine dispersion coefficients for the model. At each time step, the diffusion from one model grid square to the next was calculated. The distance r (center of one grid and center of adjacent grid) will always be the length of the side of a grid, or 200 m; thus r=200 m, q=1, $\delta=.045$ m/sec and $D_r=\delta r^q=9$ m^2/sec. This corresponds reasonably well with the values found by various experimentors and tabulated by Kullenberg [10].

Heat Budget

The heat budget of an estuary is affected by the prevailing meteorological conditions as well as by direct input by the discharge of heated water. In any given time period the temperature at some fixed point in an estuary will increase, decrease, or remain constant depending on the flux of heat through the water surface and on the mixing with surrounding water that occurs during that period.

The temperature change due to mixing is determined by solution of the constituent mass balance equation. The heat flux through the water surface, on the other hand, can be expressed as

$$q_H = (q_{sn} + q_{atm}) - (q_w + q_c + q_e);$$

where

q_{sn} = net solar radiation flux;
q_{atm} = net atmospheric radiation flux;   (13)
q_w = water surface radiation flux;
q_c = sensible heat flux;
q_e = evaporative heat flux.

The "energy received" terms q_{sn} and q_{atm} can be measured together as total net incoming radiation q_R. These two terms are indpendent of the water surface temperature and were determined by field measurement. Since a single-layer, two-dimensional model was employed, all net incoming radiation was assumed to be absorbed and distributed uniformly throughout the water column. This allowed calculation of the resultant temperature change (ΔT). The relationship between ΔT and the surface heat flux is

$$\Delta T = \frac{\Delta q}{C_p H}$$ (14)

The details of the calculation of these terms are reported by Klausewitz et al. [11].

As a verification technique for the heat exchange model, temperature data collected on June 15, 1975 were used as initial conditions. Meteorological data collected between June 15 and June 19 were then used in the model to predict the temperature at each of the test stations during the survey conducted on June 19.

A comparison of the model predictions and the observed data are presented in Table 2. The temperature values from the model after five days of simulation had a mean value 0.5°C greater than those from the field. These values were reasonably close considering the number of factors affecting water temperature. Which factors were responsible for this increase was not determined.

However, the net radiometer malfunctioned and values of total incoming solar radiation were used instead of net incoming solar radiation. Since the model requires a measure of net solar radiation which takes into account reflected light from the sea surface and the shallow bottom, this is the most likely source of the increase in the ambient temperature of the model over that found in the field.

MODEL VERIFICATION

A five day survey of the Crystal River Estuary was conducted from June 15, to June 19, 1975. During that time continuous records of meterological parameters, tide heights and effluent characteristics were maintained. These records were transcribed into numerical form for use as driving functions in the model. A salinity, temperature, depth (STD) survey on June 15 provided the initial temperature distribution seen in Fig. 4. The five day period was then simulated with the model and the predicted thermal plume (Fig. 5) was compared to the results of an STD survey conducted on June 19 (Fig. 6).

The general shape and location of the modeled plume were similar to those of the field results with the major discrepency being the isotherms near the Cross Florida Barge Canal. Apparently more water was exchanged between the discharge basin and the Cross Florida Barge Canal than was considered by the model. Also, the model plume contained higher temperatures near the outfall than were found in the field data. This could have been caused by the 3/4 mile long discharge canal and the associated atmospheric cooling effects which were not included in the model due to computer storage limitations. Also, the discharge basin was required to be at least two feet deep in order that the hydraulics model remain stable (no bottom exposure was allowed during low tidal conditions). Since in fact most of the salt marsh and mudflat region north of the canal is much shallower than two feet, significantly more nocturnal cooling can occur than the model simulated. However, if the simulated and observed thermal plumes cover the same regions of a vertically well-mixed estuary then the ratio of the surface areas of the two plumes provides a quantitative measure of their relative "closeness in extent". Since the field data points did not cover the entire Crystal River estuary, only those regions of the estuary covered by the field survey

can be compared. The portions of the estuary considered are within the region marked by the dotted lines on Figs. 5 and 6. The areas containing water with temperatures between the various isotherms are listed in Table 3.

Taking into account the fact that the ambient water temperatures resulting from the model simulations were about 0.5°C warmer than they should be, a second table was created as shown in Table 4. In this case the modeled and observed areas with similar temperatures were much closer. The mean plume temperatures were 32.10°C for the observed plume and 32.05°C for the calculated plume.

CONCLUSIONS

The similarity in shape and location between the modeled and field plumes after simulation of five days indicates that the hydraulics portion of the model was generally adequate to describe the water movements in this highly complex estuary.

The overall plume size (area with temperatures >31°C) calculated by the model was within 15% of the field plume size once corrections for ambient temperatures were made. Also the mean calculated plume temperature was 32.10°C, compared to a mean observed plume temperature of 32.05°C. However, the model exaggerated the size of the warmer portions of the plume, due to bathymetric approximations in the model and the absence of heat loss to the atmosphere in the discharge canal.

Predictions of the plume size and configuration over a tidal cycle have also been made for the FPC Anclote power plant [12]. Comparison of model results with field data indicates that the thermal prediction model is readily adaptable to other estuaries that are similar to the Crystal River Estuary.

REFERENCES

1   Reid, R. and B. Bodine, 1968. Numerical Model for Storm Surges
         In Galveston Bay. Proc. J. of Waterways and Harbors Div.,
         Am. Soc. Civil Engr., Vol. 94, No. WW1, pp. 33-57.

2   Sobey, R. J., 1970. Finite-Difference Schemes Compared for Wave-
         Deformation Characteristics in Mathematical Modeling of Two-
         Dimensional Long-Wave Propagation. Technical Memorandum
         No. 32, U.S. Army Corps of Engineers Coastal Engineering
         Research Center, Washington, D.C., 22 pp.

3   Leendertse, J. J., 1967. Aspects of a Computational Model for Long
         Period Water Wave Propagation. Memorandum RM-5294-PR, the Rand
         Corporation, Santa Monica, California. 164 pp.

4   Chow, Ven Te, 1959. Open Chanel Hydraulics. McGraw-Hill Book
         Company, New York, New York. 680 pp.

5   Dronkers, J. J., 1964. Tidal Computations in Rivers and Coastal Waters. North Holland Publishing Company, Amsterdam. 518 pp.

6   Palmer, S. L., K. L. Carder, B. A. Rodgers and P. J. Behrens, 1975. Calibration of a Thermal Enrichment Model for Shallow, Barricaded Estuaries: Annual Report 1974-1975. Dept. of Mar. Sci., Univer. of So. Fla., St. Petersburg, Florida. 141 pp.

7   Kolmogorov, A. N., 1941. The local structure of turbulence in an incompressible viscous fluid for very large Reynolds numbers. C. R. Acad. Sci., USSR 30, 301.

8   Joseph, J. and H. Sendner, 1962. J. Geophys. Res., 67:3201.

9   Oamidov, R. V., 1965. Izv. Atmos. Oceanic Phys. Ser., 1:257.

10   Kullenberg, G., 1974. An Experimental and Theoretical Investigation of the Turbulent Diffusion in the Upper Layer of the Sea, Report #25, Kobenhavas Universitet Institut for Fysisk Oceanografi.

11   Klausewitz, R. H. S.L. Palmer, B.A. Rodgers and K.L. Carder, 1974. Natural Heating of Salt Marsh Waters in the Area of the Crystal River Power Plant. Independent Environmental Study of Thermal Effects of Power Plant Discharge, Technical Report #3, Dept. of Mar. Sci., Univer. of So. Fla., St. Petersburg, Florida, 31 pp.

12   Palmer, S. L., 1975. Predicted Summer Isotherms for Anclote Ancharge after Power Plant Initialization. In: Anclote Environmental Project Report 1974. G. F. Mayer and V. Maynard (eds.) Dept. of Mar. Sci., USF, St. Petersburg, Fla. pp. 36-65.

NOTATION

c	Chezy coefficient	R_1	Vertically integrated reaction rate coefficient
c_g	Shallow water wave speed		
C	Constituent concentration	R_2	Vertically integrated source/ sink
C_0	Initial concentration		
C_p	Specific heat capacity	U	x directed mass transport
D_r	Radial dispersion coefficient	V	y directed mass transport
f	Coriolis parameter	δ	Empirical coefficient
g	Gravitational acceleration	Δq	Surface heat flux
H	Total water depth	Δs	Finite-difference space increment
H_{max}	Maximum expected water depth	Δt	Finite-difference time increment
K_c	Dispersion coefficient	ΔT	Temperature change
q	Empirical coefficient	η	Sea surface variation
Q	Water mass source/sink	ρ	Sea water denisty
r	radial distance	τ_s	Surface stress
r_1	Constituent reaction rate	τ_b	Bottom stress
r_2	Constituent source/sink		

Bottom type	Literature n	Calculated n	Δn
Mud	0.035	0.0358	−0.0008
Shell	0.035	0.0306	0.0094
Limestone	0.015	0.0043	0.0107
Grass	0.022	0.0244	−0.0024
Algae	0.025	0.0295	−0.0045
Sponge	0.032	0.0335	−0.0015
Patchy Grass	0.027	0.0244	0.0026
Sand	0.030	0.0292	0.0008

Sta. No.	Field Results	Model Results	Δt ($^{\circ}$C)
19	30.1	31.3	+1.2
18	30.3	30.8	+ .5
16	30.5	30.7	+ .2
17	30.3	31.2	+ .9
1	30.6	30.3	− .3
$\overline{T}$	30.36	30.86	0.50
σ	0.19	0.40	0.59

Table 1 Comparison of calculated and literature values for the Manning number.

Table 2 Comparison of ambient field temperatures (June 19, 1975) with ambient model temperatures after four days of simulation. (See Fig. 6 for Station Locations)

124

SLP

Interval (°C)	Field (km^2)	Model (km^2)	Ratio
> 34	.24	.36	.67
33-34	.42	.75	.56
32-33	.56	1.89	.30
31-32	2.62	4.02	.65

Interval (°C)	Field (km^2)	Model (km^2)	Ratio
> 34	.24	.22	1.09
33-34	..42	.51	.82
32-33	.56	1.01	.55
31-32	2.62	2.77	.95

Table 3   Comparison of field and Model plume areas.

Table 4   Comparison of field and adjusted model plume areas.
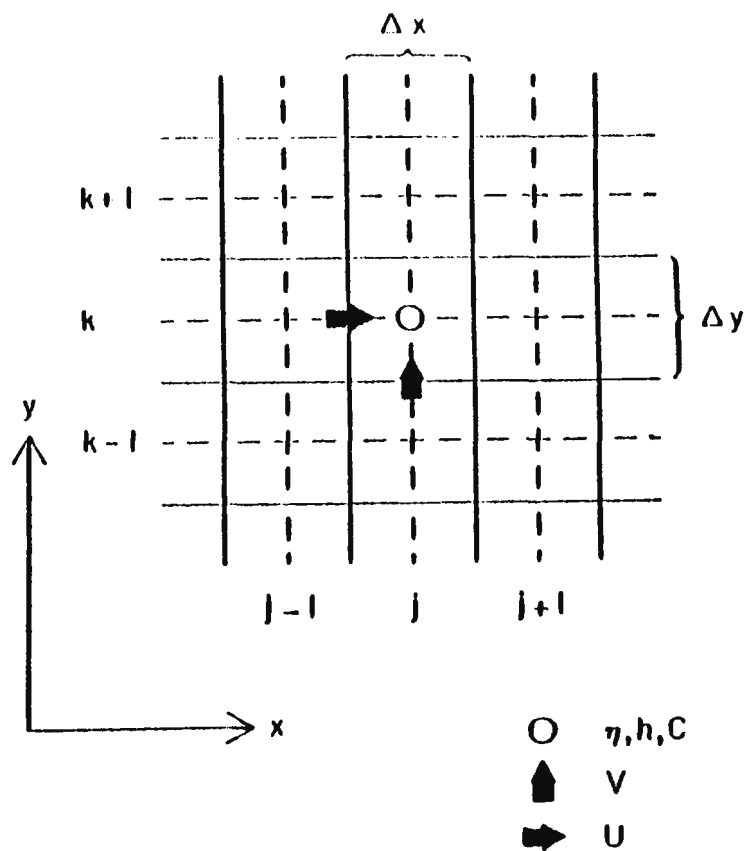
Fig. 1 Finite-difference grid scheme.
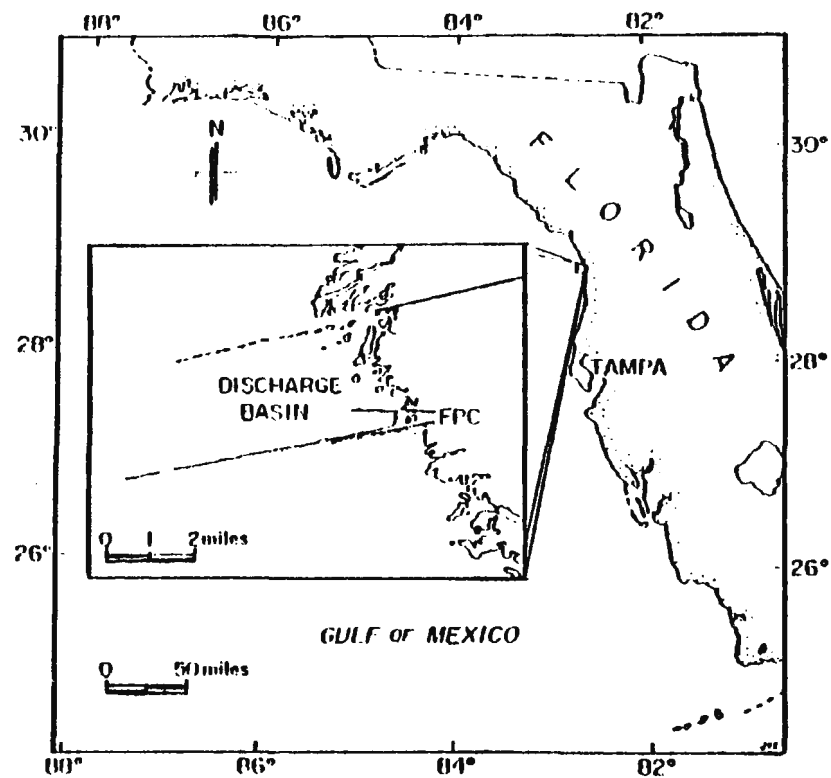
Fig. 2 Location of Crystal River Estuary

III-B-65
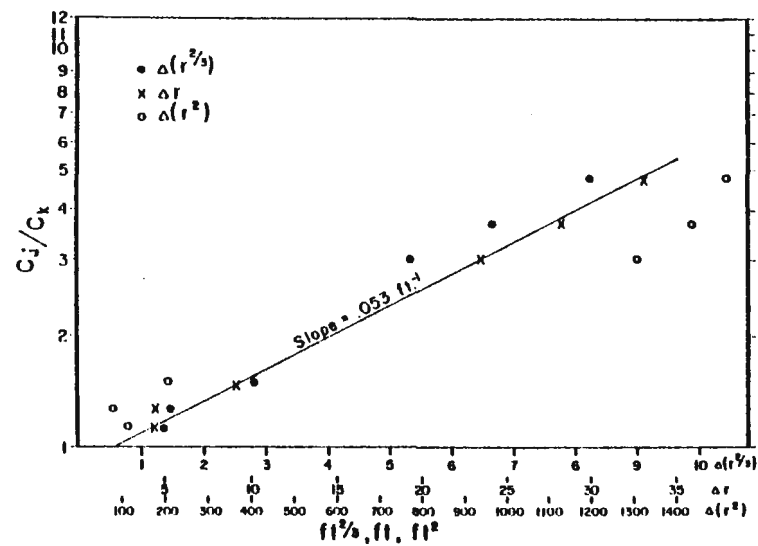
Fig. 3   Dispersion data compared to empirical
relationships.
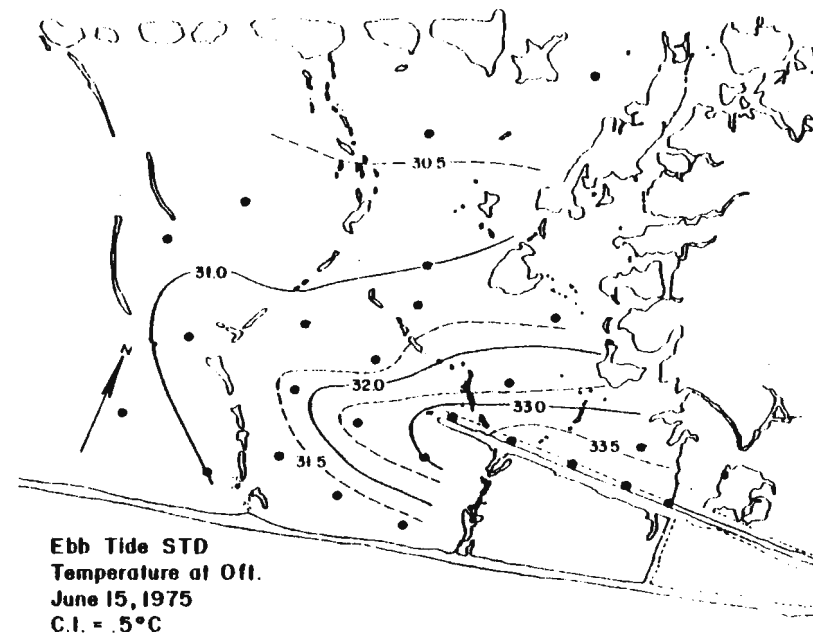
Ebb Tide STD
Temperature at Oft.
June 15, 1975
C.I. = .5°C

Fig. 4   Initial temperature distribution

Model Temperature Results
For Early Flood Tide
June 19, 1975

···· Region compared with
field results.

Fig. 5   Predicted temperature distribution

FLOOD TIDE STD
Temperature at 3 ft.
June 19, 1975
C.I. = .5 °C
···· Region compared with
model results.
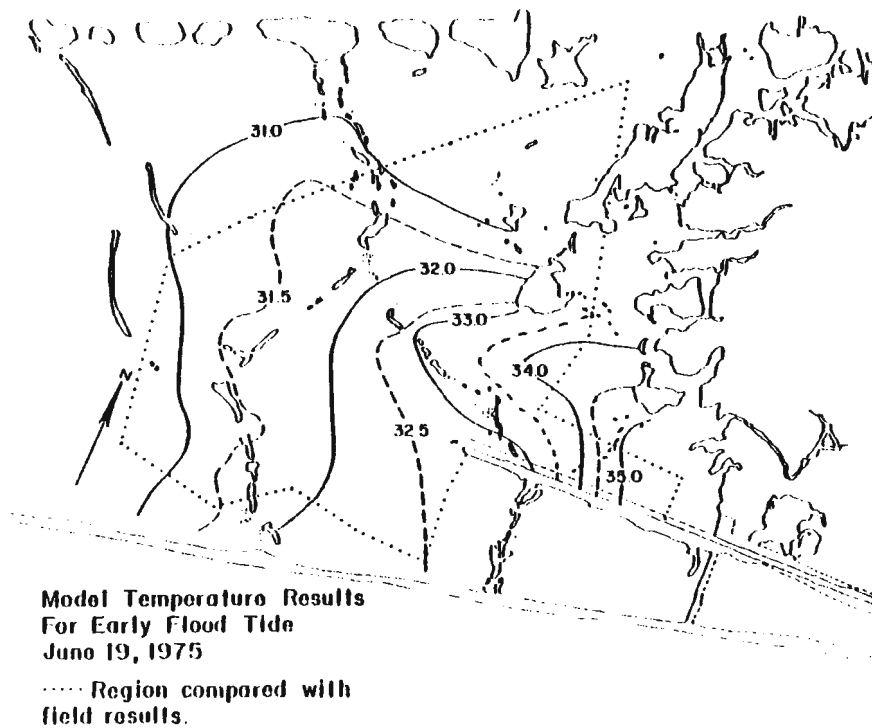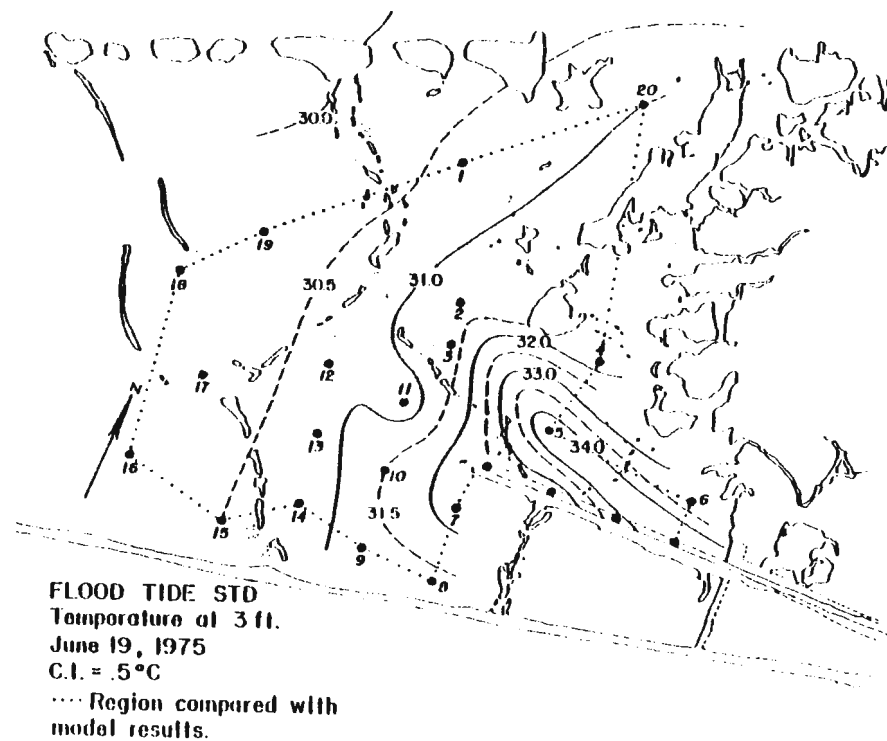
Fig. 6   Final measured temperature distribution

FARFIELD MODEL FOR WASTE HEAT
DISCHARGE IN THE COASTAL ZONE

D. N. Brocard and J. T. Kirby, Jr.
Alden Research Laboratory
Worcester Polytechnic Institute
Holden, Massachusetts, USA

ABSTRACT

Waste heat discharges in coastal areas with alternating tidal currents may lead to a background temperature rise due to insufficient flushing of the area. In this case, the discharge dilution water, and possibly also the intake water, will have a rise above ambient.

This long term heat buildup cannot be predicted by the types of models typically used for nearfield temperature calculations; either physical models or integral type jet models. Large scale circulation models using finite differences or finite elements numerical methods are capable of predicting this heat buildup. These models, however, remain costly to use and do not, as yet, alleviate the need for separate nearfield studies.

The model presented in this paper is designed to permit rapid evaluation of long term heat buildup near a heat discharge. Isotherm shapes are assumed and their areas are calculated as a function of surface heat flux, turbulent diffusion, and net current speed (flushing). Combined with nearfield temperature rise predictions, the background temperature rise can be estimated. A case study is presented as well as dimensionless plots of results.

INTRODUCTION

Coastal areas are widely used for the disposal of waste heat from power generation. Typical disposal schemes involve rapid mixing of the heated effluent with ambient water intended to limit the size of the higher temperature rise isotherms. This mixing is achieved by using turbulence associated with the initial momentum and buoyancy of the discharge. These forces also transport heat away from the discharge point. The discharge momentum, however, decays due to interfacial or bottom friction and the discharge buoyancy decreases with plume dilution so that beyond a "discharge controlled zone," these mechanisms are no longer effective in transporting heat away from the discharge area. Ambient currents, surface heat transfer, and turbulent diffusion become the dominant heat transport mechanisms. In coastal areas with alternating tidal currents, the net ambient current which provides flushing may be only a fraction of the maximum observed current. With little flushing, it is possible that a long term heat buildup will develop in the general area of the discharge. This heat buildup will result in a background temperature rise, raising the temperature of the ambient water used for nearfield dilution and possibly also the temperature of the intake water.

The design of discharge structures is based on compliance with nearfield thermal criteria and uses models for the prediction of the nearfield distribution of temperature rises. These models are either hydraulic scale models or mathematical models for jets and plumes. Neither of these allows the prediction of the background temperature rise which is actually independent of the discharge scheme. Large scale circulation models using finite differences or finite elements numerical methods are capable of predicting the long term heat buildup. These models, however, remain costly to use and do not, as yet, alleviate the need for separate nearfield studies.

The model presented in this paper calculates the farfield distribution of temperature rises due to a source of heat of given intensity as a function of net current, surface heat flux, and turbulent diffusion characteristics. This model allows a rapid evaluation of the farfield temperature distribution and, if combined with nearfield results, gives an estimate of the background temperature rise.

MODEL DEVELOPMENT

Consider a power plant cooling system with intake and discharge structures located on, or a short distance off, a straight shore. For the farfield analysis, this system can be idealized as a source of heat on the frontier of a semi-infinite body of water. If the net longshore current speed, V_n, is small compared to the maximum tidal current speed, the heat will spread in the offshore direction as well as alongshore. Self similar temperature rise isotherms are, therefore, assumed. For simplicity and flexibility, the isotherm shape is selected as rectangular with an aspect ratio "a", as shown in Figure 1. The aspect ratio, as yet undetermined, is expected to increase with increasing net current speed, V_n, which stretches the patch of heat in the alongshore direction.

With these isotherms, the rate of heat transfer across the water surface between the ΔT and $\Delta T + d\Delta T$ isotherms, located at x and x + dx is:

$$d \Phi_s = 2 \, K \, a \, x \, dx \, \Delta T \qquad (1)$$

where K is the surface heat flux coefficient.

For ocean applications, the vertical diffusion of heat is negligible compared to lateral diffusion, and a constant thickness, H, for the heated layer can be assumed [1], as shown in Figure 1. With vertically uniform temperatures in this layer, the net rate of head advection (flushing) out of the volume bound by the ΔT isotherm is:

$$\Phi_f = \rho C_p \, H \, x \, \Delta T \, V_n \qquad (2)$$

The rate of heat transport out of this same volume by turbulent diffusion is:

$$\Phi_D = -\rho C_p \, D \, H \, (a + \frac{4}{a}) \, x \, \frac{d\Delta T}{dx} \qquad (3)$$

130

in which D is a diffusion coefficient. At steady state, the rate of heat transport out of the volume enclosed in the ΔT isotherm should equal the rate of heat input into this volume. The latter is equal to the plant heat discharge rate; $\rho C_p Q_D \Delta T_D$, where Q_D and ΔT_D are the plant discharge flow-rate and temperature rise. The following heat balance equation results:

$$\int_0^x 2K\,a\,x\,dx + \rho C_p\,H\,x\,\Delta T\,V_n - \rho C_p\,DH\,(a + \frac{4}{a})\,x\,\frac{d\Delta T}{dx} = \rho C_p\,Q_D\,\Delta T_D \qquad (4)$$

This integral equation is rewritten in dimensionless form as follows:

$$2R \int_0^\eta \eta\Delta T^*d\eta + F_\eta\,\Delta T^* - \eta\,\frac{d\Delta T^*}{d\eta} = 1 \qquad (5)$$

where $\eta = x/H$, and

$$R = \frac{a\,K\,H}{\rho C_p\,D\,(a + \frac{4}{a})} \qquad F = \frac{V_n\,H}{D(a + \frac{4}{a})} \qquad \Delta T^* = \frac{H\,D(a + \frac{4}{a})}{Q_D\,\Delta T_D}\,\Delta T \qquad (6)$$

Differentiating Equation (5) with respect to η leads to the following second order differential equation:

$$\frac{d^2\,\Delta T^*}{d\eta^2} + (\frac{1}{\eta} - F)\,\frac{d\Delta T^*}{d\eta} - (2R + \frac{F}{\eta})\,\Delta T^* = 0 \qquad (7)$$

Two conditions are required to solve this equation. One is given by Equation (5) while the other is that ΔT should go to zero as η goes to infinity.

In the general case, solving the above boundary value problem requires a numerical approach. However, Equation (5) shows that when η goes to zero, ΔT will go to infinity. While this result is clearly in contradiction with physical reality, it will also lead to numerical difficulties. At $\eta = 0$, which can be interpreted as the location of the discharge, turbulent jet mixing (not included in the above derivation), becomes dominant. This mixing could be modeled here by artificially increasing the dispersion co-efficient, D, as η goes to zero. For the purpose of the farfield analysis, however, it is sufficient to limit the calculations to a region outside of the discharge nearfield, taken at $\eta = \eta_o$. In the nearfield region ($\eta < \eta_o$), the temperature will be assumed constant so that Equation (5) applied at $\eta = \eta_o$ gives:

$$R\,\eta_o^2\,\Delta T_o^* + F\,\eta_o\,\Delta T_o^* - \eta_o\,\frac{d\Delta T}{d\eta}\bigg|_{\eta=\eta_o} = 1 \qquad (8)$$

in which ΔT_o^* is the nearfield temperature. This equation replaces Equation (5) as boundary condition to the problem. The size, η_o, of the nearfield region could be estimated based on nearfield temperature studies. The value of η_o, however, was shown to have little effect on the farfield results for practical values of the parameters.

<u>Special Case: No Current</u> $(V_n = 0)$

In the special case when the net current velocity would be equal to zero, $(V_n = 0 \rightarrow F = 0)$, Equation (7) can be transformed to the following form:

$$\frac{d^2 \Delta T^*}{d \xi^2} + \frac{1}{\xi} \frac{d \Delta T^*}{d\xi} - \Delta T^* = 0. \tag{9}$$

where $\xi = \eta\sqrt{2R}$. This equation is a modified Bessel equation of order zero. The solution of Equation (9) with the boundary conditions discussed above is:

$$\Delta T^* = \frac{K_o (\eta \sqrt{2R})}{R\eta_o^2 K_o (\eta_o \sqrt{2R}) + \eta_o \sqrt{2R} K_1 (\eta_o \sqrt{2R})} \tag{10}$$

where K_o and K_1 are modified Bessel functions or order zero and one. Numerical values of these functions are available in Tables [2] and in standard computer subroutine packages [3]. For $\eta_o = 0$, the above equation simplifies to

$$\Delta T^* = K_o (\eta \sqrt{2R}) \tag{11}$$

For practical applications, numerical values given by Equations (10) and (11) are very close.

MODEL RESULTS

In the general case of $F \neq 0$, Equation (7) was solved numerically. An exponential transformation was done on η to properly treat the boundary condition at $\eta \rightarrow \infty$ while keeping small discretization steps near $\eta = \eta_o$ where the other boundary condition is specified. For $F = 0$, Equation (11) was used. Solutions are presented in Figures 2 to 4 in terms of the dimensionless parameters defined in Equation (6). The plots of ΔT^* versus η are equivalent to plots of temperature rise versus offshore distance. Values of the flushing parameter, F, and of surface heat loss parameter, R, span the range of practical applications.

Figures 2 and 3, which have constant values of F and several values of R, show the effect on the temperature of changes in the surface heat flux coefficient, K. It is interesting to note that the reduction of temperatures obtained for a given increase of K is smaller when the net flushing current is larger.

Figure 4 shows the effect of varying the flushing parameter, F, for a given value of the heat flux parameter. As expectable, temperatures decrease for increased flushing.

MODEL APPLICATION

For a practical application, and once the necessary coefficients have been determined, the graphs in Figures 2 to 4 can be used to obtain estimates of the extend of the farfield temperature rise isotherms. If nearfield results are available, these graphs can also give the background temperature rise to be added to the predicted nearfield values. Such an application is examined in the following section.

The estimation of some of the parameters involved in this model requires further attention, in particular, the diffusion coefficient, D, the isotherm aspect ratio, a, and the depth of the heated layer, H.

The diffusion coefficient can be evaluated using the following "4/3 law" first proposed by Richardson [4]:

$$D = A \sigma^{4/3} \qquad (12)$$

where σ is the standard deviation of the patch of heat and A is a coefficient which has the dimension of length to the 2/3 power per unit of time. Okubo [5] showed that the coefficient, A, actually varies to a small extent, with the dimension of the patch of heat, represented here by σ. For σ between 2000 ft and 10000 ft, a value of $A = 0.002$ to 0.003 $ft^{2/3}/sec$ is appropriate. The standard deviation, σ, should be established by trial and error.

The aspect ratio of the isotherms, a, can be estimated as follows: The distance needed for the momentum of the discharge plume to be dissipated by friction was shown by Lee et al [6] to be approximately 8H/f where f is the applicable friction factor (interfacial or bottom). This distance is approximately the distance that the plume will travel in the offshore direction (if the initial discharge is directed offshore). The distance travelled alongshore is approximately equal to the tidal excursion, i.e., $Tu_T/\pi +$ $TV_n/2$, taking the net current into account. T is the tidal period and u_T the longshore tidal velocity amplitude. An estimate of the isotherm aspect ratio, therefore, is:

$$a = \frac{T \left(\dfrac{u_T}{\pi} + \dfrac{V_n}{2}\right) f}{8H} \qquad (13)$$

The depth of the heated layer, H, is best estimated based on nearfield results. In the absence of such results, judgement is required. It should be noted that a complete finite difference or finite elements model of the area would also require the input of a layer depth.

CASE STUDY

Consider a proposed generating plant which will discharge 4.4×10^6 BTU/sec near a straight shore. Field studies indicate that the net current speed in the area varies from 0.0 to 0.2 ft/sec and using Equation (12) with $\sigma = 10,000$ ft, a value of $D = 500$ ft^2/sec is obtained. A representative

133

value of the surface heat loss coefficient for summer conditions is $K = 200 \text{ BTU/ft}^2/\text{day}/°\text{F}$. In addition, nearfield studies showed that the thickness of the heated layer in the dispersion region is 15 ft. Finally, the procedure outlined above leads to an isotherm aspect ratio $a \simeq 1$. With these values, the flushing and surface heat loss parameters are $F = 0$ to 1.2×10^{-3} and $R = 2.2 \times 10^{-7}$.

The areas of the temperature rise isotherms, as calculated by the above farfield model, are plotted in Figure 5 for net current speeds of 0.0, 0.1, and 0.2 ft/sec. Also, an isotherm aspect ratio $a = 2$ was considered and the corresponding isotherm areas are plotted in dotted lines.

On the same plot, results of a nearfield thermal study are indicated. These results are averages of nearfield results at different times during the tide cycle. Temperatures predicted by the nearfield model are significantly lower near the discharge point than those predicted by the farfield model. As already pointed out, this is due to the fact that nearfield turbulent mixing is not included in the farfield model. The results of the two models should, however, match at an intermediate point. This can be obtained by adding to the nearfield temperatures a constant background temperature rise. The point where the two models should match is not clearly defined. This point should correspond approximately to the distance from the discharge where the initial momentum is lost by friction. The distance was earlier seen to be $8H/f$; here approximately 12,000 ft if f is taken equal to 0.01, a typical value for interfacial friction. The corresponding area is 3,300 acres. With this value, and an isotherm aspect ratio $a = 1$, the background temperature rise would be zero for $V_n = 0.2$ ft/sec and $0.7°\text{F}$ for $V_n = 0.0$ ft/sec. A larger aspect ratio, which is probable for $V_n = 0.2$ ft/sec, would lead to background temperature rises about $0.2°\text{F}$ larger than the previous values.

In the particular case study considered here, the near and farfield results are almost parallel near the matching point. Therefore, a change in the location of the matching point would not result in significantly different values of the background temperature rise.

REFERENCES

1. Csanady, G.T., "Turbulent Diffusion in the Environment," D. Reidel Publishing Company, 1973.

2. Abramowitz, M., and Stegum, I.A., editors, "Handbook of Mathematical Functions," U.S. Department of Commerce, National Bureau of Standards, Applied Mathematics Series 55, 1964.

3. IBM Scientific Subroutine Package.

4. Richardson, L.F., "Atmospheric Diffusion Shown in a Distance Neighbor Graph," Proceedings of the Royal Society of London, A110, 1926.

5. Okubo, A., "Oceanic Diffusion Diagrams," Deep Sea Research, Vol. 18, 1971.

6. Lee, J.H., Jirka, G.H., and Harleman, D.R.F., "Modelling of Uni-directional Thermal Diffusers in Shallow Water," Report No. 228, R.M. Parsons Laboratory for Water Resources and Hydrodynamics, MIT, 1977.
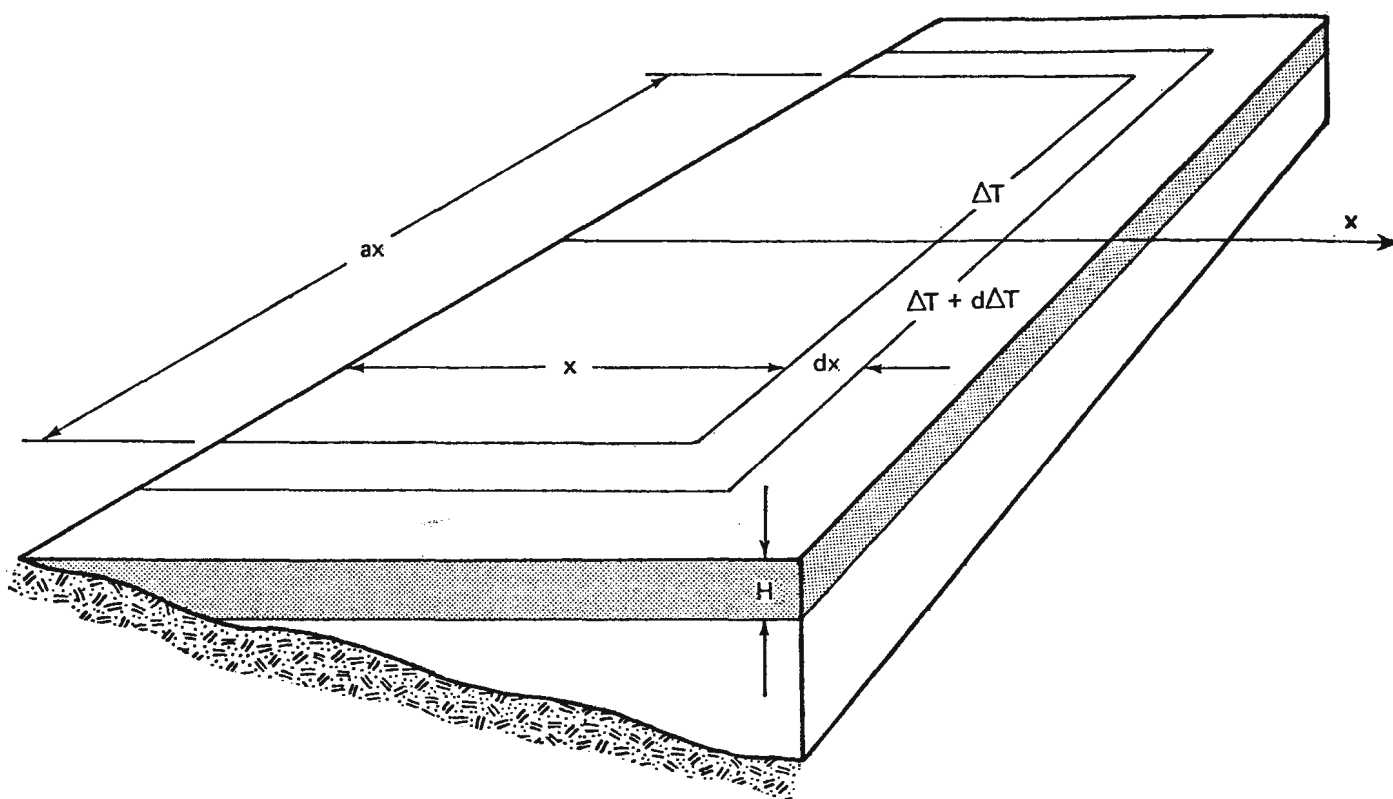
FIGURE 1   FARFIELD MODEL ISOTHERMS
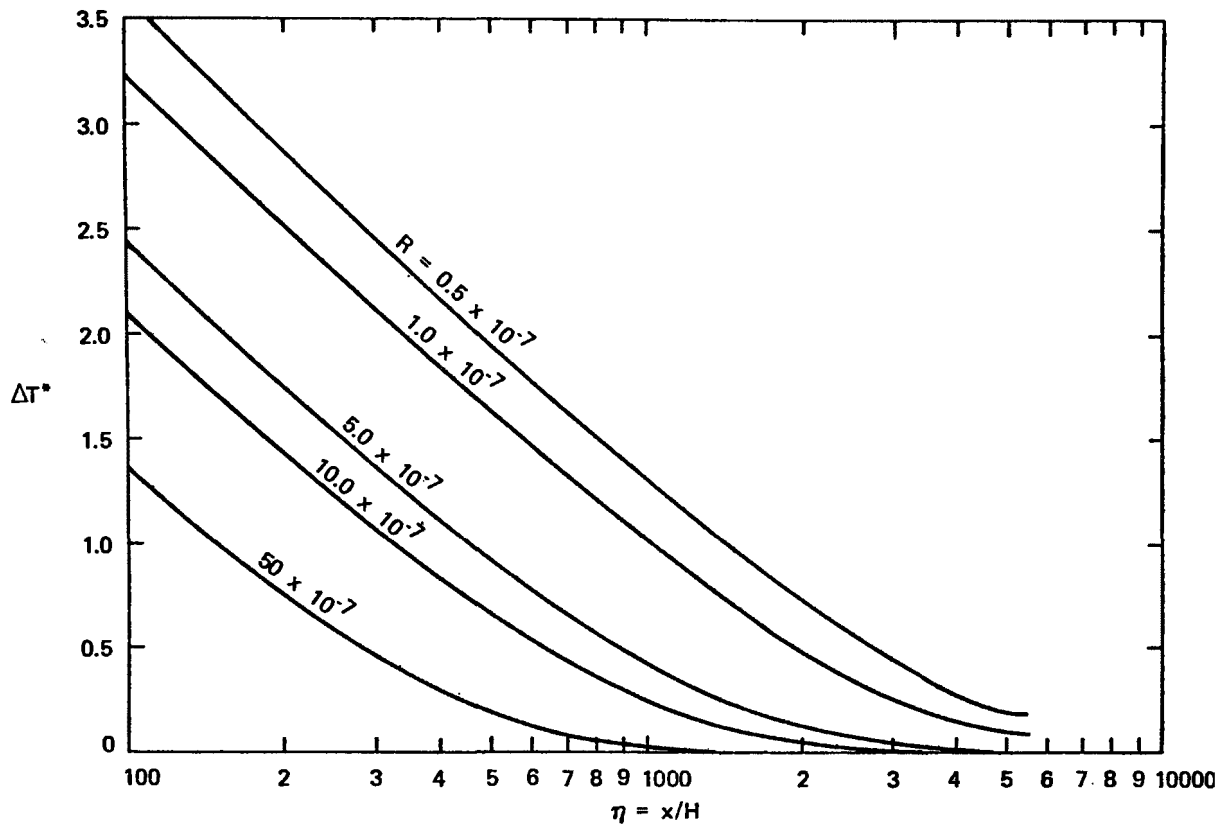
FIGURE 2   FARFIELD MODEL RESULTS FOR F = 0 AND A RANGE OF R
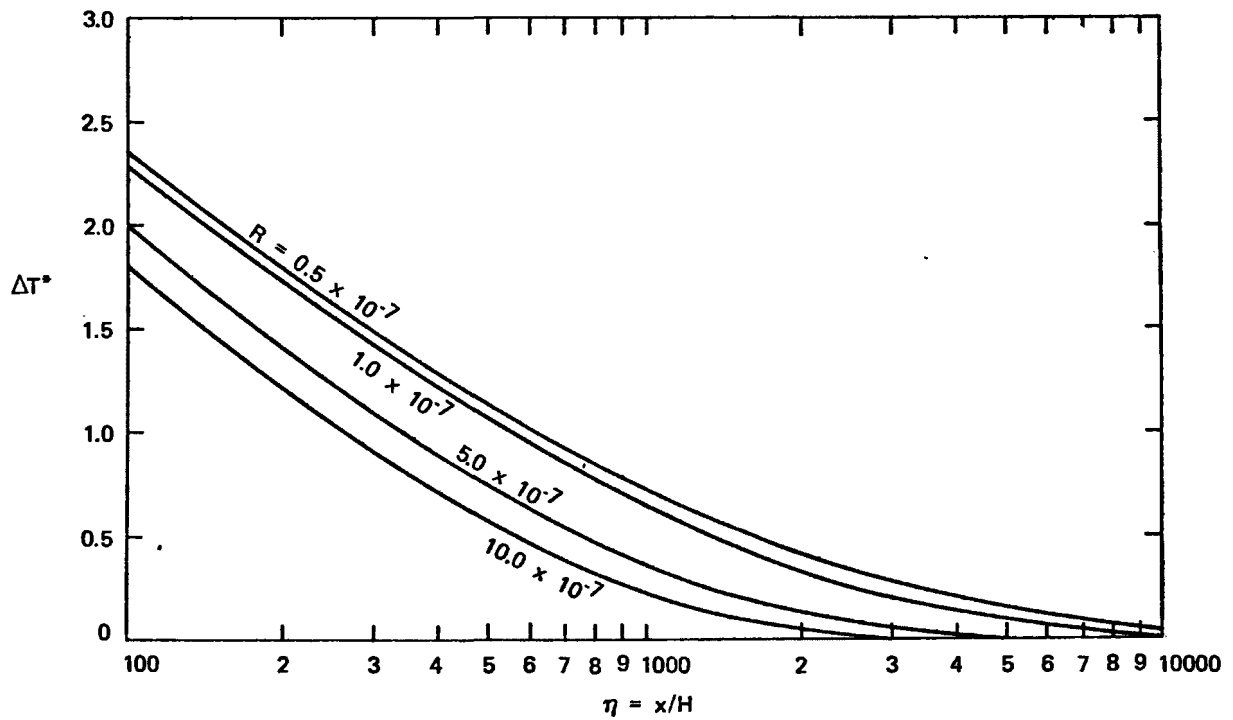
FIGURE 3   FARFIELD MODEL RESULTS FOR F = 6 x 10⁻⁴ AND A RANGE OF R
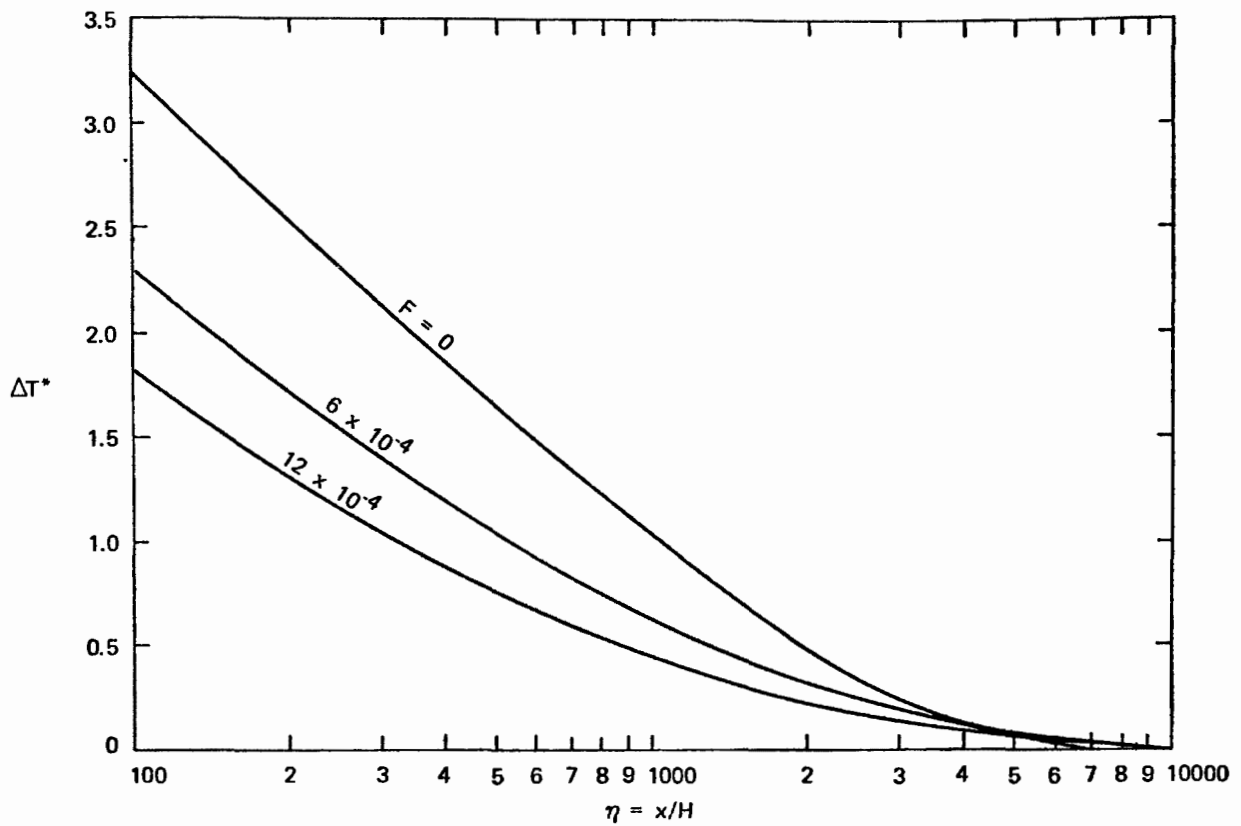
FIGURE 4   FARFIELD MODEL RESULTS FOR R = 1 x 10^{-7} AND A RANGE OF F
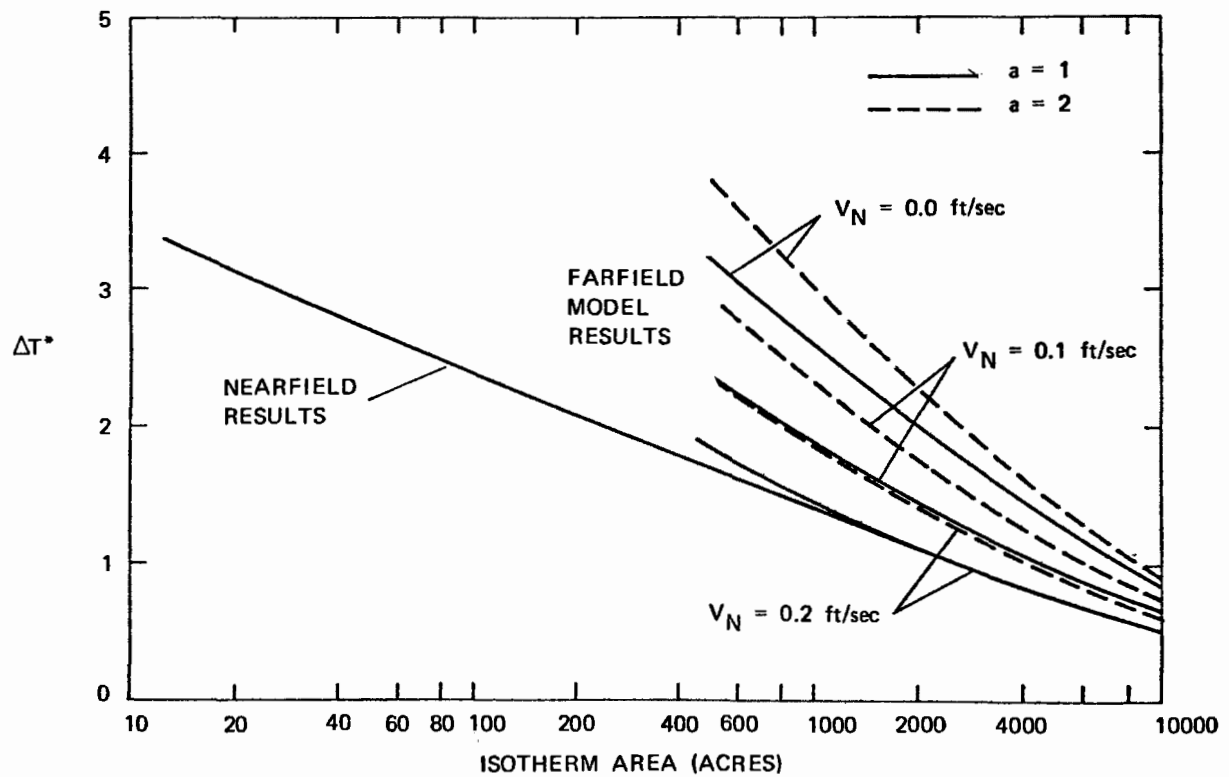
FIGURE 5   MATCHING OF NEARFIELD AND FARFIELD RESULTS FOR CASE STUDY

138

THERMAL CHARACTERISTICS OF DEEP RESERVOIRS
IN PUMPED STORAGE PLANTS

J J Shin and N S Shashidhara
Envirosphere Company
A Division of Ebasco Services Incorporated
New York, New York, USA

ABSTRACT

Temperature distribution of the upper and lower reservoirs of pumped stor-
age hydroplants is governed by (1) the pumping characteristics of the re-
servoirs, (2) heat transfer through air-water interface and (3) tempera-
ture and flow rates of water flowing into and out of the reservoirs.
The differences in the thermal characteristics of the upper and lower re-
servoirs would depend upon the relative elevations of inlet and outlet
ports and the rates of discharge during "generating cycle" and "pumping
cycle".

Mathematical models are presented in this paper to estimate the tempera-
ture distribution in the upper and lower reservoirs of a pumped storage
project, with an assumed schedule during "generating and pumping cycle".
The results of the mathematical model are utilized also to establish the
temperature distribution characteristics in deep reservoirs without a
pumped storage plant. The mathematical formulations take into account the
influential effects of solar radiation, natural heat convection due to den-
sity differences, forced heat convection by inflow and outflow, heat diffu-
sion, surface heat losses by evaporation and conduction, and surface heat
gain by long wave radiation. Reservoir discharge temperatures with and
without pumping from the lower reservoir are also provided.

INTRODUCTION

A pumped storage plant is an arrangement whereby electric power is generated
during peak load periods of an electric system by utilizing water previously
pumped into a storage reservoir during off-peak periods, utilizing excess
energy from the same system. Pumped storage plants besides having low
operating/maintenance costs and outage rates have also a low unit invest-
ment cost. They are able to transpose low-value off-peak energy into high-
value on-peak energy. In pumped storage plants, the energy required to
pump water during off-peak periods helps to maintain a steady load on the
thermal plants.

However, installation of pumped storage facilities on existing reservoirs
or natural water bodies can alter their thermal structure significantly.
Such thermal alterations are of great importance to the existing biologi-
cal communities and species. In deep reservoirs, strong thermal stratifi-

cation may develop during certain seasons, and the isotherms are horizontal during most of the year. [1] [2] The pumped storage operation between two existing deep reservoirs disturbs their thermal stratification. This disturbance affects the life support system of many forms of aquatic life in the pumped storage project.

This paper establishes the thermal stratification in pumped storage reservoirs, with and without pumping. Variation of outlet/tailrace temperature from the lower reservoir due to pumped storage operation is also analyzed.

DEEP RESERVOIR THERMAL MODEL

The thermal model used in this study is based on the deep reservoir temperature prediction model developed by Harleman and his associates. [1] [3] [4]

The deep reservoir thermal stratification process is governed by a heat balance involving solar radiation, natural heat convection due to density difference, forced heat convection by inflow and outflow, heat diffusion, surface heat losses by evaporation, back radiation and conduction, and surface heat gain by long wave radiation.

Some important assumptions have been made to set up the governing equations, such as:

1) The isotherms in a stratified reservoir are horizontal.

2) The existence of horizontal isotherms in a reservoir suppress the vertical motion to the extent that turbulent transfer of momentum or heat can be neglected.

3) Solar radiation is transmitted in the vertical direction only.

4) Heat transfer through the sides and the bottom of the reservoir is negligible.

5) Specific heat at constant pressure and the heat diffusion coefficient are constant through all space and time concerned. In addition, the Boussinesq approximation for the density is also made.

The conservation of heat energy equation becomes:

$$\frac{\partial T(y,t)}{\partial t} = \frac{D}{A(y)} \frac{\partial}{\partial y} \left(A \frac{\partial T}{\partial y}\right) - \frac{1}{\rho CpA} \frac{\partial}{\partial y} (A\phi(y,t))$$

(1)

$$- \frac{1}{A} \frac{\partial}{\partial y} (V(y,t)AT) + \frac{B(y)}{A(y)} (Ui(y,t)Ti(y,t) - Uo(y,t)T)$$

where:

T(y,t)   temperature at elevation y and time t

140

y   elevation

t   time

D   heat diffusion coefficient

A(y)   cross-sectional area of reservoir at elevation y

ρ density

Cp   specific heat at constant pressure

$\emptyset(y,t)$ heat flux of internally abosrbed radiation at elevation y and
            time t

V(y,t)   vertical velocity component at elevation y and time t

Ui(y,t)   inflow velocity at elevation y and time t

Uo(y,t)   outflow velocity at elevation y and time t

Ti(y,t)   inflow water temperature at elevation y and time t

Equation (1) is a transient, one-dimensional, second order partial differential equation. Therefore, two boundary conditions and one initial condition are necessary in order to formulate a solution.

The thermally homogeneous state of a reservoir in the early spring season is provided as the initial condition.

(2) $T = T_o$ at $t = 0$ for all y

The heat energy balance at the reservoir surface is achieved between the incoming radiation $\emptyset_o$, atmosphere radiation $\emptyset_a$, surface heat loss $\emptyset_L$ and the amount of heat diffused into the reservoir from the water surface.

(3) $CpD \dfrac{\partial T}{\partial y}\Big|_{y=y_s} = \beta\emptyset_o + \emptyset_a - \emptyset_L$

The heat transfer through the bottom of the reservoir is negligible.

(4) $\dfrac{\partial T}{\partial y} = 0$ at $y=y_b$ for all t

A numerical scheme is employed to solve the governing equation. Harleman's approach was written in an explicit and finite element schematization.

The numerical stability criteria, owing to an explicit scheme, are:

(5) $D \dfrac{\Delta t}{(\Delta y)^2} \leq 1$

141

(6) $V \dfrac{\Delta t}{\Delta y} \leq 1$

where Δt and Δy are time and elevation intervals.

MODEL VERIFICATION

The mathematical model discussed above was verified using field measurements.

Since direct measured data for solar radiation and long wave radiation were not available, they were calculated from a modification to Kennedy's method. [5] [6]

Prior to temperature prediction analysis, it was necessary to examine the validity of the basic model. Comparison of the predicted reservoir temperature profile (using the model) with actual measurements made in the field was performed.

Figure 1 shows the measured and the predicted reservoir temperature profiles for the upper reservoir. [2] An examination of Figure 1 indicates that the predicted and measured data agree well.

TEMPERATURE PREDICTION DUE TO PUMPED STORAGE OPERATION

The modified pumped storage thermal model was utilized to establish the thermal structure of the upper reservoir about 90 m deep and lower reservoir about 70 m deep. The outlet temperature of the lower reservoir is also presented. Reservoir temperature profiles are predicted and compared for two modes of operation: with and without pumping. It is seen that the temperature profiles of the two reservoirs are closely related to pumping schedules, inflow and outflow rates and levels of pumping ports.

The existing penstock of the upper reservoir is located at 25 m depth from the surface and the new pumping port is assumed to be located at about 13 m depth. Similarly for the lower reservoir, the outlet/tailrace port is located at 28 m depth and pumping port is located at 4 m depth. The ports are located such that during the (power) generation mode, the outlet water from the upper reservoir enters subsurface layers of the lower reservoir. During the pumping mode, the surface water of the lower reservoir is pumped to the upper reservoir.

The pumping schedule was assumed such that the upper reservoir loses two feet in elevation per day during the week (cumulative). Water was pumped back during the weekend (approximately 15 hour generation and 9 hour pumping during a weekday and 24 hour pumping a day through the weekend). During the generation mode, equal amounts of water were assumed to be discharged through the existing and the new generation (pumping) outlets. When inflow from other sources into the upper reservoir is greater than the outflow, no pumping was done. For the lower reservoir, it was assumed that the minimum outflows could always be maintained throughout the genera-

tion and pumping modes. This is in order to maintain minimum flow requirements in the river on the downstream side.

DISCUSSION OF RESULTS

Predicted reservoir temperature profiles with and without pumping are plotted in Figure 2 for the upper reservoir and Figure 3 for the lower reservoir for different monthly conditions. Site specific meteorological data for the year 1961 has been adopted in this analysis. However, plant operational details assumed in the analysis are preliminary. Temperature profiles for both upper and lower reservoirs are presented for the same time period.

For the upper reservoir (Figure 2), surface temperature is not affected significantly by pumped storage operation; however, temperature near the pumping port region (13 m depth) is affected by pumping and shows considerable increase when compared to similar temperatures without pumping operation. This is primarily the result of the location of the new pumping and discharge outlets. During generation mode, relatively cooler water from the upper reservoir is discharged through the new outlet to the lower reservoir while during pumping mode, the upper reservoir receives relatively warmer water from the surface layer of the lower reservoir. As a result, the upper reservoir continuously gains thermal energy through pumped storage operation and temperature increase is as much as 5°C at 13 m depth. On the other hand, temperature of the 25 m depth region (existing outlet position) decreases only slightly by pumped storage operation. This is because of the reduced mixing between the cooler deep waters (below 25 m depth) and warmer surface waters. Water temperature at depths below 25 m remains essentially unchanged.

Figure 3 shows four different temperature profiles with and without pumping for the lower reservoir. Temperatures at depths greater than 28 m remain unchanged while surface temperatures show a significant decrease (up to 8°C) due to pumping. This result is discussed here. During the generation mode, relatively cool water enters from the upper reservoir. However, during the pumping mode, warm surface water from the lower reservoir is pumped to the upper reservoir before surface heat can be transferred to the lower layers. As the seasonal effect of solar radiation on the water surface becomes stronger in late spring, more heat is transferred to the lower layers. As a result, water temperature in the lower layers increases with time, until early fall (September). The surface layer of the lower reservoir gains thermal energy during daytime generation mode, but this warm water will be pumped back to the upper reservoir during nighttime pumping mode. Thus the lower reservoir continuously loses thermal energy due to pumped storage operation. This exchange of thermal energy between two reservoirs affects the outlet/tailrace temperature of the lower reservoir as discussed below.

Figure 4 shows a comparison of lower reservoir outlet/tailrace

temperatures with and without pumping for March through December 1961. In general, it is seen that the outlet/tailrace temperature is always lower with pumping when compared to the same without pumping. However, the temperatures are almost identical in March. From April through the rest of the year outlet/tailrace temperature with pumping is 2 to 4°C lower when compared to the outlet/tailrace temperatures without pumping. Outlet/-tailrace temperatures with pumping remain almost unchanged until May, while for the same period (April and May) outlet/tailrace temperatures without pumping shows an increasing trend. Starting in June, temperature both with and without pumping shows an increasing trend until October followed by a decreasing trend from October through December. The reasons as to why temperatures with pumping show an increasing trend from June, while without pumping temperatures show an increasing trend in March/April itself is explained here. As explained earlier, during daytime the surface layer of the lower reservoir gains thermal energy mainly from radiation. However, during nighttime this warm surface layer will be pumped up before the surface heat can be transferred to the lower layers. As time passes and the effect of radiation gets stronger, more of surface heat is transferred to the lower layers even though most of it is lost due to pumping. As a result, outlet/tailrace temperature eventually becomes affected by radiation and starts to increase after May. With no pumping the same effect is felt earlier.

During the fall months, heat gain within the reservoir surface is reduced and the temperature profile becomes more uniform prior to onset of "reservoir turnover" which happens during early winter. Temperature difference between the surface and the outlet layers further decreases and outlet/tailrace temperatures with and without pumping become almost identical by mid winter. When the reservoir "turnover" occurs, outlet/ tailrace temperatures with and without pumping would be identical. The new warming cycle begins again in April and the annual cycle is repeated.

Thermal energy of the upper reservoir gained due to pumped storage operation will be lost to the atmosphere during winter months. Because of this additional thermal energy in the upper reservoir, the fall turnover of the upper reservoir will be delayed, while the lower reservoir turns over earlier than in a typical reservoir.

CONCLUSIONS

Based on one specific pumping schedule, and one set of specific inlet, outlet and pumping port positions, thermal structure has been established for two deep reservoirs of the pumped storage plant. When pumping schedules and port positions are changed, the temperature details will also change accordingly.

For the specific case analyzed here, some interesting conclusions may be drawn. The upper reservoir gains thermal energy by releasing cooler water to the lower reservoir and receiving warmer water. On the contrary the lower reservoir loses thermal energy by releasing warmer water to the

upper reservoir and receiving cooler water. Thus, for the upper reservoir, temperature increases with pumping while for the lower reservoir the same is true when there is no pumping. This behavior in temperature pattern is more significant during late spring and summer months. Outlet/tailrace temperatures of the lower reservoir are generally lower with pumping. Temperatures (with or without pumping) gradually increase with time. However, at the start of the spring cycle, there is a two month time lag. That is, the temperatures without pumping exhibit an increasing trend starting in March/April while the same is true with pumping in May/June. After this, the two temperatures continuously increase at the same rate until the end of the year, while maintaining a difference of 2 to 4°C between them at all times. After the fall turnover the two temperatures will be identical. Temperatures will remain identical until March of the following year and then the new cycle starts again.

As an outcome of these considerations, it is possible to minimize the thermal impact by installing the pumping ports of the two reservoirs at the same depths from the surfaces so that the same amount of water with similar temperature characteristics would be exchanged between the two reservoirs. It should also be possible to control the reservoir and outlet temperatues by providing an adjustable outlet/tailrace. Engineering details of such a scheme is beyond the scope of this paper.

REFERENCES

1   Huber, W C, D R F Harleman and P J Ryan, "Temperature Prediction in Stratified Reservoirs", Journal of the Hydraulics Division, Proceedings of the American Society of Civil Engineers, April 1972.

2   Shin, J J, "The Alteration of Thermal Stratification of the Deep Reservoir Due to the Operation of a Pumped Storage Hydropower Plant", Engineering Foundation Conference, August 1975.

3   Ryan, P J and D R F Harleman, "Temperature Prediction in Stratified Water Mathematical Model - User's Manual", MIT Ralph M Parson's Lab, Supplement to Report 16130 DJH01/71, April 1971.

4   Parker, F, B A Benedict and C Tsai, "Evaluation of Mathematical Models for Temperature Prediction in Deep Reservoirs", Environmental Protection Agency, EPA-660/3-75-038.

5   Kennedy, R E, "Computation of Daily Insolation Energy", Bulletin, American Met Society, Volume 30, Number 6, June 1949.

6   Huber, W D and D R F Harleman, "Laboratory and Analytical Studies of the Thermal Stratification of Reservoirs", MIT Ralph M Parson's Lab, TR 112, October 1968.
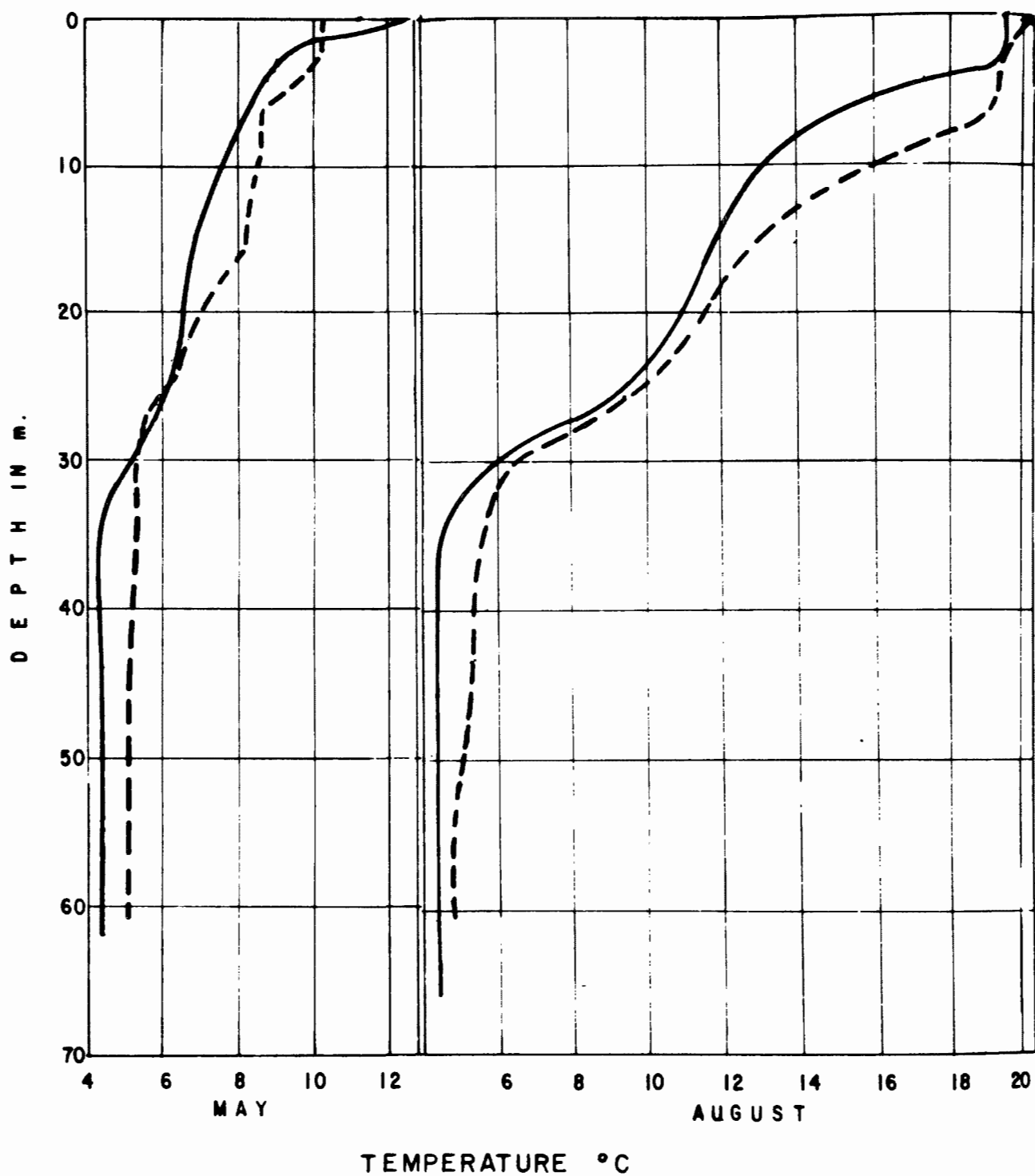
FIGURE 1 MEASURED AND PREDICTED TEMPERATURE PROFILES FOR THE UPPER RESERVOIR

P R E D I C T E D · · · · · · · ———————

MEASURED   – – – – – –   146

WITH PUMPING ————

WITHOUT PUMPING ● ● ● ● ● ●

DEPTH m.

0 10 20 30 40 50 60 70

4 6 8 10 12 14 16 18 20

JUNE

4 6 8 10 12 14 16 18 20 22

JULY

4 6 8 10 12 14 16 18 20

AUGUST

4 6 8 10 12 14 16 18

SEPTEMBER
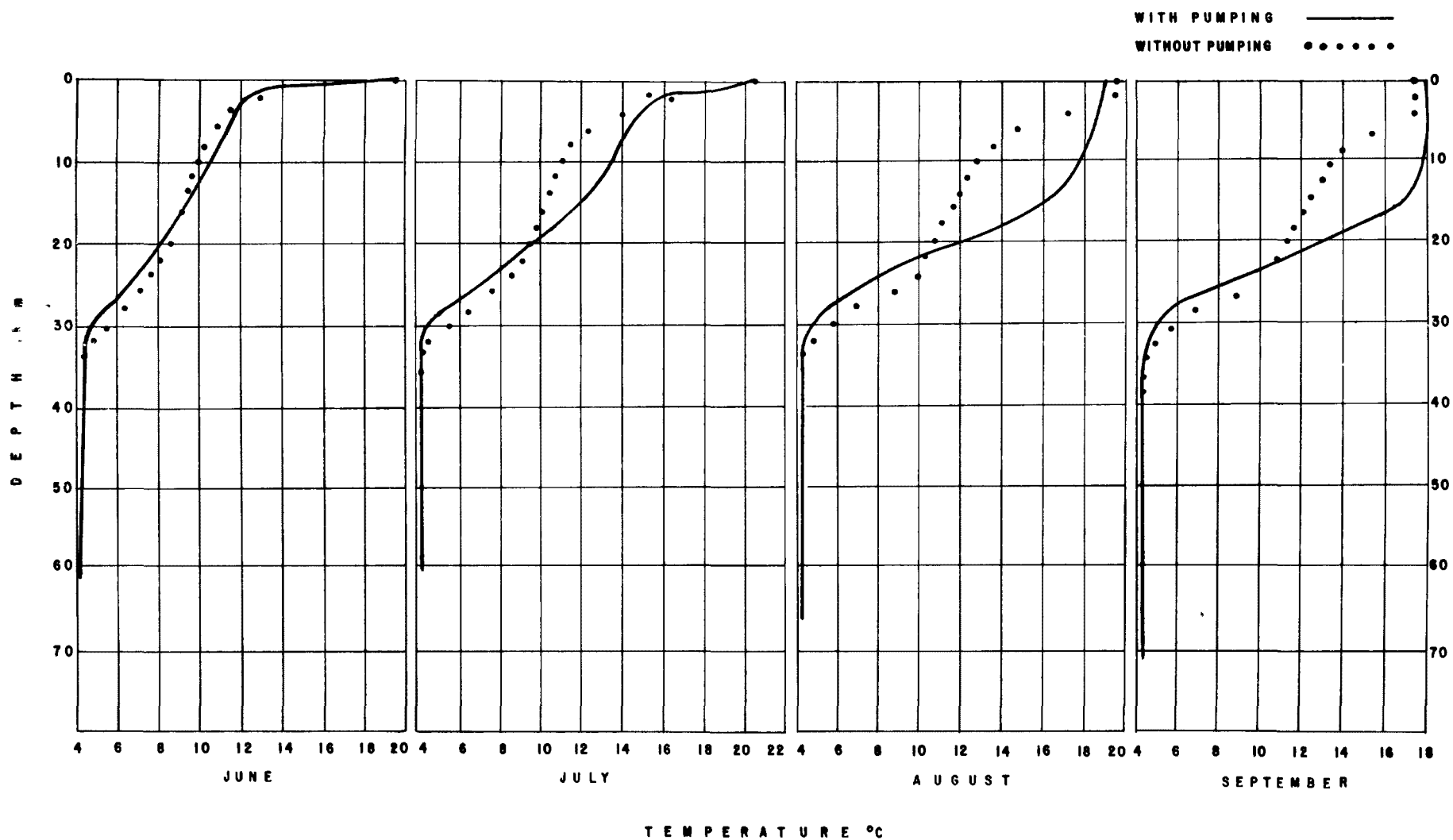
TEMPERATURE °C

FIGURE 2 – PREDICTED RESERVOIR TEMPERATURE PROFILES WITH AND WITHOUT PUMPING FOR THE UPPER RESERVOIR
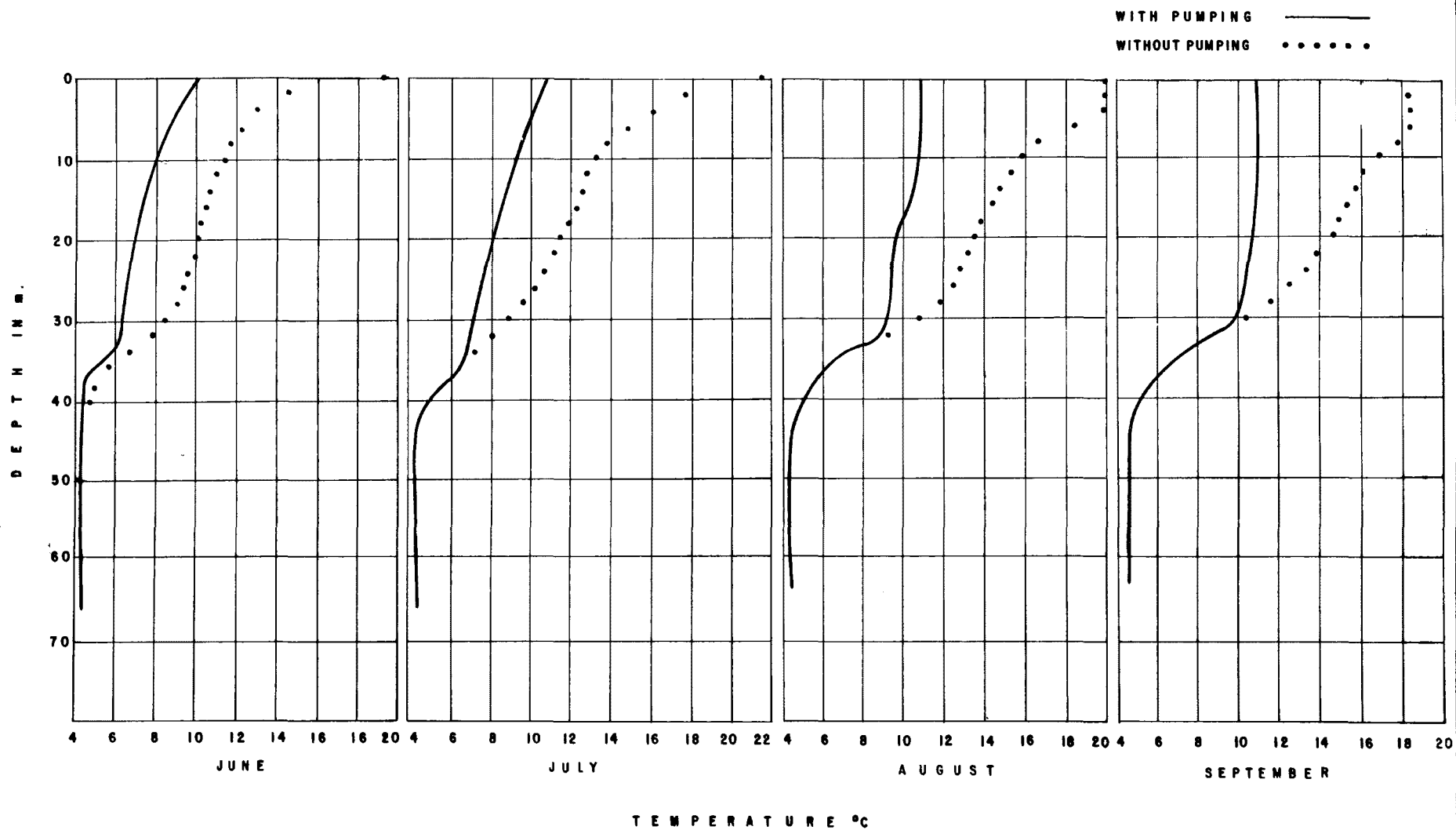
FIGURE 3 - PREDICTED RESERVOIR TEMPERATURE PROFILES WITH AND WITHOUT PUMPING FOR THE LOWER RESERVOIR

148
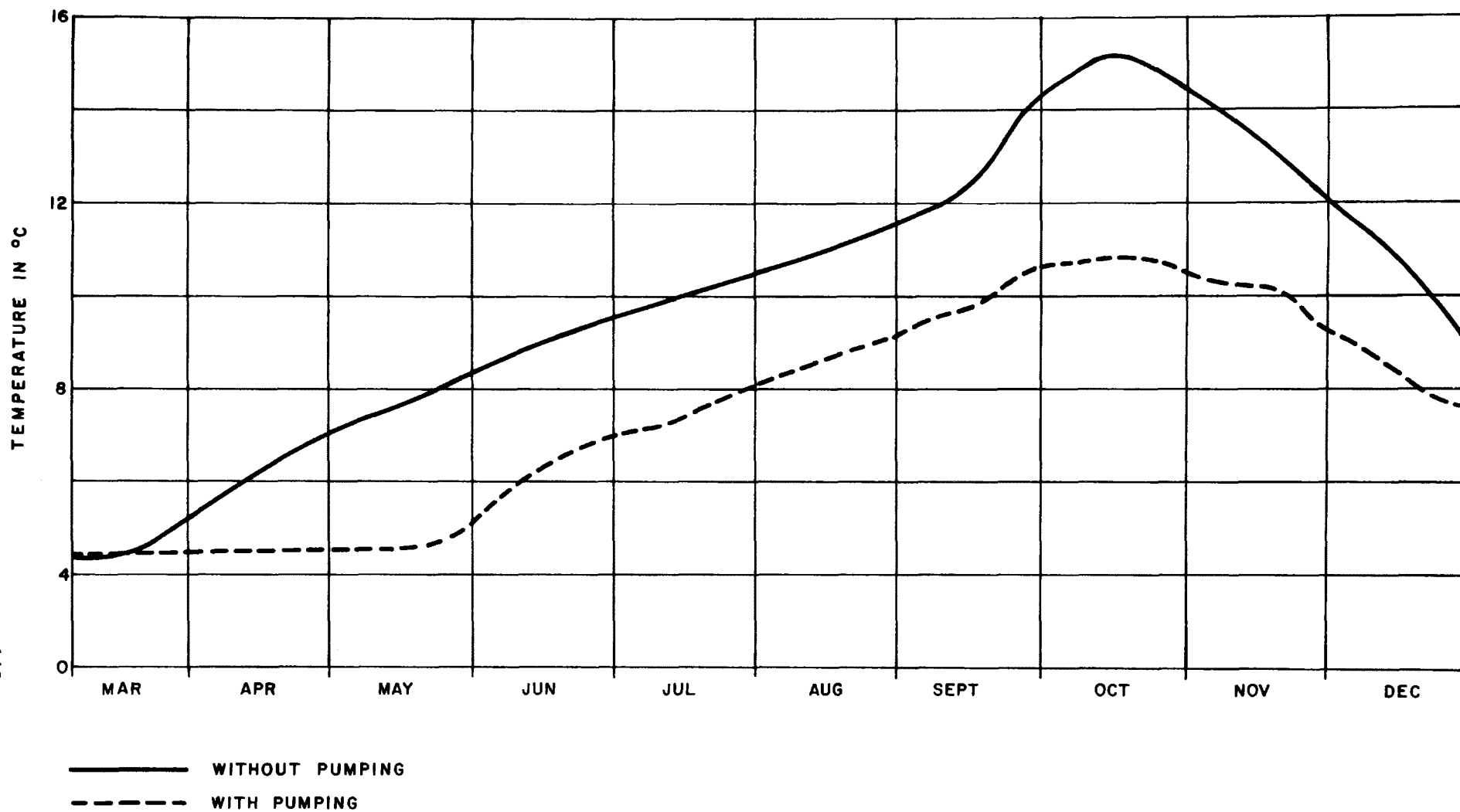
FIGURE 4 - PREDICTED LOWER RESERVOIR OUTLET TEMPERATURE PROFILES WITH AND WITHOUT PUMPING

ALGORITHMS FOR A MATHEMATICAL MODEL TO PREDICT ENVIRONMENTAL EFFECTS FROM THERMAL DISCHARGES IN RIVERS AND IN COASTAL AND OFFSHORE REGIONS

J. Häuser
Institut für Physik
GKSS
2054 Geesthacht/FRG

F. Tanzer
1. Phys. Institut
Universität Giessen
6300 L-Giessen/FRG

ABSTRACT

The ecological response of aquatic biota is a very important factor to be considered in assessing the consequence of thermal effluents. Therefore a model is necessary to predict the temperature as a function of time and position in the specified region and then, to predict the accompanying temperature ecological effects. The corresponding transport processes are described by partial differential equations which are solved numerically.

In the numerical simulation of these processes for a flow region with complex shoreline geometries four main problems arise, viz. (a) the description of the boundary (b) the determination of all discrete elements lying within the solution area together with their corresponding shapes (c) the treatment of boundary conditions, and (d) the numerical solution of the transport equation.

The present paper describes the development of algorithms for the solution of all points (a) through (d) for two-dimensional multiconnected regions.

DESCRIPTION OF THE ALGORITHMS

Mathematical models are of particular interest to assess the environmental impact of power plant operations in tidal estuaries, coastal regions, and rivers including the effects of recirculation and reentrainment of the heated discharge water. The ecological response of the aquatic bioata to the discharged cooling water is a very important factor, and a model predicting the consequences of thermal effluents will be of great use.

In Germany, at present [1], the following standards are being applied to once-through river cooling: maximum temperature at the end of the condenser discharge canal 30 °C, maximum temperature in surface water after mixing 28 °C, maximum temperature increment in surface water after complete mixing 5 K. The above temperature limits are valid only for waters of sufficiently good quality. In any case, dissolved oxygen should not fall below 5 mg/ℓ.

In situations of practical relevance the specified river, coastal or offshore region will be an area, which is irregularly shaped. Hence, a complete solution of the simulation problem requires algorithms for the following steps:

(a)   description of the boundary,

(b)   determination of all discrete elements lying within the solution area together with their corresponding shapes,

(c)   treatment of boundary conditions,

(d)   numerical solution of the transport equation.

The solution of the points (a) through (d) is performed by algorithms SPLNE, INAREA, SHAPE, and SOLVE [2].

As tidal effects play an important role the integral form (see Eq. 1 below) of the transport equation is preferred to the differential equation because of its conservative property; i.e. in order to allow adaptation to flow situations with a time and spatially varying water depth. For the purpose of this paper the transport equation is considered to be of the form

$$\frac{\partial}{\partial t} \int_V \Psi(\vec{x},t)\,dV + \oint_{A(V)} \Psi(\vec{x},t)\vec{v} \cdot d\vec{A} = \oint_{A(V)} \nabla\Psi(\vec{x},t) \cdot d\vec{A} + \int_V q'(\vec{x},t)\,dV \qquad (1)$$

where the integrations are to be carried out over the volume V and over the closed surface of V, denoted by A(V). $\Psi(\vec{x},t)$ can be some property of a medium, such as temperature T or one of the velocity components, and q', for instance, may be an additional heat flux vector if Ψ represents the temperature.

As mentioned before rivers and coastal or offshore regions may have complex shoreline geometries so it is normally not sufficient to approximate these boundaries by step functions only, i.e. to allow only discrete elements of rectangular shape. This leads to an incomplete description of the real solution area, resulting in errors for the flow field which, in turn,

affect the temperature distribution. In order to avoid these errors it is necessary to accurately model the specified region. Hence, our program allows completely arbitrary cross-sectional areas for discrete elements, a denotation used in [3, 4].

The user wishing to describe the boundary of his solution area (possibly multiconnected) does this by specifying a set of closed curves. Each curve consists of a number of segments each formed by a set of splines which describe the boundary curve between two successive data points. At the intersection of two segments the boundary curve need not be differentiable as indicated in Fig. 2. In general the closed boundary curves cannot be described as a function $y = f(x)$, so we use a parameter representation $x(t)$, $y(t)$.

Together with the data points the initial and final slopes of the tangent for each segment have to be specified. The complete input of a sample boundary curve, representing the Lower Elbe geometry between river-kilometers 641 and 667, is shown in Table 1, and Fig. 1 depicts the graphical output, constructed by SPLNE, for this region including the grid structure utilized.

The method used in this algorithm, is a cubic spline interpolation in that different cubic polynomials $x = x_i(t)$, $y = y_i(t)$ represent the boundary curve between different pairs of data points $(x_i, y_i) - (x_{i+1}, y_{i+1})$. The coefficients are chosen such as to ensure continuity of $x_i(t)$, and $y_i(t)$ as well as the first and second derivative at each data point. However, no system of linear equations is solved, rather the coefficients are determined by matrix multiplication. Here it is interesting to note that the same cubic splines are used for the spatial approximation of Eq. (1).

After the construction of the boundary all mesh points lying within the solution area (interior mesh points) must be determined. This is performed by algorithm INAREA. INAREA relies heavily on the spline representation, discussed above.

A special difficulty for the algorithm arises, when the intersection point of two segments coincides with an intersection point of a boundary curve and a line $x = x_i$ (Fig. 2). In order to determine whether an interval I on that line, which normally contains several mesh points, lies within the specified region it is necessary to know the slope of the tangent vectors of the two intersecting segments. Here it should be noted that the boundary curve - for the sake of simplicity we consider only a single curve - is followed in a clockwise direction such that the interior of the curve lies to the right. We now shift the origin of the coordinate system so that its new origin coincides with the coordinates of the afore mentioned intersection points; i.e. the interval I lies always on the negative y'axis (Fig. 2).

Since the solution area lies to the right of the curve, we can state the following rule (Fig. 2).

> Assuming the tangent of the second segment to be fixed, and rotating the tangent of the first segment counter-clockwise (positive sense) until they coincide, an interval I belongs to the solution area if the negative y'axis is intersected.

Fig. 3 shows three sample cases and Fig. 4 shows the computer printout for the Lower Elbe geometry. An asterisk indicates an interior mesh point.

One of the fundamental advantages of the employed method is its complete flexibility in considering discrete elements of any arbitrary geometry. Although the general formulation uses a Cartesian index (i, j) the method does not require the approximation of a boundary by rectangular elements. SHAPE constructs discrete elements exactly matching an irregular boundary. Here, again, the spline representation is essential. The enclosure surface of each discrete element may be computed using the spline representation.

From the algorithm INAREA we know all interior mesh points. To each interior mesh point we associate a discrete element, here called an incomplete discrete element and denoted by $IDE_{i,j}$. However, the area covered by all these incomplete discrete elements is less than the solution area due to the omission of the boundary areas $BA_{i,j}$ (Fig. 5). We wish to extend and reshape all incomplete discrete elements out to the boundary curve, thus constructing a set of variable-sized, irregular-shaped discrete elements that span the specified region.

A boundary area is associated to an incomplete discrete element if their common side length has the maximal value out of all IDEs also adjacent to this boundary area. The principle of this relation is shown in Fig. 5. Since a discrete element is three-dimensional we denote its cross-section, as depicted in Fig. 5, by $SDE_{i,j}$ which stands for surface discrete element.

Since the solution algorithm used reduces Eq. (1) to a system of coupled, ordinary first-order equations in time, it is necessary to specify initial conditions at all discrete elements. On the other hand, according to the formulation of the method, there are no boundary conditions in the sense of boundary value problems, since the conservation laws are integrated over each discrete element or its enclosure surface; i.e. the effects of the boundary are imposed on the half-point surfaces of the discrete element or on the irregular-shaped boundary of a boundary discrete element. For computational simplicity we assume that a fluid boundary coincides with lines $x = x_{i+1/2}$ or $y = y_{j+1/2}$. This is in no way a restriction, since a fluid boundary can be freely chosen. Values on the half-point boundary, however, cannot be approximated by second upwind differencing, since the corresponding adjacent discrete element may lie outside the solution area. In the case of temperature we obtain the values for the temperature and the normal derivatives on half-point surfaces by a simple Taylor expansion having second order accuracy. Eqs. (2) then represent the general mathematical formulation of our system.

$$\frac{\partial \Psi_{i,j}(t)}{\partial t} = F_{i,j}(t, \Psi_{i\pm1,j}(t), \Psi_{i,j}(t), \Psi_{i,j\pm1}(t)) \qquad (2)$$

$$\Psi_{i,j}(t_o) = (\Psi_o)_{i,j}$$

For the spatial approximation of the right-hand side of Eqs. (2), performed by algorithm SOLVE, one can use the donor cell method or second upwind differencing which is both conservative and transportive. However, this method is only of second order accuracy when employed to the approximation of half-point values, since the mathematical forms are based on linear averaging

between two discrete elements. Considering the approximation of derivates $\left(\frac{\partial \Psi}{\partial x}, \frac{\partial \Psi}{\partial y}\right)$ these are approximated by finite forms which are only of first-order accucary.

It is, however, desirable, as is pointed out in [5], to improve the spatial approximation, since this will lead to considerably increased time steps. Reducing the mesh size from Δx_1 to Δx_2 in a two-dimensional space, and using the FTCS explicit method for the diffusion problem, increases the computer time by a factor $(\Delta x_1/\Delta x_2)^4$. Hence, it is clear that methods with improved accuracy allowing greater mesh sizes are highly desirable. For this purpose we again use the cubic spline representation to improve the accuracy for the approximation of half-point values and derivatives. Discrete points of support are the center-points (mesh points) of the discrete elements. To obtain computational simplicity through decoupling of coordinates a cubic spline function is constructed separately for each row and column.

The final result is a numerical procedure having fourth-order accuracy for the approximation of half-point values and third-order accucary for approximation of derivatives $\left(\frac{\partial \Psi}{\partial x}, \frac{\partial \Psi}{\partial y}\right)$, that is the truncation error is of degree two higher than for the donor cell method.

In conclusion, the above mentioned algorithms SPLNE, INAREA, SHAPE, and SOLVE can be used for all transport processes including complex shoreline geometries. The detailed results and mathematical formulations of this extensive study are being prepared for presentation.

REFERENCES

[1] LAWA   −   Grundlagen für die Beurteilung der Wärmebelastung
                        von Gewässern, 2. verbesserte Auflage 1977, pp.116

[2] HÄUSER, J.   −   Algorithms for the Different Steps in the Numerical
    TANZER, F.   Solution of Partial Differential Equations and
                        Application to the Design of an Ion Extraction System,
                        IEEE International Conference on Plasma Science,
                        15-17 May 1978, Monterey, California

[3] ERASLAN, H.A.   −   A Transient, Two-Dimensional, Discrete-Element,
                        Far-Field Model for Thermal Impact Analysis of Power
                        Plant Discharges in Coastal and Offshore Regions.
                        Part 1: General Description of the Mathematical Model
                        and the Results of an Application, ORNL-4940, Feb.
                        1975, Oak Ridge

[4] ERASLAN, H.A.   −   Systematic Application of Transient, Multi-Dimensional
    KIM, K.H.   Models for Complete Analysis of Thermal Impact in
    HARRIS, J.L.   Regions with Severe Reversing Flow Conditions,
                        Waste Heat Management and Utilization, 9-11
                        May 1977, Miami Beach, Florida

[5] ROACHE, P.   −   Computational Fluid Dynamics, Hermosa Publishers,
                        1976

```
*    H E T R A N  -G-SS- 78/08/27/          1 101 101 101   59.6 8.4
*    LOWER ELBF RIVER FROM STREAM-KM         777
*    641 TO STREAM-KM 667.                   *    11. SEGMENT
*                                            1 101 101 101   59.4 10.2
*    INPUT DATA TO SPECIFY SOLUTION          777
*    AREA.THE FIRST NUMBER OF DATA           *    12. SEGMENT
*    CARD INDICATES A SOLID (1)              1 101 101 101   67.3 12.3
*    OR A FLUID (0) BOUNDARY.                1 101 101 101   75.8 12.7
*    BOUNDARY CONDITIONS,THEN,CALCULATED     1 101 101 101   80.0 16.0
*    FROM THESE INFORMATIONS.                777
*    THE FOLLOWING THREE NUMBERS MAY         *    13. SEGMENT
*    BF USED TO STATE SPECIAL                0 101 101 101   80.0 8.0
*    CONDITIONS FOR TEMPERATURE AND          777
*    VELOCITY COMPONENTS.                    *    14. SEGMENT
*    THE FOLLOWING TWO NUMBERS SPECIFY       1 101 101 101   78.7 7.7
*    X AND Y COORDINATES,RESPECTIVELY.       1 101 101 101   73.4 7.5
*    EACH CURVE IS RUN ALONG IN A            1 101 101 101   70.3 6.3
*    CLOCKWISE DIRECTION.                    777
*                                            *    15. SEGMENT      LUEHE
*    777 END OF SEGMENT                      0 101 101 101   70.0 6.3
*    888 END OF BOUNDARY CURVE               777
*    999 END OF COORDINATE INPUT             *    16. SEGMENT
*      1. CURVE                              1 101 101 101   65.4 5.3
*        1. SEGMENT                          1 101 101 101   60.9 2.2
1 101 101 101   0.  15.3                     1 101 101 101   57.5 2.0
1 101 101 101   7.1 18.9                     1 101 101 101   56.3 1.4
1 101 101 101   13.5 20.6                    1 101 101 101   53.8 1.4
777                                          1 101 101 101   49.6 1.7
*        2. SEGMENT      KRUECKAU            1 101 101 101   47.8 0.6
0 101 101 101   13.8 20.6                    1 101 101 101   44.5 0.4
777                                          1 101 101 101   39.2 2.1
*        3. SEGMENT                          777
1 101 101 101 14.35 20.8                     *    17. SEGMENT      SCHWINGE
1 101 101 101 14.9 21.1                      0 101 101 101   39.0 2.0
1 101 101 101   15.7  20.9                   777
1 101 101 101   22.3 19.3                    *    18. SEGMENT
1 101 101 101   29.4 17.7                    1 101 101 101   34.0 3.0
777                                          1 101 101 101   29.9 4.7
*        4. SEGMENT                          1 101 101 101   24.5 6.5
1 101 101 101   29.3 16.8                    1 101 101 101   20.1 8.0
777                                          1 101 101 101   17.7 8.3
*        5. SEGMENT      PINNAU              1 101 101 101   15.5 8.6
0 101 101 101   29.4 16.6                    1 101 101 101    9.1 8.0
777                                          1 101 101 101   0.0 7.2
*        6. SEGMENT                          777
1 101 101 101   31.6 16.4                    *    19. SEGMENT
1 101 101 101   34.0 12.5                    0 101 101 101   0.0 15.3
1 101 101 101   38.2 10.9                    888
1 101 101 101   42.1 10.4                    *    2. CURVE      PAGENSAND
1 101 101 101   45.7 11.1                    *    20. SEGMENT
777                                          1 101 101 101   11.5 16.8
*        7. SEGMENT                          1 101 101 101   18.4 16.4
1 101 101 101   45.7 10.6                    1 101 101 101   21.7 16.3
777                                          1 101 101 101   22.8 15.8
*        8. SEGMENT                          1 101 101 101   23.8 15.4
1 101 101 101   43.8 8.8                     1 101 101 101   26.0 13.4
1 101 101 101   44.4 7.6                     1 101 101 101   29.4 10.2
1 101 101 101 44.6 5.7                       1 101 101 101   19.4 14.2
777                                          1 101 101 101   13.7 16.1
*        9. SEGMENT                          1 101 101 101   11.2 16.2
1 101 101 101   45.2 4.7                     1 101 101 101   11.5 16.8
777                                          888
*        10. SEGMENT                         *    3. CURVE      AUGBERG,DROMMEL
1 101 101 101   53.2 7.3                     *    21. SEGMENT
```

Table 1: Input data for the Lower Elbe geometry

156

```
 1 101 101 101   32.7 12.4
 1 101 101 101   37.4 9.2
 1 101 101 101   42.0 8.5
 1 101 101 101   43.9 5.C
 1 101 101 101   44.4 6.6
777
*       22. SEGMENT
 1 101 101 101   43.6 5.5
777
*       23. SEGMENT
 1 101 101 101   41.5 6.9
 1 101 101 101   38.8 6.7
 1 101 101 101   35.7 7.4
 1 101 101 101   33.7 9.1
 1 101 101 101   35.1 10.1
 1 101 101 101   32.7 12.4
888
*      4. CURVE        CUEHESAND
*      24. SEGMENT
 1 101 101 101   53.0 3.4
 1 101 101 101   57.1 4.7
 1 101 101 101   59.9 5.1
 1 101 101 101   63.3 5.3
 1 101 101 101   60.1 3.3
 1 101 101 101   54.1 2.8
 1 101 101 101   53.0 3.4
888
*      5. CURVE       HANSKALBSAND
*      25. SEGMENT
 1 101 101 101   76.3 9.5
 1 101 101 101   76.8 9.8
 1 101 101 101   77.2 9.9
 1 101 101 101   77.5 10.2
 1 101 101 101   80.0 12.6
777
*      26. SEGMENT
 1 101 101 101   80.0 11.5
777
*      27. SEGMENT
 1 101 101 101   78.3 10.6
 1 101 101 101   77.9 9.6
 1 101 101 101   76.4 9.3
 1 101 101 101   76.3 9.5
999
*  INITIAL AND FINAL SLOPE FOR EACH
*  SEGMENT [DEGREES].ANGLES ARE
*  MEASURED FROM THE X-AXIS;
*  CONSIDERED POSITIVE IN
*  COUNTER-CLOCKWISE DIRECTION.
  27   15
   0    0
  28   12
 -93  -93
 -74  -74
  -6   10
 -85  -85
  44   96
 121  121
  18    9
  96   96
  14   37
 -90  -90
-166 -159
-168 -168
-168  162
-169 -169
 171 -175
  90   90
   3   67
 -34  -73
-125 -125
 146  135
  18  155
  34   43
 -90  -90
-153  100
```
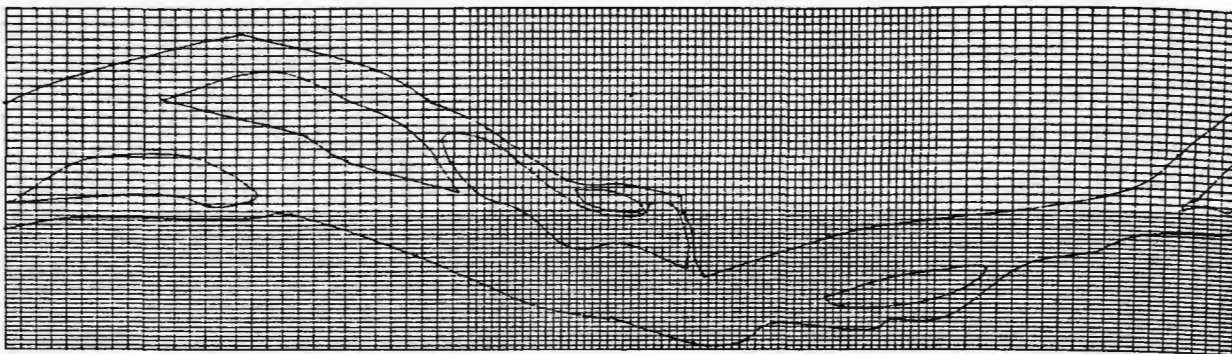
Fig. 1: Top view of the Lower Elbe River between river-kilometers 641
and 667 including the grid structure utilized
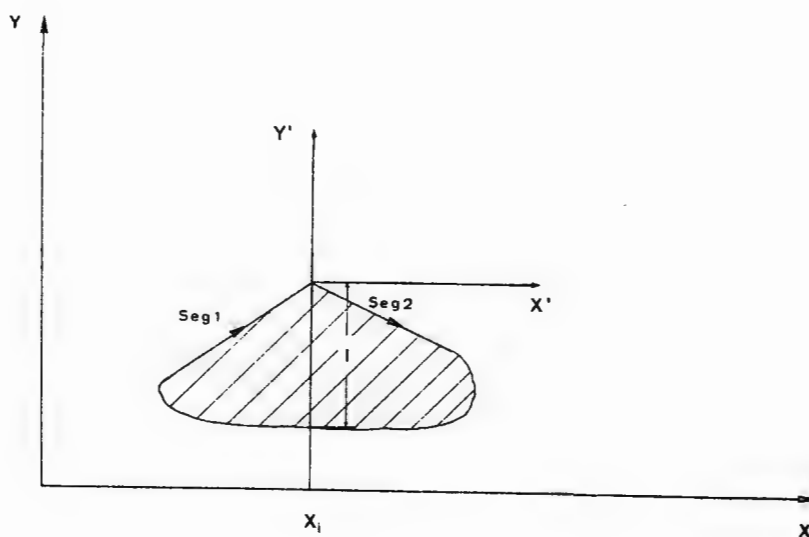
Fig. 2: Determination of interior mesh points. The shaded area denotes
the solution area S
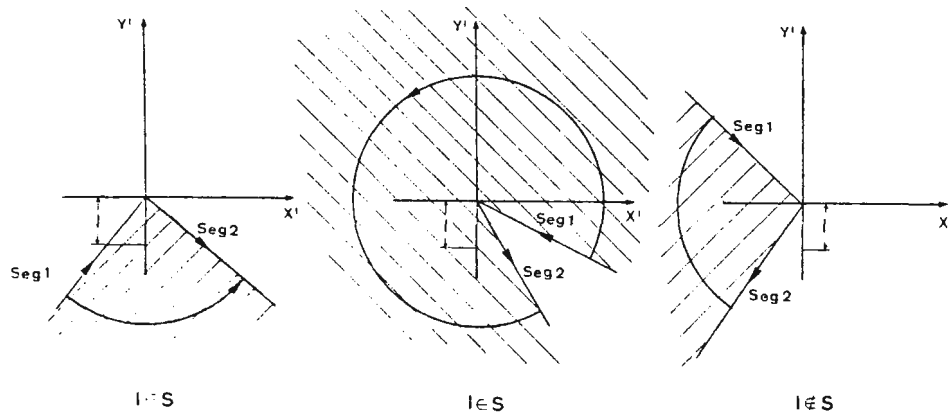
Fig. 3:   Sample   cases for the location of the solution area with respect
to interval I. The shaded areas denote the solution areas
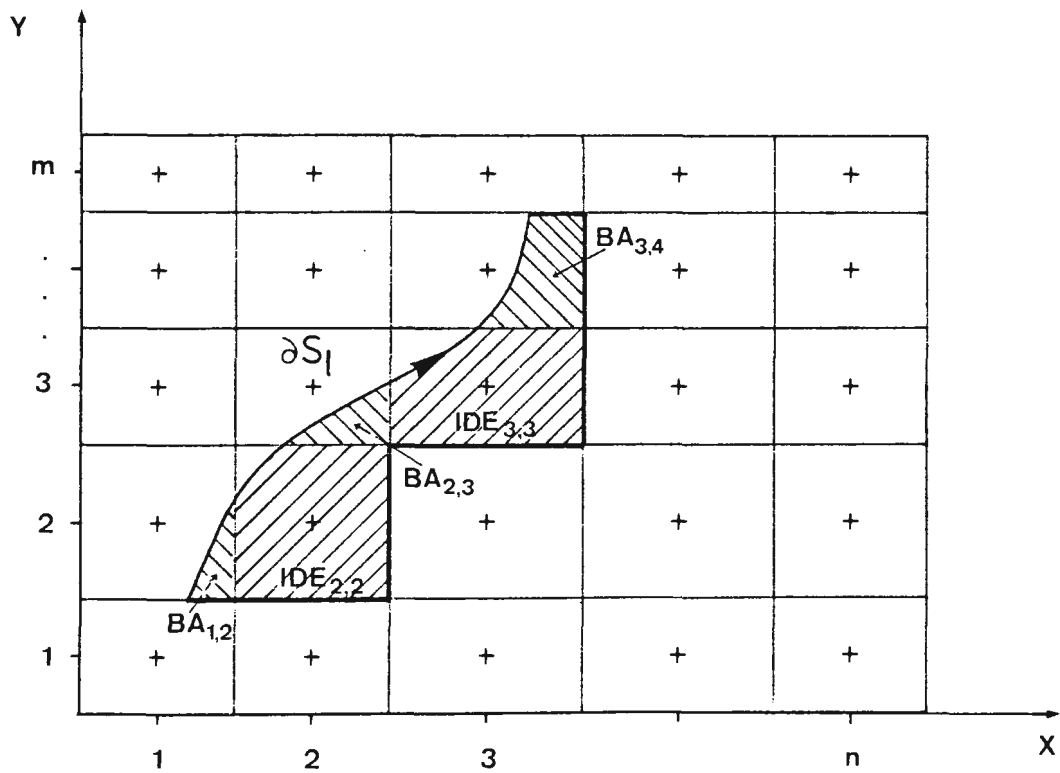
Fig. 5:   Construction of discrete elements $DE_{i,j}$. For instance,
$SDE_{2,2} = IDE_{2,2} \cup BA_{2,3} \cup BA_{1,2}$ and $SDE_{3,3} = IDE_{3,3} \cup BA_{3,4}$

Fig. 4:   Computer printout for the Lower Elbe geometry. An asterisk marks an interior mesh point

EFFECT OF SALT UPON HOT-WATER DISPERSION IN WELL-MIXED ESTUARIES. PART 2. LATERAL DISPERSION

R. Smith
Department of Applied Mathematics and Theoretical Physics,
University of Cambridge, U.K.

ABSTRACT

The dispersion of heat in shallow water differs from that of
passive contaminants in that the buoyancy can modify the flow
and hence can effect the dispersion. This has the serious
implication that on-site experiments with dyes are of limited
use in helping to predict the thermal impact of any proposed
industrial developments. For estuaries the task of modelling
the dispersion of heat is further complicated by the fact that
there are already buoyancy-driven currents due to the salinity
distribution. Thus, not only does the heat change the flow
directly, but also it changes the flow indirectly by modifying
the salinity distribution. Here it is shown that in a
vertically well-mixed estuary the interactions are such as to
disperse heat preferentially towards the shoreline for an ebb
tide and away from the shoreline for a flood tide. In extreme
cases the asymmetry in the lateral dispersion coefficient
can be several hundred percent.

INTRODUCTION

From dye experiments in shallow water there is ample evidence
of the diffusion-like character of the dispersion process [1].
Thus the natural mathematical model with which to describe
dispersion is a linear diffusion equation with an appropriately
chosen value of the effective diffusivity. Indeed, it has
become conventional to quantify dispersion in terms of this so-
called dispersion coefficient.

The explanation as to why a diffusion equation should arise,
rather than some more complicated equation, dates back to a
classic paper by G.I. Taylor in 1921 [2]. However, it was
not until several decades later that he was able to give a
quantitative theory for the particular case of a neutrally
buoyant contaminant in pipe flow [3, 4]. This work revealed
that the dispersion coefficient depends upon effects, such
as diffusion perpendicular to the dispersion direction, which
are negligible as regards to other aspects of the flow.
Furthermore, contrary to intuition, the dispersion coefficient

reduces as the transverse diffusion increases.

It is this dependence upon readily overlooked effects that
has made it so difficult for engineers to conjecture simple
empirical formulae for dispersion coefficients [5] . For
example, Fischer's [6] calculated and observed values for the
longitudinal dispersion coefficient in non-rectangular
channels can be several orders of magnitude greater than
Elder's [7] results for channels of constant depth.

Buoyancy effects

Another facet of this sensitivity of the dispersion process
is that the dispersion of a buoyant contaminant, such as heat
or fresh water, is different from that of a passive contaminant.
Close to an outfall the induced vertical stratification
suppresses the turbulence and can delay considerably the
achievement of complete vertical mixing [8] . Then further
away from an outfall the difference in hydrostatic pressure
between the centre of a buoyant plume and the surrounding
denser water drives a secondary flow (see Fig . 1) which
accelerates the lateral dispersion [9] . Finally, in confined
flows when cross-sectional mixing is not quite complete, this
same secondary flow augments the transverse turbulent diffusion
and leads to a reduced rate of longitudinal dispersion [10] .
The net result is that on-site experiments with dyes are of
limited use in helping to predict the thermal impact of any
proposed industrial development.

In an important paper, Erdogan and Chatwin [11] extended
Taylor's analysis [3] to apply to buoyant contaminants in pipe
flow. They found that the dispersion is still governed by a
diffusion equation, but with the significant difference that
the dispersion coefficient is a nonlinear function of the den-
sity gradient. For reasons of (vertical) symmetry the
dispersion coefficient is an even function. Thus, for weak
gradients the contaminant distribution $c(z,t)$ satisfies the
"Erdogan-Chatwin" equation

$$c_t = \left(\left(D_0 + (\alpha c_z)^2 D_2 \right) c_z \right)_z \qquad (1)$$

Here D_0 is the dispersion coefficient for passive contaminants,
α is the constant of proportionality between the density
change and the concentration c, and D_2 is a constant.

The same equation (1) was derived by Prych [9] for the lateral
dispersion of buoyant contaminants in open-channel flow, t
being the advection time downstream of the outfall and z being
the cross-stream coordinate. In that context there is no
need for the restrictive assumption that the gradients be weak.

162

Unfortunately, there is poor agreement between Prych's theory and his experiments. Smith [12] showed that this is remedied when Prych's "laminar" calculation of the D_2 coefficient is replaced by a more appropriate "turbulent" calculation (see Fig. 2). The revised and much increased estimate for D_2 is

$$D_2 = h^5 g^2 / 96 u_*^3 k^3 ,$$

(2)

where h is the water depth, g the acceleration due to gravity, u_* the friction velocity, and k the von Karman constant (typically .4). From a wide range of experimental results [13] a reasonable formula for D_0 is

$$D_0 = .15 h u_*$$

(3)

Heat and Salt

For a thermal discharge situated in an estuary there is dispersion of two contaminants, heat and salt, both of which change the density. If the turbulent intensity were weak, then the different lar 'iffusivities of heat and salt could give rise to th acular double-diffusive phenomena described in cha . Turner's monograph [14] . Here we shall restrict : tontion to vertically well-mixed estuaries, where by implica .ou the flow is highly turbulent and the eddy diffusivities for heat and salt are approximately equal. Thus, although there are interactions between the heat and salinity distributions, they are not so severe as to lead to the steepening of temperature gradients.

The assumption in this paper is that the dispersion takes place predominanatly across the estuary, the case of longitudinal dispersion having been addressed in part 1 [15] . Thus, here we are concerned with the middle field, where vertical mixing has been achieved but the hot-water plume extends only a small way across the estuary. Other implicit assumptions are that the estuary is sufficiently straight and free from jetties for the primary flow to be unidirectional. The mathematical task therefore is to extend equation (1) to incorporate a second contaminant and to investigate the nature of the solutions.

A striking feature of the solutions obtained below is that the interactions between heat and salt lead to the heat's being preferentially dispersed towards the saltier region of the estuary. To a first approximation the salinity distribution in a wide estuary is carried along with the tidal current. Thus, at high tide the fluid in the faster-moving, deeper

163

central region of the estuary originates further out to sea, and is saltier, than the fluid close to the shore. This means that at high tide a hot-water plume in a wide estuary would tend to be deflected away from the shoreline. At low tide the opposite is the case. For narrower estuaries (less than about 200m wide) the more complete cross-sectional mixing of salt means that the lateral salinity gradient depends upon the tidal direction rather than the tidal height [6] . Thus, in a narrow estuary heat is dispersed preferentially towards the shoreline when the tide is going out.

QUALITATIVE DEDUCTIONS

Although the heat and salt both modify the flow, there is never-the-less a single flow which disperses the two contaminants. Thus, if the turbulent eddy diffusivities for the two constituents are equal, then it follows that the two dispersion processes are dynamically identical, and that there is a common dispersion coefficient for both heat and salt. In view of the results (1,2,3) for a single buoyant contaminant, we infer that the common dispersion coefficient is simply a function of the total density gradient

i.e.
$$D = D_0 + (\beta s_z - \alpha \theta_z)^2 D_2 \tag{4}$$

The opposite signs of the β and α terms allow for the fact that the salinity s and the temperature θ have opposite effects upon the water density.

Even without any calculations we can now infer that heat is preferentially dispersed across the estuary in the direction of increasing salinity. The effect of heat is to reduce the density locally; this results in a locally reduced density gradient on the fresh side of the plume and an increased gradient on the salty side. The dispersion coefficient is a rapidly increasing function of the density gradient. Thus, the dispersion of heat is reduced on the fresh side of the plume and is increased on the salty side.

Modified salinity distribution

A similar argument enables us to infer that the middle of the plume become saltier with a compensating reduced salinity at the tails of the temperature distribution. Upstream of the outfall the salinity distribution across the estuary is in equilibrium, the cross-stream flux of salt being balanced by the non-uniform longitudinal advection [6] . This equilibrium is disturbed by the hot-water plume. At the fresh side of the plume the lateral dispersion of salt is reduced. Thus the

164

flux of salt from the centre of the plume is less than that needed to maintain the equilibrium of the salinity distribution, and the water is therefore even fresher than it would have been in the absence of the plume. At the salty side of the plume the flux of salt towards the centre of the plume is in excess of the equilibrium flux, and there too the water is fresher than it would have been in the absence of the plume. The missing salt accumulates in the central part of the plume (see Fig. 3).

It is this perturbation of the salinity distribution that is the distinctive feature of hot-water dispersion in estuaries. Not only is the lateral dispersion coefficient (4) changed by the heat directly, but also it is changed indirectly by the thermally-induced salinity perturbation. Thus, we cannot study the temperature distribution without simultaneously determining the salinity distribution.

DISPERSION EQUATIONS

In order to focus attention upon the thermally-induced changes we regard the pre-existing (locally constant) salinity gradient $\bar{s}_z$ as being known. It then follows that the salinity anomaly s' and the temperature θ satisfy the coupled nonlinear diffusion equations

$$s'_t - (D s'_z)_z = D_z \bar{s}_z \ , \tag{5}$$

$$\theta_t - (D \theta_z)_z = 0 \ , \tag{6}$$

with

$$D = D_0 + (\beta \bar{s}_z + \beta s'_z - \alpha \theta_z)^2 D_2 \ . \tag{7}$$

The form (7) of the dispersion coefficient makes it convenient to change the dependent variables from s' and θ to ρ' and θ, where ρ' is the density perturbation. Thus equation (5) is replaced by

$$\rho'_t - (D' \rho'_z)_z = 0 \ , \tag{8}$$

where the "pseudo-dispersion coefficient" D' for the composite quantity ρ' is given by

$$D' = (D_0 + 3 \bar{\rho}_z^2 D_2) + 3 \rho'_z \bar{\rho}_z D_2 + \rho'^2_z D_2 \ . \tag{9}$$

The virtue of this change of variables is that there is no coupling between the θ distribution and the nonlinear diffusion equation for ρ'.

We note that D' is always positive. This makes it possible for us to infer that for a buoyant discharge ρ' will be everywhere negative. The asymmetry of D' means that perturbation density gradients, with the same sense as the pre-existing density gradient $\bar{\rho}_z$, will be dispersed most rapidly. Consequently, the ρ' distribution is skew (see Fig.3) and the centroid moves towards the salty side of the plume. On average D' exceeds the dispersion coefficient D for heat. Thus the temperature distribution is narrower and more highly peaked than the ρ' distribution. The physical reason for this difference is that in the centre of the plume the accumulation of salt counters the density-lowering effect of heat, while at the edges of the plume the reduced salinity and the heat both tend to lower the density.

With ρ' and θ as the dependent variables, the dispersion coefficient D becomes independent of θ

i.e.
$$D = \left(D_0 + \bar{\rho}_z^2 D_2\right) + 2\rho'_z \bar{\rho}_z D_2 + \rho'^2_z D_2 \quad (10)$$

Thus, once equation (8) has been solved for the density perturbation ρ', we can evaluate D and equation (6) becomes a linear equation for θ. The only difficulty is that created by the dispersion coefficient's being non-constant. For example, if in the absence of heat the salinity-driven secondary flow doubles the lateral dispersion coefficient (i.e.

$$D_0 = \bar{\rho}_z^2 D_2$$

) and if the presence of the plume leads to perturbation density gradients of $\pm\frac{1}{2}\bar{\rho}_z$, then D varies by a factor of 2.6.

HERMITE SERIES REPRESENTATION

Formally the equation (8) for ρ' only differs from the Erdogan-Chatwin equation (1) in that the dispersion coefficient has linear as well as quadratic dependence upon the perturbation density gradient. Thus, we can use to advantage the mathematical methods recently used by the author to study the Erdogan-Chatwin equation [12].

Extremely far downstream we can expect the concentration gradients to become weak, and equations (6,8) both to reduce to constant coefficient diffusion equations. In turn this implies that the concentration profiles eventually become

Gaussian (assuming that the shorelines are distant). A natural way of representing the evolution towards normal distributions is by means of Hermite series

$$\rho' = \frac{(\beta S - \alpha Q)}{uh} \frac{1}{\sigma (2\pi)^{\frac{1}{2}}} \sum_n \frac{a_n}{n!} He_n\left(\frac{z}{\sigma}\right) \exp\left(-\frac{1}{2}\frac{z^2}{\sigma^2}\right) \;, \quad (11)$$

$$\theta = \frac{Q}{uh} \frac{1}{w(2\pi)^{\frac{1}{2}}} \sum_n \frac{b_n}{n!} He_n\left(\frac{z}{w}\right) \exp\left(-\frac{1}{2}\frac{z^2}{w^2}\right) \;. \quad (12)$$

Here S and Q are the rates at which salt and heat are being discharged from the outfall, h is the water depth and u the locally constant tidal velocity. By definition the leading coefficients a_0, b_0 are equal to 1. Also, if $\sigma(t)$ and $w(t)$ are chosen to be the exact standard deviations then a_2 and b_2 are both zero. The formulae for the first few Hermite polynomials $He_n(x)$ are

$$1 \;,\; x \;,\; x^2 - 1 \;,\; x^3 - 3x \;,\; x^4 - 6x^2 + 3 \;. \quad (13)$$

Representing the nonlinear terms

Our object is to replace all the terms in the dispersion equations for the density anomaly and for temperature by Hermite series of the forms (11) and (12) respectively. It is only the ρ'_z dependence of the dispersion coefficients which presents any difficulties. For the ρ'^2_z term this entails the introduction of the constants $G(i,j;k,n)$ such that

$$He_i(\mu x) He_j(\mu x) He_k(x) \exp\left(-\mu^2 x^2\right)$$
$$= i! \, j! \, k! \sum_n G(i,j;k,n) He_n(x) \quad (14)$$

[12]. Since μ has either of the values w/σ or 1, we shall simply denote the corresponding constants by G and G'. For the ρ'_z terms in D' and D we introduce the further constants F' and F where

$$He_i(\mu x) He_k(x) \exp\left(-\frac{1}{2}\mu^2 x^2\right)$$
$$= i! \, k! \sum_n F(i;k,n) He_n(x) \quad (15)$$

167

In [12] it is explained how G can be evaluated from Mehler's formula

$$\left(1+2y^2\right)^{\frac{1}{2}}\exp\left(-y^2x^2\right)=\sum_m \frac{(-1)^m}{m!}\left(\frac{y^2}{1+2y^2}\right)^m \mu. \qquad (16)$$

The same methods permit F to be evaluated. The properties which we shall subsequently make use of are that

$$G(1,1;1,2m+1) = \frac{(-1)^{m+1}(m-3\mu^2)}{(1+2\mu^2)^{5/2}\, m!}\left(\frac{\mu^2}{1+2\mu^2}\right)^m , \qquad (17)$$

$$F(1;1,2m) = \frac{(-1)^{m+1}(2m-\mu^2)}{\mu(1+\mu^2)^{3/2}\, m!}\left(\frac{\frac{1}{2}\mu^2}{1+\mu^2}\right)^m , \qquad (18)$$

$$F(1;2,2m+1) = \frac{(-1)^{m+1}(2m-2\mu^2+\mu^4)}{\mu(1+\mu^2)^{5/2}\, m!}\left(\frac{\frac{1}{2}\mu^2}{1+\mu^2}\right)^m , \qquad (19)$$

$$F(2,1,2m+1) = \frac{(-1)^{m+1}(2m+1-2\mu^2)}{(1+\mu^2)^{5/2}\, m!}\left(\frac{\frac{1}{2}\mu^2}{1+\mu^2}\right)^m , \qquad (20)$$

and that F, G are zero when the sum of their arguments is odd.

Proceeding as in [12] , we achieve the desired Hermite series representations of the dispersion equations (8) and (6). From the He_n coefficients we obtain equations for the rates of change of $a_n(t)$ and $b_n(t)$:

$$\sigma^2\, da_n/dt + \left\{n a_n + n(n-1)a_{n-2}\right\}\tfrac{1}{2}\, d\sigma^2/dt$$

$$= n(n-1)\left\{D_0 + 3\bar{p}_z^2 D_2\right\}a_{n-2}$$

$$- \frac{3\bar{p}_z D_2(\beta S - \alpha Q)\, n!}{(2\pi)^{\frac{1}{2}}\sigma^2\, h u}\sum_{i,k} i k\, F'(i;k,n-1)a_{i-1}\, a_{k-1}$$

$$+ \frac{D_2(\beta S - \alpha Q)^2\, n!}{2\pi\sigma^4\, h^2 u^2}\sum_{i,j,k} i j k\, G'(i,j;k,n-1)a_{i-1}\, a_{j-1}\, a_{k-1} \qquad (21)$$

168

$$\omega^2 \, db_n / dt + \left\{ n \, b_n + n(n-1) b_{n-2} \right\} \tfrac{1}{2} \, d\omega^2 / dt$$

$$= n(n-1) \left\{ D_o + \bar{\rho}_z^2 D_2 \right\} b_{n-2}$$

$$- \frac{2 \bar{\rho}_z \, D_2 (\beta S - \alpha Q)}{(2\pi)^{\frac{1}{2}} \sigma^2 \, h \, u} \, n! \sum_{i,k} i \, k \, F(i;k,n-1) \, a_{i-1} \, b_{k-1}$$

$$+ \frac{D_2 (\beta S - \alpha Q)^2}{2\pi \, \sigma^4 \, h^2 \, u^2} \, n! \sum_{i,j,k} i \, j \, k \, G(i,j;k,n-1) a_{i-1} \, a_{j-1} \, b_{k-1}$$

<div align="right">(22)</div>

We recall that F', G' are used to denote the case $\mu = 1$, while F, G denote the case $\mu = \omega/\sigma$. It deserves emphasis that equations (21) and (22) are exact. The advantage over the equivalent equations (8) and (6) becomes apparent when we seek approximations.

APPROXIMATE EQUATIONS

As shown in [12] there are a number of ways of approximating equations of the form (21) or (22). One particularly tempting procedure is to truncate the F and G summations after the leading term (i.e. to neglect a_j, b_j for $j \neq 0$). It can be shown that for large σ^2 or ω^2 this yields the correct results for the dominant contributions to the odd Hermite coefficients a_{2m+1}, b_{2m+1}. Furthermore, the shape of the concentration profile is given correctly. However, the width is wrongly estimated. For the Erdogan-Chatwin equation, with the F terms missing, it was the even Hermite coefficients and the width scale that were correct [12]

The modified procedure which we shall use here to truncate the F and G summations, is to include those terms which are linear but not quadratic in a_1, b_1. This yields the correct asymptotic forms for all the Hermite coefficients and for the standard deviations (see appendix).

169

For practical purposes it often suffices to know the simplest global properties of the contaminant distribution, such as the centroid and the standard deviation. Thus, if a_2 and b_2 are chosen to be zero, then the required information is contained in the four quantities a_1, σ^2, b_1, w^2. With the particular .truncation described above, the $n = 1$, 2 equations involve just these key variables:

$$\frac{d}{dt}(\sigma a_1) = \frac{-3\bar{\rho}_z D_2 (\beta S - \alpha Q)}{\pi^{1/2} 4\, h\, u\, \sigma^3} \quad , \tag{23}$$

$$\frac{d}{dt}\sigma^2 = 2\{D_0 + 3\bar{\rho}_z^2 D_2\} - \frac{3\bar{\rho}_z D_2 (\beta S - \alpha Q)(\sigma a_1)}{\pi^{1/2} h\, u\, \sigma^3}$$

$$+ \frac{D_2 (\beta S - \alpha Q)^2}{3^{3/2} \pi\, h^2\, u^2\, \sigma^4} \quad , \tag{24}$$

$$\tag{25}$$

$$\frac{d}{dt}(w b_1) = \frac{-2\bar{\rho}_z D_2 (\beta S - \alpha Q)}{(2\pi)^{\frac{1}{2}} h u\, (w^2 + \sigma^2)^{3/2}} \quad , $$

$$\frac{d}{dt} w^2 = 2\{D_0 + \bar{\rho}_z^2 D_2\} + \frac{3 D_2 (\beta S - \alpha Q)^2}{\pi h^2\, u^2} \frac{w^2}{\sigma(\sigma^2 + 2w^2)^{5/2}}$$

$$- \frac{8\bar{\rho}_z D_2 (\beta S - \alpha Q)}{(2\pi)^{\frac{1}{2}} h u\, (w^2 + \sigma^2)^{5/2}} \left[(2\sigma^2 - w^2)(w b_1) + (2w^2 - \sigma^2)(\sigma a_1) \right]$$

$$\tag{26}$$

Before we proceed to solve these equations it is interesting to note some qualitative results. First, in the limit of no lateral salinity gradient the centroids σa_1, $w b_1$ remain at $z = 0$ and we find that the common standard deviation $w = \sigma$ grows as per the Erdogan-Chatwin equation [12] . Secondly, equations (23) and (25) show that for a buoyant discharge, with $(\beta S - \alpha Q)$ negative, the centroid positions σa_1 and $w b_1$ are displaced in the $\bar{\rho}_z$ direction (i.e. towards the salty wide of the plume). Finally, in equations (24) and (26) the interactions between the density anomaly and the pre-existing salinity gradient are represented by the linear $\bar{\rho}_z$ terms. The formal negative sign, together with the further negative sign in the approp- riate centroid equation, shows that these interactions tend to increase the rate of dispersion. Thus, not only do the salinity gradient and the discharge of heat separately increase the

170

rate of spreading of a plume [16] , but also their interactions make the plume grow even faster.

ILLUSTRATIVE EXAMPLE

Equations (23-26) represent a considerable simplification from the coupled dispersion equations (5-7), which in turn are vastly more simple than the full equations of motion for two buoyant contaminants in a turbulent flow. Furthermore, as is evidenced by the results shown in figure 2, there is not an undue loss of accuracy. The simplifications result more from focussing attention upon what is regarded as being the primary information, rather than from the approximations which are made. The limiting factor to this process of simplification is the intrinsic complexity of the interactions between heat and salt.

Equations (23-26) do not seem to admit of exact analytic solutions. Also, the large number of degrees of freedom (e.g. lateral salinity gradient, source strength, initial standard deviation) precludes any simple non-dimensional classification of numerical results. Instead, we shall illustrate the effects of salt upon the dispersion of heat for an arbitrarily selected situation.

Figure 4 shows the calculated shape of the temperature plume (i.e. one standard deviation either side of the centroid) for a 20MW heat discharge with initial standard deviation 5m when the estuary conditions are:

$$h = 5\,m \;, \quad u = \cdot 1\,m\,s^{-1} \;, \quad u_* = \cdot 01\,m\,s^{-1} \;, \quad \partial_z \bar{s} = 1\,^o/_{oo}\,km^{-1}.$$

There is a ten-to-one exaggeration of the plume width. For comparison purposes the plume shapes are also shown for an unheated discharge, and for a heated discharge in the absence of any salinity gradient.

Several general features are worthy of comment. First, close to the outfall the rate of spreading, but not the sideways displacement, is independent of the salinity gradient. Secondly, at moderate distances the rate of spreading is significantly greater than that in either of the two limiting cases of no heat or of no salinity gradient. Thirdly, far from the outfall the plume evolves as per a dye plume emitted into the estuary from a virtual source far upstream of the actual source position and displaced into the saltier water. In the particular case shown in figure 4, the virtual source would be nearly 500m upstream and displaced by 9m away from the outfall into the saltier water.

CONCLUDING REMARKS

The parameter values in the illustrative example are quite modest, yet the effect of salt upon heat dispersion remains very noticeable even a kilometre from the outfall. Nuclear power stations can have cooling requirements several orders of magnitude larger than the example [8]. Thus the effect discussed in this paper would remain significant at much greater distances from the outfall.

Two methods which have been used to predict the thermal impact of hot-water discharges in estuaries are: on-site dye experiments, and hydraulic scale models. The first of these neglects any effects due to the buoyancy of the discharge, while the second method neglects any effects of the salinity distribution (due to scaling difficulties). The present work reveals that both of these methods err on the side of safety and under-estimate the overall dispersion. Furthermore, the effects of salt and heat are not merely additive, their interactions also contribute to the rate of spreading of the plume. In the proximity of a shoreline, another important aspect of the effect of salt upon dispersion of heat is that the plume tends to be deflected towards the saltier side. Depending upon the state of the tide, this can lead to higher shoreline temperatures than might have been expected.

ACKNOWLEDGEMENT

APPENDIX - CONCENTRATION PROFILES

Although the position and width of the plume are the most important and useful items of information, it is never-the-less of interest to determine the concentration profiles in more detail. For any particular initial discharge profile this could be done by solving numerically the nonlinear diffusion equation (8) for the density anomaly ρ' , and the coupled linear diffusion equation (6) for the temperature θ . However, if we are to distinguish general features from the particular, then solutions would need to be computed for a range of situations. Here we take a simpler course of action and seek instead approximate analytic solutions valid far downstream of the outfall (assuming, as above, that shorelines are distant).

For the density anomaly ρ' , the starting point for our calculations is the equation (21) for the Hermite coefficients a_n . If we take σ to be the exact standard deviation, then $a_2 = 0$ and the $n = 2$ equation can be used to replace t by σ^2 as the independent variable. The resulting equations for a_1, a_3, a_4 .... take the form

$$\sigma^2 da_n / d\sigma^2 + \tfrac{1}{2} n a_n = \left(F' \text{terms} \right)/\sigma^2 + \left(G' \text{terms} \right)/\sigma^4 \qquad (27)$$

where the right-hand-side terms involve summations of double and triple products of the Hermite coefficients. These terms are even more cubersome than those in equation (21) due to the change of independent variable.

An order-of-magnitude estimate of the solutions of equations (27) suggests that a_n decays at the same rate as the larger of σ^{-n} and the nonlinear forcing. In particular, $a_0 = 1$ (by definition), σa_1 tends to a constant, and the higher-degree coefficients are, at most, of order σ^{-2}.

These qualitative results, together with the explicit formulae (18-20) for the constants F', permit us to evaluate the dominant contributions to the forcing terms in equation (27). It is then straightforward to solve for the asymptotic approximations to the Hermite coefficients a_3, a_4 et seq.

$$\frac{a_{2m+1}}{(2m+1)!} = \left(\frac{3 \bar{\rho}_z D_2 (\alpha Q - \beta S)}{2 (D_0 + 3 \bar{\rho}_z^2 D_2) h u (2\pi)^{\frac{1}{2}} \sigma^2} \right) \frac{1}{\sqrt{2}} \frac{(-1)^{m+1}}{m! \, 4^m} \qquad , \quad (28)$$

$$\frac{a_{2m}}{2m!} = \left(\frac{3 \bar{\rho}_z D_2 (\alpha Q - \beta S)(\sigma a_1)}{2 (D_0 + 3 \bar{\rho}_z^2 D_2) h u (2\pi)^{\frac{1}{2}} \sigma^3} \right) \frac{1}{\sqrt{2}} \frac{(-1)^m}{(m-1)! \, 4^{m-1}} \qquad (29)$$

We observe that the odd coefficients decay at the rate σ^{-2}, while the even coefficients decay at the faster rate σ^{-3}. Hence, sufficiently far downstream the concentration profile is determined by just the odd coefficients. Furthermore, from equation (28) we see that these coefficients depend only upon such bulk properties as the buoyant output. Thus, the shape of the asymptotic concentration profile is a general feature, and for a given flow situation the width scale varies as the square-root of the buoyancy output.

From equation (29) we see that for the even Hermite coefficients the influence of the detailed conditions close to the outfall are contained in the single factor (σa_1). Thus, to improve upon the asymptotic concentration profile it suffices to

determine this one extra piece of information. More crucially, it is the even n = 2 equation which determines the standard deviation of the plume:

$$\frac{d\sigma^2}{dt} = 2\left\{D_0 + 3\bar{\rho}_z^2 D_2\right\} - \frac{3\bar{\rho}_z D_2 (\beta S - \alpha Q)(\sigma a_1)}{\pi^{\frac{1}{2}} h u \ \sigma^3} + \bigcirc(\sigma^{-4}) \tag{30}$$

Thus, the asymptotic influence of the buoyancy upon the plume width is proportional to (σa_1). Hence, it is not possible to calculate σ^2 accurately without also calculating (σa_1). This is the motivation for the two-term approximation used in the main body of the paper. However, the range of validity of equations (23-26) used above is not necessarily restricted to asymptotically large distances downstream of the outfall.

For the temperature θ, the starting point for the calculations is equation (22) for the Hermite coefficients b_n. The pattern of calculations is as described above, the presence of the σ^{-2} terms being dealt with simply by noting that $d\sigma^2/dw^2$ asymptotes to a constant. The resulting asymptotic approximations to the Hermite coefficients are that

$$b_0 = 1 \ , \quad w b_1 = \text{constant} \ , \quad b_2 = 0 \ , \tag{31}$$

$$\frac{b_{2m+1}}{(2m+1)!} = \frac{N}{w\sigma} \frac{(2m - \mu^2)(-1)^{m+1}}{(m - \frac{1}{2})(1+\mu^2)^{3/2} \ m!} \left(\frac{\frac{1}{2}\mu^2}{1+\mu^2}\right)^m \ , \tag{32}$$

$$\frac{b_{2m}}{2m!} = \frac{N \ (-1)^m}{(m - \frac{3}{2})(m-1)! (1+\mu^2)^{5/2}} \left(\frac{\frac{1}{2}\mu^2}{1+\mu^2}\right)^{m-1} \times$$

$$\left\{\frac{(a_1 \sigma)}{\sigma^3}\left(2m - 1 - 2\mu^2\right) + \frac{(b_1 w)}{w^2 \sigma}\left(2m - 2 - 2\mu^2 + \mu^4\right)\right\} \tag{33}$$

$$\tag{34}$$

where $\mu = w/\sigma$, $N = \bar{\rho}_z D_2 (\alpha Q - \beta S) \Big/ (D_0 + \bar{\rho}_z^2 D_2) h u (2\pi)^{\frac{1}{2}}$.

The corresponding asymptotic approximation to the equation for the standard deviation of the temperature distribution is

$$\frac{dw^2}{dt} = 2\left\{D_0 + \bar{\rho}_z^2 D_2\right\} \qquad -$$

174

$$- \frac{8 \bar{\rho_z} D_2 (\beta S - \alpha Q)}{(2\pi)^{\frac{1}{2}} h u (w^2 + \sigma^2)^{3/2}} \left[(2\sigma^2 - w^2)(w b_1) + (2w^2 - \sigma^2)(\sigma a_1) \right] \quad (35)$$

Arguing as above, we assert that it is not possible to calculate accurately the standard deviation w of the temperature distribution without also calculating the centroid position ($w b_1$) and the standard deviation and centroid of the density perturbation. Hence the need for the four equations (23-26) to give a quantitative mathematical description of the effects of salt upon the lateral dispersion of hot water.

REFERENCES

1. J.W. Talbot and G.A. Talbot "Diffusion in shallow seas and in English coastal and estuarine waters". Rapport. P.-v. Reunion,Conseil international pour l'Exploration de la Mer 167 (1974) 93-110.

2. G.I. Taylor. "Diffusion by continuous movements". Proc. Lond. Math. Soc. Ser. 2. 20 (1921) 196-212.

3. G.I. Taylor. "Dispersion of soluble matter in solvent flowing slowly through a tube". Proceedings of the Royal Society A 219 (1953) 186-203.

4. G.I. Taylor. "The dispersion of matter in turbulent flow through a pipe". Proceedings of the Royal Society A 223 (1954) 446-468.

5. H. Liu. "Predicting dispersion coefficient of streams". J. Environ. Eng. Div. A.S.C.E. 103 (1977) 59-69.

6. H.B. Fischer. "The mechanics of dispersion in natural streams." J. Hyraul. Div. A.S.C.E. 93 (1967) 187-216.

7. J.W. Elder. "The dispersion of marked fluid in turbulent shear flow." J. Fluid Mech. 5 (1959) 544-560.

8. G.C.C. Parker. "Study of factors affecting sea water temperatures at Sizewell power station - An appraisal of the 1975 Sizewell hydrographic survey data." C.E.G.B. report: GDCD (1977).

9. E.A. Prych. "Effects of density differences on lateral mixing in open channel flows." Keck. Laboratory of Hydraulics and Water Resources, California Institute of Technology Report KH-R-21 (1970).

10. R. Smith "Longitudinal dispersion of a buoyant contaminant in a shallow channel." J. Fluid Mech. <u>78</u> (1976) 677-689.

11. M.E. Erdogan and P.C. Chatwin. "The effects of curvature and buoyancy on the laminar dispersion of solute in a horizontal tube." J. Fluid Mech. <u>29</u> (1967) 465-484.

12. R. Smith "Asymptotic solutions of the Erdogan-Chatwin equation." J. Fluid Mech. <u>88</u> (1978) 323-337.

13. H.B. Fischer. "Longitudinal dispersion and turbulent mixing in open channel flow." Ann. Rev. Fluid Mech. <u>5</u> (1973) 59-78.

14. J.S. Turner. <u>Buoyancy Effects in Fluids</u>. Cambridge University Press (1973).

15. R. Smith "Effect of salt upon hot-water dispersion in well-mixed estuaries. Part 1. Longitudinal dispersion." Estuarine and Coastal Marine Science <u>6</u> (1978).

16. S.M. Sumer "Transverse dispersion in partially stratified tidal flow." Hydraulic Engineering Laboratory, California Berkeley, Report WHM-20 (1976).
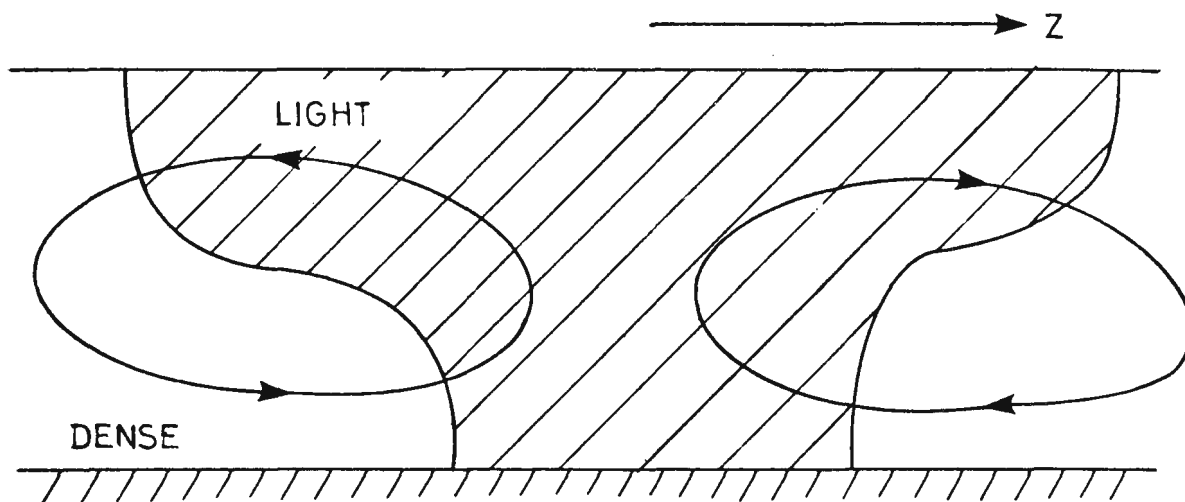
Figure 1. Cross section illustrating the secondary flow.
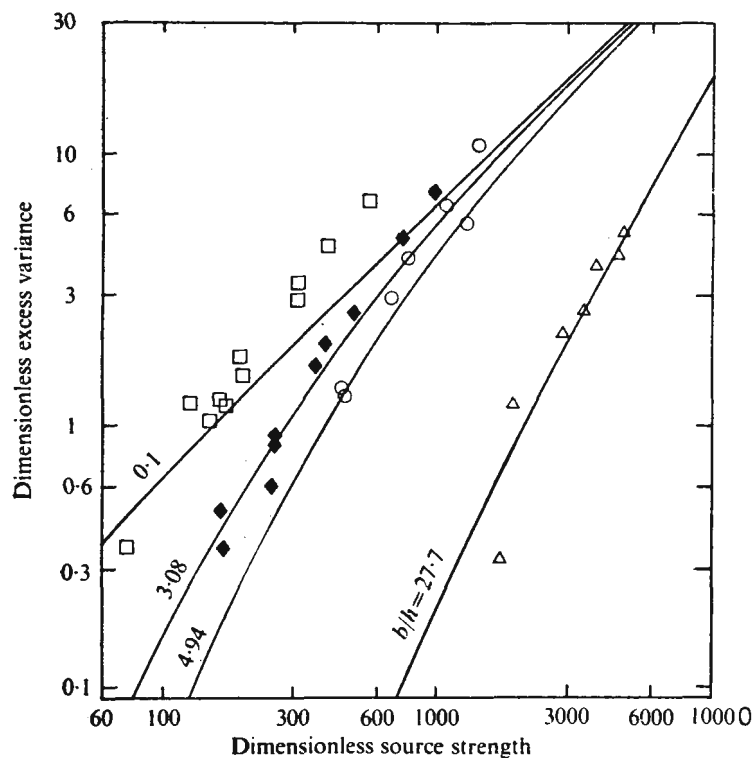
Figure 2. Comparison between Smith's [12] theory and Prych's [9] experimental results for the excess variance due to buoyancy as a function of the strength and width of the source.
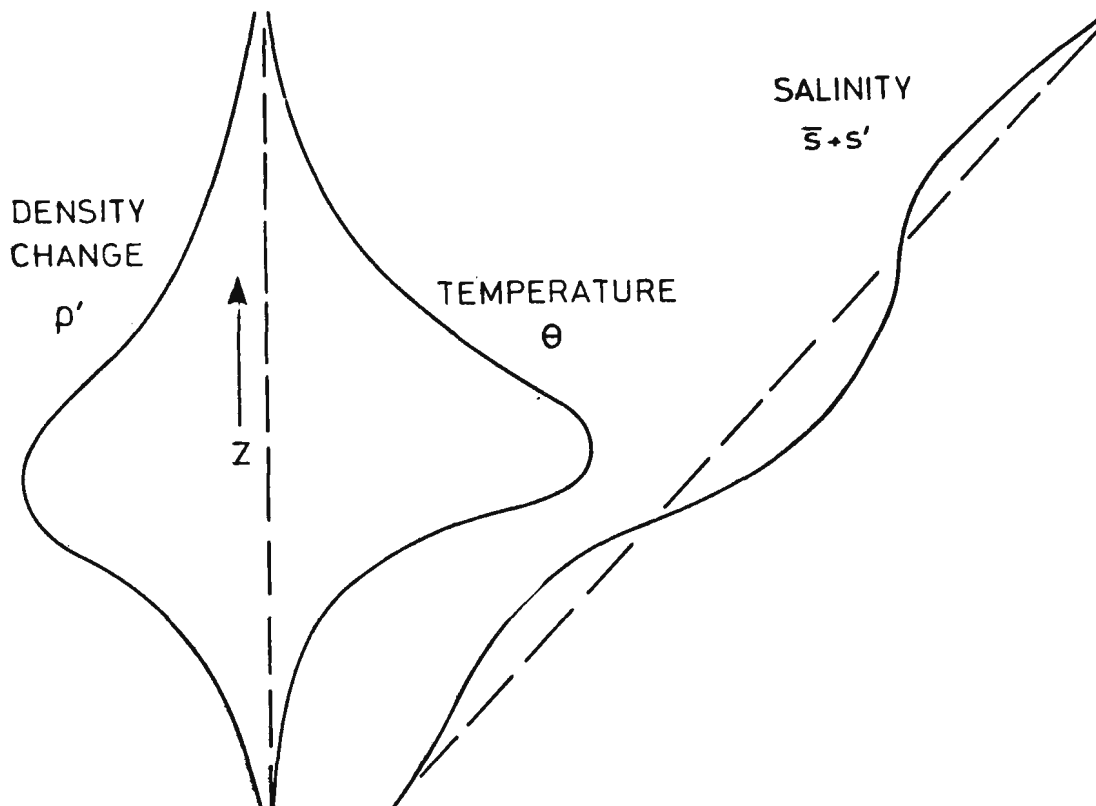
Figure 3. Distributions of salinity, temperature and density anomaly across a hot-water plume in an estuary.
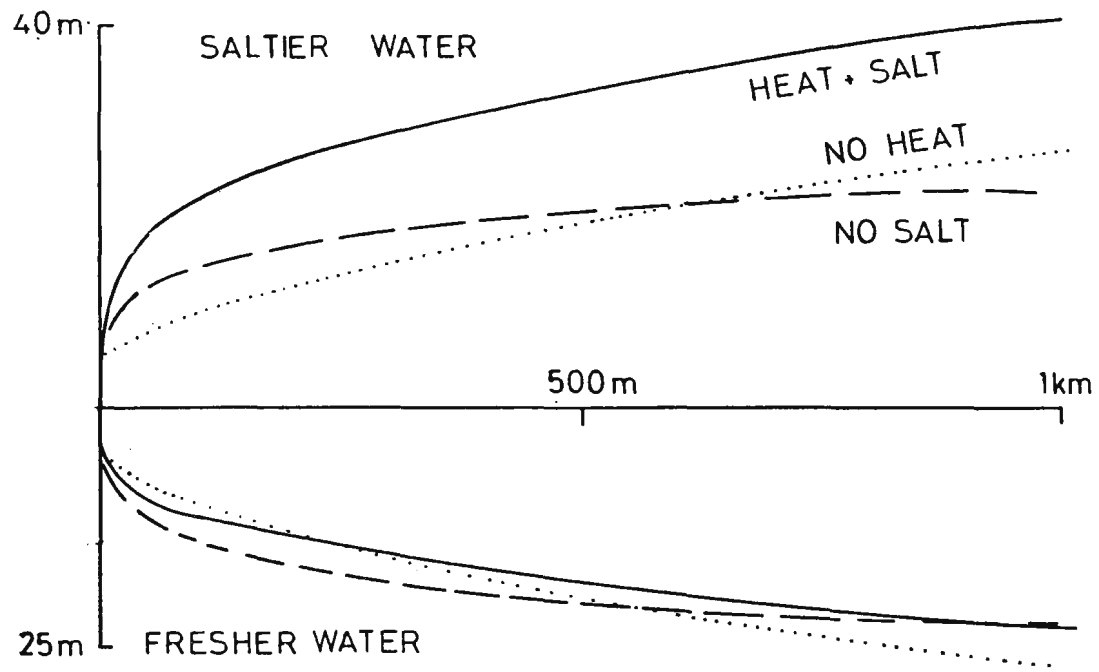
Figure 4. Plume shapes for a hot-water discharge in an estuary.

COST-EFFECTIVE MATHEMATICAL MODELING FOR THE ASSESSMENT

OF HYDRODYNAMIC AND THERMAL IMPACT OF POWER PLANT

OPERATIONS ON CONTROLLED-FLOW RESERVOIRS[1,2]

A. H. Eraslan[3,4] and K. H. Kim[5]

The University of Tennessee
and
Oak Ridge National Laboratory[4]

The operation of a large power plant can substantially alter the natural hydrodynamic and thermal conditions in a controlled-flow reservoir depending on the reversing flow conditions, and the condenser flow rate and the condenser temperature rise of the cooling water system. The realistic assessment of the thermal impact usually requires long-term (days) real-time simulations of the hydrodynamic and thermal enditions in the reservoir. The direct applications of the transient, multi-dimensional, coupled hydrodynamic and thermal mathematical models (without exception) require large amounts of computer time (dictated by the computational stability requirements of the hydrodynamic solution) in order to be able to produce results with acceptable quality of resolution in sufficiently large regions. In the licensing of a proposed power plant, the assessment of its potential thermal impact is usually based on analyses which must consider a multitude of scenarios for natural and plant operational conditions. Hence, from computer cost considerations, the repetative applications of the multi-dimensional, coupled, hydrodynamic and thermal models generally become extremely costly (usually prohibitive) for simulating the required number of different scenarios in the assessment of the thermal impact.

An alternate approach to the assessment of the thermal impact of power plant operations on controlled-flow reservoirs is to employ the recently-developed zone-matching methodology [1] based on the systematic applications of different transient, multi-dimensional, discrete-element hydrodynamic and thermal transport models [2-9]. The application of the

zone-mathcing methodology enables the implementation of the complex multi-dimensional hydrodynamic models only as needed and only for relatively short periods of real-time simulations of the necessary general class of flow conditions. The results of the hydrodynamic simulations can be used as the flow input data to the transient, multi-dimensional discrete-element thermal transport models for the necessary long-term (days) simulations of the temperature conditions in controlled-flow reservoirs.

The systematic zone-matching methodology was applied to the assessement of the hydrodynamic and thermal impact of the operation of a typical power plant (Peach Bottom Atomic Power Station) [10] on a typical controlled-flow reservoir (Conowingo Reservoir) [10] where the flow conditions in the particular section of the Susquehana River are controlled by the upstream and downstream hydro-electric power plants (at the Holtwood and Conowingo dams, respectively) and by the intermitantly operating pump-storage facility (Muddy Run).

The transient, one-dimensional, discrete-element hydrodynamic and thermal transport model (ESTONE) [2, 3] was applied to simulate 27 days of continuous flow and temperature conditions in the reservoir during the period 25 June 1974 - 21 July 1974. The results of the computer simulations and the field-measured data indicated excellent agreement during the period of the simulations (see Fig. 1).

The two-dimensional simulations of the quasi-steady, plant-induced flow conditions were obtained by the applications of the fast-transinet, two-dimensional hydrodynamic model (SLOFLO) [4, 5] as shown in Fig. 2. The dam-controlled and pump-storage-controlled natural flow conditions in the reservoir were simulated for relatively short periods (24 hrs) by the application of the fast-transient, two-dimensional, multi-layer discrete-element hydrodynamic model (HYDRO3) [6, 7]. The results of the two- and three-dimensional hydrodynamic simulations for the short periods (24 hrs) were extended, by the applications of the zone-matching methodology and the results of the one-dimensional hydrodynamic simulations to construct the necessary approximate flow fields for the long-term (10 days) termperature simulations with the fast-transient, two-dimensional (including vertical variations) discrete-element thermal transport model (TEMPER) [8, 9] as shown in Fig. 3. The results of the computer predictions for the two-dimensional multi-layer distributions of temperature conditions (depth-averaged, surface and bottom) agreed very well with the available field-measured data (within the limitations of the accuracy of the measurements) throughout the 10-day period of the simulations (see Fig. 4).

The results of the study concluded that the application of the zone-matching methodology is significantly more efficient in computer time and cost than the applications of transient, multi-dimensional coupled hydrodynamic and thermal transport models for repetative long-term simulations of the hydrodynamic and temperature conditions that are usually needed for the assessment of the thermal impact of power plant operations on controlled flow reservoirs.

REFERENCES

1. A.H. Eraslan, W.L. Lin, and K.H. Kim, "A Systematic Near-Field/Far-Field Zone-Matching Methodology Based on Uniformly-Valid Singular Perturbation Theory for Generating Complete, Two-Dimensional Natural and Plant-Induced Unstratified Flow Conditions in Lakes, Estuaries, and Coastal Regions" ORNL/NUREG-41, (in press).

2. A.H. Eraslan and K.H. Kim, "A Fast-Transient, One-Dimensional, Discrete-Element Transport Model for Predicting Hydrodynamic, Thermal and Salinity Conditions in Controlled Rivers and Tidal Estuaries for the Assessment of the Impact of Multiple Power Plant Operations" ORNL/NUREG-21, (in press).

3. A.H. Eraslan, K.H. Kim, S.K. Fischer, R.D. Sharp, and M.R. Patterson, "ESTONE: A Computer Code for Simulating Fast-Transient, One-Dimensional Hydrodynamic, Thermal and Salinity Conditions in Controlled Rivers and Tidal Estuaries for the Assessment of the Impact of Multiple Power Plant Operations" ORNL/NUREG-22, (in press).

4. A.H. Eraslan and K.H. Kim, "A Transient, Two-Dimensional Approximate Hydrodynamic Model for Simulating Natural and Plant-Induced Flow Conditions in Lakes, Estuaries, and Coastal Regions" ORNL/NUREG-42, (in press).

5. A.H. Eraslan, K.H. Kim and A.K. Atakan, "SLOFLO: A Computer Code for Approximate Simulations of Transient, Two-Dimensional Natural and Plant-Induced Flow Conditions in Lakes, Estuaries, and Coastal Regions" ORNL/NUREG-43, (in press).

6. A.H. Eraslan, W.L. Lin and K.H. Kim, "A Fast-Transient, Two-Dimensional, Multi-Layer Discrete-Element Hydrodynamic Model for Predicting Flow Conditions in Estuaries, Lakes, and Coastal Regions" USDI Report (in press).

7. A.H. Eraslan, W.L. Lin and K.H. Kim, "HYDRO3: A Computer Code for Simulating Fast-Transient, Two-Dimensional, Multi-Layer Flow Conditions in Estuaries, Lakes, and Coastal Regions" USDI Report (in press).

8. A.H. Eraslan and K.H. Kim, "A Fast-Transient, Two-Dimensional, Discrete-Element Thermal Transport Model for Predicting Temperature Distributions in Lakes, Estuaries and Coastal Regions for the Assessment

of the Thermal Impact of Power Plant Operations" ORNL/NUREG-23, (in press).

9. A.H. Eraslan, K.H. Kim, S.K. Fischer, R.D. Sharp and M.R. Patterson, "TEMPER: A Computer Code for Simulating Fast-Transient Two-Dimensional Temperature Distributions in Lakes, Estuaries and Coastal Regions for the Assessment of the Thermal Impact of Power Plant Operations" ORNL/NUREG-24, (in press).

10. A.H. Eraslan and K.H. Kim, "A Comprehensive Mathematical Modeling and Computer Simulation Study of the Hydrodynamic and Thermal Conditions in the Conowingo Reservoir and Comparisons of the Results with Field-Measured Data in the Vicinity of the Peach Bottom Atomic Power Station" ORNL/NUREG-TM-32, (in press).
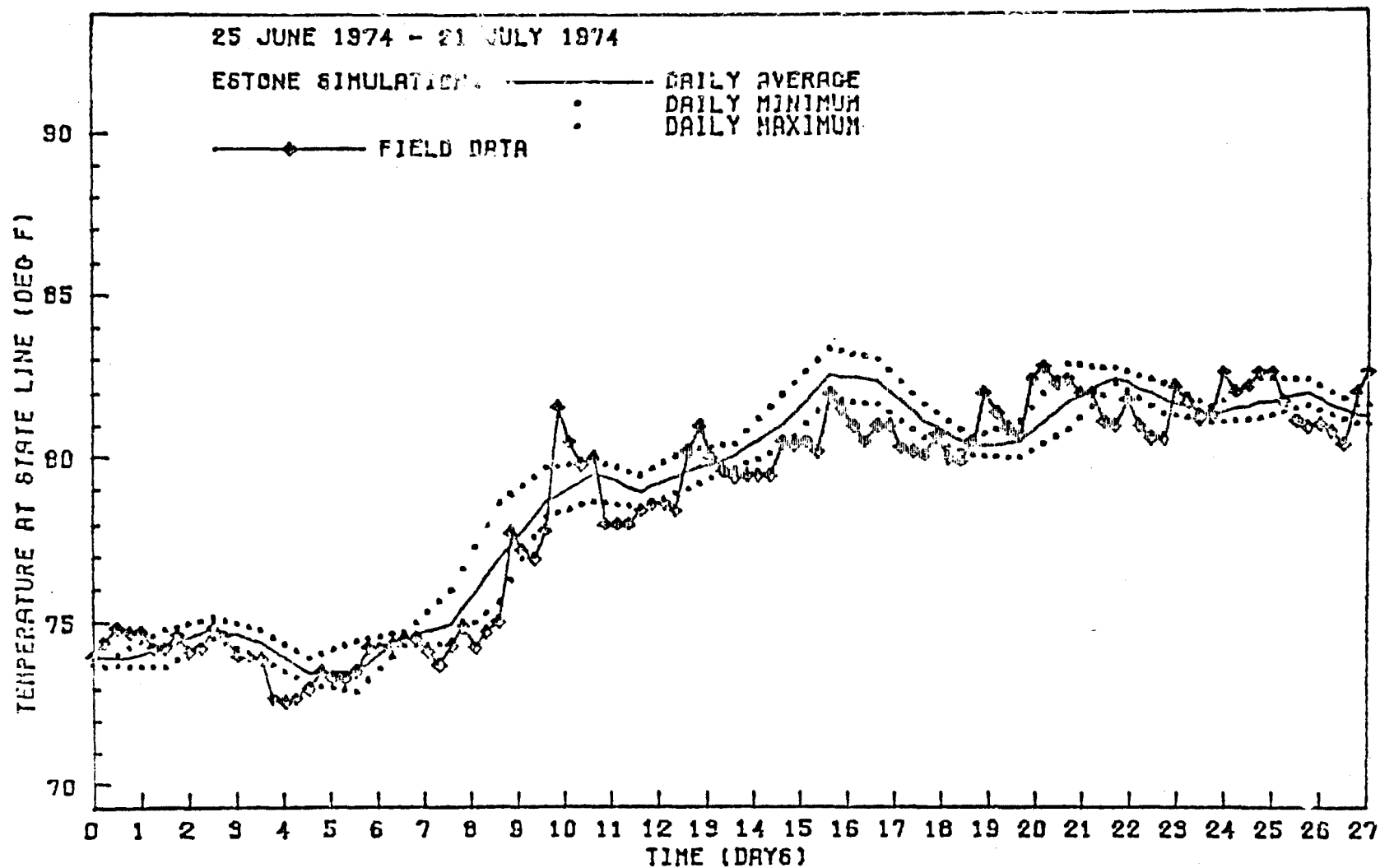
Fig. 1. Comparison of Computer Simulation Results and Field-Measured Data for Temperature Conditions at the State Line in the Conowingo Reservoir during 25 June 1974 - 21 July 1974.
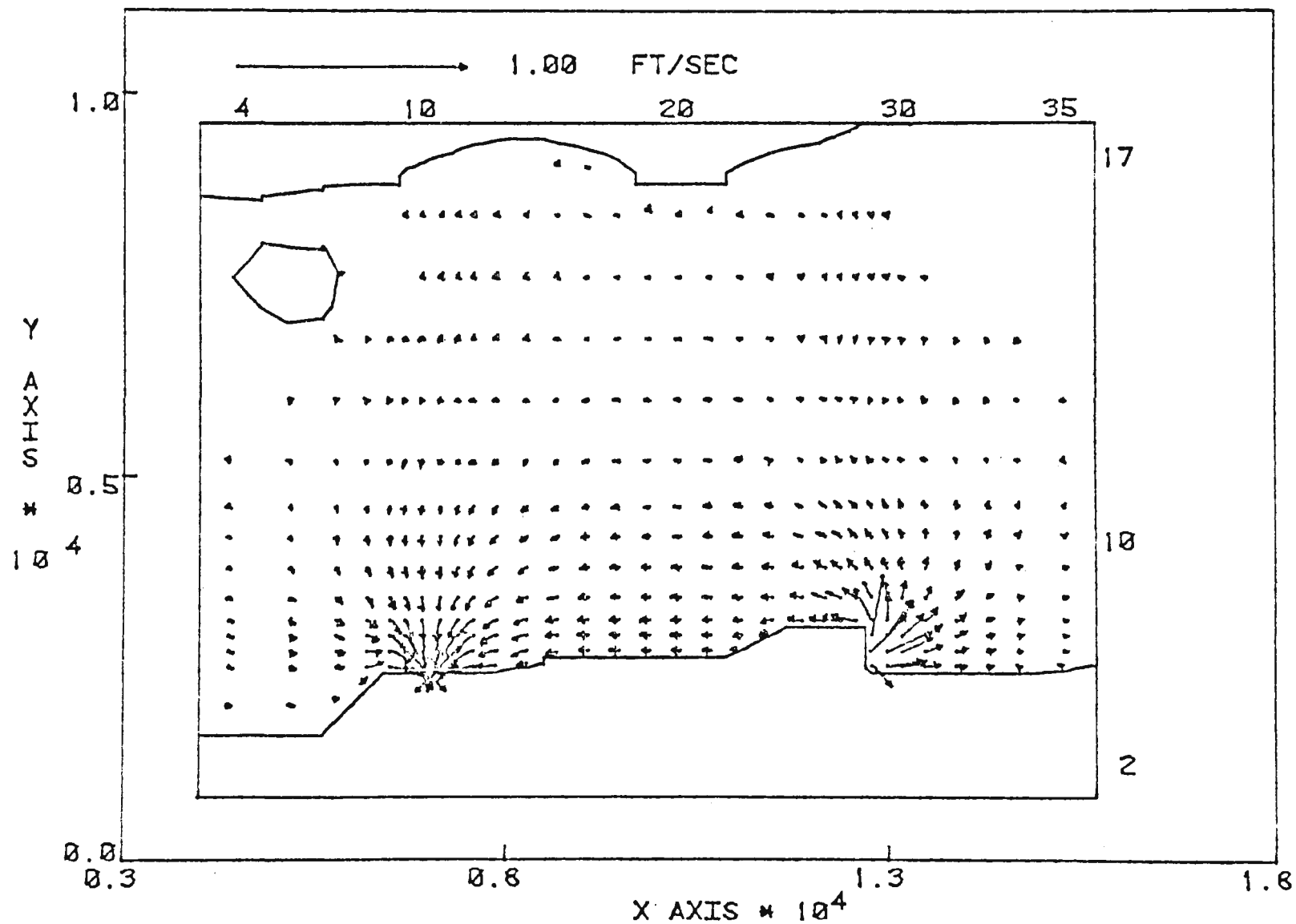
Fig. 2. Two-dimensional computer simulation results of the plant-induced flow conditions in the Conowingo Reservoir in the vicinity of Peach Bottom Atomic Power Station (exploded view of the sub-region in the vicinity of the power plant).
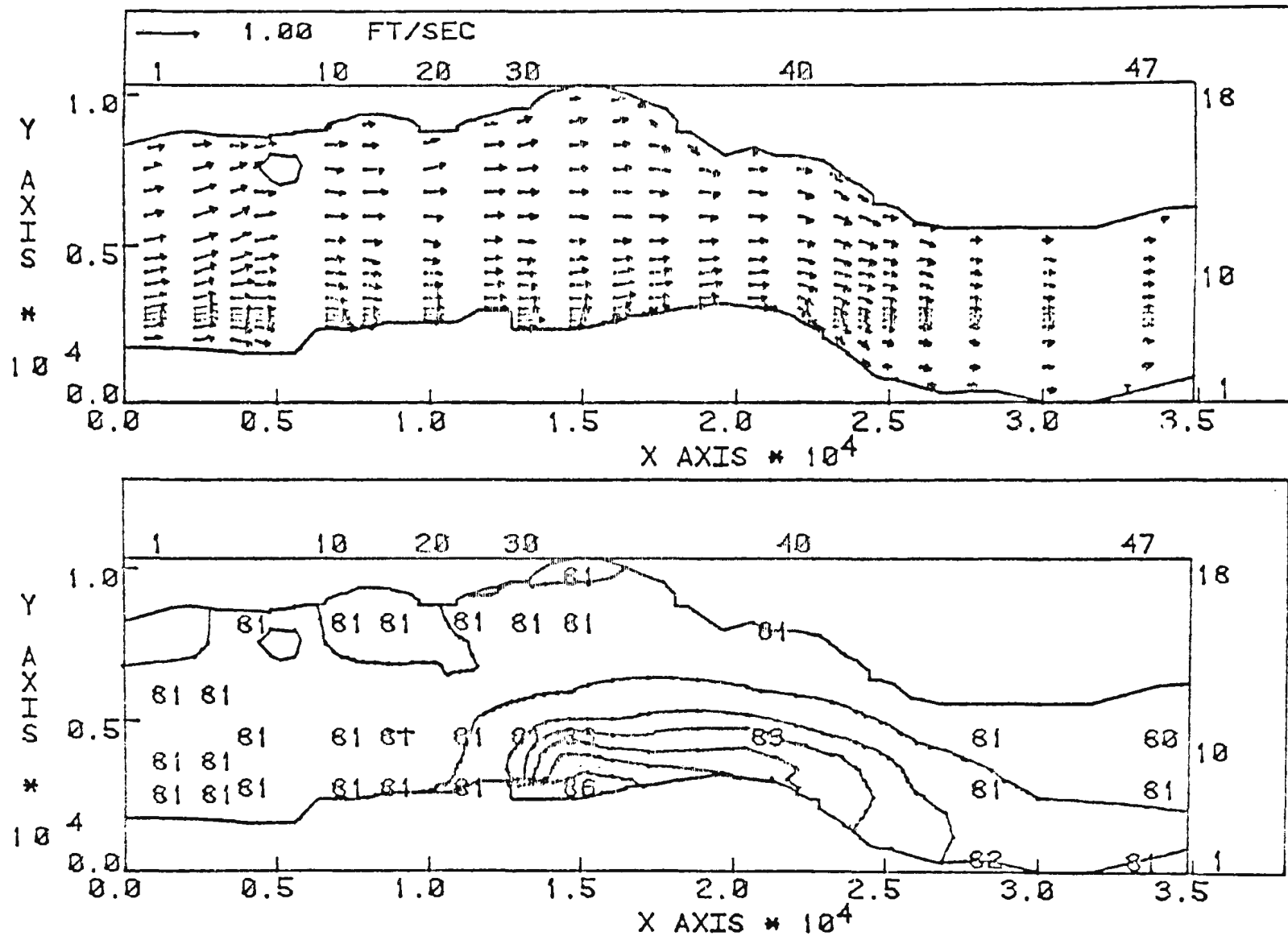
Fig. 3. Two-dimensional computer simulations (with self-similar vertical variations) of the velocity and temperature conditions in the Conowingo Reservoir in the vicinity of Peach Bottom Atomic Power Station at 11:00 hr on 15 July 1974.
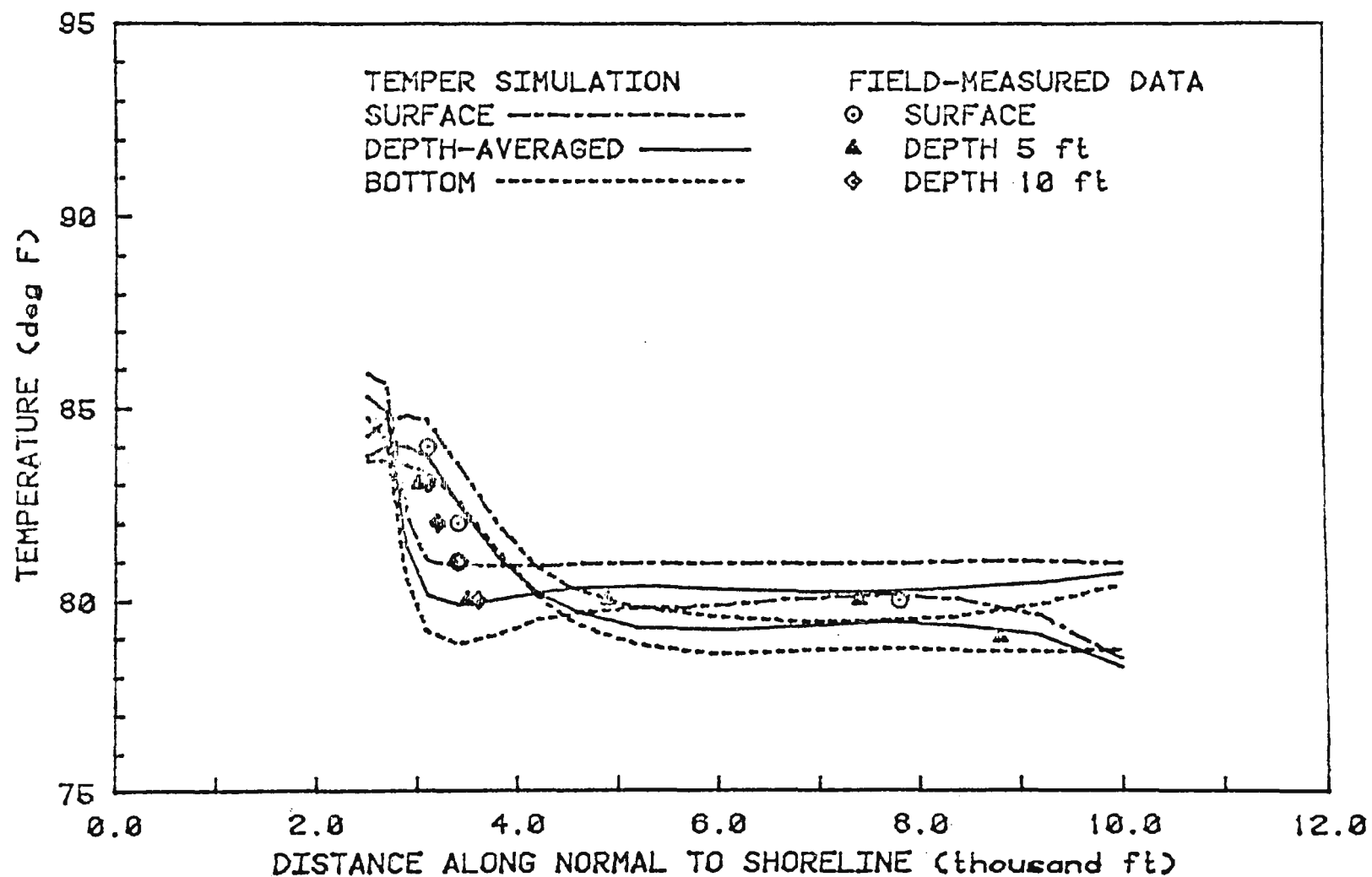
Fig. 4. Comparison of Computer Simulation Results and Field-Measured Data for Temperature Conditions along a Line Normal to the Shoreline at 1200 ft Downstream of the Discharge of Peach Bottom Atomic Power Station in the Conowingo Reservoir at 12:00 hr on 18 July 1974.

HEAT LOAD IMPACTS ON DISSOLVED OXYGEN:
A CASE STUDY IN STREAM MODELING

A.K. Deb, Ph.D., P.E. and D.F. Lakatos
Weston Environmental Consultants-Designers
West Chester, Pennsylvania, U.S.A.

ABSTRACT

The impacts of heat loads from a power generating station on the receiving waters are two fold: 1) raise the temperature, and 2) depress the dissolved oxygen of the receiving water. Both parameters are sensitive to the biological life of the receiving waters.

The objective of this study is to find the impact of heat loads from Picway Generating Station of Columbus and Southern Ohio Electric Company on the dissolved oxygen and temperature of the Scioto River. The study was primarily comprised of two parts: 1) temperature prediction using the one-dimensional COLHEAT computer model; and 2) dissolved oxygen analysis of temperature effects using the QUAL II model. A linear relationship of changes in ΔT was obtained.

INTRODUCTION

The Picway Generating Station, located on the east bank of the Scioto River approximately 10 miles south of Columbus, Ohio, has three coal-fired generating units, all of which use once-through cooling. Two of the units, numbers 3 and 4, rated at 30 MWe each, are scheduled to be removed from service in 1980. Unit 5 is a cycling unit rated at 100 MWe. The Scioto River is the source of cooling water for unit 5. The maximum withdrawal of water is 156 cfs.

The Scioto River is grossly polluted for a distance of 40 to 50 miles by sewage treatment plant effluents entering the river upstream of the Picway Station. This study was conducted for a 316(a) demonstration analysis for unit 5 and included existing and predicted temperature and dissolved oxygen (DO) distributions under low-flow conditions in the Scioto River.

The thermal effluent from the Picway Generating Station raises water temperature in the Scioto River, and there is considerable concern about the impact of this heat load on biological life and dissolved oxygen levels in the river, particularly in view of the relatively poor overall quality of the river water. Two large municipal wastewater treatment plants, the Jackson Pike STP and the Southerly STP, which are upstream of the Picway Station (see Figure 1), will decrease their monthly average effluent BOD concentration to 8 mg/L in 1981 or 1982. The Waste Load Allocation Report

(WLAR) for the Scioto River includes a statement to the effect that the reduction of these loads will significantly improve the water quality of a 40- to 50-mile stretch of river below Columbus. The Picway Station is located approximately 10 miles downstream of the Jackson Pike STP and 1.4 miles downstream of the Southerly STP. It is of concern that the projected improvement in dissolved oxygen levels in this stretch of the Scioto River resulting from the reduction in BOD load may be compromised by the heat load from the Picway Station.

This study was conducted to identify and evaluate the impacts of higher river temperatures on the biological life and dissolved oxygen levels in the stream below the Picway Station. Since conditions of low river flow and high heat load are infrequent and thus cannot readily be measured in the field, use of predictive mathematical models has been recommended.

This study was conducted in two phases: 1) temperature prediction in the downstream side of the Scioto River; and 2) dissolved oxygen prediction in the Scioto River in the upstream and downstream sides of the power plant. It was intended that the results of the first phase modeling study, i.e., the predicted temperatures under low river flow and high-heat load conditions, will be used in the second phase to predict the depression of dissolved oxygen as a result of these heat loads.

THERMAL MODELING

The model to be used for the thermal modeling study was to effectively simulate the stream characteristics of the Scioto River as well as respond to various waste heat loadings, river flows, and atmospheric conditions.

During low-flow conditions, the Picway Station discharges a heat load which occupies the entire width of the river and mixes completely (top to bottom and side to side) with the river water. Under these conditions, only one-dimensional models (which assume complete mixing) are appropriate.

The COLHEAT model, developed by the Hanford Engineering Development Laboratory, was used in this study to predict the mixed water temperature of the Scioto River downstream of the power plant.

COLHEAT Model

The COLHEAT River Simulation model is a far-field, one-dimensional model designed to simulate temperatures in the portions of the river in which complete mixing can be assumed.

The river is divided into various segments of fixed volume, through which water is transported. The water temperature is modified by the local atmospheric environment, which is introduced into the model by means of a heat budget. The advected heat, if any, in a particular segment is introduced and mixed completely with the river water of that segment. The

188

temperature rise of the mixed water of the segment caused by the introduction of advected heat and atmospheric heat exchange is calculated and assumed to be uniform throughout the whole segment. The model's routine provides temperatures at an upstream location and simulates the subsequent temperature changes at one or more downstream locations.

To evaluate the far-field temperature distribution due to thermal discharges into a stream, the following information is required as input to COLHEAT:

River dimensions, reduced to equivalent trapezoidal cross-sections.

Daily average water temperatures at the upstream end of the reach under study.

Daily river flows.

Meteorological data, including daily average values of wind velocity, air temperature, dew point, sky cover, and incoming short-wave radiation.

Daily advected heat discharge information.

Tributary flows and temperatures.

COLHEAT uses a heat budget to simulate the effect of the local atmospheric environment on the rate of heat exchange between the water body and the atmosphere. The process used in COLHEAT for heat exchange between air and water can be written as:

Net heat added = (net insolation) - (back radiation) - (evaporation) $\pm$ (conduction) + advection

Convergence of the Model

COLHEAT's transport mechanism uses the relative magnitude of the flow out of a river segment to determine the average water temperature. If the time step is not selected properly, the water from one river segment can travel through several segments in one time step. In selecting the time step and the length of each segment of the river, it is necessary to insure that the travel time of the water through each segment is greater than the time step used in the computation. This can be expressed as

$$\Delta t > \frac{\text{Min Vol}}{\text{Max Flow}} \tag{1}$$

Where:

Δt = Time step used in the model
Min Vol = Volume of smallest river section
Max Flow = Maximum of flow rate during period of simulation

189

If the convergence criterion set up in equation (1) is not satisfied, the numerical solution will not converge to the correct solution and could lead to instability in the computed temperatures.

Wind-Speed Function

In evaluating the surface heat exchange caused by evaporation and conduction, the COLHEAT model utilized the Lake Hefner wind-speed function. In their summary of the results of various studies on wind-speed function (as shown in Figure 2), Edinger, Brady, and Geyer [1, 2] indicated that the Lake Hefner wind-speed function equation underpredicts the wind-speed function by about 50 percent at low speeds and by about 30 percent at higher wind speeds. These underpredictions lead to an underprediction of heat transfer by evaporation, which in turn leads to an overestimation of summer temperatures and underestimation of winter temperatures. Figure 2 shows the considerable discrepancies among the various wind-speed function formulations.

Brady, Graves, and Geyer [3] in their study pointed out that if a water surface is warmer than its overlying atmosphere, "...the air adjacent to the water surface would tend to become both warmer and more moist than that above it, thereby becoming less dense. The resulting vertical convective air currents...might be expected to achieve much higher rates of heat and mass transfer from the water surface (even in the absence of wind) than would be possible by molecular diffusion alone."

They developed the following wind-speed function:

$$f(w) = 73.43 + 0.74 \ w^2, \quad \text{in } (\frac{Btu}{sq \ ft - hr - in \ Hg}) \quad (2)$$

$$w \quad = \text{Wind speed in mph}$$

In the Scioto River downstream of the Picway discharge, the water surface temperature under low-flow conditions in summer is high in relation to the air temperature. The average wind speed during July and August is about 2.6 mph. Under such conditions, there will be a considerable amount of evaporative loss as a result of convective air currents above the water surface, which is neglected in the Lake Hefner wind-speed function. Therefore, it would be more appropriate to use the wind-speed functions of Brady, et al.

In the present study the COLHEAT model was modified by replacing the Lake Hefner wind-speed function with that of Brady, et al., to calculate heat loss by evaporation and conduction. A duplicate set of computer runs, one with the Lake Hefner function and one with that of Brady, et al., shows that the Brady, et al., function results in lower absolute temperature and lower temperature rises (ΔT) (Figure 3).

The COLHEAT model was run to simulate the temperature rise of the Scioto River as a result of heat load under various low-flow and high-heat load

190

conditions. The results were used to predict the dissolved oxygen depression of the Scioto River downstream of the power station as a result of heat load.

DISSOLVED OXYGEN PREDICTION MODELING

The objective of the dissolved oxygen modeling study was to identify and evaluate the impacts of higher river temperatures on the dissolved oxygen levels in the stream below the Picway Station using mathematical modeling.

There are many models available for simulating dissolved oxygen in streams. The model which was selected for this study was to effectively simulate the dissolved oxygen characteristics of the Scioto River and be capable of responding to varying flows, wasteloads from sewage treatment plants, and heat loads from the Picway Station.

The QUAL II model was used in this study primarily because it has been applied and tested on many rivers throughout the United States and has performed reliably and accurately. It is a simple, steady-state, stream-quality-analysis computer model, and has been recognized by the U.S. Environmental Protection Agency (EPA) as being capable of predicting water quality (particularly dissolved oxygen) with a relatively high degree of accuracy.

The QUAL II model basically integrates the advection-dispersion mass-transport equation for all the water quality constituents to be modeled. This equation includes the effects of advection, dispersion, individual constituent changes, and sources and sinks.

The QUAL II model is very comprehensive and can simulate biochemical oxygen demand (BOD) and dissolved oxygen in streams, as well as the dynamic behavior of conservative minerals, nitrogen, and nine other parameters. The program determines the interactions of the nutrient cycle, algae production, benthic oxygen demand, and carbonaceous oxygen uptake, and their effects on the behavior of dissolved oxygen.

APPLICATION OF QUAL II TO THE SCIOTO RIVER

Adapting the QUAL II model to function as a predicting mechanism for water quality conditions in the Scioto River around the Picway Station required considerable acquisition and evaluation of data, and calibration of the model for a selected set of representative river conditions.

The scope of the data-acquisition effort in this study essentially was defined by the input data requirements of QUAL II:

Identification and description of the stream reaches involved.

Temperature profile of the stream reaches.

191

Headwater data.

Inflow data (freshwater and wastewater).

Coefficients and exponents for hydraulic equations relating river flow to the depth and linear velocity.

Various reaction coefficients for in-stream reactions.

Two very important input data items that must be identified to accurately apply QUAL II for this type of analysis are:

1. Temperature Profile of Stream - This is used in calibrating the model, and establishes the initial condition of the stream system being modeled. This data was available from sampling stations on the Scioto River, along with the results of the COLHEAT study previously discussed.

2. Model Coefficients - The particular coefficients of interest for the QUAL II model are the rate coefficients and the hydraulic coefficients and exponents. Data on hydraulic coefficients and exponents were derived from the C&SOE Thermal Discharge Study and from a stream survey conducted specifically for this study. However, certain limitations of the available data indicated the need for development of assumptions of conditions at various points where the data were missing. These assumptions, based on detailed information concerning flow-depth-velocity relationships at the U.S. Geological Survey stream-gauging stations (the upper and lower boundaries of the river stretch under study), were the basis for interpolated values for the intermediate reaches.

Initial values for rate coefficients for biochemical oxygen demand (BOD) and stream reaeration were based on generally-accepted values in the technical literature. During the calibration of the model, these coefficients were adjusted on successive runs to provide a better match of the simulated and measured data.

CALIBRATION OF THE MODEL

For calibration purposes, the QUAL II model was set up to simulate the 25-mile stretch of the Scioto River on a particular day for which detailed flow monitoring and water quality sampling and analyses were readily available. Since the critical condition for evaluating the impact of the generating station's heat load on dissolved oxygen is that of low river flow, the date selected from those available was one on which the river flow was comparatively low. The heat load from the Picway Station was introduced as input in the form of the temperature rise of the mixed water downstream, as

derived from the COLHEAT model results. The proper boundary and initial conditions were established by using the flow and quality data of the headwaters, and the temperature profile of the Scioto River throughout the study stretch.

During the calibration process, the rate coefficients for different reaches of the stream were adjusted (within accepted limits) to match the model-predicted dissolved oxygen values with the corresponding measured values.

Figure 4, a graphical summary of the calibration results, shows that the model-predicted dissolved oxygen values are generally somewhat lower than the corresponding measured values, but the differences are small. The coefficients used in the model were all within the scientifically acceptable limits, were internally consistent, and consequently it was felt that they could be used with confidence for accurate prediction of dissolved oxygen behavior.

MODEL APPLICATION

The stream characteristics (i.e., physical characteristics and model reaction coefficients) developed for calibration were used for dissolved oxygen simulations under several different stream-flow and heat-load conditions. Low flows, such as those which typically occur during the summer months, are critical to the dissolved oxygen regime. Therefore, four low-flow conditions were analyzed, and two heat-load situations were simulated. The first (with heat load added) was the historical seven-day peak load of the three generating units at the Picway Station. The second (without heat load added) represented the situation where the station was not in operation.

In developing the required input data for the modeling runs, values for initial temperature conditions in each study reach had to be determined. The flows selected for the model runs are those for which temperature predictions were generated by the COLHEAT model. The COLHEAT temperature predictions were therefore used in the QUAL II modeling runs.

DISCUSSION OF MODELING RESULTS

The results of the QUAL II model runs for the Scioto River in the vicinity of the Picway Station were presented in the form of plots of dissolved oxygen versus stream length. Examples of these plots for both the low- and high-flow runs are given in Figures 5 and 6. This type of plot was presented for all flow and heat load situations that were analyzed.

In these figures, two curves are plotted downstream of the Picway Station: the solid line shows dissolved oxygen when the Picway Station is operating, while the broken line represents dissolved oxygen without the Picway heat load. The difference in ordinate between these two curves represents the effect of the Picway heat load on dissolved oxygen, as determined by QUAL II.

The model-predicted dissolved oxygen plots show that under the lower flow conditions the dissolved oxygen concentration of a considerable length of the Scioto River below Columbus will be zero, and that the water quality of this segment will not improve very much with the projected reduction of wasteloads from the upstream sewage treatment plants. This lack of improvement is attributed to the fact that the entire river flow at low flow is essentially sewage effluent.

In order to find a relationship between the maximum temperature rise at the Picway discharge and the maximum reduction in dissolved oxygen accruing from the heat load, Figure 7 has been plotted from computer outputs of various runs. This figure illustrates the primary result of the QUAL II modeling study of the river, and shows a relationship indicating the anticipated change in the dissolved oxygen characteristics of the stream (at its most critical location) for a wide range of heat waste loads that could be introduced to that stream.

ACKNOWLEDGEMENTS

REFERENCES

1. Edinger, J.E., Brady, D.K. and Geyer, J.C. "Heat Exchange and Transport in the Environment," Electric Power Research Institute Report No. 12, 1974.

2. Edinger, J.E., Brady, D.K. and Geyer, J.C. "Heat Exchange and Transport in the Environment," Electric Power Research Institute Report No. 49, 1974.

3. Brady, D.K., Graves, W.L. and Geyer, J.C. "Surface Heat Exchange at Power Plant Cooling Lakes," Cooling Water Discharge Project Report No. 5, Edison Electric Institute, Publication No. 69-901, New York, 1969.
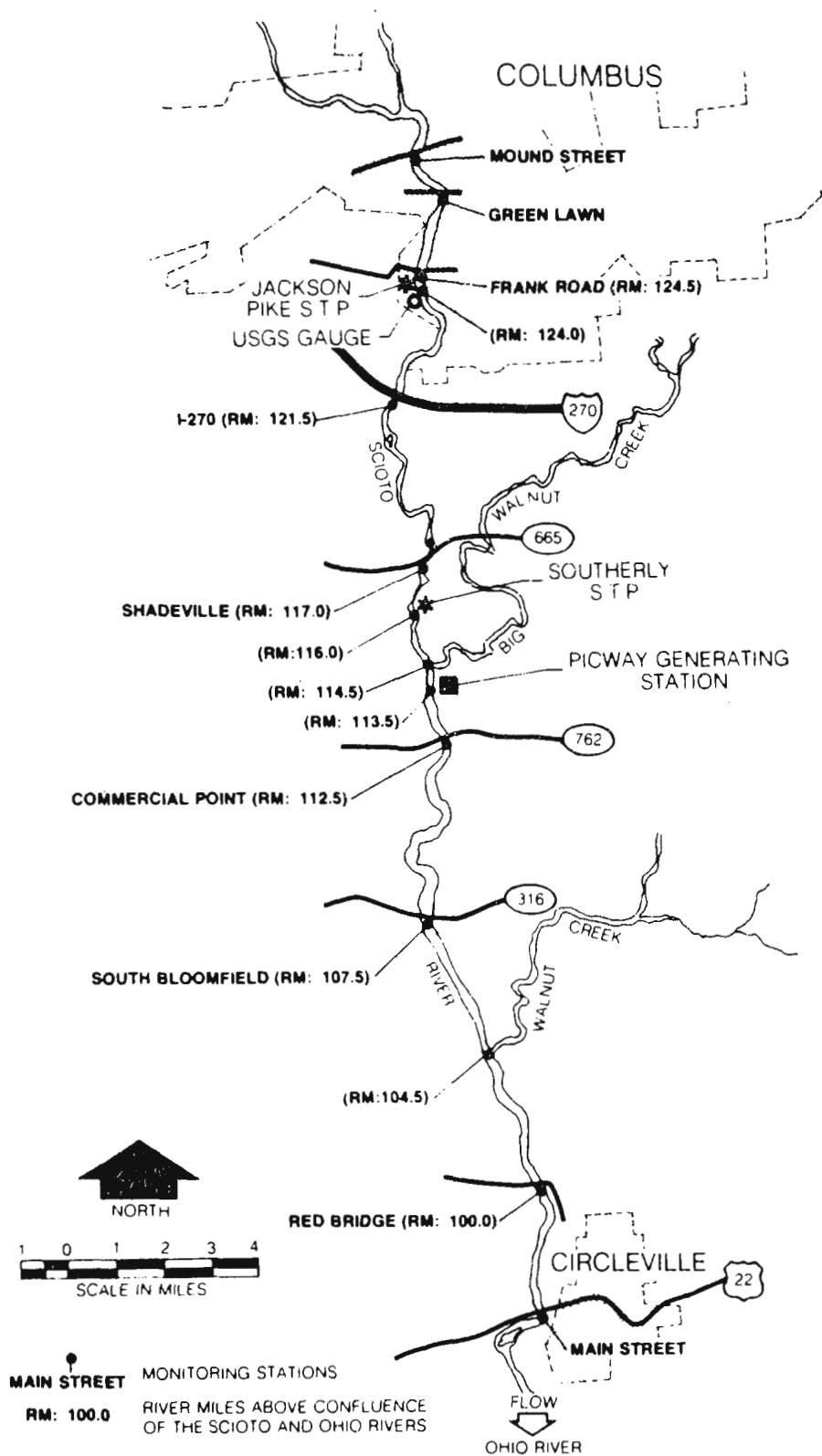
Figure 1   Schematic Diagram of the Scioto River System from Columbus, Ohio to Circleville, Ohio
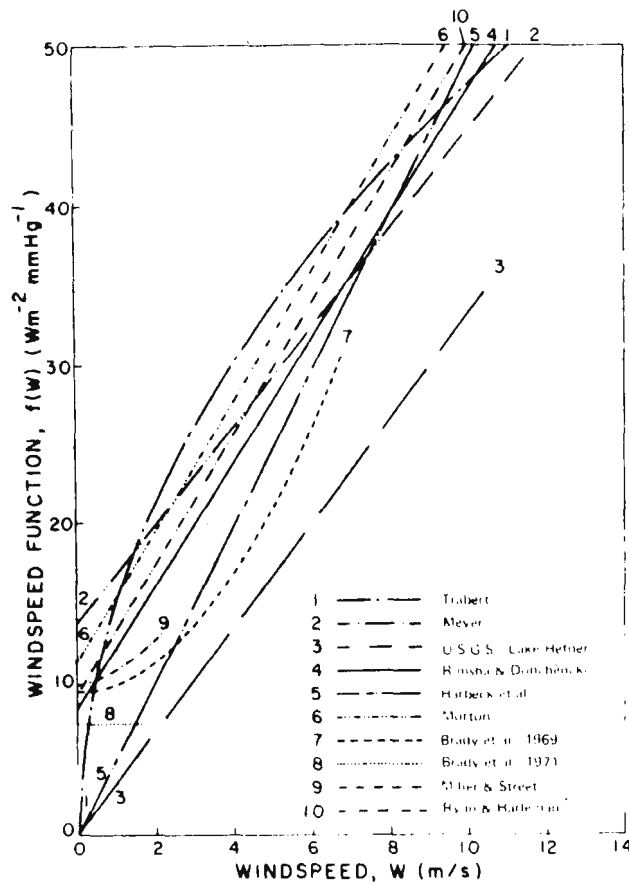
SOURCE: EDINGER, BRADY AND GEYER (1974)

**Figure 2   Comparison of Empirical Formulae for the Wind Speed
Function, from Edinger, Brady and Geyer, 1974**
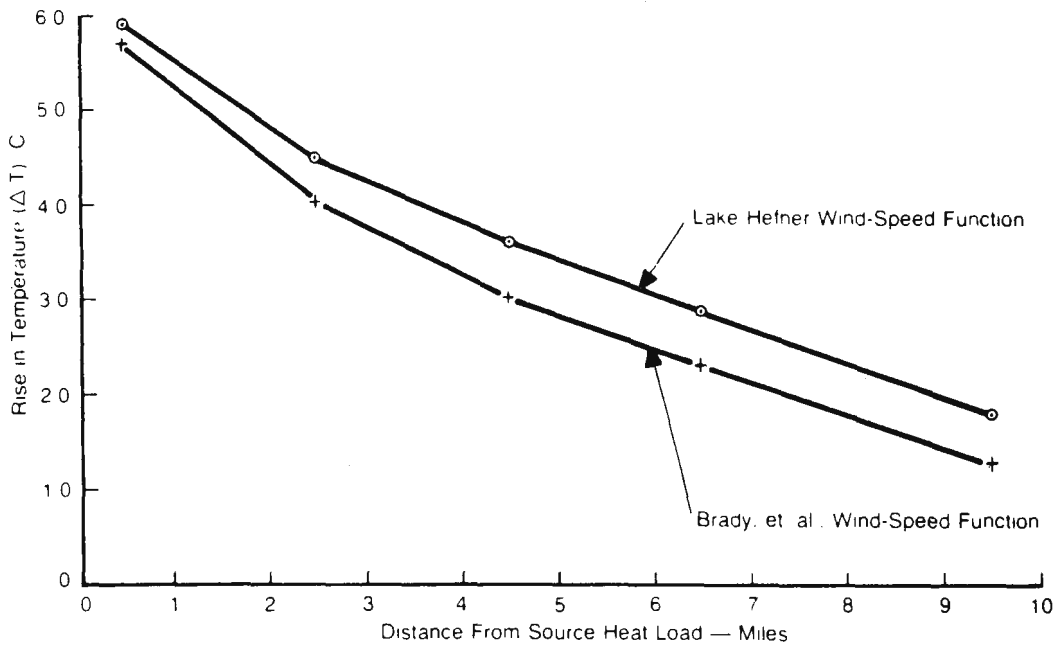
**Figure 3   COLHEAT Temperature Prediction at Low Flow (150 cfs)
with Unit 5 Operating at the Load Exceeded 10 Percent of
Time (80 MWe)**

196
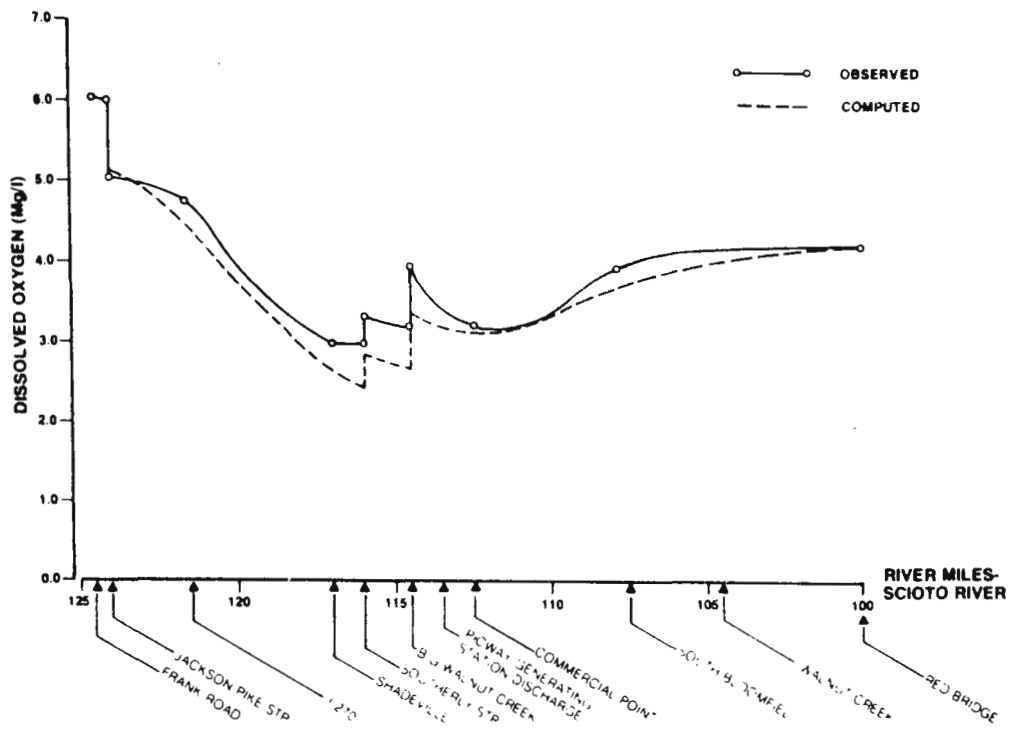
Figure 4   Results of Calibration of QUAL II Using 22 June 1977
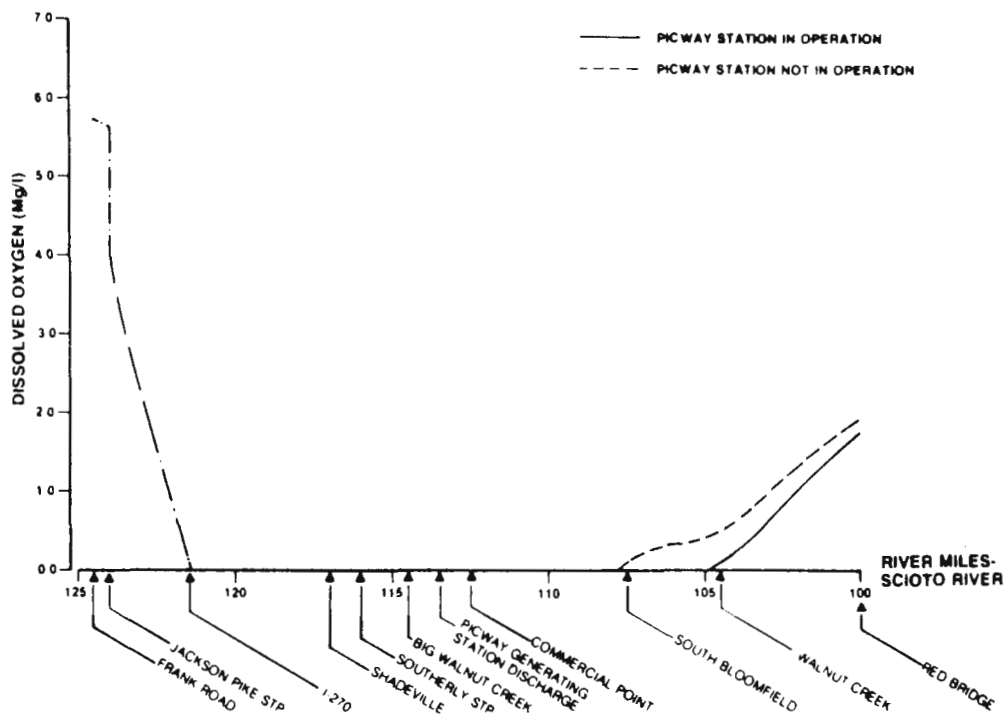
Figure 5   "Model" Prediction of Dissolved Oxygen in the Scioto River With a River Flow at the Picway Generating Station of 150 cfs and Existing Upstream Sewage Treatment Plant Loads

197
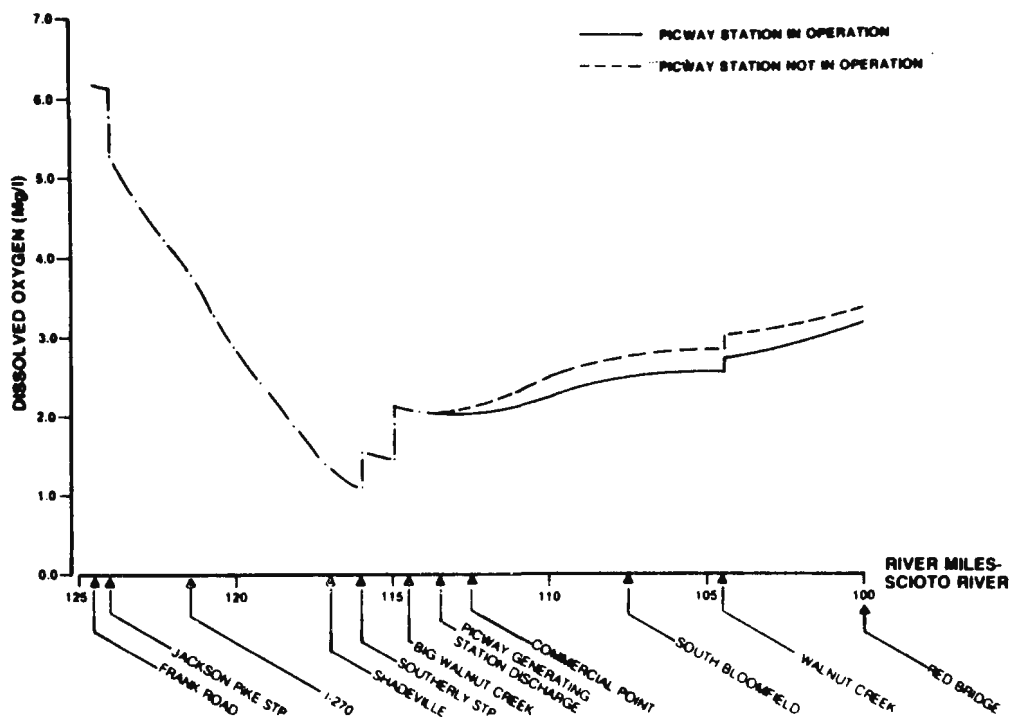
Figure 6   "Model" Prediction of Dissolved Oxygen in the Scioto
            River With a River Flow at the Picway Generating Station
            of 534 cfs and Existing Upstream Sewage Treatment
            Plant Loads
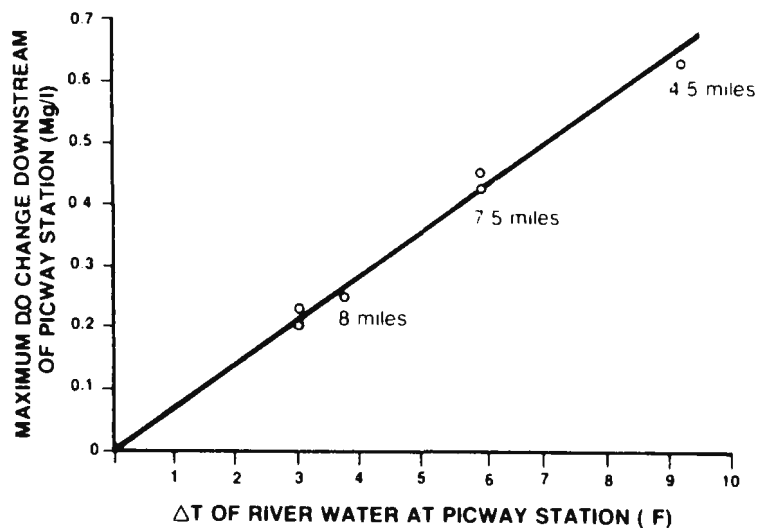
Figure 7   Sensitivity of Changes in Dissolved Oxygen to Changes
            in Temperature (Δ T) Downstream of the Picway
            Generating Station

A STOCHASTIC METHOD FOR PREDICTING THE
DISPERSION OF THERMAL EFFLUENTS IN THE ENVIRONMENT

Alan J. Witten
Energy Division
Oak Ridge National Laboratory*
Oak Ridge, Tennessee 37830

John E. Molyneux
University of Rochester
Rochester, New York 14627

A STOCHASTIC METHOD FOR PREDICTING THE DISPERSION OF THERMAL EFFLUENTS IN THE ENVIRONMENT

Alan J. Witten
ENERGY DIVISION

and

John E. Molyneux
UNIVERSITY OF ROCHESTER

ABSTRACT

The equation governing the distribution of waste heat in a receiving medium is the advective diffusion equation. Historically, this equation has been studied deterministically employing either analytical methods requiring unrealistic simplifications, or more realistic numerical schemes which are to costly for extended simulations. An attractive alternative method to deterministic techniques is the stochastic approach. Here the same advective diffusion equation is considered, however, one or more of the coefficients is assumed to be random. The appeal of the method is two-fold. First it provides a computationally efficient scheme for realistic long-term predictions by taking advantage of the reduced input data requirements, and second, it inherently has the capability to deal with accidental releases where ambient conditions are unknown.

This problem has been formulated in one-dimension with the advection velocity being a random function of time. If it is assumed that the time integral of this random velocity is gaussian, then all the excess temperature statistics can be expressed in terms of the mean flow and the autocorrelation of the random fluctuations. This assumption is not particularly restrictive, since it is imposed on the integral of the random variable, and is necessary to make the problem tractable. Using this method, general expressions for all the moments of the excess temperature have been derived. In addition, a number of closed-form special cases have been solved for the probability distribution.

Results to date have proved to be quite interesting. In particular this work demonstrates the nonlinear dependence of the excess temperature on the advective flow. Therefore, using a long-term averaged flow does not produce the same result as solving the transient problem and then averaging. In fact, if the rms velocity fluctuations are large, a simple solution using the mean flow could underestimate the excess temperature by a factor of two.

I. THE SHORT-TERM RELEASE

In this section, we model the short-term release of a passive contaminant into a river. This model has application to the problem of an accidental release or other situations in which the river flow is unknown. The model assumptions are listed below:

1. The short-term release of a contaminant is represented by an instantaneous discharge.

2. The receiving river has a constant cross-sectional area.

3. All quantities are averaged over river cross-section.

The mathematical formulation is now given by the initial value problem

$$\frac{\partial c}{\partial t} + u(t) \frac{\partial c}{\partial x} - \kappa \frac{\partial^2 c}{\partial x^2} = 0 \tag{1}$$

$$c(x = \pm \infty) = 0, \quad c(t = 0) = c_0 \, \delta(x) \ .$$

This equation can immediately be integrated

$$c(x,t) = \frac{C_0}{2\pi} \int_{-\infty}^{\infty} d\alpha \, e^{-\alpha^2 \kappa t - i\alpha[x - \int_0^t u(\tau)d\tau]} \tag{2}$$

however, this result is of little value since the river flow $u(t)$ is, by design, unknown. To extract information from equation (2) we let $u(t) = U_0 + u'(t)$ where u is the zero-mean random fluctuations. In equation (2), the river flow appears only as an integral over time. It, is therefore, appropriate to introduce a new stochastic function

$$\theta = \int_0^t u'(\tau)d\tau \ , \tag{3}$$

and introduce the final model assumption by allowing the statistics of θ to be Gaussian. This assumption is not particularly restrictive since it is imposed upon β rather than u It can be argued, by virtue of the Central Limit Theorem (Batchelor, 1953), that the statistics of u' are still quite general. With this assumption, equation (2) can be solved for all the one-point statistical moments of the concentration.

The first statistical moment is the mean and this can be written

$$c(x,t) \quad = \frac{c_o}{\sqrt{2\pi(2\kappa t + \langle\theta^2\rangle)}} e^{-(x-U_o t)^2/2(2\kappa t+\langle\theta^2\rangle)} \tag{4}$$

Comparing this to the non-random result

$$c(x,t) = \frac{c_o}{\sqrt{4\pi k t}} e^{-(x-U_o t)^2/4kt} \tag{5}$$

two conclusions can be made. First the random velocity fluctuations appear in the solution as an effective diffusivity $\kappa_{eff} = \frac{1}{2t}\langle\theta^2\rangle$ and second, using the time-averaged input data U_o does not produce the same result as using the transient input data $u(t)$ and then averaging. Through this result, the non-linear dependence of the concentration on the advecting flow is quite evident.

To present the higher order statistical moments, we introduce a change of variables which renders the results more compact. The new independent variables are

$$a = c_o/\sqrt{4\pi k t}$$

$$b = \langle\theta^2(t)\rangle /2kt \tag{6}$$

$$\xi = (x - U_o t) /\sqrt{4kt}$$

Here a is a relative magnitude of the concentration, b is the ratio of the effective diffusivity to the actual diffusivity and ξ is a nondimensional distance relative to the position of the mean advective front scaled by the diffusion length. Now the one-point Nth order statistical moment is given by

$$\langle c^N(x,t) \rangle = a^N (1 + Nb)^{-\frac{1}{2}} e^{-N\xi^2/(1 + Nb)} \tag{7}$$

The most useful result for predictive applications is the probability distribution. This distribution is related to the statistical moments by the equation

$$c^N \ (x,t) = \int_0^\infty c^N \ f_1(c;x,t) \ dc \ , \tag{8}$$

where f_1 is the probability distribution formally defined as Prob $\{c \leq c(x,t) < c + dc\}$. Equation (8) can be inverted to obtain an expression for f_1. This is

$$f_1(c; \ x,t) = c^{-1}[\pi b \ \ln(a/c)]^{-\frac{1}{2}} \ e^{- \ [\ln(a/c) \ + \ \xi^2]/b} \ \cosh \left\{ 2b^{-1} \xi[\ln(a/c)]^{\frac{1}{2}} \right\}$$

$$o < c < a \tag{9}$$

This equation is the principal result of this section.

This result is shown graphically in Figures 1 and 2. Figure 1 is a series of plots of the produce af_1 versus c/a for several values of the nondimensional position ξ. Moving away from the position of the mean advection front $\xi = 0$, the peak of the probability curve moves towards lower concentration while the curve becomes broader

and more symmetric. For increasing distances, the curve again becomes skewed as the peak approaches zero concentration. Although it was assumed that the stochastic function θ is Gaussian it is clear from this figure that the dependent variable c, the concentration, is not Gaussian. This further demonstrates the nonlinear relationship between the advecting flow and the concentration.

Figure 2 shows plots of the most probable concentration versus position for two values of the randomness parameter $b(t)$, along with a plot of the mean concentration versus position. This figure demonstrates the importance of higher order statistical moments by illustrating the inadequacy of the mean in characterizing the concentration field. For both values of b, the mean underpredicts the concentration for small distances and overpredicts the concentration for large distances.

A more complete discussion of this initial value problem is given in Molyneux and Witten (1979).

II. THE CONTINUOUS RELEASE

In this section, we model the continuous release of a passive contaminant into a river. This model can be applied to problems with unknown river flow. In addition, it is particularly useful for problems involving the long-term characterization of the contaminant concentration resulting from a continuously discharging source. In this case the time history of the flow may be specified, however, treated as an unknown for computational efficiency. Rather than solving the transient problem deterministically, a steady-state stochastic approach could provide the long-term concentration statistics

204

at a minimal cost. The model assumptions here are similar to the short-term release with the exception that the source is continuous with time and a delta function in space.

The model equation is

$$\frac{\partial c}{\partial t} + u(t) \ \frac{\partial c}{\partial x} - \kappa \ \frac{\partial^2 c}{\partial x^2} = S_0 \delta(x) \tag{10}$$

subject to the boundary and initial conditions

$$c(x = \pm\infty) = c(t = 0) = 0 \tag{11}$$

Again we take the advecting flow to be the sum of a mean plus zero mean random fluctuations given by

$$u(t) = U_0 + u'(t) \tag{12}$$

The solution to equation (10) subject to the specified conditions is

$$\tag{13}$$

$$c(x,t) = \frac{S_0}{2\pi} \int_{-\infty}^{\infty} d\alpha \int_0^{t} dt' \ e^{-\alpha^2 \kappa (t-t') \ + \ i\alpha [x - U_0 (t-t')] \ - i\alpha \int_{t'}^{t} u'(\tau) d\tau}$$

By defining a new random function·

$$\theta = \int_{t'}^{t} u'(\tau) dt \quad ,$$

the mean concentration can be written

$$\langle c(x,t) \rangle = \frac{S_o}{2\sqrt{\pi}} \int_0^t dt' \; [(\kappa + \kappa_e)(t - t')]^{-\frac{1}{2}} \; e^{-\frac{[x - U_o(t-t')]^2}{4(\kappa + \kappa_e)(t-t')}}$$ (14)

where the effective diffusivity κ_e can be written

$$\kappa_e = \frac{1}{2(t - t')} \langle \theta^2 \rangle = \frac{1}{2(t - t')} \langle \int\!\!\int_{t'}^{t} u'(\tau_1) u'(\tau_2) d\tau_1 d\tau_2 \rangle$$ (15)

The effective diffusivity defined above is time dependent. If θ is
assumed to be stationary, equation (15) asymtotically approaches

$$\kappa_e = \frac{1}{2} \langle u'^2 \rangle \tau_c$$ (16)

for large time, where τ_c is the correlation time. This is the result
obtained by Taylor (1954) for turbulent longitudinal dispersion in
pipes. Although the effective diffusivity becomes a constant for large
time, as given by equation (16), it is clear from equation (14) that
the mean concentration is a function of the time-history of the advective
diffusion process and, therefore, the transient behavior of κ_e cannot
be ignored even in steady-state applications.

Higher order one-point statistical moments have been derived from
equation (13). The nth order moment in nondimensional form is

$$\langle \overline{c}^n(\overline{x}, \overline{t}) \rangle = \left(\frac{P}{2\pi}\right)^{\frac{n}{2}} \int_0^{\overline{t}} d\eta_1 ... \int_0^{\overline{t}} d\eta_n [\det (D + \Theta)]^{-\frac{1}{2}} e^{-\frac{P}{2} Y^T (D+\Theta)^{-1} Y}$$ (17)

206

where the vectors, matrices, and functions in this equation are defined by

$$Y = [\ \bar{x} - n_1,\ \bar{x} - n_2, \ldots,\ \bar{x} - n_n]^T - \text{Distance} \qquad (18)$$

$$D_{ij} = 2n_i \delta_{ij} - \text{Diffusion}$$

$$\theta_{ij} = P_r \int_{n_i}^{\bar{t}} d\bar{\tau}_1 \int_{n_j}^{\dot{\bar{t}}} \cdot d\bar{\tau}_2\ R(\bar{\tau}_1 - \bar{\tau}_2) - \text{Random advection}$$

$$P = \frac{U_0^2 \tau_c}{\kappa} - \text{Non-random Peclet No.}$$

$$P_r \quad \frac{\langle u'^2 \rangle \tau_c}{\kappa} - \text{Random Peclet No.}$$

$$R(\bar{\tau}) - \text{Autocorrelation function for } u'(\tau)$$

Equation (17) has minimal computational value since the numerical determination of the nth order moment requires the inversion of an n x n matrix and then an n-fold numerical integration. However, by virtue of the fact that the nonrandom Peclet No. P is large for most environmental applications, the integrand of equation (17) can be asymptotically represented and n–1 integrals can be evaluated analytically, without loss of accuracy. Now the determination of any one-point statistical moment has been reduced to a single numerical integration and the formula for the nth moment is given by

$$\langle \overline{c^n(x,t)} \rangle = \qquad (19)$$

$$\frac{1}{2} \sqrt{\frac{nP}{\pi}} \int_0^{\bar{t}} dn\ \frac{e^{-\frac{nP}{4}\frac{(\bar{x}-n)^2}{(n+nP_r\psi)}}}{(n+nP_r\psi)^{\frac{1}{2}}} \left\{ \left[1 + \frac{n}{2}\frac{(1 + P_r\psi')}{(n + nP_r\psi)}(\bar{x}-n) \right]^2 \right.$$

$$\left. + \frac{nP_r n}{2}\frac{(\psi_0'' - \psi')}{(n+nP_r\psi)^2}(\bar{x}-n)^2 \right\}^{-(\frac{n-1}{2})}$$

where

$$\psi = \int_0^\eta (\eta - \sigma) \, R(\sigma) d\sigma \qquad\qquad (20)$$

$$\psi' = \frac{\partial \psi}{\partial \eta}$$

$$\psi'' = \frac{\partial^2 \psi}{\partial \eta^2}$$

$$\psi_0'' = \psi''(o) = R(o)$$

Equation (19) has been used to generate several plots of the steady-state mean concentration as a function of position for four values of the ratio of the random Peclet No. to the nonrandom Peclet No. P_r/P, and these are shown in Figure 3. The curve for $P_r/P = 0$ corresponds to the deterministic nonrandom result. For larger values of P_r/P, the mean concentration becomes greater. This feature demonstrates that transients in the flow field cannot, in general, be ignored even in state-state applications. It is important to reiterate the well known fact that the state-state concentration is independent of any constant value of the longitudinal dispersion coefficient. The only way that transient flows can properly be modeled is. by solving the transient problem deterministicall or by using a time-varying diffusivity.

III. ADDITIONAL REMARKS

In this paper, two simple stochastic models have been presented. Several of the simplifying assumptions made in the mathematical formulations can be, to some extent, relaxed. The point source assumption was purely a mathematical convenience. The problems can now be solved without additional difficulty for any Fourier transformable source distribution.

It is also possible to allow the river cross-section to vary with downstream position and allow the river flow to vary with position so as to conserve mass. Ths can be accomplished by formulating the problem using the volume of river between the source and some arbitrary downstream location x as the spatial variable rather than simply the distance. This will result in a Fourier transformable differential equation only if diffusion is neglected. The neglect of diffusion is justified since the effective diffusivity resulting from the random velocity fluctuations dominates any small-scale diffusion except at very short times. The presence of diffusion at short times after the source is turned on is only necessary with a point source. In this case, the diffusion is required for initial smoothing of the singularity. However, this difficulty can be avoided by considering the more realistic case of a distributed source. As was previously mentioned, such a source can readily be included.

Finally, the models presented assumed the release of a passive contaminant. This again was a mathematical convenience. It is possible to introduce a simple sink or first order reaction rate. In this case, a chance of variables will result in this term being transformed out of the problem producing the identical differential equations considered in the previous sections.

REFERENCES

Batchelor, G. K., The Theory of Homogeneous Turbulence. Cambridge
     University Press, Cambridge, England, 1953.

Molyneux, J. E. and A. J. Witten, Diffusion of a Passive Scalar with
     Random Advection, submitted to Water Resources Research, 1979.

Taylor, G. I., The Dispersion of Matter in Turbulent Flow Through a
     Pipe, Proc. Roy. Soc. A223, 446, 1954.
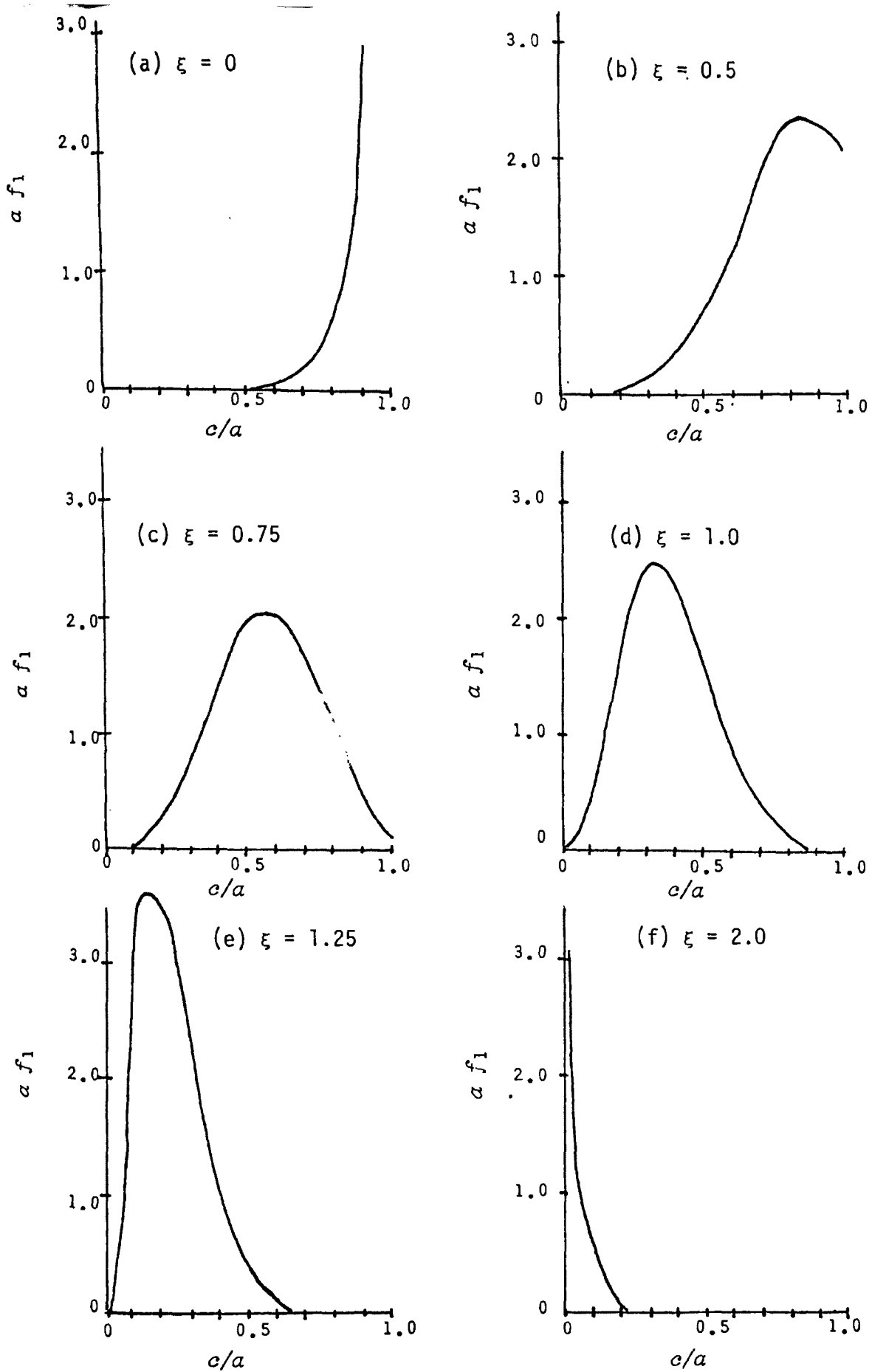
Figure 1. Probability as a function of concentration for several positions
relative to the mean advection front.
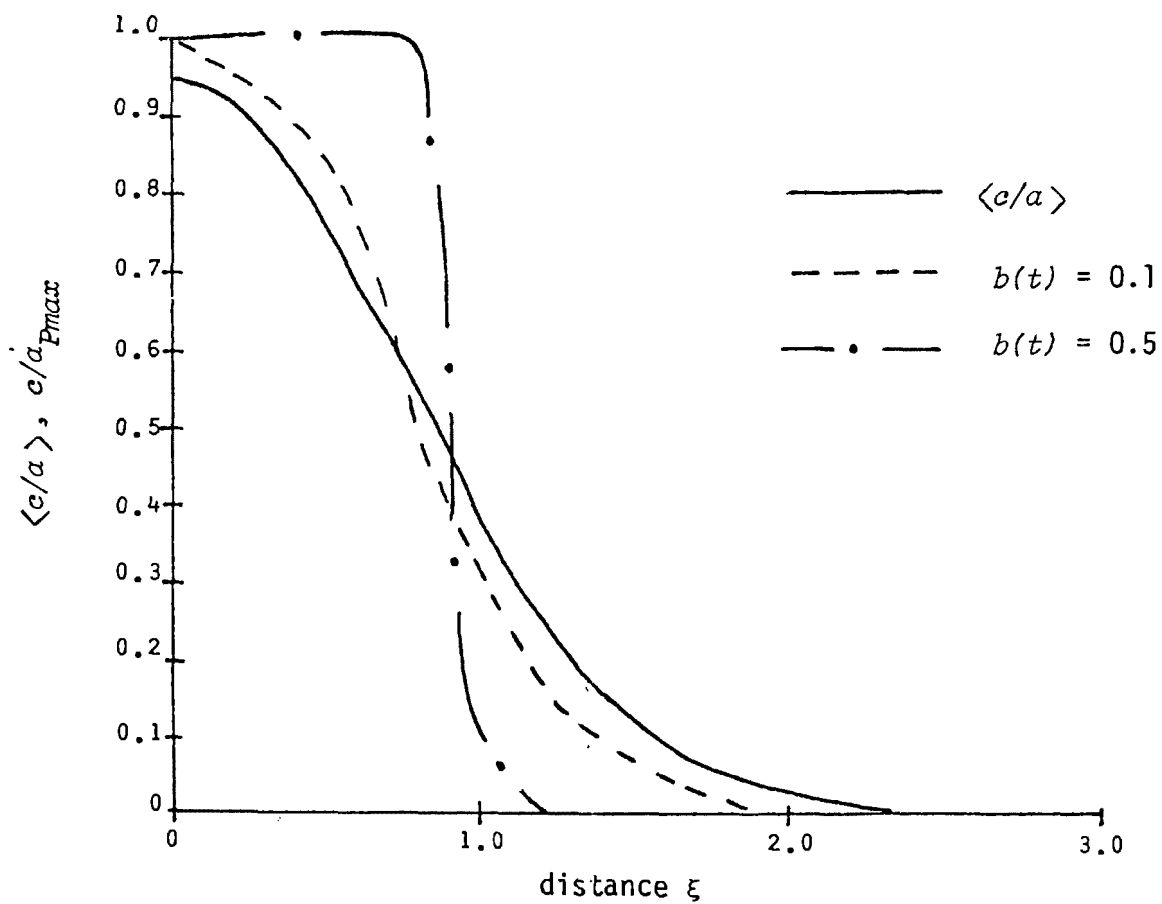
Figure 2. Plot of mean concentration versus position, and plots of most probable concentration versus position for two values of the randomness parameter.
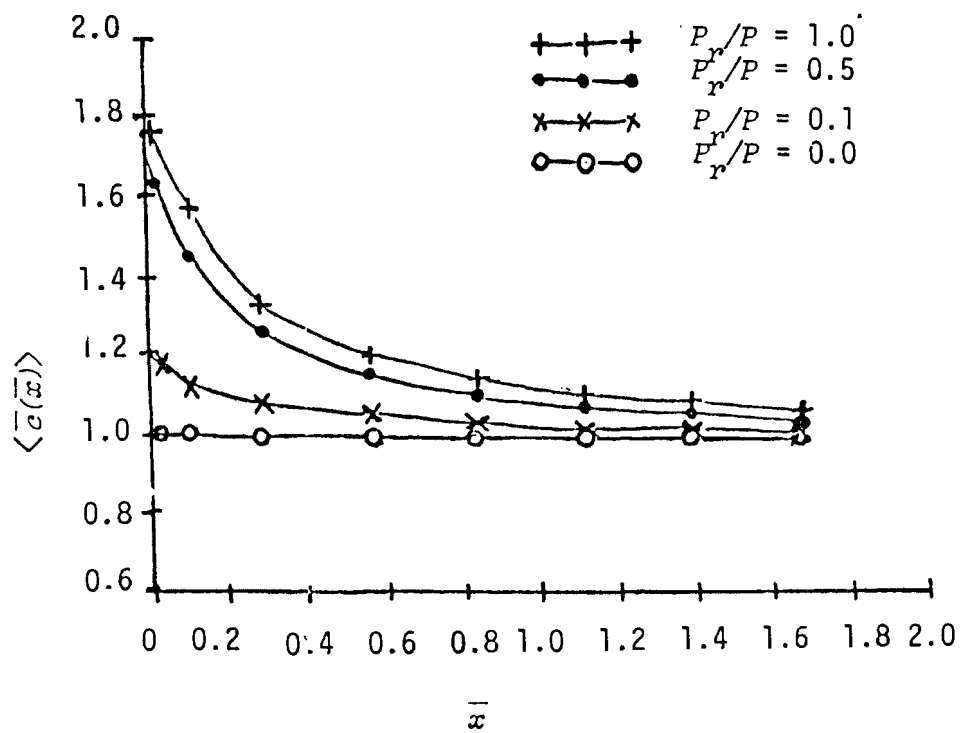
Figure 3. Plots of mean concentration versus position for several values of Pr/P.

A TWO-DIMENSIONAL NUMERICAL MODEL FOR SHALLOW COOLING PONDS

S Chieh and A Verma
Envirosphere Company
A Division of Ebasco Services Inc
New York, New York USA

ABSTRACT

A two-dimensional time dependent finite-difference numerical model is developed to describe the thermal performance of a shallow cooling pond. The terms in the governing heat transport equation include convection, dispersion and non-linearized form of surface heat loss to the atmosphere. The water body is grided in a finite number of cells and heat balance is satisfied exactly for each of these cells. The flow distribution in the pond caused by the circulating water flow is determined by a linearized formulation of the hydrodynamic equations of motion and continuity. This approach is reasonable for a low velocity regime (away from the outlets) normally encountered in typical cooling ponds associated with power plant discharges.

The model is applied to a real cooling pond situation with variable depth and irregular boundary. Based on the circulation pattern in the pond, several zones of flow can be discerned. Model results indicate that in relatively stagnant zones the role of lateral dispersion is predominant and its neglect would result in unrealistic temperature gradients. To verify this conclusion, the results of the present model were compared with those of a Langrangian type model which considers only the convection and heat loss terms in the heat transfer equation.

INTRODUCTION

A numerical model for predicting the transient temperature distribution in an irregular shaped shallow cooling pond is proposed. The model yields vertically averaged velocity and temperature distributions thus providing a tool in evaluation of cooling pond performance. This model represents an improvement over Yeh, Verma and Lai's [1] shallow cooling pond model by incorporating the longitudinal and lateral dispersive heat transfer in the equation of heat transport. Results of the proposed model are compared with those of the non-dispersive model of Yeh, et al to highlight the role of dispersion on cooling pond temperature distribution and intake water temperature predictions.

HYDRODYNAMIC MODEL

As input to the convective-dispersion equation of heat transport, velocity

214

distribution caused by the heated discharge in the cooling pond has to be determined. Yeh, et al [1] have developed a mathematical model to describe the steady state flow field in a shallow pond with irregular boundary and variable depth. Three major assumptions, upon which their model is based are: (1) convective acceleration terms in the equation of motion are small in comparison to friction and pressure terms, (ii) bottom stresses are expressible as linear functions of velocity, and (iii) pressure is hydrostatic. After vertically averaging the continuity equation and the simplified equations of motion, they obtained:

$$-g \; \partial \eta / \partial x \; + \; \frac{\tau_{xs}}{\rho h} \; - \; \frac{KU\bar{u}}{h} \; = \; 0 \tag{1a}$$

$$-g \; \partial \eta / \partial y \; + \; \frac{\tau_{ys}}{\rho h} \; - \; \frac{KU\bar{v}}{h} \; = \; 0 \tag{1b}$$

$$\frac{\partial(\bar{u}h)}{\partial x} \; + \; \frac{\partial(\bar{v}h)}{\partial y} \; = \; 0 \tag{1c}$$

where: ρ = density of fluid, K = friction factor, U = a scaling velocity, g = acceleration due to gravity, η = surface displacement, τ_{xs} and τ_{ys} are surface stresses and x, y are spatial coordinates, $\bar{u}$ and $\bar{v}$ are averaged velocity components in x, y directions and h = water depth.

Introducing a stream function ψ (x,y) such that:

$$\bar{u} = - \; \frac{1}{h \; (x,y)} \; \frac{\partial \psi}{\partial y} \quad \text{and} \quad \bar{v} = \frac{1}{h \; (x,y)} \; \frac{\partial \psi}{\partial x} \tag{2}$$

The continuity equation (1c) is automatically satisfied and equations (1a) and (1b) can be combined to give:

$$\frac{\partial^2 \psi}{\partial x^2} + \frac{\partial^2 \psi}{\partial y^2} = \frac{2}{h} \left[\frac{\partial h}{\partial x} \frac{\partial \psi}{\partial x} + \frac{\partial h}{\partial y} \frac{\partial \psi}{\partial y} \right] + \frac{h}{\rho KU} \left[\frac{\partial}{\partial x} \left(\frac{\tau_{ys}}{h} \right) - \frac{\partial}{\partial y} \left(\frac{\tau_{xs}}{h} \right) \right] \tag{3}$$

Equation 3 is solved by over relaxation techniques subject to shoreline values of ψ, prescribed by the locations of intake and discharge points. Once ψ (x,y) has been obtained, the flow field is determined by the use of Equation 2.

TWO-DIMENSIONAL DISPERSIVE THERMAL MODEL

Assuming no internal sinks or heat exchange across solid boundaries the vertically averaged thermal transport equation can be written as:

$$\frac{\partial}{\partial t} \ (hT) = \frac{\partial}{\partial x} \ (h\bar{u}T) \ + \ \frac{\partial}{\partial y} \ (h\bar{v}T) \ =$$

$$\frac{\partial}{\partial x} \left(h \ D_x \frac{\partial T}{\partial x} \right) + \frac{\partial}{\partial y} \left(h \ D_y \frac{\partial T}{\partial y} \right) + \frac{\dot{Q}}{\rho c_p} \qquad (4)$$

where: D_x, D_y = thermal dispersion coefficients along the x and y axis, respectively

$\dot{Q}$ = rate of heat exchange per unit area between the water surface and the atmosphere

ρ = specific weight

c_p = specific heat

A difference formulation, based on the "cell method", is proposed. The procedure generates a set of algebraic equations which satisfy the homogeneous, conservative and transportive properties for each cell of a spatial grid network. In the context of this thermal transport model, the homogeneous property assumes an average temperature condition within a cell, the conservative property requires that the heat flux of any cell is balanced exactly, and the transportive property ensures that a temperature is advected in the direction of flow.

Figure 1 illustrates a typical network of equally sized rectangular cells. During any time interval Δt, the heat balance for cell (i, j) can be expressed as:

$$\Delta t \cdot H_c \qquad + \qquad \Delta t \cdot H_d \qquad + \qquad \Delta t \cdot H_s \qquad = Acc \qquad (5)$$

Net Heat Transport   +   New Heat Transport   +   Net Heat Transfer   = Accumula-
  By Convection   By Diffusion   at the Water   tion
                                                    Surface

Each of the heat terms, H_c, H_d, H_s and Acc are expanded below:

Accumulation

$$Acc = \rho c_p \ (T'_{i,j} - T_{i,j}) \ \Delta x \ \Delta y \ \overline{h i,j} \qquad (6)$$

where: $T'_{i,j}$ = temperature at $t + \Delta t$

$T_{i,j}$ = temperature at t

$\overline{h}_{i,j}$ = average water depth of the cell i, j

Δx = cell length

Δy = cell width

Heat Transfer at the Water Surface

$$H_s = \dot{Q} \, \Delta x \, \Delta y \tag{7}$$

$\dot{Q}$ is the net heat flux and includes energy exchanges due to the various types of incoming and c   'ng radiation and losses due to evaporation and convection.

$\dot{Q}$ can be written as:

$$\dot{Q} = (1-\gamma_s) H_s + (1-\gamma_a) H_a - H_{br} - H_c - H_e$$

where H_s is the short wave r ⁻⁻ radiation, H_a the atmospheric long wave radiation, H_{br} the back rad₁   from waterbody, H_c the sensible heat flux due to convection and H_e ₜₕₑ latent heat of evaporation. γ_s and γ_a are reflection coefficients for short and ⁻ng wave radiations. For expressions of these heat transfer terms, refer to Edinger and Geyer[2] and Ryan and Harleman [3].

Dispersion

$$\frac{H_d}{\rho c_p} = \Delta y \; \bar{h}_{i+1} \cdot D_x \; \frac{T_{i+1,j} - T_{i,j}}{\Delta x}$$

$$+ \Delta y \; \bar{h}_i \cdot D_x \; \frac{T_{i-1,j} - T_{i,j}}{\Delta x}$$

$$+ \Delta x \; \bar{h}_{j+1} \cdot D_y \; \frac{T_{i,j+1} - T_{i,j}}{\Delta y}$$

$$+ \Delta x \; \bar{h}_j \cdot D_y \; \frac{T_{i,j-1} - T_{i,j}}{\Delta y} \tag{8}$$

where $\bar{h}_{i+1}$ etc represent the average depth along appropriate faces of the cell i,j and D_x, D_y are dispersion coefficients in x, y directions.

Convection

$$\tag{9}$$

$$H_c = H_{cr} + H_{cl} - H_{ct} + H_{cb}$$

where: H_c = heat flux by convection
   r,l,t,b = subscripts which indicate the right, left, top and bottom faces, respectively, of an individual cell

From Equations (2), the flow rates through a cell face can be expressed as:

$$q_x = h(x,y) \, \Delta y \, \bar{u} = -\Delta \psi_y$$

$$\text{and} \quad q_y = \Delta \psi_x$$

Hence, the following difference expressions can be written for terms on the right hand side of Equation 9:

$$\frac{H_{cl}}{\rho c_p} = (\psi i,j-1 - \psi i,j) \, T_{i-1,j} \quad \text{if } \psi i,j-1 > \psi i,j$$

$$= (\psi i,j-1 - \psi i,j) \, T_{i,j} \quad \text{if } \psi i,j-1 < \psi i,j$$

$$\frac{H_{cr}}{\rho c_p} = (\psi i+1,j - \psi i+1,j-1) \, T_{i,j} \quad \text{if } \psi i+1,j < \psi i+1,j-1$$

$$= (\psi i+1,j - \psi i+1,j-1) \, T_i{+1,j} \quad \text{if } \psi i+1,j > \psi i+1, \, j-1$$

$$\frac{H_{cb}}{\rho c_p} = (\psi i+1,j-1 - \psi i,j-1) \, T_{i,j-1} \quad \text{if } \psi i+1,j-1 > \psi i,j-1$$

$$= (\psi i+1,j-1 - \psi i,j-1) \, T_{i,j} \quad \text{if } \psi i+1,j-1 < \psi i,j-1$$

$$\frac{H_{ct}}{\rho c_p} = (\psi i,j - \psi i+1,j) \, T_{i,j} \quad \text{if } \psi i,j > \psi i+1,j$$

$$(\psi i,j - \psi i+1,j) \, T_{i,j+1} \quad \text{if } \psi i,j < \psi i+1,j \quad (10)$$

Model Equation

Substituting Equations 6-9, into Equation 5 yields the following difference expression for the heat transport equation:

$$T'_{i,j} = T_{i,j} + \frac{\Delta t}{\rho c_p \, \Delta x \, \Delta y \, \bar{h}_{i,j}} \left[\dot{Q} \, \Delta x \, \Delta y + H_d + H_c \right] \quad (11)$$

Thus, knowing the flow field $(\psi(i,j))$, Equation 11 can be integrated in time to find the temperature distribution in a cooling pond as a function

of time for changing meteorological conditions.

MODEL APPLICATIONS

A proposed closed cycle (recirculating) cooling pond to receive 1585 cfs of cooling water with a condenser rise of 20.8°F (reject heat of 7.4 x 10⁹ BTU/hr) is investigated. The pond has an average depth of 12.68 feet and a surface area of 2500 acres and has been created by diking the periphery of a natural terrain.

Figure 2 shows the shape of the pond and the predicted flow pattern in terms of stream lines-ψ = constant curves. The stream functions have been normalized by the total flow rate. Thus 90% total flow is contained with ψ = 0.05 and ψ = 0.95 curves.

Although the thermal model is formulated and is capable of solving the unsteady temperature distribution with varying meteorological conditions, a steady state example is only presented for the present discussion. Figure 3 shows the isothermal distribution resulting from the given flow rate of 1585 cfs, condenser rise of 20.8°F, and the following assumed steady state meteorological parameters:

$$H_s \text{ (solar radiation)} \quad = \quad 2714 \text{ BTU/ft}^2/\text{day}$$

$$T_a \text{ (Air temperature)} \quad = \quad 88.4°F$$

$$\text{Dew point} \quad = \quad 70.2°F$$

$$W \text{ (Wind speed)} \quad = \quad 7.9 \text{ mph}$$

Dispersion coefficients were arbitrarily chosen as: D_x = 1.0 ft²/s and D_y = 1.0 ft²/s.

Superimposed on the same Figure 3, are the temperature distribution predicted by the Lagrangian approach of Yeh, et al based on a non-dispersive model (D_x = D_y = 0). This comparison between the results of the present and Yeh, et al models illustrates the role of dispersion on the temperature distribution for cooling ponds of irregular shapes.

The intake water temperature calculated by the dispersive (present) and non-dispersive (Yeh, et al) models are 93°F and 93.5°F respectively, which agree closely. However, the isotherms predicted by the two models within the pond are quite different. An immediate implication of this result is that the non-dispersive Lagrangian model is adequate to predict the intake water temperature. However, a two-dimensional dispersive model should be used to determine the temperature distribution more realistically.

Examination of the temperature distribution (Fig 3) reveals that:

(1) Near the discharge, the temperature predictions by the dispersive and

non-dispersive models agree closely. This is because this region is convection dominated and the effects of dispersion is not significant.

(2) In the stagnant zones of the pond (located near the left and bottom right corner) the dispersion is dominant and the temperature predictions differ by more than $2^{\circ}F$.

(3) In the vicinity of the intake, the isotherms predicted by the non-dispersive model become almost parallel to the stream lines and the lateral temperature gradients are very large. The dispersive model on the other hand removes this anomaly.

CONCLUSIONS

A method for determining temperature distribution in shallow cooling ponds by numerical modeling techniques has been presented. The "cell method" was applied to solve the two-dimensional vertically-averaged diffusive heat flux equation. Although the model in its present form has not been verified, it has been applied to study the role of dispersion on thermal distribution cooling ponds. Numerical experiments indicate that the non-dispersive Lagrangian model is probably sufficient to predict condenser intake temperature in irregular shaped ponds. However, significant difference was found for the temperature distribution predicted by the two-dimensional dispersive and non-dispersive Lagrangian models.

REFERENCES

1. Yeh, G T, Verma, A P and Lai, F H, "Unsteady Temperature Prediction for Cooling Ponds," Water Resources Research, Vol 9, No. 6 (1973).

2. Edinger, J R and Geyer, J C, "Cooling Water Studies for Edison Electric Institute, Project No. RP-49 - Heat Exchange in the Environment," The John Hopkins University, June 1, 1965.

3. Ryan, P J and Harleman, Dr F, "An Analytical and Experimental Study of Transient Cooling Pond Behavior," Technical Report No. 161, Ralph M Parsons Laboratory for Water Resources and Hydrodynamics, Dept of Civil Eng, MIT, January 1973.
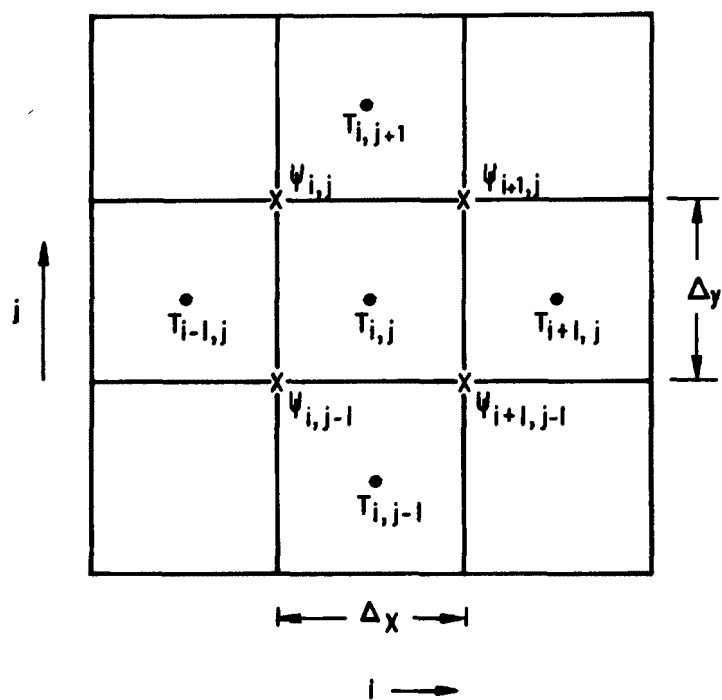
Fig 1 - NETWORK OF RECTANGULAR CELLS
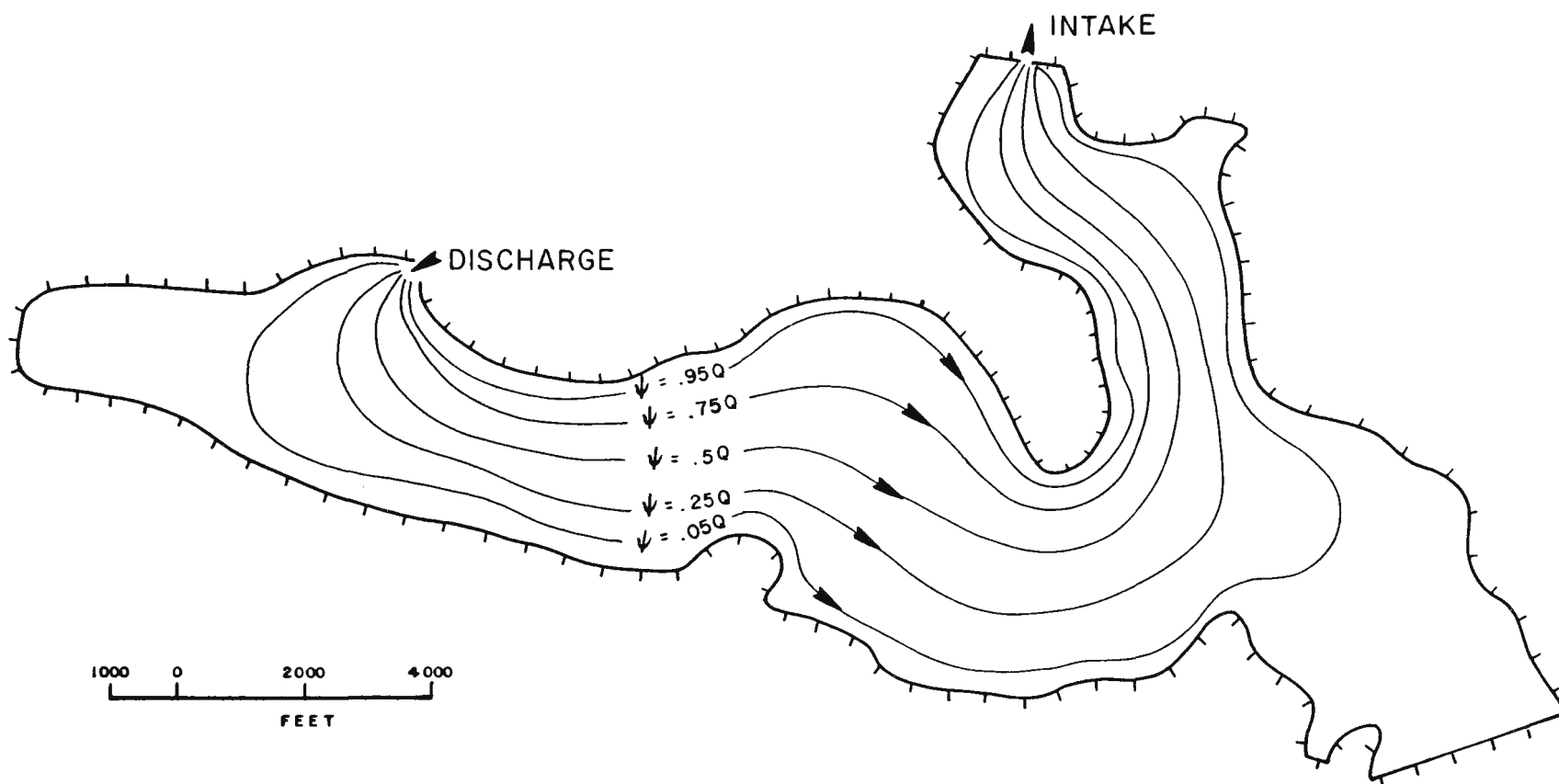
Fig. 2 .- COOLING POND SHAPE AND STREAMLINE PATTERN
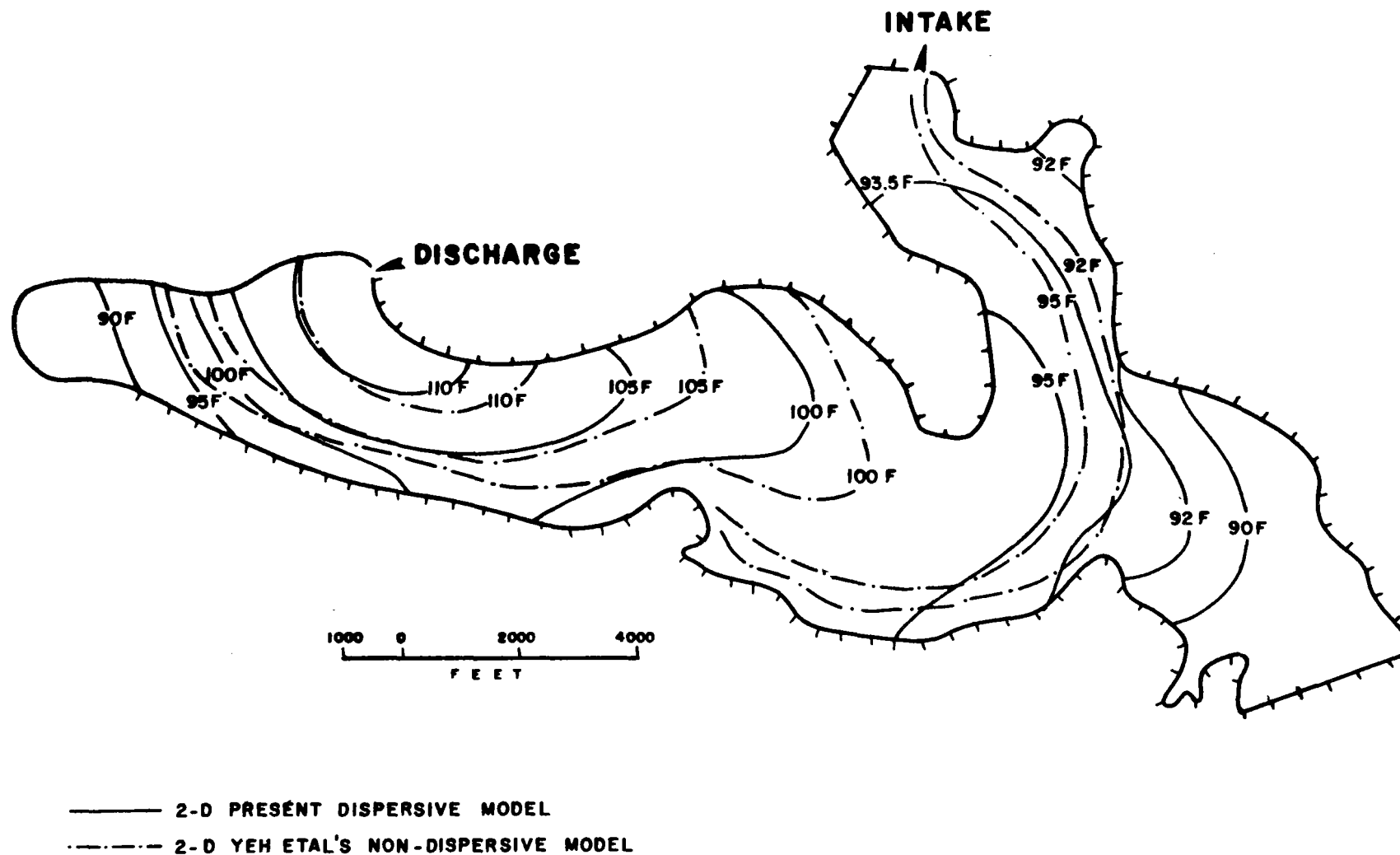
Fig 3 - TEMPERATURE DISTRIBUTION IN THE COOLING POND

WASTE HEAT FOR ROOT-ZONE HEATING - A PHYSICAL STUDY OF HEAT AND MOISTURE TRANSFER

D. L. Elwell, W. L. Roller and A. Ahmed
Department of Agricultural Engineering
Ohio Agricultural Research and Development Center
Wooster, Ohio 44691

ABSTRACT

A study of the use of power plant waste heat for root-zone heating in green-houses is being undertaken. As the first part of this study, the physical properties of a system that supplies heating water through buried pipes and irrigation water through a constant level water table have been characterized. Three different soils (sand, peat-vermiculite and silt-loam) have been investigated at heating water temperatures of 25, 30, 35 and 40°C. The resultant heat and moisture transfer figures are internally consistent and in good agreement with comparable results of other investigators, where available. The water table irrigation system is capable of maintaining suitable soil moisture content for plant growth up to the highest tempera-tures investigated, and the soil heating system can supply up to 30% of the total, seasonal heating load of a greenhouse while producing root-zone temperatures up to 32°C (89°F). These results will now serve as a base for continuing study with lettuce growing on the system.

INTRODUCTION

The fact that rejected, or waste, heat from electric power generating plants is basically a low temperature thermal resource leads to both physical and economic restrictions on the practical utilization of this large and potentially valuable resource. One possible application that shows consi-derable promise for overcoming these difficulties is greenhouse heating. Space heating requirements can be met from a low temperature resource. If, in addition, at least some of the heat is applied through the soil of the greenhouse, thus raising the temperature of the root-growth-zone, then the economic benefits can be twofold. First, overall heat load require-ments can be partially met and second, plant growth and yield can be en-hanced if other soil criteria can be maintained. Because of these poten-tial advantages both total greenhouse heating [1] - [3], and soil heating applications of waste heat [4] - [7] are being studied by various inves-tigators at this time.

The present study is directed toward the evaluation of heat and moisture transfer in heated soils of various types (as described below) that are irrigated from below, through the maintenance of a water table at an appro-priate depth. It is based on the previous work of Shapiro [5]. It is part of a three-year study, supported by EPRI (Contract No. RP1110-1), and is designed to provide detailed information about the effects of soil hea-ting and sub-surface irrigation on soil conditions and about plant growth under these conditions.

EXPERIMENTAL

One bay (5.5 x 29m (18.5 x 96 ft.)) of a two bay, double plastic greenhouse
was separated into an independent heating chamber by dividing the green-
house with a sheet of transparent plastic. Independent gas consumption
records were maintained for the heating units in each bay. This bay was
equipped with four small soil plots designed for the proposed heating and
irrigation studies of the experiment. Three of these plots were equipped
with sub-soil heating and sub-irrigation systems while the fourth plot was
unheated and surface-irrigated to serve as a control for comparison pur-
poses. The three heated plots contained "soils" that consisted of Wooster
silt-loam, a peat-vermiculite mixture, and sand, respectively and the un-
heated, control plot contained Wooster silt-loam. Each of these plots was
2.9 m (9.5 ft.) wide by 3.0 m (10 ft.) long and was sealed at a depth of
0.6 m (24 in.) by means of a plastic liner as shown in Fig. 1. The bottom
0.1 m (4 in.) of each of these plots was filled with pea gravel topped with
coarse sand, to allow for rapid, horizontal, water table equalization. A
constant water table was maintained at a depth of 0.5 m (20 in.) by an auto-
matic irrigation system.

Constant-temperature heating water, heated to 25, 30, 35 and 40°C for suc-
cessive intervals, was supplied to the heated plots by means of a mixing
valve controlled by a Honeywell air pressure regulator. This heated water
was circulated through each plot at a nominal rate of 0.16 liters/sec
(2.5 gal/min) by means of 0.1 m (4 in.) i.d. headers that supplied 0.025 m
(1.0 in.) i.d. ABS plastic pipes as shown in Fig. 2. These pipes passed
through the soil at a depth of 0.3 m (12 in.) and with a separation of 0.3 m
(12 in.). The plots were insulated on all four sides with 0.05 m (2 in.)
of styrofoam insulation in order to minimize edge effects in heat flow in
the soil.

Temperatures throughout the soil of the heated plots were recorded from
thermocouples at the locations indicated in Figs. 1 and 2. A similar, but
less-extensive, set of thermocouples existed in the control plot. A Kaye
Instruments System 8000 recorder was used to read selected thermocouples
every 30 minutes continuously. All thermocouples were read at least once
a day, and all readings of both types were fed to a teletype paper-tape-
punch unit for transfer to a computer for analysis.

Ten-junction thermopiles were connected across the inlet and outlet sides
of the heating water circulation system for each plot, and regular read-
ings from these thermopiles were combined with heating water flow infor-
mation to provide total rates of heat input at each heating level. Radio-
meters, both inside and outside the greenhouse, were used to record light
levels at various times throughout the day. And moisture distribution in-
formation was obtained by taking core samples at various locations in the
plots.

RESULTS

The soils used in the plots had the following properties. The Wooster

silt-loam soil was composed of 25% sand (primarily very fine sand - 0.1 to 0.05 mm), 60% silt and 15% clay, had a dry density of 1.32 g/cm³, and had a porosity (based on saturated water content) of 0.44. The sand "soil" was composed of 99+% quartz with approximately 55% of the particles being in the medium sand range (0.5 to 0.25 mm) and the remaining 45% being fine sand (0.25 to 0.1 mm), had a dry density of 1.63 g/cm³, and had a porosity of 0.38. And the peat-vermiculite "soil" was composed of roughly 50% (by volume) commercially available sphagnum peat moss (no further analysis was attempted) and 50% vermiculite particles, had a dry density of 0.16 g /cm³, and had a porosity of 0.81.

Moisture

The system is designed so that all moisture supplied to the water table in each plot must, at equilibrium, be balanced by an equivalent amount of evaporation from its surface. Irrigation water supply rate is shown in Fig. 3. It should be noted that 1.0 liters/day (0.26 gal/day) is equivalent to 1.13×10^{-4} m/day (0.031 in/wk) of water level change so that even at the highest consumption rates shown the irrigation demand is modest. The values for the silt loam soil are in excellent agreement with the previous work of Sepaskhah et al. [8] but the present values for moisture consumption in sand are approximately fifteen times smaller than is reported there. This difference may be readily attributed to the differences in the moisture application techniques involved which result in great loss of water to the subsoil in the case of Sepaskhah, due to high hydraulic conductivity of sand.

Moisture content at various depths in each type of soil was determined by taking core samples from two locations in each plot at regular intervals throughout the experimental period. The resultant moisture profiles are shown in Fig. 4. There was a distinct tendency for the upper layer of the peat-vermiculite to lose moisture as solar radiation increased. This loss amounted to a 50% decrease from 0.32 g/cm³ water content in January to 0.16 g/cm³ in May. There was no detectable change in this period in the upper layers of the other two soils.

The effect of heating on moisture content in the region of the hot water pipes was examined carefully. There was no detectable drying in the sand at any of the temperatures used in this experiment. There was also no drying in the peat-vermiculite through the 35°C heating level, but there was limited drying - from 0.58 to 0.51 g/cm³ - in the region of the heating pipes when the heating water was held at 40°C. Similarly, there was no drying in the Wooster silt-loam at 25 or 30°C, but there was some drying at the higher temperatures - from 0.39 to 0.35 g /cm³ and 35°C and from 0.39 to 0.30 g/cm³ at 40°C. In both of these cases, the drying was no longer detectable within two weeks after heating had been terminated. It should be noted that these drying effects seemed to apply equally to core samples that were taken midway between two heating pipes and those that were taken as close to a heating pipe as possible.

The moisture consumption (Fig. 3) and moisture profile (Fig. 4) results

for sand have been compared with the work of deVries [9] and of Jury and Miller [10]. In the notation of the latter paper, total steady-state moisture flow can be represented by

$$Q_m = -L_{mm} (\theta,T) \frac{d\theta}{dZ} -L_{mT} (\theta,T) \frac{dT}{dZ} -K(\theta,T) \tag{1}$$

where Q_m is total moisture flow (cm^3/cm^2 sec), K is hydraulic conductivity (cm/sec), θ is volumetric moisture content (cm^3 H_2O/cm^3 soil), T is temperature (^oC), and L_{mm} and L_{mT} are transport coefficients. The most useful comparison is in terms of these coefficients, and while the present experiment was not designed for this particular calculation and did not independently obtain hydraulic conductivity values, the general agreement is quite good. The only significant difference lies in the fact that the steep portion of the sand moisture profile occurs at somewhat lower moisture contents (θ = .10 to .20) than would be expected from Jury and Miller's (10) data (θ = .14 to .24). No suitable comparisons were obtained for either of the other two soils. A crude calculation, based on a value of K = 1.7 x 10^{-5} cm/sec obtained from Van Wijk and deVries [11], yielded for the silt-loam at θ = 0.35; L_{mm} = 6.1 x 10^{-3} cm^2/sec, and L_{mT} = 4.5 x 10^{-6} cm^2/sec ^oC. These values are roughly a factor of 40 less than corresponding values for sand and should be ~~ed only .f ~rude estimates.

Wet bulb and dry bulb air temperatures were recorded at various locations in the greenhouse and no systematic effect of the irrigation system on humidity was detected.

Heat

Fig. 5 gives the rate of heat absorption from the hot water pipes in each of the soils. The values shown are averages of daily values that were calculated from thermopile and flow rate records, and they have been corrected for losses in the headers. The daily values show r.m.s. deviations from the average that are less than 10%, and the calculated uncertainty in these averages is $\pm$ 5%.

The largest temperature drops recorded across the plots were 1.46, 1.10, and 2.43^oC for the sand peat-vermiculite and silt-loam respectively. These drops occurred during a two week interval when flow rates were allowed to drop be v desirable levels, and in general, temperature drops were less than h. hese amounts. Thus, the heating pipes were approximately isothermal ¹ lateral temperature variations could be neglected.

Fig. 6 shows a portion of one of the weekly computer plots of temperatures recorded from the thermocouples. Days 99 through 102 are April 9 to April 12, 1978 at which time the heating water was at T = 40^oC, and channels 20 and 22, and 30 and 32 are records from the 0.1 m (4") and 0.3 m (12") depths in the sand and peat-vermiculite soils respectively. Fig. 7 shows one of the temperature profile plots drawn by the computer from all of

228

the thermocouple readings recorded. This particular one is for the sand plot at 8:38 AM on April 9, 1978. Both of these figures represent very typical data.

The temperature profiles, with compensation for diurnal variations obtained from the weekly temperature plots, were analyzed for heat flow using thermal conductivities given by deVries [12] and Nakshabandi and Kohnke [13]. The values thus calculated were then compared with the heat absorption values given in Fig. 5. For the sand (using $\lambda = 4.1$ and 6.1×10^{-3} cal/cm sec $^{\circ}$C at average values of $\theta = 0.09$ and 0.28 respectively, and using $\Delta\lambda/^{\circ}C = 2.3 \times 10^{-5}$ cal/cm sec $^{\circ}$C/$^{\circ}$C) the agreement was within $\pm$ 3% in all cases, and it was further determined that $57 \pm 3\%$ of the heat coming from the pipes was carried upward to the greenhouse air while the remaining 43% was carried downward to the deep soil. For the silt-loam (using $\lambda = 2.9$ and 3.2×10^{-3} cal/cm sec $^{\circ}$C at average values of $\theta = 0.35$ and 0.43 respectively) the agreement is equally good at 25°C, and the rate of increase of thermal conductivity with temperature (which cannot be determined from available references) was found to be 4.4×10^{-5} cal/cm sec $^{\circ}$C/$^{\circ}$C for an agreement to within $\pm$ 7% at the higher temperatures. In this case $62 \pm 3\%$ of the heat was carried upward. Finally, for the peat vermiculite the closest comparison available is for a peat soil given by deVries (12). Use of the thermal conductivities for this peat yields a total heat flow that is 21% less than that obtained experimentally. Thus it must be concluded that $\lambda = 0.95$ and 1.27×10^{-3} cal/cm sec $^{\circ}$C at $\theta = 0.52$ and 0.71 respectively in this peat-vermiculite sample. These values yield agreement with the total heat flow data to within $\pm$ 5% and there is no indication of a significant increase in thermal conductivity with temperature rise. And, in this case $50 \pm 3\%$ of the heat was carried upward.

The thermal conductivities obtained above were used to calculate penetration of diurnal temperature variation into the soil following the methods of Wierenga et al. [14]. The calculated penetration (corrected for non-uniformity in moisture content, thermal conductivity and specific heat) at 0.3 m (12") was compared with actual penetrations into the sand and silt-loam soils. In both cases the calculated values were roughly 8% higher than the observed values, but there was an uncertainty of at least $\pm$ 10% in these experimental values and therefore there is at least marginal agreement at this point. No useful comparison could be made in the case of the peat-vermiculite due to excessive damping at the relatively low conductivities involved.

The effect of the heating on the temperature of the soil in the three plots was determined from the various computer drawn temperature profiles. The smallest amount of warming occurred in the peat-vermiculite where the average root-zone temperature increase varied from $\Delta = 5^{\circ}$C at a heating temperature of 25°C to $\Delta =10^{\circ}$C at 40°C. The warming in the silt-loam was in each case, from 2 to 2 1/2°C greater than these values, and the warming in the sand was a similar increment greater still. Thus, in general terms, average root-zone temperature of the heated soils varied from a minimum of 17°C (62°F) to a maximum of 32°C (89°F) which is an ideal range for future plant growth studies.

The maximum heating requirement for the greenhouse in which the experiments were carried out was determined both from calculations and from gas consumption records to be 215 watts/m^2 (1650 BTU/ft^2/day). At this high level the heat transfer from the soil heating pipes to the greenhouse air represents a maximum, for the various heating levels, of 4.1 to 7.1% of the total heat load for the peat-vermiculite; of 8.7 to 17.7% for the silt-loam; and of 9.3 to 15.3% for the sand. Thus, on a lower, season average basis, a root-zone heating scheme of the same configuration as the one studied and utilizing actual power plant cooling water should be able to supply from 10 to 15% of total heat load when peat-vermiculite is used as the growth medium, and from 20 to 30% when either sand or silt-loam are used.

It should be noted that the three soil heating plots have a total area that is only 16% of the area of the experimental bay of the greenhouse and that, therefore, even at the highest heating levels only a small percentage of the heat load was being met through soil heating. This percentage was not directly detectable from gas consumption records.

DISCUSSION

From the results given above, the peat-vermiculite soil was a relatively poor medium both in terms of its heat transfer properties and on the basis of root-zone temperature increase. Both the sand and silt-loam soils were better than twice as effective heat transfer agents, and while the sand reached somewhat higher root-zone temperatures, both achieved the full range of soil temperatures (up to 30°C (85°F)) that is desirable for plant growth studies. In addition, in none of the cases, as was expected, were the heat transfer rates sufficient to meet the full heating load. However, in the two more favorable media at least the heat transfer rates were high enough to suggest that root-zone heating combined with nighttime insulation techniques and reduced air temperatures could substantially reduce aerial heating requirements. Thus root-zone heating must presently be evaluated primarily in terms of increased plant productivity but in the future could also become a major factor in heat load considerations.

Both moisture transfer and general soil moisture content were lowest in the sand. It remains for the next portion of the present study to indicate whether or not these moisture levels will be adequate for plant growth. The peat-vermiculite and the silt-loam soils both showed limited drying at high temperatures. However, this drying was not sufficient to alter the generally favorable moisture levels, and in these two soils at least, the present irrigation system appears, from a physical standpoint, to be a very suitable one for maintaining excellent growing conditions.

Thus, the basic physical characteristics of the three diverse but representative soils used have been characterized in considerable detail for the irrigation and soil heating scheme that is under investigation and for a range of temperatures appropriate to power plant waste heat application. This information will now serve as a base for continuing studies of the system with lettuce growing on it, and it will be determined both

how the system parameters serve to modify the growth of the lettuce and how this growth in turn affects the physical characteristics of the system.

REFERENCES:

1. Boyd, L.L., R.V. Stansfield, G.C. Ashley, J.S. Hietala, and T.R.D. Toukinson. Greenhouse Heating With Warm Water from Electric Generating Plants. A Demonstration Project. Proceedings of an International Symposium on Controlled Environment Agriculture: 169-183. The University of Arizona, Tucson, Arizona, 1977.

2. Bond, B.J., E.R. Burns, R.S. Pile and C.E. Madewell. The Use of Waste Heat in Greenhouse Agriculture. Proceedings of an International Symposium on Controlled Environment Agriculture: 151-168. The University of Arizona, Tucson, Arizona, 1977.

3. Rotz, C.A. and R.A. Aldrich. Feasibility of Greenhouse Heating in Pennsylvania with Power Plant Waste Heat. American Society of Agricultural Engineers. Paper No. 77-4530. Chicago, Illinois.

4. Boersma, L., L.R. Davis, G.M. Reistad, J.D. Ringle, and W.E. Schmisseur. A Systems Analysis of the Economic Utilization of Warm Water Discharge from Power Generating Stations - Final Report. Bulletin No. 48, Oregon State University. 1974.

5. Shapiro, H.N. Simultaneous Heat and Mass Transfer in Porous Media with Application to Soil Warming with Power Plant Waste Heat. Ph.D. Thesis. The Ohio State University. 1975.

6. Sondern, J.A. Soil Warming in the Open. Research Report 77-5. Institute of Agricultural Engineering, Wageningen, The Netherlands.

7. Wells, L.G., A.D. Ward, J.N. Walker, and J.W. Buxton. Heat Loss From Heated Greenhouse Soil Beds. American Society of Agricultural Engineers. Paper No. 77-4529. Chicago, Illinois. 1977.

8. Sepaskhah, A.R., L. Boersma, L.R. Davis, and D.L. Slegel. Experimental Analysis of a Subsurface Soil Warming and Irrigation System Utilizing Waste Heat. American Society of Mechanical Engineers. Paper No. 73-WA/HT-11. Detroit, Michigan.

9. deVries, D.A. Simultaneous Transfer of Heat and Moisture in Porous Media. Trans. Amer. Geophysical Union, 39:909-916. 1958.

10. Jury, W.A. and E.E. Miller. Measurement of the Transport Coefficients for Coupled Flow of Heat and Moisture in a Medium Sand. Soil Sci. Soc. Amer. Proc. Vol. 38:551-557, 1974.

11. Van Eijk, W.R. and D.A. deVries. The Atmosphere and the Soil, Pages 17-61 in: W.R. Van Wijk (ed.). Physics of Plant Environment. North Holland Publishing Company, Amsterdam. 1963.

12. deVries, D.A. Thermal Properties of Soils. Pages 210-235 in: W.R. van Wijk (ed.) Physics of Plant Environment. North Holland Publishing Company, Amsterdam. 1963.

13. Nakshabandi, G.A. and H. Kohnke. Thermal Conductivity and Diffusivity of Soils as Related to Moisture Tension and Other Physical Properties. Agr. Meteorol. 2:271-279. 1965.

14. Wierenga, P.J., D.R. Nielsen, and R.M. Hagan. Thermal Properties of a Soil Based Upon Field and Laboratory Measurements. Soil Sci. Soc. Amer. Proc., Vol. 33:354-360. 1969.
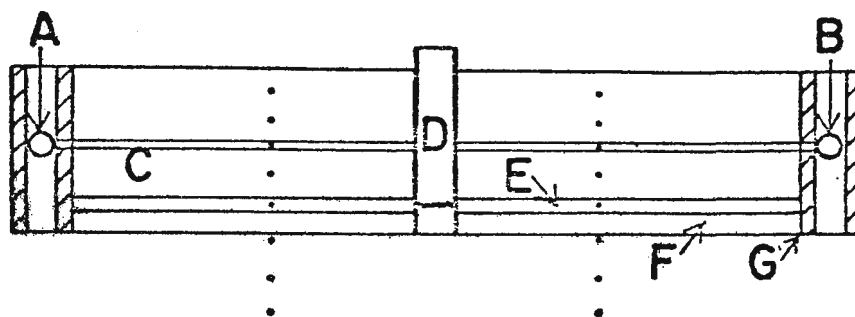
Fig. 1. Vertical section of an experimental soil warming plot showing
the depths at which the thermocouples (·) are located. The hatch
marks represent styrofoam insulation. (A) is the supply header,
(B) is the return header, (C) is one of the ten heating pipes,
(D) is a stand pipe for controling the water level, (E) is two
inches of fine sand, (F) is three inches of pea gravel and
(G) is an impermeable membrane.
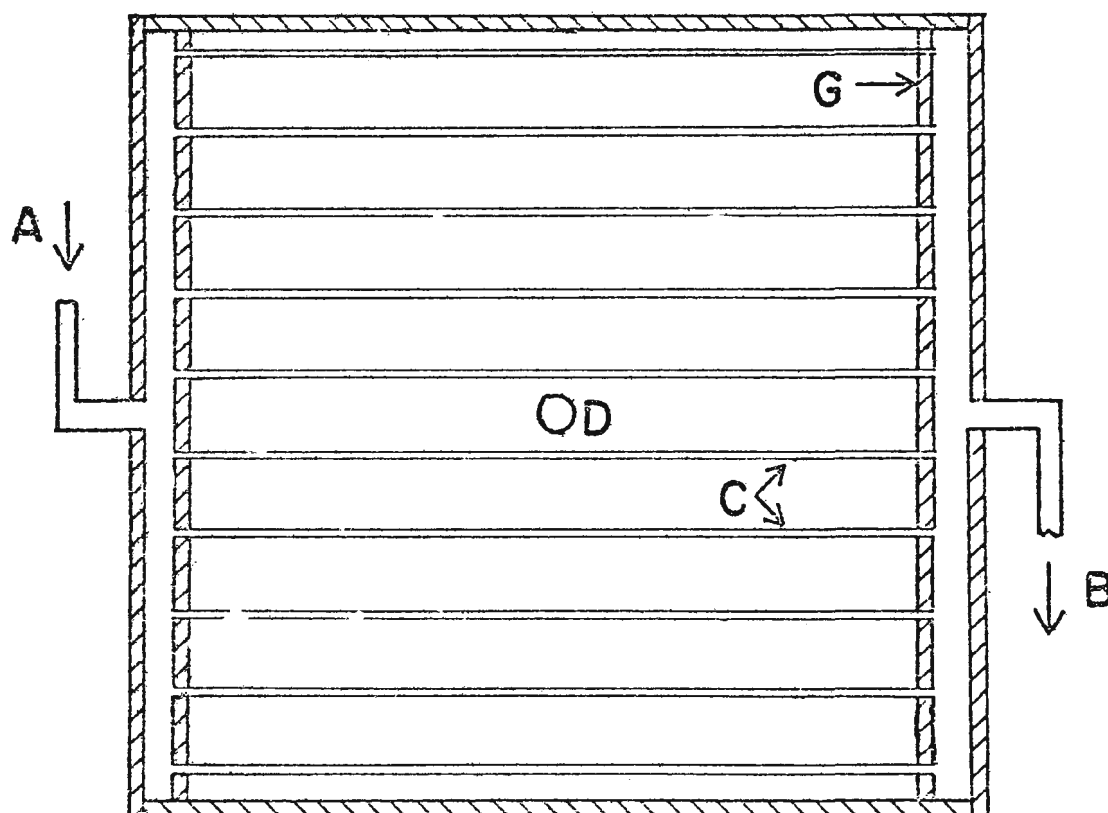
Fig. 2. Horizontal view of a plot showing two sets of thermocouples
on the pipes and two sets between the heating pipes. The labeling
is the same as in Fig. 1.
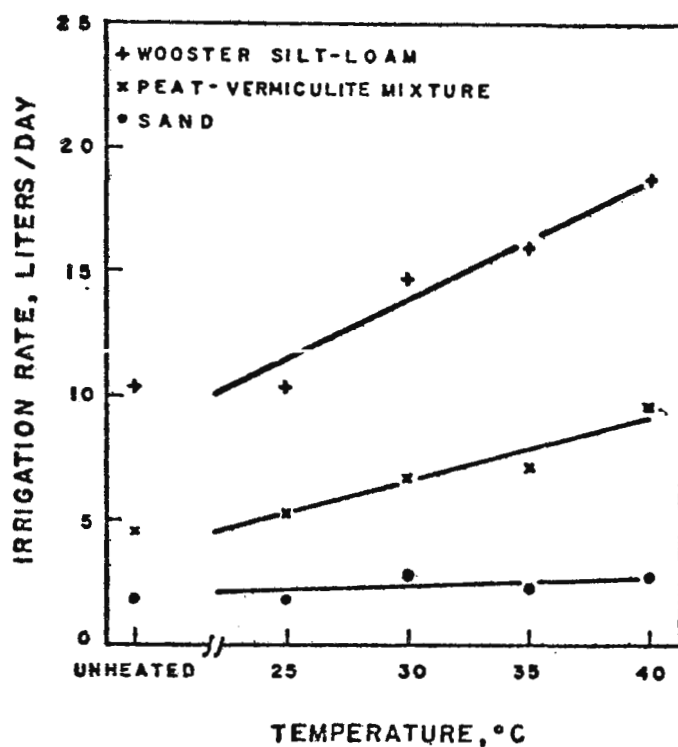
Fig. 3. Irrigation water supply rate at the different heating levels.
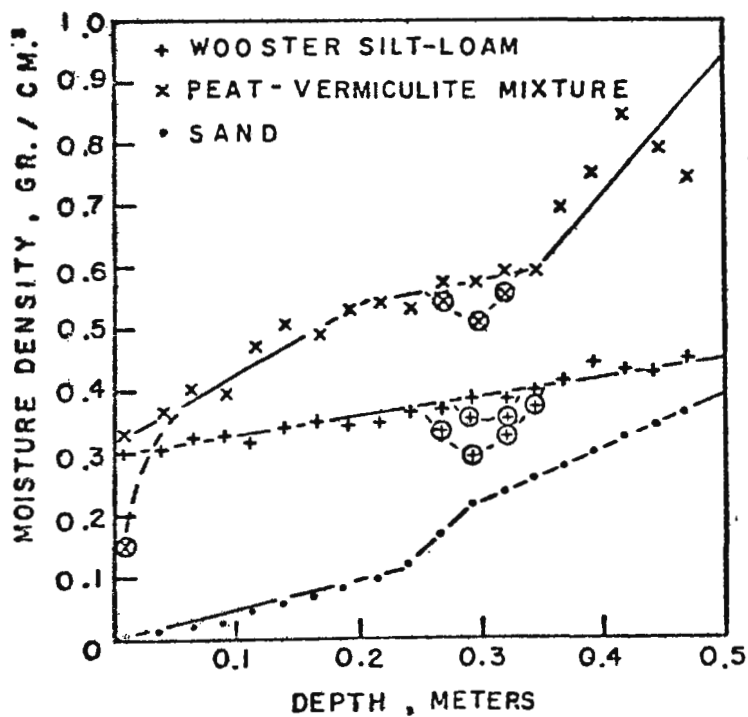
Fig. 4. Moisture Profiles. The circled points indicate the drying
effects that are discussed in the text.
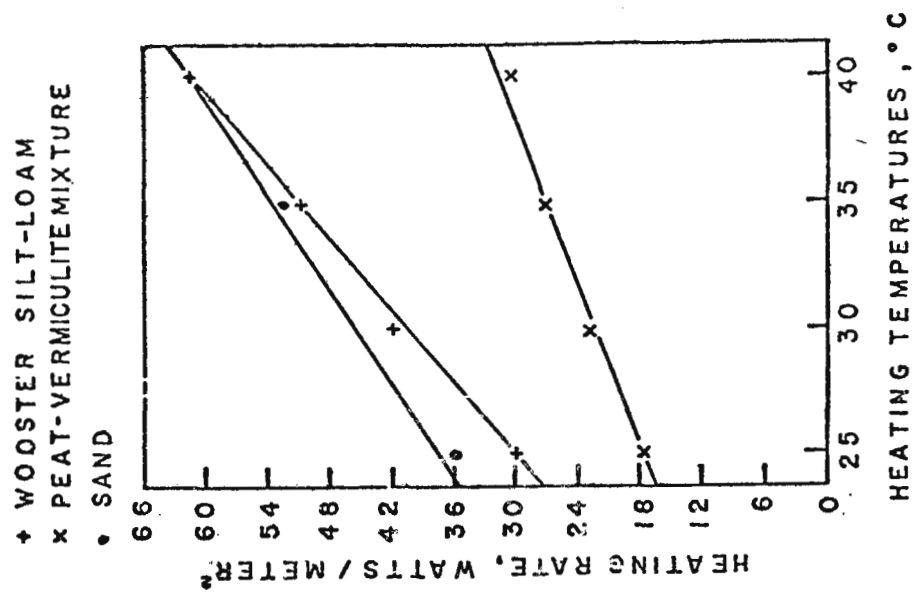
Fig. 5.   Rate of heat absorption in each of the soil plots.
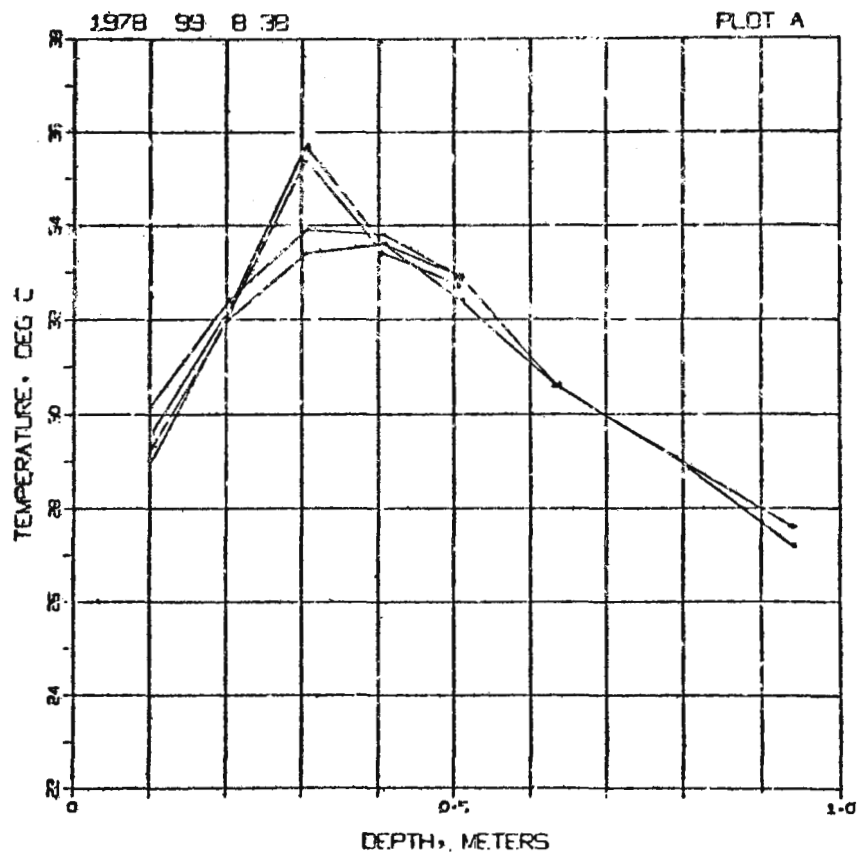
Fig. 7.   Computer plotted temperature profile.
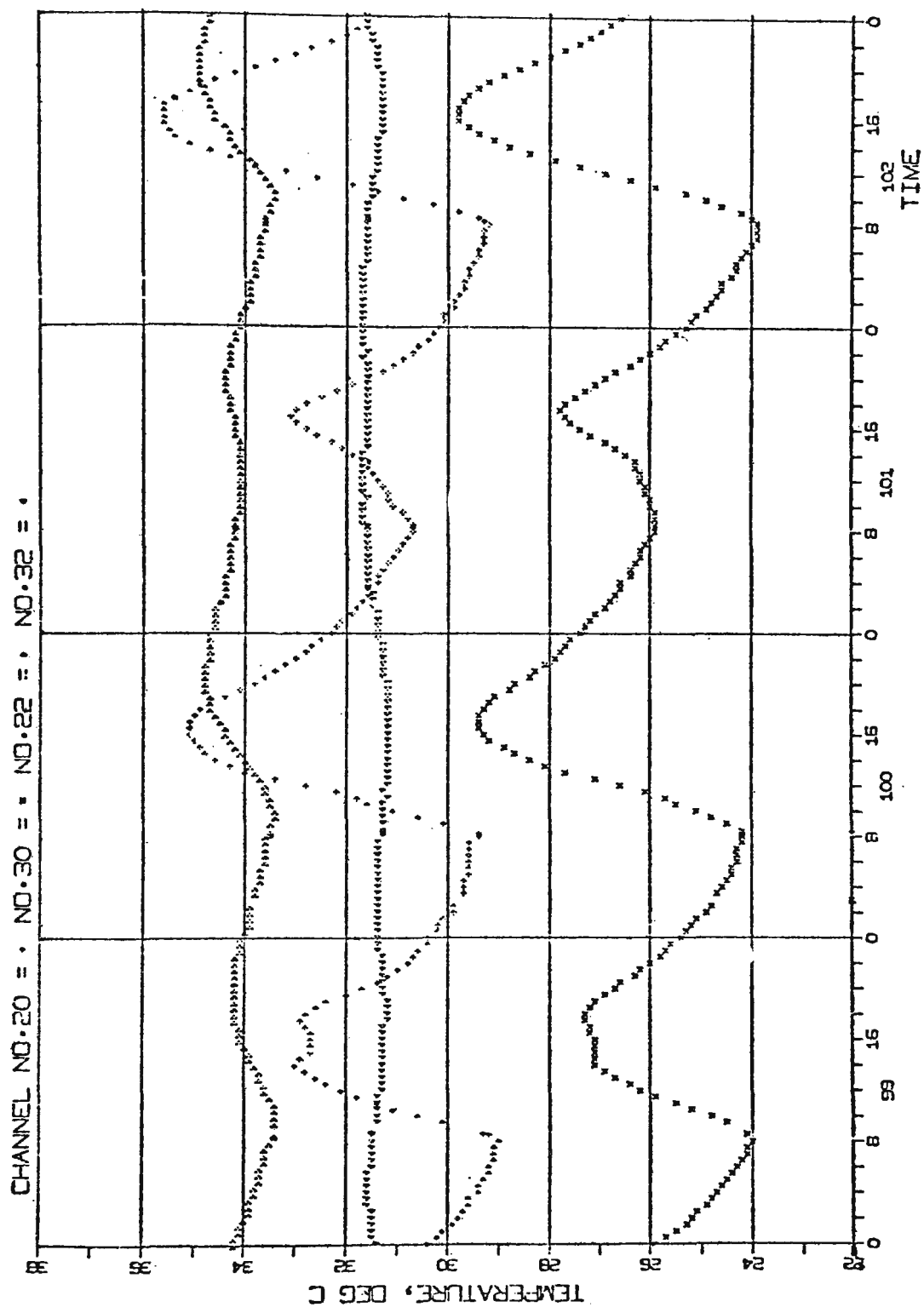
Fig. 6. Computer plot of various thermocouple readings versus time.
See text for discussion.

BENEFICIAL USE OF REJECTED HEAT
IN MUNICIPAL WATER SUPPLIES

R. A. Wynn Jr. and R. W. Porter
Illinois Institute of Technology
Chicago, Illinois U.S.A.

ABSTRACT

The relatively low temperature of thermal discharges from
steam-electric power plants makes waste-heat utilization
difficult without modification of the power cycle and atten-
dant reduction in electrical-energy generating efficiency.
The present paper concerns in situ beneficial use of waste
heat by direct once-through condenser discharge into a
municipal water supply. Computations are presented regarding
the matching of flow rates, heat losses in distribution and
energy savings. A number of benefits and penalties are also
assessed qualitatively including legal and operational aspects
and reliability. Especially attractive are improvements in
generating efficiency, alleviation of water-pipe freeze up,
savings in water-heater energy, and improvement in wastewater
treatment effectiveness. Disadvantages include the need for
careful control of condenser water quality and the question
of public acceptance of water heated by about 13 C. Two
cases with operating experience are briefly discussed,
although the installations were not developed for energy
conservation purposes.

INTRODUCTION

It is well known in power engineering that for every unit of
electrical energy generated in a steam-electric power plant,
approximately two units of heat energy must be rejected to the
environment. Nearly 30% of the total U.S. energy consumption
is for generating electricity, and almost all of this in
thermal plants [1]. Consequently, about 20% of the total
U.S. energy consumption goes into waste heat of electric
generating stations. The possibility of recovering even a
small portion of this energy, perhaps the largest locally
concentrated source of waste heat, is attractive.

Unfortunately, the relatively low temperatures required in
conventional steam condensers preclude many utilization
schemes. Cooling water is typically heated by only about 14 C
in most plants. The present paper concerns the possibility

of alleviating these problems, while still deriving benefits, by discharging heated once-through cooling water from condensers directly into a municipal supply. The principal direct beneficial use of waste heat in this scheme is the savings in water-heater energy input. Perhaps equally important is the energy savings in using once-through cooling of power-plant condensers rather than closed-cycle cooling towers or cooling ponds which result in higher turbine back pressures, reduced thermal efficiency and greater fuel consumption. By-product benefits include alleviation of water-pipe freeze up in winter, and slightly elevated wastewater temperatures, which will reduce the cost of sewage treatment. Multiple use of water resources and the elimination of evaporative consumption in power-plant cooling are attractive in the larger view of conservation. Also significant is the elimination of local environmental effects of heat and humidity discharges to the atmosphere near the plant site.

Potential Energy and Water Conservation

About 4% of the U.S. energy consumption is due to residential and commercial water heating [2-4]. Overall efficiencies are currently 50-62% [5]. In newer gas units, the efficiency is about 72% less 1%/hour of storage while for electric it is 98% less 4%/hour [6.7]. The average per capita water consumption is 568 L/day [8]. Based on 33% thermal efficiency, 1 kw(e) per capita electrical consumption, and a 14-C rise in cooling water, the per capita condenser flow is 2990 L/day which is about 5 times the water supply rate. Thus only plants near filtration plants or water conduits need be utilized to preheat much of the water-supply capacity. Considering the increasing requirements of the Federal Water Pollution Control Act [9], increases in electrical demand and shortages of water [10, 11], multiple use of water resources is attractive.

Legal and Operational Problems

There appears to be no legal temperature restriction on discharges from power plants into municipal water supplies [12]. However, there are limits on Ph, residual chlorine, rust inhibitors, etc. as governed by the Safe Drinking Water Act [13]. Recent developments in anti-surface-tension agents allow the necessary chlorine dosages to be reduced to extremely low levels and still prevent biological fouling[14]. Chlorine is also added during water-supply treatment, and it is necessary to maintain a residual concentration throughout the distribution system for sanitary purposes. However, in the event of accidents involving contamination, provisions should be made to alert the filtration plant in order to adjust treatment or switch to an alternate supply. Indeed, the presence of a full-capacity back-up cooling system and an

alternate water intake for the municipality would be highly
desirable in order to avoid a combined shut down. According
to Oliker [15], a nuclear plant in Europe is currently
providing district heating, and more such plants are under
design and construction.

Typical power plants operate at 70-80% capability [16] whereas
municipal supplies are seldom out of service. The flow in
a municipal supply may peak on a daily basis at 150% of the
annual average and range on a hourly basis from 25-300% of the
daily average [4, 17]. While there are similarities in power
and water demand patterns, alternate stand-by systems would
be useful in matching requirements, in addition to providing
reliability.

Obtaining the necessary cooperation between the power and
water utilities would be facilitated in municipalities where
they are commonly owned and, ideally, commonly located.
If mechanical closed-cycle cooling is employed, such as
mechanical-draft towers and atmospheric sprays, operating
costs would be reduced for the private or public utility. In
any case, once-through cooling will increase thermal efficiency
and avoid de-ratings under extreme environmental conditions.
Therefore, there may be an economic advantage to the electric
utility to finance the venture. The advantage to the water-
supply system is essentially one of alleviating pipe freeze
up in winter in northern regions. No difficulty is anticipated
in handling water elevated by only 14 C or less, at least
in the northern U.S. The direct benefit to consumers is
reduced energy consumption for hot-water heating. Electric
utility rates could also be reduced, preferably in those areas
where the system is actually employed in order to further
offset the inconvenience of heated water in summer. Bottled-
water companies indicate that a family of four uses about 38
liters per month of water for drinking purposes which
could be refrigerated or simply left to stand in order to cool.

THERMAL EFFECTS

The present analysis is not all inclusive and many simplifying
approximations have been made. Further details are given in
Ref. 18.

Power Plant Efficiency

For the purpose of the evaluation, two modern double 1000-Mw(e)
boiler-turbine combinations were assumed, one nuclear [19]
and one fossil [20] fueled, since there is considerable
difference in thermal characteristics. The steam condensers

238

were analyzed using the NTU method and recommended design criteria of the Heat Exchanger Institute [21]. The sizes were fixed with a 13.9-C rise in cooling water temperature at the design point and required 2.23 and 4.41 ML/min (million liters/minute) of water coolant for fossil and nuclear fuel, respectively. Alternative atmospheric-spray systems, evaporative cooling towers and cooling ponds were sized according to simple one-parameter models [22, 23, 24] and meterological conditions [25,26] not exceeded more than 5% of the time during summer in Chicago. All three systems behaved similarly, and are represented here by a single hypothetical cooling system. the tabulated heat-rate data and the steam-condenser and cooling-sytem equations were solved iteratively [27].

Results are summarized in Table 1. The major interest for energy conservation is the advantage in heat rates of once-through cooling over that of closed-cycle systems. The savings range from 0.6-1.5% for fossil fuel and 1.5-2.5% for nuclear with the most advantage in summer. The annual savings is 1% for fossil fuel and 1.9% for nuclear, which is larger due to its lower efficiency. However, fossil fuel is usually far more expensive.

Transmission

If the plants are not co-located, transmission could be by buried pipe or open channel. Heat transfer from buried pipe is complex involving possible mass transfer due to thermal and moisture gradients and capillary action, which are all affected by the type of soil [28]. The heat transfer rate per unit length from a buried pipe of diameter d, depth D to the top of the pipe, temperature T, ground surface temperature T_G and thermal conductivity K_G is ideally $-S \; k_G(T-T_G)$ where S is the shape factor and $2\pi/S$ = arc cosh $(2D/d + 1)$ [29]. The thermal conductivity for soil typically ranges from 0.35 to 2.6 w/m-C [30]. Here k_G = 0.87 w/m-C is used. Therefore, an energy balance may be performed on the flowing water. The result is cooling of the mass flow rate $\dot{m}$ from temperature T_1 to T_2 over a length L. Thus

$$(T_2 - T_G)/(T_1 - T_G) = \exp(-S \; k_G \; L/(\dot{m} \; c_w)) \qquad (1)$$

where c_w is specific heat of water (4.19 kJ/kg -C).

In order to estimate the importance of the loss between the power plant and filtration plant, we assume average conditions in the Chicago area [17] where there are two filtration plants.

239

Each is assumed to receive half the total Chicago flow with T_1 = 26.7 C, T_G = 12.8 C, $\dot{m}$ = 1.94 x 10^9 L/d, d = 6.10 m, D^1= 3.05 m,and therefore S = 3.57. For example, the resulting temperature drop T_1 - T_2 = 0.07 C over a length L = 160 km. If open channel flow were used, the losses would be much greater. If each channel were 24 m wide, and we assume a surface exchange coefficient [24] of 35.5 w/m^2- C and a natural equilibrium temperature of 12.8 C, the temperature drop over only 16 km is 1.9 C. In the remaining analyses, we assume that the plants are either connected with large buried pipes or are co-located, such that no significant interconnection loss is present.

Filtration

Renn [31] has summarized the effects of increased temperature on municipal supplies. The rates of organic decomposition and activity of disinfectants are increased while pathogenic organisms survive shorter periods. The cost of all chemicals except alum used for coagulation is about $0.30/year on a per capita basis, or $1,350,000 for the entire Greater Chicago system [17]. Evaluation of possible savings is complicated by the effect of pH which often simultaneously changes with temperature. In the case of chlorine, the chemical dosage needed for disinfectant at the plant decreases but dosage to maintain a residual concentration throughout the system increases. The production of odorous blue-green algae is increased. The optimal temperatures of blue-green algae are 16-27 C while Chicago water is currently about 2-21 C. Applying a 14-C rise brings the Chicago range to 16-35 C, and odors would be favored in winter rather than summer. The effect of temperature on density and viscosity is such to favor settling and permit more rapid filtration. A detailed experimental study by Camp, Root and Bhoata [32] noted that the alum coagulant requirement at optimal pH was virtually unchanged with temperature. If so, no advantage in alum dosage can be claimed. Further, no advantage can be gained for the overall size of facilities because of the need for full capacity in the event of power-plant outages.

Distribution

Steady state operation is assumed, and the calculations are performed for average summer, spring-fall and winter conditions. It is assumed that the power plant elevates the ambient water by either 13.9 (high ΔT) for perfectly matched flows with maximum condenser heating or 8.3 C (low ΔT) which might represent conditions where there is a 60% load factor or a 40% dilution with ambient water. Ambient (T_i) and heated water (T_i + ΔT) temperatures are listed in Table 2. For the present calculations, the flow rates and distribution config-

uration of the City of Chicago were utilized [17]. The average Chicago system flow rate is 3.876 x 10^9 L/d with a seasonal adjustment, $\bar{m}/\bar{m}$(annual), shown in Table 2. Consideration of the City of Chicago system as a balanced series-parallel network resulted in the overall SL = 12,943 km. Temperature drops to the end of the system were computed to be nearly uniform at 0.7 and 0.4 C for high and low ΔT, respectively (Table 2).

Computations were also performed on a quasi-unsteady basis where steady conditions at 150% of the average steady flow rate were first analyzed. Then, water was presumed to stand for 8 hours (nightime) and the heat transfer was computed. Finally flow at 150% of the average rate was assumed for 16 hours. The system residence time is about 4 hours. The reduced temperature change during the periods of increased flow very nearly compensates for the transient heat transfer at night under stagnation conditions. The net reduction in elevated temperature ranged from only 0.3-0.8 C on the daily average [18]. The neglected heat capacity of the ground and pipes should reduce this effect even further.

Water Heater-Energy Savings

In the present section, we use one half the maximum distribution-system losses in order to simulate the average system condition.

First, we estimate the losses in the home from the intake point to the water heater. It is assumed for the sake of the present calculations that a single line carries the water to be heated over substantially the entire distance involved. For the purposes of estimating the above losses, we assume a 7.6 m long, 2.5-cm outside-diameter line carrying the water to be heated in the home. The standard correlation for horizontal pipes was employed [29] in order to determine the film coefficient for natural convection for the expected laminar-flow regime. Because most cold-water lines are presently insulated to avoid condensation and because reducing losses is favorable using preheated water, the use of insulation is assumed for both unheated and heated water.

The heat input to the water heater used directly for elevating water temperature is essentially proportional to the water temperature rise. This includes certain losses but not those associated with maintaining water temperature levels during storage. For the present calculations we use an average water-heater temperature setting of 62.8 C as given in the proposed U.S. water-heater test standards (Federal Register, October 4, 1977). The percentage savings in heat energy required to raise the water temperature (but not maintain it) by using preheated water are shown in Table 2. The annual average savings is 24% for the high ΔT and 14.5%

241

for the low ΔT. However, as discussed previously, there is an additional heat-energy input which is independent of preheating. The ratio of heat input including certain losses used to elevate water temperature (but not maintain it) to useful energy rise which actually increases the energy of water is $1/\eta_o$ where, according to the aforementioned Rheem Company data, $\eta_o = 0.72$ and 0.98 for gas and electric units, respectively. The overall heat input ratio is related to the service efficiency which includes a decay in efficiency due to losses during storage. Thus for a residence time t, the ratio of total heat input to useful energy rise is $1/\eta_o + 0.5t\, d\eta/dt$ on the average. Using the referenced rate of change of efficiency with storage residence time t, $d\eta/dt = -0.04$ and -0.01 hr^{-1} for new gas and electric units, respectively. Assuming a standard 151-liter tank and the flow rates of Table 2, the seasonal flow residence times t are 12.8, 15.6 and 16.3 hrs. for summer, spring-fall and winter, respectively. As a result, the ratio of heat-energy input required to elevate water temperature to total heat-energy input for service requirements, is found to be 0.64, 0.57 and 0.55 for gas in summer, spring-fall and winter, respectively, and about 0.93 for electric. The difference between gas and electric units is due to electric heaters being nearly 100% efficient in directly heating the water, whereas gas units have stack and other losses. The resulting savings in total heat input are given in Table 2. The annual average savings are reduced to 14% and 22%, for gas and electric units, respectively, with the high ΔT and 8% (gas) and 14% (electric) for the low ΔT. Assuming equal numbers of each type unit, the overall annual savings is 18% of total water-heater energy input for the high ΔT and 11% for the low ΔT.

Wastewater Treatment

Data were obtained from the Metropolitan Sanitary District (MSD) of Greater Chicago for flow rates and (unpreheated) temperatures of wastewater [33]. The data indicate that the average run-off water added is 38% of the Chicago water supply (Table 2). It is estimated that the run-off water is added at approximately the air temperature (Table 2). Measured wastewater temperatures were 22.8, 18.9 and 14.3 C, respectively, for summer, spring-fall and winter. The City of Chicago sewer system using unpreheated water was analyzed for heat transfer based on the flow and temperatures after the aforementioned run-off water was added. This was done using the shape-factor method and an equivalent full-flow pipe diameter for each section based on the estimated average six tenths of full flow probably encountered. The resultant temperatures at the average intake to the sewer system, including run-off water, were computed as 22.9, 19.3 and 15.1 C, respectively, for summer, spring-fall and winter. Subtracting the effect of run-off water, the

242

corresponding user discharge temperatures were found to be quite uniform at 22.8, 22.8 and 21.6 C, respectively. Indeed, the data seem to show that the water comes to essentially equilibrium at the user environmental temperature. It is not clear how much the water would have to be preheated before being discharged at elevated temperatures. Based on the temperature data of Table 2 for the average intake to the user $\bar{T}_o$ and based on 22% of the flow being heated to 62.8 C in the water heater [4], the resultant mixed flow of heated and unheated water apparently was cooled 7.2 C in summer and was heated 1.8 and 6.6 C, respectively, in spring-fall and winter. These increments can be approximated by a straight line versus the average intake water temperature $\bar{T}_o$. The computations were repeated using preheated water and the same function, resulting in annual average increases in wastewater temperatures of 0.8 and 0.2 C, respectively, for high and low ΔT.

CASE STUDIES

At Henderson, Kentucky [34], located on the Ohio River, local conditions made construction of new water intakes very expensive for a new filtration plant. Instead, the discharge from an existing municipal power plant on the same site was used successfully. Serving a 17,000 population, the filtration plant employs walking beam flocculators and rake-type sludge collectors. Chemicals added include hydrated lime and dry aluminum sulphate for coagulation and color and turbidity removal. Chlorine for disinfection and taste and odor control, activated carbon for taste and odor control, and sodium silicofluoride for fluoridation are added at one or more points in the system. At Edmonton, Alberta (Canada) a power-plant discharge at an average of 18 C is blended with 0.6 C river water in order to produce an intake averaging 13 C all winter [35]. An average flow of 227 ML/da serves a population of 550,000. The use of heated water has minimized the occurence of water-main breaks and virtually eliminated domestic freeze-ups.

REFERENCES

1. "Energy in Focus, Basic Data", Federal Energy Administration, Washington, DC, May 1977.
2. Behrens, C., "AHAM Offers Energy Savings to the Public", Appliance Manufacturer, Vol. 22, No. 10, p. 80-82, October 1974.
3. Rimberg, D., Utilization of Waste Heat from Power Plants; Noyes Data Corp., Park Ridge, NJ, 1974.

4. Kammerer, J. C., "Water Quality Requirements for Public Supplies and Other Uses", Handbook of Water Resources and Pollution Control, Van Nostrand Reinhold Co., New York, 1976.
5. Babbitt, H., Plumbing, McGraw-Hill, New York, 1960.
6. Rheem Manufacturing Co., Private Communication to R. Wynn by Mr. Haag, Engineer, Chicago, December 29, 1977.
7. Consdorf, A. P. and Behrens, C., "Appliance Energy Efficiency: The Trials of a Test", Appliance Manufacturer, Vol. 25, No. 3, 40-59, March 1977.
8. Beall, S., "Uses of Waste Heat", ASME Paper 70-WA/Ener-10, 1970.
9. "Federal Water Pollution Control Act Amendments of 1972", United States Code, Public Law 92-500, October 18, 1972.
10. Parker, F. L. and Krenkel, P. A., Physical and Engineering Aspects of Thermal Pollution, CRC Press, Cleveland, 1970.
11. Norton, R. C., Westre, W. J. and Larsen, G. L., "Dry Cooling Design Characteristics of a Large Power Plant", Proceedings of American Power Conference, Vol. 37, p. 591-597, 1975.
12. Lum, J., Private Communication to R. Wynn, U.S. Environmental Protection Agency, January 10, 1978. See also Federal Register, Vol. 39, No. 196, pp 36186-36207, October 8, 1974.
13. "Safe Drinking Water Act", United States Code, Public Law 93-523 (1974). See also Interim Primary Regulations in Federal Registers of March 14, 1975, December 24, 1975, July 9, 1976 and July 11, 1977.
14. Grier, J. C. and Roensch, L. F., "The Achievement of Slime Control in Utility Condensers without Impairing Discharge Water Quality", Proceedings of American Power Conference, Vol. 39, 1978 (to be published).
15. Oliker, I., "Cogeneration Power Plants Serve District Heating Systems", Mechanical Engineering, Vol. 100, No. 7, p. 24-29, July 1978.
16. Spencer, D. and Gildersleeve, O., "Market Potential for New Coal Technologies", EPRI Journal, Vol. 3, No. 4, p. 19-26, May 1978.
17. Pavia, R. A., "Annual Report 1976 Operating Statistics", City of Chicago, Department of Water and Sewers, Chicago, 1977.
18. Wynn, R. A. Jr. and Porter, R. W., "Beneficial Use of Waste Heat in Municipal Water Supplies", IIT Waste Energy Management Report (in preparation).
19. "Heat Rates for Fossil Reheat Cycles Using General Electric Steam Turbine-Generators 150,000 kw and Larger", General Electric Steam Turbine-Generator Products Division, Schnectady, NY, February 1974.
20. Ortolano, L. and Smith, F. A., "Costs of Thermal Effluent Standards for Power Plants", Journal of the Power Division, ASCE, p. 15-31, July 1974.

21. Steam-Its Generation and Use, Babcock and Wilcox Co., New York, p. 6-18, 1972.
22. Porter, R. W. and Chaturvedi, S., "Atmospheric Spray-Canal Cooling Systems for Electric Power Plants", Proceedings of Waste Heat Management and Utilization Conference, Vol. 2, University of Miami, p. IV-C-121 to 161, May 1977.
23. Fraas, A. P. and Ozisik, M. M., Heat Exchanger Design, Wiley, NY, p. 241-255, 1965.
24. Lorenzi, D. L. and Porter, R. W., "Simplified Analysis of Surface Energy Exchange from Heated Bodies of Water", ASME Paper, WAM, December 1978.
25. Bennett, I., "Monthly Maps of Mean Daily Insolation for the United States", Solar Energy, p. 145-158, July-Sept. 1965.
26. Ruffner, J., The Weather Almanac, Gale Research, Detroit, 1974.
27. Rao, D. and Porter, R. W., "Effect of Alternate Cooling Systems and Beneficial Use of Waste Heat on Electric Power Plant Performance, IIT Waste Energy Management Report (in preparation).
28. Baladi, J. Y., Schoenhals, R. J. and Ayers, D. L., "Transient Heat and Mass Transfer in Soils", ASME Paper 78-HT-31, May 1978.
29. Holman, J., Heat Transfer, McGraw-Hill, NY, 1976.
30. Kreith, F., Principles of Heat Transfer, Intext, NY, 1973.
31. Renn, C. E., "Warm Water Effects on Municipal Supplies", Journal of the American Water Works Association, Vol. 49, p. 405-413, April 1957.
32. Camp, T. R., Root, D. A. and Bhoota, B. V., "Effects of Temperature on Rate of Floc Formation", Journal of the American Water Works Association, Vol. 32, 1913-1927, November 1940.
33. Lue-Hing, C., Metropolitan Sanitary District of Greater Chicago, Private Communication to A. Obayashi, April 1978.
34. Highland, J. T., "Power Plant Cooling Water Provides Domestic Supply", Public Works, p. 101-104, November 1962.
35. Gyurek, L., Private Communication to R. Porter, The City of Edmonton, Alberta, Canada, Water Treatment Plants, January 6, 1978.

Table 1. Comparison of Seasonal Performance of Typical
2000 Mw(e) Power Plants with Alternate Cooling near Chicago.

	Fossil Fuel		Nuclear Fuel	
	Once-through	Closed-cycle	Once-through	Closed-cycle
Summer				
Condenser Intake(C)	23.2	29.9	23.2	29.9
Turbine Back Pres.(k P_a)	7.6	10.5	7.6	10.5
Thermal Efficiency(%)	43.4	42.8	31.7	30.9
Savings in Heat Rate(%)	1.5	-	2.5	-
Spring Fall				
Condenser Intake(C)	13.3	25.7	13.3	25.7
Turbine Back Pres.(k P_a)	4.2	8.5	4.2	8.5
Thermal Efficiency(%)	43.6	43.2	32.1	31.5
Savings in Heat Rate(%)	0.9	-	1.8	-
Winter				
Condenser Intake(C)	1.4	22.5	1.4	22.6
Turbine Back Pres.(k P_a)	3.4	7.3	3.4	7.3
Thermal Efficiency(%)	43.7	43.4	32.2	31.7
Savings in Heat Rate(%)	0.6	-	1.5	-

Table 2. Steady-State Data for Unpreheated and Preheated
Water Supply Based on Chicago Configuration. (Bracketed data
refer to high initial ΔT = 13.9 C (Upper) and low initial
ΔT = 8.3 C (lower).)

	Summer		Spring-Fall		Winter	
	Unheated	Heated	Unheated	Heated	Unheated	Heated
Ambient Water T_i(C)	21.1	21.1	9.4	9.4	0.6	0.6
Intake T_i + ΔT(C)	21.1	[35.0 / 29.4]	9.4	[23.3 / 17.8]	0.6	[14.4 / 8.9]
Ground T_G(C)	20.0	20.0	10.6	10.6	2.2	2.2
ṁ/ṁ(annual)	1.17	1.17	0.96	0.96	0.92	0.92
Supply Discharge T_o(C)	21.1	[34.3 / 29.0]	9.5	[22.6 / 17.3]	0.7	[13.7 / 8.5]
Distribution Max ΔT(C)	0.0	[-0.7 / -0.4]	0.1	[-0.7 / -0.5]	0.1	[-0.7 / -0.4]
Overall Max ΔT(C)	0.0	[13.2 / 7.9]	0.1	[13.2 / 7.9]	0.1	[13.1 / 7.9]
Avg. User Intake $\bar{T}$(C)	21.1	[34.6 / 29.2]	9.4	[22.9 / 17.6]	0.6	[14.1 / 8.7]
Water-Heater Inlet T_c(C)	21.1	[33.4 / 28.5]	10.7	[22.7 / 17.9]	2.9	[14.9 / 10.1]
Water-Heater Flow (L/d)	285	285	233	233	223	223
Useful-Energy Savings (%)	-	[30 / 18]	-	[23 / 14]	-	[20 / 12]
Gas-Heater Savings(%)	-	[19 / 11]	-	[13 / 8]	-	[11 / 7]
Electric-Heater Savings(%)	-	[28 / 17]	-	[21 / 13]	-	[18 / 11]
User Discharge(C)	22.8	[24.8 / 24.2]	22.8	[23.5 / 22.6]	21.6	[22.5 / 21.9]
Run-Off(C)	22.8	22.8	10.6	10.6	0.6	0.6
ṁ(run-off)/ṁ(supply)	0.27	0.27	0.40	0.40	0.47	0.47
Initial Sewer(C)	22.9	[24.5 / 24.0]	19.3	[19.8 / 18.9]	14.9	[15.6 / 15.2]
Final Sewer(C)	22.8	[24.3 / 23.8]	18.9	[19.4 / 18.6]	14.4	[15.1 / 14.6]

Title: Super Greenhouse Project Utilizing Waste Heat from Astoria #6
         Thermal Power Plant*

Author: R. G. Reines

Abstract:

    The energy demands for heating greenhouses in the Northeastern Region
of the United States has increased significantly in the past 3 years. This
has created interest in means to both conserve energy in greenhouses as well
as search for alternative sources of heat. Presently, greenhouse heating
systems convert high quality fossil energy to provide the temperature
portion of the energy requirements for photosynthesis. The notion that
discharge temperatures from thermal power plants are relatively coincident
with botanical temperature requirements, creates a potential large scale use
of low quality energy now discarded at all thermal power plants in New York
State. Traditional utilization of waste heat for greenhouses has been from
thermal power plants which rely on cooling towers rather than once through
cooling. Little work has been done on the investigation of using once
through power plants as potential sources of heat for greenhouses due to
low temperature heat that is available. The purpose of this discussion
paper is to present a conceptual design of a super greenhouse utilizing
waste heat from a thermal power plant, Astoria Unit #6, in Astoria, New York.

    This paper will include considerations in economic and energy require-
ments of new low cost energy efficient greenhouse design and new low cost
heat exchanger configurations which would utilize this low quality heat.

In addition, potential energy and economic impact and scenarios of
implementation of large scale utilization of super greenhouses utilizing
waste heat in New York State will be discussed.

Author Affiliation:

Department of Agricultural Engineering, Cornell University
(now with ILS Laboratory, Tijeras, New Mexico)

*This paper was not presented.

EXPERIENCE WITH THE NEW MERCER
PROOF-OF-CONCEPT WASTE HEAT AQUACULTURE FACILITY

Bruce L. Godfriaux,[1] Robert R. Shafer[2]
Albert F. Eble,[3] Mark C. Evans[3] Tom
Passanza,[3] Connie Wainwright,[3] and
Hal. L. Swindell,[3]

ABSTRACT

At the First Waste Heat Management and Utilization Conference, a paper was given that summarized the results of our pilot waste heat aquaculture research program and explained the concept of sequential (diseasonal) aquaculture. The design of a proposed proof-of-concept aquaculture facility was also discussed. This design was subsequently modified.

In April, 1978, construction of the modified Mercer Proof-of Concept Aquaculture Facility was completed. Facility process water can be derived wholly or in part from five sources: generating station discharge water, ambient river water, well water, tempering pond (reservoir) water, and recirculated facility process water. The operation of the overall system is discussed.

Results through the use of this system for the rearing of rainbow trout, Salmo gairdneri, (Richardson), completed on June 6, 1978, in addition to the results to date (August, 1978) for the other species presently being cultured at the facility are discussed. These species include the American eel, Anguilla rostrata, (Lesueur) and channel catfish, Ictalurus punctatus (Rafinesque). Projected harvest densities for the latter two species are briefly outlined.

[1] Public Service Electric and Gas Company, Newark, NJ

[2] Buchart-Horn: Consulting Engineers, York, PA

[3] Trenton State College, Trenton, NJ

INTRODUCTION

The proposed new proof-of-concept waste heat aquaculture fac-
ility was described in [1] given at the First Conference on
Waste Heat Management and Utilization in May 1977. Since
then the Mercer Proof-of-Concept has been built and operated
for some five months as of August 1978.

Several modifications have been made to the original proposed
design due to monetary constraints and site specific charac-
teristics which were only discovered after aquaculture facility
construction commenced. These modifications are briefly des-
cribed later in the "Introduction" section of this paper.

The Mercer Aquaculture Facility (Fig. 1) at the Public Service
Electric and Gas Company Mercer Generating Station is four
miles south of Trenton, New Jersey, on the Delaware River. The
station which is coal-fired, generates some 600MW of power and
discharges approximately 1.7 million liters per minute of
heated discharge water at a maximum of $6^{\circ}C$ above the ambient
Delaware River water temperature.

The recently constructed Mercer Proof-of-Concept Aquaculture
Facility is shown in Fig. 2, with piping layout. Changes
in the constructed facility as compared to the proposed fac-
ility as described in [1] include the elimination of two
outdoor concrete raceways 30.5 m long x 2.4 m wide by either
2.4m or 1.2 m deep and the substitution of six 12.2 m long
x 1.8 m wide x 1.2 m deep nursery raceways by two nursery
raceways 18.3 m long x 1.8 m wide x 1.2 m deep. Also, a
recirculation chamber was added to the temperature moderation
pond (Fig. 2). The chamber is really the "heart" of
the new facility and allows aquaculture personnel tremendous
flexibility in using and blending different water sources.
The function and operation of this structure will be described
in greater detail later in the paper and in [2].

Other modifications in the constructed facility from the pur-
posed facility include the elimination of separate piping
for well water to raceways/ponds and the elimination of the
aeration lagoon in the waste treatment system for the process-
ing of raceway/pond cleaning wastes. One of the originally
purposed 5,700 liters/min discharge canal intake pumps was
also eliminated, since two of the originally proposed main
grow out raceways were dropped. The aforegoing modifications
were required when the bids on the proposed facility were
higher than anticipated.

After the wells were drilled, it was discovered that the well
water contained extremely high levels of iron (17 to 23 ppm)

and manganese (3·5 to 3·8 ppm). This proved toxic to trout, and plans to set up a trout hatchery have been postponed until such time or a suitable treatment method for the removal of iron and manganese from the well water can be determined. Without the well ater, trout cannot be reared all year round at the Mercer Aquaculture Facility. During the summer months the only cool water source for trout culture was well water.

DESIGN, LAYOUT AND OPERATION OF THE MERCER PROOF-OF-CONCEPT AQUACULTURE FACILITY

The facility is a combination of previously existing pilot facilities as described by Godfriaux et. al. [3] and shown in Figure 2 by hatching, and recently completed proof-of-concept facilities.

DESIRED OPERATIONAL FEATURES

From the experience of a pilot research program in the utilization of heated condenser cooling water in aquaculture, it was discovered that when the generating station cooling water was chlorinated, it proved toxic to rainbow trout. Subsequently, all aquaculture facility intake pumps withdrawing station discharge canal water were stopped automatically during this period.

This discontinuous aquaculture process flow proved to be the limiting factor in obtaining high density trout production due to the rapid depletion of dissolved oxygen in the process water. This problem was accentuated since discharge water temperatures and the trout biomass increased through the spring season.

For the present proof-of-concept facility, a continuous process flow was desired through the chlorination cycles of the generating station. This could be achieved by recirculating the existing aquaculture facility process water entirely during these periods, adding additional non-chlorinated heated discharge water to the aquaculture facility from a storage reservoir area (tempering pond - see Fig. 2) or by adding ambient river or well water (now not feasible) during the station chlorination period or any combination of the above.

RECIRCULATION CHAMBER

This was designed to provide a continous flow of process water to the aquaculture facility even during generating station chlorinations periods. In addition, the recirculation chamber allows aquaculture facility personnel to use singly or in

combination generating station discharge water,ambient temperature Delaware River water, aquaculture facility process water (through recirculation) or tempering pond (reservoir) water.

The design and operation of the recirculation chamber is shown in Figure 3. Under normal operations, water from the river, station,discharge canal and well is pumped into the tempering pond for mixing and blending. The tempering pond overflows the distribution chamber inlet weir. The water then flows by gravity to the various aquaculture facility raceways, ponds and laboratories. When flow into the tempering pond is less that the outflow from the distribution chamber, the water level begins to fall in the distribution chamber upending the float switches (Fig. 3). This triggers the operation of the submersible, recirculation pumps. If the water level of the distribution chamber falls below the level of the bypass chamber, them a checkvalve opens allowing the effluent aquaculture process water to flow into the distribution chamber for circultion. At the same time, a restricted flow of new water continues to flow from the tempering pond through the tempering pond drain into the distribution chamber even though the tempering pond water level is below the level of the distribution chamber inlet weir (Fig. 3).

Once normal flow is restored to the tempering pond, the tempering pond water level rises and eventually overflows the distribution chamber inlet weir. The water level within the distribution chamber rises and the checkvalve to the bypass chamber closes. Next,the float switches are immersed in the water and this turns off the recirculation pumps. Water flow to the aquaculture facility then returns to normal operation by gravity flow. For further detailed information on the disign and operation of the recirculation chamber, see [2].

FACILITY PUMP AND PIPING SYSTEM

Figure 4 shows a simplified flow schematic of aquaculture facility process water system. Most facilities only receive the blended water from the tempering pond. However, the nursery raceways not only receive blended water, but also river ambient, well water (not being used at the present time) and supplementary heated water from the heat exchanger. These additional water sources were provided to the nursery raceways, since they would often be rearing juveniles of species that would be"out-of-season" in the main grow out raceways and would require water sources with different temperature regimes. Therefore,trout fry and fingerlings would require cool water during the summer months and American eels, shrimp

250

<u>Macrobrachium</u> <u>rosenbergii</u> and catfish would require warm, heat exchanger water during the winter months for growth.

All waste aquaculture facility process water is routed back to the bypass chamber of the recirculation chamber for possible re-use before being discharged to the generating station discharge canal.

AERATION SYSTEM

Subsequent to the writing of the first paper [1], an aeration system with two Gardner-Denver positive displacement blowers, each capable of delivering 5.23 m ^{3}/min of air at 9 psig were installed as part of the proof-of-concept aquaculture facility. A supplementary of pure oxygen bubbling system was also installed for use during emergencies. Gaseous oxygen is introduced into the raceways via Schramm bioweve diffusers fitted to a liquid oxygen container. Further, the regulator of the oxygen container was fitted with a solenoid valve that was opened by the same pulse that triggered the generating station chlorine program.

By November 1978,we expect also to have installed a sidestream oxygen injection system. The reason this system will be needed is to supply additional oxygen when catfish and rainbow-trout start approaching densities of 190 kg/m^3. The water flow alone to the main grow out raceways will not supply sufficient dissolved oxygen at these rearing densities.

With the sidestream oxygen injection system, a predetermined quantity of water from the supply line,feeding each raceway is further pressurized, thereby increasing the water dissolved oxygen carrying capacity. Gaseous oxygen from a nearby liquid oxygen storage container is injected into the pressurized water which is then injected at different points in the rearing ponds and raceways.

WATER MONITORING AND ALARM SYSTEM

An alarm system is used to provide notifications to the aquaculture project manager, the generating station control operator (in the power plant control room), and outside aquaculture personnel in the event of any abnormal environmental conditions in the project. The various parameters are being monitored (water temperature, water pressure), by Asco temperature and pressure switches. When a reading is out of bounds, they activate electrical switching devices. The electrical output of these devices is sent to a common control relay. This relay is used to initiate an electronic telephone dialer system. The telephone dialer uses a pre-recorded

magnetic tape cartridge that contains telephone numbers and a message. It is used to call and inform outside people that an alarm condition exists. The dialer system is a modification of a commercially available system made by Dryton, Inc. for fire and security uses in residential and industrial applications.

AQUACULTURE WASTE WATER TREATMENT

As stipulated in the EPA Draft Development Document for Proposed Effluent Limitations Guidelines and New Source Performance Standards for the Fish Hatcheries and Farms (1974) [4], process water flow may be discharged directly back into the water source. However, water used for raceway cleaning should be settled (particulates removed) before effluent is returned to receiving waters. The waste settling basin shown in Figure 2 was constructed for removing particulates from raceway cleaning waters.

CHLORINE CONTROL SYSTEM

The Fisher-Porter chlorine control equipment has been modified to include an electrical interlock with the heated discharge water intake pumps. The operation of the interlock system depends on the opening of the chlorine dilution water valve. Upon activation of the control relay for the dilution water valve, an auxiliary relay causes the heated discharge water pump contactor to open thereby stopping the pumps. An additional feature of this system is the ability to operate only one pump at a time or to override the system completely in the manual mode.

SEQUENCE OF CULTURE OPERATIONS

Due to the large seasonal temperature fluctuation in the Delaware River from $0^{o}C$ to $31^{o}C$ in addition to a maximum of $6^{o}C$ thermal increment from the Mercer Generating station, both a warm and cold water fish species were selected to be reared during the warmer and colder seasons of the year. This new aquaculture concept is called "diseasonal aquaculture". The initial species selected for culture were rainbow trout Salmo gairdneri (cold water species) and the freshwater shrimp (Macrobrachium rose bergii).

However, a venture analysis [5] indicated that the production level from Macrobr chium rosenbergii would not be sufficient to cover operating expenses. Therefore, starting in July 1978, channel catfish Ictalurus punctatus is being experimentally

cultured at high densities to determine suitability both bio-
logically and economically as the replacement warm water
species.

Figure 5 shows the sequence of rainbow trout and catfish cul-
ture operations through the year. This schedule is idealized
at the present time, since the facility well water can not
be used due to its high iron and manganese content. There-
fore trout culture during the summer months can not take
place at the Mercer Aquaculture Facility. However, this cycle
as shown would be followed during the warmer months for trout
at any off-site trout hatcheries which might be developed in
the near future.

CULTURE RESULTS WITH NEW AQUACULTURE FACILITY
RAINBOW TROUT AND CHANNEL CATFISH

From the beginning of April to August 16, 1978, the recirc-
ulation chamber has been fully operational. During this period
rainbow trout and channel catfish were being reared in two
concrete raceways, each 30.5m x 3.6m by either 1.2m or 1.8m
deep. These raceways were divided longitudinally and rainbow
trout were placed in one side of each raceway. With catfish
the raceways were divided transversely and the catfish were
placed in the upper end of each raceway. The deep raceway
was supplied with a process water flow rate of 5,700 liters/
min. (1,500 GPM) and the shallow raceway received 2,600
liters/min. (700 GPM). Density of rainbow trout during this
two month period varied from $26.7kg/m^3$ (1.7 lbs./ft.^{3}) at
stocking to $51.1kg/m^3$ (3.2 lbs./ft^3) at harvest. Catfish
density to date has varied between $13.2kg/m^3$ (0.8 lbs./ft.^{3}
to $14.8kg/m^3$ (0.9 lbs./ft^3).

Initially, at the beginning of April, when rainbow trout were
cultured, ambient river water temperatures were sufficiently
low that only heated discharge water from the generating sta-
tion was used (TABLE 1). During the chlorination period, pro-
cess effluent water from the aquaculture facility was recir-
culated with the addition of new, fully oxygen saturated water
via the 25cm. line from the adjacent tempering pond (Fig.
3). This arrangement kept dissolved oxygen values above 5
ppm at the discharge end of both raceways during this period.

By the beginning of May (TABLE 1), the ambient water temper-
atures had risen to a level that temperature moderation of the
station heated discharge water was required for trout culture.
During this period 7,200 liter/min. (1,900 GPM) of water
from the station discharge canal was blended with 1,900 liters/
min. (500 GPM) of ambient river water. During station chlor-
ination periods the discharge canal pumps were shut down and

a 5,700 liter/min. (1,500 GPM) recirculation pump was automatically activated. During the chlorination periods the 1,900 liters/min. ambient river pump was left running. Since part of the process flow rate was recirculated and the flow rate was reduced during the recirculation period, pure oxygen was bubbled in through a 2cm diameter PVC pipe alone the bottom of each raceway.

Slightly later in May (not shown in TABLE 1), another 1,900 liters/min. ambient river pump was added to further dilute the heated discharge water from the Mercer Generating Station.

By May 15th, with increasing Delaware River ambient water temperatures, the heated discharge water intake pump was shut down and only the ambient river pumps (3,800 liters/min.) were left running. A 5,700 liter/min, recirculation pump was also brought into service and left running constantly until trout harvest on June 5 and 6, 1978. TABLE 1 indicates that with a combination of fresh ambient river water blended with recirculated process water, dissolved oxygen values were maintained above 5.8 ppm at the discharge end of each raceway during this period before harvest . During this period, however, the lower two-thirds length of each raceway was continuously aerated by a 7.5cm diameter PVC pipe supplied with air at 9 psig from 185 ft.^{3}/ min . Gardner-Denver positive displacement blower (Model 5PDR6).

It was also noted that as the effluent water from each raceway dropped over the weir boards, the water picked up between two and three ppm of dissolved oxygen.

On July 11, 1978, some 60,000 17 to 20cm long catfish fingerlings were delivered to the Mercer Aquaculture Facility from Arkansas. Approximately 3,000 were lost due to the handling stress of the long journey. There have been some disease problems including infestations of Epistylis. On July 28, 1978 during a formaldehyde treatment for Epistylis approximately 7,000 additional catfish were killed. The reasons for this were not readily apparent. The treatment was effective in eliminating the Epistylis infestation. However, we are now having bacterial infections of Aeromonas and Pseudomonas which is being treated with Terramycin mixed in the catfish feed.

TABLE 2 shows operational data for the aquaculture facility during the catfish culture period to date (August 16, 1978). The reason that the catfish biomass has not increased over the one month culture period is that there has been mortalities of approximately 11,000 catfish of 60,000 originally stocked.

One reason for the higher incidence of disease among catfish than we originally expected is that since July we have on a partial water recirculation mode. This has been due to two reasons: the ambient river water temperature plus thermal increment from the generating station has resulted in the station discharge water being higher that the catfish optimam growth temperature, and our new 5,700 liter/min. (1,500 GPM) discharge canal intake pump unexpectedly broke down. Both ambient river and remaining discharge canal water flows are not sufficient to meet agriculture process water flow requirements. Thus, partial recirculation of aquaculture process is required .

STRIPED BASS AND EELS

Approximately 6,000 5cm long striped bass fingerlings weighing 3.2kg were picked up from Edenton National Fish Hatchery in Edenton, North Carolina on June 28, 1978. Remaining fish as of August 8, 1978 now weigh 12.7kg and vary in length from 6cm to 10cm. Mortality rate to date has been 2,562 fish or 42.7%. All mortalities have been attributed to fungal infections of Saprolegnia. Treatments to control these infestations have been with formaldehyde at 125 ppm for one hour. Feeding of striped bass has consisted of 35% protein trout feed four times per day every two hours at 6.9% of their total body weight.

On April 4, 1978, some 3,000 to 3,500 early juvenile eels 1g to 2g in weight were received at the Mercer Aquaculture Facility. An additional 15,500 juvenile eels were delivered to the facility on May 27, 1978 and placed in the nursery raceways (Fig. 2) for grow out. At the present time (August 15th) the juvenile eels weigh on average approximately 10g each. Projected goals for the grow out of eels are to realize harvest densities of 35 to 50kg/m^2 in the nursery raceways. We hope to harvest 8,250 eels at 200g each over a time period of 8 to 10 months with a cumulative mortality of 50-55%

DISCUSSION AND CONCLUSIONS

The new Mercer Proof-of-Concept Aquaculture Facility has given aquaculture personnel great versatility in maintaining various operational modes at the installation. This operational flexibility of the Mercer Proof-of-Concept Aquaculture Facility is made possible by the recirculating chamber. Over the first five months of use, the recirculation chamber has allowed aquaculture facility personnel to choose between a wide variety of operating options by selecting the blend and source of aquaculture facility process water. This has allowed for the maintenance of water temperatures as near optimum as possible for the culture of species being reared

at the time. These operating options are listed below.

1. Use of heated discharge water only
2. Use of ambient river water only
3. Blend (in varying proportions) of ambient and station discharge waters
4. Recirculation of any of the above waters
5. Recirculation of any of the above waters with additional water from the adjacent tempering pond which acts as a temporary water storage reservoir
6. Partial recirculation of process water with balance of required facility process flow coming from one or both of the above water sources (discharge or ambient river water)

Another attractive feature of the proof-of-concept aquaculture system is that it can maintain process flow by gravity for 30 to 60 minutes by using the tempering pond water supply in the event of an electric power failure. We temporarily lost electric power to the aquaculture facility for 20 minutes. This feature was greatly appreciated at the time.

Results with rainbow trout culture which achieved densities up to $50.9 kg/m^3$ indicate that water flow rates alone will not supply sufficient dissolved oxygen if trout and catfish harvest densities are nearly quadrupled to $178.2 kg/m^3$. A supplementary oxygenation through a sidestream oxygen injection system will be required.

To date channel catfish have shown greater susceptability to disease than rainbow trout with consequent higher mortality rates. The initial long truck journey from Arkansas to New Jersey no doubt severly stressed these fish. It can not be determined at the present time whether transportation stress is responsible for a good portion of the disease outbreaks with catfish.

ACKNOWLEDGMENTS

REFERENCES

1. Guerra, C. R., B. L. Godfriaux and C. J. Sheahan 1977:
    Utilization of waste heat from power plants by sequential
    culture of warm and cold weather species in (Lee, S. S.
    and S. Sengupta (Eds.) Proceedings of the Conference
    on Waste Heat Management and Utilization, Vol. 2,
    May 9-11, 1978 in Miami Beach, Florida. pp. V-C-213
    to V-C-232.

2. Godfriaux, B. L. and R. R. Shafer in press: A method
    of maintaining aquaculture process flow during chlorina-
    tion of electric generating station cooling water. in
    (Godfriaux, B. L. et al, eds.) Proceedings of Power
    Plant Waste Heat Utilization in Aquaculture - Workshop II,
    March 29-31, 1978, Rutgers University.

3. Godfriaux, B. L., H. J. Valkenburg, A. Van Riper and
    C. R. Guerra 1975: Power plant heated water use in
    aquaculture in Proceedings of the Third Annual Pollution
    Control Conference of the Water and Wastewater Equipment
    Manufacturer's Association, April 1-4, 1975. pp. 233-50.

4. Schneider, R. F. 1974: Development document for proposed
    effluent limitations guidelines and standards of per-
    formance for the fish hatcheries and farms. Prepared
    by the Environmental Protection Agency, Office of Enforce-
    ment, National Field Investigations Center, Denver,
    Colorada. 237 p.

5. Godfriaux, B. L., C. R. Guerra and R. E. Resh 1977:
    Venture analyses for intensive waste heat aquaculture.
    in (Avault, J. W., (eds) Proceedings of the Eighth
    Annual Meeting of the World Mariculture Society,
    January 9-13, 1977, San Jose, Costa Rica. pp. 707-22.

Raceway	Date	Dissolved Oxygen (ppm) Raceway Inlet	Raceway Outlet	Process Water Source liters/min. (GPM) Discharge Canal	Ambient River	Recirculation	Trout Biomass kg/m^3	$lbs./ft.^3$	Process Flow Temperature $(C°)$
Shallow	4/7/78	10.4	7.4	9,100 (2,400)	-	-	33.0	2.0	13.9
Shallow	4/7/78[a]	10.2	8.9	-	-	5,700 (1,500)	33.0	2.0	13.9
Deep	4/7/78	10.4	8.0	9,100 (2,400)	-	-	35.0	2.2	14.0
Deep	4/7/78[a]	10.4	9.5	-	-	5,700 (1,500)	35.0	2.2	14.0
Shallow	5/6/78	10.2	6.5	7,200 (1,900)	1,900 (500)	-	43.9	2.7	15.0
Shallow	5/6/78[a]	8.7	6.1	-	1,900 (500)	5,700 (1,500)	43.9	2.7	15.0
Deep	5/6/78	10.2	4.5	7,200 (1,900)	1,900 (500)	-	43.2	2.7	15.0
Deep	5/6/78[a]	8.4	4.4	-	1,900 (500)	5,700 (1,500)	43.2	2.7	15.0
Shallow	5/21/78[b]	9.6	5.8	-	3,800 (1,000)	5,700 (1,500)	50.9	3.1	17.4
Deep	5/21/78[b]	9.6	5.8	-	3,800 (1,000)	5,700 (1,500)	51.1	3.2	17.5

[a]Pure oxygen was bubbled through 2cm diameter PVC pipe at the bottom of each raceway during water recirculation periods.

[b]The lower two-thirds length of each raceway was continuously aerated by a 7.5cm diameter PVC pipe supplied with atmospheric air at 9 psig from $5.25m^3$/min. positive displacement blower.

259

| Raceway | Date | Dissolved Oxygen (ppm) | | Process Water Source liters/min. (GPM) | | | Catfish Biomass | | Process Flow Temperature (C°) |
		Raceway Inlet	Raceway Outlet	Discharge Canal	Ambient River	Recirculation	kg/m³	lbs./ft.³	
Shallow	7/12/78	7.2	6.8	5,700 (1,500)	3,800 (1,000)	11,300 (3,000)	7.4	0.4	28.0
Deep	7/12/78	7.2	6.6	5,700 (1,500)	3,800 (1,000)	11,300 (3,000)	14.5	0.9	28.0
Shallow	8/1/78[a]	8.4	7.4	3,000 (800)	3,800 (1,000)	11,300 (3,000)	9.2	0.6	25.0
Deep	8/2/78[a]	7.5	6.2	3,000 (800)	3,800 (1,000)	11,300 (3,000)	14.7	0.9	24.0
Shallow	8/17/78[a]	7.4	5.9	3,000 (800)	3,800 (1,000)	11,300 (3,000)	9.7	0.6	29.0
Deep	8/17/78[a]	7.2	4.5	3,000 (800)	3,800 (1,000)	11,300 (3,000)	18.9	1.2	29.0

[a]Pure oxygen was bubbled through 2cm diameter PVC pipe at the bottom
of each raceway.

69-74&75
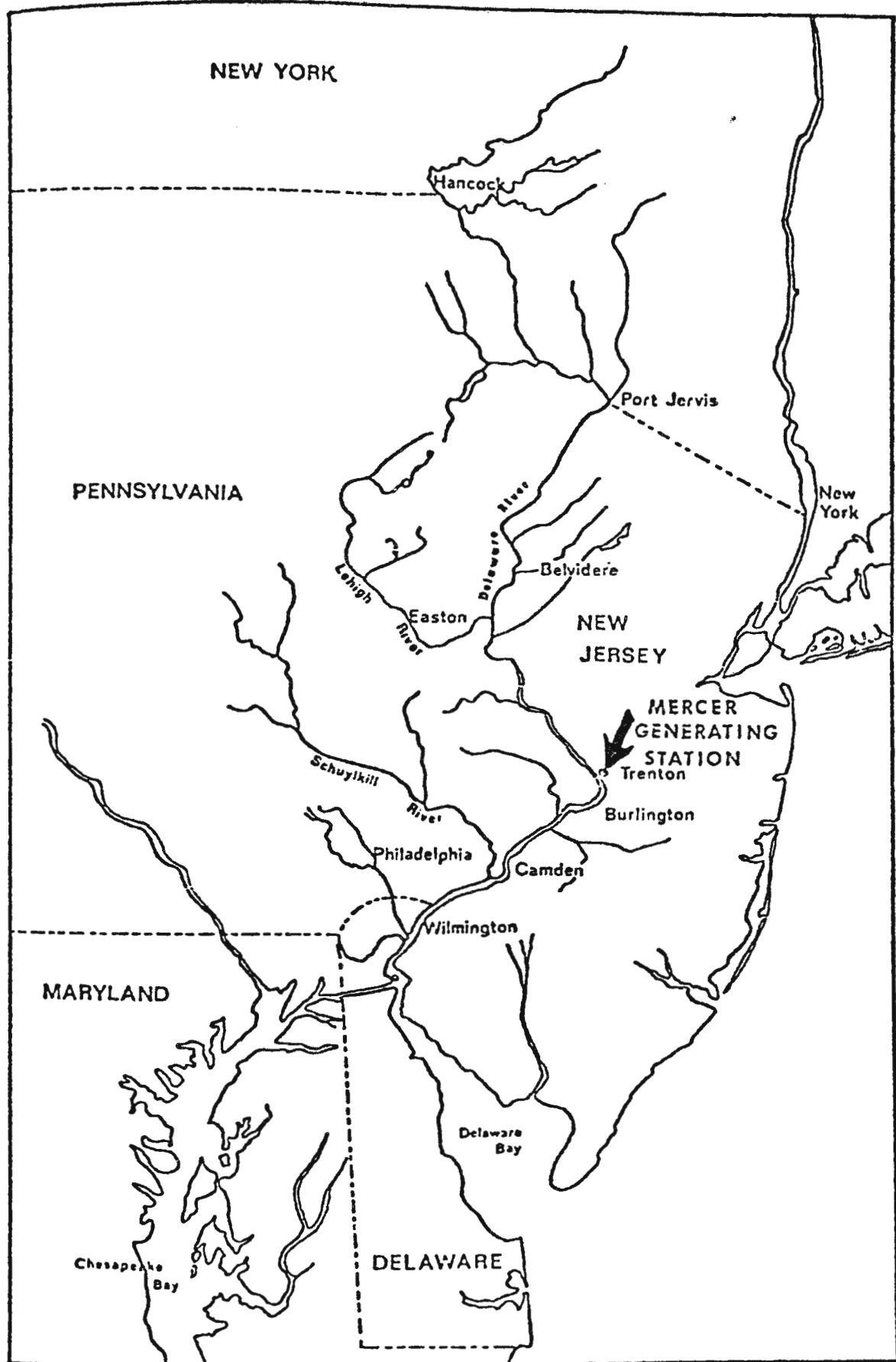
Figure 1.   Map of the Delaware River Drainage Basin Showing
the Location of the Mercer Generating Station

261

Figure 2. Scheme of
Renovated Aquaculture Facilities,
Mercer Generating Station,
Trenton, NJ

previously
existing
pilot aqua-
culture facilities

262
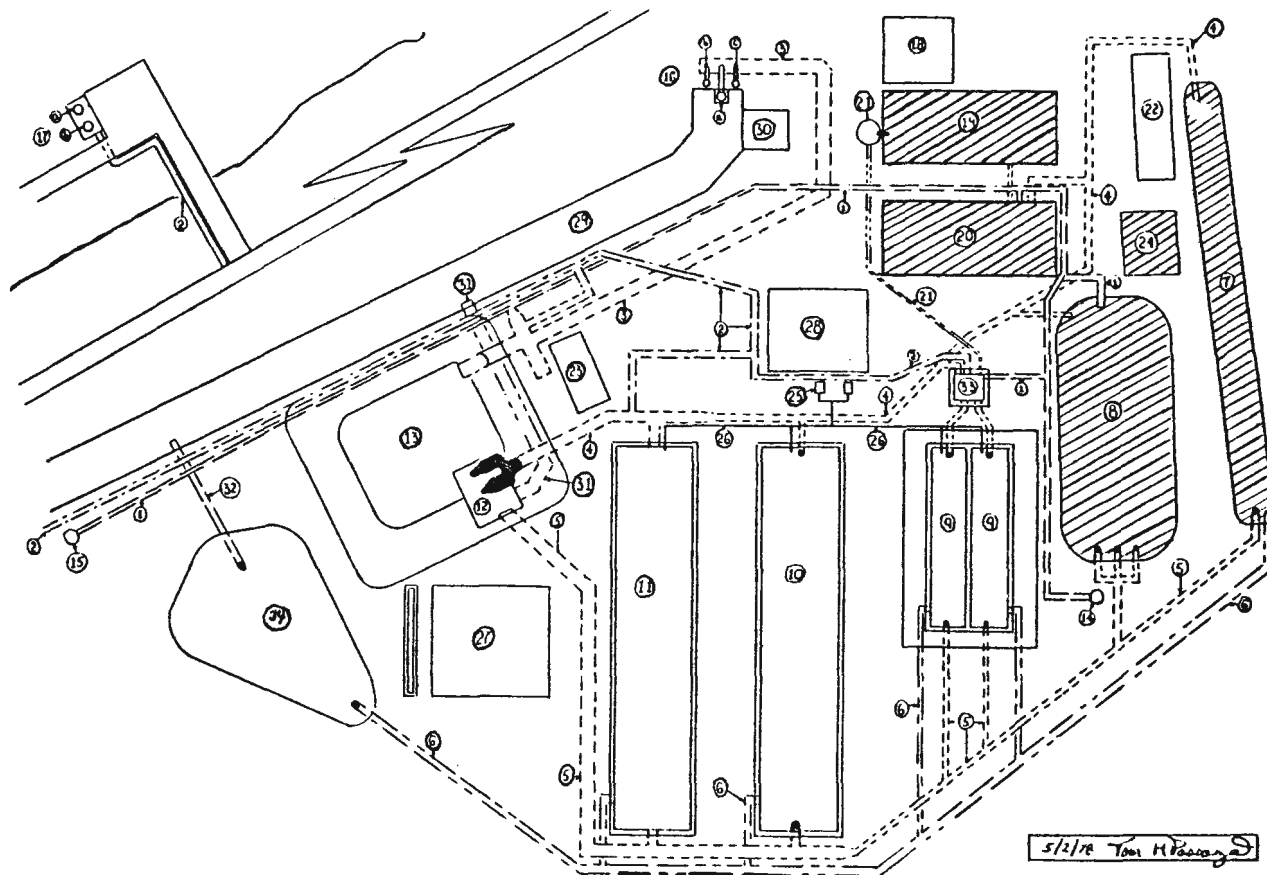
1. Lines from Well 1 and Well 2 to laboratories and raceways
2. Line from Delaware River to Aquaculture System
3. Line from Mercer Station discharge canal to Temperature-Moderation Pond
4. Line from Recirculation Chamber to raceways and laboratories.
5. Line from raceways to Recirculation Chamber
6. Line from raceways to Waste-Settling Pond
7. Raceway I
8. Pond I
9. Enclosed Raceways A, B
10. Raceway II
11. Raceway III
12. Recirculation Chamber
13. Temperature-Moderation Pond
14. Well No. 1
15. Well No. 2
16. Pumps for Mercer Station discharge canal to Aquaculture System
   a - 1,500gpm pump
   b - 800gpm pump
   c - 800gpm pump

17. Delaware River Pump Station
   a - 500gpm pump
   b - 500gpm pump
18. Maintenance Building - also houses alarm system
19. Laboratory I
20. Laboratory II
21. Line from Laboratory I to Mixing Chamber for Enclosed Raceways
22. Office-Laboratory Trailer
23. Office Trailer
24. Food-Storage Shed
25. Compressed - Air Blowers
26. Air lines for compressed air
27. Greenhouse
28. Mercer Station Transformer
29. Mercer Station discharge canal
30. Mercer Station Fire House
31. Drainage line from Recirculation Chamber to Mercer Station discharge canal.
32. Line from Waste-Settling Pond to Mercer Station discharge canal.
33. Mixing Chamber for Enclosed Raceways
34. Waste-Settling Pond

DORSAL VIEWS OF RECIRCULATION CHAMBER

GRAVITY DRAIN FROM ALL RACEWAYS, POND & G.H.

SUBMERSIBLE PUMPS

CHECK VALVE

WOODEN WEIR FOR WATER LEVEL CONTROL

DRAIN TO RIVER

VALVE FROM RECIRCULATING POND

LOWER CHECK VALVE TO RACEWAYS, POND, G.H.

TOP VIEW OF PIPING ON RECIRCULATING CHAMBER

FLOATATION ON AND OFF SWITCHES

WATER FROM SUBMERSIBLE PUMPS TO RACEWAYS, POND, & G.H.

LATERAL VIEW OF SYSTEM

WOODEN WEIR

GRAVITY DRAIN FROM ALL RACEWAYS, POND, & G.H.

POND LINER

TEMPERING POND

DRAIN TO RIVER

BYPASS CHAMBER

TEMPERATURE MODERATION POND DRAIN

VALVE TO REGULATE WATER FROM RECIRCULATING POND

CHECK VALVE, PIPE LEADS TO RACEWAY, POND, G.H.

SUBMERSIBLE PUMPS

CANAL WATER 3,100 GPM TOTAL

TOTAL GPM POSSIBLE 5,100 GPM

RIVER WATER 1,000 GPM TOTAL

WELL WATER 1,000 GPM TOTAL

DISTRIBUTION CHAMBER

263

Figure 3. Operation of Tempering Pond - Recirculation Chamber System
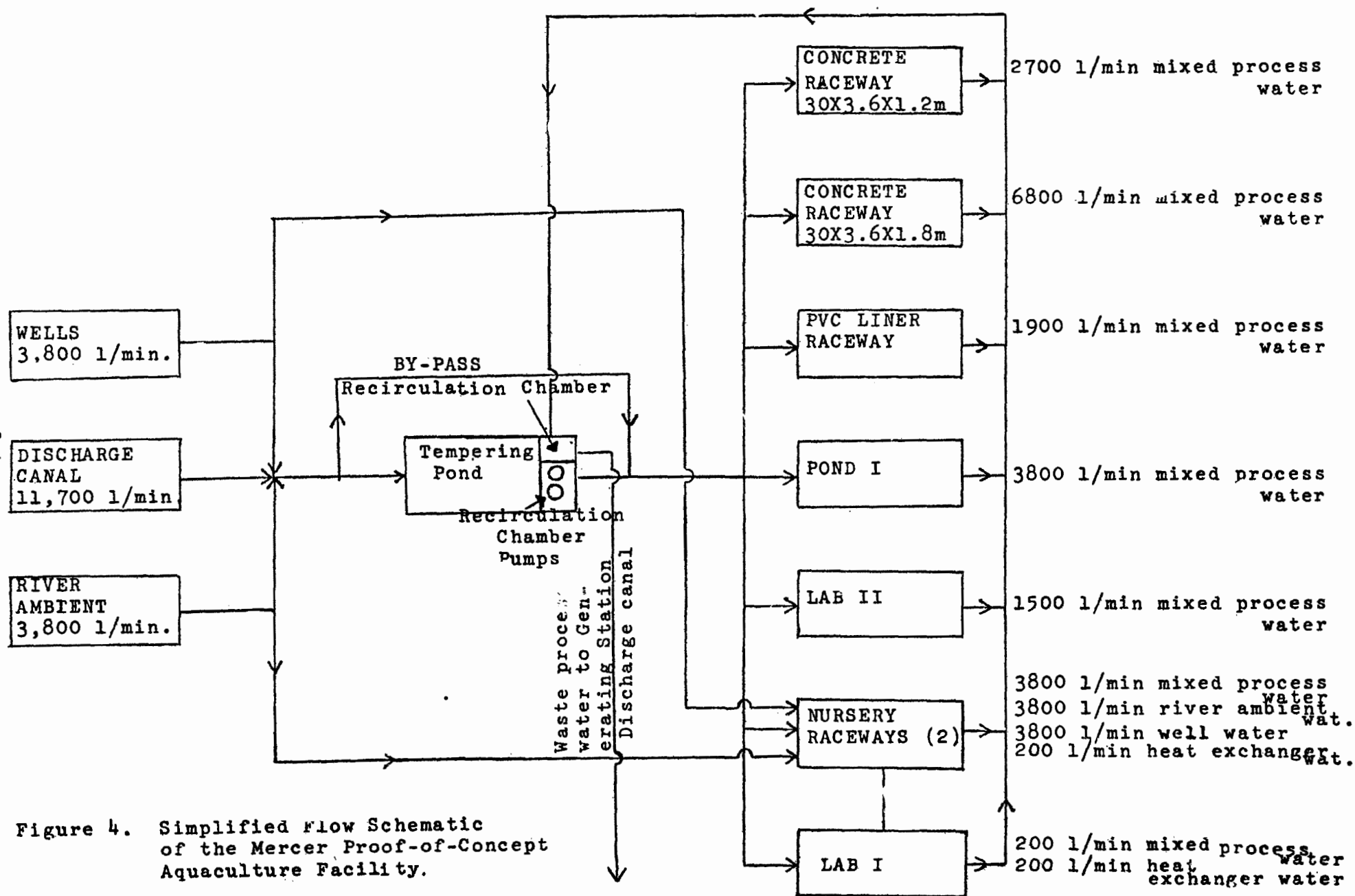
Figure 4. Simplified Flow Schematic of the Mercer Proof-of-Concept Aquaculture Facility.

	ACTIVITY	LOCATION	MONTHS
			J F M A M J J A S O N D

Ictalurus punctatus

	ACTIVITY	LOCATION
1.	Brood Stock Spawned	Laboratory I
2.	Eggs Hatched & Larval Cycle Completed	Laboratory I
3.	Early Fry Reared	Laboratory I
4.	Fry-Early Fingerling Grow Out	Laboratory II
5.	Fingerling Grow Out	Insulated Nursery Raceways
6.	Final Grow Out & Harvest	Outdoor Ponds & Raceways
7.	Brood Stock Recruited & Maintained	Laboratory II

Salmo gairdneri

	ACTIVITY	LOCATION
1.	Eyed Eggs Received	Laboratory II
2.	Eggs Incubated & Hatched	Laboratory II
3.	Early Fry Reared	Laboratory II
4.	Fry Grow Out (9 cm at stocking)	Nursery Raceways
5.	Fingerling Grow Out (20 cm at stocking)	Outdoor Ponds & Raceways
6.	Harvest 30 cm Trout	Outdoor Ponds & Raceways

S = Start, H = Harvest

Figure 5. Sequence of Shrimp and Trout Culture Operations at the Mercer Aquaculture Facility

WASTE HEAT RECOVERY IN THE FOOD PROCESSING INDUSTRY

W. L. Lundberg and J. A. Christenson
Westinghouse Electric Corporation
Advanced Energy Systems Division

F. Wojnar
H. J. Heinz Company
U.S.A. Division
Pittsburgh, Pennsylvania U.S.A.

ABSTRACT

A project is described which evaluated the potential for waste heat recovery in the food processing industry. The work was performed by Westinghouse Electric Corporation under a Department of Energy contract and with the cooperation of the H. J. Heinz Company. In particular, applications of thermal storage were sought. However, the project was not restricted to those applications, and attention was also given to satisfying immediate energy needs with recovered waste heat. The primary purpose of the work was the study of waste heat recovery systems and methods that could have a significant impact upon the nation's energy consumption if the food industry applied them on a large-scale basis. The paper discusses the technical aspects of potential waste heat recovery systems and the economics of installing them at selected survey factories.

INTRODUCTION

Westinghouse recently completed a nine month study project to assess the potential for economical waste heat recovery in the food industry and to evaluate prospective waste heat recovery systems. The project was funded by the U.S. Department of Energy (DOE) and was conducted by Westinghouse with the cooperation of the H. J. Heinz Company. Heinz arranged access to two of their manufacturing plants within the Heinz U.S.A. Division and permitted Westinghouse personnel to analyze factory and food system operations. At each factory, a waste heat availability study was performed and the resulting data were then applied as the basis for recovery system conceptual design. The system studies focused on thermal performance and economic evaluations and in this paper, the results of that effort and project conclusions regarding feasibility are presented.

SURVEY SITES AND SELECTION RATIONALE

The Heinz U.S.A. Division operates eleven factories engaged in a variety of thermal food processes. Two of those factories, located in Pittsburgh and Lake City, Pennsylvania, were selected as survey sites for our project. The Pittsburgh Factory is a large multi-building facility employing over 2,000 production people and specializing in foods processed with steam and hot water. The factory's main products are baby foods and juices, canned soups and canned bean products. At the Lake City Factory, approximately 150 employees are engaged in the preparation of dessert products that are quick-frozen as the last step in the process. Lake City operations are conducted in a modern, single-story building having a total floor area of approximately 70,000 ft^2.

The products manufactured by the Pittsburgh Factory place it in the Canned Specialties (SIC 2032) industry but the processes used are also common to Canned Fruits and Vegetables (SIC 2033) as well. Similarly, the Lake City products would place that factory, strictly speaking, within the Ice Cream and Frozen Desserts (SIC 2024) industry. However, similar food processes are also employed in the Frozen Specialties (SIC 2038) and Frozen Foods and Vegetables (SIC 2037) industries. Based upon food industry data, the annual energy consumption by these five industries (SIC 2032, 2033, 2024, 2038, and 2037), which are represented by our Pittsburgh and Lake City survey sites, totals to nearly 120×10^{12} Btu (Canned to Frozen Ratio $\approx 60/40$) and accounts for 13% of the total food industry (SIC 20) energy usage. If waste heat recovery systems were implemented to reduce energy consumption in those five industries by 10%, the annual savings, nation-wide, would amount to 0.012 quad or approximately 1.3% of the current SIC 20 usage. This potential industry impact is significant and therefore it appeared that survey and conceptual system design work at the Pittsburgh and Lake City Factories would be very worthwhile. This was the main reason for selecting those particular factories for use as survey sites.

WASTE HEAT AVAILABILITY

At each factory, operations were analyzed and waste heat production rates were estimated. At the Pittsburgh Factory, hot waste water is the main waste heat source and the estimates were based, in the case of several contributing systems, upon actual measurements of waste water flow rates and temperatures. Where only temperatures could be conveniently measured, the flow rates were estimated by applying the temperature data and known values of product temperatures and flow rates to a system energy balance. In several cases, neither waste water flow nor temperature could be determined conveniently and in those situations, the systems were modeled mathematically to produce estimates of the required parameters.

At the Lake City Factory, the refrigeration system condensers represent the waste heat source of most interest during this project. For conceptual system design purposes, average refrigerant flow rates and condenser heat dissipation rates were predicted based upon estimated compressor electrical loads and assumed refrigerant cycle state points. In this section, the food processing systems at the two survey sites are described and the results of the waste heat availability study at each site are summarized.

Pittsburgh Factory

The Pittsburgh Factory operates several food systems that produce hot waste water. To eliminate the possibility of product contamination, waste water from the processes is not recycled nor is waste heat recovery attempted. Instead, the waste water streams are collected by a drain system that transports them from the factory via clear water and sanitary sewer systems. The various waste water sources evaluated at the Pittsburgh Factory and waste water conditions for individual units are identified in Table 1. To assess the total waste heat availability, the unit data from Table 1 were combined with operational data (cycles per shift, cycle times, number of units in operation, etc.) supplied by Heinz U.S.A. The resulting information was compiled by shift and on a building-by-building basis and

is summarized in Table 2. The table entries apply to those systems selected for waste heat recovery. Systems not represented in Table 2 were neglected due to low temperature and/or low volume reasons and to high fouling potential in the case of the blowdown heat source.

Lake City Factory

The Lake City Factory has two major refrigeration requirements - blast freezing and cold storage. Pie and cake products complete the preparation process on a conveyor line that transports them through a blast freezer maintained at -35°F. When they exit the freezer in 20 - 40 minutes, the frozen products are placed in a storage freezer (-5°F) to await shipment. The refrigeration effect for both freezers is provided by an ammonia system driven by ten rotary and reciprocating compressors. On the discharge side of the compressors, the refrigeration system is arranged in two separate parts. Eight compressors (five blast freezer, two storage and one ice bank unit)* discharge to six manifolded condensers while the two remaining compressors (Group 2) are staged units that serve a storage freezer and discharge to their own condenser. Since blast freezer operation only occurs during the one or two production shifts of each day, waste heat rejection at the first condenser group peaks during those shifts and declines to a minimum (imposed by the ice bank and storage load) during the night time hours. Heat rejection at the independent condenser, however, is more uniform over the entire day due to its storage function. The point of this discussion is that two independent sources of refrigeration waste heat exist at the factory that behave differently with time. Therefore, they could be linked with two independent waste heat applications whose energy demands also follow different time patterns.

At the compressor discharge, the assumed ammonia vapor conditions were 185°F at 150 psia. An average refrigerant flow rate for each compressor was calculated based upon factory electrical data, compressor on-time estimates and nameplate horsepower, assumed state-points and a compressor mechanical efficiency of 0.85. The resulting refrigerant flow rate for the Group 1 compressors during production hours is 7,390 lb/hr and for Group 2, 1,860 lb/hr. On the basis of these flow rates and other system data, the annual heat dissipation at the condensers totals 4.0×10^{10} Btu. For comparison, this quantity is larger than the factory's annual total energy consumption (gas and electricity combined) by approximately 50%.

WASTE HEAT APPLICATIONS

Pittsburgh Factory

Three applications of waste heat were selected for study at the Pittsburgh Factory. They involve the heating of boiler make-up water, fresh water for food processes and factory clean-up water. The main method of heating process water at the factory is by the direct injection of cold water with steam. Since process water is not recycled, condensate losses are high and must be matched by make-up. By Heinz U.S.A. estimates, nearly two-thirds of the boiler feedwater flow is composed of make-up water and

---

*Referred to subsequently as the Group 1 compressors.

268

preheating that water would be an excellent use of waste heat. In this case, conventional heat exchange could be used and the timing is opportune since the highest demand for make-up occurs during production when waste heat availability also peaks. A similar application exists in the case of food processing water.

Production area clean-up is a daily operation that requires significant energy input. While spot clean-ups occur as needed during the production hours, the major clean-up effort is performed during third shift when production hardware is disassembled and washed or cleaned in place. Heinz U.S.A. estimates that the factory requires 200,000 gal. of heated clean-up water (150-180°F) per day and meeting that demand is responsible for 3-4% of the plant's total energy consumption. Waste heat could be used to satisfy a portion of the required energy. However, since this particular need and the waste heat supply are not in phase, thermal energy storage would be required.

Lake City Factory

The Lake City Factory also has a daily need for heated clean-up water (8,000 to 10,000 gal. at 150°F) and waste heat from the refrigeration system could satisfy it. Again, thermal storage would be needed since the waste heat supply and the demand for energy in this case are not in phase.

A second waste heat application involves the heating of air which is blown beneath the freezer floors. A potential problem with ground floor freezers is that the earth beneath the floor will freeze eventually and cause the floor to heave. To eliminate or minimize the problem, freezer plants usually install floor insulation and warm the earth beneath the floor electrically or by circulating a warm non-freezing liquid through a piping grid. A third method to prevent freezing is to blow warm air through ducts installed below the floor. This method is employed at Lake City. Outdoor air is drawn in through a roof-mounted system composed of a vaneaxial fan and an air temperature controlled gas-fired heater. The modulated heater is activated whenever the outdoor temperature falls below 70°F. The system is rated at 7000 scfm and the annual air heating load is 1.4 x 10^9 Btu or approximately 5% of the factory's total energy need.

WASTE HEAT RECOVERY SYSTEM DESIGN AND EVALUATION

Pittsburgh Factory

Several recovery system concepts to satisfy the waste heat applications discussed above are being considered for use at the Pittsburgh Factory. Features of the reference system, shown schematically in Figure 1, will be discussed herein. In that concept, waste water streams at various temperatures are collected from processes occurring in three production buildings. The high temperature streams (i.e., those above 140°F) are collected in the high temperature accumulator (HTA) while all low temperature streams are channeled to a low temperature accumulator (LTA). The LTA and HTA will be insulated and they serve as surge tanks between the waste water

source and application points. All of the waste water sources identified in Figure 1 produce continuous waste water streams except the retorts. Retort operation occurs on a batch basis and the temperature of the waste stream emitted by a retort varies with time. It is intended, therefore, that the retort drain system will be equipped with temperature-sensing, three-way valves. The valves will direct waste water to the HTA during the high temperature part of the cooldown and to the LTA when the waste water temperature falls below a set-point value. In studies performed to date, the set-point has been 140°F. The purpose in separating the waste water streams by temperature as opposed to mixing them pertains to the storage part of the system. Using high temperature waste water to prepare the highest temperature stored water decreases the cost/benefit ratio for storage and causes it to approach that for the entire system.

From the HTA, waste water flows on demand to the high temperature heat exchanger (HTHX) located in the Power Building. At the HTHX, heat is transferred to incoming fresh water as it flows to various food processes. When those demands diminish while hot waste water is still available at the HTA, the system will automatically divert the flow of heated fresh water to storage. Water that accumulates in storage during the production period would then be used during third shift for clean-up purposes.

Waste water collected in the LTA will flow to two low temperature heat exchangers (LTHX) also lcoated in the Power Building and mounted in parallel. Waste heat will be applied at that location to preheat fresh water for food processing and for boiler make-up. The parallel heat exchanger arrangment is necessary since the food processing and make-up applications require water from two different sources — on-site wells and the city water main, respectively.

Estimated materials and installation costs for the reference waste heat recovery system are identified in Table 3. Allowing an additional 15% for engineering brings the total system cost to $413,300. At current fuel prices, Heinz U.S.A. estimates the delivered value of energy at $3.05 per million Btu's and in one year's time (220 production days, 2 shifts per day, 7 hours per shift), it is further estimated that the reference system described above will recover approximately 7.0×10^{10} Btu thereby reducing factory energy consumption by 5 - 6%. Thus, the projected dollar savings produced annually by the system are $214,000 which would return the capital investment at the rate of 35% per year. The return on investment (ROI) calculation is based upon the Heinz ten-year, discounted cash flow method and assumes a 10% investment tax credit, a 12% depreciation rate and a 50% income tax. The calculation made no allowance for fuel price escalation.

Lake City Factory

For the Lake City Factory, two independent systems have been evaluated. The first system, shown schematically in Figure 2, will apply refrigeration waste heat from the Group 1 compressors to heat fresh water for later use during third shift clean-up operations. The system will be located in an existing water distribution system at a point between the softener exit and the first clean-up station take-off. The thermal storage tank and its

circulation loop will be solid at water main pressure with a storage capacity of approximately 6,000 gallons which would be sufficient to supply the factory's daily clean-up water needs. System control will center on the storage tank temperature and the refrigerant temperature at the heat exchanger exit. For tank temperatures less than a set point value (say 150°F), the centrifugal circulation pump will energize provided the refrigerant temperature is greater than a set point value representing its saturation temperature. With those conditions satisfied, the temperature sensing flow control control valve will open and water will circulate from storage to the heat exchanger and back to storage. The water will enter the thermal storage tank via a low velocity distribution ring near the tank top and horizontal baffling arranged along the height of the tank will promote stratification. The circulating pump will take its suction from the low temperature zone at the bottom of the tank and water to be delivered to the clean-up stations would be withdrawn at the top.

The system heat exchanger will operate as a desuperheater and under normal conditions, vapor will exit the unit with 5 - 10°F of superheat still remaining. The vapor will then flow to the existing condensers to complete the heat rejection process.

Table 4 presents materials and installation cost estimates for the water heating system. The total system cost, including engineering, would be $36,900 and the system would displace natural gas at the rate of nearly 1900 MCF annually. This reduction in fuel consumption is valued, at current fuel prices, at $3,870 per year and it would reduce the factory's total energy input (gas and electricity) by 7% and its natural gas consumption by 13%. Again based upon the Heinz project evaluation method and assumptions, the annual ROI for the water heating system will be 8%.

A second waste heat recovery system for the Lake City Factory is shown schematically in Figure 3 and would apply refrigeration waste heat to warm freezer floor air. As the figure indicates, outdoor air is presently warmed by an existing gas-fired heater and distributed to floor ducts by a fan. The fan operates continuously and air temperature control is achieved by regulating the flow of natural gas to the heater. Waste heat from the Group 2 compressors could be utilized to preheat or completely heat floor air by installing an air-cooled condenser at the heater inlet. Refrigerant vapor from the storage freezer system would be routed through the condenser on its way to the existing evaporative condenser. The system control would cause the incoming air to bypass the new condenser in any proportion to maintain the gas heater inlet tmeperature at a setpoint value. Thus, the fraction of the refrigerant condensing load handled by the new condenser would also be a variable ranging from zero during warm weather operation to nearly one-fourth under design, cold-weather conditions. It is noted that the function of the recovery system would be to supplement the existing gas-fired system. Thus, any portion of the air heating load not satisfied by waste heat will be supplied automatically by the gas heater which will continue to operate with its own control system and independent of the waste heat recovery system.

271

Costs to procure and install an air heating system are identified in Table 4 and the total estimated cost, with engineering, is $17,700. The system would displace natural gas at the yearly rate of 1390 MCF (valued at $2,880) and reduce the factory's natural gas and total energy consumption by 10% and 5%, respectively. The air heating system ROI is estimated at 14%.

CONCLUSIONS

Based upon our study, it is concluded that waste heat recovery from certain food processes is feasible and can be performed economically using available, off-the-shelf hardware. This conclusion is certainly valid for the large Pittsburgh Factory where both the anticipated ROI and the predicted fuel and energy savings are especially attractive. In fact, the predicted performance of the Pittsburgh Factory system is sufficiently attractive that plans are being developed to design and install an instrumented demonstration system at the factory. The purpose of the DOE supported project will be to evaluate actual hardware performance, to optimize system design and to determine actual costs and benefits resulting from the waste heat recovery system. The results of the project will then be publicized to encourage the application of similar waste heat recovery concepts within the food industry.

While the predicted economic performance of the Lake City systems is less than desired, it is believed that the project results do warrant additional system studies. This is especially true in the system scaling area and the results of the study should be extrapolated to refrigeration plants of other sizes. In fact, a similar effort should also be undertaken for the hot water systems of the Pittsburgh Factory type. Through such efforts, it will likely become evident that retrofit projects within a certain heat recovery range are more feasible than others and plant sizes and conditions most appropriate for such projects could therefore be identified.

TABLE 1.   INDIVIDUAL UNIT WASTE WATER CONDITIONS — PITTSBURGH FACTORY

Source	Flow Rate (gpm)	Temperature (°F)
Continuous Can Washer	12	175
Continuous Bottle Washer	7	175
Continuous Cooker/Cooler	60	140
Horizontal Stationary Retorts		
Canned Products	100	100
Glass Products	100	140
Continuous Pasteurizer	80	170
Continuous Cooler	55	120
Horizontal Rotary Retorts		
Type 1	10	135
Type 2	30	125
Continuous Boiler Blowdown	12	212

TABLE 2.   WASTE WATER SUMMARY — PITTSBURGH FACTORY

	Average Flow Rate & Temperature	
	First Shift	Second Shift
Power Building		
Continuous Cooker/Coolers	120 gpm - 140°F	60 gpm - 140°F
Can Washers	37 gpm - 175°F	12 gpm - 175°F
Meat Products Building		
Horizontal Stationary Retorts (Glass Products)	316 gpm - 140°F	316 gpm - 140°F
Can Washers	25 gpm - 175°F	12 gpm - 175°F
Bottle Washers	7 gpm - 175°F	7 gpm - 175°F
Continuous Pasteurizer	80 gpm - 170°F	80 gpm - 170°F
Bean Building		
Can Washers	25 gpm - 175°F	12 gpm - 175°F
Continuous Coolers	110 gpm - 120°F	55 gpm - 120°F
Total Flow Rate & Average Temperature	720 gpm - 145°F	554 gpm - 145°F

TABLE 3. ESTIMATED COSTS — PITTSBURGH FACTORY SYSTEM

Item	Materials ($)	Installation ($)
Tanks	90,000	—
Heat Exchangers	44,400	6,700
Pumps	13,400	6,000
Strainers	10,000	4,000
Valves	15,500	12,800
Piping	27,300	92,200
Instrumentation/Controls	17,800	19,300
	218,400	141,000

Total Materials & Installation — $359,400

TABLE 4. ESTIMATED COSTS — LAKE CITY WATER HEATING SYSTEM

Item	Materials ($)	Installation ($)
Thermal Storage Tank (6000 gal)	8,300	3,000
Heat Exchanger	3,500	1,200
Pump	500	500
Water Flow Control Valve	1,100	200
Temperature Sensor & Transmitter	3,500	400
Piping	2,300	5,000
	19,200	10,300

Total Materials & Installation — $29,500

TABLE 5. ESTIMATED COSTS — LAKE CITY AIR HEATING SYSTEM

Item	Materials ($)	Installation ($)
Condenser	2,800	1,800
Piping	600	1,100
Air Ducting	{ 3,000	1,200
Controls		800
Fan Motor	500	—
	6,900	4,900

Total Materials & Installation — $11,800

MEAT PRODUCTS BUILDING

PASTEURIZER

CAN WASH

RETORTS

T

HTS L

BEAN BUILDING

CAN WASH

COOLER

L LTA

POWER BUILDING

COOKER COOLER

CAN WASH

DRAIN

WELL WATER

LTHX

FOOD PROCESSES

BOILER MAKEUP

DRAIN

WELL WATER

HTA

HTHX

LTHX

CITY WATER

DRAIN

FOOD PROCESSES

CLEAN-UP STATIONS

100,000 GALLON THERMAL STORAGE

– – – HIGH TEMPERATURE WASTE SYSTEM (>140°F)
– · – · LOW TEMPERATURE WASTE SYSTEM (< 140°F)
——— THERMAL STORAGE SYSTEM
– – – HOT PROCESS WATER
········· BOILER MAKEUP

HTA – HIGH TEMPERATURE ACCUMULATOR
HTHX – HIGH TEMPERATURE HEAT EXCHANGER
HTS – HIGH TEMPERATURE SUMP
LTA – LOW TEMPERATURE ACCUMULATOR
LTHX – LOW TEMPERATURE HEAT EXCHANGER

275

Fig. 1. Waste Heat Recovery System - Pittsburgh Factory
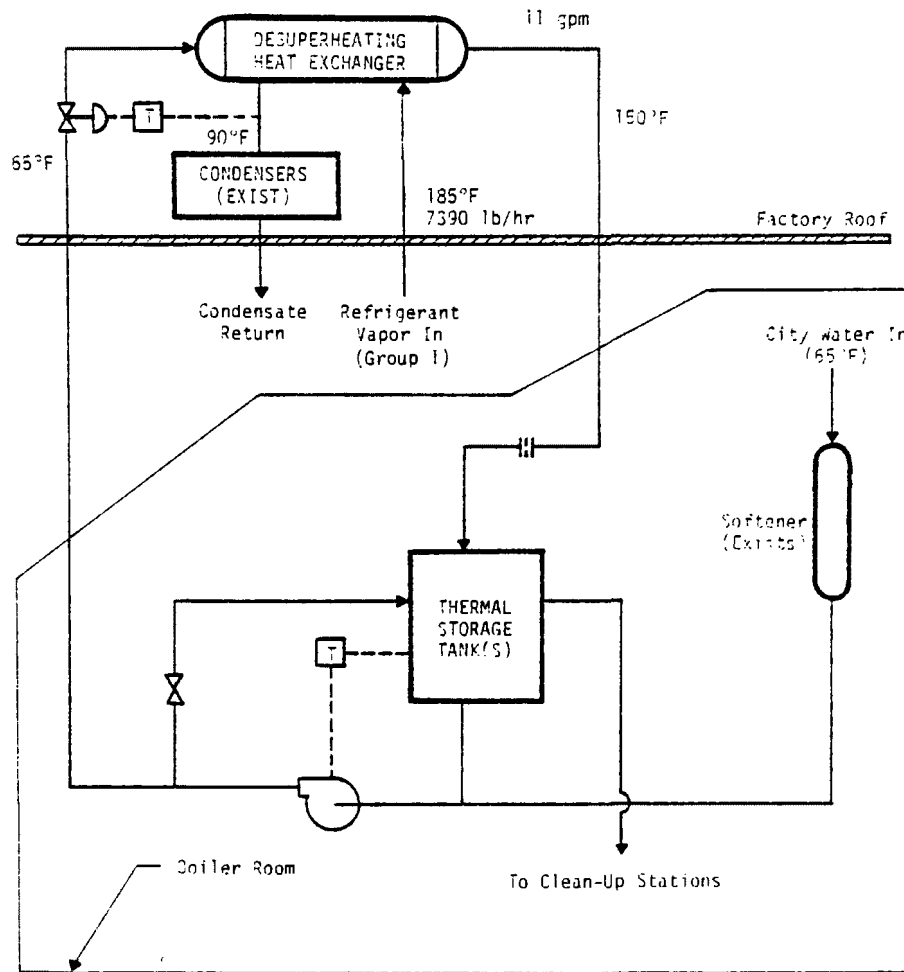
Fig. 2. Waste Heat Recovery System for Water Heating - Lake
City Factory
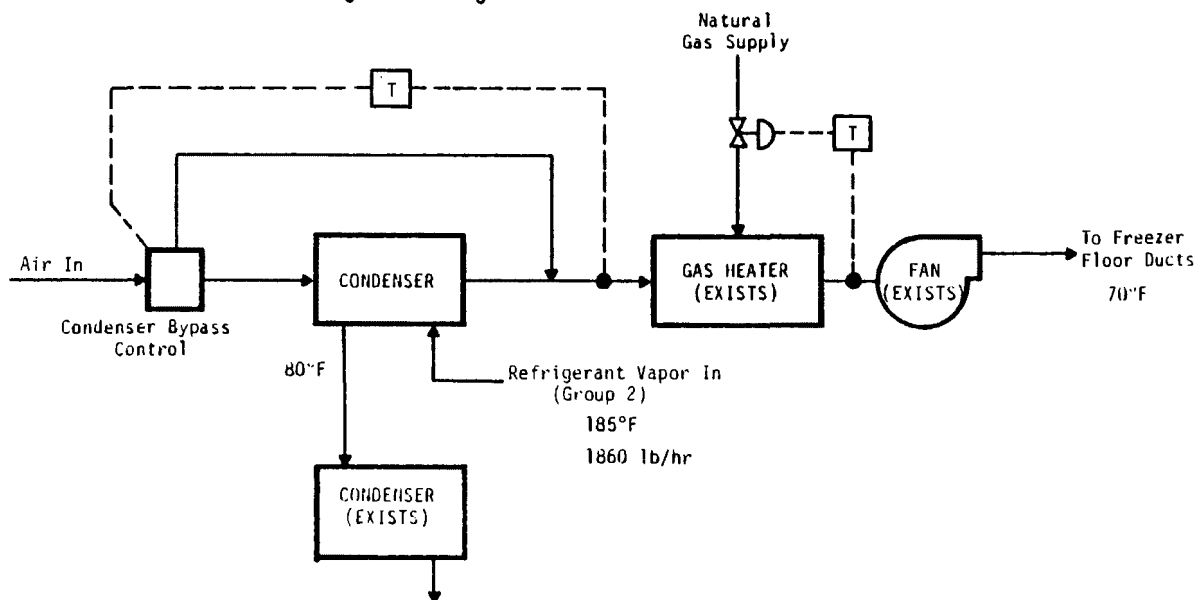
Fig. 3. Waste Heat Recovery System for Air Heating - Lake City Factory

276

GENERATION OF CHILLED WATER FROM CHEMICAL PROCESS WASTE HEAT

Jack Entwistle
Fiber Industries, Incorporated
Charlotte, North Carolina U.S.A.

ABSTRACT

Recovery of waste heat from a chemical process column, and the conversion of waste heat into chilled water, was accomplished at the Palmetto, S. C. plant of Fiber Industries, Inc. by the installation of a waste heat boiler/absorption chiller system. Overhead vapors, at 40 psig, from two columns,provide the heat source. Two waste heat boilers were installed adjacent to the columns. Each waste heat boiler is capable of generating 13900 pounds of steam per hour at 16 psig when the plant is operating at maximum production. The absorption chiller has a nominal capacity of 1140 tons and at maximum rating requires 21000 pounds of steam per hour at 12 psig. Lithuim bromide is the absorbent.

INTRODUCTION

Expansion of plant production facilities required an additional chiller to supply $45^{o}F$ water to air conditioning units. Two alternatives were evaluated.

1. Installation of an additional electrically driven centrifugal chiller, similar in design to existing equipment.

2. Installation of a waste heat boiler/absorption chiller system utilizing waste heat in the overhead vapors of a plant process column.

The study estimated that the waste heat boiler/chiller installation would cost $600,000, the centrifugal chiller installation would cost $300,000 and the annual operating costs would be $100,000 lower, at existing electrical rates, if the absorption chiller was installed. A present-worth analysis determined that the absorption chiller was the best economic choice.

The actual installation cost was $450,000 and electrical rate increases have paralled the original estimate so that project economics have proved to be better than the study predicted.

SYSTEM DESCRIPTION

General

Prior to installation of the waste heat recovery system, 28 million Btu/hour of energy was wasted in the condensation of process column overhead vapors, using cooling tower water as the method of removing heat. The waste heat recovery system makes a large fraction of the energy contained in these column vapors available for generation of chilled water in the absorption chiller. Because of the fear of contamination either by or to the process it is not practical to use these vapors as a direct makeup to the plant steam system.

The system recovers this energy by use of the two waste heat boilers located adjacent to the columns. Vapors from the column overheads exit the column at 40 psig and 289°F. These vapors are piped to the channel (tube) side of the waste heat boiler, where they are condensed by boiler feed water surrounding the tubes (relatively colder at 252°F). The latent heat released by the condensation is transferred to the surrounding water, and 16 psig steam is produced. The condensed overheads are then returned to the column overhead piping, upstream of the water-cooled condenser. The water level outside the tubes within the waste heat boiler is maintained by use of centrifugal pumps which transfer feed water from the utility boiler deaerator system. Solids control within the waste heat boiler is achieved by manual intermittent blowdown from the boilers.

Steam is piped to the lithium bromide cycle absorption chiller which is located alongside the centrifugal chillers in the plant utilities building. This location enabled convenient connections to be made to the existing cooling water and chilled water systems. Figure 1 shows the arrangement of the complete waste heat recovery system.

Waste Heat Boilers

The waste heat boilers recover most of the heat content of the column overhead vapors and convert the energy into a usable form. i.e. low pressure steam. One waste heat boiler has been provided for each column in order to preserve the integrity of the self-contained concept of the process equipment. Each waste heat boiler is a large U-tube kettle type reboiler with condensate sump on the tube side, and mist eliminator head on the shell side. Table 1 summarizes the design parameters.

The design maximum steam rate for each unit is 13,900 pounds/hour. However, the actual steam rate which can be delivered by each waste heat boiler is a function of the following:
  (a) Percentage of column overheads flow bypassed directly to the condenser for pressure control.
  (b) Plant production rate.
  (c) Column reflux ratio.

Initially the control system was set up to bypass about 10% of the vapor flow directly to the condenser so that precise column pressure control could be maintained by varying the flow rate to the condenser. This method protects the production process from column upsets but also reduces the amount of recovered energy. After three months of satisfactory operation it was found that the column could be protected from adverse pressure fluctuations, even with 100% vapor flow to the boiler, by controlling the steam pressure.

Steam Piping

The steam generated by the waste heat boilers is transported some 400 feet to the plant utility building in a 12 inch diameter pipe. Since the rate of steam generation is a function of plant production, and at maximum production the rate of steam generation is greater than the absorption chiller demand, piping connections were made to the plant low pressure steam piping system. Thus total plant low pressure steam requirements can be balanced.

To ensure that the absorption chiller was placed in service without production upsets a piping connection was made to the 300 psig utility boilers. The chiller was initially operated with steam supplied from the utility boilers. After chiller operation was satisfactorily established this connection was permanently closed.

Absorption Refrigeration Machine

The absorption chiller is a lithium bromide cycle York, model EM1130, machine. Design conditions are summarized in Table 2. The chiller uses the combined output of both waste heat boilers as its source of steam. The operating characteristics of the process column and the absorption machine were analyzed to derive the relationship of refrigeration tonnage to steam output.

$$T = \frac{(S_1 + S_2) - 2620}{15.88}$$

Where   T = Net refrigeration, tons

S_1 = Steam rate, waste heat boiler #1, pph

S_2 = Steam rate, waste heat boiler #2, pph

A graphical representation of this relationship is shown in Figure 2.

Operation of an absorption refrigeration machine is based on four factors.
1. A refrigerant, in this case water, which boils at a temperature below that of the liquid, also water, being chilled. Since water is used as a refrigerant and a coolant the refrigerant evaporator must be at a pressure of 5 to 10 mm Hg for the boiling temperature to be low enough to chill the coolant.
2. An absorbent, in this case lithium bromide, which possesses a great affinity for the refrigerant. This affinity enables the refrigerant vapor to be converted to the liquid phase while still at low pressure.

279

3. A source of energy, steam from the waste heat boilers, to drive an endothermic reaction.
4. A source of cooling water to remove heat from an exothermic reaction.

A schematic representation of the cycle is shown in Figure 3.

Water is pumped over the chilled water coil and is evaporated by the heat in the chilled water; this transfer of heat reduces the temperature of the chilled water. Water vapor from the evaporator is absorbed by an intermediate concentration of LiBr thus diluting the solution. Since this is an exothermic reaction heat must be removed by cooling water. The dilute solution is pumped to the generator, via a heat exchanger, where the water and LiBr are separated. This is an endothermic reaction so that heat, in the form of steam from the waste heat boilers, is required. The water vapor is condensed by cooling water and flows back to the evaporator. The strong solution of lithium bromide flows through a heat exchanger back to the absorber. The heat exchanger transfers heat from the LiBr leaving the generator to the LiBr being pumped from the absorber to improve cycle efficiency. A vacuum pump purges the unit of non-condensible gases and a de-crystallization pipe prevents the formation of solid LiBr.

COOLING AND CHILLED WATER

The existing cooling water pumps and towers were capable of handling the machine cooling requirements. A cooling water recirculation pump was installed to maintain a minimum cooling water inlet temperature of 75°F. If inlet water temperature drops below this value crystallization of the LiBr solution may occur.

One additional chilled water pump was installed in the existing chilled water sump. Existing pumps provide back up capability in case of pump failure.

CONCLUSION

Although the thermodynamic performance of an absorption refrigeration machine is not very high, three very real practical reasons supported its selection;
1. Availability of an un-utilized machine from a sister plant. This obviously reduced the capital cost of the installation.
2. Compatability with the production process. When tying together production and utilities functions it is essential that constraints are not placed on the operation of production facilities. The absorption machine has a large turn-down ratio, and an ability to operate over a 10 psig range of steam supply pressure, therefore it operation imposes no constraints on production requirements.

3. Compatability with existing utility systems. The absorption
   chiller operates in parallel with the centrifugal chillers,
   is located alongside them in the utility building and is con-
   venient to cooling water, chilled water and electrical systems.
   Although the machine has a complex thermodynamic cycle the
   operating techniques are relatively simple. This latter point
   is very important to the successful implementation of an energy
   management program. Improving energy efficiency or recovering
   waste heat in an industrial plant generally adds equipment to
   the plant facilities. Ensuring that complexities are minimized
   is of paramount importance. Operating personnel must be well
   trained, but successful operation is only assured if they are
   not overwhelmed by complex equipment and controls.

TABLE 1. WASTE HEAT BOILER DESIGN PARAMTERS

T.E.M.A. Designation	32/50-214 BKU
T.E.M.A. Class	C
Design Press./Temp.	75 psig/600°F
Material of Constr.	C.S. shell/304 S.S. Tubes
Total design heat transfer rate	13,798,500 BTU/Hr.
Condensing fluid,tubes	Process Vapors
Condensing rate, max.	15,000 pounds/hour
Boiling fluid, shell	Water
Boiling Rate, Max.	13,900 pounds/Hr.
Design solids content in boiler water	10 ppm by wt.
Design moisture content in steam, max.	1% by wt.
Operating Temp. shell in/out	202°F/252°F
Operating Press., shell	16 psig
Operating temp., tubes in/out	289oF/287°F
Operating press., tubes	40 psig
Maximum shell diameter	50 inches
Straight length of tubes	214 inches

TABLE 2. ABSORPTION CHILLER DESIGN PARAMETERS

Design capacity	1,000 tons (1140 maximum)
Steam Consumption	18,500 lb/hr. (21000 lb/hr. max.)
Steam Pressure	12 psig
Steam control valve pressure drop	3 psi
Chilled water temp., inlet	52°F
Chilled water temp., outlet	42°F
Chilled water flow rate	2,400 GPM
Chilled water pressure drop	35 ft. (15.2 psi)
Condenser water temp., inlet	85°F
Condenser water temp., outlet	98.3°F
Condenser water flow rate	4,500 GPM
Condenser pressure drop	24 ft. (10.4 psi)
Maximum chill water Δ T	14°F
Maximum steam pressure	15 psig
Minimum chill water flow	890 GPM
Cooling water temp. (minimum)	75°F

282

FIGURE 1. WASTE HEAT RECOVERY SYSTEM

FIGURE 2. STEAM CONSUMPTION VS NET REFRIGERATION
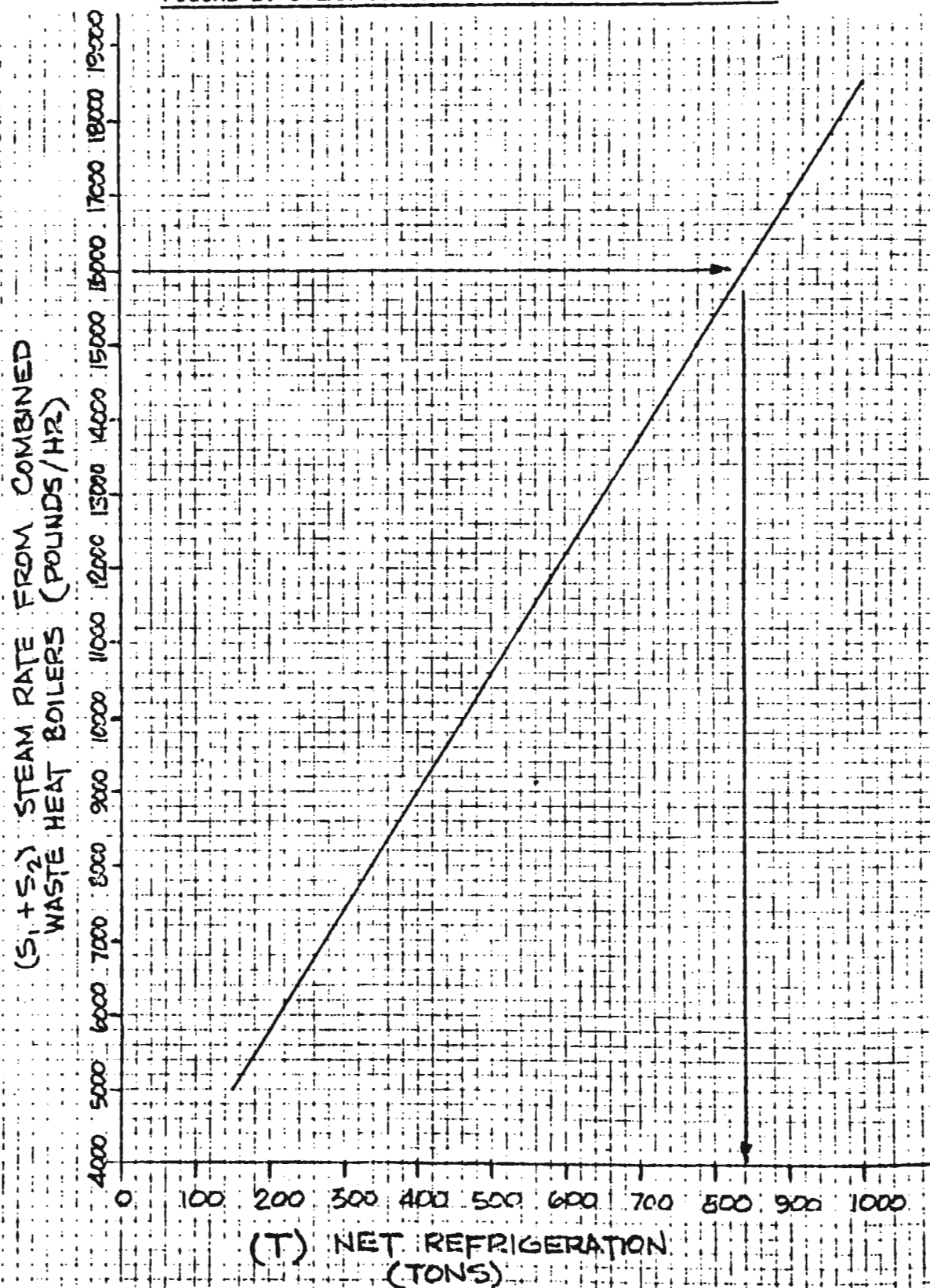
FIGURE 3   SCHEMATIC OF ABSORPTION CYCLE
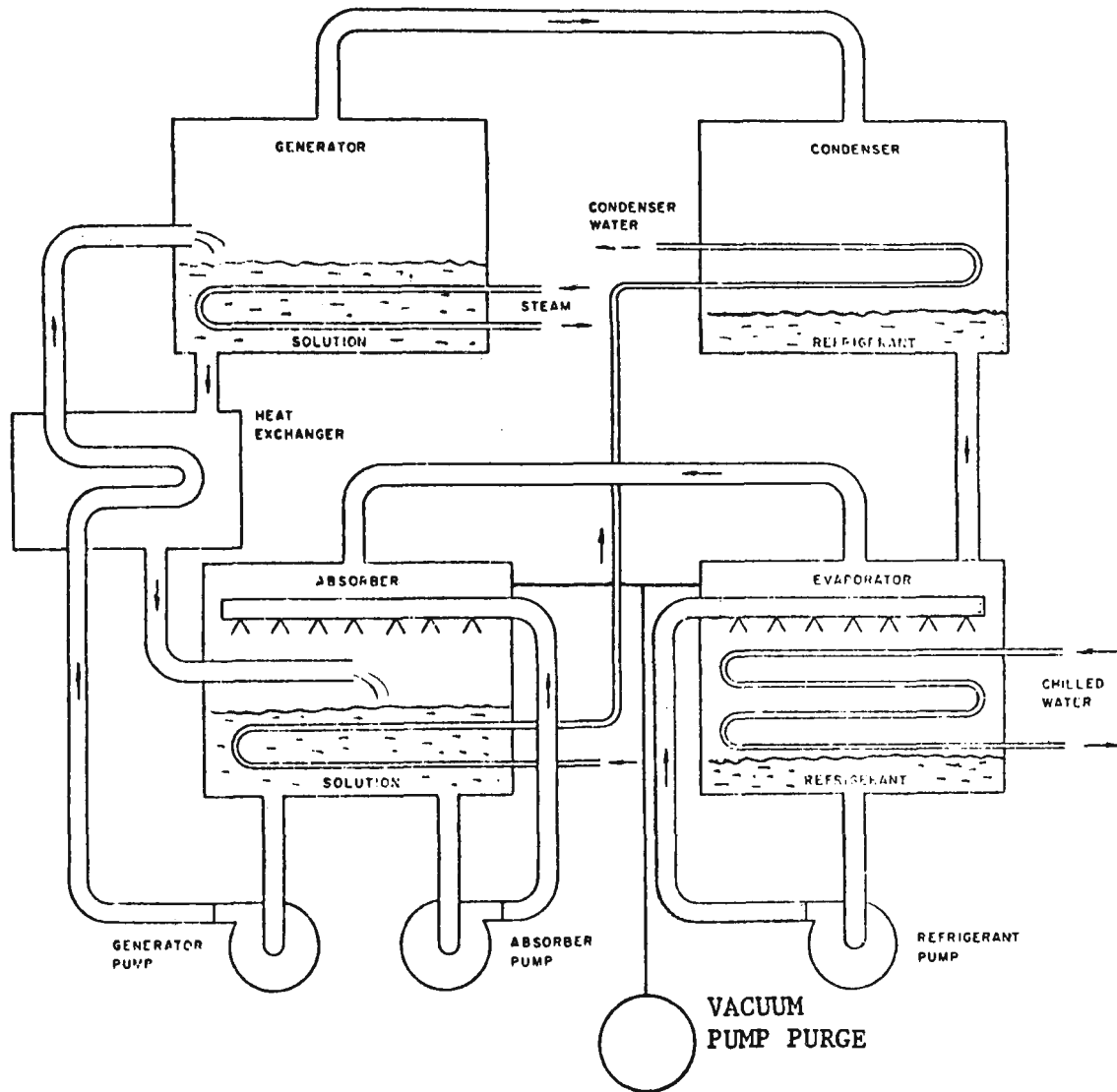
THE SHERCO GREENHOUSE PROJECT: FROM
DEMONSTRATION TO COMMERCIAL USE OF CONDENSER
WASTE HEAT

G. C. Ashley
Northern States Power Company
Minneapolis, Minnesota U.S.A.

J. S. Hietala
Northern States Power Company
Minneapolis, Minnesota U.S.A.

R. V. Stansfield
Northern States Power Company
Minneapolis, Minnesota U.S.A.

ABSTRACT

Northern States Power Company's Sherburne County Plant produces both elec-
tricity and waste heat for commercial sale. As a result of nearly ten
years of research, development and demonstration, it is now technically and
economically feasible to utilize condenser reject heat for commercial
greenhouse heating in Minnesota. A three-year demonstration project
jointly funded and sponsored by Northern States Power Company, the Univer-
sity of Minnesota, and the U.S. Environmental Protection Agency has lead
the way for commercial adoption of the concept. Experience during the
demonstration project proved that condenser waste heat available at
approximately 85°F was suitable to maintain a greenhouse growing environ-
ment of 55 to 60°F when outside air temperatures fell as low as -43°F.
During the first year of operation of the pipeline system serving waste
heat to commercial greenhouse customers, an overall availability of service
of 97% was achieved. The savings in heating costs to commercial operators
using waste heat have amounted to nearly $5,000 an acre year compared to
conventionally heated greenhouses. While there are presently three commer-
cial operators with 1.7 acres in production, the experiences of these
operators have been sufficiently satisfactory that future expansion of
waste heat service at the Sherburne County Plant site is expected.

INTRODUCTION

Since 1970, Northern States Power Company (NSP) has been investigating
beneficial uses of the heat energy available in condenser cooling water at
electric generating plants. The concept of utilizing condenser cooling
water for agricultural heating applications, proposed initially by re-
searchers at Oak Ridge National Laboratory (ORNL) in the late 1960's, was
of particular interest to NSP; since new generating plants were then in
the planning stages that would utilize closed-cycle cooling systems.
Closed-cycle cooling system designs result in condenser outlet water temp-
eratures of generally not less than 85°F during the winter heating season.

With this knowledge, NSP approached the University of Minnesota Agricultural Experiment Station requesting their assistance to determine the best potential application for utilizing condenser cooling waters in agriculture. After extensive investigation into the field of waste heat utilization and several visits to waste heat related projects, the University of Minnesota advised that the concept of utilizing this waste heat for greenhouse heating appeared promising.

Based on the University of Minnesota's recommendations and research efforts with evaporative pad heating systems conducted at ORNL and also at TVA, NSP decided to test the concept of greenhouse heating in a 2,000 ft^2 commercially operated greenhouse in Minneapolis during 1974 and 1975. Encouraging results from this research effort eventually lead to an award from the U.S. Environmental Protection Agency (EPA) to demonstrate the technical and economic feasibility of using power plant waste heat in a larger scale, one-half acre greenhouse. The Sherco Greenhouse, as it i⁻ now known, was a cooperative effort of NSP, the University of Minnesota, and EPA. The EPA grant was for a two-year period completed in May 1977; but because of the success and the interest of EPA in commercial adoption of the concept, the project was extended through June, 1978.

The Sherco Greenhouse was built in the Fall of 1975 and heated during 1975-76 with simulated waste heat, since the power plant was still under construction. In September 1976, the Sherco Greenhouse began using condenser reject heat from Sherburne County (Sherco) Unit I condenser cooling water. The Sherco Greenhouse was heated from the waste heat source in the 1976-77 heating season and in the 1977-78 heating season. Due to the success and publicity of the Sherco Greenhouse, a commercial florist and a commercial vegetable operator approached NSP in 1977 requesting suitable sites and warm water service to heat commercially operated greenhouses. Therefore, in the Summer of 1977 NSP decided to provide warm water from the Sherco Plant on a commercial service basis to greenhouse operators. Presently warm water service is being provided to three commercial operators with a total acreage in production of about 1.7 acres. This paper describes only the experience and economic projections of NSP in providing waste heat service in the form of warm water to commercial greenhouse operators. A more complete description of the Sherco Greenhouse Project can be found in references 1 and 2.

EXPERIENCE WITH COMMERCIAL GREENHOUSES

As a result of the successful experience of the Sherco Greenhouse project, NSP was approached by commercial operators in the Spring of 1977 and asked to provide a site and warm water service to a one-acre commercial floral operation and to a .2 acre commercial vegetable operation. Both commercial facilities began construction in 1977 and warm water was first sold commercially to the one-acre floral operation in November, 1977. The smaller, .2 acre, vegetable operation did not require warm water service until February, 1978.

Description of Facilities

The one-acre commercial floral greenhouse is an arch roof, gutter connected plastic covered structure like the Sherco Greenhouse; however, it has a bay width of 17.5 feet and length of 144 feet with 17 gutter-connected bays to provide a total enclosed area of 42,840 ft^2, or just less than one acre. (See Figure 1). The greenhouse was erected in mid-summer 1977 and initially planted partially in roses and chrysanthemums in August, 1977. Following the first grow out of the mums, the greenhouse was fully cropped in roses and is now producing only roses. The heating systems for the commercial greenhouse facility include both soil heating and air heating of a design similar to that used in the Sherco Greenhouse. The commercial floral operation began taking warm water service for greenhouse heating in November, 1977 and has now experienced an entire heating season utilizing warm water from the operating power plant.

The commercial vegetable producer's facilities are two quonset style greenhouses that are covered with a double layer of polyethylene. Each unit measures 30 feet wide by 150 feet long. The commercial vegetable producer is using a hydroponic culture method and the first crops produced were lettuce and spinach. The heating system employed in the vegetable operation is conceptually the same as that used in the Sherco Greenhouse in that it utilizes dry fin tube heat exchangers and packaged air handling units. However, the air distribution system is under the growing beds rather than above the growing beds as in the Sherco Greenhouse and the commercial rose range.

In order to serve warm water reliably, NSP decided in the Summer of 1977 to make an interconnection between the two generating units so that waste heat could be provided from either of the units. In order to do this, a tie into the Unit II riser pipe near the cooling tower was made and a pipeline was constructed to interconnect to the previously existing pipeline from the Unit I cooling tower. It was deemed necessary to have an interconnected pipeline system from the two units to provide sufficiently reliable warm water service to maintain commercial interest in condenser waste heat for greenhouse heating. The pipeline installed in 1977 was an 18" diameter cast iron pipe that was uninsulated and buried to a nominal depth of about 5 feet. The 18" diameter pipeline was intentionally over-sized to allow for future expansion of commercial warm water service. The pipeline chosen is capable of delivering sufficient flow to heat up to 14 acres of greenhouses at the Sherco site.

Warm Water Service Operating Experience

Warm water service first became commercially available for greenhouse heating on November 2, 1977. From that time until the end of May, 1978 the warm water service system operated with an overall availability of 96.6%. On a weekly basis during the first heating season, there were only four weeks out of thirty when warm water was unavailable for part of the time. Unavailable service to the commercial greenhouse operations was primarily

288

due to pipeline failures. There were two pipeline failures experienced during the heating season; one was the failure of a service line from the main pipeline into the commercial floral operation; the other failure was the failure of a main 12" diameter plastic pipeline. In the former case, a four-day outage occurred; in the latter case a 26-hour outage occurred. The only time that a two-unit generator outage made warm water unavailable was during May when Unit I was scheduled out for a month for annual maintenance; and Unit II was simultaneously scheduled out for weekend maintenance. Thus, for a period of 56 hours, warm water was unavailable due to a simultaneous two-unit outage. Fortunately, this occurred in May when the heating requirements of the greenhouses were not great.

While the warm water was available 96.6% of the time, it was not always available at temperatures high enough for maintaining the greenhouse environment desired by the commercial operators. This was due primarily to reduction in electrical load on the two-unit station over night and also, to some extent, resulted from frozen coal problems experienced at the power plant. Figure 2 indicates the effect of unit loading on warm water temperature. It can be seen that as the generator unit load varies from about 200 MW to 700 MW, which is the normal load range, the condenser outlet water temperature can vary over a range of about 20°F. Due to the nature of the electrical system loads of NSP; a unit like Sherco, designed to load follow, reduces load over night which reduces the condenser outlet water temperature. Even so, over the first heating season, the waste heat was available at the condenser outlet above 85°F for 83% of the time. Figure 3 indicates the measured warm water temperature distribution for all of January, 1978. As indicated, 73% of the time the temperature was greater than 85°F; at least entering the pipeline. After taking into account pipeline heat losses for delivery to the customer, the temperature available at the customer point of use was reduced 3°F.

Supplemental Heat Energy

The commercial greenhouse operations utilizing warm water heating also have a backup heating system in the event of pipeline system failure or a two-unit generating station outage. While the backup heating system is primarily designed for standby and emergency heating, it can also be used to supplement heat energy available from the warm water source. The back-up heating systems used by the commercial operators at the Sherco site are propane fired unit heaters. Propane was selected as the fuel over oil, partly because propane would be required in any event for CO_2 generation; and, partly because the cost of propane fired heating equipment is less than the cost of oil-fired heating equipment.

Even though the warm water was available to the customers 97% of the time during the first commercial heating season, the one-acre floral range consumed 8,700 gallons of propane. While about 1,700 gallons of this propane consumption was for CO_2 generation, the balance was used to provide standby heat during pipeline failures and a two-unit outage; as well as supplemental heat at times when the warm water temperature was too low to

maintain the desired greenhouse temperature. The total propane consumed represented less than 10% of the annual heat requirements of the green-house and that used only for supplemental heat amounted to 5%. It is expected that as the pipeline system is operated in the future, the operat-ing availability of the pipeline system will improve and the supplemental and standby heat energy requirements will be diminished.

Electrical Energy Consumption

Because of the relatively low temperature difference between the heating source and the desired space temperature, a significant amount of elec-trical energy is required by the fans and pumps to produce the required heat transfer rate. For example, in the case of the one-acre commercial operation, the heating system fans have a total motor horsepower of 85, while the liquid pumping requires 10 Hp. Thus, a total of 95 Hp or approx-imately 70 KW of electrical load results from the full load operation of the heating system. Because the heating fans cycle on and off by thermo-static control, the actual daily utilization of energy is significantly less than the full load operating requirement. The total measured elec-trical consumption in the one-acre commercial floral range during the first heating season was 237,000 KWH. It is estimated that about 85% of this electrical consumption was directly attributable to the operation of the warm water heating system. Based on NSP electrical rates, the cost of electric energy to drive the warm water heating system is one of the most significant operating cost items. The others, of course, are the cost of delivering the warm water to the customer and the cost of supplemental heating fuel. Presently the cost of electric energy to operate a warm water heating system for a typical acre is about $7,000 per year; while the cost to deliver warm water is about $8,000 per acre-year. Though the electric energy requirement to operate the warm water heating system has a significant cost impact, compared to a heat pump system extracting heat from the same low temperature water source, the greenhouse direct heat transfer heating system is more than three times as efficient, utilizing one-third as much electric energy as a heat pump system.

Economic Feasibility

The economic feasibility of utilizing condenser reject heat for greenhouse heating is dependent upon many variables. The most important of these are site specific variables such as distance from the waste heat source to the greenhouse acreage served, climatic conditions, electric rate structures, land cost, and distance to market. Because of these highly site specific variables, generalizations about the economic feasibility of utilizing waste heat for greenhouse heating are of limited value.

However, it has been found that at least at the Sherco site, conditions are such that the concept appears to be economically feasible. For example, the most recent cost estimates to install the necessary pipeline services to serve a 14 acre greenhouse complex located within roughly one-half mile of the waste heat source, reveal a pipeline investment of about $35-40,000

290

per acre of greenhouse served. Depending on cost of money and other considerations, the investments in pipelines generate a requirement for a return of about $6-8,000 per acre per year to recover the investment.

In addition to the capital cost of pipelines, there is an operating cost associated with pumping the warm water from the waste heat source to the user; and, there is a cost associated with the overall operation and maintenance of the pipeline network. At the present time, NSP estimates that the total variable operating cost will run roughly 1¢/thousand gallons of water delivered to the user. At this rate, a typical one-acre greenhouse operation in Minnesota would realize an operating cost of $1,500 per acre-year.

The approximate total capital and operating cost associated with delivery of waste heat at the Sherco site is now $8,000 an acre-year. NSP has adopted a philosophy of providing waste heat on a cost-of-service basis with a return on investment that is equivalent to the rate of return on investment for other utility services provided by the Company. That is to say, there is no energy value placed on waste heat. No portion of the fuel cost of the power station of any capital investment normally associated with a power plant are allocated to the cost of serving waste heat. The cost of serving waste heat is based on incremental investment and incremental operating costs only. This cost-of-service pricing philosophy may or may not be unique in the utility industry.

Since a major portion of the cost of serving waste heat is related to investments in pipelines, it is possible to offer long-term fixed-price contracts to pay for the fixed cost associated with the waste heat service. So in much the same way as sewer and water are assessed to individual users in municipal water systems, the commercial greenhouse operators are essentially assessed their portion of the cost of the pipeline network and then allowed to pay for it over a period of 20 years. The variable cost of operating, maintaining, and pumping the water in the pipeline are subject to yearly price changes based on actual operating experience. The effect of the long-term fixed-price contract for waste heat energy is to make the waste heat system more and more attractive in the future as other energy costs escalate.

In addition to the investments incurred by the utility to supply warm water to a commercial greenhouse, the greenhouse operator incurs a significant investment in the warm water heating system; the coils, fans, and pumps required to transfer sufficient heat to the greenhouse. For the Minnesota climatic conditions, the estimated installed cost of a complete one-acre warm water heating system including controls, electrical work, and a back-up heating system is about $85,000 per acre. This compares to conventional greenhouse heating systems that, on the same basis, might cost about $50,000 per acre.

The comparative operating costs of utilizing waste heat versus conventional heating are indicated in Table 1. The figures presented are based on a one

acre, double plastic greenhouse located at the Sherburne County Plant site. The total operating costs on a per acre year basis for the waste heat system in 1978 are estimated to be $17,000, which includes $8,000 for waste heat, $7,000 for electricity, and $2,000 for standby propane. A typical conventional greenhouse using No. 2 fuel oil has an estimated heating cost of $28,000 per year.

There is an apparent savings of $11,000 per acre year by utilizing the waste heat system in 1978 dollars. But, the big advantage of the waste heat system is more apparent in the future as fuel costs escalate. The waste heat system would realize an escalation in the cost of propane and electricity; but, the waste heat costs would not increase very much due to the fact that the pipeline investment had been made 20 years previously. In 1998, at a compound escalation of 6% for all utilities and variable operating costs, the waste heat system shows a cost advantage of $51,000 per acre-year. These comparative operating costs are projections based in part on operating experience and anticipated future operating experience at the Sherco plant site. The actual operating costs for all utilities for the one acre commercial floral range totaled 37¢/ft^2 for the period November-May. This compared to 65¢/ft^2 for a glass greenhouse owned by the same company. While part of the savings is attributable to the fact that one greenhouse is double polyethylene and the other is glass, probably only 30% of the savings results from that difference. The remaining savings, about 8¢/ft^2, directly result from the use of warm water for heating. This actual experience in the first year of commercial operation of the warm water heating system falls considerably short of the projected annual savings of roughly $11,000 an acre year, but the greenhouse to which the comparison was made received 62% of its energy as interruptible natural gas. Had the other greenhouse been heated only with oil, the comparative savings would be about $13,000 per acre-year.

In terms of overall commercial acceptance of waste heat, there are other considerations that are very important. One of these is the transportation distance from the market. Most new modern electric power stations are located some distance from major metropolitan centers for reasons of air quality and other considerations. Therefore, the source of waste heat is not close to the market for the output of the greenhouse producers. The increased transportation costs must be considered by the prospective greenhouse operator in determining whether he can relocate to a power plant site to use waste heat. A second consideration is the cost of land and the manner in which land acquisition is handled. At Sherco NSP owns all of the land in and about the power plant; and, the land on which the commercial greenhouses are located is leased to the greenhouse operators at a nominal fee. Because the operators are on leased land, though, they will never benefit from the appreciation in land values which in the past has generated significant long-term capital gains for greenhouse owners. Thus, in cases where land will be owned by a utility and leased to greenhouse operators, there need to be significant savings in operating costs to offset the disadvantage of leased land. Another consideration may be the local property tax structure. Generally speaking the value of a power

station is so great as to impact local property tax mill rates to the extent that property taxes tend to be low in areas in which power plants are located. This can have a beneficial financial effect on the commercial greenhouse operation.

While it appears economically feasible to provide waste heat service to greenhouse customers and it appears reasonable for the greenhouse customers to make additional investments in heating systems to save in future heat energy costs, it is still too early to predict whether this trend will hold true at many power plant sites in the U.S. or whether this will prove to be a relatively unique situation.

CONCLUSIONS

Based on the experiences over a three-year period with the Sherco Greenhouse, it is apparent that condenser reject heat, available at the relatively low temperature of 85°F, is a wholly satisfactory heat energy source for greenhouse heating in northern climates. The concept of utilizing this waste warm water has been accepted and adopted by commercial greenhouse operators in Minnesota. Though the commercial acreage in production now is only 1.7 acres, depending upon future fuel cost escalation and market conditions, an expected initial expansion of up to 14 acres at the Sherburne County Plant site is reasonable. Whether the concept demonstrated can be expanded throughout the U.S. will depend on a myriad of site specific and market related variables, but at this time the prognosis is good.

REFERENCES

1. Ashley, G. C. and Hietala, J. S. "The Sherco Greenhouse: A Demonstration of the Beneficial Use of Waste Heat". Proceedings of the Waste Heat Management and Utilization Conference. May 9-11, 1977.

2. Boyd, L. L. et. al. "Use of Waste Heat from Electric Generating Plants for Greenhouse Heating". Proceedings of the ASAE 1977 Winter Meeting. Paper No. 77-4531. December 13-16, 1977.

TABLE I
COMPARATIVE OPERATING COSTS OF WASTE HEAT VERSUS CONVENTIONAL HEATING

	- 1978 Costs -		- 1998 Costs -	
	Waste Heat	Conventional	Waste Heat	Conventional
Fuel Cost Standby Propane	2,000	27,000	6,000	86,000
Electricity	7,000	1,000	22,000	3,000
Waste Heat Cost	8,000	_____	10,000	_____
Total Per Acre Per Year	17,000	28,000	38,000	89,000

Basis: #2 Fuel Oil @ $.384/gal
Propane Cost @ $.43/gal
Electricity Cost @ 3.5¢/kwh

Fig. 1 Commercial Floral Range, Vegetable Range, and Sherco
Greenhouse in Foreground. Power Plant in Background.
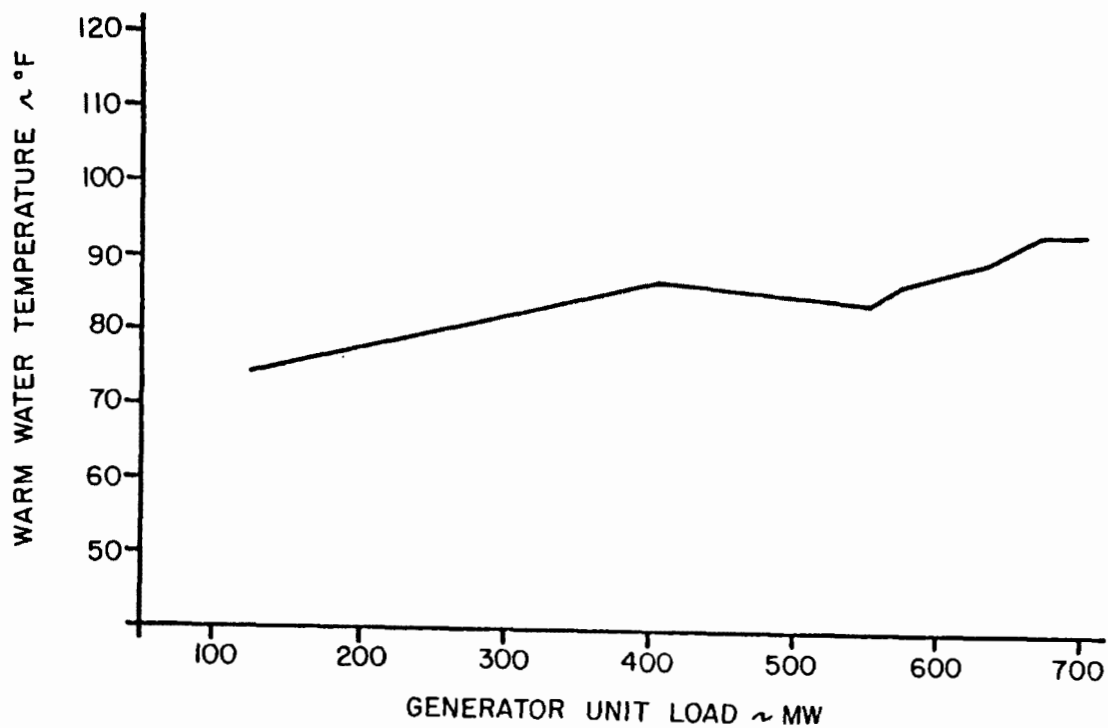
Fig. 2 TYPICAL WARM WATER TEMPERATURE
VARIATION WITH UNIT LOAD

73% of
Time
Temperature
Greater than
85°F
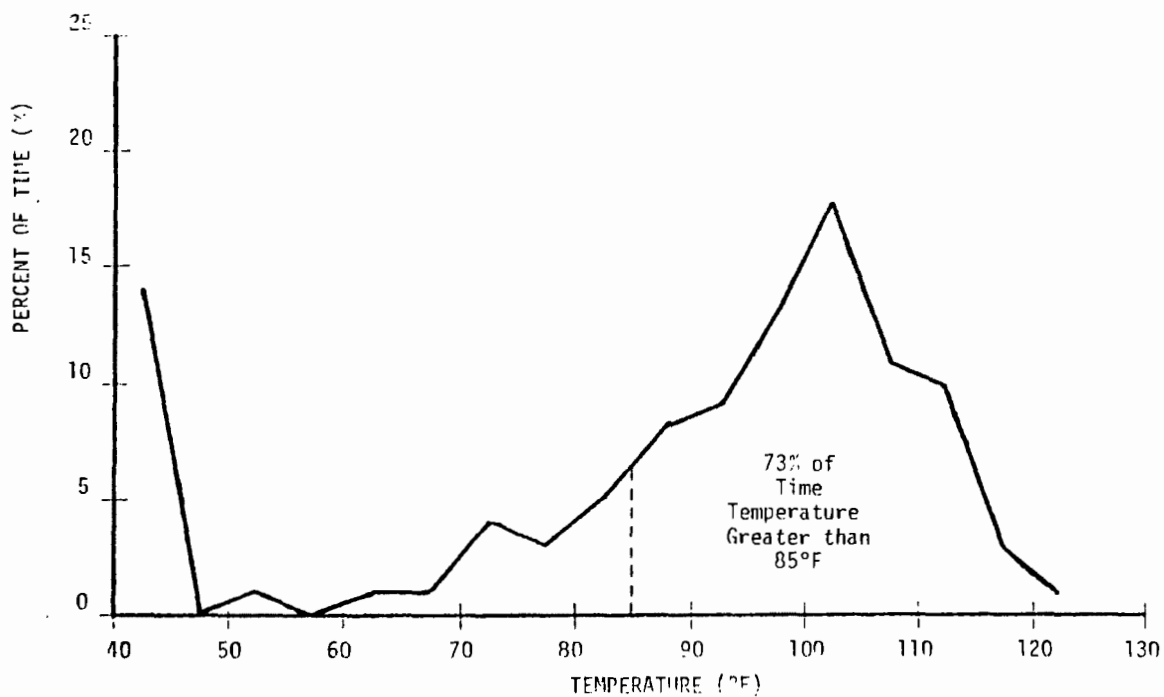
Fig. 3 CONDENSER OUTLET WATER TEMPERATURE DISTRIBUTION
JANUARY, 1978
COMPOSITE OF UNIT I AND UNIT II

ANALYSIS OF ECONOMIC AND BIOLOGICAL FACTORS OF
WASTE HEAT AQUACULTURE

J. S. Suffern and M. Olszewski
Oak Ridge National Laboratory*
Oak Ridge, Tennessee 37830

ABSTRACT

A waste heat aquaculture system using extensive culture techniques is
currently under investigation at the Oak Ridge National Laboratory. The
system uses nutrients in waste water streams to grow algae and zooplankton
which provide feed for fish and clams. A tilapia polyculture association
and the freshwater clam Corbicula are the animals cultured in the system.

The investigations detailed in this study have been performed to determine
the economic and biological feasibility of the system and examine energy
utilization. A net energy analysis identified the energy saving potential
for the system. This analysis included all energy costs (both direct and
indirect) associated with building and operating the system.

The economic study indicated that fish production costs of $0.55/kg
($0.24/lb) were possible. This cost, however, depends upon the fish pro-
duction rate and food conversion efficiency and could rise to as much as
$1.65/kg ($0.75/lb).

The biological studies have examined growth relationships and production
potential of the cultured organisms. In the laboratory, growth-tempera-
ture optima have been defined (32°C, with good growth rates between 26 and
34°C) for tilapia hybrids. In addition, growth rate acceleration experi-
ments have been carried out, developing techniques which yield 40% higher
growth rates in experimental fish as compared with controls. Using cage
culture techniques in sewage oxidation ponds, we have obtained production
estimates in excess of 50,000 kg/ha/yr (50,000 lb/acre/yr).

The energy utilization study indicated that, when all energy costs are
included, fish from the aquaculture system may require only 35% of the net
energy now required for fish products from the ocean. However, the energy
requirements also depend on system parameters and could be as large as the
energy required for ocean caught products.

The analyses indicate that the system is economically feasible. They also indicate that significant energy savings are possible if waste heat aquaculture products replace ocean caught products.

INTRODUCTION

A waste-heat utilization strategy must meet basic feasibility criteria in order to be considered viable. [1] At ORNL, we have been carrying out multidisciplinary studies to evaluate the economic and technological feasibility of aquaculture as a waste heat utilization strategy, and have reached some very interesting conclusions. This paper presents the results of our studies to date, outlining the conceptual design we have found to be optimal, and the biological, economic and energetic analyses we have carried out.

SYSTEM DESIGN

The basic precept of current aquaculture research at ORNL is that production systems should be designed to produce low-cost protein. Our basic thinking is that, although protein supplies are adequate in the United States at present, a large part of the world is already protein poor, and conditions of surplus are not likely to last much longer. The design of such a system is a radical departure from the capital-intensive monoculture techniques in vogue in the United States today. First, for reasons of system efficiency and stability, polyculture, that is, growing several species at once, should be used. Second, instead of using expensive high-protein feed, waste streams, such as sewage, animal wastes, or food processing wastes, could provide nutrient input.

Based on these ideas, a preliminary system concept was developed and subjected to extensive engineering and economic analyses. The current conceptual design (Fig. 1) is a sequential pond system, involving a succession of ponds dedicated to different cultures: algae, mixed species of fish, crustaceans, or rooted vegetation, into which controlled amounts of heated water and waste-stream nutrients are fed. Although details may change as a result of future research, the basic concept is expected to remain.

BIOLOGICAL STUDIES

Several different species arrays may be used in the system, [2], and of these, one based on tilapia appears most promising. They are excellent food fish and are readily marketable. Second, they have been cultured extensively around the world and enjoy a reputation of having few disease problems. Third, as a result of worldwide culture activities, a good data base exists on many aspects of their biology. Fourth, literature reports on several species indicate growth-temperature optima from 25 to 35°C.

This is substantially above that recorded for temperate-latitude fish, a factor that suits the genus well to waste heat systems where relatively high temperatures might be expected. Also, all tilapia species have about the same body shape and size, allowing some standardization of harvest and processing techniques.

Tilipia have one major drawback as a food culture organism: they become reproductively active at a small (<100 g) size. This could result in a crop of fish too small to market as human food, and is a problem which must be solved if the fish are to be practical for use in a commercial operation. At present, there are two ways around this dilemma. The first is sex reversal by hormone injection. This technique involves the administration of androgenic hormones to young fish, accomplishing sex reversal with about 95 to 99% effectiveness. The second method is hybridization. Several of the species, when crossed, produce monosex hybrids. Done carefully, this technique is 100% effective in some crosses.

We chose to use a monosex hybrid, the all-male cross of ♂ Tilapia hornorum by ♀ Tilapia mossambica, in our initial experimental program. This hybrid is known to be a plankton feeder, and appeared to be a promising candidate to fill that feeding niche in a polyculture array.

Our experimental efforts have been designed to answer questions which are fundamental to commercialization of the waste nutrient-waste heat aquaculture concept. A primary bit of needed information is the thermal regime necessary to maintain maximum growth rates in cultured organisms. In order to assess the optimum growth temperature of Tilapia mossambica ♀ x Tilapia hornorum ♂ hybrids, fish between 45 and 55 mm standard length were divided into sixteen groups of ten fish each. Two groups of ten fish each were placed in each of eight glass aquaria, 45 x 89 x 38 cm, and separated by wire mesh partitions. Each aquarium was maintained at a different temperature: 20, 23, 26, 28, 30, 32, 34, or 37°C, with a continuous flow-through of about 3.5 liters/minute. Purina trout chow (#2) was fed to the fish ad libidum and the tanks were vacuum-cleaned daily.

At the initiation of the experiment, tilapia were acclimated to test temperatures for one week. Laboratory lighting throughout the experimental period was maintained at a seasonal (summer) photoperiod; activated by an outdoor photocell. All fish were weighed and measured biweekly after anesthesia in tricane methanesulfonate. The experiment ran for 39 days.

Growth at all temperatures was approximately linear throughout the experiment (Fig. 2). The largest increase in biomass occurred with those fish maintained at 32°C with the fish at 26, 28, 30 and 34°C also showing substantial growth. Even though the fish at 32°C produced the most biomass, the confidence intervals on percent increase in weight per day (Fig. 3) indicate that there is not a statistically significant difference between the growth rates at 26, 28, 30, 32 and 34°C. Statistical sifnificance may not be the most important criterion for selecting aquaculture temperatures, however, when the trend of the results is so clear.

In order to test the utility of our waste-stream nutrient concept, the Oak Ridge National Laboratory (ORNL) sewage oxidation ponds were used as an experimental facility. It was felt that they were an excellent simulation of a waste-nutrient-loaded pond system, and would produce results similar to a system devoted to aquaculture.

The two ORNL sewage ponds are sequential. Raw sewage flows from a preliminary mechanical chopper into the first pond, resides there for about six days, then flows into the second pond, is retained for another six days, then is discharged (receiving chlorination during the process) to a stream. Table 1 lists some salient characteristics of this pond system during the experimental period. The sewage ponds are rectangular, and are lined with polyvinyl chloride. To facilitate the oxidation process each pond is equipped with large bubble aerators, designed and installed to produce a short turnover time. This aeration system is very effective; in several months of observation, dissolved oxygen readings did not drop below 5.5 ppm. During the experimental period (July and August) average daily temperatures were 26-34°C, found to be favorable in the laboratory growth-temperature experiments. Due to the rapid turnover caused by the aeration system, the ponds were isothermal.

The tilapia were stocked in the ponds at a density of $53/m^3$ in floating cages made of 6 mm mesh Vexar netting and wood frames, and were weighed and measured biweekly after anesthesia in tricane methanesulfonate.

The plankton assemblages in the two ponds were strikingly different. The first pond, into which raw sewage was discharged from the preliminary treatment facility, was almost a monoculture of Euglena for the duration of the experiment. This condition appears to be the "natural" equilibrium situation. The second pond was a fairly stable zooplankton culture, dominated by a large strain of Daphnia pulex. Numbers of this organism declined during the peak temperatures in mid-July, but became re-established as temperature began to fall in August, again dominating the plankton assemblage.

Change in mean weight of the tilapia is shown in Figure 4. As can be seen by inspection, average weight gain was essentially linear over time; about 7.5 g/week (~ 1.07 g/day). Although the differences are not statistically significant, it appears that the fish in pond 2 (the one dominated by zooplankton) grew faster than those in pond 1. Lodge, et al. [3] have recorded growth rates between 1.7 and 2.0 g/day with tilapia weighing 60-150 g in the same system.

The production potential of a waste-nutrient system was calculated from the results, and is quite large. From these experimental data, we calculate production rates of 397 g/m^2/wk or 3970 kg/ha/wk or 206,440 kg/ha/yr.

This production estimate must be viewed with caution, as it is based on extrapolation from experimental results, not the operation of a full-scale system. Several assumptions underlie the estimate, some of which make it

excessive. The first is that the entire pond surface is assumed to be covered with cages. This is unreasonable, as it allows no room for harvesting equipment (boats). Assuming one half of the pond surface to be open allows room for boats and reduces the production estimate by a factor of two. We also assumed that the fishes' daily growth increment remained constant up to marketable size (300 g). Our experimental data indicate no decrease in growth increment as fish size increases up to around 150 grams, but we feel that such a decrease is likely in larger fish, and that production estimates should be reduced by a factor of two to account for this. We have assumed that the system operates near the optimum growth temperature for the fish year-round, a situation which is feasible in temperate latitudes only with the addition of heat for much of the year, making our production estimates applicable only to waste heat aquaculture systems (any other source of heat, excepting geothermal, would be too expensive).

It is probably not necessary to reduce production estimates to account for density-dependent effects if pond design and stocking densities are similar to those discussed in this paper. Density-dependent effects may alter production rates in two basic ways. First, fish crowding may lower growth rates. This is probably not the case at the stocking densities postulated here; experiments carried out by the senior author (Suffern, unpublished) indicated no difference in growth rate between fish stocked in the sewage ponds at $10/m^3$ and those stocked at $53/m^3$. A second density dependent effect on production is the effect of fish feeding on food organisms. If consumption by the fish exceeds food organism production rates, fish production rates will decline. Assuming Golueke, et al.'s [4] reported production rates for algae in hypereutrophic, intermittently aerated ponds, a conversion effeciency from algal biomass to fish biomass of 10%, rapid mixing, half the surface area covered with cages, and a pond depth of about 2.5 meters, fish production between 25,000 and 50,000 kg/ha/yr could be supported. This is probably a low estimate of supportable production because Goleuke's estimates were based on ponds which were aerated only during the winter as versus all-year round aeration in our proposed system. Also, the support estimate does not account for aufwuchs utilization by the fish, a component of their ration in this cage culture system. Given all these considerations we feel it is reasonable to expect production on the order of 50,000 kg/ha/yr from a waste-heat waste-nutrient aquaculture system.

We carried out growth acceleration experiments to explore ways of boosting production rates in waste-heat aquaculture systems. There is evidence that changes in growth rates in some animals can be caused by exposure to moderate doses of hard radiation. [5] This effect was tested on tilapia hybrids.

Twenty-five young tilapia hybrids (mean weight 2.7 g, mean standard length 4.60 cm) were exposed to 500 rads of gamma radiation in a cobalt[60] source. From previous experiments at ORNL with channel catfish (Ictalurus punctatus) (Blaylock, unpublished) there was evidence that this dosage might enhance growth rates. The irradiated tilapia were placed in a flow-through

tank kept at 30°C. A control group of 25 fish was kept in an adjacent tank with identical flow and temperature conditions. Both groups were fed ad libidum with Purina #2 trout chow.

The results of this experiment are shown in Figure 5. The mean weights of the fish for the control and treated groups are tabulated in Table 1. The data clearly show that up to week 8 there was no difference in the growth patterns of the two groups. After that time, however, one observes a possible pattern with the irradiated group gaining faster than the control group.

Using the Subhatme d-statistic [6] we find the mean weights significantly different at the 0.05 level at fourteen weeks; an indication of real divergence. This trend continues through week 52, at which time the irradiated fish average about 40% heavier than controls.

At the present time, detailed autopsies are being performed on the fish in an attempt to ascertain the mechanism whereby gamma radiation causes growth rate changes. Our hypothesis is that the administered radiation caused gonadal atrophy resulting in growth rate changes parallel to, for example, those seen in cattle which have been made steers.

Several aspects of this system's biology remain to be examined. For example, heavy metal accumulation, pathogen transmission and effluent characteristics are all areas of potential concern to commercialization. Fitzgerald and Suffern [7] have examined heavy metal uptake in sewage pond raised fish. While results are still being analyzed, preliminary indications are that heavy metal accumulation may not be a major problem. Lodge, et al. [3] have examined nutrient processing and effluent characteristics of a sequential pond cage culture system, and find dramatic reductions in nutrient levels in successive ponds. Pathogen transmission, a subject of concern with the FDA, has yet to be explored adequately.

ECONOMIC ANALYSIS

The previous discussion of the system's operation indicates that the fish and clam production systems can be considered to be independent systems. Results from the preliminary analysis [8] of the system indicated that the clam system was the major income center for a combined system. However, the experimental efforts described above have indicated that the fish production system has the potential to match the clam system profitability. Therefore, this report will be limited to an economic feasibility analysis of the fish production system.

System Size

Analysis of the system was performed for an 0.4 ha (1 acre) fish pond. To determine if an auxiliary plankton production pond was required it was

necessary to estimate fish production (and corresponding food intake) and plankton growth rates.

Fish production rates for tilapia polyculture systems of this type have not been firmly established. Annual yields of 7378 kg/ha (6500 lb/acre) have been reported for tilapia grown in sewage enriched ponds in Africa. [9] The investigations at ORNL suggest that an annual yield of up to 85, 125 kg/ha (75,000 lb/acre) is possible for cage culture in aerated ponds if sufficient algae is provided. [10] Because of these fish production uncertainties, the system was analyzed over this range.

Food conversion rates are similarly unknown. However, it is generally accepted that conversion efficiencies of 10% (wet weight to wet weight) are typical when moving from one trophic level to the next. Assuming the algal feed is approximately 80% water and using a 10% conversion efficiency yields a food conversion ratio of 2:1 [2 kg (dry weight) algae converted to 1 kg (wet weight) of fish]. Since there are a number of uncertainties in arriving at this ratio, the system was analyzed using food conversion ratios of 2.5:1 and 5:1.

From values reported in the literature [4, 11] it appeared that average algal production rates of 10 to 20 g/m^2-day (90 to 180 lb/acre-day) are achievable in ponds using animal manures as their source of nutrients. Since it was assumed that sufficient nutrients would be available to sustain this production, the system design was based on an average daily algal production of 15 gr (dr wgt)/m^2 (135 lb/acre).

Based on the above assumptions, the required algal pond sizes were computed for an 0.4 ha (1 acre) fish growth pond. These results are shown in Table 2.

The capital cost for construction of ponds were based on constructing them by using bulldozers to push up levees. Costs for this type of construction range from $2625 to $3250 per hectare. ($1050 to $1300 per acre) [12, 13, 14]. Therefore, a cost of $3000/ha ($1200/acre) was used.

The fish production rates obtained in our studies were obtained using cage culture techniques in an aerated pond. Thus, equipment costs for the fish pond system included aerators and cages in addition to the usual fish handling equipment.

It was assumed that cylindrical cages constructed from Conwed fabric were used. The cost for these cages, including a flotation system, was estimated at 10¢/ft^3. [15] For design purposes it was assumed that half the surface area of the pond was taken up by cages. The aerator costs were based on data available in commercial fish farming journals. [16] Assuming a shipping cost of 5% of the purchase price, a cost of $300 was used for a (350 gpm) aerator. The power required by the aerator is 0.8 kw.

302

The number of aerators required depend upon the volume of the fish pond and the pond circulation rate desired. The pond circulation rate is defined as the average time required for the entire pond volume to be pumped through the aerators. Based on an 0.4 ha (1 acre) surface area and a 2 m (6 ft) pond depth the aerator requirements over a range of pond circulation rates is given in Table 3.

A summary of the fish pond capital costs is given in Table 4. It was assumed that the ponds were constructed to utilize gravity flow so large pumps for emptying ponds were not necessary. The equipment costs include fish handling equipment and ohter miscellaneous equipment needs.

The capital costs for the auxiliary algal pond are also given in Table 4. To prevent light transmission problems and maintain high algal productivity these ponds are only 0.6 m (2 ft.) deep. Small circulation pumps are also provided to ensure mixing of the water.

Since the algal ponds are not as deep as the fish ponds, they are less expensive to construct. Based on crawfish pond (usually 1 m deep) construction costs [17] experience, algal pond construction costs were estimated at \$1600/ha (\$400/acre).

A plastic heat exchanger was designed to transfer 8790 kw (30×10^6 Btu/hr) to the ponds. In sizing the heat exchanger an overall heat transfer conductance of 369 W/m^2-°C (65 Btu/hr-ft^2-°F) and a log mean temperature difference of 5.6°C (10°F) were used. The heat exchanger material is a polypropelene copolymer extruded in the form of a honeycomb with the flow channels in the interior of the plate. The material cost is \$1.90/m^2 (\$0.24/ft^2). The fabricated heat exchange cost was estimated to be \$8.07/m^2 (\$0.75/ft^2) of heat exchange area.

The heat loss for an acre of pond area varies with climatic conditions and temperature of the pond. Experimental data from Oregon [18] indicates heat losses of 5.8 MW (20×10^6) Btu/hr) from an acre algal pond maintained at 35°C (95°F). Accounting for cooler climates a heat loss of 8.8 MW (30×10^6 Btu/ha) per acre was used for this study. This results in a capital cost of \$10,800 ha (\$27,000/acre) of pond surface area for the heat exchanger.

These capital costs were annualized using a fixed charge rate (FCR) of 15%. The fixed charge rate includes minimum return on investment, capital item depreciation, taxes, insurance, project lifetime and a number of other items. Using a FCR of 15% for a project with a 20-year lifetime yields a return on investment of 8%. For the purposes of this study, tax credit considerations were not included in the FCR. Including an investment tax credit of 10% (which is typical) yields a return on investment of about 14%. Thus, neglecting the tax credit results in a conservative economic analysis. A summary of the annual fixed charges for each pond is given in Table 5.

A summary of the operating costs for the system components is given in Table 6.

The total annual fish production costs were then obtained by summing the annual fixed charges and the annual operating costs from Tables 5 and 6. These costs were then applied to the system sizes given in Table 2 to yield the total annual fish production cost. The production cost was divided by the fish production rate to yield the unit production cost. These results are plotted in Figures 6 and 7, and indicate production costs between $0.55/kg ($0.24/lb) and $1.65/kg ($0.75/lb); depending on production rates and food conversion efficiencies.

NET ENERGY ANALYSIS

The energy required, directly and indirectly, to produce fish by the aquaculture method described has been estimated and compared with the energy used in harvesting an equal amount of fish by conventional fishing. The electrical energy required for operating the pumps and aerators is estimated directly from the projected water flow rates and pressure heads. Other direct and indirect energy requirements, such as those for pond construction, heat exchanger fabrication and installation, and labor, are calculated using tabulated net energy intensities. The energy intensity, defined as the energy required to make a dollar's worth of products or services, has been calculated from economic census data and tabulated for each major economic sector. [19] For example, in 1967 a dollar's worth of concrete products required 117.2 MJ (117.234 Btu). This includes all energy expended from the time when the constituents were in the ground as minerals through the final fabrication. Energy embodied in machinery or facilities used, in supplies consumed, in transportation, etc., is included. The energy required for each portion of the aquaculture installation has been calculated using the energy intensity for the broad economic sector which corresponds best to it.

A summary of the energy requirements determined in this manner is given in Table 7. The net energy of the feed stream and the discharge water stream are assumed to be free inputs and are not included. In addition, each acre of pond requires 1908 GJ (1908 million Btu) for the heat exchanger. The use of fingerling stocking fish has been assumed; an additional cost of 1675 KJ/kg for stocked fish.

The energy requirements in Table 7 are used with the pond areas in Table 2 to calculate the total energy requirements for fish production. The results are plotted in Figure 8. The energy needed to obtain an equal amount of fish by conventional fishing, estimated at 52.9 GJ/kg (24,000 Btu/lb), is also shown. The results plotted in Figure 8 give the ratio of the net energy required by extensive aquaculture to that required by conventional fishing. These numbers suggest that, for large enough production rates, aquaculture may produce fish at considerably lower net energy expenditures than fishing.

REFERENCES

1. Gross, A. C. and M. C. Cordaro. 1977. Waste Heat Utilization from a Utility Standpoint. The Problem of Implementation. In: The Proceedings of the Conference on Waste Heat Management and Utilization, S. S. Lee and S. Sengupta, eds. p9A-29-39.

2. Beall, S. E., C. C. Coutant, M. Olszewski and J. S. Suffern. 1977. Energy from Cooling Water. Industrial Water Engineering 14(6): 8-14.

3. Lodge, D. M., J. S. Suffern and S. M. Adams. In preparation. Growth of all-male hybrid Tilapia in sewage pond cage culture. Oak Ridge National Laboratory, Oak Ridge, Tennessee.

4. Golueke, C. G., W. J. Oswald, G. L. Duan, C. E. Rixcord and S. Scher. 1973. Photosynthetic reclamation of agricultural solid and liquid wastes. Environmental Protection Agency Ecological Research Series, Report #EPA-R3-73-031. 83 pp.

5. Donaldson, L. and K. Bonham. 1964. Effects of low-level chronic irradiation of chinook and coho salmon eggs and alevins. Trans. Am. Fish. Soc. 93(4): 333-341.

6. Finney, D. J. 1971. Statistical Method in Biological Assay. Griffin, London. 668 pp.

7. Fitzgerald, C. and J. S. Suffern. In preparation. Trace metal analysis of a sewage-aquaculture system. Oak Ridge National Laboratory, Oak Ridge, Tennessee.

8. Olszewski, M. 1977. The Potential Use of Power Plant Reject Heat in Commercial Aquaculture, ORNL/TM-5663. Oak Ridge National Laboratory, Oak Ridge, Tennessee.

9. Anon. 1974. Sewage for Tilapia, Fish Farming Int. 2: 108-109.

10. Suffern, J. S., et al. 1978. Growth of Monosex Hybrid Tilapia in the Laboratory and Sewage Oxidation Ponds. In: Symposium on Culture of Exotic Fishes, R. O. Smitherman, W. L. Shelton and J. H. Grover, eds. Fish Culture Section, American Fisheries Society. Pp. 65-82.

11. Boersma, L., et al. 1974. Animal Waste Conversion Systems Based on Thermal Discharges, Special Report 416, Agricultural Experimental Station, Oregon State University.

12. Robert Snow Means Company, Building Construction Cost Data 1978, p. 19.

305

13. Dupree, H. 1978. Fish Farm Experimental Station, Stuttgart Arkansas, personal communication with J. S. Suffern, Oak Ridge National Laboratory, January 1978.

14. Crawford, K. 1978. Personal communication with J. S. Suffern, Oak Ridge National Laboratory, January 1978.

15. Sipe, M. 1978. Personal communication with J. S. Suffern, Oak Ridge National Laboratory, January 1978.

16. Commercial Fish Farmer and Aquaculture News 4(4), p. 21 (May 1978).

17. Bean, R. 1978. Louisiana State University, personal communication with J. S. Suffern, Oak Ridge National Laboratory, January 1978.

18. Gasper, E., et al. 1975. Utilization of Waste Heat in a Biological System. The Conversion of Swine Manure to Single Cell Protein and Methane Gas, presented at the American Society of Agricultural Engineers, Chicago, Illinois, December 15-18, 1975.

19. Bullard, C. W., P. S. Penner, and D. A. Rilati. 1976. Energy Analysis: Handbook for Combining Process and Input-Output Analysis, ERDA-77-61.

Table 1

Weight Gain of Irradiated (500 rads ^{60}Co gamma)
and Control Tilapia

Week	Irradiated Mean Weight, Std. Dev.	Control Mean Weight, Std. Dev.
0	2.70 ± 0.54	2.78 ± .36
2	5.19 ± 0.9	3.94 ± .87
4	12.60 ± 2.54	11.48 ± 2.59
6	19.29 ± 4.59	15.28 ± 3.25
8	22.38 ± 5.46	21.46 ± 5.50
14	59.48 ± 8.79	51.80 ± 12.99
20	72.57 ± 10.18	58.32 ± 15.92
48	218.55 ± 17.34	144.91 ± 22.71
52	238.06 ± 22.27	161.47 ± 22.01

Table 2

Algal Pond Sizes for 0.4 ha (1 Acre) Fish Pond

Fish Production Rate (Kg/yr)	Food Conversion Ratio	
	5:1	2.5:1
	Algal pond size (ha)	
2,948	-	-
4,536	0.004	-
11,340	0.6168	0.1098
22,680	1.639	0.616
34,020	2.6629	1.129

Table 3

Pond Aerator Requirements

Circulation Rate (hours)	Req. Aerator Flow Rate (gpm)	# Aerators	Cost ($)	Power (Kw hr/day)
24	1,350	4	1,200	77.2
12	2,700	8	2,400	154.4
6	5,400	16	4,800	308.8
3	10,800	31	9,300	598.3
1.5	21,600	62	18,600	1196.6
0.75	43,200	124	37,200	2393.2

Table 4

Pond Capital Cost Summary

Item	Fish Pond Cost ($/acre)	Algal Pond Cost ($/acre)
Pond Construction	1,200	400
Equipment	850	100
Cages	13,100	
Aerators	See Table 2	
Misc. Equipment (Pumps)	200	200
Subtotal	15,350 + Aerators	700
Contingency (@ 25%)	3,840 + (0.25) Aerator	175
Total	19,190 + (1.25) Aerator	875

Table 5

Summary of Annual Fixed Charges for 0.4 ha Pond

System	Annual Fixed Charges
Fish Pond 12 hour Aerator Circulation	$ 3,338
Fish Pond 3 hour Aerator Circulation	4,631
Algal Pond	130
Heat Exchanger	4,050

Table 6

Summary of Annual Operating Costs

	Operating Cost ($ 1 acre-year)			
	Fish Pond		Algal Pond	Heat Ex.
Item	3 hour	12 hour		
Management & Labor	750	750	100	
Materials	100	100	100	150
Electricity @ 2.5¢/km hr	5,460	1,410	60	
Stocking	($0.03)	(Stocking rate)		
Total	6,312 + stocking	2,260 + stocking	260	150

Table 7

Net Energy Requirements for 0.4 ha Ponds

Item	Energy Required (GJ)		
	3 hour Fish Pond	12 hour Fish Pond	Algal Pond
Capital Items			
Construction	27	27	27
Pumps	5	5	5
Equipment	385	127	
Cages	1589	1589	
Total Capital	2006	1748	33
Operating Items			
Electricity	14741	3831	30
Labor	20	20	20
Total Operating	14761	3851	50
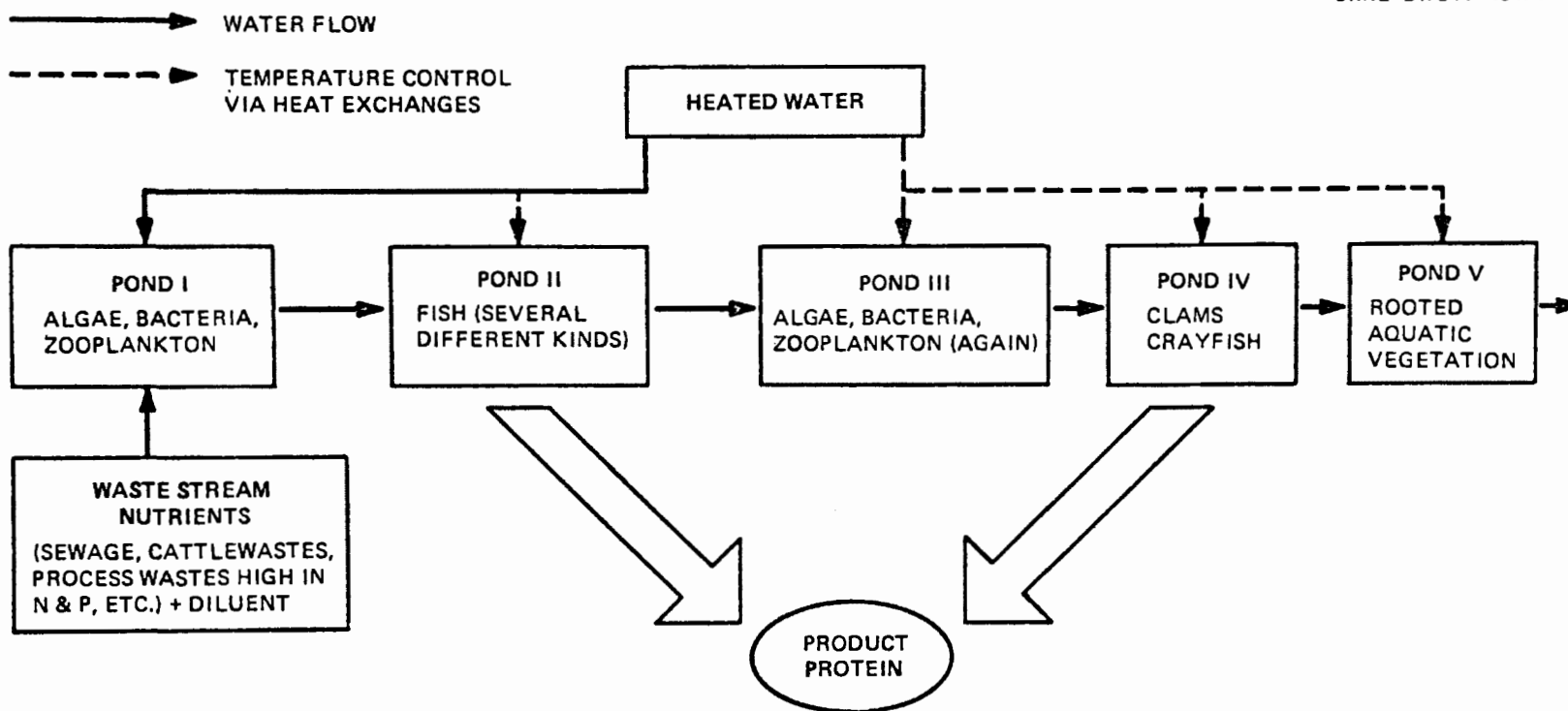
Figure 1.   Conceptual design of the ORNL waste-heat aquaculture system.
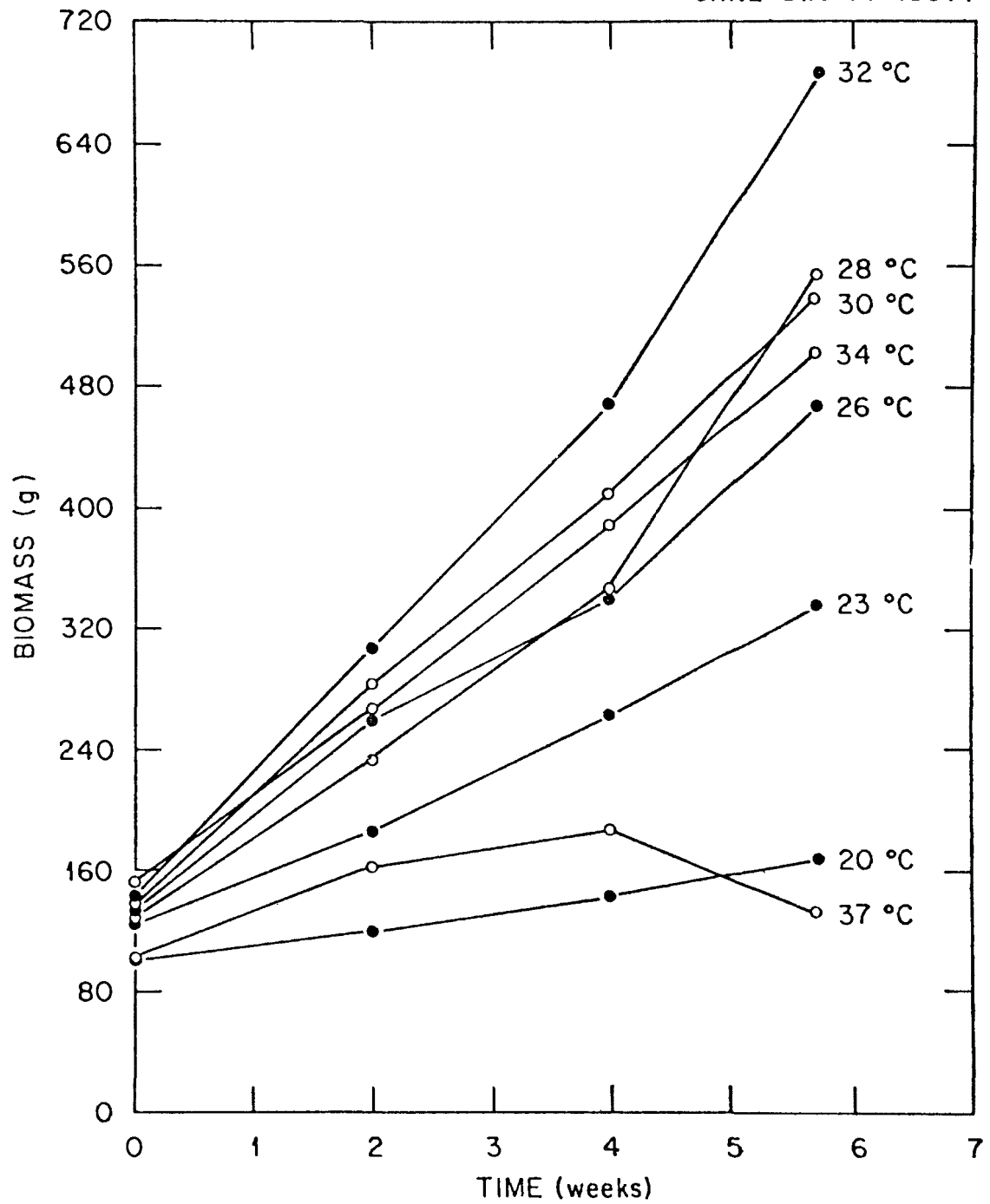
Figure 2. Growth of tilapia hybrids at different temperatures in the laboratory.
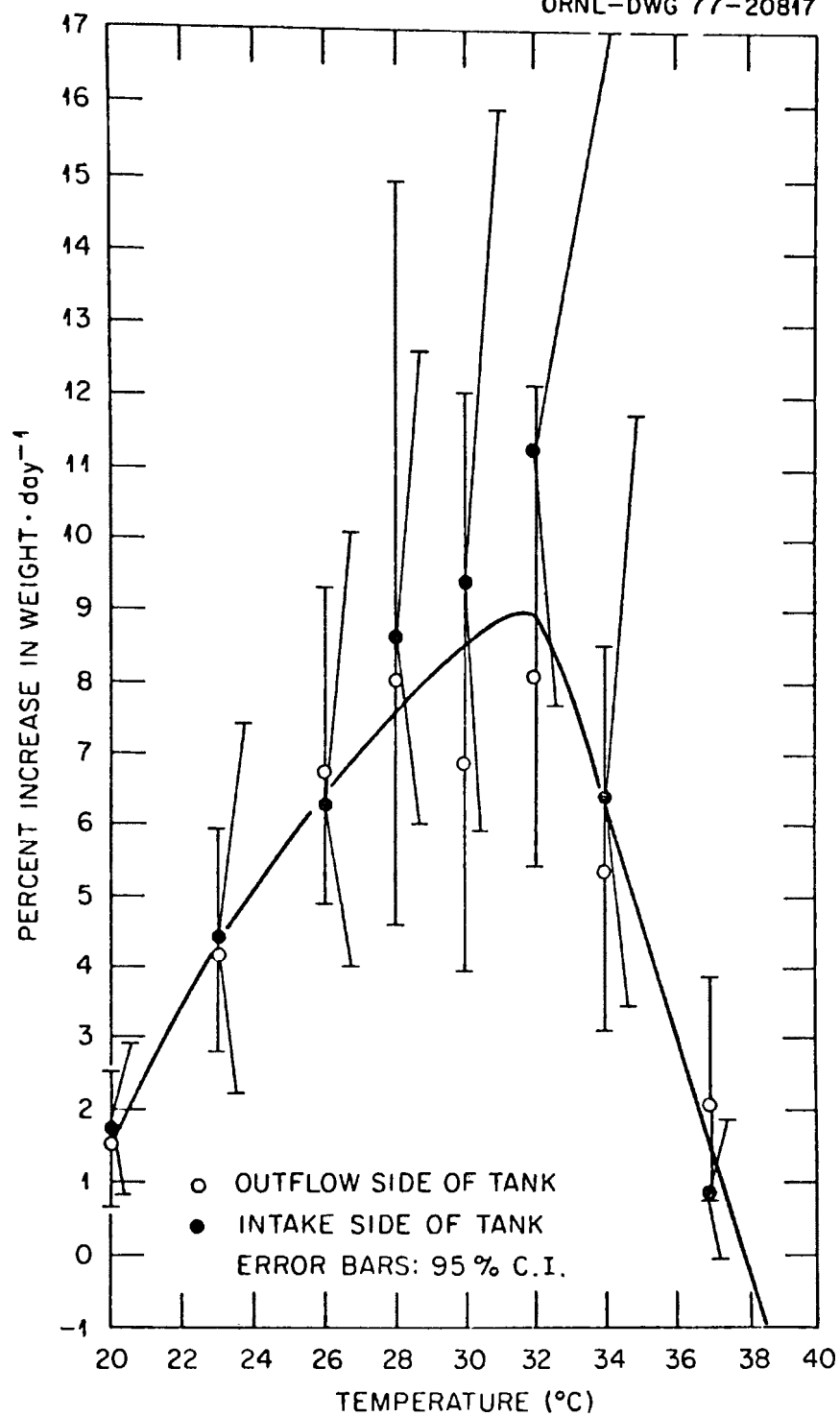
Figure 3. Tilapia growth versus
temperature after 39 days.

313
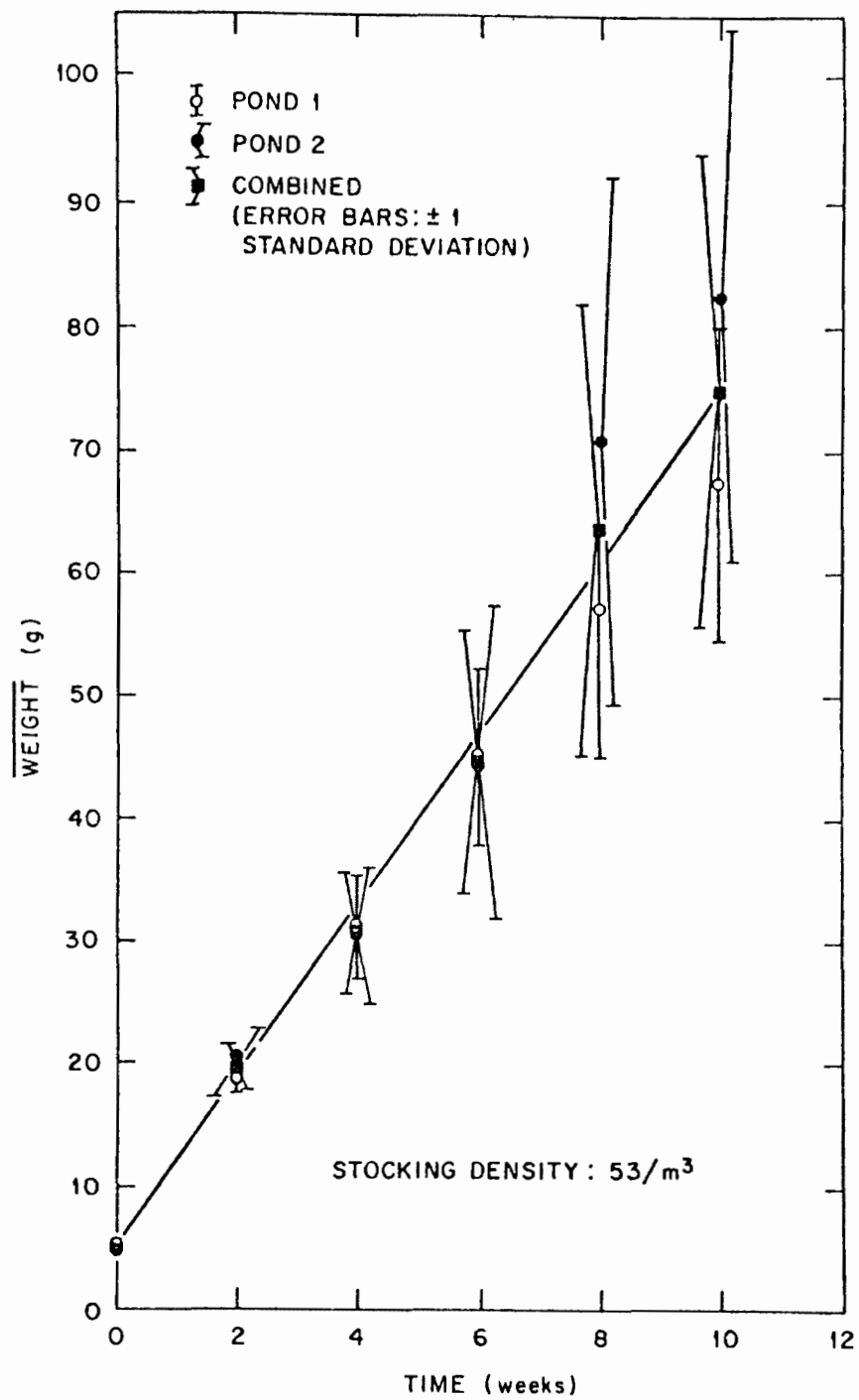
Figure 4. Growth of tilapia hybrids in sewage pond cage culture.
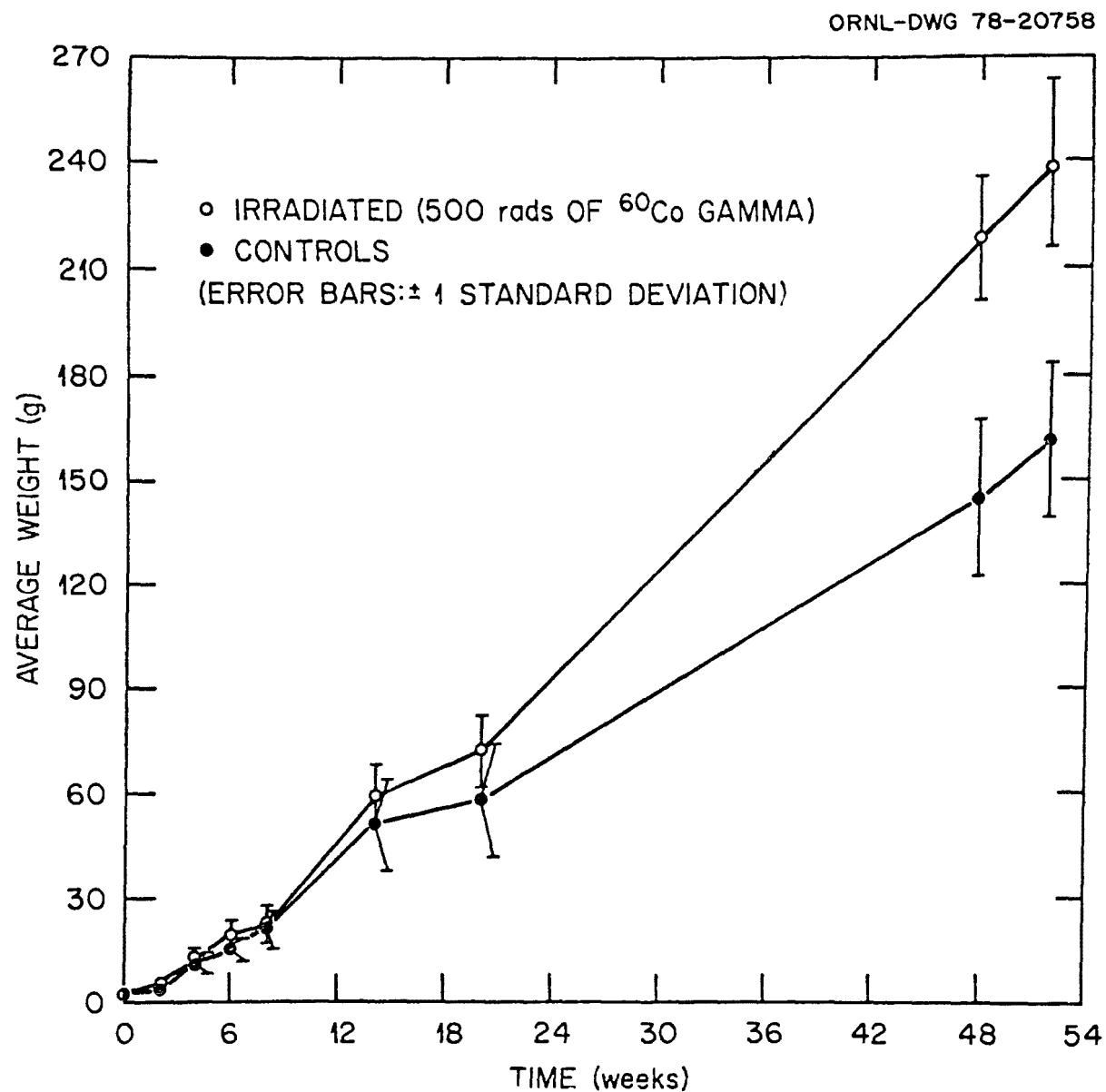
Figure 5. Growth of irradiated and control tilapia hybrids in the laboratory.

316
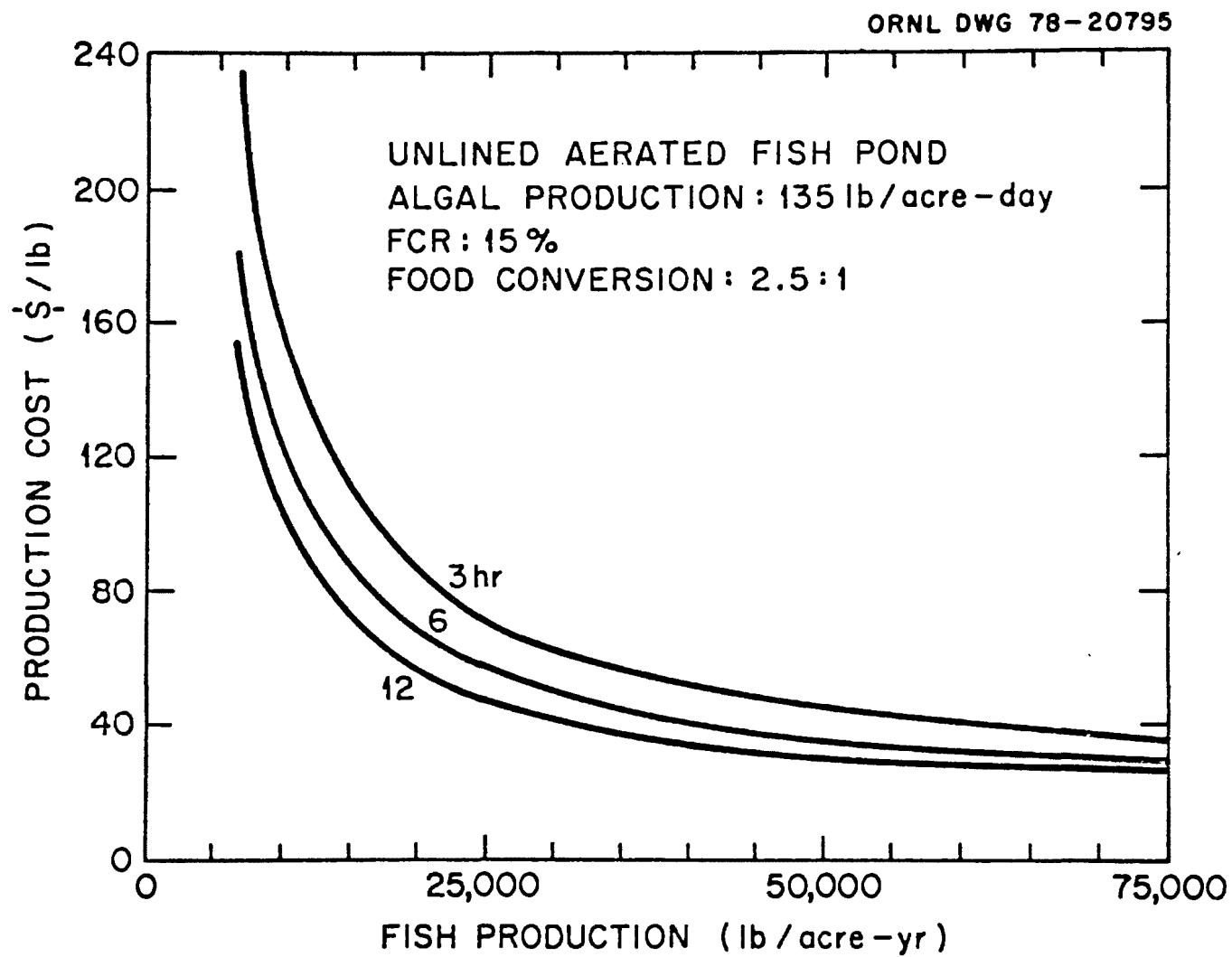
Figure 6. Production costs for fish assuming a
2.5:1 food conversion ratio.
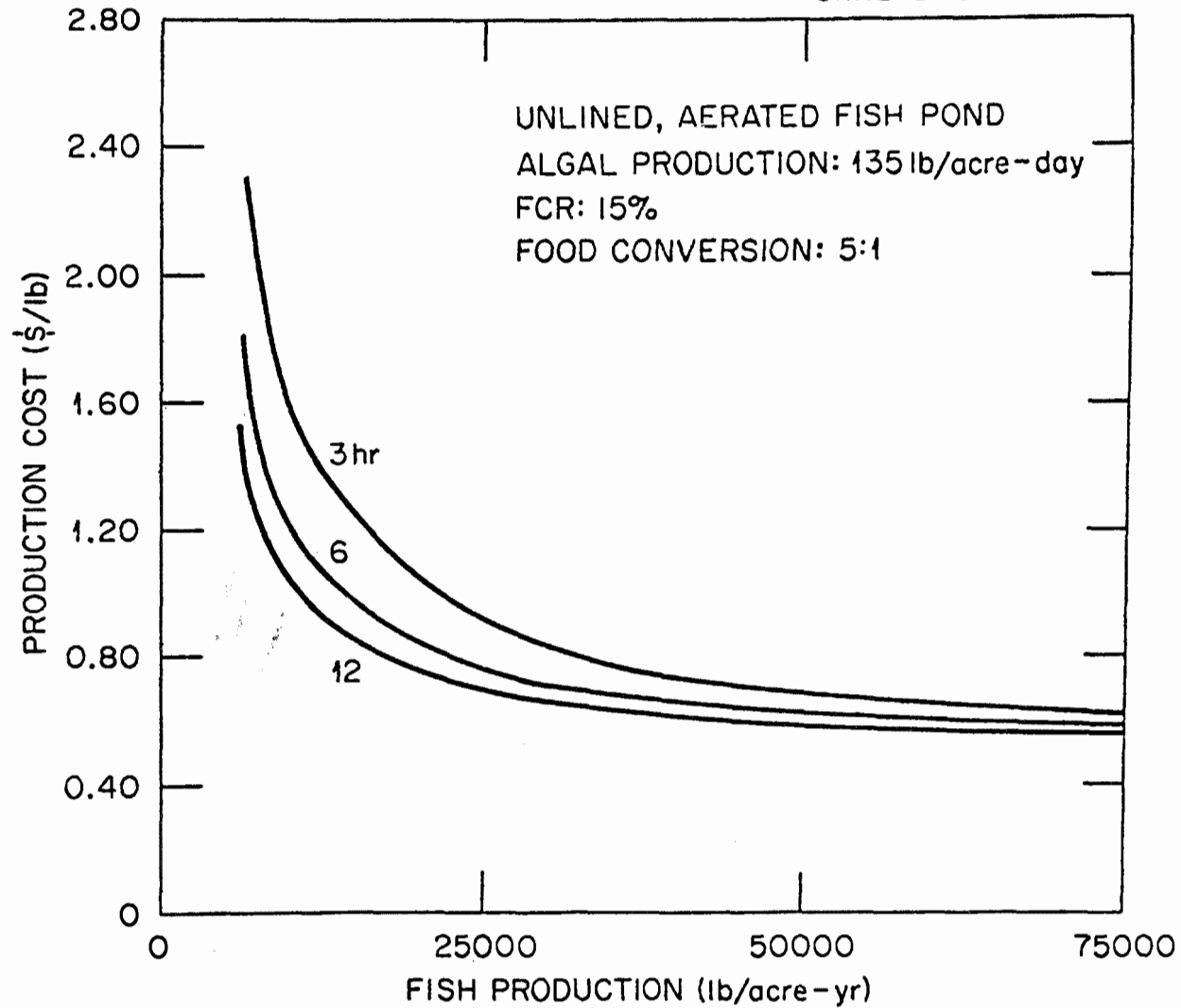
Figure 7. Production costs for fish assuming a
5:1 conversion ratio.
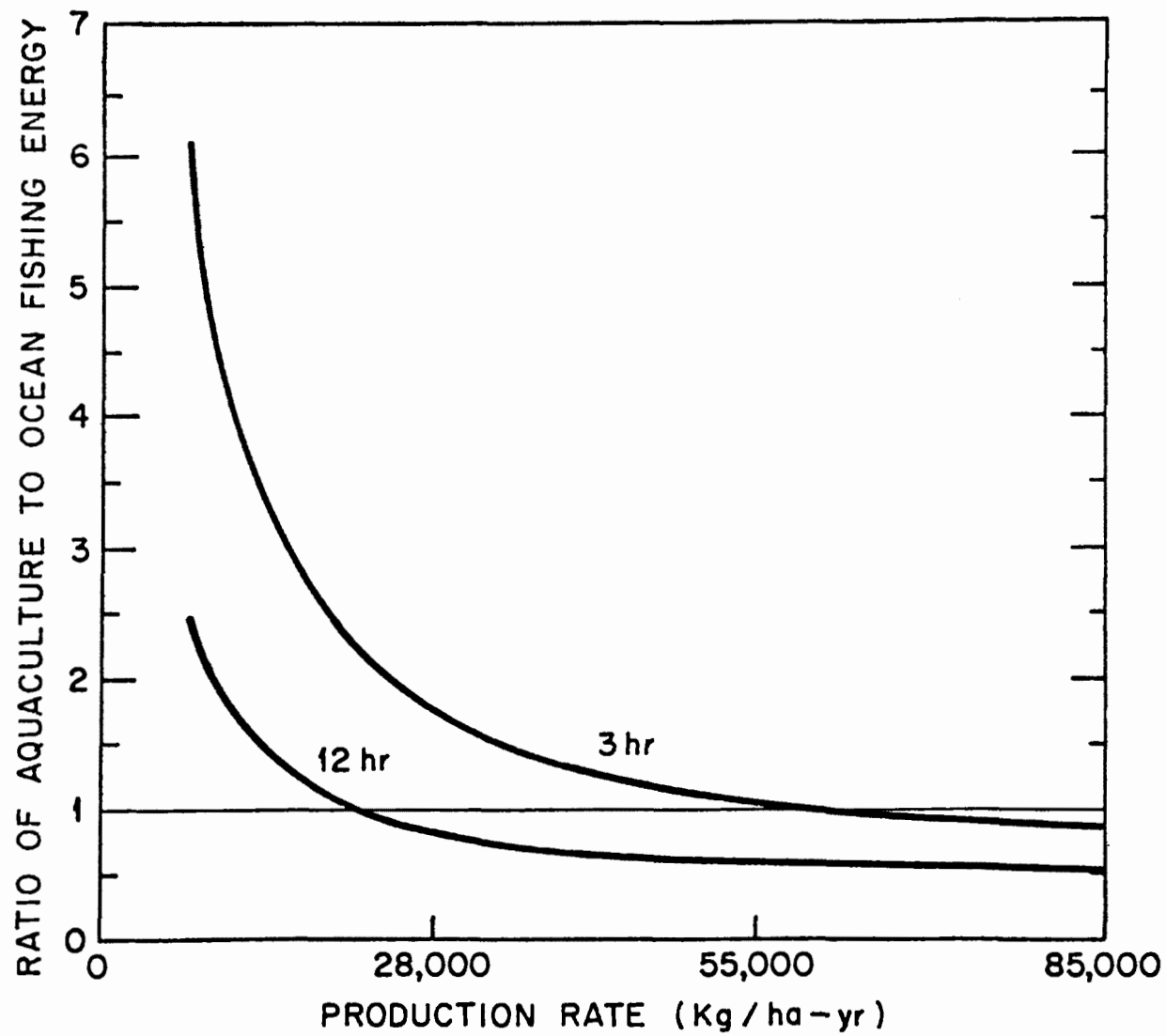
Figure 8. Ratio of energy required for aquaculture to that required by ocean fishing.

A QUALITATIVE/QUANTITATIVE PROCEDURE FOR ASSESSING THE BIOLOGICAL EFFECTS OF WASTE HEAT ON ECONOMICALLY IMPORTANT POPULATIONS*

John M. Thomas
Ecosystems Department
Pacific Northwest Laboratory
Operated by Battelle Memorial Institute
Richland, WA 99352

ABSTRACT

Recent research suggests statistical procedures which can be used to detect changes in populations of aquatic biota due to the operation of nuclear power plants. However, the effect of such changes on future populations must be assessed. I have devised a procedure in which a probable model, not necessarily a mathematical model coded for a computer, for economically important populations is derived and modified in conjunction with field monitoring studies, beginning in the preoperational period.

The advantages of my proposal are fourfold:

a) Field studies will be terminated (i.e., good quality field work is rewarded) after an agreed time.

b) Imaginative scientists, currently doing routine monitoring, can design and carry out studies which investigate key questions in population ecology.

c) Both statisticians and modelers have the opportunity to suggest the directions of, or institute, new field work.

d) The adversary mode used to establish and assess the adequacy of current monitoring programs (i.e., involving litigation) is bypassed.

JMT

Various features of the plan are amplified in this paper and the specific portions discussed include: 1) the amount of population decline which might be ecologically acceptable, 2) the precision needed for measuring crucial parameters, 3) the interpersonal problems which may result during frequent meetings of a "negotiating team" over many years, and 4) equilizing monitoring costs among power plant sites.

INTRODUCTION

Recent research (Eberhardt [1], Thomas [2,3], Thomas et al., [4], Gore et al., [5,6], Murarka et al., [7], Adams et al., [8], McKenzie [9], McKenzie et al., [10], and McCaughran [11]) has suggested several possible methods for field designs, statistical analysis, and useful field techniques necessary for the conduct and assessment of biological effects derived from monitoring studies at nuclear power plants. Thomas and Thomas et al., [3,4] suggested that sampling all trophic levels diluted efforts to assess population effects on economically important species and devised a scheme whereby monitoring studies would be stopped after a finite time.

The purpose of this paper is to amplify portions of the plan and to discuss certain aspects in more detail. Additional features discussed include possible interpersonal conflicts resulting from the use of a negotiating committee charged to direct studies during the course of a long term (up to eight years) program and cost equitability among monitoring studies.

RECOMMENDED CHANGES FOR CURRENT MONITORING PROGRAMS

Currently, intervenor charges of population impacts on economically important fish and shellfish has resulted in the construction and refinement of computer simulations of mathematical models for most life stages of species of concern. These models are impossible to defend (as correct) on a scientific basis partly because: 1) they employ estimates of parameters and either no data or data poorly measured data perhaps obtained at some other site, usually ecologically dissimilar, and 2) a generally limited understanding of ecosystems. To circumvent these difficulties, I advocate that a representative model, not necessarily a model constructed to run on a computer, be derived and modified in conjunction with field studies beginning in the preoperational period. The results and understandings gained from the model can then be used to design additional field studies to obtain either information identified as needed or better estimates of previously studied parameters (i.e., number currently in

various life stages, age specific mortalities, etc.). Since the basic plan is designed to replace current monitoring programs, I envision that the resources expended now can be devoted to implementing the current ideas. If monitoring requirements under NEPA are changed by regulatory agencies in the future (i.e., less monitoring effort), then my proposal must be reevaluated in terms of cost. One idea might be to require "pool" funding by nuclear and nonnuclear power plant operators.

Clearly, the studies outlined above will be expensive so most monitoring efforts on lower trophic levels should be abandoned. If circumstances arise whereby monitoring lower trophic levels is mandated, then only outfall areas should be considered (with appropriate matched control stations [9]). The latter action is not without justification (Thomas and Thomas et al., [3,4]). In the second paper [4] we have proposed that such efforts must be terminated in a finite time both as an incentive for plant owners and to ensure continuing and adequate financial support. In addition, I propose that expenditures should be of about the same magnitude at most power plant sites. Power plants sited in locations where no economically important species reside probably should contribute to studies at other sites to attain approximate cost sharing. Clearly, the public pays (via higher power bills) for studies as currently conducted as well as under this plan. Since the population effects issue is universal, it seems reasonable to expect the public to share the costs. This is necessary because the answer to the question, "What are the effects on future biological populations?" will not likely result from studies at any single site but instead will take many years of sustained effort at many sites utilizing diverse ecological studies and new field techniques. This is due, in part, to current lack of adequate field procedures to obtain data on ecological parameters in situ and because we cannot usually separate power plant effects from other life span insults (i.e., oil pollution, changed fishing pressure, carrying capacities), and sometimes our inability to define the size and range of spawning populations.

Thus, we must develop improved understandings of population ecology and much better field procedures. Given enough time, both objectives can emanate from my suggested monitoring program because: 1) power plant operators are rewarded by terminating monitoring in a known time, 2) ecological scientists are freed from routine monitoring currently required, and 3) quantitative scientists will have a continuing input into the design and day-to-day operation of field programs.

THE SUGGESTED MONITORING SCHEME

Figure 1 contains an expanded version of the plan first
proposed in Thomas et al [4]. While the example is oriented
toward a fishery where several years may elapse before progeny
such as salmon and herring return to spawn; an extension to
shellfish or other species could readily be made. Studies
may be necessary to approximate numbers and assess parameters
relevant to population dynamics of all life stages of the
species of concern when a projection of future population
numbers is to be made. Thus, while I do not advocate studies
of lower trophic levels in general, these will be necessary
when immature forms of the species of concern are a portion
of such trophic levels. In addition studies of other lower
trophic level species may be necessary because of their
particular influence(s) on the population of concern. The
logical plan shown in Figure 1, which includes negotiation to
define the content of the monitoring, discrete field studies
and the number of years of study, constitutes the basis for a
stopping rule for power plant ecological impact studies.

The first feature deserving special attention is the pre-
liminary assessment during the first preoperational year.
Since this is a "guessing stage," considerable credance
should be given to local experts, such as fish and game
personnel and local ecologists in order to guesstimate future
effects. In addition, some attention needs to be given to
emotional concerns of persons considered something less than
experts (i.e., fishermen) as a means to anticipate possible
future intervenor questions. For example, if catch effort
data are available for prior years, it should be pointed out
that wide fluctuations have occurred in the past, for which
we may or may not have any clues as to causes. In constrast,
the local experts should be used to provide insight for
a word model (box and arrow diagram?) of the population of
concern; useful input may also come from fishermen. Some
examples of guesstimates needed are included in Figure 1.

During the second preoperational year the full negotiating
committee should be established. The exact number of members
and their professional training may be partially reflective
of a site specific problem. However, the suggested membership
in Figure 1 should perhaps be a minimum. The use of con-
sultants should reflect the committee's particular needs
based on their collective technical inadequacies. However,
they should have the power to employ specialists as needed,
independent of any power company influence. As soon as
organizational matters are decided preliminary limits, both
statistical and biological, that the initial studies can be
expected to attain should be negotiated. The reality of the

expectations will be assessed and reevaluated during the third preoperational year. Further, during the third preoperational year both the size of the population change(s) and the statistical precision desired for essential parameters needed to project changes should be promulgated, even though these may still be partly educated guesses.

Current experience in ecology indicates that coefficients of variation (standard deviation divided by the mean expressed as a percentage) can vary from 20 to over 100 percent and that some variables may be nearly impossible to measure in situ (i.e., natural mortality of fish eggs or larvae) except in a crude way. Because of these factors, I propose that even crude estimates of the size of confidence intervals for key parameters and the size of population change that the monitoring programs might detect should be deferred to the third preoperational year. Thus, second year efforts should be designed to assess what is possible. Studies instituted during the third preoperational year should mimick those for operational years. Clearly, if adults of the species of concern migrate and return more than one year later, additional preoperational years of study may be required. In such cases, the financial resources should be spread out and some ancillary studies considered essential may have to be cancelled. Thus, the size of the difference to be detected between operational and preoperational years will be wider and possible site specific effects may be more difficult to assess. However, since monitoring results from many sites collected during many years will be necessary to address the population effects issue, the data, techniques and experience will make a contribution to the overall assessment.

I advocate the cost spreading above, so all sites incur costs of a similar amount, only in cases where power plants are not sited in an ecologically unsuitable location. Otherwise, particular power companies should be assessed the increased cost when additional preoperational data are needed. One function of the negotiating committee might be to make the initial assessment of site suitability.

In the absence of any experience with the plan outlined in Figure 1, a discussion of how it should function in operational years may be premature but the features given can be an adequate starting point. However, some realistic limits for the size of population changes to be detected and confidence bounds for key parameters must be an integral feature and need to be based on preoperational studies. Since there may not be enough adequate data from preoperational studies, I suggest that the population projection made using some representation of the system (i.e., model) should result in

323

an estimate at least one order of magnitude below that presumed to be ecologically detrimental. In light of the fact that the confidence with which we can expect to measure field parameters is dependent on many factors, any suggested a priori recommendations about their possible precision may be premature. However, the negotiating committee should insist on replicated studies which at least correspond to state-of-the-art, and in some cases, should require research which will allow improving the reliability of field measurements. Finally, the committee must define the length of the operational study. For lack of other guidance, I suggest one complete reproductive cycle for migratory species with a long reproductive cycle, of three to four years or more, and a three year period for others with shorter cycles. Additional years should be required if inadequate studies are conducted and ameliorative schemes maybe instituted if damage to the population is judged unacceptable.

It should be noted that while at times the negotiating committee may operate in somewhat of an adversary mode, that decisions about the overall conduct of the program and important questions needing further research, will be the result of a consensus of views. Currently, one often hears utility, intervenor, and regulator alike state, "If we could just get away from the lawyers, lock the people with genuine concerns and the scientists in a room, we could hammer out (negotiate) a reasonable program to assess impact." The proposal depicted in Figure 1 goes a long way toward attaining that goal.

POTENTIAL PROBLEMS OF A FUNCTIONING NEGOTIATING COMMITTEE

It is essential that the negotiating committee function in a manner whereby decisions taken have not emanated from divisive, as opposed to "considered", deliberations. Since the members will have diverse backgrounds, biases, and expectations and because at times they will need to operate in a collective bargaining atmosphere, strong differences of opinion can and will develop. Figure 2 illustrates some "people problems" such a committee may encounter and offers the suggestion that a return to the goalsetting and mutual understanding phases may be necessary since the period of interpersonal involvement may be up to eight years. To aid in recognizing phases where harmful disagreement is either beginning or has become divisive, I suggest that a disinterested leader or committee chairman be appointed to direct committee business. The sole function of this individual will be to recognize the points of possible friction shown in Figure 2 which could delay attaining the goal of finishing a quality study in Y-years.

.

Gore, K. L., Thomas, J. M., Kannberg, L. D., Watson, D. G. (1977c). Evaluation of nuclear power plant environmental impact prediction, based on monitoring programs. BNWL-2152, NRC-1, Battelle, Pacific Northwest Laboratories, Richland, Washington. 31 pp.

6. Gore, K. L., Thomas, J. M. and Watson, D. G. (1978). Quantitative evaluation of environmental impact assessment based on aquatic monitoring programs at three nuclear power plants. J. Environ. Mgt. 6, in press.

7. Murarka, I. P. Policastro, A. J., Ferrante, J. G., Daniels, E. W. and Marmer, G. P. (1976). An evaluation of environmental data relating to selected nuclear power plant sites. ANL/EIS-1 (Kewaunee), ANL/EIS-2 (Quad-Cities), ANL/EIS-3 (Duane Arnold), ANL/EIS-4 (Three Mile Island), ANL/EIS-5 (Zion), ANL/EIS-6 (Prairie Island), ANL/EIS-7 (Nine Mile Point). Argonne National Laboratory, Argonne, IL.

8. Adams, S. M., Cunningham, P. A., Gray, D. D., Kumar, K. D. and Witten, A. J. (1977). A critical evaluation of the nonradiological environmental technical specifications. ORNL/NUREG/TM-70 (Surrey Power Plant Units 1 and 2); ORNL/NUREG/TM-71 (Peach Bottom Atomic Power Station Units 2 and 3); ORNL/NUREG/TM-72 (San Onofre Nuclear Generating Station Unit 1). Oak Ridge National Laboratory, Oak Ridge, Tennessee.

9. McKenzie, D. H. (1978). A review of statistical analysis methods for benthic data from monitoring programs at nuclear power plants. Proceedings of this conference.

10. McKenzie, D. H., Kannberg, L. D., Gore, K. L., Arnold, E. M., and Watson, D. G. (1977). Design and analysis of an aquatic monitoring program at nuclear power plants. PNL-2423, NRC-1. Battelle, Pacific Northwest Laboratories, Richland, Washington. 125 pp.

11. McCaughran, D. A. (1977). The quality of inferences concerning the effects of nuclear power plants on the environment. In Proceedings of the Conference Assessing Effects of Power-Plant Induced Mortality on Fish Populations, Gatlinburg, Tennessee, May 3-6, 1977. (W. Van Winkle, ed.) pp. 229-242. Pergamon Press.

ACKNOWLEDGMENTS

REFERENCES

1. Eberhardt, L. L. (1976). Quantitative ecology and impact assessment. J. Environ. Mgt. 4,27-70.

2. Thomas, J. M. and Eberhardt, L. L. (1976). Ecological impact assessment. In Proceedings of the Conference to Computer Support of Environmental Science and Analysis. Albuquerque, New Mexico, July 9-11, 1976. (S. Fernbach and H. M. Schwartz eds.) pp. 181-197. CONF-750706, U.S. Energy Research and Development Administration, Washington, D.C.

3. Thomas, J. M. (1977). Factors to consider in monitoring programs suggested by statistical analysis of available data. In Proceedings of the Conference for Assessing Effects of Power-Plant-Induced Mortality on Fish Populations, Gatlinburg, Tennessee, May 3-6, 1977. (W. Van Winkle, ed.) pp. 243-255. Pergamon Press.

4. Thomas, J. M. (1978). Statistical methods used to assess biological impact at nuclear power plants. J. Environ. Mgt. 6, in press.

    Gore, K. L., Thomas, J. M. Kannberg, L. D., and Watson, D. G. (1976). Evaluation of Monticello Nuclear Power Plant, environmental impact prediction, based on monitoring programs, BNWL-2150, NRC-1, Battelle, Pacific Northwest Laboratories, Richland, Washington. 127 pp.

    Gore, K. L., Thomas, J. M., Kannberg, L. D., Mahaffey, J. A. and Watson, D. G. (1977a). Evaluation of Haddam Neck (Connecticut-Yankee) Nuclear Power Plant, environmental impact prediction, based on monitoring programs. BNWL-215, NRC-1, Battelle, Pacific Northwest Laboratories, Richland, Washington, 181 pp.

5. Gore, K. L., Thomas, J. M., Kannberg, L. D. and Watson, D. G. (1977b). Evaluation of Millstone Nuclear Power Plant, environmental impact prediction, based on monitoring programs. BNWL-2152, NRC-1, Battelle, Pacific Northwest Laboratories, Richland, Washington. 120 pp.

FIGURE 1. A PROCEDURE FOR A QUANTITATIVE/QUALITATIVE
ASSESSMENT OF THE EFFECTS OF WASTE HEAT ON A FISHERY.

327
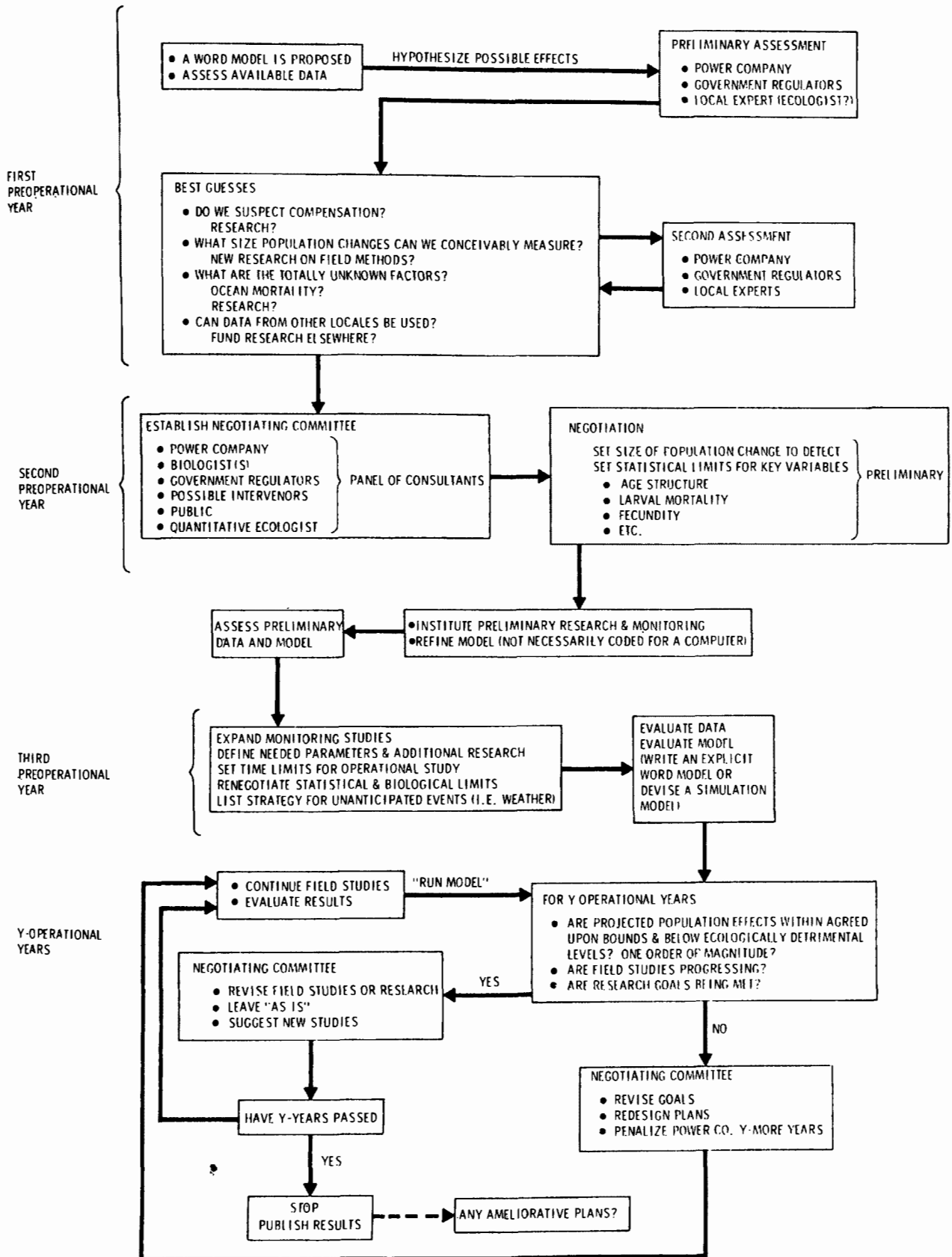
FIGURE 2. POSSIBLE RESOLUTION OF "PEOPLE PROBLEMS" ENCOUNTERED BY A NEGOTIATING COMMITTEE FUNCTIONING FOR Y-YEARS

- WILLINGNESS TO SHARE INFORMATION BY MEMBERS
- EXPECTATION OF VARIOUS MEMBERS
- BIASES OF VARIOUS MEMBERS
- EDUCATIONAL LEVEL OF MEMBERS
- CREDIBILITY OF CONSULTANTS

Y-YEARS STUDIES TERMINATE

- UNDERSTANDING OF EACH MEMBERS ROLE
- VARIOUS DEGREES OF COMMITTMENT

- STABLE FIRST FEW YEARS

- DISAGREEMENT-PROBLEMS (RESOLVABLE WITHOUT GREAT FRICTION)

- TOTAL DISAGREEMENT-FRICTION [HARD TO RESOLVE,PRESSURE (OUTSIDE PRESSURE?)]
- STUDIES GO POORLY

- COMMITTEE BEGINS TO LOSE MEMBERS
- AMBIGUITY-UNCERTAINTY

PLAN FAILS

328

A REVIEW OF STATISTICAL ANALYSIS METHODS
FOR BENTHIC DATA FROM MONITORING PROGRAMS
AT NUCLEAR POWER PLANTS*

D. H. McKenzie
Ecosystems Department
Pacific Northwest Laboratory
Battelle Memorial Institute
Richland, WA 99352
United States of America

ABSTRACT

Recent reviews of the monitoring programs at nine nuclear power plants have attempted to evaluate the aquatic impacts thought to be due to thermal discharges. These reviews have provided an opportunity to compare and evaluate some of the statistical approaches used a posteriori to analyze data from such programs. This paper addresses three major areas or questions that must be answered when attempting to analyze these data: What data do we analyze to assess impact? What statistical analysis technique should we employ? and What is an appropriate experimental unit and how do we select error rates? Each of these areas is discussed and evaluated based on the benthic data collected at the nine power plant sites.

In general, considerably more taxonomic detail was present in the data base than was utilized in the statistical analyses and recommendations are developed that will increase the cost effectiveness in these areas. The advantages and disadvantages of three statistical approaches, analysis of variance, regression, and time series, are discussed and illustrated with examples from the nine power plant sites. The selection of statistical error rates and experimental units is discussed and arguments presented for establishing appropriate values.

INTRODUCTION

The primary objective of an environmental monitoring program can be simply stated as the measurement of the environmental changes induced by the operation of the power plant. A recently concluded effort by the staff of three laboratories [Argonne National Laboratory (ANL), Oak Ridge National Laboratory (ORNL), and Pacific Northwest Laboratory (PNL)] examined nine nuclear power plant monitoring programs and evaluated the degree to which the above objective was met. The ANL group evaluated the environmental monitoring data for Zion [1], Prairie Island [2], and Nine Mile Point [3] Nuclear Power Plants. The ORNL group examined the results of the Surry [4], Peach Bottom

---

[5], and San Onofre [6] Nuclear Power Plants' environmental monitoring programs. The monitoring programs conducted at Monticello [7], Haddam Neck [8], and Millstone [9] Nuclear Power Plants formed the basis for the PNL evaluations. These reviews provide an opportunity to compare and evaluate the statistical methods and approaches used to analyze data from such programs. While it is tempting to ascribe state-of-the-art precedent to the techniques used in these reviews, the temptation should be resisted due to the a posteriori nature of these efforts. The techniques chosen by each of the groups was primarily dictated by the availability or lack of data. In general, the three groups concluded that the ability of the monitoring program to measure impact is dependent upon many things, but probably of greatest importance is the design or planning approach taken when establishing the monitoring program.

This paper examines the results of the three laboratories and addresses what would be appropriate if the analysis was not constrained by the a posteriori approach. Three major areas or questions are discussed that should be answered during the design or planning stages for a monitoring program. The first question is: What data are appropriate for the assessment of impact? The second important area is the selection of the statistical analysis technique(s). The third area concerns the appropriate experimental unit and selection of error rates. Each of these areas is discussed and evaluated based on the benthic data presented in the nine power plants reviewed by the three laboratories.

Data Collected

There is considerable uncertainty or at least lack of consistency concerning what abiotic and biotic data are to be recorded as exemplified by the nine monitoring programs. The same uncertainty goes unresolved through the analysis and interpretation stages. Uniformity in the entire assessment program will increase the effectiveness of the overall efforts.

The approach to resolving the issue should be to look at the information needed to assess impact and not what can be measured. In general, the reviewed studies appear to have been based on the "measure everything" approach. However, the analysis and interpretations can be based on only a small subset of that data.

The biotic characteristics that were examined in the nine impact evaluations were the numbers of benthic organisms per area in one or more of the following categories: total numbers, phylum, class, order, genus, species and total biomass. No rationale was presented to support the selection of the specific level of taxonomic identification chosen. In addition, the results of the individual analyses of the various categories were given equal value in the interpretation of impact. Thus, there does not appear to be a consensus among the reviewers on the level of taxa identification needed for impact assessment (or perhaps the approach was to try everything and hope that something would "turn-up"). However, the reviewers were constrained by the a posteriori nature of their studies and had to use what was available, not necessarily what was needed, or most desirable for the impact assessment.

330

The following scheme is recommended for establishing the level of taxonomic identification, analysis and interpretation. First, it should be realized that identification to the species level of all benthic organisms is unwarranted. The maximum number of analyses of benthic categories was seven and only five were fully discussed and interpreted [8]. The majority of the nine benthic program analyses examined total organisms and one or two subdivisions. Thus, it appears that the authors from the three laboratories considered this level of analysis to be appropriate for the assessment of impact on the benthos. While it is impossible to conclude that what the three laboratories used is ideal, it does appear to be consistent with the general state-of-the-art of impact assessment for benthic communities. However, a priori establishment of an overly simplified or restrictive number of taxonomic units for recording the data is probably unwise. This number will be site specific and will depend on the complexity of the benthic community, its economic values, and the amount and detail of the information that exists during the design phase.

Although site specific characteristics may indicate a need for adjustments in the general rule, it is recommended that not more than five to seven subdivisions of the benthic taxa be recorded, analyzed and interpreted. This appears to be consistent with the general state-of-the-art of impact assessment for benthic communities.

Another biotic parameter that was considered in three of the nine studies was the biomass of the benthic organisms. The Peach Bottom benthic data analysis and impact assessment were conducted solely on biomass data [5]. Changes in methods restricted the usefulness of Surry benthic biomass data to comparisons among stations within individual years [4]. Gore et al. [8] concluded on the basis of a correlation analysis of the Haddam Neck benthic data that counts, wet and dry weights contained much the same information and analyzed only the count data. Thus, it appears that count data is to be preferred over biomass data, and that when both are available, the biomass data add very little to the analysis. However, this must be balanced by the relative costs of obtaining the two types of benthic data. In general, biomass measurements are less costly and can be obtained more quickly than count data; dry weights are usually preferred over wet weights because their measurement endpoint can be more precisely obtained.

Another factor that warrants consideration during the design and establishment of the benthic monitoring program is the expected frequency of zero organism counts in the samples. These should be avoided when possible by increasing the area sampled or decreasing the number of taxonomic categories or both. The reasoning behind this recommendation is primarily statistical, although the biological interpretation of the data base is also complicated by increasing frequencies of zero counts. The usual underlying statistical assumptions that are made in order to analyze the data include the assumption of a normal distribution or alternatively that the data can be transformed into the normal distribution. Data sets with substantial numbers of zero counts cannot be assumed or transformed to follow the normal distribution and alternative techniques (often more complicated or less powerful)

331

must be utilized. Thus, it is desirable to avoid for statistical reasons, whenever possible, data sets containing substantial numbers of samples with zero organisms. If the true density of organisms is such that zero count samples occur frequently, it follows that there is also a low probability of detecting a plant impact that reduces the number of these benthic organisms.

Abiotic measurements are frequently made along with the collection of benthic data and are usually based on point estimates, e.g. grab samples of water or sediment. Only the review of Haddam Neck Nuclear Power Plant [8] attempted to use these measurements in the data analysis. Their conclusions, based on correlations with water and sediment temperatures and dissolved oxygen, indicate that these measurements were of little value in explaining changes in the benthic communities. However, this does not provide good evidence that abiotic data should not be collected. To be of greatest use in assessing impacts on the biota, physical and chemical measurements should be made on a very frequent or continuous basis in order to define the variations in these factors and to obtain an integrated measure of potential stressors. The expense and difficulties in maintaining the instrumentation necessary for the continuous monitoring of these parameters will preclude their measurement at more than a very few stations. Physical and chemical measurements also are necessary in plant monitoring to obtain evidence that effluent discharge to surface waters are within applicable state and Federal water quality standards.

REVIEW OF STATISTICAL TECHNIQUES

Analysis of Variance

The reviews by both ANL and PNL relied heavily upon analysis of variance techniques to test the hypothesis of no impact from the operation of the power plant. In general, time, space, stations, and operating status were included as fixed effects in the model. The data were assumed to be log-normal and were transformed prior to the analysis. The major term of interest was the interaction term representing the operating status x sites (control, treatment, or exposed). Multiple observations at a station taken at the same time were considered to be replicates. Descriptions of the models, assumptions, and test results are presented [1,8].

This approach is probably the best available methodology when faced with data bases that contain the following types of problems: missing observations, unbalanced sample sizes, confounding of effects and no a priori design. Often the required underlying assumptions are not fully satisfied, with the investigator relying upon the robustness of the technique and the acknowledgment that the tests are only approximate. However, if we look beyond the problems of analyzing "inadequate" data bases and consider this analysis of variance approach to well-designed monitoring programs, some items for consideration emerge.

The first item to be considered is the manner in which the analysis tests the impact hypothesis. The effect of the plant cannot be represented in the

factorial design. The hypothesis testing occurs by examining the significance of the interaction term, operating status x sites. The interaction for the determination of environmental changes can be depicted as follows:

| | Stations | |
	Control	Effected
Status		
Preoperational	M_{11}	M_{12}
Operational	M_{21}	M_{22}

where M_{ij} is the mean of all observations taken with operating status i and at station category j. The interaction hypothesis that is tested is $M_{11} - M_{12} = M_{12} - M_{22}$ and is performed with a single degree of freedom test [10,11].

A disadvantage of this test is the uncertainty that is introduced by the nonnormal underlying probability distributions. The problem of nonnormal data is generally recognized but a satisfactory solution has not been achieved. McCaughran [11] points out that interaction effects are influenced by the scale of measurement; thus, transformations may introduce or remove significant interaction effects. He recommends that the data not be transformed, therefore relying on the robustness of the analysis to mitigate the effects of the nonnormal data distribution. Thomas [12] takes the alternative approach and reasons that the effects from nonnormality are more important and transforms the data prior to analysis. He acknowledges that this may alter the significance of the interaction terms. Thus, the judgment of a significant effect (impact) may be dependent upon the choice of scale adopted by the investigator.

A second and major disadvantage is the interpretation of a statistically significant interaction effect. One of the underlying causes for a significant interaction effect can be the impact resulting from the power plant operations. However, there are also numerous other causes that can give rise to a significant interaction term. In general, the interaction term may be significant whenever the main factors, operating status and sampling sites, are not strictly additive. The following quote from Winer [13] summarizes the problem:

> In some cases there is an intrinsic interaction between the factors which cannot be considered a function of the choice of the scale of measurement. These cases are not always easily distinguished from cases in which the interaction is essentially an artifact of the scale of measurement.

Thus, a test for significance of the interaction term may not be a true test of impact.

As pointed out by McCaughran [11] the above problems disappear when a one-way analysis of variance design is used. In two-way designs, the problems

are formidable but tractable. The majority of the designs considered by Gore et al. [7,8] and Murarka et al. [1] were on the order of three- to five-way analyses, often with a nesting of factors. These designs, therefore, include higher order interaction terms that can be statistically significant and, thereby, confound the interpretation of the interaction effect of interest. Thus, the interpretation of a significant interaction term as a significant power plant induced impact does not have the desired quantitative statistical foundation that is to be preferred for making environmental decisions.

An additional problem associated with using analysis of variance techniques to evaluate monitoring data is sufficient computer resources. When the model contains several main effects and several levels for each effect, the number of cells required to estimate the complete model can easily surpass the available memory of most computers. A major contribution to the increased number of cells results from using each station as a level. Two methods have been used in the analysis of monitoring data by Gore et al. [7,8] and Murarka et al. [1] to circumvent the problem. Gore et al. [7,8] suggests that the monthly effects be treated by separate analyses. They constructed 12 analysis of variance tables, one for each month, and tested for impact within each month to reduce computer core requirements. The major drawback appears to be that the number of hypotheses and tests escalates beyond reasonable limits. For example, in analyzing the Haddam Neck benthic data, 4 species and 3 phylum groups were analyzed for 11 monthly data sets, a total of 77 analysis of variance tables. Thus, the solution to the computer space problem has created a problem in controlling the experimentwise error rates (i.e., the probability levels for the F-tests).

Murarka et al. [1] resolved the problem of limited computer core by reducing the number of factors in the model. He omitted month, depth zones and repeated samples at the same stations and greatly reduced the number of cells and, thus, computer core requirements. This technique requires the additional assumption that years represent "random" observations of the preoperational and operational periods. The consequences of this approach, mainly the effect on the estimate of the error variance, need to be further explored and tested before the usefulness of omitting factors can be established.

Regression Techniques

Regression techniques were used by Adams et al. [4,5] to test hypotheses of impact from the power plant. In general, they attempted to estimate the relationship between the control and treatment area station densities by fitting a linear regression line to the paired observations. Murarka et al. [14] proposed a multiple regression model in which data from all the control stations were used to predict the density at the treatment station with the plant operating.

The assessment of a plant impact with the Surry data was severely constrained by the lack of useable preoperational monitoring data [5]. The authors attempted to fit the following general model to the operational data:

334

$$R_s = k \, (R_c)^\alpha \prod_{j=1}^{p} (f_j)^{\beta_j}$$

where R_s and R_c are the density at the stressed and control stations, respectively, k and α are coefficients that estimate the relationship between the two stations, the f_j's are the stress factors, and β_j the associated coefficient. The model is linearized by a logarithmic transformation and the resulting model fit to the benthic data.

$$R_s = \ln k + \alpha \ln R_c + \beta_1 \, \delta_0 + \beta_2 \, \delta_2$$

where δ_0 is the ln (T_s/T_c) at lag zero and δ_2 is ln (T_s/T_c) at lag two; where T_s and T_c represent temperatures at the discharge and control areas, respectively. The units for the time lag or the reasons for omitting a lag one term are not given by the authors. The model is fit by ordinary least-square methods and the coefficients β_1 and β_2 are interpreted as indicating deleterious effects when they are negative. We believe such an interpretation can lead to serious errors. The problems with the above procedure are twofold, one with the application of the methodology and the other with the interpretation of the statistical analysis.

The major exception to the above procedure is the interpretation of the model parameters to indicate cause and effect (i.e., impact). Adams et al. [4] imply that the inclusion of the term, α ln R_c, accounts for the natural variability in the system and that if β_1 is statistically nonzero, then a significant effect due to f_i is present. Such an interpretation is unwarranted based on this statistical method. The model is fit using least squares, which uses all the independent variables simultaneously, and with equal weight. The method does not attempt to first explain as much variability as possible using only the control station density, i.e., account for naturaly variation, and then attempt to explain the pure noise component. The contribution to the linear regression of the individual variables cannot be adequately assessed by using this technique. Also, it is unclear what effect the inclusion of the lagged terms had and what criteria were used to select the lag 0 and lag 2 terms. A method which examines the correlation and partial correlation coefficients, for example a stepwise regression procedure, is needed to evaluate the relative importance of the individual terms in the model. In addition, the authors do not establish that a deleterious effect can be expected to produce a negative coefficient (β_1 or β_2) within the multiple regression equation. Thus, I am not convinced that an assessment of impact can be based on the sign of β_1 or β_2.

The use of the above linear regression models is dependent upon assumptions about the distributions and associated error structures of both the $X(R_c)$ and $Y(R_s)$ variables. Snedecor and Cochran [15] list the following three assumptions that are made about the relationship between X and Y for ordinary linear regressions:

1) For each selected X there is a normal distribution of Y from which the sample value of Y is drawn at random.

2) The population values of Y corresponding to a _selected_ X has a mean μ that lies on the straight line $\mu = \alpha + \beta X$.

3) In each population, the standard deviation of Y about its mean $\alpha + \beta X$ has the same value, assumed constant as X varies (emphasis added).

These assumptions are likely to be satisfied by the monitoring data, except that values of X were not selected. The values of X are subject to the same errors of measurement and inherent variability as the values of Y. Ricker [16] reviews a number of different applications of linear regression in fisheries research and concludes that estimates based on ordinary predictive regressions are biased to some degree. In addition, he gives a number of the relevent statistical procedures that can be applied to obtain unbiased estimates under certain other assumptions. Thus, although these problems are often ignored by many authors, we believe that the resultant analyses can be biased and additional efforts are required to establish their validity.

Murarka et al. [14] proposes a multiple regression model of the form:

$$\hat{Y}_{ij} = \hat{\theta} + \hat{\phi}\, X_{ij}$$

where the subscript j indicates a specific time point in the operational period at station i. The model was fit to preoperational data to estimate $\hat{\theta}$, $\hat{\phi}$ and the variance σ^2. The test of impact is performed by calculating the predicted value of $\hat{Y}_{ij}$ based on the operational period observations at X_{ij} and comparing these to the observed data Y_{ij}. While this approach is seemingly attractive, it has two major drawbacks. As pointed out by Murarka [10] further testing and evaluation of the problems associated with the fact that both the X and Y variables are subject to error must be accomplished before accepting the technique. Additional problems may arise in those cases where the operational control station densities are considerably beyond the range of the preoperational densities. In these cases, the variance, which depends on the difference between the operational and the preoperational mean density, may become large with a resulting decrease in sensitivity of the tests.

Another linear regression approach is suggested by Adams et al. [5] in their analysis of the data from the Peach Bottom Atomic Power Station. Their approach considers the following model for the preoperational and operational data sets for each pair of treatment-control stations:

$$T = C^\beta \text{ or } \ln T = \beta \ln c$$

where T and C are the densities at the treatment and control stations, respectively, and β is slope of the regression line. Thus, the data are transformed by logarithms and a zero intercept regression line fit by least squares techniques. The hypothesis that the regression coefficient, β_p (preoperational) and β_0 (operational) are equal is tested to evaluate the impact of the power

plant operation. This method contains the same uncertainty as the previous regression methods because both T and C are measured with approximately the same error structures.

In addition, no explanation or rationale is presented for choosing the zero intercept models in logarithmic units. Therefore, we are left to speculate about the underlying assumptions. A model which is slightly less restrictive could be written as $T = \alpha C^\beta$. The above formulation assumes that $\alpha = 1$ for all cases. The model transformed by logarithms would then be of the form $\ln T = \ln \alpha + \beta \ln C$, and a test of the hypothesis that $\alpha = 1$ could be made. This preliminary test should be made because, although it may be logical to assume that whenever $\ln C$ approaches zero, $\ln T$ should also approach zero, it is not clear that it is a straight line relationship throughout the entire range of $\ln C$ and $\ln T$ values. As pointed out by Snedecor and Cochran [15]:

> This model (zero-intercept) should not be adapted without careful inspection of the data, since complications can arise. If the sample values of X are all some distance from zero, plotting may show that a straight line through the origin is a poor fit, although a straight line that is not forced to go through the origin seems adequate. The explanation may be that population relation between X and Y is curved, the curvature being marked near zero but slight in the range within which X has been measured. A straight line of the form (a + bx) will then be a good approximation within the sample range, though untrustworthy for extrapolation.

This advice seems appropriate in the present situation. It would seem reasonable to expect that the relationship between T and C could well be different as C approached zero. An additional implied caveat is that extrapolation beyond the observed range of preoperational densities may lead to extraneous conclusions.

Another problem arises when we consider the experimentwise error rate of the above procedure. For example, the benthic monitoring data was collected at one control and ten treatment stations at the Peach Bottom facility [5]. Subsequently, 18 β values are estimated and 8 comparisons of $\beta_p = \beta_0$ are made. Since a Type I error rate of 0.10 or 0.05 for all of these tests should be maintained, the individual tests should be conducted at an adjusted α level. These authors combined the preoperational and operational data sets and estimated a single β for stations where $\beta_p = \beta_0$. However, it would seem more beneficial to combine stations with similar preoperational and operational relationships, i.e., where $\beta_{p_i} = \beta_{p_j}$ and $\beta_{0_i} = \beta_{0_j}$. These combined data sets would then increase the sensitivity of the test of interest, $\beta_p = \beta_0$ in addition to reducing the overall number of tests.

Time Series Analysis

The use of time series analysis technique was proposed and utilized by Murarka et al. [1,2] and Murarka [3] as an alternative to the linear models

approach. Lettenmaier and Murry [17] also investigated the applicability of intervention analysis, a method based on the time series approach, to the monitoring of nuclear power plant environmental impacts. On the surface, these models appear to provide a very useful technique for examining the impact hypothesis.(a) Instead of assuming that the data meet the underlying assumptions for the classical analysis of variance approach, the data are treated as a time series and the integrated moving average process given by Box and Tiao [19] is applied.

The major disadvantage of the approach appears to be the requirement for moderate to large data sets. The length of the data set as well as the frequency of observation required to successfully apply the method with sufficient precision severely limit its application to monitoring data. With regards to the frequency of sampling, Box and Jenkins [18] suggest that the interval should be fairly short compared with the time constants expected for the system. The time constants are a measure of the speed with which the system approaches a new state following a shift in the input conditions. Since it is likely that many of the aquatic organisms respond fairly rapidly to certain kinds of changes, a sampling interval of daily or every few days appears to be needed. With the possible exception of impingement and physical-chemical monitoring, sampling at this level is both economically and biologically not feasible.

Another aspect of the method that needs further investigation before the time series approach can be fully evaluated is the modeling of the impact itself. Murarka et al. [1] investigated a model which assumed that impact could be represented by an immediate and constant effect upon the time series. Undoubtedly this represents an over simplification of the actual impact function and additional work and investigations are needed to define more realistic formulations.

STATISTICAL CONSIDERATIONS

Error Rates

There are three important factors to consider when setting out to establish the number of samples to collect on a monitoring program. The first of these is to evaluate the consequences of concluding that an impact exists, when in actuality none exists, and to assign an acceptable probability to this happening. The second factor is the reverse of the first, that is, to assign an acceptable probability to concluding that no impact exists, when one actually is present. The third factor that must be considered is the size or magnitude of an impact or change that the monitoring program should be capable of detecting. With these three factors and an estimate of the variance or coefficient of variation, it is possible to answer the often asked question: How many samples should be collected?

(a) A complete review of time series is beyond the scope of this paper, the interested reader is referred to Box and Jenkins [18], Box and Taio [19,20].

An alternative way to establish sample sizes, and we suspect the most univer-
sal, is to start with a level of effort or price range and calculate how many
samples can be collected within those constraints. This approach often relies
heavily upon approximating the expenditures of previous monitoring programs
and what the market will bear. If the previous studies were well-designed
and conducted at an appropriate level and were similar to the current situa-
tion, then reasonable results can be anticipated. However, when using this
method, the program designer should be aware of the resultant probability
levels and detectable changes that the program is capable of producing.

The selection of the α error rate for testing hypothesis has routinely been
set at 0.05 by scientists and engineers. However, by comparison those
experiments generally were characterized by: 1) controlled experimental con-
ditions; 2) consequences of a wrong decision easier to quantify; 3) signifi-
cance and interpretation of statistical differences uncomplicated; 4) greater
certainty about the underlying distributions; 5) relatively small coefficients
of variation; 6) sampling relatively easy and cheap. The area of testing
impact hypotheses has few, if any, of these characteristics. Therefore, we
recommend that a slightly larger α error rate of 0.10 be used for testing
impact hypotheses. This also provides a better balance between α and β error
rates within the limited range of feasible sample sizes.

Additional consideration should be given to the problems of controlling the
experimentwise error rates. If we assume that each taxonomic group represents
the experimental unit, then the above error rates are appropriate for each
analysis. However, if the experimental unit is assumed to be a trophic level
assemblage that potentially will be impacted, then the error rates of the
analysis for each of the individual taxonomic groups should be adjusted to
control the overall experimental error rates. Thus, if more than two taxono-
mic groups are tested, the investigator should be concerned about the
experimentwise error rates.

An example of the consequences of using taxa level error rates when a trophic
level error rate is appropriate will illustrate the problem. If we were to
use an α level of 0.10, 10% chance of making a Type I error, 90% probability
of not making a Type I error on each analysis of a single taxa, then the
formula: $p = 1 - (1 - \alpha)^n$ where α = Type I error rate and n = number of
analyses, can be used to calculate the probability of making at least one
Type I error for the n taxa groups. Thus, if $\alpha = 0.1$ and $n = 6$, then $p = 0.49$
or stated simply, we have approximately a 50% chance of concluding there is
a significant impact on at least one taxa group when, in fact, there is no
impact. A similar line of argument can be made for the probabilities asso-
ciated with making at least one Type II error. That is, if we have a power
of 0.80 on the above six individual analyses, we are likely to fail to
detect a significant impact, i.e. make at least one Type II error, from the
power plant approximately 75% of the time. Thus, whenever the trophic level
is the appropriate experimental unit the investigators must adjust the error
rates on the individual analyses to achieve acceptable experimentwise error
rates.

The magnitude of the β error rate or power levels for testing impact hypothe-
sis was not addressed in any of the nine case studies conducted by ANL, ORNL
and PNL. In general, acceptable power levels have not been established and
are generally ignored in the evaluation of impact hypotheses. McCaughran [11]
infers by example that a power of 0.90 is to be preferred. Nearly equal pre-
ference is given to power of 0.70, 0.80 and 0.90 by Thomas [12]. It would
appear reasonable to assume that the consequences of making either a Type I
or II error are potentially of similar magnitudes. When we make a Type I
error, the power customers pay for unneeded environmental controls at the
nuclear power plant. On the other hand, if we make a Type II error, the
general public incurs an added loss due to the undetected environmental
impact. If we guard against serious Type II errors by requiring continuing
monitoring programs, then perhaps we can allow increased Type II error rates.
However, it would not seem advisable to make decisions based on tests that
have a power of less than 80%. I recommend that the power of the tests impact
hypothesis be 0.80. The selection of the power for testing the impact hypo-
thesis includes the following considerations: 1) consequences of making a
β error; 2) the uncertainity of the experimental data; 3) cost of the field
program; and 4) our ability to reevaluate the decision periodically during
the life span of the power plant. The β error rates that are greater or less
than this appear to require excessive sample sizes or are too insensitive to
provide a sound basis for decision making. While the selection of a power
level of 0.80 is qualitative, I believe it will aid in focusing attention on
this statistical attribute of impact assessment.

The third consideration in establishing sample sizes is the magnitude of
change to detect that which is appropriate for impact assessment. As was
pointed out to each of the three laboratories' studies, ANL, ORNL and PNL,
research is needed to provide information on the biological significance of
an observed change and what constitutes a significant change. Thus, while
no site specific or generic value can be recommended, it appears that the
detection of 50% changes in density for the data sets reviewed in this report
is a reasonable level.

SUMMARY AND CONCLUSIONS

The review of the nine power plant environmental impact assessment programs
has indicated that there is very little uniformity or consistency in the
quantitative approach. This extends beyond the site specific requirements
imposed by the habitat and ecosystem. In addition, a difference exists
between the objectives as established for the monitoring program and the
inferences that can be based on the data actually collected. Three aspects
of the impact quantification and assessment were examined and the following
conclusions reached for the benthic populations.

The identification of benthic organisms to the "lowest possible taxon" is
generally unwarranted for the current state-of-the-art of impact assessment.
Rather, organisms should be classified into a maximum of five taxonomic or

.

functional groups. In addition, collecting data on abiotic water quality parameters solely to establish ecological relationships is unrealistic for the scope of a monitoring program.

Of the three analytical methods reviewed in detail it appears that the analysis of variance approach offers the best available framework for testing impact hypothesis. This technique, although likely requiring further refinement, offers the greatest probability of correctly identifying impacts.

The testing of impact hypothesis should be done with known error rates, including a definition of the experimental unit and the probabilities of making Type I and Type II errors. It is recommended that benthis studies be designed to detect at least 50% changes in population density with an α rate of 0.10 and a β rate of 0.20. These three parameters should be evaluated and clearly stated in the environmental impact statement.

REFERENCES

1. Murarka, I. P., A. Policastro, E. Daniels, J. Ferrante and F. Vaslow. 1976. An Evaluation of Environmental Data Relating to Selected Nuclear Power Plant Sites; The Zion Nuclear Power Station Site. ANL/EIS-5, Argonne National Laboratory, Argonne, IL.

2. Murarka, I. P., J. G. Ferrante, E. W. Daniels, E. E. Pentecost. 1976. An Evaluation of Environmental Data Relating to Selected Nuclear Power Plant Sites: Prairie Island Nuclear Generating Plant Site. ANL/EIS-6, Argonne National Laboratory, Argonne, IL.

3. Murarka, I. P. 1976. An Evaluation of Environmental Data Relating to Selected Nuclear Power Plant Sites: The Nine Mile Point Nuclear Power Station Site. ANL/EIS-7, Argonne National Laboratory, Argonne, IL.

4. Adams, S. M., P. A. Cunningham, D. D. Gray and K. D. Kumar. 1977. A Critical Evaluation of the Nonradiological Environmental Technical Specifications, Vol. 2, Surry Power Plants Units 1 and 2. ORNL/NUREG/TM-7 Oak Ridge National Laboratory, Oak Ridge, TN.

5. Adams, S. M., P. A. Cunningham, D. D. Gray, K. D. Kumar and A. J. Witten. 1977. A Critical Evaluation of the Nonradiological Environmental Technical Specifications, Vol. 3, Peach Bottom Atomic Power Station Units 2 and 3. ORNL/NUREG/TM-71. Oak Ridge National Laboratory, Oak Ridge, TN.

6. Adams, S. M., P. A. Cunningham, D. D. Gray and K. D. Kumar. 1977. A Critical Evaluation of the Nonradiological Environmental Technical Specifications, Vol. 4, San Onofre Nuclear Generating Station Unit 1. ORNL/NUREG/TM-72. Oak Ridge National Laboratory, Oak Ridge, TN.

7. Gore, K. L., J. M. Thomas, L. D. Kannberg and D. G. Watson. 1976. Evaluation of Monticello Nuclear Power Plant, Environmental Impact Prediction, Based on Monitoring Programs. BNWL-2150/NRC-1. Battelle, Richland, WA.

8. Gore, K. L., J. M. Thomas, L. D. Kannberg, J. A. Mahaffey and D. G. Watson. 1976. Evaluation of Haddam Neck (Connecticut Yankee) Nuclear Power Plant, Environmental Impact Prediction, Based on Monitoring Programs. BNWL-2151/NRC-1. Battelle, Richland, WA.

9. Gore, K. L., J. M. Thomas, L. D. Kannberg and D. G. Watson. 1977. Evaluation of Millstone Nuclear Power Plant, Environmental Impact Prediction, Based on Monitoring Program. BNWL-2152/NRC-1. Battelle, Richland, WA.

10. Murarka, I. P. 1977. Statistical Analysis of the D. C. Cook Preoperational Environmental Monitoring Program. ANL/EIS-9. Argonne National Laboratory, Argonne, IL.

11. McCaughran, D. A. 1977. The quality of inferences concerning the effects of nuclear power plants on the environment, pp. 229-242. In: Proceedings of the Conference on Assessing the Effects of Power Plant Induced Mortality on Fish Populations. Van Winkle (ed), Pergamon Press, NY.

12. Thomas, J. M. 1977. Factors to consider in monitoring programs suggested by statistical analysis of available data, pp. 243-255. In: Proceedings of the Conference on Assessing the Effects of Power Plant Induced Mortality on Fish Populations, Van Winkle (ed). Pergamon Press, NY.

13. Winer, B. J. 1971. Statistical Principles In Experimental Design. Second Edition. McGraw-Hill, NY, 907 pp.

14. Murarka, I. P., A. J. Policastro, J. G. Ferrante, E. W. Danials and G. J. Marmer. 1976. An Evaluation of Environmental Data Relating to Selected Nuclear Power Plant Sites: A Synthesis and Summary With Recommendations. ANL/EIS-8. Argonne National Laboratory, Argonne, IL.

15. Snedecor, G. W. and W. G. Cochran. 1967. Statistical Methods, Sixth Edition. Iowa State University Press, IA., 593 pp.

16. Ricker, W. E. 1973. Linear regressions in fishery research. J. Fish. Res. Bd. Can. 30:409-434.

17. Lettenmaier, D. D. and L. C. Murry. 1977. Design of Nonradiological Aquatic Sampling Programs for Nuclear Power Plant Impact Assessment Using Intervention Analysis. UW-NRC-6. University of Washington, Seattle, WA.

18. Box, G. E. P. and G. M. Jenkins. 1970. Time Series Analysis Forecasting and Control. Holden Day, CA., 553 pp.

19. Box, G. E. P. and G. C. Tiao. 1965. A change in level of a nonstationary time series. *Biometrika* 52:181-192.

20. Box, G. E. P. and G. C. Tiao. 1975. Intervention analysis with applications to economic and environmental problems. *J. Am. Stat. Assoc.* 70:70-79.

FURTHER STUDIES IN SYSTEMS ANALYSIS OF COOLING LAKES: HYDRODYNAMICS AND ENTRAINMENT

Kenneth D. Robinson and Robert J. Schafish
R.W. Beck and Associates
Denver, Colorado

George Camougis
New England Research, Inc.
Worcester, Massachusetts

ABSTRACT

The effects of entrainment on semi-closed ecosystems in cooling lakes are not clearly understood. A methodology is presented wherein entrainment assessment is based on power plant induced hydrodynamics and biological population dynamics. Entrainment probability distributions are developed for important areas (habitat) in cooling lakes. These are compared with regeneration times and critical development times for specific biota which allows a semi-quantitative evaluation of the effects of entrainment on the entire ecosystem.

INTRODUCTION

Entrainment is a factor that must be accounted for in the overall biological evaluation of cooling lakes. Rather than consider entrainment as a separate issue in cooling lake ecosystem analysis, that evaluation must include the relationships among entrainment effects, lake hydrodynamics and thermal effects. A systems approach to cooling lake analysis provides an important assessment tool. This paper is a further development of systems concepts applied to cooling lakes which was presented as a paper at the 1977 Waste Heat Management and Utilization Conference (1).

Federal 316 (b) guidelines to meet the requirement that intake structures reflect the best technology available for minimizing adverse impact, classify potential impact designs according to the volume of intake flow relative to the volume of the source water body (2). The guidelines further define a zone of potential involvement for entrainment as that portion of the source water body that is likely to be drawn into an intake structure. These concepts are inappropriate for intakes in closed ecosystems such as those found in cooling lakes. Hydrothermal analysis shows that the entire volume of a moderately loaded cooling lake can be entrained, even in lakes with control arms.

Mortality resulting from entrainment can be viewed as a predatory process in the cooling lake ecosystem. How this predation affects the various trophic levels in the lake is a function of intake variables such as location, cooling water flow rate, intake configuration and design. It is also a function of the cooling lake hydrodynamics which dictate how the prey arrives in the vicinity of the predator. A more complete understanding of the relationship between hydrodynamics and entrainment shows that there is not a uniform progression of the entire lake contents toward the intake.

344

Rather there is a very wide variation in the residence time of any particle of water which is dependent upon the lake hydrodynamics. This variation can be described and analyzed.

COOLING LAKE ECOSYSTEMS

As with most lacustrine systems, cooling lakes develop a complex biological community consisting of various trophic levels and biotic groups. The final community depends upon the physical and chemical factors in the lake ecosystem.

Representative Biota

No single method has been accepted universally as the procedural approach to assessing the aquatic biota in environmental studies. However, based upon general ecological principles by Odum(3) and the useful manual by Weber (4) and the pertinent guidelines from the USEPA (5) it has become customary to assess the following aquatic biota in environmental studies of cooling lakes:

- (1) phytoplankton
- (2) periphyton
- (3) macrophyton
- (4) zooplankton
- (5) benthic macroinvertebrates
- (6) fishes

The trophic relationships among these various biotic groups are generally well understood. Also the major genera and species can be predicted with some degree of confidence, although each ecosystem has its own unique characteristics. Cooling lake ecosystems may differ from those of natural lakes because of power plant induced flow patterns and thermal structures. Heat addition can increase productivity due to longer growing seasons while entrainment can act upon certain biota in a predatory way.

Habitat Assessment

Of great practical importance is the assessment of the various habitats in the cooling lake ecosystem. For example, the physical conditions such as lake morphometry, depth, light, temperature, dissolved oxygen and other factors greatly influence the types of biota that grow in the various locations within the lake. The importance of habitat assessment to arrive at some estimate of biological importance is discussed in the USEPA guidance document (5) on entrainment studies. An important concept is that some aquatic biota (e.g., phytoplankton) tend to be homogenous in their distribution throughout the water mass; in contrast, other biota (e.g., macrophyton, fishes) tend to have more localized habitats.

Thus, as examples, the shallow areas with macrophytes, the deeper areas of the lake, and the areas with different substrates can all be identified and mapped. This permits a graphic presentation of specific habitat zones. Finally, the types of biota (especially fishes) that are likely to use the habitat zones can be identified. Some estimate of the probability of entrainment of the various biota within the various habitat zones can

then be made by correlating habitat, regeneration capacity and the influence of the cooling lake hydrodynamics.

Regeneration Capacity

Another important factor in the assessment of entrainment is the regeneration capacity of the various biotic groups. Organisms representative of all biotic categories may be entrained, including phytoplankton, zooplankton, larval forms of benthic macroinvertebrates, and fish eggs and larvae. The microbiota (e.g., phytoplankton) have short regeneration times, and the effects of entrainment are generally not critical to the maintenance of viable populations. On the other hand, the entrainment of fish eggs and larvae with longer incubation and development times may be potentially more adverse to fish populations, especially where spawning generally occurs on a yearly basis. However, population dynamics are also based on fecundity and density-dependent factors, and are important compensation considerations. Consequently, any realistic assessment of regeneration capacity must consider these other factors along with the regeneration times. The following table presents some typical times for various reproduction parameters for major biotic groups (Table 1).

TABLE 1

Biotic Groups	Various Reproduction Parameters	Time
Bacteria	Typical Doubling Time	Less than 1 hr
Phytoplankton	Typical Doubling Time	10 hr – 100 hr
Zooplankton	Brood Interval	2 – 5 days
	Maturation Time	5 days
Fish Eggs	Typical Incubation Time	2 – 10 days
Fish Larvae	Typical Development Time for Larval Stages	More than one month
Juvenile Fish	Typical Maturation Time	More than one year

It is important to recognize that cooling lakes function as closed systems with respect to entrainment, in contrast with riverine systems where the through-put is large. Because the entire contents of the cooling lake may be subject to entrainment which can result in high mortality, the concepts of regeneration time or critical development time for various biotic components are especially important in assessing the effects of entrainment. Should a particular group of organisms be subject to entrainment with a frequency close to or greater than regeneration time (or critical development time), the effects on the balance of the ecosystem could be significant.

COOLING LAKE HYDRODYNAMICS

Cooling lakes are hydrothermally distinct from natural lakes or reservoirs because of the relatively large volumes of heated water which are circulated through them. In natural impoundments, seasonal variation causes cyclical stratification and destratification due to density differences between warm and cool water. Cooling water discharge from a power plant superimposes additional thermal conditions and creates unique flow patterns which can significantly affect water quality and influence aquatic habitat. The pumping-induced circulation can also affect the way in which organisms are entrained by the intake structure.

Residence Time Distribution

Residence time is generally regarded as the time for water to flow from the discharge to the intake. An average residence time for the discharge flow is calculated on a flow-through basis (lake volume/flow rate). For purposes of entrainment assessment this concept can be expanded to include the time for water to flow to the intake from any specific area (habitat) in a lake.

The flow dynamics in a cooling lake can be very complex; because of the induced hydro-thermal structure, an average residence time may not be meaningful since the discharge flow will more likely be re-entrained over a range of residence times. Depending on the lake configuration, part of the discharge flow could be "short-circuited" with a re-entrainment time much shorter than the average residence time. Conversely, another part of the discharge could take much longer. For this reason it is more realistic to consider a residence time distribution over a range of entrainment time intervals in order to account for the actual flow patterns.

A residence time distribution is equivalent to an entrainment probability distribution for water (or organisms) in the vicinity of the thermal discharge. Using the same circulation patterns, entrainment probability distributions can also be developed for any area (habitat) in a cooling lake. Thus, for aquatic organisms in a particular location with respect to the cooling water intake, an entrainment probability distribution can be compared with regeneration times for biota such as zooplankton or phytoplankton, or for critical development times in the case of fish eggs and larvae.

Cooling Lake Model

Hydrothermal analysis can be used to predict the complex flow structures in cooling lakes (1). Circulation patterns can range from simple plug flow in long, narrow lakes to complex, multilevel circulations in wide, strongly stratified lakes. Studies have shown that, with proper design, cooling water discharge from a power plant will tend to form a distinct, heated surface layer (due to density differences) which will remain intact and tend to spread over the entire surface of a cooling lake.(6)

Ryan and Harleman (7) have developed a mathematical model for an idealized cooling pond which separates the water body into a discharge mixing region, a warm surface layer and a cooler sublayer as shown in Figure 1. This constitutes the primary flow pattern in many cooling lakes and forms the basis for calculating residence time distributions. In the model, heated discharge water enters the surface layer where it entrains cooler subsurface water and then flows to the far end of the reservoir. At the

end of the surface layer, destratification causes down-welling of surface water to the sublayer. The sublayer can be stratified due to heat input from the down-welling and also from solar radiation not absorbed in the surface layer.

The actual detailed behavior of flows and temperatures in such lakes will be somewhat more complex than in the idealized mathematical model. Some of the variations can be accounted for by considering important secondary flow patterns. Research has shown that a buoyancy-driven circulation pattern can be established in dead ended sidearms causing warmer surface water to flow into the arms.(8) As the surface flow in the sidearm cools, the more dense water sinks to the sublayer and causes a return flow to the main water body. This creates a flow residence time within the sidearm which becomes one component of the residence time distribution for the cooling water flow in the entire lake. Watershed runoff, pumped makeup water and wind-driven currents may create other secondary flow patterns which can add components to the residence time distribution.

Model Application

The analysis described above was applied to a 1500-acre cooling lake (shown in Figure 2) to calculate probabilities of entrainment at specific locations within the lake. The calculations were based on a plant capacity of 1000 MW_b a condenser cooling water flow of 800 cfs and a condenser temperature rise of 27.5^b F. Based on analysis, the discharge will produce a heated surface layer 3 feet thick. The intake, located on the lower side of the lake, draws water from both the surface layer and the sublayer. This produces a complex circulation pattern in which only a portion of the surface layer is entrained. The remainder of the surface flow continues to the lower end of the lake where down-welling to the sublayer occurs. Part of this sublayer flow will return to the intake, while the remainder will flow in the sublayer to the upper end of the lake to be re-entrained in the discharge mixing region. Other secondary flows such as sidearm circulation will add components to the flow patterns.

For a reservoir volume of 14,000 acre-feet, the discharge flow will have an average residence time in the reservoir of about nine days on a flow-through basis. However, because of the complex flow pattern, some of the discharge water will flow via the surface layer to the intake while the remainder may follow any one of the other patterns discussed above. Using the hydrothermal analysis discussed above, representative entrainment probability distributions were developed for three locations in the lake: the discharge area, a midlake area and a side arm (as shown in Figure 2). Because of the simplifications necessary for the analysis, these distributions are somewhat idealized. They are, nevertheless, useful for evaluating the potential impact of entraiment on the ecosystem of the cooling lake. As the figure shows, the area near the discharge has a relatively high probability of entrainment within 1 to 5 days. This is in contrast to the areas near the end of the lake which have the residence time distributions displaced towards the longer residence times.

ENTRAINMENT ASSESSMENT

The integration of the entrainment probability distributions with regeneration and development times can provide a semi-quantitative basis for assessing the effects of entrainment. Since the mortality from entrainment predation can be very high, the

regeneration times for various biota are important. Comparison of regeneration times for the smaller organisms (e.g. bacteria, plankton) with residence time distributions as presented in the illustrative example can indicate whether or not entrainment will adversely affect populations. The same interpretations can be applied to fish eggs and larvae. However, for these organisms, the entrainment probabilty is further complicated by factors such as spawning habitat, egg buoyancy, mobility and preferred habitat of immature forms. Fish eggs and larvae are not always uniformly distributed in the water column. Thus correlation of habitat with the entrainment probability of the adjacent water mass becomes an important assessment tool.

The use of this technique can be illustrated by considering Table 1 and Figure 2. The probability of entrainment within 1-5 days for the upper end of the lake is high compared with the lower end of the lake. This may have some effect on populations of biota with short regeneration times. However, there is still adequate regeneration time available to assure that these biota can sustain viable populations, perhaps at somewhat reduced levels. Also, the analysis implies that there is a considerable portion of the lake where these organisms will be subject to a low probability of entrainment for the duration of their reproductive time span. Figure 2 shows that the probability of water mass entrainment within 30 to 90 days is quite high for all locations within the lake. This may have significant implications to biota with reproductive paramenters within that time range. However, as discussed above, it is necessary that other factors (e.g. spawning habitat, egg buoyancy) be considered in the overall assessment of the probable effects of entrainment.

CONCLUSIONS

The overall approach of this analysis has the advantage of looking at a cooling lake as an integrated system. Residence times correlated with habitat zones can provide realistic estimates of the probability of entrainment of the various biota and thus permits an assessment of the significance of entrainment to the lake ecosystem as a whole.

This approach to entrainment evaluation in cooling lakes has implications in several areas of cooling lake ecosystem analysis. A thorough understanding of lake hydrodynamics in the early planning stages can allow selection of the design features with the purpose of controlling entrainment effects. An intake system could be designed as a selective predator by integrating hydrodynamics, habitat of important biota and cooling water intake location and design. In this way, entrainment mortality for certain biota could be selectively increased and could actually benefit the lake ecosystem. This approach is divergent from the present regulatory framework for analysis of entrainment effects which requires that the intake system be selected so as to minimize environmental effects. It is apparent that guidelines developed for entrainment evaluation in cooling lakes should be re-evaluated to reflect these concepts.

REFERENCES

1. Robinson, K.D., Schafish, R.J. and Camougis, G. 1977. A Systems Approach to Biological and Thermal Considerations in Cooling Lake Analyses. Proceedings of the First Annual Waste Heat Management and Utilization Conference, Miami Beach. May 1977.

2. U.S. Environmental Protection Agency (USEPA). 1976. Development Document for Best Technology Available for the Location, Design, Construction and Capacity of Cooling Water Intake Structures for Minimizing Adverse Environmental Impact. Effluent Guidelines Division, Office of Water and Hazardous Materials. Washington, D.C.; Government Printing Office.

3. Odum, E.P. 1971. Fundamentals of Ecology. Third Edition. Philadelphia: W.B. Saunders Company.

4. Weber, C.I. (ed.). 1973. Biological Field and Laboratory Methods for Measuring the Quality of Surface Waters and Effluents. National Environmental Research Center, Office of Research and Development. Cincinnati: U.S. Environmental Protection Agency. (EPA 670/4-73-001).

5. U.S. Environmental Protection Agency (USEPA). 1977. Guidance for Evaluating the Adverse Impact of Cooling Water Intake Structures on the Aquatic Environment: Section 316 (b), P.L. 92-500 (draft).

6. Jirka, G.H.; Abraham G.; and Harleman, D.R.F. 1975. An Assessment of Techniques for Hydrothermal Prediction. Ralph M. Parsons Laboratory for Water Resources and Hydrodynamics Report No. 203. Cambridge: The Massachusetts Institute of Technology.

7. Ryan, P.J. and Harleman, D.R.F. 1973. An Analytical and Experimental Study of Transient Cooling Pond Behavior. Ralph M. Parsons Laboratory for Water Resources and Hydrodynamics Report No. 161. Cambridge: The Massachusetts Institute of Technology.

8. Brocard, P.; Jirka, G.H.; and Harleman, D.R.F. 1975. Buoyance-Driven Circulations in Side Arms of Cooling Lakes. Presented at American Society of Civil Engineers' Convention, Denver, Colorado, November 1975.

MIXING REGION

DISCHARGE

SURFACE LAYER

SUBLAYER

INTAKE
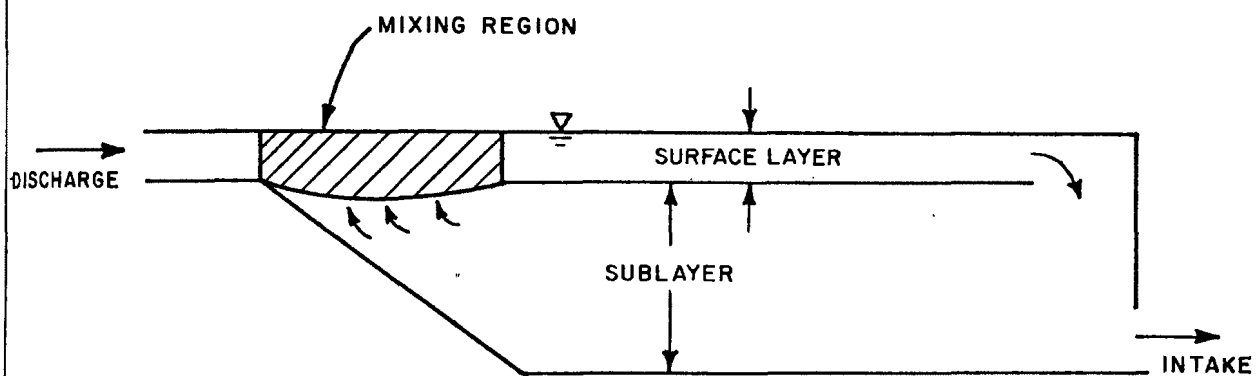
IDEALIZED COOLING POND MODEL

FIGURE I
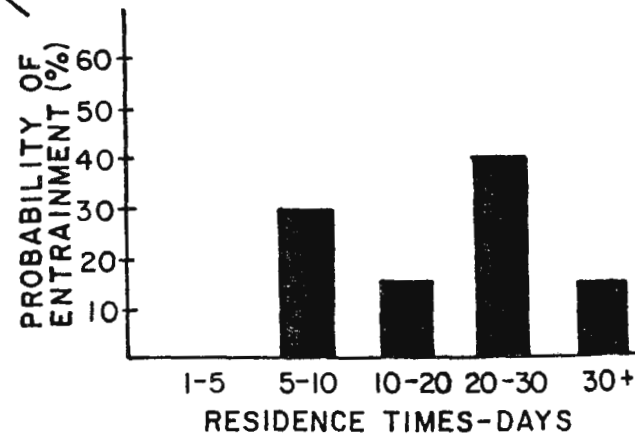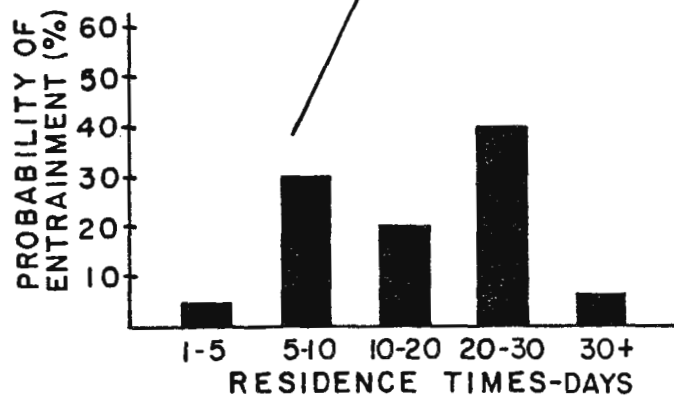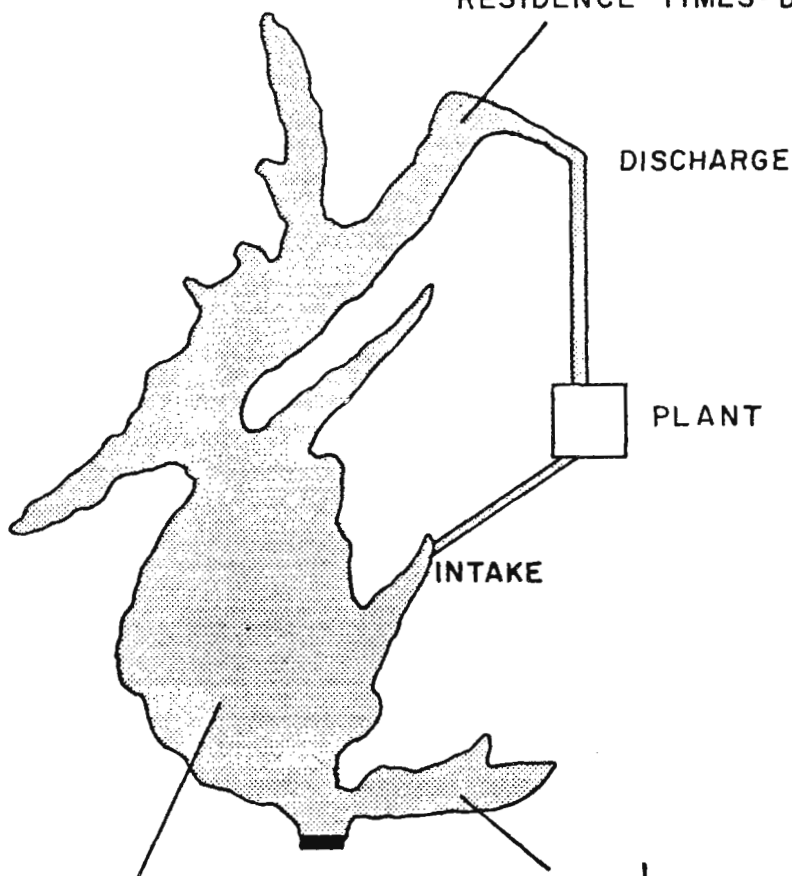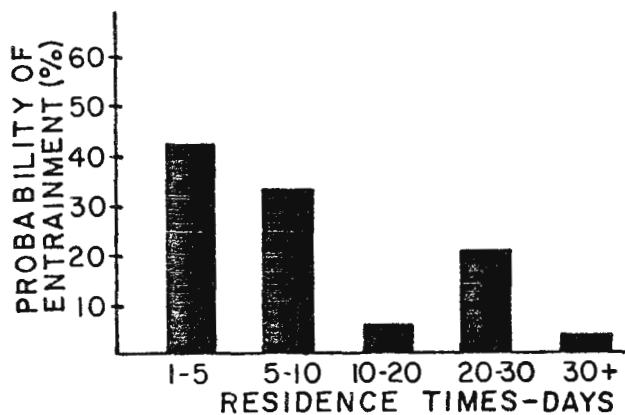
PROBABILITY DISTRIBUTIONS
FOR
ENTRAINMENT IN A COOLING LAKE

FIGURE 2

SYNTHESIS AND ANALYSES OF EXISTING COOLING IMPOUNDMENT INFORMATION ON FISH POPULATIONS*

K. L. Gore and D. H. McKenzie
Battelle Memorial Institute
Pacific Northwest Laboratory
Richland, Washington U.S.A.

ABSTRACT

This paper presents the results of a literature review and assessment study undertaken to examine the effects of a once-through cooling mode of power plant operation on small, essentially closed aquatic ecosystems, represented by cooling impoundments. Fourteen cooling impoundments were selected based on physical criteria and availability of suitable ecological references. No major detrimental effects appeared from power plant operation on fish populations inhabiting the cooling impoundments. Some direct qualitative effects were indicated among fish inhabiting areas that received heated effluents, such as earlier seasonal spawning or faster growth rates. Increased water velocity associated with effluent discharge apparently had more controlling influence on fish distribution and abundance than did temperature, particularly during spawning seasons. Statistical analyses were performed on data sets of gill net catch data. Comparisons between control impoundments and heated impoundments were based on correlation matrices and/or Wilcoxon's Signed Rank Test. Results indicated there were no statistically significant differences in fish populations between heated and control impoundments attributable to plant operation.

INTRODUCTION

It is the common practice of the National Environmental Policy Act of 1969 to require assessment and evaluation of the potential impacts of power plant operation. In addition, power plants must also abide by the provisions of Sections 316(a) and 316(b) of the Federal Water Pollution Control Act Ammendments of 1972, which are concerned with the attainment of best available technology of plant design to minimize adverse environmental impacts attributable to thermal effluents, impingement, and entrainment.

The traditional way of disposing of waste heat from power operation has been direct discharge (once-through) into various aquatic ecosystems. However due to the above legislative actions, artificial cooling impoundments are feasible alternatives to the problem of waste heat disposal.

The objectives of our study were (a) to synthesize existing fish population information from cooling impoundments, (b) to analyze the data to extract rational conclusions on fish population effects of condenser cooling systems, and (c) to identify effects that cannot be assessed with existing data.

For the purpose of this paper, a cooling impoundment was identified as a semi-confined water body used to provide recirculation water to cool condensers of electric power plants in freshwater ecosystems. Load ratio was defined as impoundment surface area in acres divided by rated plant generating capacity in MWe. A load ratio of ten or less was arbitrarily selected as the upper limit where impacts at the ecosystem level would be expected to occur. In some cases where suitable ecological data from cooling impoundments were available, sites with load ratios greater than ten were included.

Site Selection Criteria

Selection of sites for ecological assessment required: (1) identification of power plants utilizing freshwater cooling impoundments in their generating cycle, (2) determination of impoundments that were essentially closed systems and the surface area of each, (3) compilation of basic plant operational data, and calculation of load ratios, (4) referencing available ecological publications for each impoundment, and (5) initial scrutiny of references to determine their value in our synthesis and assessment program.

Initial screening and evaluation of about 135 electric power plants were done by completing a data form for each prospective site. Evaluation of completed forms and the accumulated list of publications pertaining to aquatic ecological studies at each site enabled us to narrow the original list. Eventually, 14 sites were selected for intensive data synthesis and analysis (Table 1).

Data from publications acquired for each site were evaluated for completeness with ecological matrices designed to cover a wide range of various abiotic and biotic parameters. Among the options and considerations used in final site selection were: (1) impoundment load ratio, (2) number of publications available for each site, (3) quantity and quality of available ecological data, (4) extent of literature coverage of fish populations at each site, (5) geographical location, and (6) whether or not "control situations" existed.

ANALYSIS AND DISCUSSION

Analysis of potential impacts on fishery resources in cooling impoundments are divided into two main themes. The first covers what we have determined from the data collected from 14 sites in a generic qualitative manner. The second covers independent qualitative and semi-quantitative analyses of selected data sets. In this latter part, comparison is made

of two cooling impoundments with three nearby control reservoirs, in which parameters such as game to rough fish ratios, fish condition factors, and catch per unit effort are treated.

Qualitative Assessment

There are apparently no major detrimental effects from power plant operation on fish populations inhabiting closed system cooling impoundments. However, this conclusion is accompanied by several limitations.

First and most important, most available studies were highly qualitative because they were based on nonquantitative evidence. This was due mainly to sampling design deficiencies.

Second, most available studies were research projects undertaken by students to complete requirements for advanced degrees. Many projects were narrow in scope (e.g., dealing with only one aspect of the life history of a single fish species), and provided little ecological information on generic fish population parameters in relation to the ecosystem. Many available studies had a duration of one year or less, and did not examine annual seasonal variations in population abundance. Reports prepared by fish and wildlife agencies were usually not designed to detect or measure power plant effects on fish populations, but to obtain data on which to base recommendations for fish management and enhancement of the sport fishery.

Third, available data outside the southwestern United States was scanty. The majority of cooling impoundments, including the 14 sites chosen for our evaluation, were located in Texas where ambient water temperatures are historically high [1]. Fish living in Texas waters have high temperature tolerances [2]. Thus, conclusions reached concerning the effects of thermal additions on fish populations in Texas cooling impoundments did not necessarily apply to other geographical areas.

A fourth limitation to complete evaluation of possible power plant effects on fish populations was the absence of data measuring impingement, entrainment, and/or chlorination impacts. At the 14 sites we assessed, no indication was given whether these potential perturbations existed or not. The question of thermal effects on reproductive capacity of fish populations was also not addressed quantitatively, but the topic was occasionally dealt with briefly in a qualitative sense.

Any ecological study concerning the effects of stress on fish populations must determine if the majority of adults reproduce normally, if a high percentage of the eggs hatch, and if young fish have a "typical" survival rate the first year of life. This type of study is important because sound judgments on whether power plant operations are affecting the fish populations in a cooling impoundment are difficult without basic information on reproductive success and progeny survival. Survival and growth of stocked fish is an incomplete answer.

We evaluated the appropriateness of each statistical test applied by various authors in individual studies. We looked to see: (1) if a correct test was applied to the correct data set, (2) if there were deficiencies in sampling design, (3) if there was a better way to test the data, and (4) if it would be beneficial to retest the data. In most cases the appropriate statistical test was applied. However, since fishery statistical methods have evolved rapidly, in some cases a more appropriate test was available for application.

We usually did not analyze the data available in various reports again for two reasons. First, a better or newer statistical test, in our judgment, would probably not have altered the results due to limitations imposed by deficiencies in sampling design. Second, in order to make quantitative assessments, several assumptions were required that out-weighed in a negative sense the weight and power of the quantitative test. Therefore, we attempted to statistically evaluate the original data, or analyzed data not previously tested statistically, in only a few cases.

Analysis of Specific Data Sets

We obtained fishery data sets for two heated reservoirs, Lake Colorado City and Lake Nasworthy, that could be compared with nearby unheated reservoirs. Lake Colorado City was compared with Champion Creek Reservoir (control). Lake Nasworthy was compared with Twin Buttes Reservoir and San Angelo Reservoir (controls).

Data sets for 8 to 11 years were assembled for each comparison, covering the period from 1960 to 1975. Semiquantitative (correlation matrices) and nonparametric (Wilcoxon's Signed Rank Test) statistics were employed for data evaluations. Data at each location were presented as averages of one to four sampling trips per year.

A correlation matrix was used to evaluate associations among the variables for the combined data set, which included data from heated and control reservoirs as appropriate. Variables tested included: (1) game fish by number and weight; (2) rough fish by number and weight; (3) channel catfish and largemouth bass by number, percent number, weight, percent weight, average weight, and condition factor; (4) game fish to rough fish ratio by number and weight; (5) average weight of game and rough fish; and (6) percent of game fish by number and weight.

Variables showing a high correlation coefficient were investigated further by plotting individual data. Plots were made for the three following variables in the Lake Colorado City-Champion Creek comparison: (1) game to rough fish ratio by weight, to number of largemouth bass; (2) game to rough fish ratio by weight, to percent game fish by weight; and (3) game to rough fish ratio by weight, to average weight of channel catfish.

For the Lake Nasworthy - Twin Buttes and San Angelo Reservoir comparison, the following eight variables showed a high correlation value: (1) average number of game fish, to total number of game fish, (2) average weight of rough fish, to total rough fish weight per set, (3) average weight of

rough fish, to total rough fish weight per set; (3) average weight of rough fish, to average weight of channel catfish; (4) average weight of game fish, to average weight of largemouth bass; (5) average weight of rough fish, to number of gizzard shad per set; (6) average weight of rough fish, to percent shad by number; (7) average weight of rough fish, to average weight of shad; and (8) average weight of game fish, to percent number of river carpsucker.

The important relationship that the plots depicted was the comparative distribution of data points from heated and control impoundments. The distribution in most plots (Figures 1 and 2) indicated that there were no major differences in fish population parameters between heated and control impoundments. Therefore, the underlying relationships were apparently similar. We did not attach probability levels to the observed correlation coefficients because probability levels are heavily influenced by the frequency of zero values in the data sets, which did occur to some degree. Thus, our correlation matrices approach was general. However, if large differences between variables actually existed, the correlation matrix would demonstrate them. We conclude from this analysis that there were no significant differences between fish populations in heated and control impoundments.

The correlation matrix evaluation was taken one step further. We decided that even though two variables did not correlate initially, it was still possible that a real difference in fish population parameters between the two water bodies might occur. We chose variables that should show real differences if they were actually occurring, and conducted additional tests.

As expected, the variables did not correlate. Furthermore, dispersal of data points indicated that there were no large differences in fish populations between the two impoundments. If differences were to occur, a clumping of data points for each reservoir would be expected. Therefore, no detectable differences existed for noncorrelated variables.

The final approach we employed in analyzing fish population data was a nonparametric statistic. Wilcoxon's Signed Rank Test [3] was used to examine possible differences between variables. Parameters tested were those where differences due to power plant operation were most likely to occur. The following parameters were tested between heated and control reservoirs: (1) game fish number per gill net set, (2) rough fish number per gill net set, (3) game/rough fish ratio by number per gill net set, (4) channel catfish "K" factor (5) largemouth bass "K" factor, (6) channel catfish number per gill net set, and (7) largemouth bass number per gill net set.

No significant differences were found between Lake Nasworthy, Twin Buttes and San Angelo Reservoirs (Table 2). Significant differences in largemouth bass condition factors could not be established because data were lacking.

357

For the Lake Colorado City - Champion Creek Reservoir comparison, several significant differences were found (Table 3). The number of rough fish per gill net set was significant (95% level), indicating a larger rough fish population in Lake Colorado City. However, the number of game fish per gill net set between the sites was not significantly different. Since the rough fish population was larger in Lake Colorado City, the game to rough fish ratio by number was also significant (99% level). The channel catfish condition factor was significantly higher at Champion Creek Reservoir, but total number per gill net set of channel catfish was significantly higher for Lake Colorado City. Thus, Lake Colorado City apparently supported a larger population of channel catfish, but they weighed less for a given length than channel catfish from Champion Creek Reservoir. Largemouth bass populations, total game fish per gill net set, and bass condition factors between the impoundments were not significantly different. Consequently, both reservoirs appeared to support basically the same viable fish populations although Lake Colorado City had the larger population of rough fish. According to Texas Parks and Wildlife Department reports, Lake Colorado City has received heavy fishery pressure for at least 15 consecutive years, yet sustains a productive fishery with very little supplemental stocking.

In summary, we conducted independent statistical evaluations of fish population data. Available data was first analyzed from a general perspective (correlation matrix), then investigated that approach in more detail. We finally employed a specific test to data sets where expected differences from power plant operation should be readily revealed. However, the data analyzed were yearly averages of the variables tested. Fish were often collected just one time annually, while several collections were made in other years. Moreover, sampling seasonality varied from year to year and between impoundments. Thus, the data are not as representative as desired of the fish populations in each impoundment. Gill net catches over a 15 year period provided the best available data set, which did allow us to investigate some potential differences in fish populations between heated and control impoundments.

On the basis of independent statistical analyses, and the qualitative judgments and limiting qualifications mentioned earlier, we conclude that no statistically significant differences existed between fish populations of the cooling impoundments and control sites.

Based on generic information reviewed for 14 sites, it appeared that cooling impoundments represented functioning ecosystems. Fish populations are apparently maintained without the aid of management stocking programs in some cases; whereas, fish populations in other cooling impoundments needed annual supplemental stockings. However, stocking usually reflected intense fishing pressure where carrying capacity of the water body was exploited other than deficiencies in that water body for normal fish reproduction.

Whether the need for supplemental stocking in cooling impoundments was caused by extensive fishing pressure, perturbations from the power plant

or any of a number of possible other reasons could not be determined. Stocking needs were probably due to other causes, rather than power plant induced. Other lakes (without power plants) also required supplemental stocking to maintain game fish populations, sometimes when subject to less fishing pressure.

Increased water velocity associated with discharge of heated effluent apparently influenced fish distribution and abundance more than did increased temperature, especially during the spawning season, for most fish species. Fish were free to seek or avoid discharge areas as their preferences dictated, regardless of whether the controlling factor was temperature or current. The increased circulation in cooling impoundments caused by the power plant discharge was generally considered to benefit aquatic life, but there was no evidence provided to prove or disprove this hypothesis.

Without quantitative evidence to judge whether detrimental effects were occurring in cooling impoundments, our best qualitative assessment told us that there were no overriding perturbations on fish populations from power plant operations in cooling impoundments. However, this conclusion was reached without quantitative evidence. Until studies are designed and implemented to produce data amenable to quantitative assessment, only qualitative interpretations can be made.

REFERENCES

1. Drew, H. R. and J. E. Tilton. 1970. Thermal requirements to protect aquatic life in Texas reservoirs. _J. Wat. Poll. Control Fed. 42:_ 562-572.

2. Strawn, K. and J. E. Dunn. 1967. Resistance of Texas salt and freshwater marsh fishes to heat death at various salinities. _Texas J. Sci._ 19:57-76.

3. Hollander, M. and D. A. Wolfe. 1973. _Nonparametric Statistical Methods._ Wiley and Sons, New York, 503 pp.

360

TABLE 1

RESULTS OF SCREENING POTENTIAL SITES
FOR ECOLOGICAL DATA SYNTHESIS AND ANALYSIS (1)

Generating Plant (Utility)	Cooling Impoundment	Load Ratio (Surface) Acres/MWe	No. of Reports
Asheville Carolina Power & LIght	Lake Julian	0.8	13
Big Brown Texas Power & Light Co.	Fairfield Lake	2.0	6
V. H. Braunig San Antonio Public Service Bd.	Braunig Lake	1.5	9
Eagle Mountain Texas Electric Service Co.	Eagle Mountain Lake	13.0	20
Handley Texas Electric Service Co.	Lake Arlington	4.4	16
Lake Catherine Arkansas Power & Light Co.	Lake Catherine	2.6	6
Morgan Creek Texas Electric Service Co.	Lake Colorado City	1.9	20
North Lake Dallas Power & Light Co.	North Lake	1.2	13
San Angelo West Texas Utilities	Lake Nasworthy	12.0	28
Sim Gideon Lower Colorado River Authority	Lake Bastrop	1.6	10
Striker Creek Texas Power & Light Co.	Striker Creek Reservoir	3.4	6
Sundance/Wabamun Calgary Power Ltd.	Lake Wabamun	23.2	17
Thomas Hill Assoc. Electric Coop.	Thomas Hill Reservoir	9.6	18
Tradinghouse Creek Texas Power & Light Co.	Tradinghouse Creek Reservoir	1.5	7

(1)Criteria for site slection include: (a) freshwater environment; (b) low load ratio, usually <10; (c) semienclosed water bodies; (d) once-through cooling cycle; and (e) quality and quantity of ecological information.

TABLE 2

RESULTS OF WILCOXON'S SIGNED RANK TEST APPLIED TO FISH DATA FROM
LAKE NASWORTHY (HEATED) AND TWIN BUTTES RESERVOIR AND SAN ANGELO RESERVOIR (CONTROLS)

	Gamefish by number per set					Rough fish by number per set				
Year	Lake Nasworthy	Twin Buttes	Rank	San Angelo	Rank	Lake Nasworthy	Twin Buttes	Rank	San Angelo	Rank
1961	5.18	--	--	23.20	-9	21.77	--	--	48.20	-9
1962	2.20	--	--	2.20	1	8.00	--	--	16.20	-2
1963	9.58	--	--	5.30	3	28.37	--	--	18.27	4
1964										
1965	12.33	16.50	-2	--		4.17	23.75	-7	--	--
1966	10.00	12.00	-1	9.00	2	47.25	34.67	4	24.25	6
1967	18.33	7.12	7	3.17	8	51.67	37.12	6	25.33	7
1968	19.33	12.28	3	14.00	4	40.67	26.61	5	25.00	5
1969	25.06	15.17	5	10.78	7	31.72	32.50	-1	34.50	-1
1970	17.33	9.17	4	24.33	-5	51.75	44.50	3	42.33	3
1971	19.78	9.50	6	8.00	6	33.94	37.38	-2	8.33	8
			NS		NS			NS		NS

	Game/rough fish ratios by numbers					Game/Rough Fish Ratios by Weight				
Year	Lake Nasworthy	Twin Buttes	Rank	San Angelo	Rank	Lake Nasworthy	Twin Buttes	Rank	San Angelo	Rank
1961	0.24	--	--	0.48	-6.5	0.18	--	--	0.24	-1
1962	0.28	--	--	0.14	3	0.40	--	--	0.09	7
1963	0.34	--	--	0.29	1	0.21	--	--	0.42	-4
1964										
1965	2.96	0.69	7	--	--	1.82	0.07	7	--	--
1966	0.21	0.35	-3	0.37	-4	0.40	0.20	3	0.30	2
1967	0.35	0.19	4	0.12	5	0.51	0.40	1	0.21	6
1968	0.48	0.46	1	0.56	-2	0.80	0.44	5	0.43	8
1969	0.79	0.47	5	0.31	9	0.50	0.76	-4	0.33	3
1970	0.33	0.20	2	0.57	-6.5	0.44	0.89	-6	0.17	5
1971	0.58	0.25	6	0.96	-8	0.54	0.37	2	1.68	-9
			NS		NS			NS		NS

TABLE 2 (CONTINUED)

Year	Channel catfish "K" factor Lake Nasworthy	Twin Buttes	Rank	San Angelo	Rank	Largemouth bass "K" factor Lake Nasworthy	Twin Buttes	Rank	San Angelo	Rank
1961	--	--	--	1.56	--	2.25	--	c		c
1962	1.04	--	--	1.46	-8	2.90	--	a	2.52	a
1963	1.55	--	--	1.60	-1.5	2.68	--	n	2.90	n
1964								n		n
1965	1.92	2.08	-3	--	--	2.49	2.87	o	--	o
1966	1.81	1.56	5	1.35	1	--	2.30	t	--	t
1967	1.92	1.74	4	2.06	4.5	2.68	2.58		--	
1968	2.12	1.74	7	1.87	7	2.89	2.85	t	3.45	t
1969	1.90	1.62	6	1.82	3	2.68		e	3.09	e
1970	1.93	1.86	1	1.79	4.5	2.65	2.25	s	2.35	s
1971	1.89	2.01	-2	1.94	-1.5	2.91	3.36	t	--	t
			NS		NS					

TABLE 3

RESULTS OF WILCOXON'S SIGNED RANK TEST APPLIED TO FISH DATA FROM
LAKE COLORADO CITY (HEATED) AND CHAMPION CREEK RESERVOIR (CONTROL)

Year	Game fish by number per set			Rough fish by number per set		
	Champion Creek	Lake Colorado City	Rank	Champion Creek	Lake Colorado City	Rank
1960	2.9	4.7	-1	2.4	4.0	-2
1961						-2
1962	1.7	16.3	-9	2.5	8.0	-4
1963	8.5	12.7	-4	1.8	25.7	-9
1964						
1965						
1966	13.2	10.8	3	2.3	12.8	-7
1967	26.5	12.5	8	5.0	23.5	-8
1968	13.2	9.8	6	5.2	13.4	-6
1969	20.4	12.4	5	11.4	17.3	-5
1970	9.2	18.4	-7	23.2	19.1	3
1971	6.3	8.3	-2	14.9	15.6	-1
			NS			*

Year	Channel catfish "K" factor			Largemouth bass "K" factor		
1960	1.82	1.75	1	2.94	2.74	4.5
1961						
1962	--	1.47	--	1.97	2.56	-8
1963	1.71	1.52	4.5	2.02	2.28	-6
1964						
1965						
1966	1.88	1.69	4.5	2.62	2.48	3
1967	2.30	1.65	8	2.13	2.47	-7
1968	2.03	1.77	6	2.47	2.57	-2
1969	1.93	1.85	2	2.17	2.88	-9
1970	2.04	1.68	7	2.34	2.54	-4.5
1971	1.94	1.76	3	2.84	2.76	1
			**			NS

---

* = Significant at 95% level
** = Significant at 99% level

TABLE 3 (CONTINUED)

Year	Catfish by number per set Champion Creek	Lake Colorado City	Rank	Bass by number per set Champion Creek	Lake Colorado City	Rank
1960	0.23	1.58	-4	2.15	6.33	8
1961						
1962	--	4.56	--	0.50	5.00	-9
1963	0.17	4.25	-8	1.33	2.62	-7
1964						
1965						
1966	0.75	2.00	-3	0.25	0.25	1.5
1967	1.67	1.50	1	1.33	1.33	1.5
1968	1.11	2.61	-5	0.67	0.44	5
1969	1.65	3.65	-6	0.59	0.47	4
1970	2.00	4.25	-7	0.50	0.55	-3
1971	1.19	2.20	-2	0.06	0.56	-6
			**			NS

Year	Game/rough fish by number Champion Creek	Lake Colorado City	Rank
1960	0.6	0.8	-1
1961			
1962	1.3	0.6	3
1963	2.3	0.4	8
1964			
1965			
1966	5.2	0.6	9
1967	2.1	0.4	7
1968	1.4	0.6	4.5
1969	1.4	0.6	4.5
1970	1.0	0.5	2
1971	1.2	0.3	6
			**
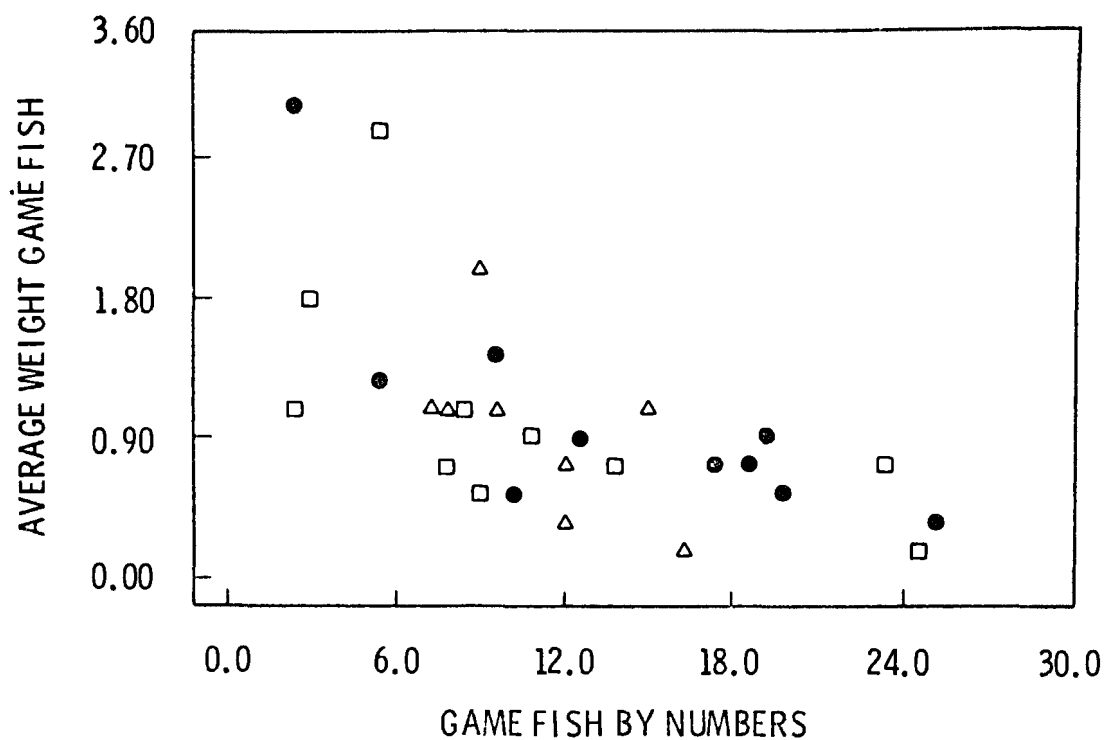
Figure 1. Average Weight of Game Fish Plotted Against Game Fish by Total Numbers for Lake Nasworthy (0), Twin Buttes Reservoir (Δ) and San Angelo Reservoir (□).
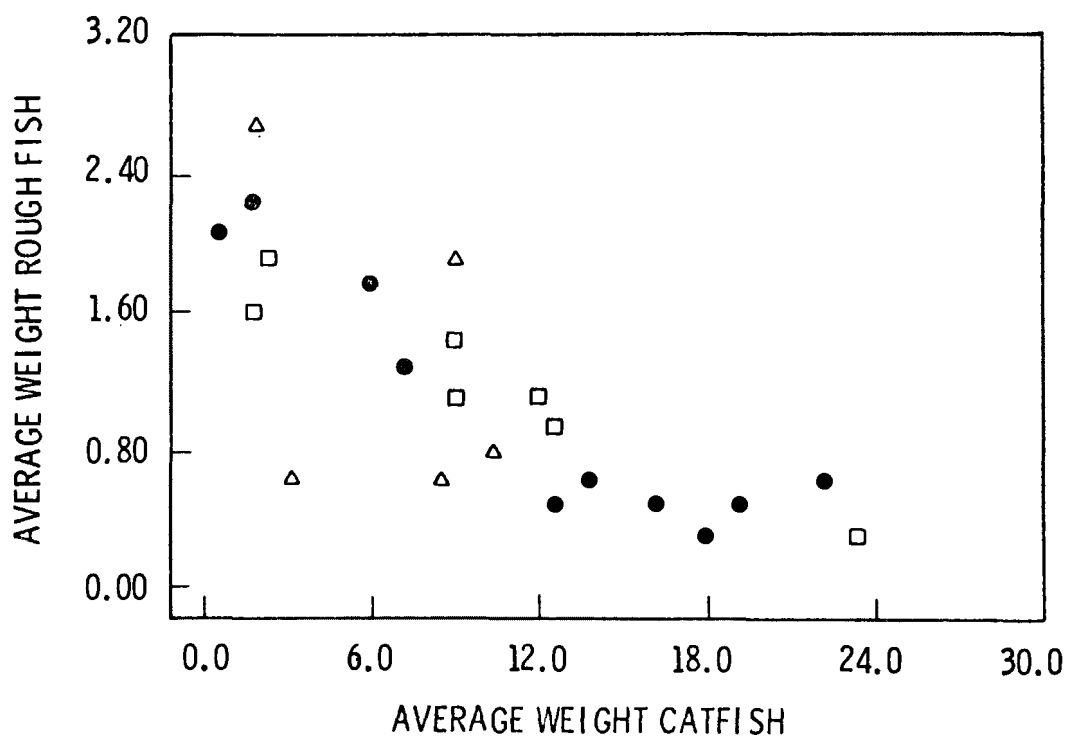
Figure 2. Average Weight of Rough Fish Plotted Against Average Weight Catfish for Lake Nasworthy (0), Twin Buttes Reservoir (Δ) and San Angelo Reservoir (□)

A SIMPLE METHOD OF PREDICTING PLUME
BEHAVIOR FROM MULTIPLE SOURCES

L.D. Winiarski, W.E. Frick*, and A. Carter
Corvallis Environmental Research Laboratory
U.S. Environmental Protection Agency
Corvallis, Oregon 97330 U.S.A.

ABSTRACT

A method for predicting the behavior of plumes from multiple sources with
the aid of a computer program or nomograph is illustrated and compared with
field data. Sources close together are treated as an equivalent single
source which is designed to have the same efflux of mass, momentum and
energy. The perimeter of the equivalent single source is taken to be the
same as the total perimeter of the multiple sources. The apparent area of
the actual sources as projected normal to the wind is used with the equiva-
lent source to determine the wind-induced entrainment.

INTRODUCTION

Complex plume behavior can be predicted with simple, logical numerical
procedures. The key to accurate yet inexpensive computation lies in the
ability to model the mass entrainment and horizontal momentum transfer
between the wind and the plume. The simple assumption that all the wind
impinging on the plume (i.e. passing through the wind projected area) is
entrained and adds its momentum to the plume has proved to be a useful
concept for single source plume predictions (1,2). It is logical to assume
that a similiar concept could be extended to deal with multiple source
plumes.

ASPECT FACTOR

The results that follow are based on two hypotheses: (1) the main difference
between the multiple plumes and a hypothetical single "equivalent plume" with
the same mass, momentum and energy flux is that the projected area and
peripheral area of the single, equivalent plume differs from that of the
multiple tower arrangement, and (2) after the plumes merge they can be approxi-
mated by an axi-symmetric equivalent plume.

A single plume model can be used to approximate multiple plume behavior by
introducing an Aspect Factor (AF) to account for the differences in pro-
jected area computation before the plumes have merged.

$$AF = \frac{\text{actual projected cylindrical area of multiple plumes}}{\text{projected area of equivalent single plume}}$$

---

* Now affiliated with the Oregon Department of Transportation, Salem.

Aspect Factor is used as a coefficient multiplying the projected area of the cylindrical part of the equivalent plume. This allows the computation of the projected area to approximate that of the actual multiple source arrangement. Although AF changes along the trajectory, consideration of the initial geometry and wind direction often indicates how this variation can be approximated. Once the relationship between AF and equivalent radius is determined, it can be input as a table to the single plume model. The following example will illustrate this.

EXAMPLE

The model predictions will be compared with data from three Neurath natural draft cooling towers (3, 4). Each tower radius is 22.4 m. The centers of the towers form an equilateral triangle 114 m on a side (Figure 1a). An equivalent source, radius 38.8 m, is also shown with its center at the centroid of the three towers. The calculation shows AF = 1.73 initially. Aspect Factor is constant until the upwind plume begins to "shadow" the downwind plumes. This occurs when the individual plume radius is about 28.5 m. At that point the equivalent plume radius is 49.35 m (Figure 1b). Once shadowing occurs, the value of AF changes. The next reference point occurs when the plumes begin to merge. From the geometry of Figure 1c this would occur when the individual plume radius is about 57 m (equivalent radius 98.7 m). Aspect Factor is calculated to be 1.15 at this point. A linear variation of AF with equivalent radius is assumed between points b and c. The last significant point (AF = 1.0) is where the plumes have merged into a single, approximately round plume. The precise point is difficult to define. In this case a simple approximation would be to consider an extrapolation until AF = 1.0, which occurs at an equivalent radius of about 111.6 m.

A more general prescription for estimating this last point where AF = 1.0 is to calculate the radius where the equivalent plume would just encompass the plume of the tower furthest from the centroid. However, in this case there is no practical advantage in using this procedure rather than the simple extrapolation shown, because AF would be so close to 1.0 in this region.

RESULTS

The model predictions are compared with data in Figures 2 through 8. An improvement has been made in the numerical procedure for calculating the psychrometric variables otherwise the model is the same as the one discussed in Reference 2. Except for high humidity cases, the new procedure yields practically the same results as presented previously (2). When the humidity is high, the point of saturation (visibility limit) is extremely sensitive to the calculation procedure. This can have a noticeable effect on visible plume length.

NOMOGRAPHS

In order to make estimates of plume behavior as well as see the overall effect of plume variables we have prepared a series of nomographs (6) like that shown in Figure 9. In addition to the aspect factor, the key parameters are

$$\text{velocity ratio, } K = \frac{V_o}{\text{wind speed}}$$

$$\text{Froude number, } Fr = \frac{V_o}{\sqrt{\frac{\rho_a - \rho}{\rho} Dg}}$$

$$\text{Neutrality number, } N = \frac{V_o}{\sqrt{\frac{\Delta\theta}{\Delta Z} g \frac{D^2}{T}}}$$

where V_o is the initial velocity, ρ_a and ρ are the ambient and plume densities respectively, D is the source diameter, g is the acceleration due to gravity, $\Delta\theta/\Delta Z$ is the potential temperature gradient, and T is the ambient temperature. The neutrality parameter is a new dimensionless parameter we have introduced to account for non-adiabatic conditions.

Large values of N (e.g., $\frac{\Delta\theta}{\Delta Z} \approx 0$) mean nearly adiabatic (neutral) conditions. Generally, nondimensional trajectories are found to be the same if N, Fr and K are the same. This is subject to the condition that density-temperature relationships of the fluids involved behave similiarly within the pertinent temperature ranges. The advantage of achieving approximate similarity is considerable, but one must be aware of potential problem areas (6).

To illustrate, the parameters of the Neurath run N49 (Figure 5) were Fr = .5, V_o = 3.5 m/s, N = 3.2. The nomograph (Figure 9) parameters approximate these. Because of similarity it can be compared to run N49 even though it is generated from a different set of conditions. A plume trajectory for K = .5 (based on an average value of the extrapolated wind speed) gives a rise of about 3 equivalent diameters (230 m) at a distance of 15 diameters (1160 m) which corresponds approximately with Figure 5.

The nomographs show the general trend of the important variables. For a given ambient temperature gradient and set of tower exit conditions, each K curve represents a centerline plume trajectory at a given ambient wind speed. Relatively speaking, K = 10 is a low wind condition, K = .5 is high. In this example, the atmospheric temperature gradient is strongly stable (i.e. N is small) so the plume reaches an equilibrium height in a relatively short distance even in a low wind situation.

SUMMARY

Three significant points of this study are:

(1) The aspect factor concept appears to be a simple, yet effective method of taking into account multiple source geometry with a single source plume model.

(2) A similarity parameter (N), akin to the Froude number, can be used to account for non-adiabatic atmospheres.

(3) Used judiciously, nomographs can be very helpful in obtaining approximate answers to atmospheric plume problems.

REFERENCES

1. Winiarski, L.D. and Frick, W.E. Cooling Tower Plume Model, USEPA Ecological Research Series, EPA-600/3-76-100, September 1976.

2. Winiarski, L.D. and Frick, W.E. "Methods of Improving Plume Models," Cooling Tower Environment--1978 Proceedings Water Resources Research Center, University of Maryland, May 1978.

3. Vereins Deutscher Ingenieure. "Untersuchungen an einem Naturzug - Nasskühlturm." Fortschritt-Berichte der VDI Zeitschriften. Reihe 15. Nr. 5. Juli 1974.

4. Policastro, A.J., Carhart, R.A. and Devantier, B. Validation of Selected Mathematical Models for Plume Dispersion from Natural-Draft Cooling Towers. Presented at the Waste Heat Management and Utilization Conference, Miami Beach, 9-11 May 1977.

5. Winiarski, L.D. and Frick, W.E. Atmospheric Plume Nomographs with Computer Model for Cooling Tower Plumes, USEPA Interagency Energy-Environment Research and Development Series, manuscript.

6. Frick, W.E. and Winiarski, L.D. Why Froude Number Replication Does not Necessarily Ensure Modeling Similarity. Second Waste Heat Management and Utilization Conference, Miami Beach, 4-6 December 1978.

a) Initial separate plumes

equivalent plume

WIND

22.4m (initial radius)

38.8m

114m

$$A.F. = \frac{3 \times 2 \times 22.4}{2 \times 32.8} = 1.73$$

b) Shadowing starts

WIND

28.5m

49.35

$$A.F. = \frac{3 \times 2 \times 28.5}{2 \times 49.35} = 1.73$$

c) Merging begins

98.7m

57.0m

$$A.F. = \frac{2 \times 2 \times 57}{2 \times 98.7} = 1.15$$

(a)   (b)
38.8 49.35

(c)
98.7 111.6

ASPECT FACTOR

2.0

1.5

1.0

.5

0

0   20   40   60   80   100   120

Separate   Shadow   Merge   Single

Equivalent radius(m)
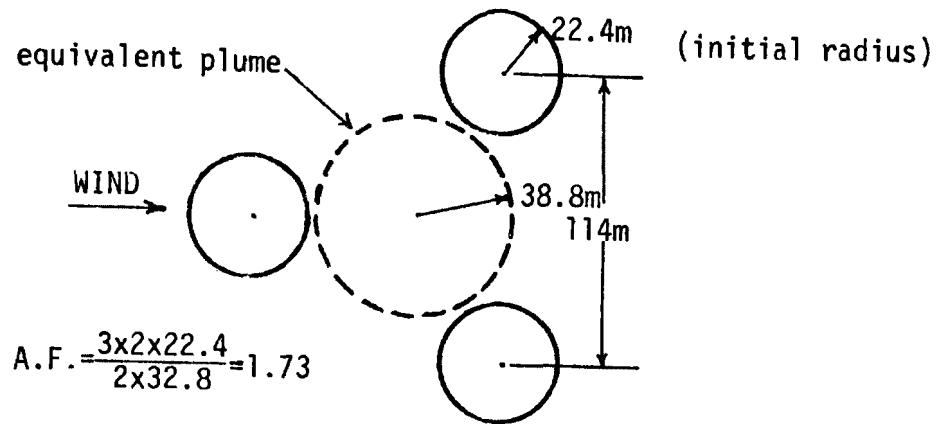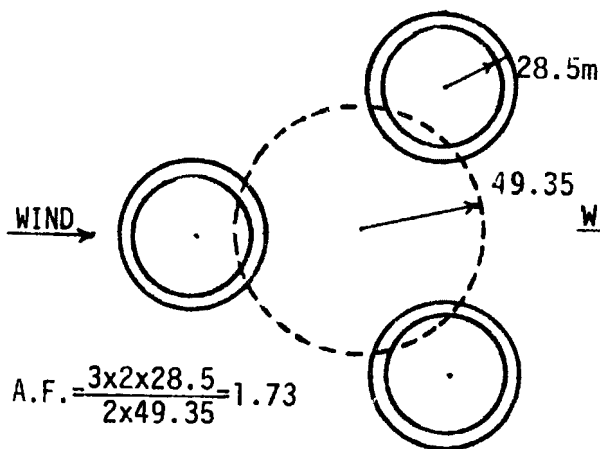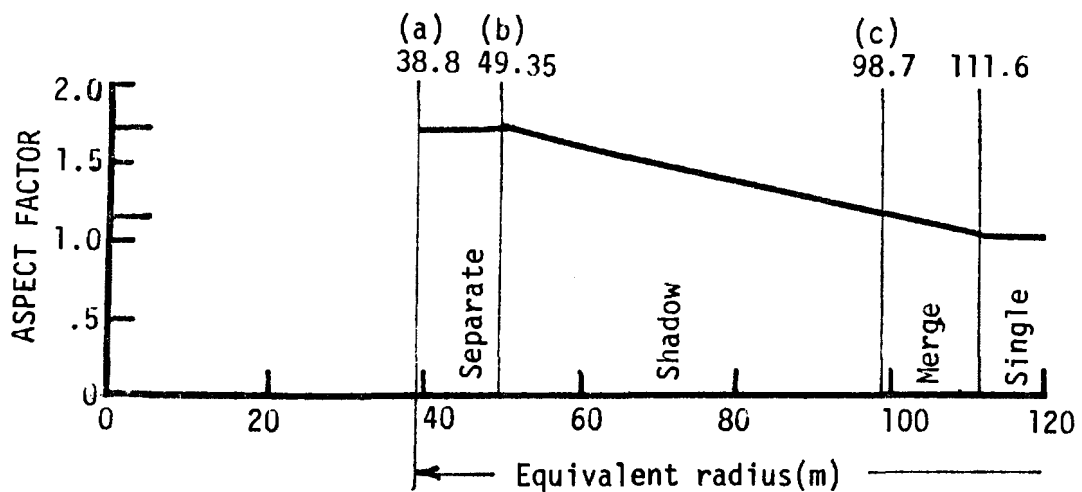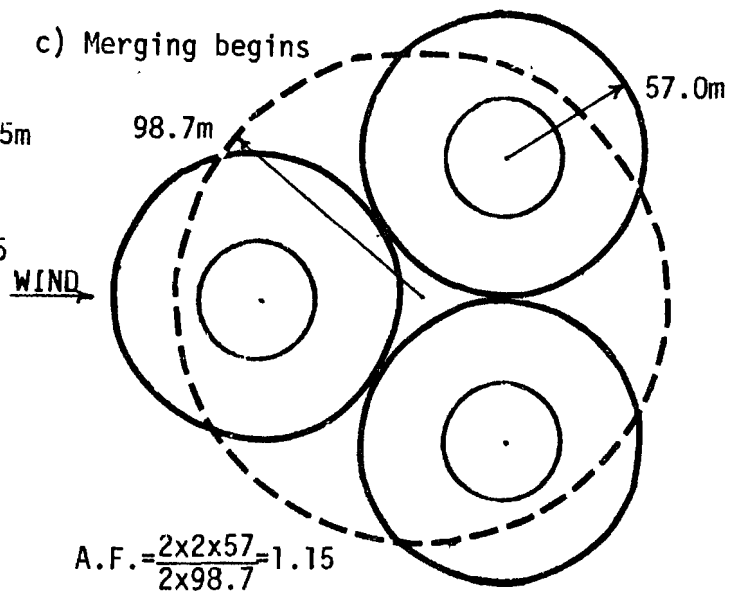
Figure 1. Approx. change in Aspect Factor as Neurath plumes grow.

371

LEGEND
——————— Trace of actual plume outline
▲——▲——▲ Predicted visible plume
· · · · · Predicted invisible plume
— — — Predicted centerline
—✗— Ambient humidity (0-1.0)
—■— Ambient temperature
—▲— Wind speed
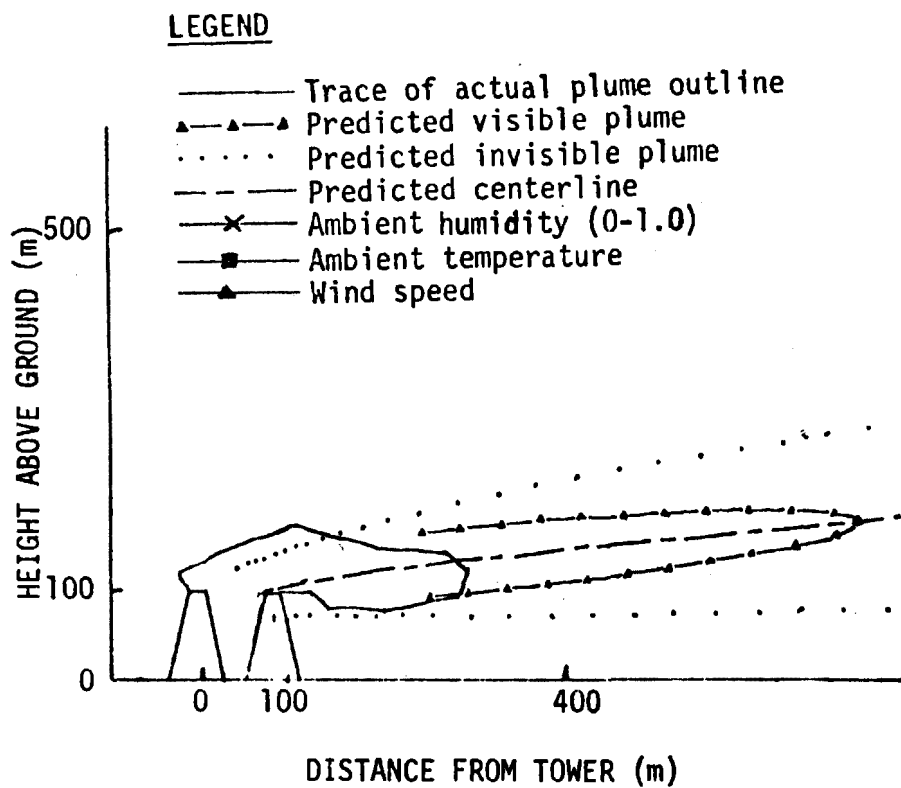
Figure 2. Neurath run N15.
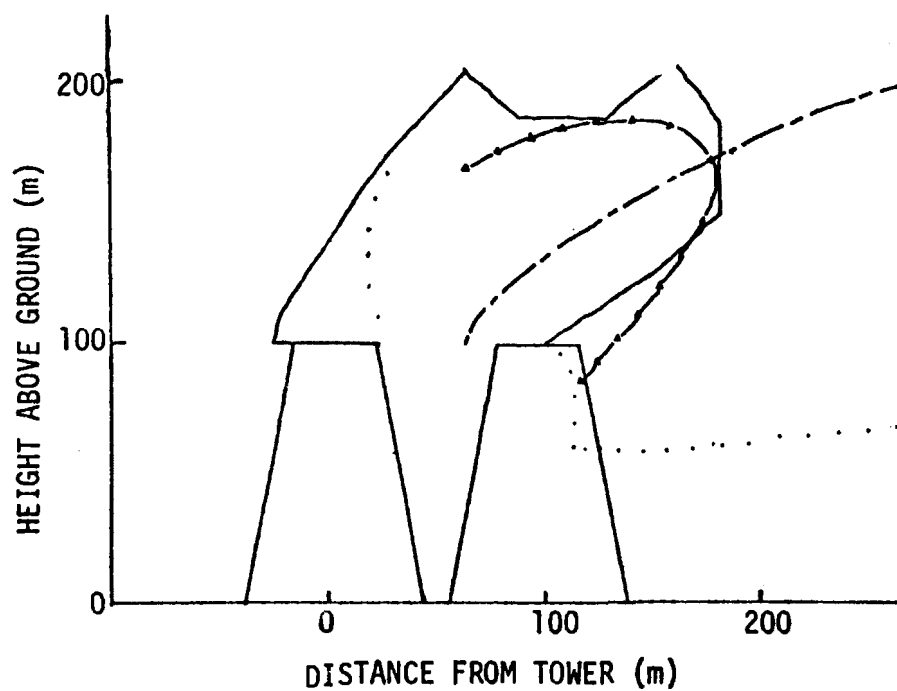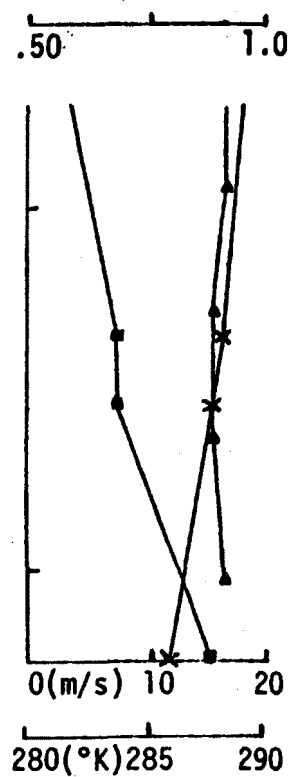
Figure 3. Neurath run N34.
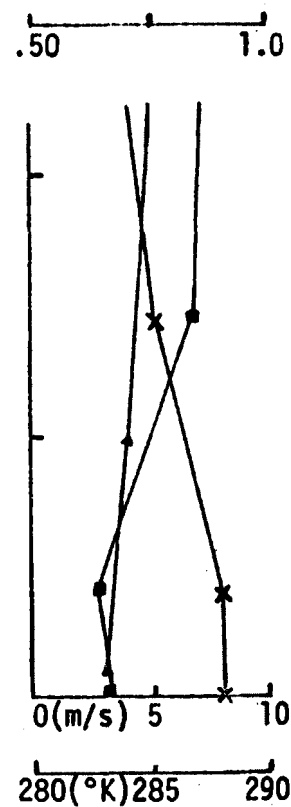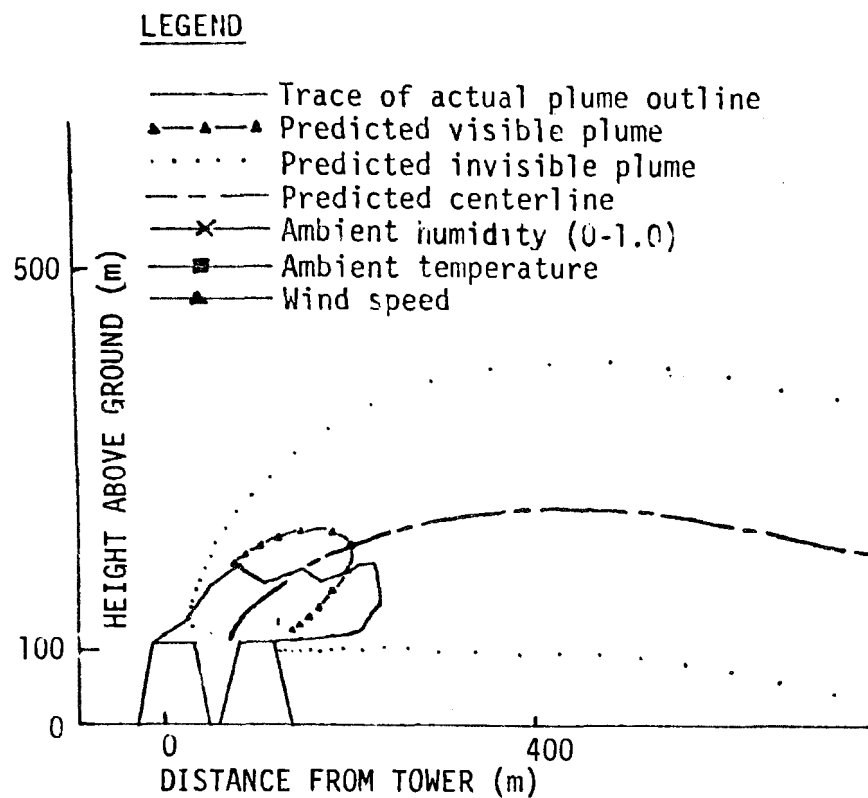
Figure 4.   Neurath run N37.

Figure 5.   Neurath run   N49.

373

LEGEND

——————— Trace of actual plume outline
▲—▲—▲ Predicted visible plume
· · · · · Predicted invisible plume
— — — Predicted centerline
—✕— Ambient humidity (0-1.C)
—▣— Ambient temperature
—▲— Wind speed
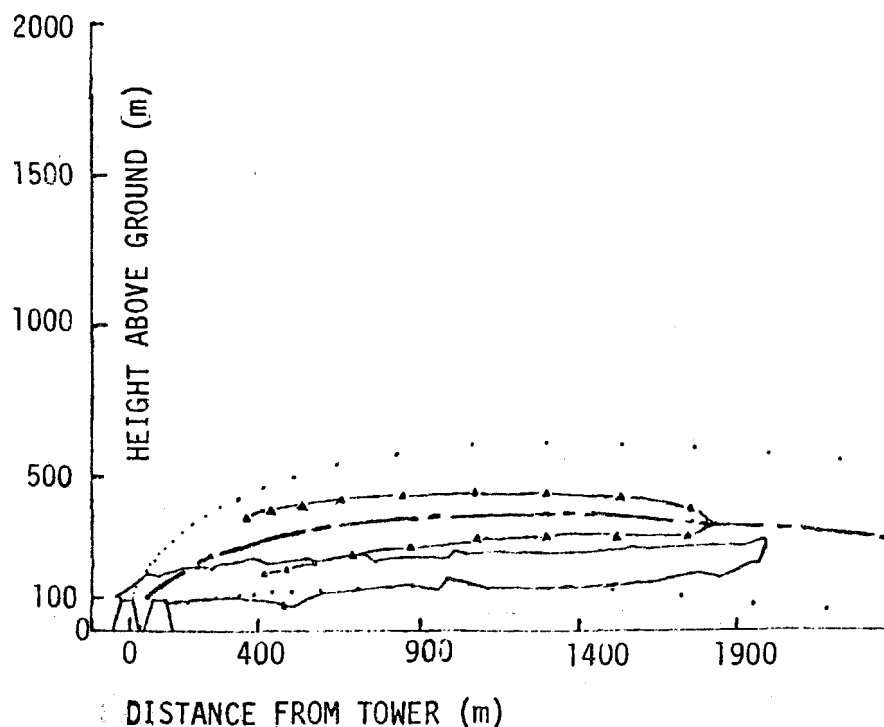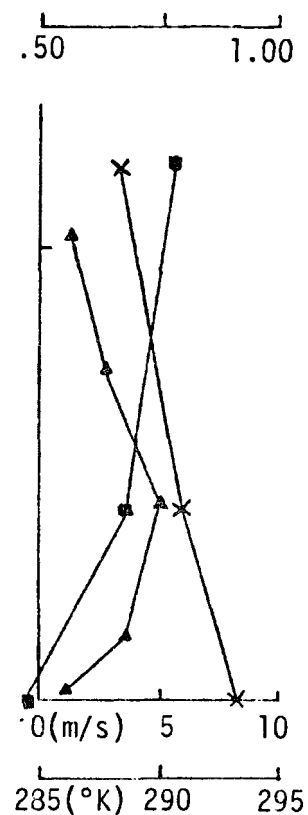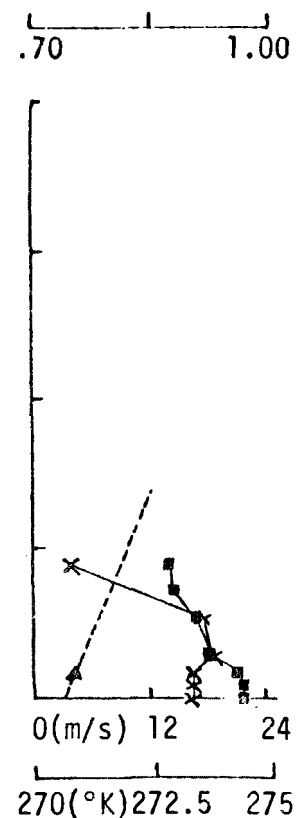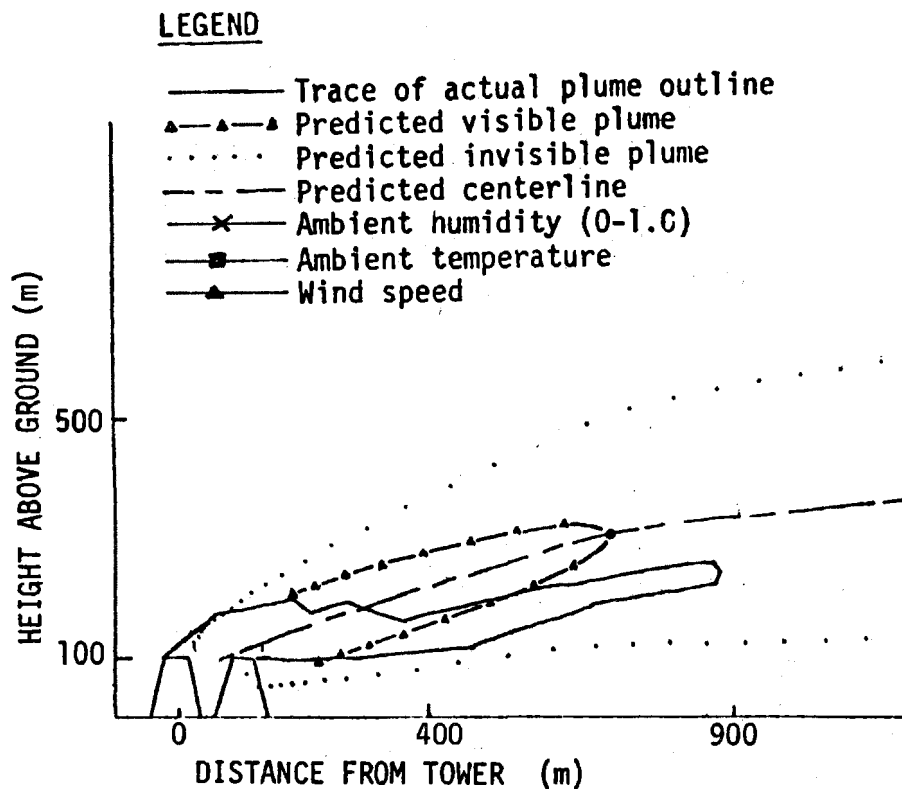
Figure 6. Neurath run N51.
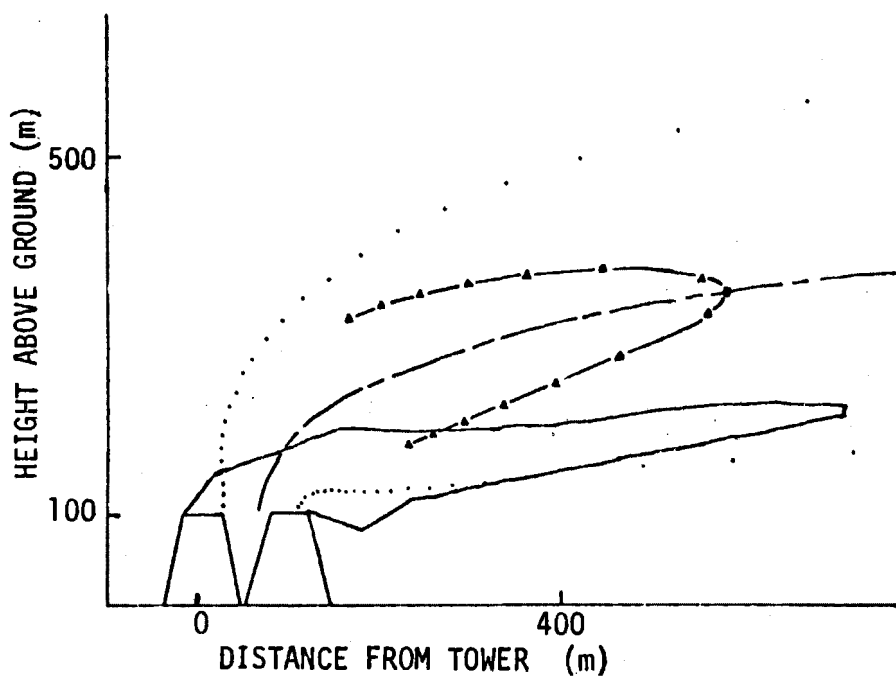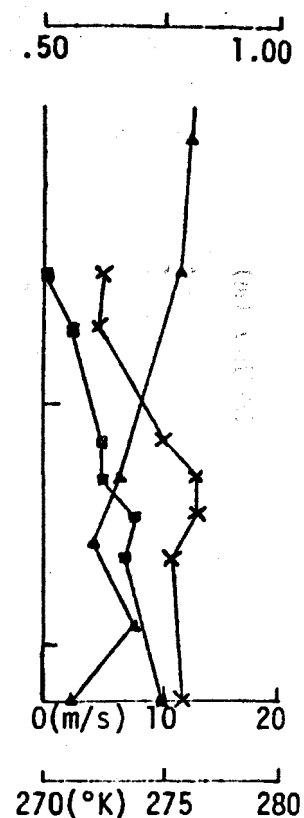
Figure 7. Neurath run N54.

374
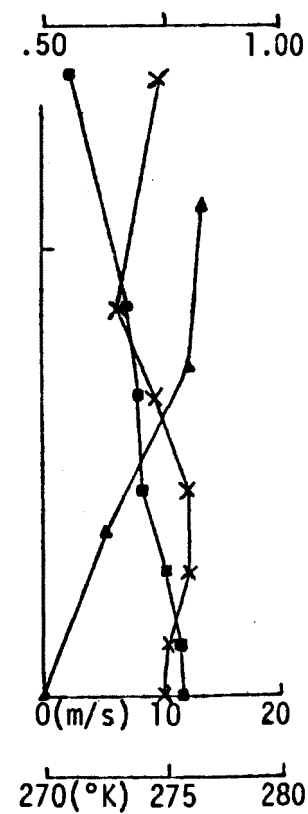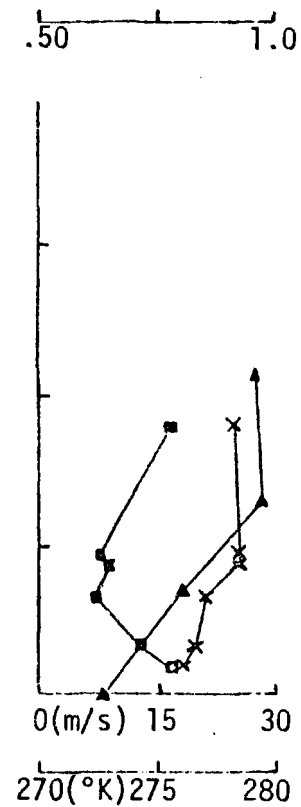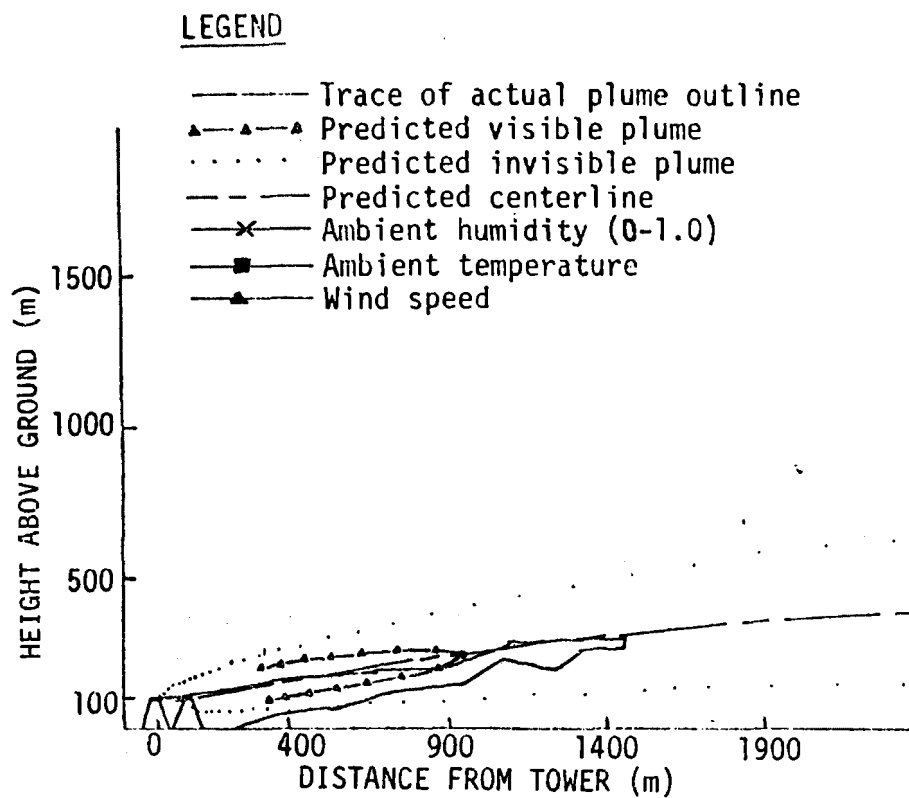
Figure 8. Neurath run N67.
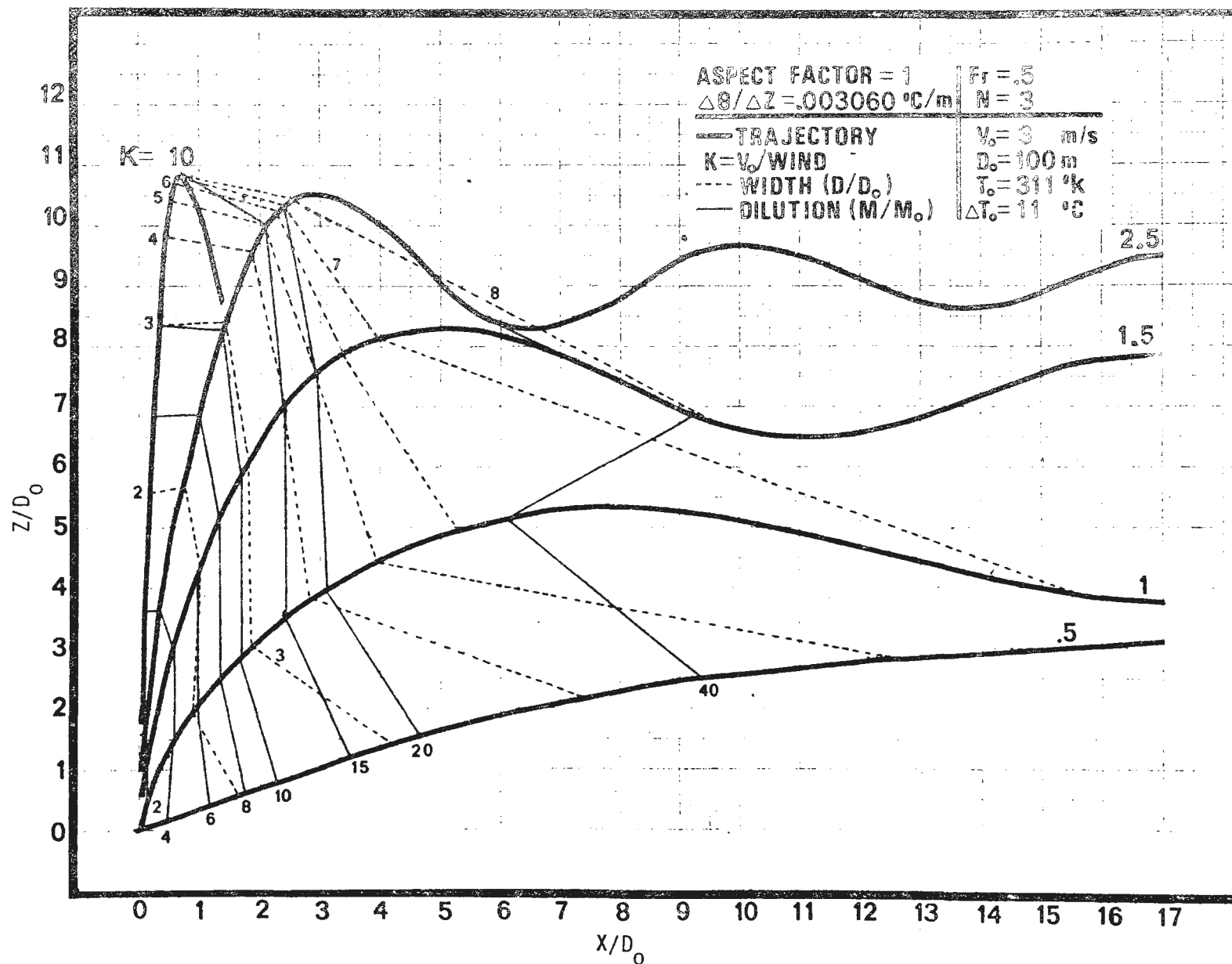
Figure 9. Nomographs for atmospheric plumes.

MODELLING NEAR-FIELD BEHAVIOUR
OF PLUMES FROM MECHANICAL DRAFT
COOLING TOWERS

T.L. Crawford[*] and P.R. Slawson
Mechanical Engineering Dept.
University of Waterloo
Waterloo, Ontario, Canada

ABSTRACT

For the purpose of analysing plume behavior from cooling towers it is convenient to distinguish two principal regions: the near-field and the far-field. In the former the plume is strongly influenced by the source geometry, effluent release height, local terrain and the presence of nearby structures of towers making mathematical description extremely complex. By comparison, in the far-field the plume behavior is relatively insensitive to details of its origin and mathematical formulation is much better understood and developed. The near-field behavior of plumes from mechanical draft cooling towers is particularly complex and often dramatically affected by the proximity of adjacent towers. This results in frequent downwash of the tower effluent which then leads to re-ingestion of a significant fraction of its own effluent (recirculation) or of the effluent of an upwind tower (interference) thus affecting tower performance.

Single camera photographic observation of the near-field behavior of plumes from the twin mechanical draft cooling towers at plant Gaston were made. A three-dimensional numerical model of the near-field plume behavior has been developed. A general overview of the model and a comparison of model prediction on the near-field plume behavior with an observed time-mean plume are given.

INTRODUCTION

Physically realistic vapor and drift plume models are required in the environmental assessment of heat dissipation technologies such as mechanical and natural draft cooling towers, spray ponds, and spray canals. In modeling vapor and drift plume behavior for these evaporative cooling devices it is convenient to distinguish two principle regions, the near-field and the far-field. The near-field plume (within about five characteristic lengths downwind) is complex in behavior because of the strong influence of source geometry, effluent release height, wind shear, local terrain, and nearby structures on the flow field. These influences disturb the near-field flow to a turbulent state that is poorly understood. As a result of the near-field complexities, development of a realistic mathematical modeling technology has been slow. In contrast, the far-field

---

plume (beyond about 10 characteristic lengths downwind) is relatively well-behaved and relatively insensitive to details of its origin. The mathematical formulation of far-field plume behavior is much better understood and developed. In the intermediate region, the complex near-field plume evolves to the simpler, self-similar far-field plume. The boundary conditions for far-field plume models depend on the integral effect of the near-field detail.

The importance of the near-field region to far-field plume behavior varies greatly and depends on the extent of the near-field disturbances. Recent full-scale studies of various cooling tower complexes have illustrated the importance of the near-field disturbances on far-field plume behavior. Slawson et al. (1975 and 1978) showed that, for a rather simple natural draft cooling tower geometry, up to a 50-percent depression in far-field plume trajectories resulted from near-field tower downwash. A recent study of twin 9-cell mechanical draft tower plumes illustrated a dynamically more complex near-field plume behavior with subsequent severe effects on far-field plume behavior. A mathematical model of near-field plume behavior would be useful for specifying boundary conditions for far-field plume models and for assessing the effects of recirculation and interference on tower performance.

Modelling Considerations

To study the highly complex behavior of such near-field flows, a computer model capable of solving the time-dependent, three-dimensional equations governing fluid motions greatly distorted by structures and none-passive plumes was developed (Crawford 1977). The validity of the model was established by comparison with a variety of physical modeling studies. Presented herein is a comparison of initial model calculations with one experiment from the full-scale study of twin 9-cell mechanical draft cooling towers. A brief overview of the modeling methodology is presented here and further details may be found in Crawford (1977).

The computer model solves the full nonlinear equations that specify the mean transport and diffusion of fully turbulent, three-dimensional incompressible flows. These equations are, the mass conservation equation,

$$\frac{\partial U_i}{\partial X_j} = 0$$

the energy or diffusion equation

$$\frac{\partial \theta}{\partial t} + \frac{\partial (\theta U_j)}{\partial X_j} = \frac{\partial}{\partial X_j}\left[K_h \frac{\partial \theta}{\partial X_j} \right] + \frac{S}{\rho C_p}$$

378

and the 3 component momentum equations

$$\frac{\partial U_i}{\partial t} + \frac{\partial (U_i U_j)}{\partial X_j} = - \frac{1}{\rho} \frac{\partial P}{\partial X_i} + \frac{\theta}{T} g \delta_{3i} + \frac{\partial}{\partial X_j} (K_m \frac{\partial U_i}{\partial X_j})$$

where the Einstein subscript notation is used. In these equations, the density ρ, hydrostatic pressure P, potential temperature θ, temperature T, and velocity components U_i may be functions of the position coordinates X_i and of time t. The parameters K_m and K_h are the eddy exchange coefficients for heat and momentum which were specified as a function of the vertical coordinate X_3. (K varied linearly with height from similarity theory.)

In order to solve the above governing equations for a particular flow, it is necessary to incorporate the pertinent initial and boundary conditions which make the problem determinate. The correct specification of these can become a significant part of the overall solution problem.

The numerical solution of the governing equations is accomplished by applying finite difference approximations to them. The solution method is fully implicit, employing velocity components and pressure as the main dependent variables. These variables are computed for one of four staggered, interlacing grid systems which fill the domain of interest. A hybrid central-upwind difference scheme is employed to improve accuracy and aid convergence. The solution of the flow dynamics proceeds in a successive guess-and-correct fashion. In the first part of each cycle, intermediate velocities are calculated from the momentum equations using the pressure distribution from the previous cycle, where a uniform pressure distribution is assumed initially. The second step adjusts these velocities and pressures such that mass conservation is satisfied. Following this balance of mass, other variables of interest are subject to their respective conservation equations.

Although it is possible to include the balance equations for liquid water and water vapor in the above set of equations, in order to predict the extent of the vapor plume. They were not included in the present model for the sake of simplicity. Since the near-field upwind, cavity and wake regions are strongly elliptic in nature, further simplifications of the equations and the subsequent solution procedure was avoided.

The computer program load module, including plotting routines and array storage for the 30 x 13 x 16 grid used, requires 386 K bytes of storage. Storage of the grid required about 292 K of this 386 K. The execution time for simultaneous solution of the flow field and the energy equation about the two towers and plotting of all results was 416 seconds on an IBM 270/165. The solution time for this simulation is increased due to the strong coupling of equations by the buoyancy force term.

Gaston Mechanical Draft Cooling Tower Study

A number of full-scale experiments investigating near- and far-field condensed plume behavior from twin mechanical draft cooling towers were conducted by Slawson and Crawford (1976). Some details of the experimental work was given by (Champion et al, 1977). Only near-field observations are pertinent to the present work. Subsequent experimental details may be found in a limited circulation report soon to be published.

The twin 9-cell cross-flow towers studied, serve an 800-mw unit of the Gaston generating station in Wilsonville, Alabama. Each tower has an overall length of 100 m, width of 22m, and height of 17m. The towers are orientated one behind the other with parallel axes spaced about 100 m apart. Each of the nine cells within a tower has a 200-hp motor driving a 9 m diameter fan to give a plume exit velocity of about 8 m/s.

The objectives of the field experiment were to (1) quantitatively document visible plume behavior, (2) measure appropriate meteorological variables, and (3) measure tower fluxes of heat and mass. The visible or condensed plume behavior was quantitatively documented by a single camera photographic technique following that given by Halitsky (1961). The meteorological data consisted of: temperature profiles (dew point and dry bulb) from an instrumented aircraft, wind speed and direction profiles from dual-theodolite tracking of 30-gm pilot balloons and wind and temperature data from instrumented on-site micrometeorological towers. Although a variety of source measurements were taken, only exit velocity and temperature measurements are used herein. Exit temperature was obtained from thermistor traverses of cell exits. Normal to the line of towers the terrain is relatively flat with variations of about 10 meters.

Figure 1 illustrates the observed wind speed and temperature profiles for the morning of January 15, 1976. The wind direction was normal to the towers and the observed profile was characterized by a U_* of 1.07 m/s and Z_0 of 1.47 m. At 0845 hours the meteorological tower ΔT indicated a transition from slightly stable to slightly unstable stratification. The dash-line plotted in the symmetry plane of figure 2 illustrates the observed time-mean near-field condensed plume boundary.

Initial and Boundary Conditions

The inflow velocity profile (log-law) was defined in the usual manner for a neutral atmospheric boundary layer characterized by $U_* = 1.07$ (m/s) and a roughness length of $Z_0 = 1.47$ m. Table 1 summarizes the initial and boundary conditions for flow about the twin towers. Simulations were run with a 30 x 13 x 16 grid which was refined about the towers. The towers were located about the Y_+ grid boundary which was defined as a symmetry plane. Use of a symmetry plane in this manner significantly reduces the grid storage requirement. The grid extended upwind of the first tower X/L = 5, downwind of the second tower X/L = 6.6, above Z/H = 5.25 and to the side Y/L = 3.6, where L is the tower half-length and H is its height.

380

The primary difficulty of this problem is its three-dimensional nature and the difficulty in applying boundary conditions. Boundary conditions about the towers were incorporated by significant software modifications in the main solution control subroutine. See Crawford (1977) for further detail.

Figures 3 and 4 illustrate the significance of observed and simulated tower downwash and flow disturbance. The coarse nature of the grid used is also illustrated by the "+" marks of figure 4. Four horizontal and three vertical grid lines intersect each tower. Little refinement in the grid is possible with present generation computers since three-dimensional grid refinement is proportional to the cube root of grid points added. Thus at present is is difficult to significantly extend the physical scale of the computer simulation in order to model more of the near field plume. One possible method of extending the modelling domain would be to hybridize a three-dimensional numerical model and the one-dimensional integral plume theory. This could be done by solving the one-dimensional simulated flow-field as a boundary condition.

Comparison of Numerical Simulation With Observations

Figure 3 compares the near-field observed plume boundary and simulated temperature distribution about the twin towers. This comparison is primarily qualitative since temperature contours cannot be rigorously compared to plume condensation boundaries with the present program. Correct computation of the condensation boundary would require adding conservation equations for vapor and liquid water as indicated earlier. The condensed boundary is usually defined where the liquid water content reaches some small value or zero. A simplified method for estimating this boundary from the computer simulated plume temperature field is as follows.

Figure 2 illustrates the saturation curve at a given pressure for air over a range of air temperatures. The point T represents the condition of air, assumed to be saturated, leaving the cooling tower, while point A is the ambient condition of the final condition of the plume after infinite dilution. The line T-A is the assumed intermediate plume conditions at varying levels of dilution. At plume temperatures between T and C the plume is supersaturated or condensed, and between C and A "dry". The visible boundary is assumed to occur at C corresponding to 2° C which agrees qualitatively well with the 2° C isotherm of figure 3 predicted by the computer model.

BIBLIOGRAPHY

Champion, E.R., C.H. Goodman, and P.R. Slawson, "Field Study of Mechanical Draft Cooling Tower Plume Behavior", Waste Heat Management and Utilization Conf., (1977).

Crawford, T.L., "Numerical Modeling of Complex Two- and Three-Dimensional Flow and Diffusion Problems in the Natural Air Environment, Ph.D. thesis, Mechanical Engineering Department, University of Waterloo, (1977).

Halitsky, J., "Single Camera Measurement of Smoke Plumes", Int. Journal of Air and Water Pollution. V. 4, No. 3/4, pp 185-198 (1961).

Slawson, P.R. and J.H. Coleman, "Natural-Draft Cooling-Tower Plume Behavior at Paradise Steam Plant", Waste Heat Management and Utilization Conf., (1977).

Slawson, P.R., J.H. Coleman, and J.P. Blackwell, "Natural Draft Cooling Tower Plume Behavior at Paradise Steam Plant", (Part I), E-AQ-76-1. Tennessee Valley Authority, Chattanooga, Tennessee, August (1975).

Slawson, P.R., J.H. Coleman, and J.W. Frey, "Natural Draft Cooling Tower Plume Behavior at Paradise Steam Plant", (Part II), Tennessee Valley Authority, Chattanooga, Tennessee, (1978).

Slawson, P.R., T.L. Crawford, C.H. Goodman, E.R. Champion, Jr., "Plume Behavior From Mechanical Draft Cooling Towers at Plant E.C. Gaston", Part I," to be published.

TABLE I

SUMMARY OF BOUNDARY CONDITIONS
FOR FLOW ABOUT TWIN MECHANICAL DRAFT COOLING TOWERS

Boundary Type	Dependent Variable			
	U	V	W	T^a
Inflow[b] (X_-)	$U_* \kappa \ \ln(Z/Z_o)$	0	0	0
Outflow (X_+)	$\dfrac{dU}{dX} = 0$	$\dfrac{dV}{dX} = 0$	$\dfrac{dW}{dX} = 0$	$\dfrac{dT}{dX} = 0$
Freestream (Y_-)	U_∞	$\dfrac{dV}{dY} = 0$	$\dfrac{dW}{dY} = 0$	0
Symmetry (Y_+)	$\dfrac{dU}{dY} = 0$	0	$\dfrac{dW}{dY} = 0$	$\dfrac{dT}{dY} = 0$
Ground (Z_-)	0^c	0^c	0	$\dfrac{dT}{dZ} = 0$
Freestream (Z_+)	U_∞	V_∞	W_∞	$\dfrac{dT}{dZ} = 0$
Tower Faces	d	0	d	d

Notes:

a. The towers were a significant source of thermal energy.

b. The inflow boundary condition is also the initial condition for the
30 x 13 x 16 grid. The velocity profile was logarithmic and character-
ized by $U_* = 1.07$ m/s and $Z_o = 1.47$ m.

c. The boundary condition for U and V at the ground was set with a wall
function having a roughness coefficient equivalent to Z_o.

d. Tower inlet and exit conditions were set to match observed momentum
and energy fluxes.

383

Figure 1 OBSERVED TEMPERATURE AND WIND SPEED PROFILES ON JANUARY 15, 1976, AT WILSONVILLE, ALABAMA

384
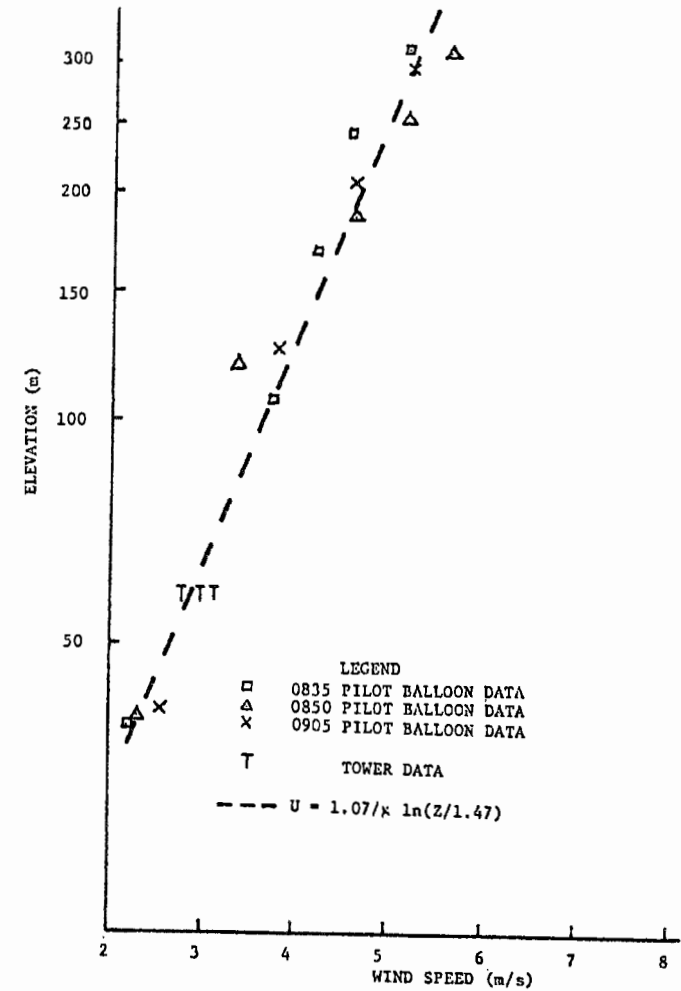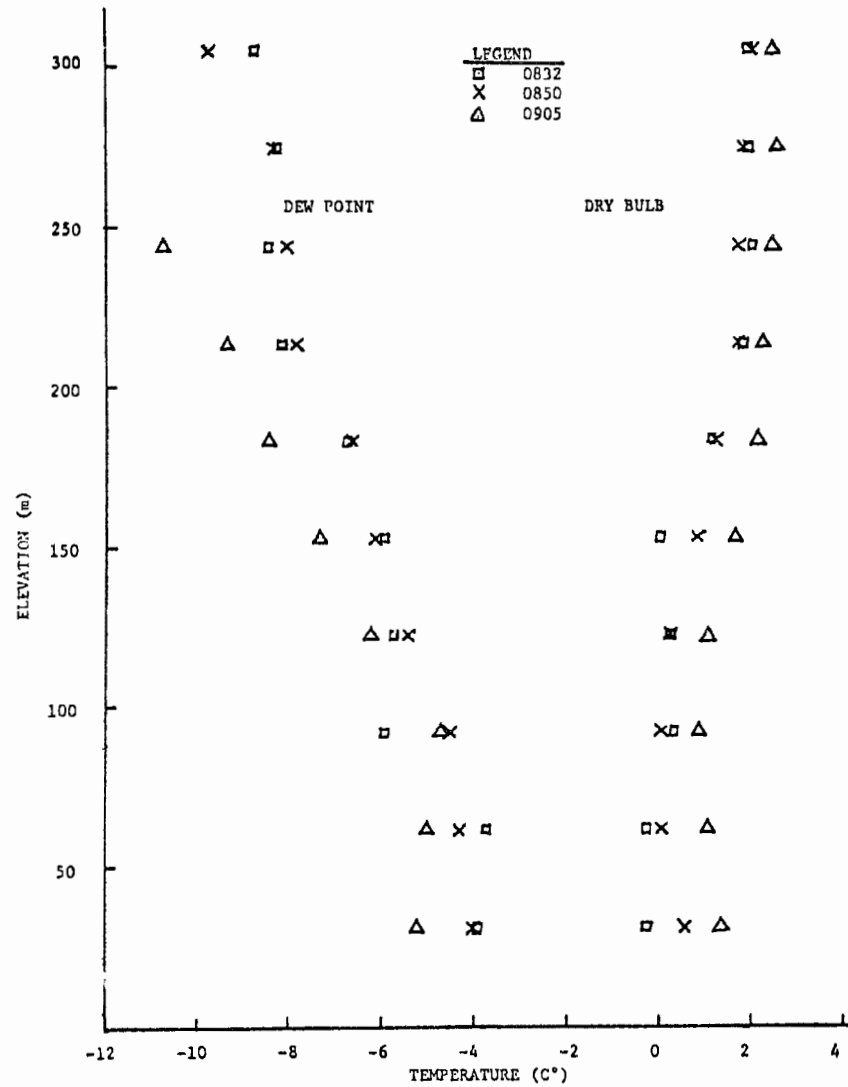
Figure 2   ESTIMATION OF CONDENSED PLUME BOUNDARY

385
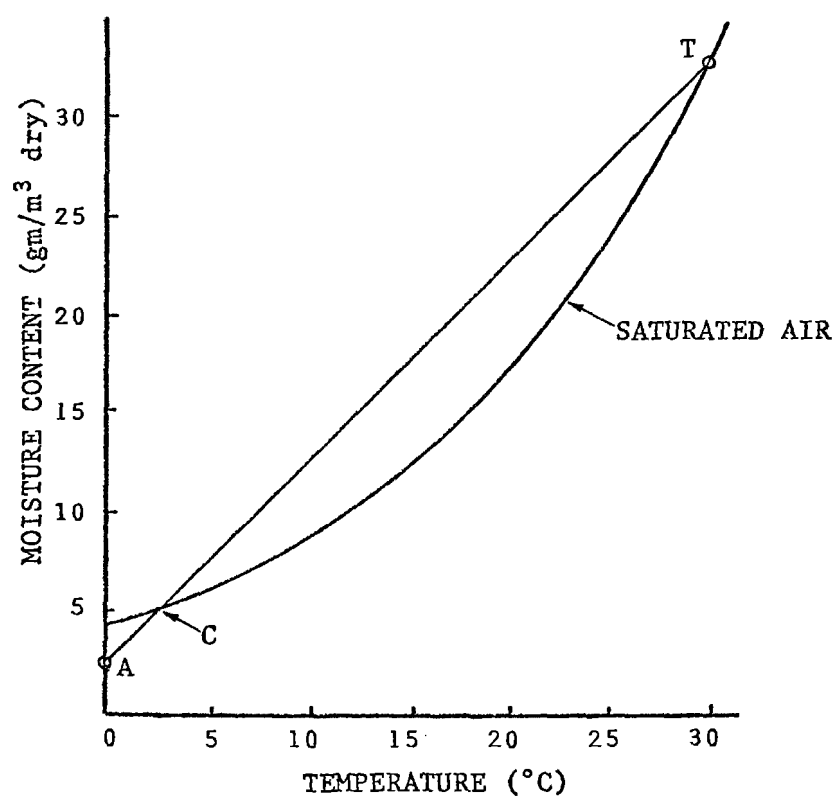
Figure 3 COMPARISON OF OBSERVED PLUME BOUNDARY AND SIMULATED TEMPERATURE DISTRIBUTION ABOUT GASTON'S TWIN MECHANICAL DRAFT COOLING TOWERS
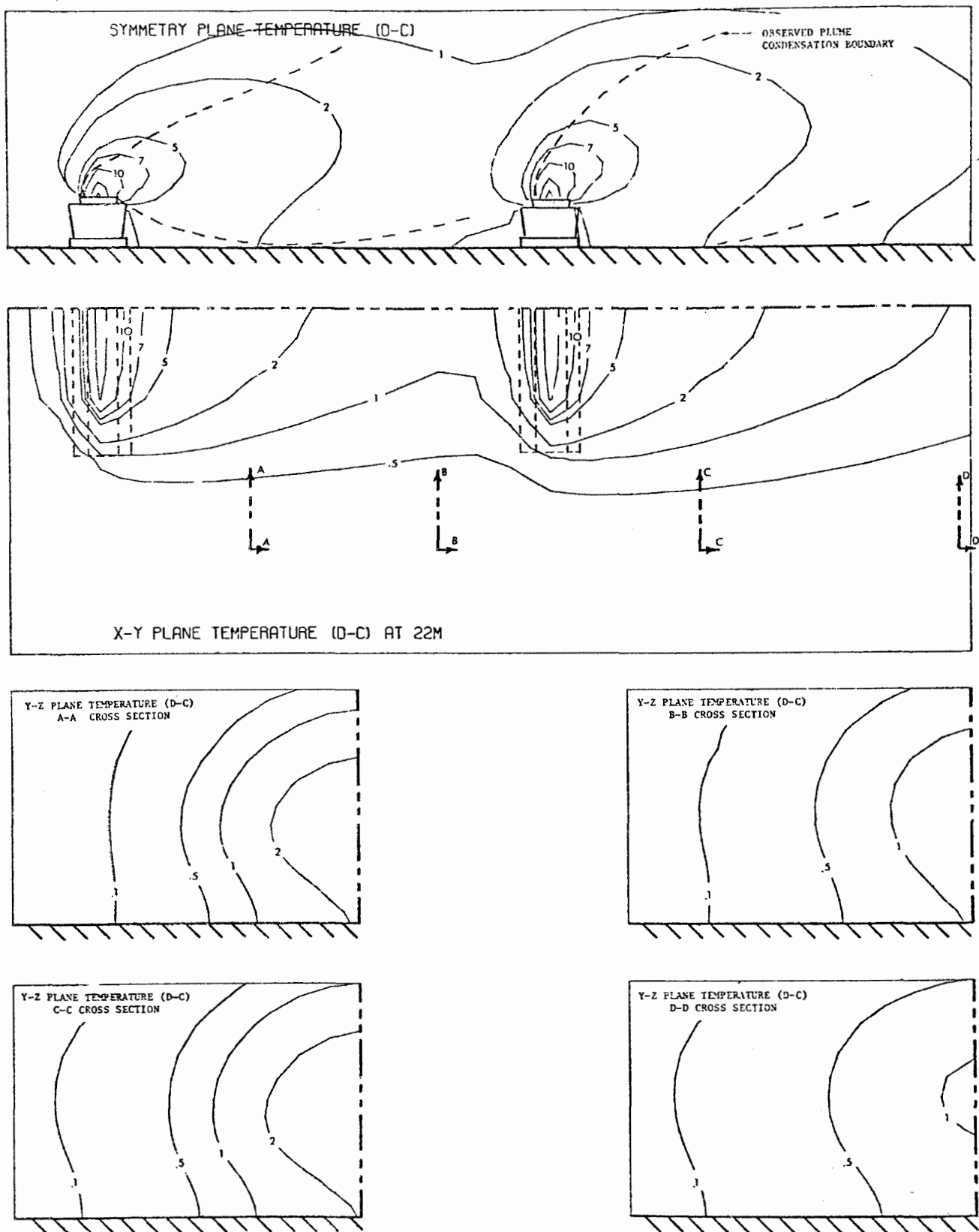
Figure 4 SIMULATED VECTOR FLOW FIELD ABOUT GASTON'S TWIN MECHANICAL DRAFT COOLING TOWERS

Symmetry Plane

Ground Plane

CROSS SECTION A-A

CROSS SECTION B-B

CROSS SECTION C-C

CROSS SECTION D-D

SCALE

50 METERS

387
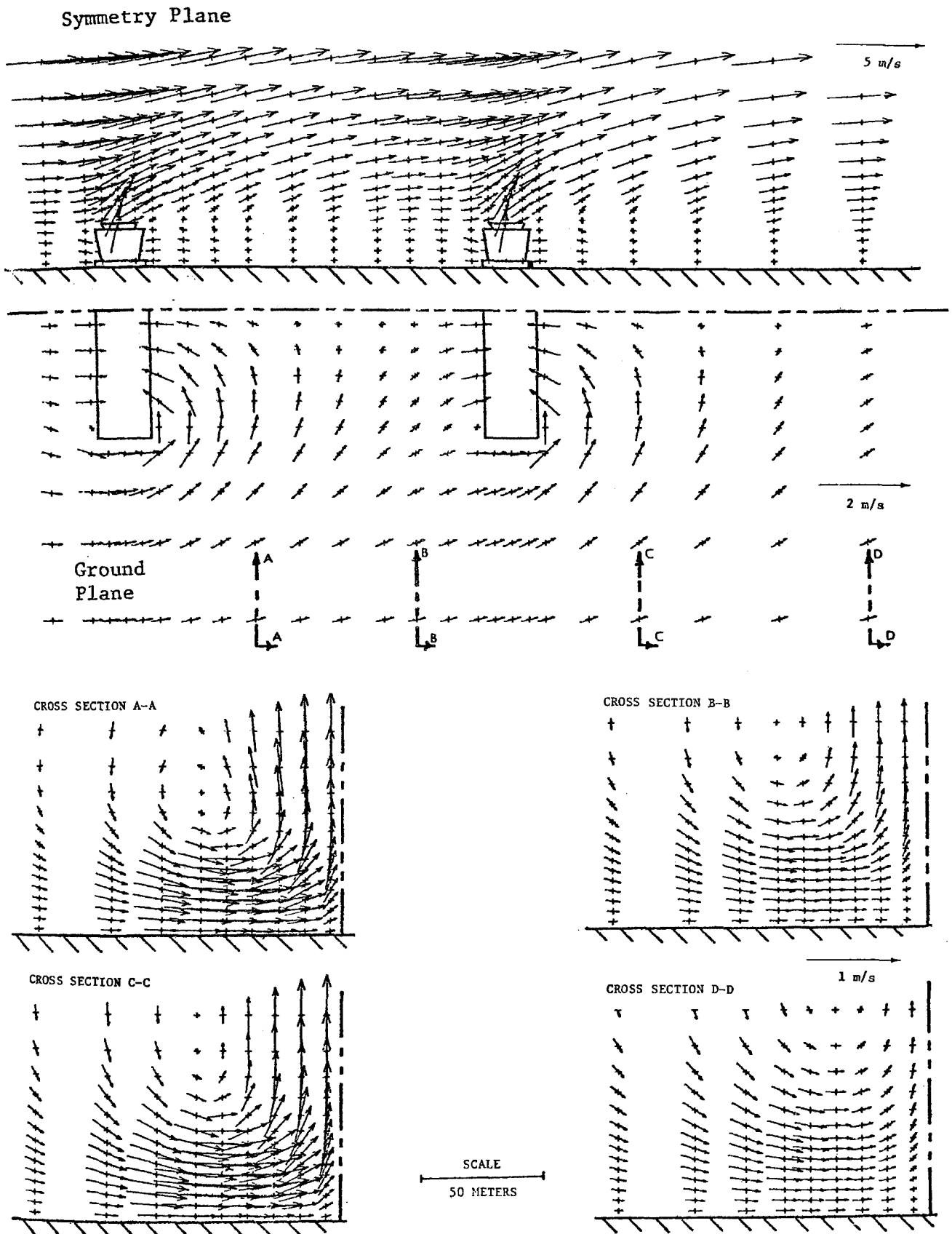
MECHANICAL-DRAFT COOLING-TOWER PLUME BEHAVIOR
AT PLANT GASTON

P.R. Slawson
Mechanical Engineering Department
University of Waterloo
Waterloo, Ontario, Canada

ABSTRACT

Field studies on the twin mechanical-draft cooling-tower plume behavior at the Gaston Steam Plant, Willsonville, Alabama, were conducted during February, 1973 and January-February 1976. Details on the experimental technique and measurements of some of the observed far-field time-mean condensed (visible) plumes are presented with corresponding source parameters and ambient air data. Predictions of far-field plume behavior and visible plume length using a slightly modified version of the closed-form model after Slawson and Coleman [1] Slawson [2] are compared with observations. The effects of elevated inversions, severe vertical wind shear and the nature of the source geometry on the observed plume behavior and subsequent predictions by the simple closed-form model are discussed.

INTRODUCTION

It is fairly well accepted that a thorough understanding of cooling tower plume behavior (both near-field and far-field) is required in order to develop mathematical models of visible plume length, trajectory and salt or other effluent deposition for purposes of environmental impact assessment. The majority of work on cooling tower plume behavior both experimental and theoretical has been associated with natural draft cooling towers. Consequentely, little comprehensive field data exists for model development on the behavior of plumes from mechanical draft cooling towers. Recent work by Slawson et al [3], [4], has shown that plume downwash around natural draft cooling towers can significantly alter far-field plume trajectory. Thus, due to the usual more complex source geometries of reduced tower height, multiple fans, and presence of adjacent towers, the near-field plume behavior from mechanical draft cooling towers can be expected to dramatically affect both operating performance through plume recirculation and interference as well as far-field plume behavior.

Southern Company Services Inc. has conducted two full-scale field study observational programs on the mechanical draft cooling tower plumes at Plant Gaston, Willsonville, Alabama, during February 1975 and January-February 1976. The objective of the field studies was to observe by photographic means the near-field and far-field behavior of the condensed (visible) portion of the cooling tower plumes. In addition, detailed

measurements on source and ambient parameters were made. Some details of the experimental technique may be found in a paper by Champion et al [5]. An attempt at modelling the observed near-field plume behavior is given by Crawford and Slawson [6].

The objective of the work outlined in this paper was to determine whether the simple integral vapor plume model of Slawson [2] could be modified or site tuned to produce consistant and reasonable agreement between the observed and theoretical far-field plume trajectories and lengths for the twin mechanical draft cooling towers at Plant Gaston.

EXPERIMENTAL DESCRIPTION

The twin Ecodyne concrete cross-flow mechanical draft cooling towers at Plant Gaston each service an 880 MWe coal-fired steam electric generating unit. Each tower has an overall length of 98.8 m width of 22.2 m and height of 16.9 m. There are 9 cells (9 fans) per tower. Each fan has a diameter of 9.2 m and rotates at 117 rpm to produce an average exit velocity of 8.14 meters per second. The towers are parallel to one another and separated by a distance of approximately 100 meters. They are aligned along a north-west south-westerly direction, and are located on the northeast side of the generating station. Measurements were made of tower exit temperature and velocity along with ambient measurements of dry bulb and dewpoint temperatures, wind speed and direction from ground level to above plume top. The source and ambient data were obtained bracketing the time period when the visible plume was being photographed from far-field and near-field camera stations. The visible plume photographs (one every minute during a given one to two hour period) were subsequentely reduced to time-mean visible plume outlines covering a period over which ambient conditions (particularly wind) were considered reasonably steady. The near-field visible plume top and bottom were much more qualitative in nature than the far-field due to the strong three-dimensional nature of the plume near the source.

MODELLING CONSIDERATIONS

As indicated above, the basis for the vapour plume model discussed here is the closed form or analytical solution of the integral equations governing moist plume behavior given by Wigley and Slawson [7], Slawson [2]. If one assumes that the plume is well bent-over and that it is rising in a uniform wind field these equations reduce to:

$$U \frac{dUR^2}{dx} = 2\alpha \frac{M}{R} \tag{1}$$

$$U \frac{dM}{dx} = F \tag{2}$$

$$U \frac{dF}{dx} = -MN^2 \qquad\qquad (3)$$

$$U \frac{dH}{dx} = -MG \qquad\qquad (4)$$

$$\frac{dz}{dx} = \frac{W}{U} \qquad\qquad (5)$$

where $M = UR^2W$, $F = UR^2b$, $H = UR^2 \Delta q$ are the fluxes of vertical momentum, buoyancy and excess specific humidity respectively. A buoyant acceleration per unit mass is given by $b = \rho \Delta T/T_a$. The plumes vertical transport velocity and wind speed are given by W and U respectively. The specific humidity gradient is given by $G = dq_a/dz$, and the Vaissalla frequency (for stable stratification) by $N = (g/T_a \; \partial\theta/\partial z)^{\frac{1}{2}}$. Further details on the development and solutions to the above equations may be found in papers by Wigley and Slawson [7], [8], [9], Slawson and Coleman [1] and Slawson [2].

Following the work of Slawson and Csanady [10] the plumes growth or entrainment of ambient air is considered to occur in two phases. In the first phase the self-generated turbulence of the plume is the dominant mechanism for growth while in the second or atmospheric phase, atmospheric turbulence is responsible. Here, we are mainly concerned with plume behavior in a stable atmosphere and following Slawson and Coleman [1] assume that the atmospheric phase of plume growth starts at the point of maximum rise. Also, for modelling purposes we assume that plume growth in the atmospheric phase is described by the Pasquill sigma's.

The vapour plume model as outlined here and described in detail in the above mentioned references had been previously used for describing the behavior of single natural draft cooling tower plume.

As noted previously, the additional complexities associated with the plume dynamics of mechanical draft cooling tower plumes must somehow be accounted for if the model was to be modified in order to adequately describe the far-field plume behavior at Plant Gaston. It was thought that the modifications to the natural draft cooling tower plume model must at least account for, (a) the existence in this case of two sources of non-circular initial exit geometry (long thin rectangular sources), (b) the stronger wind speed shear layer associated with plumes closer to the ground and (c) wind direction relative to the long axis of the towers. The detailed description of near-field plume behavior is out of the realm of any integral model and is thus the subject of the paper by Crawford and Slawson [6]. Here we attempted to account for the effects (a), (b) and (c) above by empiricle or semi-empiricle methods.

PRS

The thin rectangular geometry of the mechanical draft cooling tower source was initially incorporated into the model by simply considering a plume element to be of near-rectangular cross-section, rather than circular. The source shape was also altered to account for the projection of the real tower source into a plume normal to the wind direction. With this modification to the model it became apparent from test calculations that the rectangular source geometry (aspect ratio) of the Gaston Towers had little effect on plume behavior in the far-field (ten tower lengths from the source). Thus, for the Gaston site at least the model used a circular plume but incorporated merging of two plumes, wind speed shear and wind or plume direction effects.

The plumes from the two towers were considered to have merged together completely at the point where the edges of the two plumes were calculated to meet. At this merge point where the plumes just touched, a new plume cross-sectional area (A_m) was calculated equal to the sum of the areas of the two individual plumes. From this new area a new effective plume radius was determined. The new (merge point) momentum buoyancy and excess specific humidity fluxs were determined by combining the individual fluxes in proportion to their respective plume cross-sectional areas, thus,

$$M_m = (\frac{M_1}{A_1} + \frac{M_2}{A_2}) A_m \tag{6}$$

$$F_m = (\frac{F_1}{A_1} + \frac{F_2}{A_2}) A_m \tag{7}$$

and $$H_m = (\frac{H_1}{A_1} + \frac{H_2}{A_2}) A_m \tag{8}$$

The model also alters the trajectory from the single plume to the merged plume at the merge point. The trajectory of the merged plume starts at an elevation based on a weighted average of the previous two plume elevations at the merge point. Subsequently, virtual source variables are calculated for the now merged plume and the model re-runs as a single plume model.

A trajectory constant was used in the model of Slawson [2] to account for the effect on plume trajectory of plume downwash around the natural draft cooling tower. In the modified version used for the Gaston plumes the trajectory constant was made an empiricle function of the observed wind speed shear and the wind angle relative to the long axis alignment of the towers. It was known from the numerical integration model of Slawson [2] that a principal effect of vertical wind speed shear was to lower the plume trajectory. Also, physical modelling studies have shown that aerodynamic wakes and recirculating flows are affected by the orientation of rectangular bluff bodies to the principal flow direction. It was also felt that the entrainment of ambient air into the plume, which in the model is incorporated through the value of the entrainment constant α, would depend on the

amount of wind direction shear present over the plume rise region. Thus
the entrainment constant was made an empiricle function of the amount of
wind direction shear.

It is obvious from the previous discussion that a great deal of rather hea-
vy handed empiricism was required in order to modify the simple vapour plume
model so that it would apply to the twin mechanical draft cooling tower
plumes at Plant Gaston. The need for these or similar modifications drama-
tically emphasize the shortcomings in the physical basis of the, simple va-
pour plume model when applied to mechanical draft cooling tower plume
behaviour.

RESULTS AND DISCUSSIONS

Three far-field time-mean plumes have been selected from the data base as
examples of the observations and subsequent model comparison. Since the
model has been developed to include considerable empiricism from a limited
data base it certainly cannot in its present form be considered as a pro-
ven predictive tool. Table 2 lists the source data on tower exit velocity,
temperature (assumed at saturation) and surface pressure corresponding to
the observations given in figures 1 to 6. The ambient data on temperature
and wind profiles illustrated in these figures represents the average for
the time period corresponding to the plume observational period. Further
details on the model and specific measurements will be given in a final
report by Slawson et al [11].

In figure 1 the model trajectory well approximates the observed but the
final plume length appears to be overpredicted by some 33%. However, in
this case the visible end of the plume was obscured by cloud.

In figures 3 and 5 model trajectories and plume lengths are in good
agreement with the somewhat shorter observed plumes. During all three of
the plume observational periods the ambient profiles of wind speed and
temperature are complicated by the presence of severe "kinks" in the pro-
files. The simple top-hat distribution of plume parameters used in the
model may be too severe a restriction for such complex profiles of ambient
parameters. However, the model uses the average ambient parameter over
the predicted depth of the plume when calculating plume parameters in an
attempt to account for variability across the plume. A significant diffe-
rence between the observations of figure 1 and those of figures 3 and 5 is
the wind and or plume direction relative to the long axis alignment of the
twin mechanical draft cooling towers. In figure 1 the wind is blowing
nearly parallel to the long axis while in figures 3 and 5 it is normal to
the long axis of the towers. Again, it is doubtfull that the simple empi-
ricism developed for the present model to account for wind orientation ef-
fects on plume near-field behaviour is established well enough on the basis
of such a limited data set. One soon realizes both from observations on
near-field plume behaviour and from the complexities and uncertainties as-
sociated with modelling such behaviour, as Crawford and Slawson [6] illu-
strate, that any empiricism purporting to account for such behaviour is at
least site specific as well as denpendent on the plume model itself.

In addition to the problems of incorporating the effects of near-field plume dynamics and complex time-mean profiles of ambient parameters one must in the present model decide on the point of onset as well as a description of plume spread in the atmospheric diffusion phase. In cases of very long plumes in stable atmospheres, the atmospheric phase may become very important to predicting the observed plume length. Thus the choice of stability category and subsequent sigma's becomes important in the present model.

CONCLUSIONS

Based on the data used here we conclude that it is very difficult to model even far-field plume behaviour (to the extent of these observations) with a simple integral vapour plume model. Since considerable empiricism appears to be required in order to make the simple model work, then a much larger data base than that at our disposal is required to firm-up the functional form of any empiricism introduced to the model for mechanical draft cooling tower plume applications. It is hoped that perhaps a numerical integration model which can at least account for vertical wind speed shear may better approximate the real physics of plume behavior in the far-field.

ACKNOWLEDGEMENT

REFERENCES

1. Slawson, P.R., and Coleman, J.A. (1977): "Natural draft cooling tower plume behavior at Paradise Steam Plant", Proc. Waste Heat Management and Utilization Conf., Miami, Florida, May 9-11.

2. Slawson, P.R. (1978): "Observations and Predictions of Natural Draft Cooling Tower Plumes at Paradise Steam Plant", Atmos. Env., 12, 1713-1724.

3. Slawson, P.R., Coleman, J.H., and Frey, J.W. (1975): "Natural Draft Cooling Tower Plume Behavior at Paradise Steam Plant (Part I)", Tenn. Valley Auth., Div. of Env. Plan. E-AQ-76-1, 145 pp.

4. Slawson, P.R., Coleman, J.H., and Frey, J.W., (1977): "Natural Draft Cooling Tower Plume Behavior at Paradise Steam Plant (Part II)", Tenn. Valley Auth., Div. of Env. Plan. TVA/EP-78/01.

5. Champion, E.R., Goodman, C.H., and Slawson, P.R., (1977): "Field Study of Mechanical Draft Cooling Tower Plume Behavior", Proc. Waste Heat Management and Utilization Conf. Miami, Florida, May 9-11.

6. Crawford, T.L., and Slawson P.R., (1978): "Modelling Near-Field Behaviour of Plumes from Mechanical Draft Cooling Towers", Proc. Waste Heat Management and Utilization Conf. Miami, Florida, Dec. 3-6.

7. Wigley, T.M.L., and Slawson, P.R., (1975): "The Effect of Atmospheric Conditions on the Length of Visible Cooling Tower Plumes", Atmos. Env., 9, 439-445.

8. Wigley, T.M.L., and Slawson, P.R., (1971): "On the Condensation of Buoyant Moist, Bent-Over Plumes"", J. Appl. Meteor., 10, 253-259.

9. Wigley, T.M.L., and Slawson, P.R., (1972): "A comparison of Wet and Dry Bent-Over Plumes", J. Appl. Meteor., 11, 335-340.

10. Slawson, P.R., and Csanady, G.T., (1967): "On the Mean Path of Buoyant Bent-Over Chimney Plumes", J. Fluid Mech., 28, 311-322.

11. Slawson, P.R., Crawford, T.L., Goodman, C.H., and Champion, E.R. (1978): "Plume Behavior from Mechanical Draft Cooling Towers at Plant E.C. Gaston". To be published.

TABLE 1

DATA ON SOURCE PARAMETERS AND ATMOSPHERIC SURFACE PRESSURE

DATE	TIME	Wo (m/s)	Tpo (°C)	Po (mb)
12/2/75	0717-0757	9.64	32.24	1013.9
13/2/75	0655-0745	9.64	25.94	1023.3
15/1/76	0647-0745	9.74	28.14	1029.4
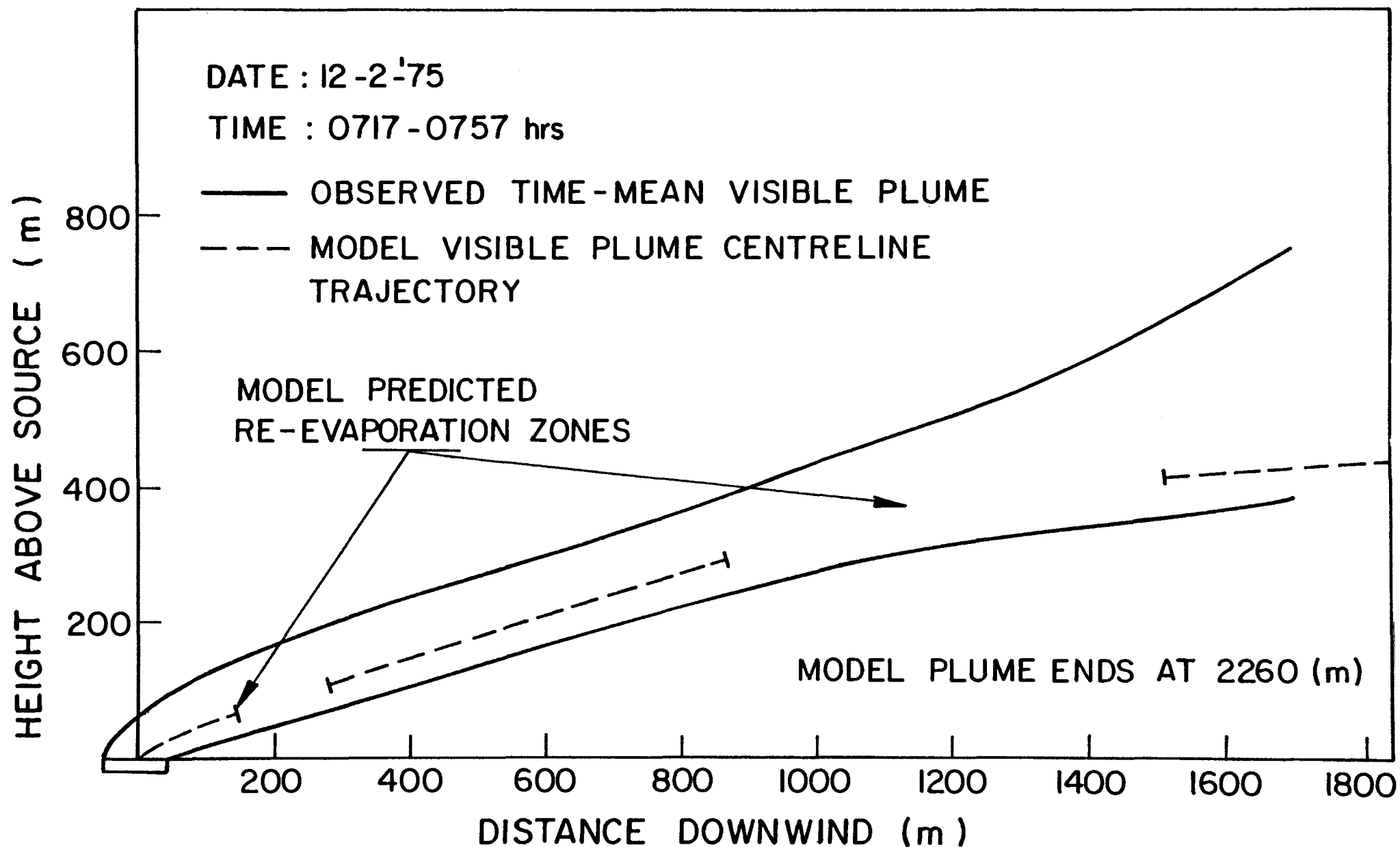
Figure 1   Comparison of Predicted and Observed
Time-Mean Plumes 12/2/75.
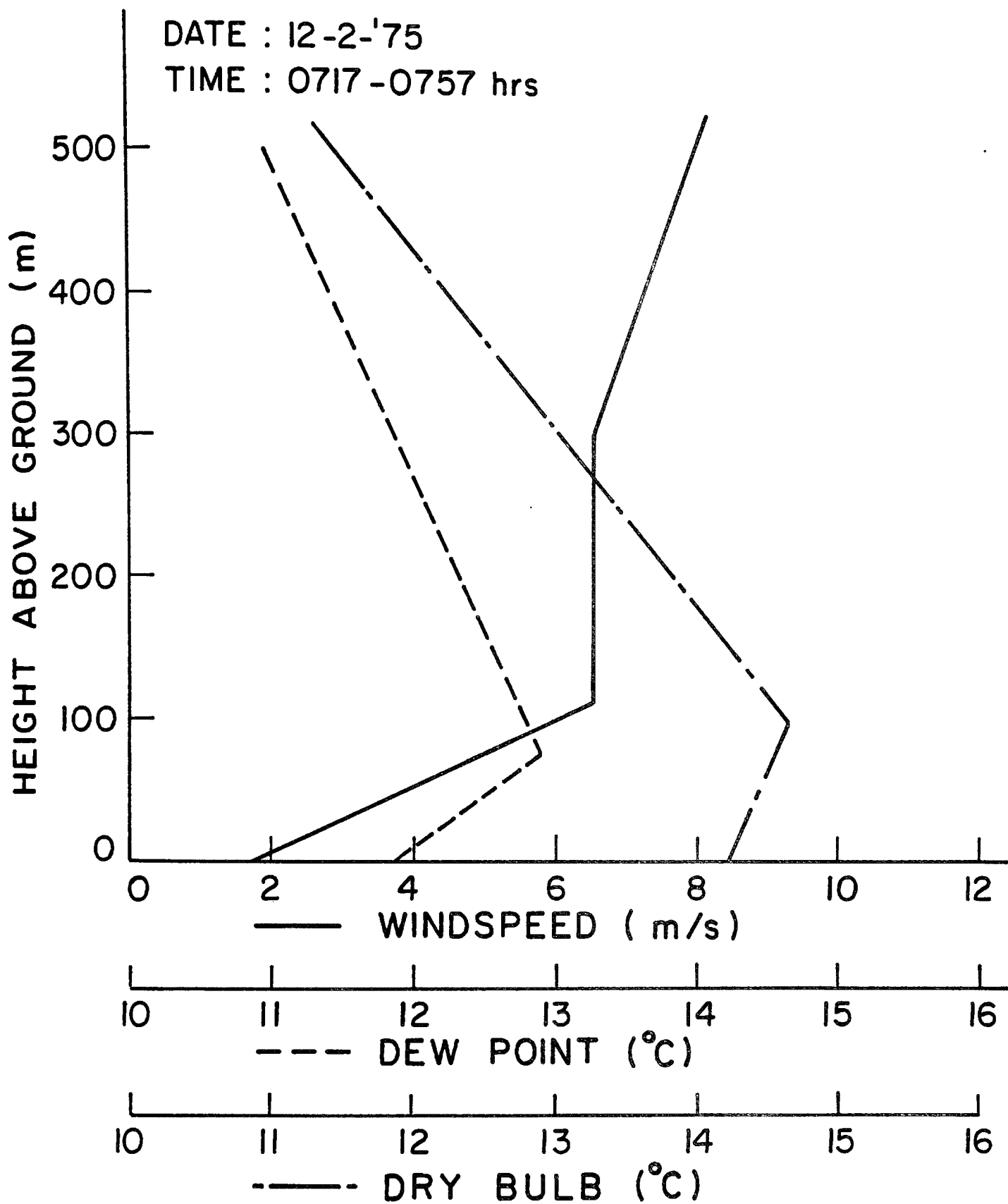
Figure 2 Observed Ambient Temperature and Wind
Speed Profiles, 12/2/75, 0717-0757 Hours.

397
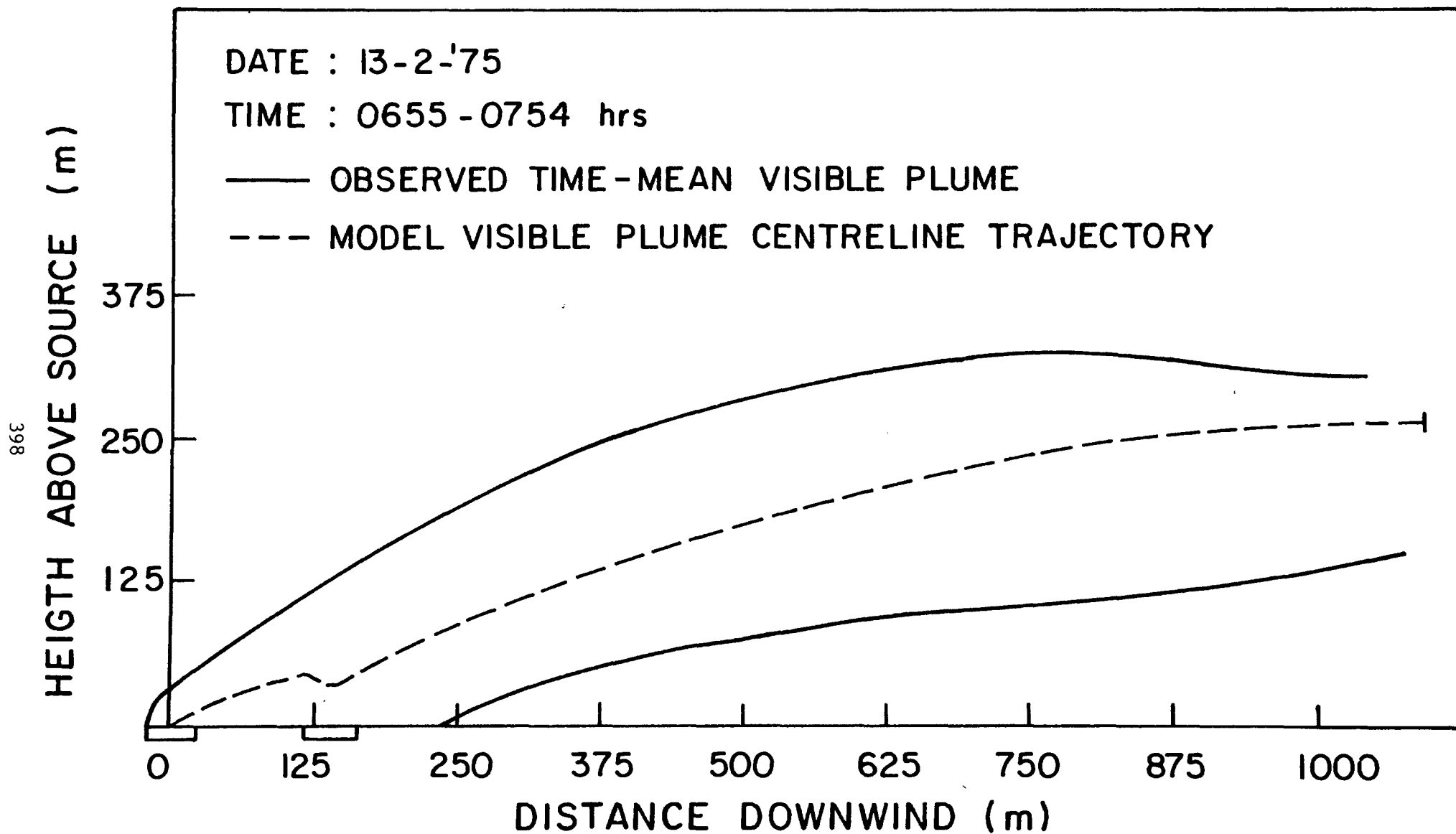
Figure 3 Comparison of Predicted and Observed
Time-Mean Plumes 13/2/75.
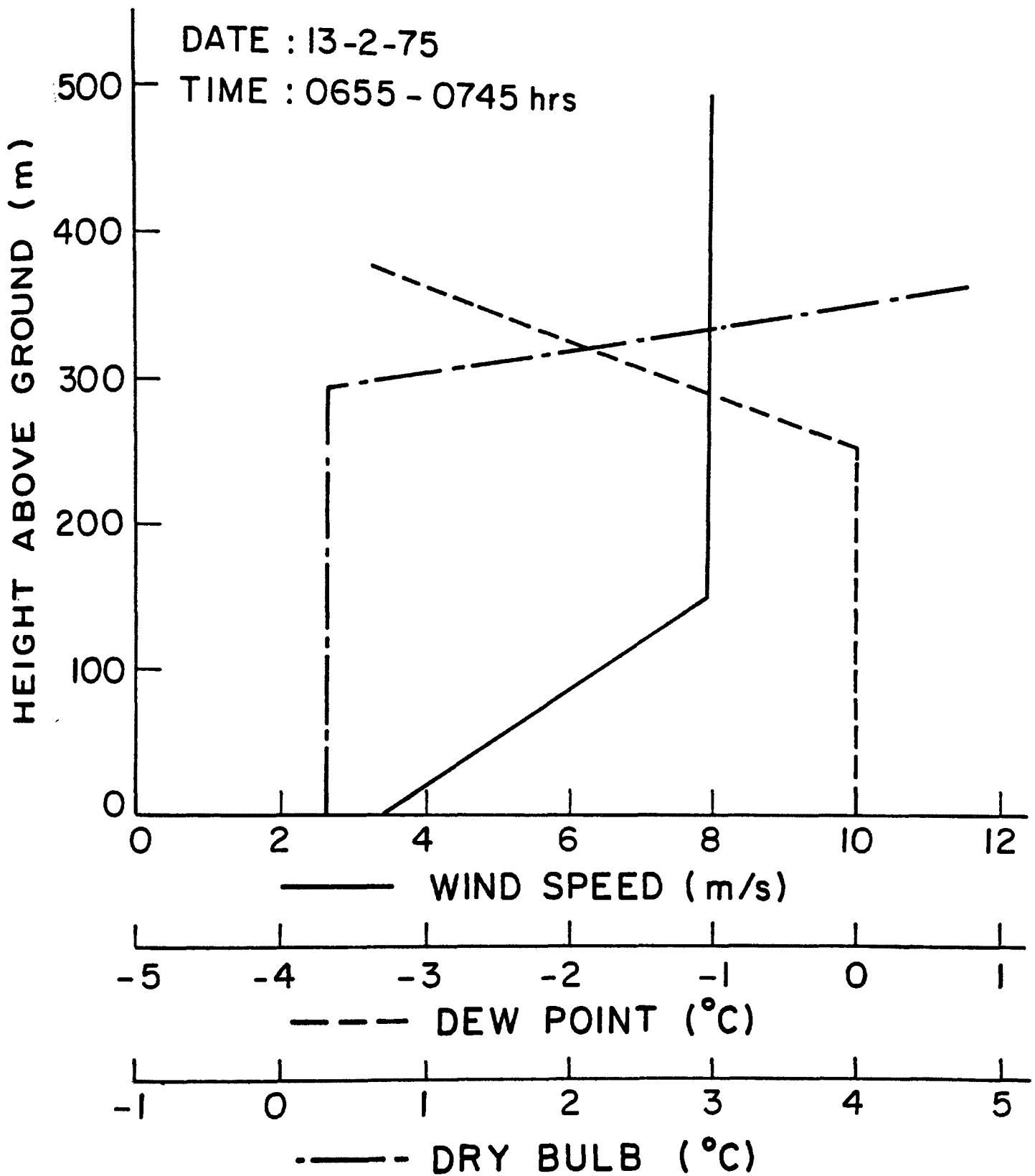
Figure 4   Observed Ambient Temperature and Wind
Speed Profiles, 13/2/75, 0655-0745 Hours.

399
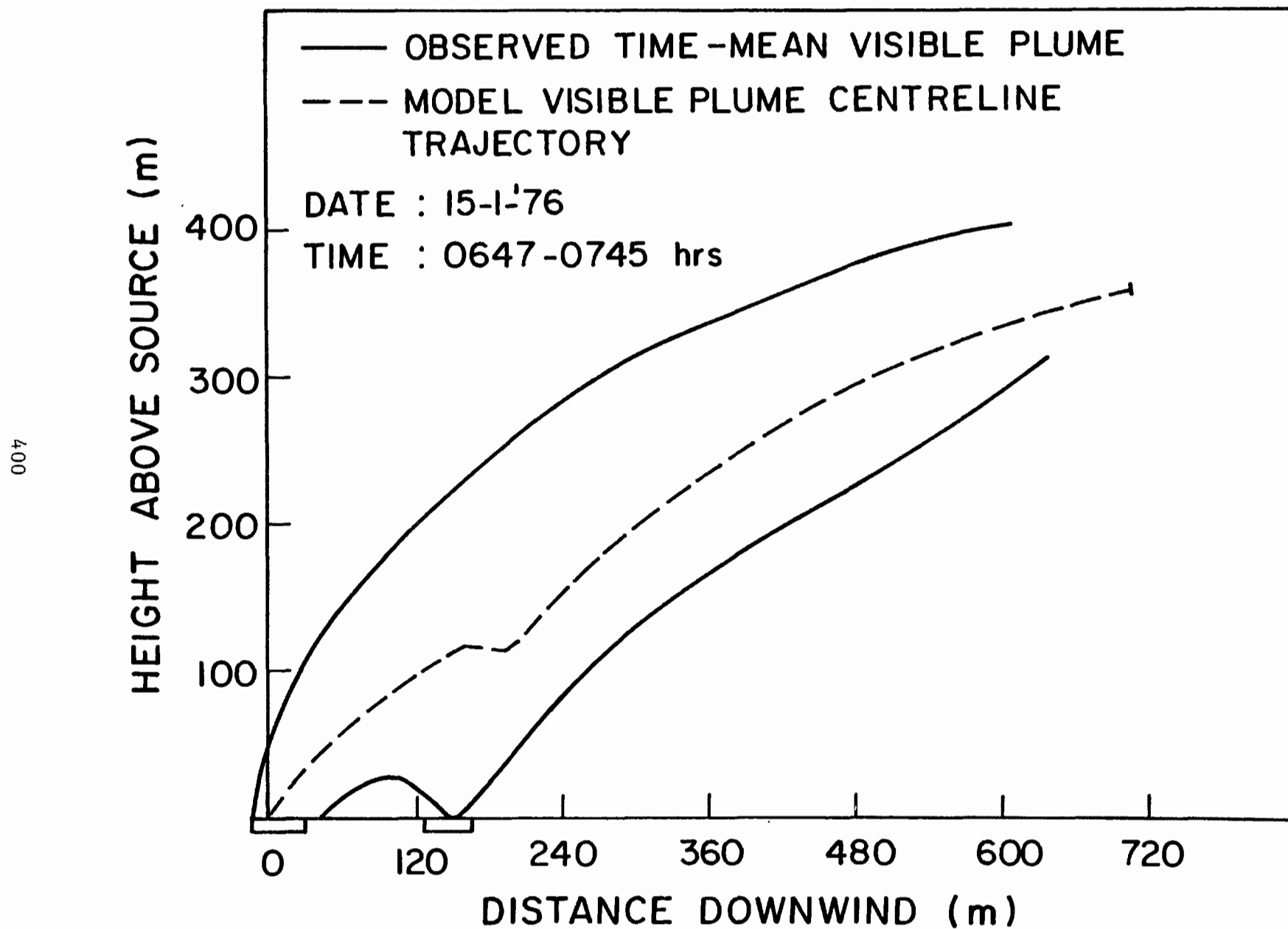
Figure 5   Comparison of Predicted and Observed
Time-Mean Plumes, 15/1/76.
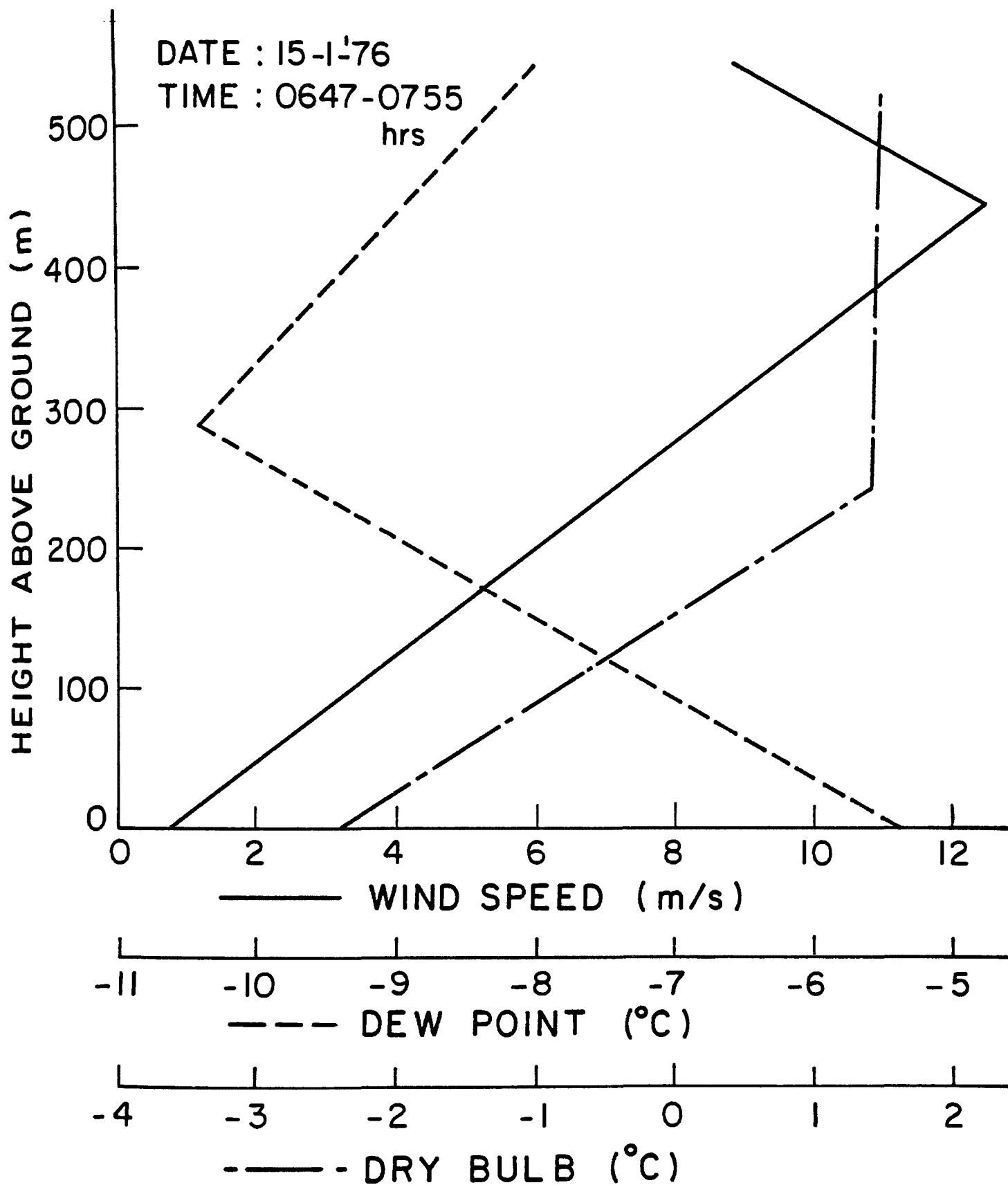
Figure 6   Observed Ambient Temperature and Wind
Speed Profiles, 15/1/76, 0647-0745 Hours.

401

CRITICAL REVIEW OF THIRTEEN MODELS FOR
PLUME DISPERSION FROM NATURAL DRAFT COOLING TOWERS

R. A. Carhart*, A. J. Policastro, S. Ziemer, and K. Haake
Division of Environmental Impact Studies
Argonne National Laboratory
Argonne Illinois, USA

ABSTRACT

Thirteen models for natural-draft cooling-tower (NDCT) plume rise are evaluated theoretically and tested with 39 sets of visible plume field data from three sites. The models evaluated have been employed or developed for use in the environmental-impact evaluation process for nuclear power plants.

Two separate theoretical approaches represent the models tested: semi-empirical and integral. The ten models using the integral approach treat the same basic phenomena through the use of conservation equations: entrainment; buoyancy; pressure drag; heat, vapor and liquid water dispersion. Each model simulates these phenomena in a slightly different manner.

It is found that a wide range in predictions occurs among the models. Models which compute plume bending by entrainment alone predict too much dilution when the plume trajectory is predicted correctly. The most successful models employ additional means for plume bending which does not result in more entrainment. Among the methods used is to add a pressure drag to bend the plume, or to treat a smaller spreading rate for the moisture portion of the plume, or to provide a rapid plume bendover in the zone for flow establishment. The correctness of each of the latter assumptions is yet to be determined.

Model performance may be divided into three categories: competitive, average, and below average. The competitive models [Winiarski-Frick, Stone & Webster, Slawson (Closed Form) and Hanna] satisfy the following criterion: the models can predict visible plume length within a factor of 2.5 (predicted visible plume length is 0.4 to 2.5 of observed) and visible plume height by a factor of 2 (predicted visible plume height is 0.5 to 2.0 of observed) in 50% of all cases tested. Seven models predict with varying lesser degrees of performance with two models (ORFAD and Frick) predicting consistently poorly. Some of the model/data discrepancies can be traced to data errors and uncertainties in the measurement of tower exit and ambient conditions. However, the models have all shown a consistent performance with the visible plume data over the 39 data sets and have presented a unified picture of their performance. Improved predictions can be made by improving model assumptions and by calibrating the improved model to the field data.

---

*Visiting Scientist. Permanent Address: Department of Physics. University of Illinois at Chicago Circle.

INTRODUCTION

The Environmental Protection Agency under the authority of the Federal Water Pollution Act Amendments of 1972 mandates the use of closed-cycle cooling for nearly all new electrical power plants. At present, utilities normally choose to install evaporative natural-draft and mechanical-draft cooling towers. Criteria used for siting new plants include considerations of tower environmental impact. The towers must be designed to minimize interference and recirculation for economic reasons, and to minimize off-site fogging, icing, shadowing and drift deposition for environmental reasons. Predictions of these environmental impacts must be presented by the utility to state and federal regulatory bodies in the licensing process. Thus the availability of reliable techniques for predicting atmospheric and ground-level disturbances produced by the tower plumes is essential.

A number of mathematical models have been developed and are in use for predicting tower environmental impacts, but none of these models has been validated using a wide range of experimental data. The Nuclear Regulatory Commission recently sponsored a program at Argonne National Laboratory to validate the popular and promising models currently available. The final report of the study is in preparation, [1] and this paper focuses on only some of the results obtained. It should be read with reference to our earlier paper for additional details not repeated here [2].

In this paper the formulations of thirteen single-tower natural-draft cooling tower plume models is intercompared in a common format along with each model's degree of success in predicting the visible plume outlines for 39 single-tower plumes from three sites. Model performance is traced to specific assumptions made in model formulation.

PHYSICAL AND MATHEMATICAL ASPECTS OF NDCT PLUME DISPERSION

The emission from a natural-draft cooling tower into an ambient environment resembles the classic problem of a jet in a free environment. More precisely, it is a problem of a vertical jet of finite size with initial momentum and buoyancy being dispersed in a crosswind. It is reminiscent of the emission of stack gases into the atmosphere from a fossil-fired plant. Unlike the stack, however, the cooling tower has a much larger exit diameter, a much smaller temperature difference with the ambient environment (i.e., less buoyancy) and a smaller exit velocity (less momentum per unit mass). As the plume disperses, it entrains ambient air which has physical properties varying with height. (Wind speed, wind direction, dry-bulb temperature, and relative humidity are usually functions of height above the ground in the natural atmosphere). The smaller exit velocity (actually densimetric Froude number) of the outlet for the cooling tower sometimes causes downwash conditions for the plume under moderate and high winds. In such case, the cavity generated behind the cooling tower due to the crosswind interaction with the tower will provide a low pressure field below the plume which has the effect of pulling the plume downward and increasing the rate of entrainment (mixing) of the plume. The effect of the tower structure thus complicates

the free-jet problem. A second complication to the free jet problem is the presence of moisture in the plume. Due to thermodynamic processes present inside the tower, the plume is generally saturated at exit and contains some liquid recondensate. Additional liquid water can form from condensation when the warm moist plume mixes with the cooler ambient air, and when the plume cools during adiabatic ascent. This condensation releases latent heat warming the plume further. Later in the plume history, the plume moisture tends to disperse below the saturation level due to ambient mixing but because of evaporation of accumulated liquid water (absorbing heat), the saturation state of the plume is maintained. A common assumption is that the plume is visible whenever liquid water is present in the plume. As long as liquid water is present, the plume state is assumed to remain on the saturation curve of the X-T psychrometric diagram, where X is the plume mixing ratio and T, the plume temperature. It should be noted that the treatment of condensation/evaporation energetics in the plume provides feedback to the plume temperature, increasing it during condensation and decreasing it during the evaporation phase. Generally, however, moisture thermodynamics significantly affects the dynamics of the plume only under extreme conditions such as very cold and/or very humid ambient atmospheres.

In our plume model validation study, thirteen models [3-15] for NDCT plumes were evaluated. Ten employ the integral formulation in which a set of conservation equations are solved to predict plume dispersion. These conservation equations can be reduced to a set of coupled nonlinear ordinary differential equations which are solved by a variety of numerical methods. From each model we have extracted eight differential equations for the following plume properties: R(plume radius), v_x(horizontal plume velocity), w(vertical plume velocity), T_p(plume temperature), X_p(plume specific humidity), σ(plume liquid water content), x(downwind coordinate), and z(vertical coordinate). The first three are dynamic equations, the next three are thermodynamic equations, and the last two are kinematic equations. A brief review of each equation follows.

    1. <u>Mass Flux Equation</u>: In this equation, the mass flow into the plume from the ambient environment is defined. If ϕ_m is the plume mass flux through a plane normal to the centerline (divided by π) and s is the distance along the centerline from the tower exit plane to this plane, then the fractional entrainment rate, μ, (called simply the entrainment rate in this work) is defined by

$$d\phi_m/ds = \mu\phi_m \tag{1}$$

The rate of entrainment of ambient air into the plume is usually expressed by means of an entrainment velocity, v_e. In top-hat models (i.e., models that assume uniform lateral profiles of plume variables) with circular plume cross-sections, there is a relationship between μ and v_e based on conservation of mass:

$$\mu = \frac{2\pi R \cdot \rho_a \cdot v_e}{\pi R^2 \cdot \rho_p \cdot v} = \frac{\text{ambient flux into jet}}{\text{plume flux along jet centerline}} \tag{2}$$

where v is the total plume velocity along the centerline ($v^2 = v_x^2 + w^2$).

For each of the ten integral models the entrainment assumption is given in Table 1. It is defined for each model in terms of a functional expression for μ or v_e. The different assumptions for μ represent major differences among the models. To obtain the relationship in Eq. (2), one must view v_e as uniform around a given plume circumference and directed radially inward.

2. Horizontal Momentum Equation: The initially zero horizontal momentum of the jet is increased through addition of the entrained momentum of plume air directed downwind and the action of a pressure (drag) force arising from the pressure difference between windward and leeward sides of the jet. Each model presents an equation for dv_x/ds, where v_x is the total horizontal plume velocity. (Note that $v_x = v \cos \theta$, where θ is the angle of the centerline above the horizontal). Major differences among the models exist in terms of their assumptions on the pressure force (its presence or not and its functional form). Some models make the bent-over plume assumption in which the plume is assumed to accelerate immediately upon exit to the wind speed. In such a case $v_x = u$ and the horizontal momentum equation is redundant. The equations used by the models are summarized in Table 2.

3. Vertical Momentum Equation: The initial vertical momentum of the plume as it exits the tower is augmented by the plume buoyancy directed upwards and the vertical component of the plume drag force (if present) directed downwards. The buoyancy force includes the additional effect of moisture in the plume (moist air is lighter than dry air) and the negative buoyancy effect of the weight of liquid water in the plume. Every model yields an equation for dw/ds, where w is the plume vertical velocity, $w = v \sin \theta$. See Table 3 for the assumed form of this equation in each model.

4. Equation for Plume Enthalpy: The plume temperature decreases with downwind distance due to the interplay of (a) mixing with ambient air, (b) adiabatic expansion and cooling as the plume rises into lower pressure regions, and (c) the energetic effects of net condensation or evaporation of liquid water. From each model, one can extract the equation used for dT_p/ds, the change of plume centerline temperature with centerline distance. Table 4 lists the version of this equation used in each model.

5. Moisture Dispersion Equation: The plume mixing ratio X_p changes due to mixing with ambient air having different moisture content. As generally drier ambient air is entrained and mixes with plume air, liquid water can condense or evaporate affecting the moisture content of the plume, so long as the plume remains at saturation at plume temperature and pressure. After liquid water has been exhausted by evaporation, further mixing will cause X_p to drop below saturation. Condensation and evaporation change the plume temperature which indirectly affects plume mixing ratio. Every model yields an equation for dX_p/ds, the change of plume mixing ratio with centerline distance. In Table 5 is given the appropriate equation for each model. Differences among models exist in the treatment of moisture thermodynamics; for example, some models treat condensation alone and neglect evaporation of liquid water while some others neglect liquid water entirely.

6. Liquid Water Dispersion Equation: The plume liquid water content begins initially as the condensate present within the plume at exit. This initial condensate is dispersed over a larger plume volume due to plume

405

mixing and is increased or decreased as a result of the condensation or evaporation that takes place in the plume. As a result, the plume liquid water content, σ, in kg/kg will vary with centerline distance. From each model, we extracted the equation chosen for $d\sigma/ds$, the change of plume liquid water content with centerline distance. Table 6 lists these equations by model.

7,8. Plume Trajectory Equations: Two kinematic equations are written to relate plume centerline distance s and the downwind and vertical coordinates x and z.

In interpreting Tables 1-6, several points must be borne in mind. Whenever a conflict arose between intentions presented in the model's theoretical description and the actual equations we derived by taking the infinitesimal limit of the steps followed in the computer code, the equations implied by the latter were chosen. This procedure guarantees that Tables 1-6 reflect the actual equations used to produce all model predictions for those models whose source codes were available to us. In all cases we ran the models with very small step sizes and in double precision to minimize truncation error. In the two models which differentiate types of liquid water (cloud-water, small drops; hydrometeor, larger drops) and include effects of freezing for low plume temperatures; i.e., the Hanna [9] and Lee (NUS) [12] models, the equations in Table 6 apply to σ as the sum of all liquid water in the plume, and apply strictly when the plume is above the ice-nucleation point. (In our studies, we find freezing effects to be small.) Also, the small effects of rainout and evaporation of hydrometeor water are neglected in the equations presented for the Hanna and Lee (NUS) models. Finally, to facilitate the comparisons, some other small terms in the model equations presented in Tables 1-6 have been dropped whenever they contributed a mere few percent relative to the terms which have been retained. No significant differences in model performance can be traced to those terms and their omission from the tables serves to focus the comparison on the essential variations among model formulations.

It is important to recognize the several most controversial areas in the modeling of single-tower NDCT plumes. Perhaps the most important is the choice of entrainment function as mentioned above since the models are very sensitive to the entrainment theory used. The presence or not of pressure drag effects on the plume and the method by which it is modeled (including the alternative of the bent-over plume assumption) is a second major area of controversy. Pressure drag affects mainly plume bending and, as a result, brings the plume in contact with different air masses depending on the local height of the plume.

Plume thermodynamics is treated differently in the models depending on the modeler's expectation of the importance of condensation and/or evaporation effects. Some models treat freezing of liquid water in the plume on very cold days and the possibility of rainout. Also, different criteria are used to define the boundary of the visible plume. A common criterion is that the visible part of the plume is defined as that region where the local liquid water content is greater than zero.

The treatment of the final atmospheric diffusion phase of plume dispersion also differs among the models. Most models ignore it while others recognize the need to treat atmospheric-turbulence-induced dispersion beyond maximum rise. A difficult phenomenon to model is tower-or building-induced downwash. The effect of wind interaction with solid bodies upwind of the plume is to increase plume bending and increase entrainment from below the plume. The treatment of such boundary-induced effects is really beyond the integral approach. Although no fundamental treatment exists, one model [4] attempts to treat it through empirical equations. Most models ignore the problem. It is the combination of alternative assumptions which distinguishes one model from the other.

METHODS OF EVALUATING NDCT PLUME MODELS

The good method to evaluate the performance of NDCT plume models is to ·compare model predictions to field data encompassing profiles of temperature, specific humidity, and velocity at numerous transects through the plume. In this way, a three-dimensional view of the plume in terms of its gross characteristics (spreading, trajectory, etc.) and its microphysics (3D temperature, moisture and velocity) can be attained. Unfortunately, no such data were available at the time of our study. Some measurements [16] of this type at Neurath and Meppen in West Germany have been made recently for a number (usually three) plume cross sections downwind. The data have just now been made available to us and will be useful in future studies.

A large body of data exists [17-21] for visible plumes at several American and European sites. A typical data set encompasses visible plume outlines (usually time averaged over a 20 minute to 1 hour period), ambient profiles of dry-bulb temperature, relative humidity, and wind speed (sometimes a single profile or at times several profiles averaged over the period of visible plume photographs) and tower exit conditions such as tower exit temperature, updraft velocity, relative humidity, and sometimes liquid water content. The better data in that category involves time-averaged measurements of tower exit conditions, ambient profiles, and visible plume outlines. The disadvantage of such data is that only the visible portion of the plume is being compared to model predictions. The invisible portion can be much larger and extend far downwind. Also, airplane measurements have revealed that the visible portion of the plume generally occupies the top portion of the plume with the bottom invisible. However, the visible plume does give a measure of the plume trajectory and spreading of the saturated moisture portion of the plume. We have accumulated 39 data sets for single NDCT plumes. Our comparison of the models to this large data base have revealed distinct trends in model performance which helped us locate model flaws from the model/data comparisons. It is the consistent performance of each model to our visible plume data base which has proven the value of our model/data comparisons to this body of data. Of course, comparisons of model predictions with in-plume data and with single-phase data (dry plumes in a dry environment) should complement the results we have obtained to date.

The scope and nature of the plume data sets have been described previously [2]. The 39 single-tower cases are listed in abbreviated form in Table 7, which gives averages of ambient dry-bulb temperature, relative humidity, wind speed, and average lapse rate for each case over the observed visible plume-rise region. These average values allow a comparison of the environmental and tower conditions for each single-tower plume case, and illustrate the range of conditions found in our data base. Our model calculations, however, employed the full ambient profiles measured.

The 12 Lünen cases represent winter conditions for the cooling tower plume from a 335 MWe fossil-fired plant located inland in West Germany. The Lünen tower represents a small source of heat and moisture release. The 14 Chalk Point data sets include 7 December cases and 7 June cases from a tower for a 630 MWe fossil-fired plant located on an estuary in Maryland. The Chalk Point tower represents a moderate source of heat and moisture release. From Paradise, Kentucky, we have 13 data sets taken in the winter at a single tower rejecting heat from a 1100 MWe fossil-fired plant. The Paradise tower represents a large source of heat and moisture release. Consequently, a balance of source sizes is represented in the field data.

Figures 1-21 summarize selected model/data comparisons for 20 sets of visible plume data. On the left-hand side of each figure is a two-dimensional presentation of the visible-plume outline. The abscissa is distance from the tower centerline along the direction of prevailing wind, and the ordinate is height above ground level. The vertical distributions of ambient conditions are given in the right-hand side of each figure; the symbols represent points of actual measurement. Note that the scales, both horizontal and vertical, are varied to illustrate the great disparity in the extent of visible plume predicted by the models.

To aid in quantifying model reliability, we have listed in Table 8 some relatively simple statistical indices of model performance, obtained from the 39 single-tower cases listed in Table 7. These indices are all based on the ratio of the predicted to observed length and height of the visible plume, which we denote by ρ. Excluded from the averages are those cases in which $\rho_i > 5$ or $\rho_i < 0.2$ so as to minimize the impact of a few very poor predictions. We have instead tabulated the number of cases that are within a factor of 5 in the column of Table 8 labeled N_5. Also tabulated is the number of times the prediction falls within a factor of 2 and 2.5 (for visible plume length). In interpreting the columns N_2 and N_5, one should note that the total number of single-tower cases was 39. The ρ_i distribution is further characterized by its range, its simple arithmetic mean, and 10 raised to a power equal to the average of the absolute values of the logarithms of the ρ_i's. (See Table 8). This latter average was used since it handles overprediction and underprediction equally and since it weighs values of ρ_i near 1 more heavily than those far from 1. These simple statistical measures are not the only sensible choices, but do give important insight.

A critique of the formulation of each model and the discussion of our model/data comparisons is summarized on a model-by-model basis below.

DISCUSSION OF MODEL FORMULATIONS AND ANALYSIS OF MODEL/DATA COMPARISONS

The formulations of the 13 models will be summarily reviewed with our critical comments. Selected comparison graphs of the more than 215 available in our complete study are presented to show the significant features of each model's performance with the data. Finally, each model's performance based on several criteria using all 39 data sets is discussed in the final section of the paper.

Slawson-Wigley Model [3]

The general version of this model assumes a plume of circular cross-section with plume variables (defined here as total values rather than excess above ambient) distributed as top hat profiles. The general version does not make the bent-over plume assumption and allows for immediate condensation of liquid water in the plume whenever supersaturation conditions are computed. The energetics of evaporation of liquid water is, however, not treated. The computer code for the model is set up to allow for several simplifying assumptions to be applied to the general theory. Of those permitted, Slawson and Wigley suggest that best results can be obtained by making two simplifying assumptions defined upon input: (a) the bent-over plume assumption, and (b) the liquid water content of the plume at any cross-section is zero. The authors recommended the use of these options within the code for our validation work.

It should be noted that the assumption of no liquid water in the plume implies a very simple treatment of plume thermodynamics. Plume temperature and plume mixing ratio are varied due only to adiabatic mixing with ambient air, and to cooling with plume rise at the dry adiabatic lapse rate (see Tables 4-6). However, if adiabatic mixing produces water vapor above the local saturation value, then X_p is allowed to exceed the saturation value; i.e., the plume relative humidity is permitted to exceed 100% with σ remaining at zero. This plume relative humidity increase above 100% will often occur in the region of the plume just beyond the exit plane. The plume relative humidity begins at 100% (saturation) at the tower exit, builds up to values exceeding 100%, and then due to further entrainment during plume dispersion the plume relative humidity falls below 100%, at which time the plume is assumed to lose visibility. Thus this version of the model conserves the flux of water vapor by allowing plume supersaturation instead of employing the common device of creating a liquid water reservoir which is increased or decreased during plume dispersion. This treatment of plume thermodynamics is simplified because it ignores the energetic effects of condensation heating and evaporation cooling. The Lee-Batty model (to be discussed later) also assumes $\sigma = 0$, but limits X_p to the saturation value and loses water by discarding all condensate as it forms. Another difference between the two models is that the Lee-Batty model includes condensation heating while the simplified Slawson-Wigley model does not; both models do not account for evaporation cooling.

Slawson and Wigley treat entrainment by using the assumption on the entrainment velocity that $v_e = \alpha|w|$, where $\alpha = 0.3$. This assumption is the most common one used for models with the bent-over plume assumption, but Slawson and Wigley employ it for the generalized version of the model as well. It should be noted that Fan's assumption [22] reduces to $v_e = \alpha|w|$ when a bent-over plume is assumed. The model does not make the Boussinesq approximation.

The Slawson-Wigley model employs a separate formulation for the diffusion phase of plume dispersion; i.e., the region in which plume momentum and buoyancy have been dissipated and ambient turbulence predominates. Slawson and Wigley employ the criterion that when the plume velocity drops below 1/10 of the wind speed, ambient turbulence dominates plume dispersion. At that plume cross-sectional location, the plume's vertical velocity is set to zero yielding a mild discontinuity in plume slope. This cross section is used to match the initial phase of plume growth (from the integral model) to a Pasquill Gaussian diffusion model representing atmospheric turbulence. The matching is accomplished by conserving mass, momentum, energy, and moisture fluxes at that cross section. Further plume dispersion is computed with the same equations as the integral model except that the plume radius is determined from the vertical and lateral widths of the Gaussian distribution which themselves grow with distance downwind at a rate dependent upon the ambient stability according to Pasquill [23] curves.

The model predictions show a uniform trend with trajectories rising faster than the observed ones. This behavior seems to be due primarily to the absence of a vertical "pressure" or "drag" force. (Note that the bent-over plume assumption is equivalent only to a very strong horizontal force proportional to (v_x-u)). Because of the $v_x = u$ assumption, the behavior of this model's trajectories emphasizes a trend we have noted. All models in our study which do not augment entrainment with some additional momentum-transfer mechanism, predict trajectories lying above the observed ones. Absence of downwash effects, as with all other models studied, also contributes to the trend, especially for high wind speeds. A study of the plume data [24] suggests that downwash effects are noticeable whenever $u_0/w_0 > 1.0$. Also, omission of the weight of liquid water in the vertical velocity equation contributes slightly, but noticeably, to the trend of higher plume trajectories which can be seen particularly for visible plumes which level off before disappearing such as the one in Fig. 1.

The predicted visible plumes in this model seem to be generally short and somewhat low. In fact, for 21 of our 39 cases, the predicted visible plume length was more than 50% shorter than the observed length. The absence of thermal inertia in the plume seems to be partly responsible, but the major effect seems to be that 0.3 for α is too large as an entrainment coefficient, and generates too great a dilution. Our experience with this form of entrainment assumption suggests lower values for better model-data agreement. Fig. 10 illustrates one of these short predictions. We found that for the cases with a low ambient humidity such as the Chalk Point cases for June, where essentially no condensation occurs, the Slawson-Wigley model shows no visible plume. On the other hand, when ambient relative humidity exceeds

410

90%, the model's predicted plumes are very long. No clear physical reason for this behavior is evident. For other comparison graphs for this model, see Figs. 2 and 11.

Slawson (Closed-Form) Model [4]

This model is a version of the Slawson-Wigley theory [3] which contains sufficient simplifying assumptions to provide a closed-form solution to the governing equations. The assumptions made are (a) bent-over plume assumption, (b) no liquid water in the plume ($\sigma=0$), (c) the Boussinesq approximation, and (d) simplified representation of ambient meteorology including uniform wind speed, constant temperature lapse rate and constant dew point lapse rate. These four simplifications are sufficient to allow an exact integration of model equations resulting in a set of algebraic equations for plume temperature, mixing ratio, vertical velocity, radius, and plume centerline height as a function of downwind distance.

The method used by Slawson to define ambient parameters is worth reviewing. The uniform wind speed (equal to plume horizontal velocity) is taken as the average value of the horizontal wind speed over the plume rise region. This average value is estimated by successive iteration. First, the tower top wind speed is used to predict maximum rise above the tower. Once this rise is obtained, a linear least-squares fit is made to the wind profile over this height and the value at half maximum is computed. Then the rise is predicted using the improved value. Two iterations are specified to avoid the possibility, which occurs in some cases, of indefinite oscillations in the value of the average wind speed calculated. Slawson also assumes that the dew point lapse rate and temperature lapse rate are constant with height. The appropriate average value is obtained by iteration and linear least-squares fitting as done for wind speed after an initial estimate is made.

The Slawson model is the only model reviewed in this study which attempts to account for plume downwash effects. This is accomplished through an empirical modification of the closed-form expression for the plume center-line trajectory. The empirical modification of the trajectory equation was fixed through fitting to 13 plume trajectories from the Paradise plumes. The expression effectively reduces the height of the plume at any downwind distance under downwash conditions. The empirical modification causes the plume height to decrease more rapidly than usual with increasing tower-top wind speed and vertical wind shear for downwash conditions. The increased effect of downwash on entrainment is not considered by Slawson. Slawson employs the same entrainment function as used in the Slawson-Wigley theory.

It should be pointed out that this closed-form model has received more attention by Slawson than the numerical Slawson-Wigley model in terms of calibration to field data. The Slawson model has been used rather extensively for environmental impact calculation due to its simplicity and to the fact that the environmental data usually available is not very detailed and is

411

thought to be adequately represented by the above simplified treatment.

The closed-form model shows better results in comparison to the field data than does the Slawson-Wigley model. This is true in spite of the more accurate treatment of ambient meteorology and plume dynamics employed in the Slawson-Wigley approach. We believe that the source of improvement seen in the Slawson model is in the calibration to actual field data of the entrainment function and downwash coefficients. [The entrainment coefficient $\alpha = 0.3$ used in the Slawson-Wigley model was actually obtained through calibration of the Slawson model to field data. The appropriateness of that coefficient to the Slawson-Wigley equations needs to be tested.] The performance statistics of the Slawson model is on a par with the most competitive models. The model performs better than 9 of the other 12 models tested. The model yielded predictions for all 39 single-tower cases, yet predicted no visible plume for one summer Chalk Point case. Predicted visible plume lengths tended to be short, consistent with the behavior of the Slawson-Wigley model. Visible plume rise predictions were more evenly distributed with both over and under predictions occurring. Trajectory predictions of the Slawson model were improved over those of the Slawson-Wigley model predictions in cases with large observed downwash (see Fig. 3). The added entrainment probably present with downwash is not represented in the model, which may help explain the length overprediction seen in this Figure. Plume trajectory predictions were generally good for the duration of observed plume visibility, and some impressive fits were achieved, as shown in Fig. 4. Further comparisons may be examined in Figs. 16-21.

Weil [5]

The model assumes a circular plume cross-section with top-hat profiles of plume variables, although a more general theoretical formulation is presented as well. Weil also introduces the Boussinesq approximation. In the buoyancy term (see Table 3) of the vertical momentum equation, several small approximations are made. The model assumes an entrainment rate proportional to $\beta |w|$ with $\beta = 0.55$. This value of entrainment coefficient is the largest value chosen for this parameter among the models reviewed that use this entrainment equation. Weil introduces no pressure or drag forces in the model and, as a result, only entrainment affects the change in the horizontal plume velocity, and only buoyancy augments entrainment in the vertical momentum equation.

The Weil model fully represents the major thermodynamic processes in the plume. The equation for temperature change in the plume (Table 4) correctly includes the effects of adiabatic mixing and the energetics of evaporation and condensation. The treatment of moisture thermodynamics leads to the factor $(1+\alpha)^{-1}$ in the equation for dT_p/ds (see Table 4); the term $-\gamma_d(1+\alpha)^{-1}$ is the saturated adiabatic lapse rate. Note that the factor $(1+\alpha)^{-1}$ affects the other two terms on the right-hand side of the dT_p/ds equation as well. In the model, liquid water is allowed to build up in the initial stages of plume dispersion due to condensation, heating the plume. As the

plume disperses, the liquid water is allowed to evaporate, cooling the plume until the plume mixing ratio drops below its saturation value. From that point on, simple mixing and adiabatic cooling govern the plume dispersion.

A comparison of model predictions to field data reveals that the Weil plumes typically rise above the observed plumes and lose visibility rather rapidly. The explanation for this is partially that the model has no pressure or drag forces to augment entrainment and buoyancy in the transfer of momentum and the consequent bending of the plume. Fig. 5 illustrates a typical Weil prediction. Due to the large entrainment in the model, the plumes spread rapidly and disperse the moisture rapidly leading to a shorter visible plume. For other plume predictions of the model, see Figs. 6, 7, and 9.

The model does not compare favorably with the better models as may be seen from the model's performance statistics given in Table 8. In fact 20 of 39 visible plume rise predictions have p_i values below 0.5 and 33 have values below 1.0. In terms of visible plume length predictions, 34 of 39 ratios p_i lie below 1.0 and 31 of 39 are less than 0.5. The model's basic formulation appears to be sound except for the items mentioned above and perhaps the need to add an atmospheric diffusion phase to the model. The model should give better predictions when corrected and calibrated to the data to determine β.

Frick Model [6]

The philosophy of the Frick model rests heavily on the assumption of an elliptical cross section at each downwind location. Several experimental observations reported in the literature indicate that single vertical jets in a crossflow have cross sections that are horse-shoe-shaped (elliptical as an approximation) rather than circular. Altering the round-plume hypothesis in favor of an elliptical plume cross section directly impacts entrainment in the Frick model since Frick assumes that entrainment is directly proportional to the area of the projection of the (elliptical) cross section on a plane normal to the wind direction. Use of an elliptical cross section will provide a larger entrainment into the plume than the corresponding round-jet assumption.

The Frick model is set up for top hat profiles of plume variables. The Boussinesq approximation is used. The semi-major axis of the plume is "a" (in the horizontal) and the semi-minor axis is "b" (in the vertical). While important in determining the actual value of the entrainment rate, the equations for the separate growth rates of a and b with centerline distance are not detailed here. The main effect of the ellipticity can be seen in the Frick model entrainment rate formula (see Table 1) where μ contains factors such as $(a/b)^{(1/2)}$ which increases the entrainment rate with increasing ellipticity. The model's equation for μ contains no adjustable constants since it is based instead on an assumption that for any given plume slice, the ambient air which impinges on the portion of that slice which is exposed to the oncoming ambient wind is fully entrained.

Since the area exposed depends on the growth of a and b, and since that growth is, in turn, dependent on µ, one must solve Frick's set of equations in a consistent manner to obtain µ. This explains the complicated form of the velocity-dependent factor in $\alpha(s)$ for the Frick model in Table 1. That factor, $\{1 - (uv_x)/(v^2)\{1 - (uv_x)/(2v^2)\}\}^{-1}$ will vary from 1.0 initially to (a) values slightly below 1.0 if $uv_x/v^2 > 2.0$, (i.e., if the windspeed greatly exceeds the plume exit velocity) and to (b) a value of 2.0 for a fully bent-over plume. During the rise of the plume, the term in the entrainment velocity $\pi^{-1} \sqrt{a/b}$ (u/v) |w| tends to dominate especially at first. The resulting values of µ are considerably larger than for other models initially and throughout the region where the plume is bending over strongly.

Our model statistics summary (Table 8) and Figures 6-7 show that this model predicts very short visible plumes compared to observed. (See also Figs. 5 and 9.) Final length predictions average 1/3 of observed values. The predicted centerline trajectories are reasonably close to the observed ones over the predicted visible portion of the plume. As expected, the model also consistently predicts a lower final visible plume rise in accord with the short final length trend. The Frick equation for vertical velocity variation is common, accounting for the expected velocity decline due to entrainment, and containing the usual buoyancy term. The model assumes no vertical drag force.

The treatment of moisture thermodynamics does not follow common practice. The model documentation suggests that the standard equation for dT_p/ds is used, allowing for (a) adiabatic mixing with ambient air, (b) adiabatic expansion with plume rise and (c) latent heat either released to (condensation) or absorbed from (evaporation) the plume. (Frick neglects the variation of saturation mixing ratio with pressure). The usual equation for this is

$$\frac{dT_p}{ds} = (1+\alpha)^{-1} \left\{ -\gamma_d \frac{w}{v} - \mu((T_p - T_a) + \frac{L}{c_p} (X_p - X_a)) \right\} \quad , \quad (3)$$

where $\alpha = (L/c_p)(dQ_s/dT)$ evaluated at $T = T_p$ and Q_s is the saturation mixing ratio at plume temperature. Eq. (3) is typically applied in computer codes in a sequence following the steps (a), (b), and (c) above. Step (c) is carried out to return the plume state to the saturation curve, if indeed the plume is saturated, and is usually carried out through an iteration procedure to properly locate the plume on the saturation curve. However, in the actual coding of the iteration for step (c) the equation used by Frick is, instead,

$$\frac{dT_p}{ds} = -\gamma_d \frac{w}{v} - \mu (dQ_s/dT)^{-1} (X_p - X_a) \quad (4)$$

The second term in Eqn. (4) is the limit as $L \to \infty$ of the term proportional to µ in Eqn. (3), and the first term is the limit as $L \to 0$ of the saturated adiabatic lapse rate, $(1+\alpha)^{-1} \gamma_d$. Since α ranges between 0.3 and 4.0 over

normal plume temperature limits, the differences between Eqn. (3) and Eqn. (4) are substantial, and use of the limits on L do not provide an accurate approximation. The plume is forced to remain at $X_p = Q_s(T_p)$ by the coded model logic, (see Table 5), but T_p will drop too fast and consequently X_p will drop too fast when Eqn. (4) is used. Effectively, then, water vapor is not conserved and disappears from the system. This effect, while secondary to the large entrainment rate in magnitude, also serves to shorten the predicted visible plume. In fact, the equation for liquid water flux effectively implied by the Frick model equations is

$$\frac{d}{ds} \left[\phi_m (X_p - X_a + \sigma) \right] = - \phi_m \frac{w}{v} \frac{dX_a}{ds} +$$

$$\phi_m \left\{ -\beta\gamma_d \frac{w}{v} + \mu \frac{c_p}{L} \left[(T_p - T_a) - \frac{1}{\beta} (X_p - X_a) \right] \right\} . \tag{5}$$

The terms containing μ are normally negative throughout the dispersion of most plumes, except for a short initial region where adiabatic mixing usually causes additional condensation. (Derivation of Eqn. (5) is obtained directly from the Frick model equations in Tables 4-6). Using the correct equations for T_p, X_p and σ which conserve total water will lead to Eqn. (5) with only the first term on the right-hand side.

Recall that the Frick model ignores the pressure dependence of the saturation mixing ratio, using a standard value of pressure of 1020 mb. Since the errors in computing X_p and X_a have the same trend, this approximation has little effect on the predictions.

The trajectories predicted from the Frick model all lie above the observed trajectories; i.e., the predicted plumes bend over too slowly. This behavior seems to be a persistent feature of all models which do not use a strong "pressure" force or bent-over plume assumption, and instead modify the plume's horizontal momentum only by means of the added momentum of entrained ambient air.

Winiarski-Frick Model [7]

This model is similar in structure to that of Frick and is a later version of the Winiarski-Frick model presented in Ref. 25. The plume is assumed to have a circular cross-section and top-hat profiles of plume variables, at least in the initial phase. The Boussinesq approximation is not used. In terms of plume dynamics, equations for the entrainment rate, horizontal velocity, and vertical velocity appear in Tables 1-3.

The model allows for two possible entrainment mechanisms: (1) impingement, in which the momentum of all of the ambient air which is directed towards the "exposed" portion of the plume surface for any given cross-sectional slice is transferred to the plume, and (2) aspiration, in which ambient is drawn into the plume as a result of the turbulence induced by the difference between the plume centerline velocity and that component of the ambient velocity parallel to the plume centerline, $|v - u \cos \theta|$, representing a

shearing action. Winiarski and Frick believe that the impingement mechanism is predominant in moderate to large wind situations and the aspiration mechanism is important in very weak wind conditions. Actually the mechanisms will overlap and it is difficult to ascertain how much entrainment is due to each one. Their numerical studies have indicated that the most fruitful assumption is that the larger of the two mechanisms at any downwind distance is to be used to represent the total entrainment mechanism. An anomaly exists in the functional form for the impingement entrainment function. The entrainment rate due to impingement near the tower exit becomes infinite when the wind speed is approximately $\sqrt{2}$ times the exit velocity and becomes negative when the wind speed exceeds this value. The negative value does not cause any computational problems since the maximum value of entrainment and impingement is used at any cross-section. The physical validity of the functional form of entrainment by impingement (see Table 1) is, however, questionable.

It is interesting to compare the magnitude of the entrainment by impingement in the Winiarski-Frick model with the entrainment rates in other models. Rewriting the Winiarski-Frick impingement-entrainment velocity as αw, we may compare the value of the complex function that defines α with the constant values of 0.3 and 0.55 as chosen by other modelers. Sample numerical evaluations of the Winiarski-Frick α reveal it to be much larger than the range 0.3-0.55. As a result, Winiarski-Frick plume predictions should be short due to excessive dilution with centerline trajectories lying somewhat above observed ones. This is based also on the fact that this version of the Winiarski- Frick model does not include any drag force mechanism to augment plume bending and does not include the "virtual mass" concept used earlier [25] which would cut down the effect of plume buoyancy. As a result, we would expect to characterize the model's predicted plumes as very short and consequently low as compared to observed plumes.

However, an additional feature of the model serves to lengthen the predicted plumes by a large amount. The top hat assumption requires the moist plume to be fully-mixed laterally so that the temperature and humidity are uniform. This complete mixing laterally may imply that the plume is below saturation at a particular cross-section. Experimental data have shown that plume variables follow more bell-shaped distributions than top-hat profiles. However, distributing the same amount of energy and moisture so that peak values occur at the center with minimum values along the edge may result in a condensed visible core with an invisible, subsaturated outer region. This smearing of the top-hat distribution into a bell-shaped distribution will clearly lengthen plume predictions. Winiarski and Frick chose the following profiles for excess temperature and water vapor,

$$\Delta T(s,r) = \Delta T_c(s) \ \frac{\cos\ (r\pi/R)\ +\ 1}{2} \ ; \ \Delta Q(s,r) = \Delta Q_c(s)\ \frac{\cos(r\pi/R)\ +\ 1}{2}$$

where s is the centerline distance from the tower, r is the lateral distance, $\Delta Q_c(s)$ and $\Delta T_c(s)$ are the centerline (peak) values of the new distributions $\Delta T(s,r)$ and $\Delta Q(s,r)$ defined above ambient values.

416

These profiles apply only for downwind distances beyond the point where the plume has lost visibility ($\sigma = 0$) with the top-hat differential equations. Winiarski and Frick define at this evaporation point the lateral profile of ΔT and ΔQ by conserving energy and moisture. (i.e., area under ΔT and ΔQ curves match the corresponding area obtained from the top-hat profile). Interestingly, ΔT_c and ΔQ_c become 3.37 times the corresponding top-hat values leading to a supersaturated central region of the plume which extends laterally to 63% of the computed top-hat radius. The original equations with the top-hat profile assumption are employed to calculate the invisible radius R with downwind distance. This R also is used to characterize the growing width of the two cosine functions above. The amount of lengthening is very significant in most cases. The Winiarski-Frick equations imply that the mass flux through the plume cross section where the cosine distribution predicts loss of visibility contains precisely 3.37 times the mass flux in the plume at the point of evaporation of the initial top-hat plume. Another limitation of the model is that ambient conditions at the point of evaporation are used in the mixing relationships defining plume visibility when the cosine distributions are operational, rather than local ambient conditions at the cross section under study. To us, the use of a bell-shaped distribution after visibility has ended, according to the top-hat differential equations, is primarily a method to extend plume length and represents part of the calibration procedure of the model to data. It should be noted that Winiarski and Frick calibrated the model to data not by adjusting coefficients but by testing numerous different physical assumptions until a combination which seems to agree with data was determined.

Model/data comparisons for the Winiarski-Frick model appear in Figs. 5-7 and 9. Note the discontinuity in the visible plume outline. The discontinuity is located at the point where visibility ends for the top-hat plume. This point of evaporation results from solving the full thermodynamic and dynamic equations describing plume development. Up to this point, plume equations were solved using the top-hat assumptions only; beyond that point, the cosine distribution for plume temperature and moisture was employed from which a smaller visible radius of the supersaturated core becomes the visible radius.

The model's performance places it in the group of the four most competitive models. Its rise predictions are the best of all models studied, and the length predictions, while usually short, place the model among the top three for visible plume length predictions. This seems surprising in view of the fact that the equations governing the visible core, which normally accounts for most of the predicted visible plume length, omit a number of physical effects usually considered important to include in predicting lengths. Recall that no liquid water reservoir or energetic effects of condensation and evaporation are involved in the use of the bell-shaped temperature and moisture distributions. However, as mentioned above, Winiarski and Frick have calibrated the model to a larger data base than other modelers have used, including single-phase data and some Lünen and Chalk Point data. Also, the calibration has not been done by selection of values for adjustable constants, but by varying the model's physical assumptions, in ways illustrated by the choice to use entrainment by impingement or aspiration, but not both.

ORFAD (Oak Ridge Fog and Drift Model) [8]

In the ORFAD model, the concentration of water vapor emitted by the cooling tower is assumed to be dispersed in the atmosphere in a Gaussian manner about a centerline trajectory computed from a Hanna-Briggs plume rise formula. The spreading rate of the Gaussian distribution depends on the Pasquill stability class estimated from local meteorological parameters. [For the model/data comparisons at Paradise, the appropriate meteorological data were not available and consequently we obtained the lapse rate from on-site soundings.] ORFAD calculations are traditionally made with reliance solely upon ground-level data for the state of the ambient atmosphere. Unfortunately, no correction of the measured ground-level wind speed is made in order to estimate its value at plume height for input into the Hanna-Briggs trajectory formula. As a result, the use of these smaller ground-level wind speeds leads to predicted centerline trajectories which rise much above the observed trajectories. Use of a power-law wind speed profile to estimate elevated winds from ground-level measurements should provide some improvement in the predicted trajectories.

Two additional theoretical weaknesses exist in the ORFAD model. First, in considering the effect of the ground as a boundary to the dispersion of water vapor, ORFAD does not reflect the Gaussian tail of the plume water vapor from the ground, but merely doubles the plume water-vapor concentrations at all heights. More importantly, the model assumes that the ambient concentration (gm/m^3) of water vapor at the ground is the same for all heights; thus, when $dT_a/dz < 0$, ORFAD predicts a "cloud layer" or fog at and above the height where the water-vapor density obtained at ground level begins to saturate the ambient air. When natural cloud layers were reported as present in some data cases, this procedure was seen to underestimate their heights severely, and it often gave cloud-layer predictions on clear days. When $dT_a/dz < 0$, the visible plume predicted by ORFAD can rise into this cloud layer without ever terminating. The ORFAD plume terminates only if the lapse rate is positive or if conditions are very dry or windy. In only 12 of 39 test cases did the model give definite predictions. These 12 cases normally had either inversions or were very stable with low humidity. The twelve definite predictions can be classed as uniformly long and high at the point of disappearance, in accord with the trajectory trend noted above and the overestimation of plume water vapor. One of these plume predictions is shown in Fig. 8. The overall predictive ability of this model for visible plume outline is the weakest of all models tested. Our major criticism of the model formulation is that the simulation of the plume as a spreading Gaussian distribution of fog about a centerline is physically incorrect. The plume spreads due to the coupled effect of plume buoyancy, momentum, interaction with the ambient wind, and plume moisture thermodynamics. The ORFAD model basically assumes that ambient turbulence is spreading the plume moisture about a pre-determined plume centerline. An additional problem with the Gaussian approach is that it ignores the possibility of natural adverse gradients of water vapor concentration near the ground that would prevent the downward dispersion of plume vapor to the ground. To us, the physical picture used in ORFAD of the dispersion of moisture is incorrect as a basis for plume or, ultimately, ground-fogging predictions.

418

Hanna [9]

The framework of the Hanna model is similar to many other models. However, a few interesting modifications have been made. Hanna recognizes the apparent paradox that a model, through entrainment alone, cannot predict the correct trajectory, spreading, and dilution simultaneously. Hanna, therefore, employs Briggs' suggestion [26] as to a possible resolution of the apparent paradox. Briggs argues that the change of the momentum flux with height depends partly on the fact that ambient air above the rising plume must also be accelerated. With this reasoning the effective radius of the "momentum plume" is therefore larger than the radius as determined from temperature differences. Hanna follows Briggs who suggests that for bent-over plumes $\partial R_m/\partial z = 0.6$ for the momentum plume (R_m = momentum radius) and $\partial R_t/\partial z = 0.4$* for the temperature plume (R_t = temperature radius). Consequently, the ratio, E_m, of the effective momentum flux to the momentum flux within the temperature plume approaches $(0.6/0.4)^2$ or 2.25. Hanna's second major modification relates to a separate radius for the moisture plume. Hanna claims that observations by Slawson et al. [27] and Meyer et al. [28] indicate that visible plume lengths are consistently underpredicted by basic plume models, due to the fact that inhomogeneities in the plume can result in locally saturated spots, even though the plume may be unsaturated on the average. So the use of a smaller R_w than R_t and R_m, is meant to represent the inhomogeneity of the plume, where only part of the disturbed-flow region is pictured as being occupied by saturated, heated plume air. Hanna simulates this by assuming that the ratio, E_w, of the cross-sectional area of the moisture plume to the temperature plume approaches 1/2. In terms of the rate of change of the radius with height, this assumption can be written $\partial R_w/\partial z = 0.71 (\partial R_t/\partial z)$ where R_w is the radius of the moisture plume.

Hanna assumes top hat plume profiles for all variables. The plume cross section is taken to have a central circular core $R \leq R_w$ and two annular regions $R_w \leq R \leq R_t$ and $R_t < R < R_m$. Each region has different properties. In the central core of radius R_w, all plume variables have their elevated values. In the first annulus, of inner radius R_w and outer radius R_t, the temperature and velocity differ from ambient values, but the vapor mixing ratio and liquid water mixing ratio have ambient values. In the second annulus, of inner radius R_t and outer radius R_m, only the plume velocity differs from the properties of the ambient flow. All three radii are initialized to $R_{eff} = R_0(w_0/u_0)^{1/2}$, where R_0 is the tower exit radius, w_0 the plume exit velocity and u_0 the windspeed at tower top. (Note that this choice of R_{eff} does not conserve mass flux, but increases it as if the exit diameter were larger. Since the model uses the bent-over plume assumption, $v_x = u$, the correct choice to conserve mass flux should be $R_{eff} = R_0 (w_0/v_0)^{1/2}$, where $v_0 = (w_0^2 + u_0^2)^{1/2}$.) As the plume disperses, the ratios of the radii approach the limits $R_w/R_t = 0.707$ and $R_m/R_t = 1.50$ alluded to above. Thus, the model really has three different entrainment rates. To compare them approximately one can consult Tables 1 and 4. The entrainment rate for the "momentum plume" (see Table 1) is approximately $2(0.6)w/(R_w v)$, whereas that for the "temperature plume", (note the $(T_p - T_a)$-term in Table 4) is approximately

---

*Hanna actually uses the equation $\partial R_t/\partial z = 0.4 - [(R_t/2u) \partial u/\partial z]$ for bent-over plumes. This last term is usually small and is meant to account for stretching of the plume as it rises through layers of wind shear.

$2(0.4)w/(R_t v)$. Since $(0.6)/R_m \to (0.4)/R_t$ as s becomes large, these two entrainment $\overline{\text{rates}}$ are comparable in effect. The entrainment rate for the "moisture $\overline{\text{plume}}$" is (as seen from the $(X_p - X_a)$-term in Table 4) $2(0.2)w/(R_w v)$. Thus, the dilution of plume moisture and liquid water occurs at about half the rate as that of the dilution through mixing and lowering of plume temperature. As a corollary, due to the different radii, the effects of condensation or evaporation on plume temperature are reduced as seen in the E_w contribution to the factor $(1+E_w \alpha)^{-1}$ for dT_p/ds, (Table 4). Otherwise the term would have represented the saturated adiabatic lapse rate of $(1+\alpha)^{-1} \gamma_d$; thus, in this model, a smaller central region of moisture is contributing energy effects over a larger region of temperature elevation.

It should be noted that the actual form of Hanna's equations as used and shown in the Tables only satisfy the conservation laws for large s, since his entrainment factors are all the constant large-s limits of the variable ones implied by the radial growth assumptions, $(dR_w/dz) = (.71) (dR_t/dz)$ and $(dR_m/dz) = (1.5)(dR_t/dz)$. It would be relatively simple to modify the code to satisfy the conservation laws exactly throu_hout plume rise.

The model generally predicts accurate plume trajectories, with a slight tendency for predicted trajectories to lie above the observed ones. (See Figs. 1,10). The visible length predictions are among the best of all models with an absolute log-mean average length ratio of 1.57, (see Table 8). Very few predictions lie below 0.2 of the observed values or above 5.0 of the observed values. Predictions of visible plume rise are likewise among the best with an absolute log-mean average rise ratio of 1.67, and only 4 of 39 predictions are incorrect by more than a factor of 5. A drawback of the model as formulated is the lack of any logic to follow plume dispersion beyond maximum rise, leading to no definite plume length predictions in 14 of 39 single-tower cases included in this study. As can be seen from Fig. 1, illustrating one of these ambiguous predictions, an added atmospheric diffusion phase could improve overall model performance by providing predictions in all cases. The model predicts long and high plumes for high wind cases; i.e., above 9 m/s average wind speed, probably due to omission of the effects of tower downwash. Also, in cases of high ambient relative humidity; i.e., above 85%, especially in neutral-to-unstable conditions, a problem exists in the performance of this model, as it tends to overpredict plume length considerably in these cases; (see Fig. 11, another non-terminating case).

It is interesting that the Hanna model is among the best performers. Undoubtedly the choice of three different radii for the plume is an important component. There is experimental evidence from studies of jet mixing in air that the turbulent spreading rate for momentum is greater than the corresponding spreading rate for heat, which supports the assumption $R_m > R_t$. But, in reviewing, our model/data comparisons for all models, there is no trend to show that predicted plume lengths are shorter than observed. This would weaken the motivation for the assumption that $R_w < R_t$.

Tsai-Huang (Stone and Webster) Model [10]

The Tsai-Huang model assumes a circular cross-section. The model is one of the two which assumes Gaussian profiles for all plume variables. The equations for the plume are actually applied after the plume has passed through a zone of flow establishment in which jet profiles change from uniform at the tower exit to Gaussian distributions at the end of the ZFE. Tsai and Huang obtain characteristics for the ZFE from the data of Fan [22] (centerline length of ZFE and trajectory angle at end of ZFE). However, the actual equation of the plume trajectory is not known; consequently, Tsai and Huang assume a parabolic equation for the plume trajectory from which the coordinates at the end of ZFE can be determined. As a result of the parabolic assumption, the empirical bending used by Tsai and Huang is made somewhat arbitrary. The density deficit at the end of the ZFE is taken as one-half the initial value. On the other hand, the plume velocity and mixing ratio are taken to be unchanged from the tower exit to the end of the ZFE. These then establish the initial conditions for the integration of the model's differential equations for ZFE which are listed in Tables 1-6.

The zone-of-established flow portion of the model uses Abraham's [29] modification of Fan's theory[22] of vertical jet discharges in a crossflow. In this theory, entrainment is defined as the sum of two terms, the first (predominant in the very near field) developed from the theory of nonbuoyant jets in stagnant ambients and the second (predominant as jet momentum subsides) taken from the theory of buoyant thermals in stagnant fluids. The model also considers a drag force operating normal to the jet centerline.

The model does not consider condensation, evaporation or liquid water effects in plume dynamics. The discharged moisture mixes with the ambient air by simple mixing as in the Slawson-Wigley model. The plume is assumed to be saturated as it leaves the tower and no longer remains visible when the mixing of the plume with colder ambient air reduces the temperature to a point at which the moisture at the plume centerline is just below saturation level for that temperature. The thermodynamics of the plume are thus greatly simplified.

It is useful to compare the Tsai-Huang equations to the more traditional equations; e.g., those of Slawson and Wigley. Examining Tables 4 and 5, the following differences occur: (a) Tsai and Huang replace the dry adiabatic lapse rate in the dT_p/ds equation by the actual ambient lapse rate, and (b) Tsai and Huang add $(w/v) \, dX_a/ds$ to the equation for dX_p/ds. Under near-neutral and well-mixed conditions these terms will give the same effects as those present in the Slawson-Wigley model. However, under stable conditions, the plume temperature will decrease too slowly and the plume mixing ratio will behave in some unpredictable fashion. The Slawson-Wigley equations represent the usual theory for a model, such as Tsai-Huang, which assumes absence of liquid water and the neglect of condensation/evaporation energetics.

Predictions of this model tend to have lower final rise values than do the

observed plumes. Of the predicted-to-observed rise ratios, 28 out of 39 lay below 1.0. The empirical trajectory used to define the zone for flow establishment seems to be responsible. Most predicted plumes show a rapid bent over, followed by an artificial "lift-off" perhaps due to residual buoyancy in the plume (see Fig. 12). Apparently the slope of the centerline at the start of the established flow region given by the parabolic trajectory is not consistent with the actual residual buoyancy and horizontal and vertical velocities of the plume. Thus, the overall plume rise would be artificially lowered. In addition, ZFE relationships are being used here outside their range of established validity, especially for small values of u_0/w_0, as represented by the case shown in Fig. 13.

An interesting feature of the Tsai-Huang model is that the predicted plume tends to be very long whenever it remains visible as it reaches fully bent-over conditions. When the slope of the plume centerline is small, the entrainment becomes nearly zero. (One term in the entrainment function drops out and the other is very small). Plumes will travel long distances downwind with very little entrainment. This tendency of very reduced entrainment is underscored in high-humidity situations (Lünen S-6, for example), leading to extremely long visible plumes. When the plume levels out, entrainment vanishes and since $\mu \to 0$ the temperature equation becomes $dT_p/ds = dT_a/ds$. Thus, the predicted plumes never show vertical oscillations at the Brunt-Vaisala frequency as they level off but rather extend to extremely great lengths with no apparent change in plume variables. Seven of the 39 predicted plumes for this model were of this type, with the plume failing to terminate at any reasonable downwind distance.

The model's length predictions were among the best, especially when both the ρ_i-ratio in Table 8 and the model's degree of reliability are jointly considered. The rise predictions should also be considered state-of-the-art as seen from the Table. For the model to be useful for environmental impact studies, the stage of the plume when it is fully bent-over needs to be treated correctly with introduction of a non-zero entrainment velocity after rise ceases.

Lee-Batty Model [11]

This model is similar in formulation to that of Weil and Slawson-Wigley. The Batty-Lee and Slawson-Wigley models both use the bent-over plume assumption. The Lee-Batty modifications of the Slawson-Wigley model are in these major areas. First, an elliptical cross section is used after maximum plume rise whenever the ambient stability class is not neutral; otherwise a circular cross-section is assumed. The eccentricity of the elliptical shape depends on the ambient stability class. Second, the entrainment velocity can differ from that used in the Slawson-Wigley model, depending on the value of certain ambient parameters -- namely, the wind speed, ambient lapse rate, and eddy-dissipation rate. Different functional forms of the entrainment velocity are used, depending upon whether neutral or non-neutral ambient stability prevails, but these are only important at or near the point of final rise.

422

Of the 39 single-tower plume length predictions given by this model, 27 were less than 50% of the observed values. We attribute this behavior primarily to overly-rapid dilution of plume air by ambient air, in view of the rather large value chosen for α of 0.4 (see Table 1). Because the model plume trajectories are also higher than the observed ones, the visible plume rise predictions, while low, are not as far below the observed values as one might expect. Figures 12 and 13 serve to illustrate typical predictions of this model.

One other major feature of model formulation contributes substantially, and sometimes predominantly, to early disappearance of the predicted visible plumes, and to the elevated trajectories. In this model, no liquid water is allowed to build up in the plume, (see Table 6), in spite of the fact that (a) the saturated adiabatic lapse rate is introduced in the dT_p/ds equation, cf. Table 4, and (b) X_p is forced to remain at saturation with associated condensation heating during the first stages of plume dispersion (see Tables 4 and 5). So when additional condensation of plume moisture is expected; i.e., $(T_p - T_a) - \beta^{-1} (X_p - X_a)$ is positive or, equivalently, the plume state after simple adiabatic mixing with entrained ambient fluid is supersaturated on the X-T diagram, then no liquid water is added to a "reservoir" for later evaporation. (The expected plume condensation should occur early in the plume dilution in most cases, when adiabatic mixing causes additional condensation of plume moisture.) Then, as soon as $(T_p - T_a) - \beta^{-1} (X_p - X_a)$ drops below zero, the model plume immediately is assumed to be subsaturated. At this point, the appropriate dry adiabatic lapse rate is used in the dT_p/ds equation, and the plume temperature and mixing ratio begin to change due only to simple adiabatic mixing. Instead of this procedure, collected liquid water should be allowed to evaporate when the plume state would otherwise fall below the saturation curve. The predicted plumes thus have no evaporative phase with attendant cooling of the plume air. Clearly, the Lee-Batty procedure fails to conserve water by a substantial amount.

In most models, the evaporative phase (during which the previously built-up liquid water gradually disappears reducing plume buoyancy) occupies the major portion of visible plume dispersion. Also, this model's visibility criterion demands that plume relative humidity falls below 97% before disappearance of the visible plume. This serves to lengthen the plumes somewhat relative to other models. Both the high trajectories and the extreme shortness of the predicted plumes can be traced in part to the omission of a liquid water reservoir in the plume and the absence of an evaporation phase.

Lee (NUS Corp.) Model [12]

The computer code for this model is proprietary to the NUS Corporation yet the major details on the model development are in the open literature. We were provided with an object deck of the computer code to run at ANL. We could not therefore verify the coding of the model, which limits the confidence we can place in results of our search for major causes of the model's predictive behavior.

The model accounts for entrainment from the theories of Morton, Taylor, and Turner [30] and Briggs [31]. A drag force is assumed to act normal to the jet centerline of the plume; the bent-over plume assumption is not made while the Boussinesq assumption is followed. Kessler's theory [32] of microphysics is applied to partition the total liquid water in the plume into cloudwater and hydrometeor components. Rainout from the plume is treated.

Visible plume rise predictions of this model rank among the top three or four (cf. Table 8). However, the plume length predictions are usually short, with 28 of 38 length predictions less than 50% of observed. Visible plume trajectories generally lie above the observed trajectories with the greatest deviations near the tower.

We converted the model's equations for plume temperature, mixing ratio, and liquid water into our standard form; these equations for plume thermodynamics appear in Tables 4-6. The equations simulate the energetics of both condensation and evaporation of liquid within a treatment of conservation of total water in the plume. After the plume has lost its liquid water through dispersion and evaporation, simple mixing equations are employed in the region of plume subsaturation.

Lee employs a common form for the vertical velocity equation (see Table 3), but an uncommon form for the horizontal momentum equation (see Table 2). The horizontal velocity equation retains a fairly weak "pressure-drag" force which increases v_x and an entrainment term, $-\mu v_x$, which actually acts to decrease v_x. The usual expression derived for a Gaussian model (such as the Lee (NUS) Model) is instead $+\mu$ $(u/2 - v_x)$ where the plume downwind coordinate satisfies $dx/dt = 2v_x$. The effect of using $-\mu v_x$ instead of $\mu(u/2 - v_x)$ should be to limit v_x to small values and prevent it from approaching the wind speed. We attempted to test this expectation through examination of the computer output for a number of cases. Although the printout of the object code does not give v_x, we were able to infer values of v_x from the plume slope and vertical velocity which were presented. We found that the horizontal velocity of the plume does not remain at small values and does indeed approach the wind speed but does so more slowly than most other models.

Two representative model predictions are given in Figs. 14 and 15, one in low winds and the other in high winds and both in cold temperatures. The model has no diffusion phase which would allow the plume to disperse beyond the first point where the updraft velocity becomes zero (maximum rise). However, it was only 4 of 39 cases in which the plume was still visible at maximum plume rise. Thus, in only those four cases, was visible plume length not predicted.

In 5 of the 39 cases, the predicted plumes showed no signs of termination after downwind integration of 5-10 km, and are regarded as yielding indefinite results. These anomalous cases occurred when the predicted plume had nearly leveled off at a height where the ambient air was saturated; the long

plumes actually result from inaccurate trajectory predictions in those cases.

Calabrese - Halitsky - Woodard (Pickard - Lowe - Garrick Inc.) Model [13]

The computer code for this model is proprietary although the details of the model formulation are in the open literature. We were not able to examine the computer code for the model, but instead we arranged to send input data for our 39 single-tower test cases to K. Woodard at Pickard-Lowe-Garrick, who ran the cases and provided us with model output. He chose not to use all of the ambient profile data for the computer runs, but instead extracted from the data only those values which would have been obtained from an on-site meteorological tower, as they would do in an assessment study for a new power plant.

The model employs a simple form of the Briggs-Hanna plume rise formulas. We do not provide details here since the proprietary values of the empirical constants are not available. A power-law extrapolation scheme is adopted to estimate elevated wind speed from ground-level values. The model uses Halitsky's empirically-derived formulas [33] for a flow establishment phase and an established flow phase of plume dispersion. The established flow formulas lead to the choice of widths for the final Gaussian diffusion phase. In the diffusion phase, where the plume has reached final rise, both excess enthalpy and excess water vapor (above ambient) follow Gaussian distributions which spread dependent upon the Pasquill stability class. The tail of the Gaussian distribution which would continue below the ground is treated by a method of reflection, which results in additional concentration added to the above-ground distribution. The model formulation is similar in spirit to the ORFAD model, but embodies a number of the improvements suggested earlier for the ORFAD treatment. The model is not formulated to provide predictions at wind speeds lower than about 1 m/s. Such plumes from NDCT's are considered by the modelers to have low environmental impact.

The predictive performance of this model was the best among the three semi-empirical models (ORFAD, Saame, and Calabrese-Halitsky-Woodard) and compares favorably with several of the integral models. The model performance is remarkable in view of the reliance on surface weather data.

The predicted plumes followed no clear trends with respect to the observed plumes, with the exception that the trajectories lay uniformly above the observed ones. This random behavior may be due to uncertainties in the extrapolation of surface weather data. Fig. 16 illustrates the inherent limitations of wind-speed extrapolation for a particular case showing an incorrect trend on plume trajectory. The 9 cases where complete predictions were not made is implied by the value of N_F in Table 8. These cases fell into two classes. First, there were extremely long predictions, where the outputs we received simply didn't include the end of the visible plumes; expanded runs would probably define these plumes. (Fig. 17 shows the model prediction for a very long case). Second, there were cases where no predicted plumes were shown at all: in summer on dry days, and in very low winds.

425

It should be noted that the first output point for the model prediction is 40 m downwind, and a finer grid would probably further define presently ambiguous cases. Thus, the model's overall reliability for giving complete (though not necessarily correct) predictions is probably better than the 9 missed cases would suggest.

Stephen - Moroz [14]

This model assumes a circular plume cross section with top-hat profiles and does not adopt the Boussinesq approximation. The bent-over plume assumption is made but the plume horizontal velocity is kept fixed at an <u>average</u> wind speed rather than being allowed to vary according to the ambient wind speed profile. The average windspeed, $\bar{u}$, is taken as the ambient wind speed at tower top.

The model's entrainment assumption is the most complicated of any studied to date. It attempts to include the additional effects of atmospheric turbulence by means of an empirical parametrization suggested by Briggs [32]. The entrainment function also includes a "cloud-phase" entrainment rate when the plume reaches heights in excess of 600 m above ground. The full degree of complexity of the entrainment assumption is apparent from Table 1.

The model adopts a Lagrangian approach to formulate the plume equations by following a plume parcel of length S into which ambient air mixes. To follow a fixed mass of (diluted) plume air, one must allow S to vary.* In the model, only the vertical mass flux, or the mass flux through a horizontal plane is conserved. A more correct choice would have been to take S/v to be a constant, where $v = (w^2 + \bar{u}^2)^{1/2}$. Thus, the mass flux through a plane normal to the plume centerline would be taken as conserved. In the model, then, as the plume vertical velocity tends to zero, so will S, and excessive radial growth of the plume is needed to "conserve" mass flux.

It is simple to translate the model's equations from a Lagrangian picture to the Eulerian picture adopted in our presentation of model equations. However, the reformulation of plume equations in terms of total mass flux, $VR^2\rho_p$, rather than mass flux through a horizontal plane, necessitates solving a system of implicit equations for the variation of primitive plume variables with centerline distance. The resulting complications in the model equations shown in Tables 1 - 6 may be a source of some of the unusual plume behavior predicted by the model. It should be noted that this model's equations do not lead to conservation of the usual fluxes. Further, the additional factors and terms do not lead uniformly to identifiable trends and effects. Thus, the discussion of this model's predictive characteristics must be more descriptive without much motivation from the manner of treatment of the physical effects.

---

*This is effected by taking S/w to be a constant throughout plume development. Thus as the plume vertical velocity tends to zero, so will S, and <u>excessive radial growth</u> is needed to "conserve" mass flux.

426

Notably, the model's radial growth is unrelated to any actual dilution of plume air taking place as in other models which define an entrainment function in an Eulerian scheme; rather, it is defined by the behavior of the vertical velocity and the conservation equation of mass flux through a horizontal plane. When the plume is still visible as w approaches zero, extreme radial growth results. See Fig. 17 for an example of this effect. However, the model does well for plumes rising in low winds, as shown in Figs. 18 and 19, as one might expect since the conservation of plume mass flux becomes better approximated by a vertical conservation equation and therefore the model treatment is more appropriate for these low wind situations.

The model trajectories tend to lie well above the observed ones, due mainly to the use of the tower-top wind speed as the average value; this tower top value is usually less than the average wind speed over the observed plume-rise region. The predicted plumes have a slight tendency to be long. This trend is strengthened by examination of the 13 out of 39 cases where w became zero before the predicted plume disappeared. Since the model makes no provision, as presently formulated, for plume dispersion after final rise is attained, these plumes can be considered as longer still. The predicted plumes also tend to have final rise values above the observed ones, for reasons mentioned above concerning the trajectories and horizontal lengths. It is interesting that the model's values for the absolute-log-mean ratio of predicted-to-observed lengths are among the best when one includes only the 23 of 39 cases where those ratios lie between 0.2 and 5.0. Also, on all measures of visible plume-rise, the model performed comparably with the best-performing models, although 28 of 39 of those ratios were above 1.0. This would seem to suggest that plume dynamics in the vertical direction are better represented by the model equations than for the horizontal direction.

Saame Model [15]

The Saame model is the third semi-empirical model tested in this study. Each of those models adopts a similar general approach. Water vapor and enthalpy are Gaussian-distributed about an empirically determined centerline. Ground-level atmospheric data are utilized and extrapolated upward as needed. Tower thermodynamics are also simulated to obtain initial water vapor and updraft velocity for the plume. These models, then, are set up to be directly useful in environmental impact assessment. However, the use of data at the ground to extrapolate to plume height and the simulation of tower flow behavior can not be as accurate as the direct use of measured values when available. Thus, much of the predictive inaccuracy of these three models, can be traced to the use of degraded input data. An interesting further study would be to test a modification of the models which would employ the best measured data for test cases, while at the same time, preserving the basic empirical formulations. This exercise would aid in discovering the inaccuracies in the formulations themselves.

In Saame's model, the usual stability-dependent Gaussian widths for the

water vapor distribution are introduced, as functions of downwind distance. Their form is based, again, on Pasquill's curves. A virtual origin upwind of the tower is located, such that the centerline water vapor concentration of the distribution through a vertical plane though the tower center equals the average water vapor concentration leaving the tower. The effective release height of the diffusing vapor is computed from the Carson-Moses formula [34] using a wind speed at tower top inferred from that at ground by a power-law assumption. The model does not attempt to follow the plume's trajectory from the tower exit to the effective stack height, but instead the plume outline begins and is directed horizontally at the effective height. Such an approximation is normally reasonable for calculation of pollutant dispersal far downwind, but corresponds poorly with visible outlines of relatively short plumes, which become invisible while still rising (cf. Fig. 12). The model uses the actual ambient relative humidity profile to delineate the region where plume water vapor saturates the ambient.

The predicted visible plume outlines in this model occur at heights uniformly above the observed outlines, even when the observed plume has reached final rise. Of the 39 ratios of predicted-to-observed visible plume rise, only 7 are less than 1.0 in value. Use of an average wind speed over the plume-rise region, rather than a tower-top value would generally improve this behavior. Also, the predicted visible plumes seem usually to be shorter than the observed plumes, with only 4 of 39 predicted-to-observed length ratios exceeding 1.0 in value. Fig. 20 shows one of the predicted plumes which is longer than the corresponding observed plume. The model fails to make a prediction in two very low wind conditions, but otherwise provides complete predictions. The model's performance statistics in Table 8 are competitive with the more inaccurate of the integral models. One of its better plume rise predictions is shown in Fig. 21.

DISCUSSION OF MODELS PERFORMANCE

Table 8 summarizes the performance statistics of each model. Numerous criteria may be established to determine which models perform best. Each criterion clearly is arbitrary to some degree. For example, we might choose the better models by the number of cases the models predicted plume characteristics within a factor of 2. On the other hand, one might want to choose a model that gave the fewest complete misses (i.e., a large N_5 count). A criterion which seems to separate the better performing models (trajectory, spreading, visible plume properites) is the following: model predictions are within a factor of 2 for visible plume height and a factor of 2 1/2 for visible plume length and maintain these factors 50% of the time. The models of Winiarski-Frick, Hanna, Slawson (Closed Form) and Tsai-Huang (Stone & Webster) satisfy this criterion. Their performance for the prediction of visible plume outlines is also best upon examination of our complete set of graphs similar to those of Figs. 1-21. The graphical (and performance statistics) results of the Frick and ORFAD models shows an overall poor performance. All other models tested provide comparatively fair predictions.

Several additional items should be noted. The four better-performing models can themselves benefit from improvement, e.g. the Hanna model can be improved with a diffusion phase added to the model along with a treatment of downwash. Each model can benefit from a calibration of its experimental coefficients to the full collection of available field data. Second, not all model/data discrepancies are caused by model errors. Uncertainties in tower exit and ambient measurements along with the transient nature of plume dispersion make the acquisition of field data difficult. Each data set contains some experimental errors in the measured model input conditions as well as in the determination of visible-plume outlines. The disappearance of the visible plume into natural cloud layers makes the plume hard to define in some cases. Also, when the plume appears as a series of puffs, the precise definition of a steady-state outline is difficult to determine. Also, time-averaging of a series of time-lapse photos inevitably induces some error. In spite of the experimental difficulties and experimental error in each data set, the models performed very consistently with the data base as a whole and this performance allowed us to trace the major model/data discrepancies to model assumptions. It should also be recalled that the visible portion of the plume is often only a small fraction of the entire plume and generally represents only the topmost portion of the plume. Consequently, our model/data comparisons test only the initial part of the plume. Only recently have some European data on in-plume measurements of the visible and invisible portions of the plume been made available which allow us to test, in a limited manner, model predictions further from the tower. Such data complements our large visible plume data base and provides additional information for model validation and model improvement.

ACKNOWLEDGMENTS

REFERENCES

1. A. J. Policastro, R. A. Carhart, W. E. Dunn, S. Ziemer, B. Devantier, and K. Haake. Evaluation of Mathematical Models for the Prediction of Plume Dispersion from Natural-draft Cooling Towers. Division of Environmental Impact Studies. Argonne National Laboratory. (in preparation). 1978.

2. A. J. Policastro, R. A. Carhart, and B. Devantier. Validation of Selected Mathematical Models for Plume Dispersion from Natural-Draft Cooling Towers. Paper presented and published in Proceedings of Waste Heat Management and Utilization Conference. Miami Beach, Florida. May 9-11, 1977.

3. P. M. Wigley and P. R. Slawson. "The Effect of Atmospheric Conditions on the Length of Visible Cooling Tower Plumes." Atmospheric Environment. 9. 1975.

4. P. R. Slawson and J. H. Coleman. "Natural-Draft Cooling-Tower Plume Behavior at Paradise Steam Plant." Waste Heat Management and Utilization Conference. Miami Beach. May 1977.

5. J. Weil. "The Rise of Moist Buoyant Plumes." Journal of Applied Meteorology. 13. p. 435-443. June 1974.

6. W. E. Frick. "The Influence of Stratification on Plume Structure." Master's Thesis. Atmospheric Sciences Department. Oregon State University. June 6, 1975.

7. L. Winiarski and W. Frick. Methods of Improving Plume Models. IN: Cooling Tower Environment -- 1978 Proceedings. A Symposium on Environmental Effects of Cooling Tower Emissions. May 2-4, 1978. Power Plant Siting Commission. Maryland Department of Natural Resources. Report PPSP-CPCTP-22. WRRC Special Report No. 9. May 1978.

8. M. E. LaVerne. "Oak Ridge Fog and Drift Program (ORFAD) User's Manual." ORNL/TM-5021. 1976.

9. S. R. Hanna. "Predicted and Observed Cooling Tower Plume Rise and Visible Plume Length at the John E. Amos Power Plant." Atmospheric Turbulence and Diffusion Laboratory. ATDL Contribution File No. 75/21. Oak Ridge, Tennessee. November 1975.

10. Y. J. Tsai and C. H. Huang. "Evaluation of Varying Meteorological Parameters on Cooling-Tower Plume Behavior." Symposium on Atmospheric Diffusion and Air Pollution. AMS Publication. Boston, Massachusetts. p. 408-411. 1972.

11. K. B. Batty. "Sensitivity Tests with a Vapor Plume Model Applied to Cooling Tower Effluents." Master's Thesis. Department of Meteorology. Penn State University. November 1976.

12. J. L. Lee. "A Numerical Simulation of Atmospheric Convection Caused by Heat Dissipation at Large Power Centers." American Meteorological Society. Third Symposium on Atmospheric Turbulence, Diffusion and Air Quality. October 26-29, 1976.

13. R. V. Calabrese, J. Halitsky, and K. Woodard. "Prediction of Temperature and Moisture Distributions in Cooling Tower Plumes." Pickard-Lowe-Garrick Inc., Washington, D.C. 1974.

14. D. W. Stephen and W. J. Moroz. "Plume Rise from Wet Cooling Towers in Strong Winds." Engineering Research Bulletin B-107. Center for Air Environment Studies. Penn State University, University Park, Pennsylvania. September 1972.

15. J. Saame. "An Analytical Investigation of the Formation and Dispersion of Fog Plumes from a Natural Draft Water Cooling Tower for Various Meteorological Conditions." Master's Thesis. Department of Mechanical Engineering. University of Pittsburgh. 1971.

16. H. Fortak. Use of a Power Glider Equipped with Instruments for Three-Dimensional Structural Study of Man-Made Thermal Convection. Translated from German. Report for the Deutschen Forschungsgemeinschaft. ORNL-tr-4101. April 1974 - May 1975.

17. Arbeitsgruppe über die meteorologischen Auswirkungen der Kühltürme "Bericht über die meteorologische Messerie am Standort Lünen vom 27.11.1972 bis 1.12.1972 Zur Teiluberprüfung and Verfeinerung des numerischen Modells SAUNA." Dienst für Luftreinhaltung der Schweizerischen Meteorologischen Zentralanstalt Payerne. 17 Mai 1973.

18. J. H. Meyer. "Chalk Point Surface Weather and Ambient Atmospheric Profile Data, First Intensive Test Period, December 15-19, 1975 (Revision)" Applied Physics Laboratory, The Johns Hopkins University. December 1976; Environmental Systems Corporation. "Environmental Systems Corporation Seasonal Test Data for the Period of December 15-19, 1975." April 7, 1976. (Chalk Point Cooling Tower Projects Documents PPSP-CPCTP-4 REV. and PPSP-CPCTP-8.)

19. J. H. Meyer and Jenkins, W. R. "Chalk Point Surface Weather and Ambient Atmospheric Profile Data, Second Intensive Test Period, June 14-24, 1976." Applied Physics Laboratory, The Johns Hopkins Univeristy. January 1977; Environmental Systems Corporation. "Environmental Systems Corporation Seasonal Test Data for the Period of October 1, 1975 - June 30, 1976." April 1977. (Chalk Point Cooling Tower Projects Documents PPSP-CPCTP-11 and PPSP-CPCTP-12. Volume 2 of 2).

20. P. R. Slawson and J. H. Coleman. "Natural Draft Cooling Tower Plume Rise Behavior at the Paradise Steam Plant, Part II." Tennessee Valley Authority. Division of Environmental Planning. (Draft). 1976.

21. P. R. Slawson. Personal Communication. Department of Mechanical Engineering University Waterloo, Waterloo Ontario, Canada, 1977.

22. L. N. Fan. "Turbulent Buoyant Jets into Stratified or Flowing Fluid." California Institute of Technology Report No. KH-R-15. 1967.

23. F. Pasquill. "Atmospheric Diffusion". Van Nostrand Monographs. London. 1962.

24. A. J. Policastro, W. E. Dunn, R. A. Carhart, M. Breig, S, Ziemer. and J. Ziebarth. Progress Report to EPRI: Model Improvement Program for Cooling Tower Plume Rise and Drift Deposition Models. January-March 1978. Argonne National Laboratory. Argonne, Illinois.

25. L. Winiarski and W. E. Frick. "Cooling Tower Plume Model." Thermal Pollution Branch. PNWRL. NERC EPA. Corvallis, Oregon. 1975.

26. G. A. Briggs. Plume Rise Predictions. IN: Proceedings of Workshop on Meteorological and Environmental Assessment. American Meteorological Society. 45 Beacon Street. Boston, Massachusetts. 1975.

27. P. R. Slawson and J. H. Coleman. "Natural-Draft Tower Plume Behavior at Paradise Steam Plant, Part II." Tennessee Valley Authority. Division of Environmental Planning. (to be published).

28. J. H. Meyer, T. W. Eagles, L. C. Kohlenstein, J. A. Kagan, and W. D. Stanbro. "Mechanical-Draft Cooling Tower Visible Plume Behavior - Measurements, Models, Predictions" IN: Cooling Tower Environment - 1974. Eds. Steven Hanna and Jerry Pell. U.S. Energy Research and Development Administration. 1975.

29. G. Abraham. "The Flow of Round Buoyant Jets Issuing Vertically into Ambient Fluid Flowing in a Horizontal Direction." Delft Hydraulics Laboratory Publication No. 81. The Netherlands. March 1971.

30. B. Morton, G. Taylor, and J. Turner. "Turbulent Gravitational Convection from Maintained and Instantaneous Sources." Proc. of Royal Society of London. Ser A. Vol. 234. p 1-23. 1956.

31. G. A. Briggs. Plume Rise. AEC Critical Review Series. TID-25075. 82 pp. 1969.

32. E. Kessler. On the Distribution and Continuity of Water Substance in Atmospheric Circulations. Meteorological Monographs. Vol. 10. 84 pp. American Meteorological Society. Boston. 1969.

33. J. Halitsky. International Journal of Air and Water Pollution. Vol. 10. pp 821-843. 1966.
34. J. E. Carson and H. Moses. "Calculation of Effective Stack Height." Argonne National Laboratory Report ANL - 7220. pp 96-99. January 1967.

Table 1. Model Entrainment Assumptions for

$$\mu = \frac{1}{\phi_m} \frac{d\phi_m}{ds}, \quad \phi_m \text{ the Mass Flux}$$

Model	Assumption for μ	Bouss. Appx.?
Slawson-Wigley	$\mu = \frac{2}{R} \frac{T^*_p}{T^*_a} \frac{v_e}{v}, \quad v_e = \alpha|w|, \quad \alpha = 0.3$	no
Neil	$\mu = \frac{2}{R} \frac{v_e}{v}, \quad v_e = \alpha|w|, \quad \alpha = 0.55$	yes
Frick	$\mu = \frac{2}{\sqrt{ab}} \frac{v_e}{v}, \quad v_e = \alpha(s)|w|$ $\alpha(s) = [1 - \frac{uv_x}{v^2}(1 - \frac{uv_x}{2v^2})]^{-1} [\frac{1}{\pi}\sqrt{\frac{a}{b}} \frac{u}{v} - \frac{w}{|w|} \frac{\sqrt{ab}}{8}$ $\frac{uv_x}{v^4} \, g \, \frac{\Delta T^*}{T^*_a}]$	yes
Winiarski-Frick	$\mu = \frac{2}{R} \frac{T^*_p}{T^*_a} \frac{v_e}{v}, \quad v_e = \max(v_{eI}, v_{eA}), \quad \beta = 0.1$ $v_{eI} = \alpha(s)w, \quad v_{eA} = \beta |v - u \cos\theta|$ $\alpha(s) = [1 - \frac{T^*_p}{T^*_a} \frac{u}{v^2}(v_x - \frac{u}{2} + \frac{w^2}{v^2} u)]^{-1} \cdot$ $[\frac{1}{\pi} \frac{u}{v} - Rg \frac{uv_x}{v^4} (\frac{\Delta T^*}{T^*_a} \sigma)]$	no
Hanna[a]	$\mu = \frac{2}{R_m} \frac{v_e}{v}, \quad v_e = \alpha(s)w, \quad \alpha_0 = 0.6$ $\alpha(s) = \alpha_0 \frac{u^2}{v^2} + \frac{gR_m}{v^2 E_m} (\frac{\Delta T}{p} E_w \sigma) +$ $\frac{1}{2} (R_m \frac{w^2}{uv^2} - \frac{R_0}{2u}) \frac{du}{dz}$	yes
Tsai-Huang[b]	$\mu = \frac{2}{R} \frac{v_e}{v}, \quad v_e = \beta_1 (v - u\cos\theta) + \beta_2 u \cos\theta \sin\theta$ $\beta_1 = .08, \quad \beta_2 = .354, \quad r = b/2, \quad v = u\cos\theta + \frac{v'}{2}$	yes
Lee-Batty[c]	$\mu = \frac{2}{R} \frac{v_e}{v}, \quad v_e = \alpha|w|, \quad \alpha = 0.4$	yes
Lee	$\mu = \frac{2}{R} \frac{v_e}{v}, \quad v_e = \alpha[w^2 + (v_x u/2)^2]^{1/2},$ $\alpha = 0.15$	yes
Stephen-Moroz	$\mu = \frac{2}{R} \frac{T^*_p}{T^*_a} \frac{v_e}{v}, \quad v_e = \frac{u^2}{v^2} \zeta_e + \frac{1}{2} \frac{wRg}{v^2} \frac{T^*_a}{T^*_p} (\frac{\Delta T^*}{T^*_a} \sigma)$ $\zeta_e = [\frac{T^*_a}{T^*_p} \frac{v}{\max(w,u)}]^{1/2} \omega_e, \quad \alpha = .093, \quad \gamma = 0.5,$ $\omega_e = \begin{cases} (\alpha^2 w^2 + \gamma^2 u^2)^{1/2}, & (w > 1.018u, \ z < 600-H) \\ \gamma w, & (w < 1.018u, \text{ stable, } z < 600-H) \\ .285 (\frac{wu}{z})^{1/6}, & (w < 1.018u, \text{ unstable and neutral} \\ & \quad z < 600-H) \\ (0.1)w [\frac{T^*_a}{T^*_p} \frac{\max(u,w)}{v}]^{1/2}, & (z > 600-H) \end{cases}$ $z = \min(z + H, 505)$	no

(a) This is the entrainment rate for the "momentum plume" the largest cross-section with radius R_m. The factor E_m is the area of the cross-section of the momentum plume divided by the area of the cross-section of the temperature plume. E_m is 1 initially and grows to 2.25 late in plume rise. R_0 is the tower exit radius. The initial mass flux is increased at the start of calculations by a factor of $[1 + w_0^2/u_0^2]^{1/2}$.

(b) This model assumes Gaussian plume profiles and should be considered as having a special set of initial conditions at the end of an empirical "zone for flow establishment". These special conditions provide initial conditions for the dynamic and thermodynamic equations solved in the model. The updraft velocity at the end of ZFE is 0.5 w_0; the corresponding temperature excess and mixing ratio excesses are both halved; $b_0 \approx R_0$; and v' is the excess plume velocity along the trajectory at the centerline.

(c) The v_e equation is modified near or at maximum rise, depending on ambient stability, and the cross-section may become elliptical. The equation given above governs the major portion of plume rise.

433

Table 2. Model Equations for Change of Horizontal Velocity with Centerline Distance.

Model	Equation for dv_x/ds
Slawson-Wigley	$\dfrac{dv_x}{ds} = \dfrac{du}{ds}$, $\quad v_x = u$
Weil	$\dfrac{dv_x}{ds} = \mu(u - v_x)$
Frick	$\dfrac{dv_x}{ds} = \mu(u - v_x)$
Winiarski-Frick	$\dfrac{dv_x}{ds} = \mu(u - v_x)$
Hanna	$\dfrac{dv_x}{ds} = \dfrac{du}{ds}$, $\quad v_x = u$
Tsai-Huang	$\dfrac{dv_x}{ds} = \mu(u - v_x) + \dfrac{2}{R}\dfrac{c_D}{\pi} u \dfrac{uw^3}{v^4}$, $\quad c_D = 0.15$
Lee-Batty	$\dfrac{dv_x}{ds} = \mu(u - v_x)$
Lee	$\dfrac{dv_x}{ds} = -\mu v_x + \dfrac{2}{R}\dfrac{c_D}{\pi} u \dfrac{u|w^3|}{v^4}$, $\quad c_D = 0.15$
Stephen-Moroz	$\dfrac{dv_x}{ds} = 0$, $\quad v_x = \bar{u}$, $\quad \bar{u}$ an average value.

Table 3. Model Equations for Change of Vertical Velocity with Centerline Distance

Model	Equation for dw/ds
Slawson-Wigley	$\dfrac{dw}{ds} = -\mu w + \dfrac{g}{v}\left(\dfrac{\Delta T^*}{T_a^*} - \sigma\right)$
Weil [b]	$\dfrac{dw}{ds} = -\mu w + \dfrac{g}{v}\left[\dfrac{T_p - T_a}{T_1} + 0.61(X_p - X_a) - \sigma\right]$
Frick	$\dfrac{dw}{ds} = -\mu w + \dfrac{g}{v}\left(\dfrac{\Delta T^*}{T_a^*} - \sigma\right)$
Winiarski-Frick	$\dfrac{dw}{ds} = -\mu w + \dfrac{g}{v}\left(\dfrac{\Delta T^*}{T_a^*} - \sigma\right)$
Hanna [a]	$\dfrac{dw}{ds} = -\dfrac{2\alpha}{vR_m}\left(\dfrac{w}{v}\right)w + \dfrac{g}{E_m v}\left(\dfrac{\Delta T}{T} - E_w \sigma\right)$, $\quad \alpha = 0.6$
Tsai-Huang [b]	$\dfrac{dw}{ds} = -\mu w + \dfrac{g}{v}\left(\dfrac{T_p - T_a}{T_1}\right) - \dfrac{2}{R}\dfrac{c_D}{\pi} u \dfrac{uv_x w^2}{v^4}$, $\quad c_D = 0.15$
Lee-Batty	$\dfrac{dw}{ds} = -\mu w + \dfrac{g}{v}\left(\dfrac{\Delta T^*}{T_a^*} - \sigma\right)$
Lee	$\dfrac{dw}{ds} = -\mu w + \dfrac{g}{v}\left(\dfrac{\Delta T^*}{T_a^*} - \sigma\right) - \dfrac{2}{R}\dfrac{c_D}{\pi} u \dfrac{uv_x w|w|}{v^4}$, $\quad c_D = 0.15$
Stephen-Moroz	$\dfrac{dw}{ds} = -\mu \dfrac{v^2}{u^2} w + \dfrac{v^2}{u^2}\dfrac{g}{v}\left(\dfrac{\Delta T^*}{T_a^*} - \sigma\right)$

(a) $\hat{T} = T(1 + 0.31x)$, $\quad .22 \le E_w/E_m \le 1.0$.

(b) T_1 is a reference temperature, the ambient dry-bulb temperature at the tower exit.

Table 4. Model Equations for Change of Plume temperature with Centerline Distance when Plume is Saturated.

Model	Equation for dT_p/ds, (Saturated Plume)[a]
Slawson-Wigley	$\frac{dT_p}{ds} = -\gamma_d \frac{w}{v} - \mu(T_p - T_a)$
Weil	$\frac{dT_p}{ds} = (1+\alpha)^{-1} \{-\gamma_d \frac{w}{v} - \mu[(T_p - T_a) + \frac{L}{c_p}(X_p - X_a)]\}$
Frick	$\frac{dT_p}{ds} = -\gamma_d \frac{w}{v} - \mu(X_p - X_a)/\beta, \quad \beta = \mu(1 + \frac{X_p}{.622})$
Winiarski-Frick	Same as Frick.
Hanna[b]	$\frac{dT_p}{ds} = \frac{1}{1+\Gamma_w^a} \{-\gamma_d \frac{w}{v} - \frac{2}{vR}(\nu w)[(T_p - T_a) + \frac{L}{c_p}(.71)\frac{R_w}{R}(X_p - X_a)]\}, \quad \nu = 0.1$
Tsai-Huang	$\frac{dT_p}{ds} = -\mu(T_p - T_a) + \frac{w}{v}\frac{dT_a}{dz}$
Lee-Batty	$\frac{dT_p}{ds} = \begin{cases} (1+\alpha)^{-1}\{-\gamma_d \frac{w}{v} - \mu[(T_p - T_a) + \frac{L}{c_p}(X_p - X_a)]\}, \\ \quad \text{if } (X_p - X_a)/(T_p - T_a) < \beta \\ -\gamma_d \frac{w}{v} - \mu(T_p - T_a), \quad \text{if } (X_p - X_a)/(T_p - T_a) > \beta \end{cases}$
Lee	$\frac{dT_p}{ds} = (1+\alpha)^{-1}\{-\gamma_d \frac{w}{v} - \mu[(T_p - T_a) + \frac{L}{c_p}(X_p - X_a)]\}$
Stephen-Moroz	$\frac{dT_p}{ds} = (1+\alpha)^{-1}\{-\gamma_d \frac{w}{v} + \frac{L}{c_p}(\frac{\mu g}{v}(\frac{\Delta T^*}{T^*} - \alpha) - \mu)^{-1} + [(T_p - T_a) + \frac{L}{c_p}(X_p - X_a)]\}$

(a) $\beta = \frac{dX_s}{dT}\Big|_{T_p}, \quad \alpha = (L/c_p)\beta, \quad \alpha(10°C) = 0.54, \quad \alpha(30°C) = 0.89$

(b) $L > L_w + 1/2, \quad L > R_w/R + 0.71; \text{ as } s \text{ becomes large.}$

Table 5. Model Equations for Change of Plume Mixing Ratio with Centerline Distance when Plume is Saturated.

Model	Equation for dX_p/ds, (Saturated Plume)[a]
Slawson-Wigley	$\frac{dX_p}{ds} = -\mu (X_p - X_a)$
Weil	$\frac{dX_p}{ds} = \beta \frac{dT_p}{ds}$
Frick	$\frac{dX_p}{ds} = \beta \frac{dT_p}{ds}$
Winiarski-Frick	$\frac{dX_p}{ds} = \beta \frac{dT_p}{ds}$
Hanna	$\frac{dX_p}{ds} = \beta \frac{dT_p}{ds}$
Tsai-Huang	$\frac{dX_p}{ds} = -\mu(X_p - X_a) + \frac{w}{v}\frac{dX_a}{dz}$
Lee-Batty	$\frac{dX_p}{ds} = \begin{cases} \beta \frac{dT_p}{ds}, \quad \text{if } (X_p - X_a)/(T_p - T_a) < \beta \\ -\mu (X_p - X_a), \quad \text{if } (X_p - X_a)/(T_p - T_a) > \beta \end{cases}$
Lee	$\frac{dX_p}{ds} = \beta \frac{dT_p}{ds}$
Stephen-Moroz	$\frac{dX_p}{ds} = \beta \frac{dT_p}{ds}$

(a) $\beta = dQ_s/dT\Big|_{T_p}, \quad \beta(-10°C) = 1.38 \times 10^{-4} \ (°C)^{-1}, \quad \beta(30°C) = 1.57 \times 10^{-3}(°C)^{-1}$

435

Table 6. Model Equations for Change of Liquid Water with Centerline Distance.

Model	Equation for $d\sigma/ds$ [a]
Slawson-Wigley	$\frac{d\sigma}{ds} = 0, \ \sigma = 0$
Weil	$\frac{d\sigma}{ds} = -\mu\sigma + \beta(1+\alpha)^{-1}\{\gamma_d \frac{w}{v} + \mu[(T_p - T_a) - \beta^{-1}(X_p - X_a)]\}$
Frick	$\frac{d\sigma}{ds} = -\mu\sigma + \mu\frac{c_p}{L}[(T_p - T_a) - \frac{1}{\tilde\beta}(X_p - X_a)],$ $\tilde\beta = \beta(1 + \frac{X_p}{.622})$
Winiarski-Frick	Same as Frick
Hanna [b]	$\frac{d\sigma}{ds} = -\beta(1 + E_w\alpha)^{-1}\{-\gamma_d \frac{w}{v} - \frac{2}{R_v}(0.4w)[(T_p - T_a) + \frac{L}{c_p}(0.71)\frac{R_w}{R}(X_p - X_a)]\}$
Tsai-Huang	$\frac{d\sigma}{ds} = 0, \ \sigma = 0$
Lee-Batty	$\frac{d\sigma}{ds} = 0, \ \sigma = 0$
Lee	$\frac{d\sigma}{ds} = -\mu\sigma + \beta(1+\alpha)^{-1}\{\gamma_d \frac{w}{v} + \mu[(T_p - T_a) - \beta^{-1}(X_p - X_a)]\}$
Stephen-Moroz	$\frac{d\sigma}{ds} = -(\frac{v^2}{u^2} 1 - \frac{w}{u^2 v} g \frac{\Delta T^*}{T_a^*})\sigma + \beta(1 + \alpha)^{-1}\{\frac{w}{v}\gamma_d - \frac{w}{u^2 v}g \cdot (\frac{\Delta T^*}{T_a^*} - \sigma)[(T_p - T_a) - \beta^{-1}(X_p - X_a)]\}$

(a) $\beta = dQ_s/dT\big|_{T_p}$, $\alpha = (L/c_p)\beta$

(b) $1 \geq E_w \rightarrow 1/2,\ \ 1 \geq R_w/R \rightarrow 1/\sqrt{2}$

Table 7. Average Ambient Conditions Over the Observed Plume-Rise Region for Single-NDCT Plume Data Cases.

Site	Label	Date	ū (m/s)	W_o (m/s)	T̄ (°C)	RH (%)	dT/dz (°C/100m)
Lünen, West Germany	LUS1	11/28/72	13.0	4.1	3.3	61	-0.84
	LUS4	11/30/72	8.0	4.6	4.0	70	-0.50
	LUS5	11/30/72	9.0	4.4	6.8	64	-0.36
	LUS6	12/ 1/72	9.3	4.5	6.1	93	-0.98
	LUSS2	12/11/72	5.1	3.5	6.6	70	-0.76
	LUSS3	12/12/72	5.3	3.4	8.0	53	-0.89
	LUSS5	12/15/72	4.8	3.5	2.9	69	-0.68
	LUSS7	12/20/72	1.3	3.7	1.4	70	+0.45
	LUSS9	12/22/72	0.9	3.9	-3.5	76	+1.24
	LUSS11	1/10/73	3.3	3.7	0.9	92	-0.64
	LUSS12	1/11/73	1.2	3.6	0.6	80	-0.89
	LUSS17	1/24/73	2.6	3.7	0.2	90	-0.57
Paradise, Kentucky	P2-1	1/31/73	10.6	4.4	4.1	72	-0.20
	P2-2	2/ 2/73	8.6	5.0	6.2	86	-0.86
	P2-3	2/ 3/73	4.1	6.2	-0.6	84	-0.74
	P2-4	2/ 4/73	10.2	6.6	3.6	68	+2.29
	P2-5	2/ 5/73	8.1	6.2	7.9	67	-0.11
	P2-6	2/ 8/73	7.0	6.4	-5.8	46	-0.91
	P2-7	2/ 9/73	4.1	7.2	-10.2	74	-0.33
	P2-8	2/ 9/73	4.8	6.9	-7.0	65	-0.94
	P2-9	2/10/73	7.1	7.2	-8.8	66	-0.30
	P2-10	2/10/73	4.9	6.8	-5.9	55	-0.86
	P2-11	2/11/73	7.1	6.8	-7.1	66	-0.42
	P2-12	2/11/73	2.8	5.8	-1.3	45	-0.85
	P2-13	2/12/73	7.0	6.0	6.7	43	-0.95
Chalk Point, Maryland	CP1D15	12/15/75	13.5	2.9	12.7	68	-0.83
	CP1D16	12/16/75	7.6	3.2	6.7	34	-1.44
	CP1D17A	12/17/75	5.8	4.0	2.3	74	-0.35
	CP1D17B	12/17/75	4.0	4.0	1.0	73	-0.79
	CP1D17C	12/17/75	2.6	4.2	5.8	46	-0.94
	CP1D18	12/18/75	16.7	3.5	-5.0	33	-1.50
	CP1D19	12/19/75	8.6	4.0	-8.9	24	-0.90
	CP2J17	6/17/76	4.8	4.0	22.2	84	-0.93
	CP2J18A	6/18/76	3.7	4.0	25.1	77	-1.01
	CP2J18B	6/18/76	6.8	3.8	26.7	61	-0.82
	CP2J19	6/19/76	4.5	4.2	25.3	73	-0.79
	CP2J22	6/22/76	4.4	4.0	23.0	82	-1.06
	CP2J23	6/23/76	2.8	4.3	25.3	69	-1.02
	CP2J24	6/24/76	4.1	3.6	25.1	64	-1.13

436

Visible Plume Rise

Model	Range of ρ_i	N_2	N_5	N_F	$\bar{\rho}=\frac{1}{n}\sum\rho_i$	σ_1	$\rho_2 = 10^{1/n\sum|\log\rho_i|}$	σ_2
Slawson-Wigley	0.0-9.3	19	33	2	1.42	1.30	1.88	0.22
Slawson (closed form)	0.0-16.8	23	32	1	1.26	1.10	1.72	0.19
Weil	0.12-6.1	15	32	0	0.80	0.78	2.13	0.19
Frick	0.0-3.83	16	36	0	0.61	0.59	2.19	0.20
Winiarski-Frick	0.13-8.6	30	36	0	0.83	0.37	1.50	0.13
ORFAD	0.56-7.9	5	11	27	2.34	1.29	2.27	0.19
Hanna	0.23-11.3	26	35	0	1.39	1.02	1.67	0.18
Tsai-Huang (Stone & Webster Engr. Corp.)	0.01-10.6	24	32	0	0.92	0.49	1.52	0.14
Lee-Batty	0.11-10.0	19	32	1	0.92	0.75	1.88	0.23
Lee(NUS)	0.0-13.0	27	35	1	1.18	0.68	1.59	0.17
Calabrese-Halitsky-Woodard (Pickard-Lowe-Garrick Inc.)	0.0-10.6	17	28	9	1.54	1.02	1.86	0.17
Stephen-Moroz	0.4-20.5	24	35	0	1.44	0.97	1.68	0.19
Saame	0.0-9.7	17	36	2	2.08	0.94	2.01	0.17

Visible Plume Length

Model	Range of ρ_i	N_2	$N_{2.5}$	N_5	N_F	$\bar{\rho}=\frac{1}{n}\sum\rho_i$	σ_1	$\rho_2 = 10^{1/n\sum|\log\rho_i|}$	σ_2
Slawson-Wigley	0.0-48.9	7	12	23	4	0.91	1.02	2.25	0.18
Slawson (closed form)	0.0-299	13	19	26	1	1.19	1.09	2.07	0.17
Weil	0.03-24.3	4	4	18	0	0.52	0.56	2.94	0.19
Frick	0.07-2.51	4	4	18	0	0.36	0.13	2.99	0.15
Winiarski-Frick	0.08-16.0	22	26	32	0	0.79	0.50	1.79	0.15
ORFAD	0.32-16.2	0	0	2	17	2.49	2.17	3.79	0.09
Hanna	0.24-2.90	18	19	23	15	1.19	0.72	1.57	0.16
Tsai-Huang (Stone & Webster Engr. Corp.)	0.01-4.9	19	20	27	7	1.64	1.08	1.79	0.19
Lee-Batty	0.05-3.9	8	13	24	2	0.85	0.90	2.27	0.15
Lee(NUS)	0.0-5.3	5	7	20	6	0.42	0.22	2.68	0.20
Calabrese-Halitsky-Woodard (Pickard-Lowe-Garrick Inc.)	0.0-5.4	13	18	26	9	1.21	0.91	1.88	0.17
Stephen-Moroz	0.1-3.8	16	18	23	13	1.41	0.98	1.60	0.19
Saame	0.0-24.4	11	18	28	2	0.75	0.81	2.21	0.15

Notes: ρ_i is defined as the ratio of predicted to observed (either length or height as indicated)
N_2 is the number of times the prediction is within a factor of 2, i.e., $0.5 < \rho_i < 2.0$
$N_{2.5}$ is the number of times the prediction is within a factor of 2.5, i.e., $0.4 < \rho_i < 2.5$
N_5 is the number of times the prediction is within a factor of 5, i.e., $0.2 < \rho_i < 5.0$
N_F is the number of failures of the model in 39 data sets
σ_1 is the standard deviation of the ρ_i distribution
σ_2 is the standard deviation of the $|\log \rho_i|$ distribution

Table 8. Performance Statistics for Thirteen Single-tower Models for Predictions of Visible Plume Rise and Visible Plume Length.

437
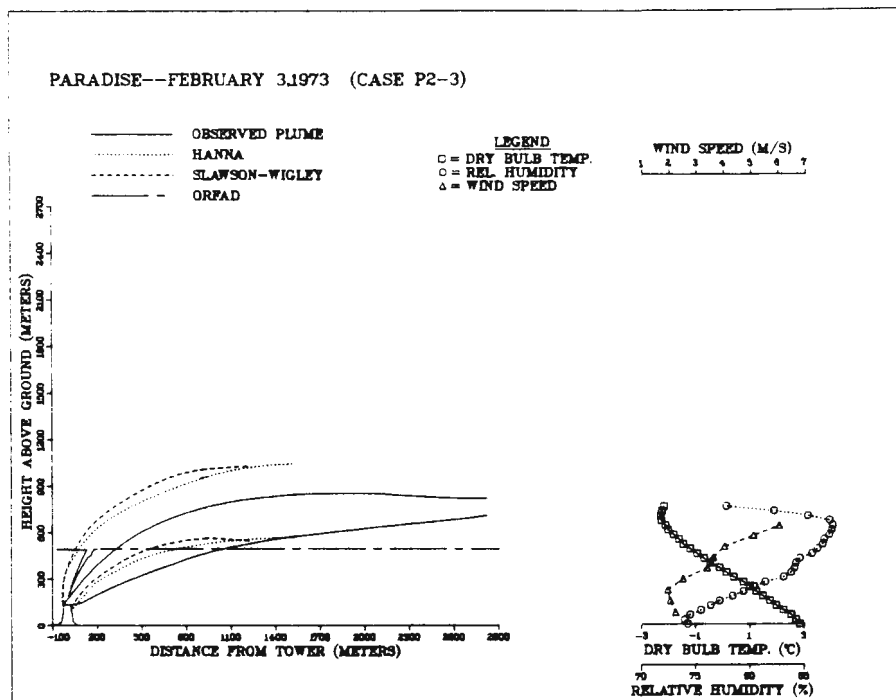
Fig. 1.   Comparison of Plume-model Predictions of Hanna, Slawson-Wigley
           and ORFAD to Observed Visible-plume Outline at Paradise: February
           3, 1973.
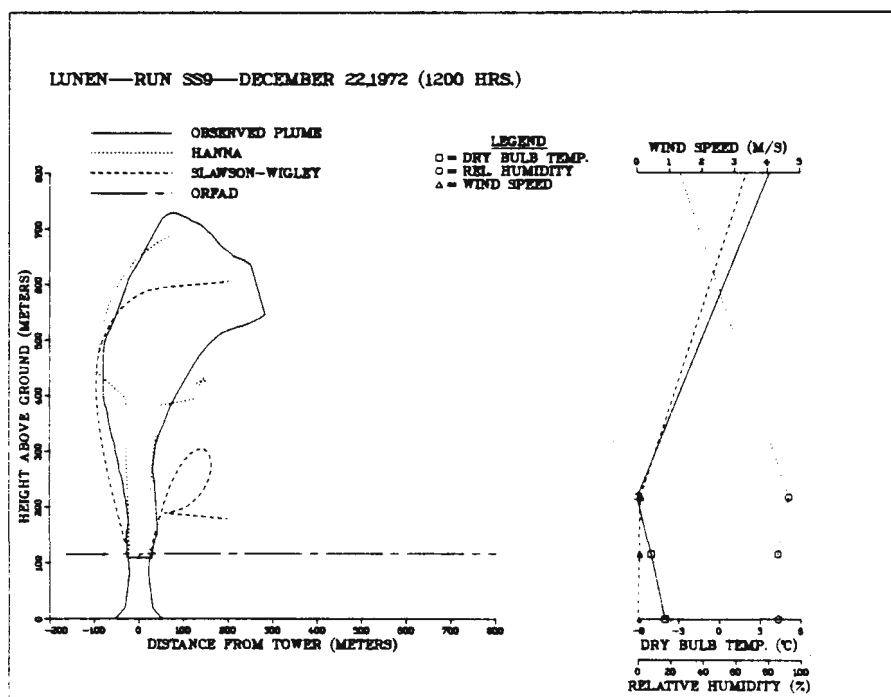
Fig. 2.   Comparison of Plume-model Predictions of Hanna, Slawson-Wigley and
           ORFAD to Observed Visible-plume Outline at Lünen: December 22, 1972
           (1200 Hrs.).

438
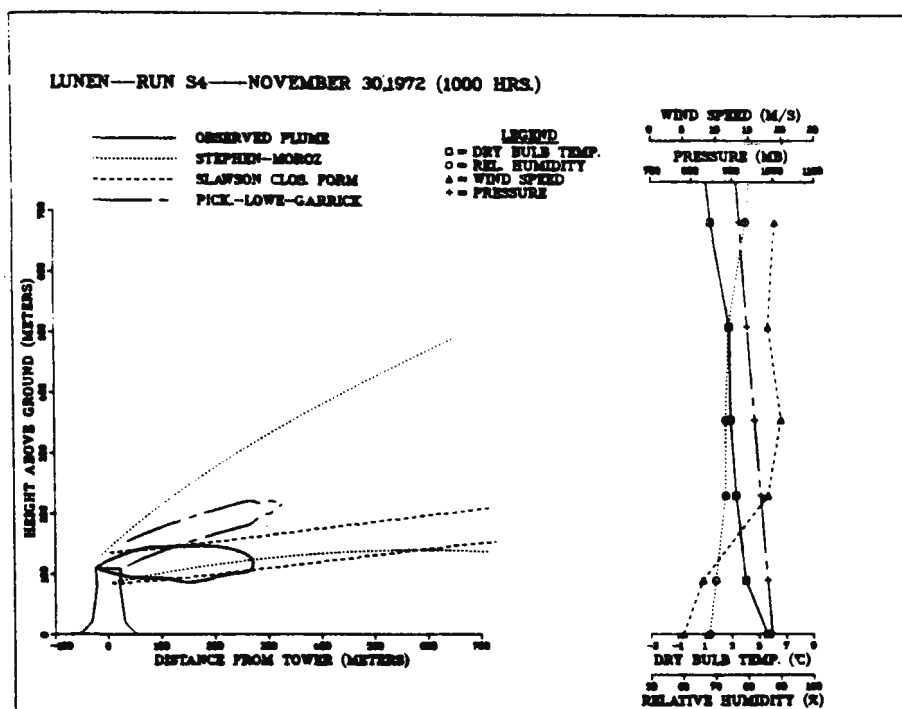
Fig. 3.   Comparison of Plume-model Predictions of Stephen-Moroz, Slawson
           (Closed Form) and Pickard-Lowe-Garrick to Observed Visible-plume
           Outline at Lünen: November 30, 1972 (1000 Hrs.).
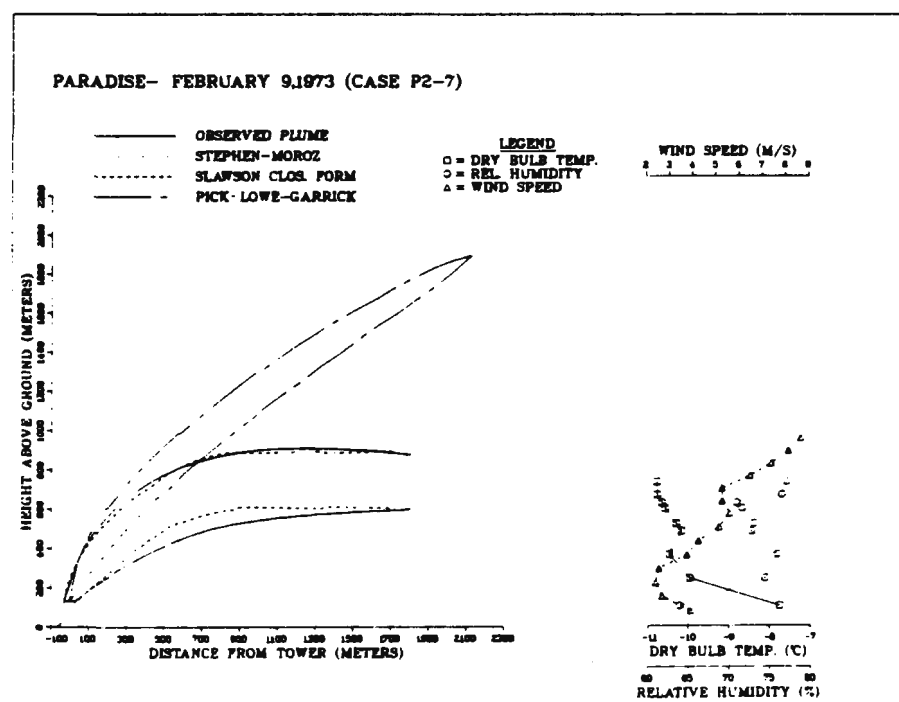
Fig. 4.   Comparison of Plume-model Predictions of Stephen-Moroz, Slawson
           (Closed Form) and Pickard-Lowe-Garrick to Observed Visible-plume
           Outline at Paradise: February 9, 1973.
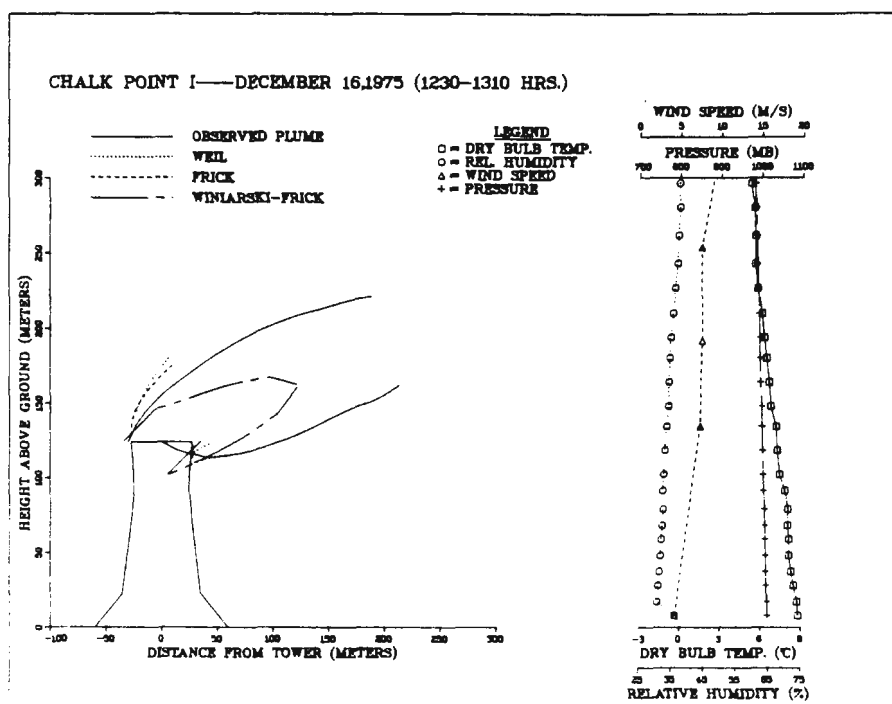
Fig. 5. Comparison of Plume-model Predictions of Weil, Frick, and Winiarski-Frick to Observed Visible-plume Outline at Chalk Point: December 16, 1975 (1230-1310 Hrs.).
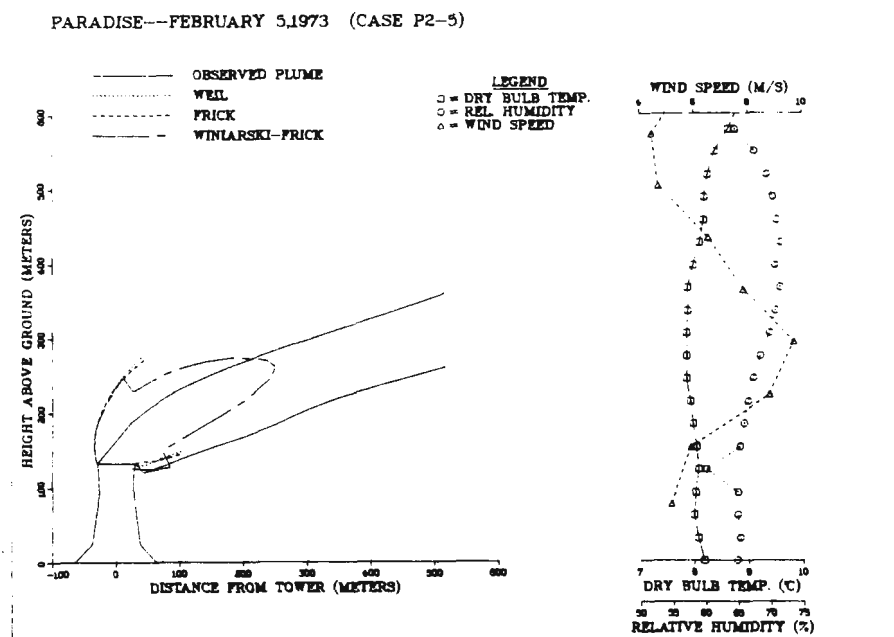
Fig. 6. Comparison of Plume-model Predictions of Weil, Frick, and Winiarski-Frick to Observed Visible-plume Outline at Paradise: February 5, 1973.

440
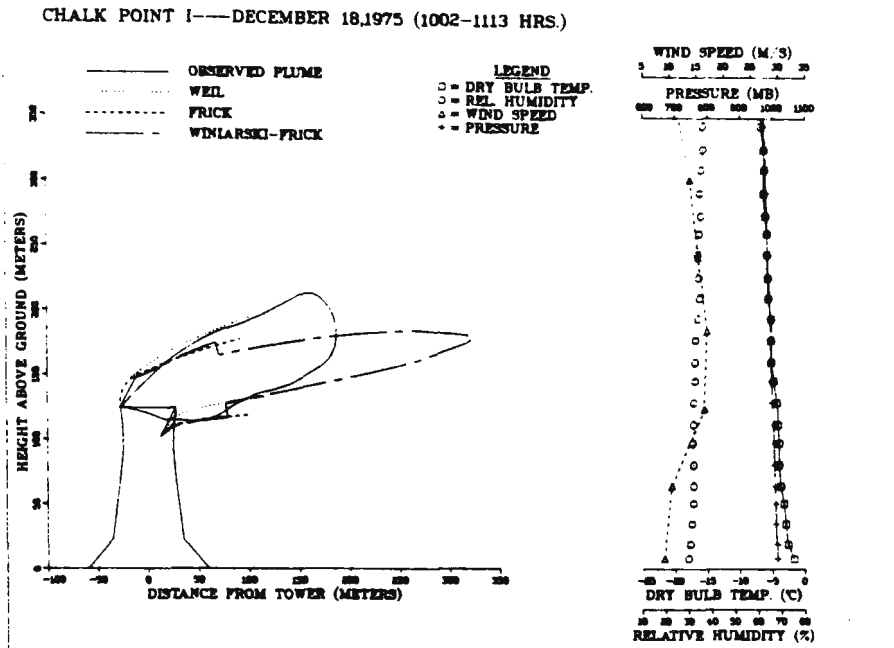
Fig. 7.   Comparison of Plume-model Predictions of Weil, Frick, and Winiarski-Frick to Observed Visible-plume Outline at Chalk Point: December 18, 1975 (1002-1113 Hrs.).
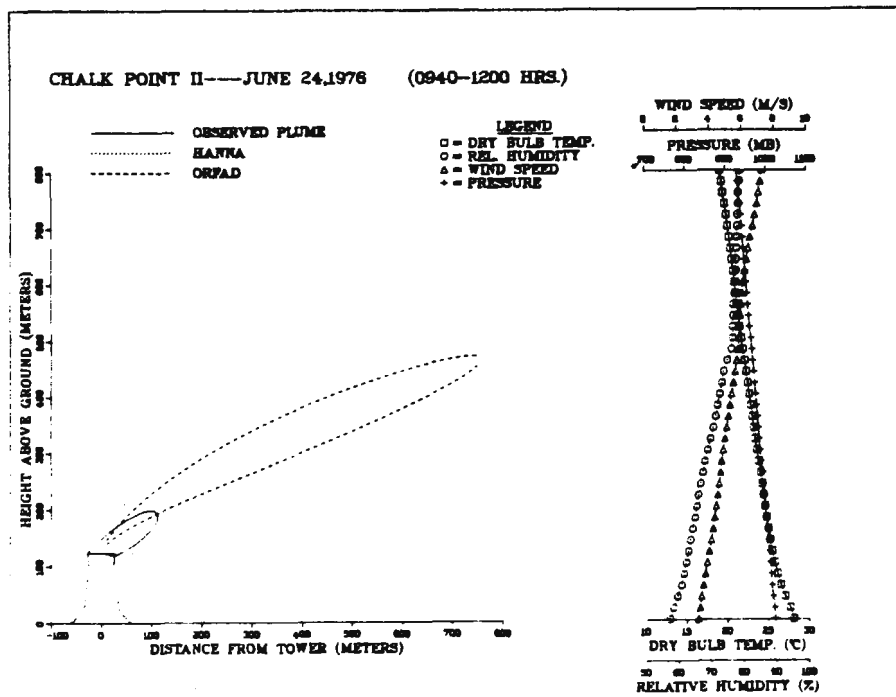
Fig. 8.   Comparison of Plume-model Predictions of Hanna, Slawson-Wigley (no plume), and ORFAD to Observed Visible-plume Outline at Chalk Point: June 24, 1976 (0940-1200 Hrs.).
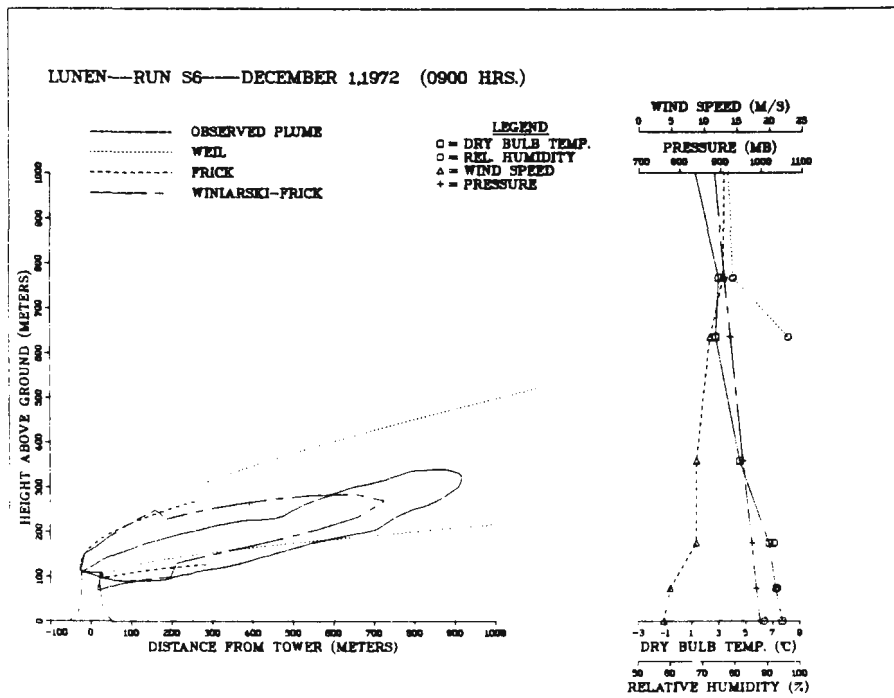
Fig. 9a. Comparison of Plume-model Predictions of Weil, Frick, and Winiarski-Frick to Observed Visible-plume Outline at Lünen: December 1, 1972 (0900 Hrs.) . . . small scale.
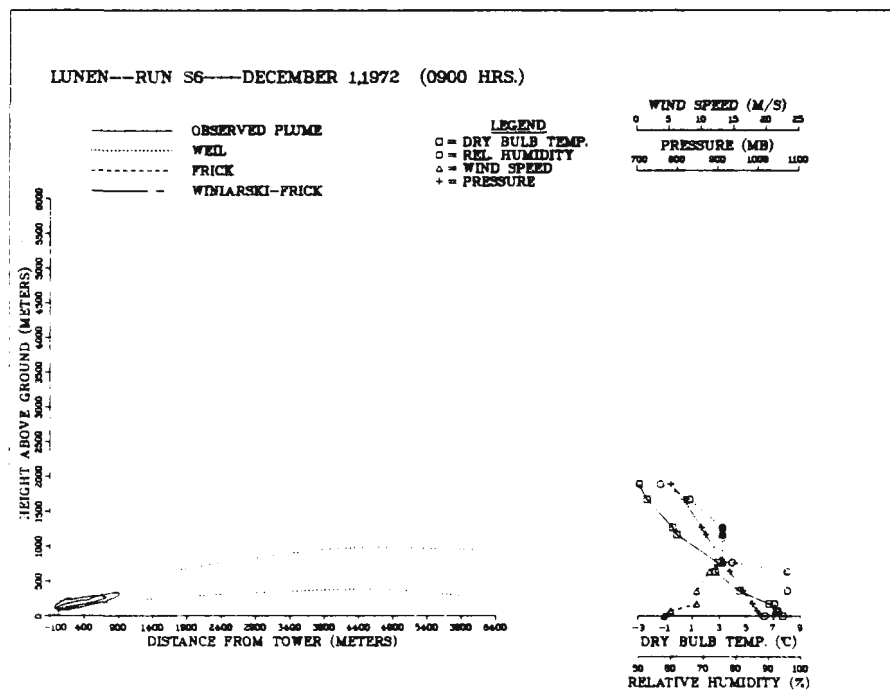
Fig. 9b. Comparison of Plume-model Predictions of Weil, Frick, and Winiarski-Frick to Observed Visible-plume Outline at Lünen: December 1, 1972 (0900 Hrs.) . . . large scale.
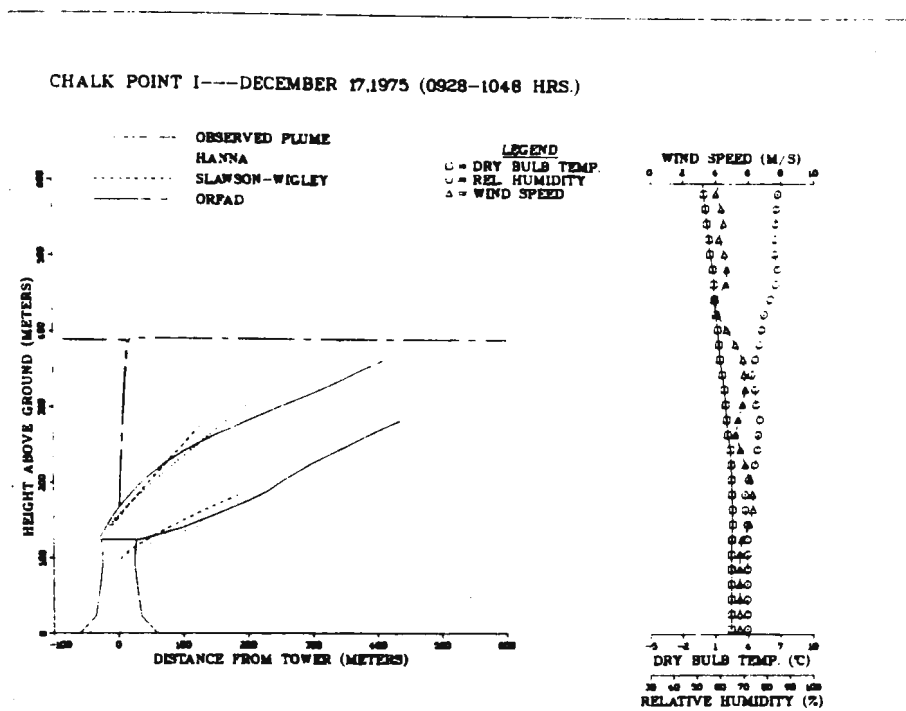
Fig. 10. Comparison of Plume-model Predictions of Hanna, Slawson-Wigley, and ORFAD to Observed Visible-plume Outline at Chalk Point: December 17, 1975 (0928-1048 Hrs.).
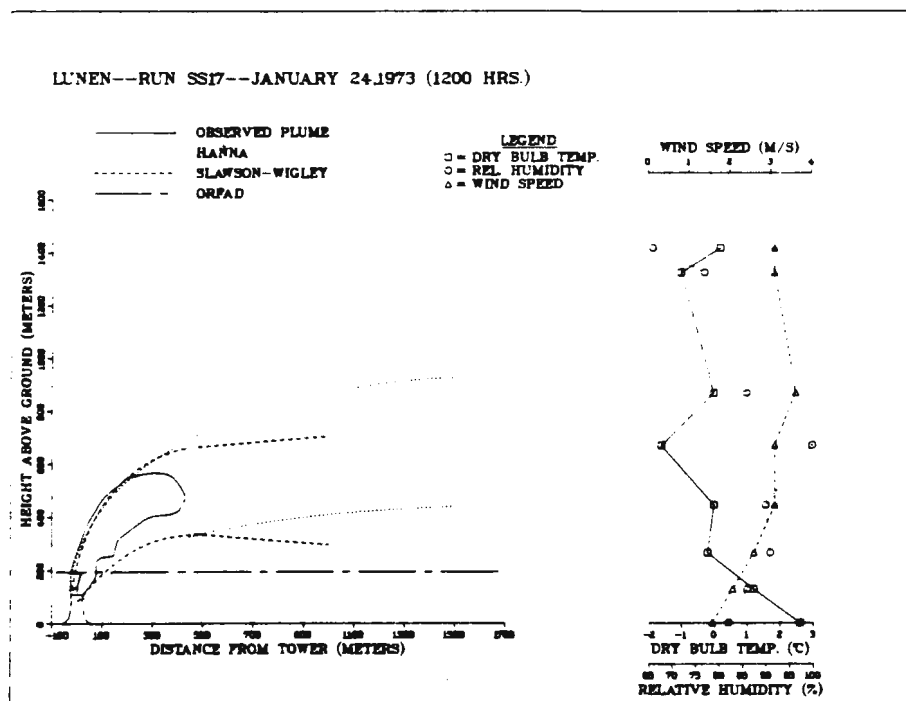
Fig. 11. Comparison of Plume-model Predictions of Hanna, Slawson-Wigley and ORFAD to Observed Visible-plume Outline at Lünen: January 24, 1973 (1200 Hrs.).
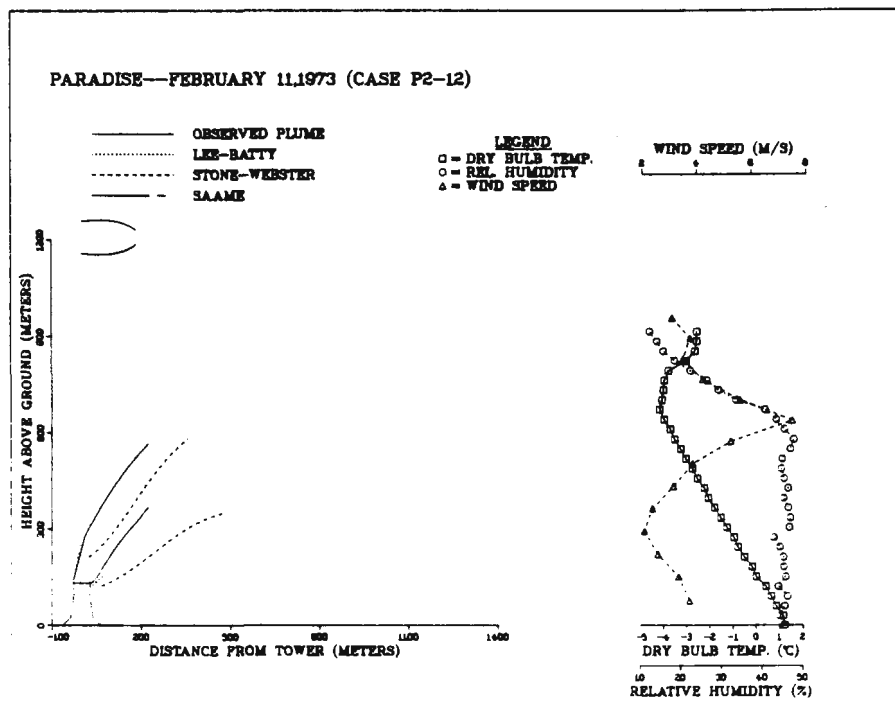
Fig. 12. Comparison of Plume-model Predictions of Lee-Batty, Stone & Webster and Saame to Observed Visible-plume Outline at Paradise: February 11, 1973.
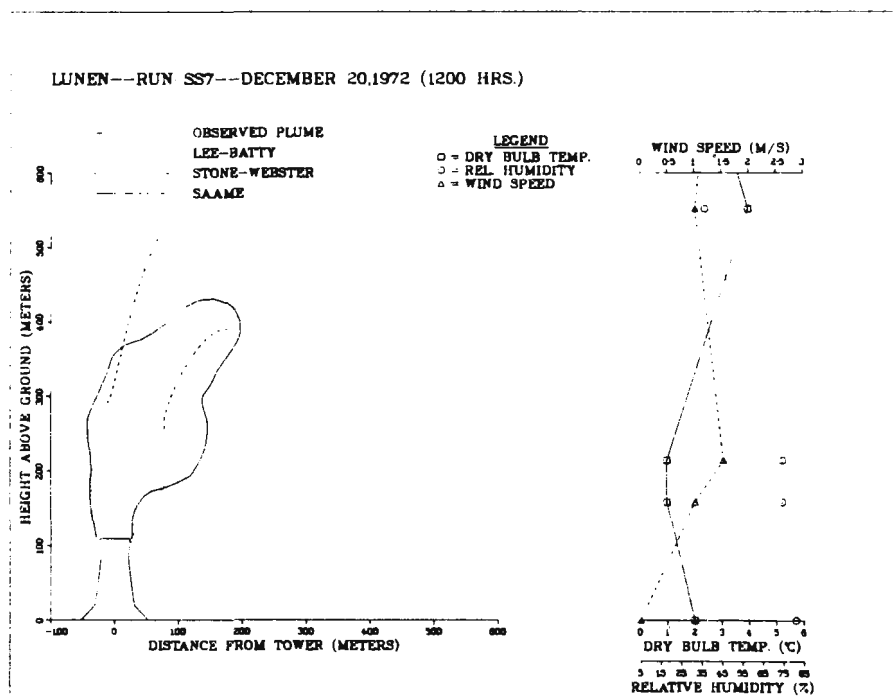
Fig. 13. Comparison of Plume-model Predictions of Lee-Batty, Stone & Webster and Saame to Observed Visible-plume Outline at Lünen: December 20, 1972 (1200 Hrs.).

444
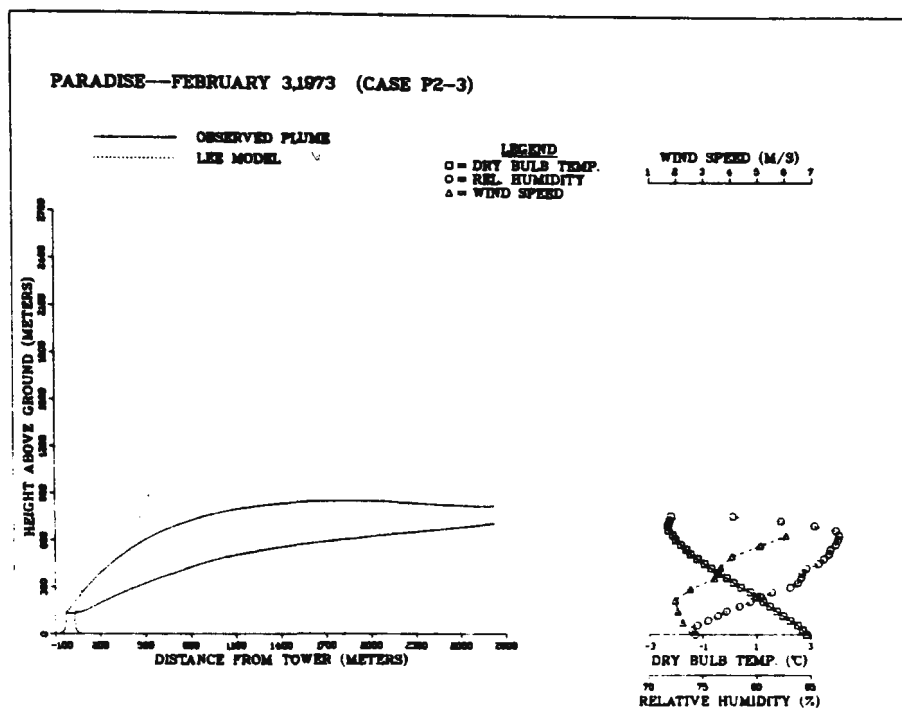
Fig. 14. Comparison of Plume-model Predictions of Lee (NUS) to Observed Visible-plume Outline at Paradise: February 3, 1973.
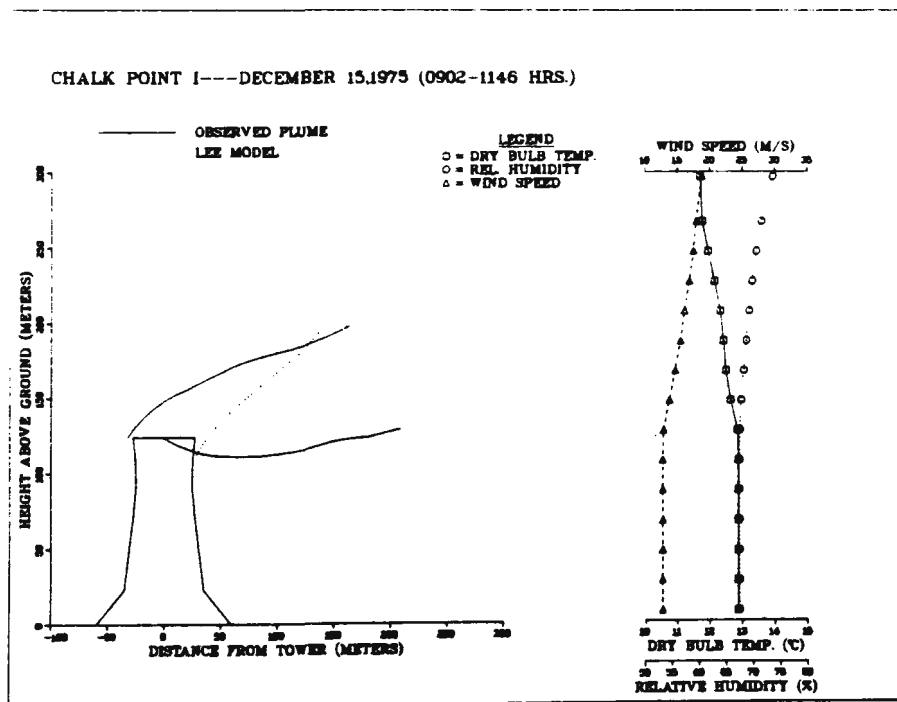
Fig. 15. Comparison of Plume-model Predictions of Lee (NUS) to Observed Visible-plume Outline at Chalk Point: December 15, 1975 (0902-1146 Hrs.).
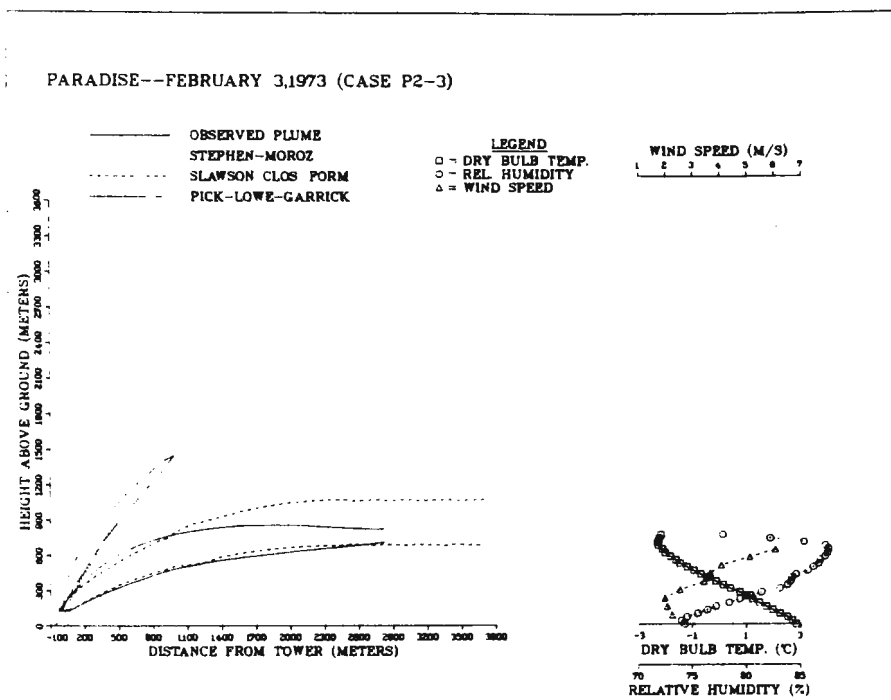
Fig. 16. Comparison of Plume-model Predictions of Stephen-Moroz, Slawson (Closed Form) and Pickard-Lowe-Garrick to Observed Visible-plume Outline at Paradise: February 3, 1973.
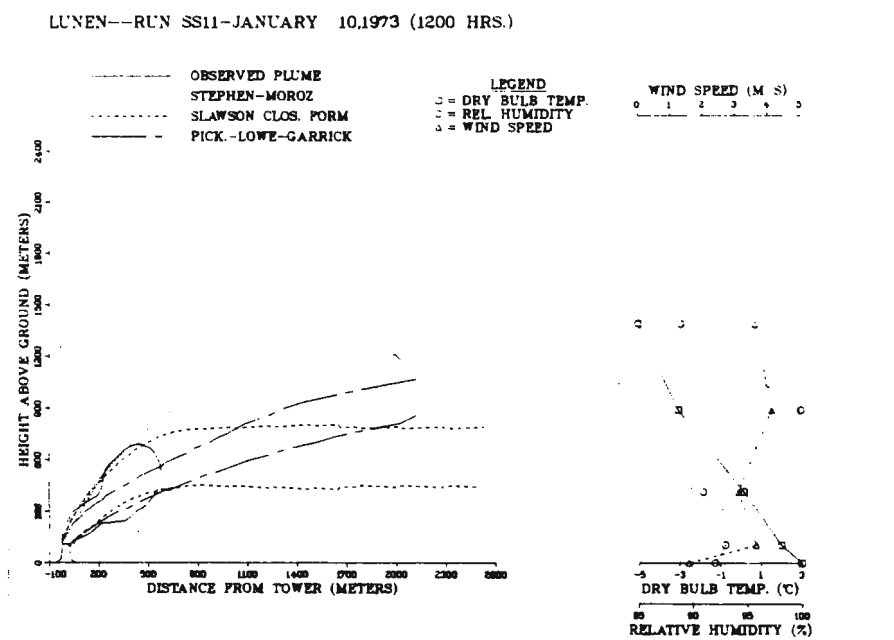
Fig. 17. Comparison of Plume-model Predictions of Stephen-Moroz, Slawson (Closed Form) and Pickard-Lowe-Garrick to Observed Visible-plume Outline at Lünen: January 10, 1973 (1200 Hrs.).
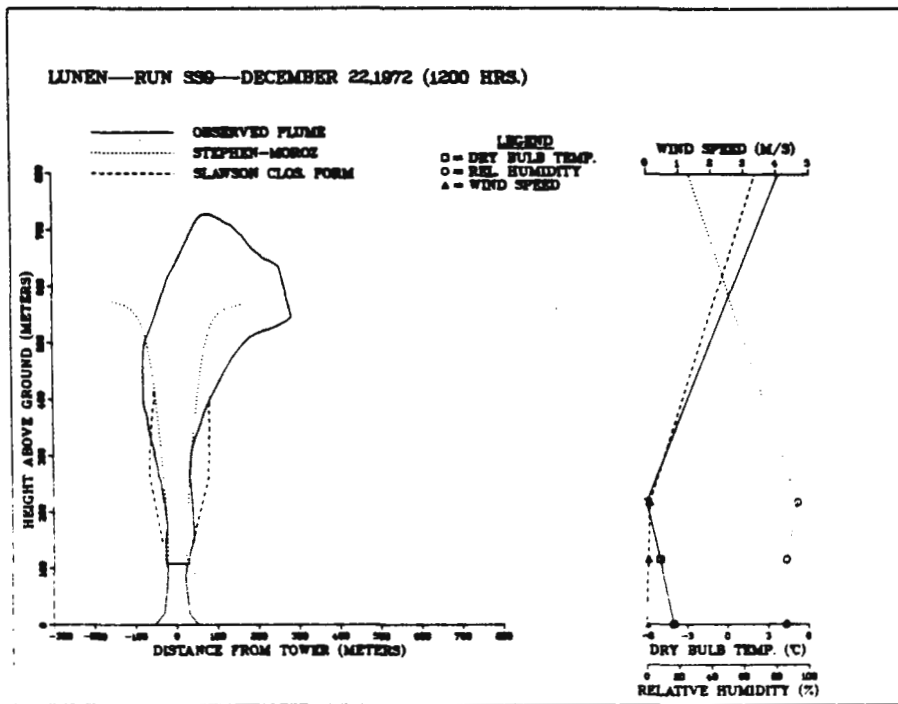
Fig. 18. Comparison of Plume-model Predictions of Stephen-Moroz and Slawson
(Closed Form) to Observed Visible-plume Outline at Lünen: December
22, 1972 (1200 Hrs.).
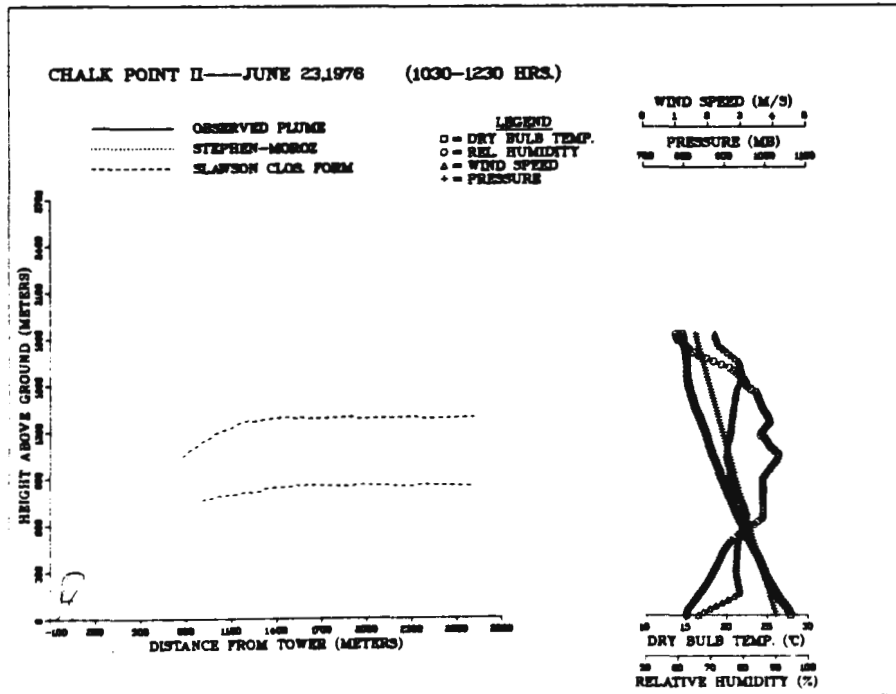
Fig. 19. Comparison of Plume-model Predictions of Stephen-Moroz and Slawson
(Closed Form) to Observed Visible-plume Outline at Chalk Point:
June 23, 1976 (1030-1230 Hrs.).
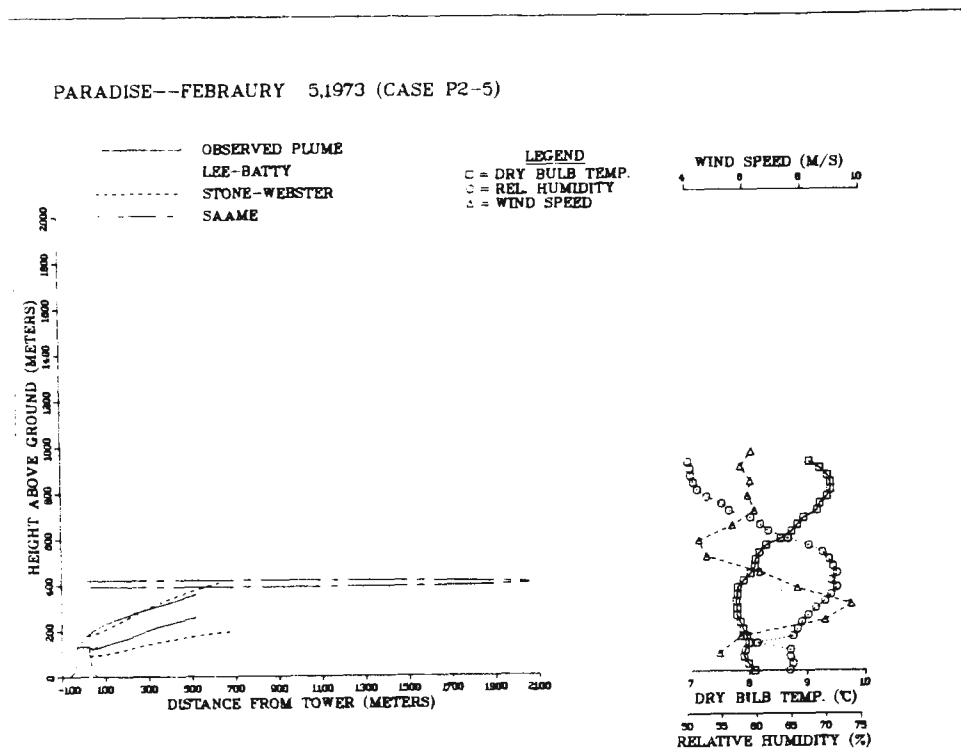
447

PARADISE--FEBRAURY 5,1973 (CASE P2-5)

Fig. 20. Comparison of Plume-model Predictions of Lee-Batty, Stone & Webster and Saame to Observed Visible-plume Outline at Paradise: February 5, 1973.

CHALK POINT I---DECEMBER 18,1975 (1002-1113 HRS.)
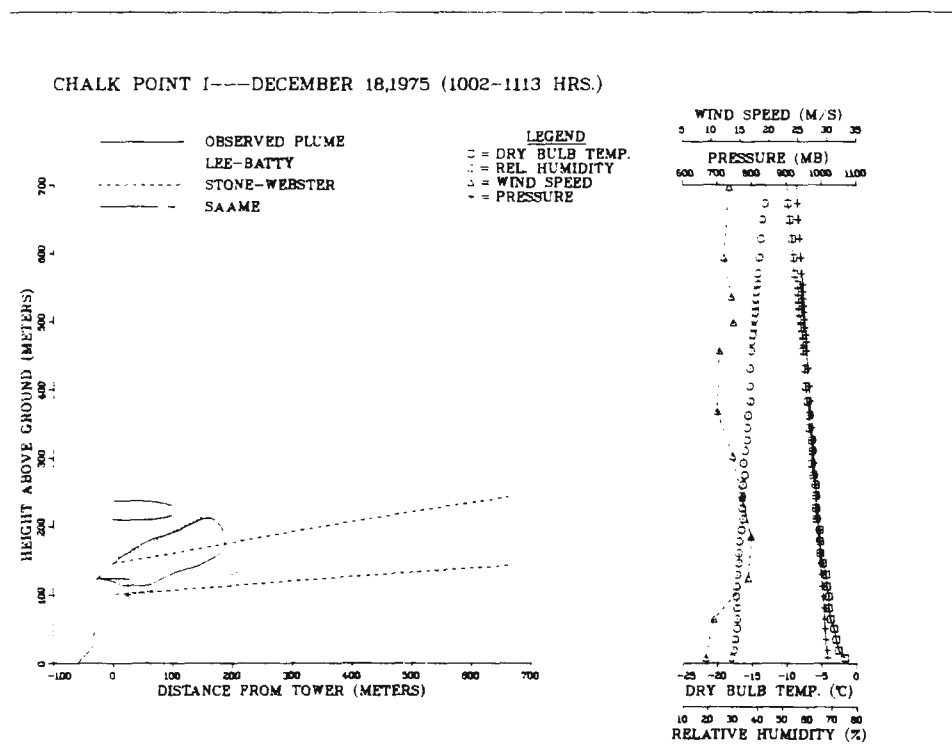
Fig. 21. Comparison of Plume-model Predictions of Lee-Batty, Stone & Webster and Saame to Observed Visible-plume Outline at Chalk Point: December 18, 1975 (1002-1113 Hrs.).

448

EVALUATION OF METHODS FOR PREDICTING
PLUME RISE FROM MECHANICAL-DRAFT
COOLING TOWERS

W. E. Dunn, G. K. Cooper* P. M. Gavin
University of Illinois at Urbana-Champaign
Urbana, Illinois U.S.A.

ABSTRACT

This paper evaluates various methods commonly used to predict the length
and height cf the visible plume produced by an array of mechanical-draft
cooling towers by comparing predictions with observational data from the
Benning Road Power Station and from a smaller array of towers at the
Purdue University Power Plant. Four different approaches - empirical,
integral, cloud-physics and finite-difference - are examined. Statistical
estimates of predictive capability are given. Problems inherent in the
application of these approaches are discussed. Observations concerning
areas of weakness and thus areas of potential improvement are made.

INTRODUCTION

Disposing of large quantities of low grade heat has long been a major
problem for industry and, in particular, the electric utility industry.
Historically, the waste heat naturally generated in the conversion of
thermal energy to mechanical energy has been rejected to nearby lakes and
rivers. In recent years, however, the shortage of available once-
through sites combined with stringent federal regulations on the use of
natural waterways has dictated the adoption of alternative methods of
cooling. The most popular alternatives, at present, are natural-draft
and mechanical-draft cooling towers.

These systems which transfer large quantities of thermal energy and
moisture to the atmosphere may also produce adverse environmental impacts.
Most of these impacts are directly or indirectly related to the vapor
plume formed in the atmosphere by the thermal energy and moisture
release. Thus, for the assessment of potential adverse effects, know-
ledge of the way in which the plume disperses in the atmosphere is
essential.

In this paper, we evaluate several different methodologies commonly used
to predict the length and height of the visible plume produced by

---

*Now at Mississippi State University.

proposed mechanical-draft cooling tower installations by comparing predictions with observational data from the Benning Road Power Station and from a smaller array of towers at the Purdue University Power Plant. This work provides a measure of the reliability with which predictions can now be made, but more importantly provides valuable insights into the weaknesses of various approaches and into methods of improvement.

THE MATHEMATICAL MODELS

The methods tested represent four different types of approach - empirical, integral, cloud-physics and finite-difference.

To some extent all models are empirical. In this context, however, an empirical model is one based solely on observational data with little or no theoretical basis. Such methods are clearly undesirable from a fundamental viewpoint, but are often the only recourse in situations for which the physics is very poorly understood. Moreover, extensive data analysis may uncover basic scaling relationships that are otherwise obscured by the complexity of the problem. Unfortunately, the one purely empirical model tested did not perform well with data from a higher power site indicating that the essential scaling relationships were not captured.

The integral and cloud-physics methods are virtually identical and it may be argued should not be distinguished. Both are one-dimensional analyses in which the dominant physical process is entrainment; the principle difference lies in their historical origins and consequent emphases. Integral models, evolved from the theory of jets, generally have no or only a simple treatment of thermodynamics. The cloud-physics models, on the other hand, include more detailed treatments of cloud processes such as condensation and evaporation and, in general, consider several different forms of liquid water.

Finite-difference models attempt to treat the physics of the problem on a microscopic level. These models, although more difficult and expensive to use, offer the potential of handling more complex tower configurations in which factors such as downwash and merging are significant problems. This potential cannot be realized, however, if the processes themselves are poorly understood or if unacceptable simplifications are necessary for computational tractability (assuming a principle direction of flow, for example). Since these models are in an early stage of development, what can now be said is subject to revision as new and better techniques become available.

The most common approach to plume modeling is based on the plume-rise theory put forth by Briggs [1] and subsequently extended by Hanna [2,3]. This theory is itself an extension of the now-classic integral analysis of jets presented principally by Morton, Taylor, and Turner [4]. Simple

algebraic relationships derived from this theory are in widespread use under the names "Briggs," "Briggs-Hanna," and "Hanna-Briggs" plume-rise formulae. These formulae represent closed-form solutions to the integral conservation equations once a great many simplifying assumptions are made. For practical application of the formulae as a predictive tool, much schematization of the problem is necessary. The ambient must be idealized in terms of a single wind speed, humidity, lapse rate, and reference temperature. The complex thermodynamic nature of the plume must be represented in terms of a single dynamic parameter, the initial buoyancy flux. Owing to the large number of ways of implementing these plume-rise formulae, all of which appear at least superficially to be reasonable, the variation among ostensibly identical formulations can be great. Moreover, the empirical coefficients inherent in these formulae can be varied on the basis of many different justifications which merely multiplies the number of predictions one can obtain.

The usual recommendation is that ambient conditions be "averaged" over the height of the "plume." Of course, when the formulae are being used in a predictive sense, the height of the plume is unknown. One common alternative is to average over some fixed height such as 500 m. A more involved procedure is to determine ambient conditions iteratively, i.e., by alternately calculating average ambient conditions and plume height until convergence is achieved. This latter approach appeared to us to be preferable and was thus used. Interestingly, this iterative procedure failed to converge in a large number of cases. Rather the calculated plume height would begin to flip-flop between two different values. In such cases, we took the simple arithmetic average of the two values as the predicted plume height. In addition, we found the common practice of using the wind speed at tower top gave very poor predictions.

Determination of atmospheric stability (stratification) can also be a source of difficulty. In general, an integrated or weighted average of temperature lapse rate over the height of the plume was found superior to the usual two point method, although the latter is typically satisfactory owing to a weak or missing dependence of predictions on stability. Moreover, use of the moist lapse rate was found to be undesirable since it made unstable some cases which were stable based on the dry lapse rate.

Exit buoyancy flux F is defined as

$$F = g \frac{\Delta \rho}{\rho} W_0 R_0^2$$

where g is acceleration of gravity, W_0 is plume exit speed, ρ is ambient density, R_0 is plume exit radius, and $\Delta \rho$ is the density difference between the ambient and the exiting plume.

In the computation of $\Delta \rho$, it has been suggested by Hanna and others that some account should be made of the latent heat of the plume. This is usually done by assuming that some fraction A of the latent heat is

converted into sensible heat. Thus, the effective plume exit temperature T_0' is given by

$$T_0' = T_0 + A(h_{fq}/C_p)\Delta\omega$$

where T_0 is the actual exit temperature, h_{fq} is latent heat of vaporization, C_p is specific heat of air, and $\Delta\omega$ is the mixing ratio of the exiting plume less that of the ambient.

We found that inclusion of latent heat gave too much buoyancy making the plume too high and short. Of course, one might argue that the entrainment coefficient should also be modified for moist buoyant plumes.

Plumes from several closely grouped sources must be treated in terms of a single source as supposed in the theoretical development of the plume-rise formulae. One extreme assumption is to simply merge all plumes instantly upon exit and sum all fluxes. A second approach is presented by Briggs [5]. He analyzes plume merging in terms of an enhancement factor which treats, at least heuristically, the relative distance between sources.

A simple computer code was written to facilitate intercomparison of the various plume-rise formulae and the comparison of plume height and length predictions with experimental data. In addition, computer codes were acquired for the models presented by Eagles and Kohlenstein [6], McVehil [7], and Commonwealth Associates [8]. These models are based in large part on the Hanna-Briggs plume-rise theory, but were modified and/or calibrated for predicting mechanical-draft tower plumes.

In addition to the several integral models tested, one model from each of the other three categories was examined. May, et al. [9], have adapted their one-dimensional cloud model to prediction of mechanical-draft cooling tower plumes. This model integrates conservation equations for vertical momentum, energy, and water content vertically using a classical entrainment hypothesis and the assumption that the plume moves horizontally at the local wind speed. Thus, this model is quite similar to the "bent-over" plume analysis of Briggs, yet handles an inhomogenous ambient and contains a more thorough thermodynamic analysis.

The model by Smith and Agee [10] was developed for Indianapolis Power and Light Company from four sets of winter plume observations. This model was included in the study since it represents an empirical model developed from mechanical-draft cooling tower data.

Compared to the above closed-form models, the two-dimensional finite-difference model presented by Taft [11] is considerably more difficult and expensive to use. Although the computer code was obtained from the author, a considerable amount of programming time was expended converting certain machine-specific operations, reworking the input format to be

compatible with the standardized format of the data and algorithmatizing and programming calculation of the "equivalent" initial conditions required by the model, a procedure originally done by hand. A typical production run of this program requires from 10 to 20 minutes of execution time on our CDC CYBER-175 and occupies about 80,000 words of memory. Owing to the significant cost involved, only a few such runs were made for comparison with available data.

THE OBSERVATIONAL DATA

A significant obstacle to the validation and improvement of mathematical models for mechanical-draft cooling tower plumes is the scarcity of observational data. For this study, we had only two sets of data available to us, one of which may be too flawed to give meaningful results.

The better of the two is the set of data collected by Meyer, et al. [12], at the Benning Road Power Plant near Washington, D. C. during the period from October 25, 1973 through February 26, 1974. The plant with a generation capacity of only 289 MWe has two linear rectangular mechanical-draft units of 8 cells each. The towers are situated on relatively level terrain near the Anacosta River. The only obstruction is a nearby incinerator. The cells are 21.3 meters high with an exit radius of 4.7 meters. The axes of the two tower structures lie in the east-west direction. The field study conducted by Meyer, et al., included measurements of (a) entrance and exit temperatures of the cooling water, plant load, and cooling water flow rate; (b) exit dry-bulb and wet-bulb temperatures for a single instrumented cell; (c) exit air speed profiles taken for the instrumented cell from which volumetric flow rates were calculated; (d) Rawinsonde profiles of ambient temperature, water vapor density, and wind speed; (e) surface-level wind direction and pressure; (f) cloud height and stability class; and (g) height and length of the visible plume obtained from photographs taken normal to the wind direction. This set of data, composed of over 50 observations, is reasonably complete and is tabulated in a form that is fairly convenient to use. One deficiency is the lack of visible plume outlines by which to test additional aspects of the models.

The second set of data employed in this study was gathered by Westlin [13] at the Purdue University Power Plant during the period between July 9, 1971 and October 10, 1971. This plant has a single tower 18.1 m high consisting of 3 cells, each with an exit radius of 4.6 m. Although the terrain is reasonably flat, the power plant which is considerably taller and longer than the tower is located directly east of the tower. Each of the 30 observations includes (a) difference between entrance and exit temperatures of the cooling water; (b) exit temperature of the plume; (c) volume flux calculated from the manufacturer's fan ratings; (d) near surface measurements of temperature, relative humidity, pressure and wind speed (with a threshold of 1 m/s); and (e) visible plume heights and

lengths extracted from photographs of the plume. Again, visible plume outlines are missing and, in addition, no ambient profile data are available. Documentation is also less complete compared with the Benning Road data. Most distressing is the fact that for many of the cases in which the wind speed was reported to be below the 1 m/s threshold of the anemometer, the length to rise ratio of the plume is much larger than in those cases for which the wind speed is reported to be greater than 2 m/s. Sadly, the original records and photographs were lost.

COMPARISON OF MODEL PREDICTIONS WITH OBSERVED PLUME HEIGHTS AND LENGTHS

A few simple statistics will be used to gage model performance. They are

δ = ratio of predicted to observed plume parameter (either length or height as indicated by subscript),

N = number of observations in data set,

δ_{max} = maximum value of δ for given data set,

δ_{min} = minimum value of δ for given data set,

γ = log-mean value of δ defined as

$$\gamma = \exp\left|\frac{1}{N}\sum_{J=1}^{N}|\ln\delta_j|\right|$$

f_2 = fraction of cases (in percent) for which $0.5 \leq \delta \leq 2.0$,

f_5 = fraction of cases (in percent) for which $0.2 \leq \delta \leq 5.0$,

f_0 = fraction of cases overpredicted, i.e., for which $\delta > 1.0$, and

f_F = fraction of cases for model failed to give a prediction for any reason.

Tables 1-3 summarize these statistics for the several models tested. An explanation of the motivation for using these statistics is in order.

The maximum and minimum values of the δ ratio are meant to indicate worst case performance. In contrast, the log-mean ratio γ is meant to characterize model performance in an average sense but one in which overprediction and underprediction are treated on equal footing and one in which an error by a factor of 4 is treated as being twice as bad as an error by a factor of 2. The fraction of cases for which the prediction is within a factor of 2 of the observation is meant to gage overall model performance taking into account the limitations of the data. Based on typical uncertainties for the measured parameters and baring major blunders on the part of the field workers, the range in predictions one might typically expect is roughly a factor of 2. Of course, model predictions are most sensitive to uncertainty in the ambient values for high relative humidity predictions. The fraction within a factor of 5 indicates the percentage of time that the model prediction is totally out of bounds as compared with the data and thus also aids in assessing worst case performance. Finally, the fractions of overprediction and model

failure are important for identifying systematic behavior in model/data discrepancies.

One may argue that these statistics do not reflect the weighting one might use in the analysis of potential environmental impact where, for example, the overprediction of short plumes by a factor of 2 is not nearly as undesirable as is underprediction of long plumes by a factor of 2. Here, however, we are most interested in determining to what extent the models reproduce the basic scaling relationships of the physical problem. In this sense, it is equally important to predict both short and long plumes accurately.

For the Benning Road data set, overall model performance is good. Only the model of Smith-Agee gives systematically poor predictions being consistently too short and low by a factor of roughly 5. Among the different models based on the Hanna-Briggs analysis, the assumption of fully merged plumes and calculation of buoyancy flux without latent heat additions proved superior. In general, we found that formulae developed and calibrated using dry-plume data perform better than those developed in an attempt to include thermodynamic effects. There may well be several compensating influences at work.

There is virtually no significant distinction among the various models (except for those already noted). Predictions are with a factor of 2 roughly 80% of the time with a mean error factor of 1.5 to 1.7. It must be pointed out that all of these models were at least partially calibrated against the Benning Road data; data from a second larger installation would be most valuable in testing model capabilities.

The model by Taft was consistently too short and low in its predictions by a factor of roughly 4 in rise and 6-10 in length for the three comparisons that were made. An explanation for this behavior is presently lacking.

Model/data discrepancies are considerably greater for the Purdue data. All of the models tend to overpredict both plume rise and length. Only the cloud-physics model of May et al. performed well with this data. These results must be viewed cautiously owing to the uncertainties in the data and to the fact that most plumes were quite short so that large factors of overprediction may not be very serious. The reason(s) for the good performance of the cloud-physics model are not presently known. The model of Smith and Agee did better with this data.

SUMMARY AND CONCLUSIONS

This paper considers and evaluates by comparison of predictions with observation data four different approaches to plume modeling. The results of this study are: (a) Among the integral formulations based

on the results of Briggs and Hanna, the "dry-plume" formulae give better predictions of plume rise and length than do the formulae which attempt to treat thermodynamic effects. (b) The integral models predicted plume character very well at the Benning Road Station but not as well at the smaller Purdue Power Plant. One explanation is perhaps that several of the models were at least partially calibrated with the former data. (c) The cloud-physics model did well at both sites although the reason for this result was not determined. (d) The empirical model tested did not do well at the Benning Road site suggesting that it did not conatin the correct basic scaling relationships. (e) The one finite-difference model gave plumes consistently too short and low. A poor understanding of the micro-scale physics treated by this model is a possible explanation. (f) Treatments of plume merging and downwash are poor. However, the common approach of instantaneous merging did well with the Benning Road data perhaps again because of favorable calibration.

REFERENCES

1. G. A. Briggs, Plume Rise, AEC Critical Review Series, Report TID-25075, 1969.

2. S. R. Hanna, Predicted and Observed Cooling Tower Plume Rise and Visible Plume Length at the John E. Amos Power Plant, AE, 10, 1043-52 (1976).

3. S. R. Hanna, Meteorological Effects of the Mechanical-Draft cooling Towers of the Oak Ridge Gaseous Diffusion Plant, Cooling Tower Environment - 1974, CONF-740302, 1975.

4. B. R. Morton, G. I. Taylor, and J. S. Turner, Turbulent Gravitational Convection from Maintained and Instantaneous Sources, Proc. Roy. Soc. (London), Ser A, 234" ;-23 (1956).

5. G. A. Briggs, Plume Rise from Multiple Sources, Cooling Tower Environment - 1974, CONF-740302, 1975.

6. T. W. Eagles and L. C. Kohlenstein, A Cooling Tower Visible Plume Prediction Model Based on Measurements, presented at Fifty-fifth Annual Meeting of American Geophysical Union, held in Washington, D.C. 1974.

7. G. E. McVehil, Personal Communication, Boulder, Colorado, May, 1977.

8. Y. H. Huang, Personal Communication, Commonwealth Associates, Jackson, Michigan, January, 1977.

9. L. E. May, H. D. Orville, and J. H. Hirsch, Application of Cloud Model to Cooling Tower Plumes and Clouds, Institute of Atmospheric Sciences, South Dakota School of Mines and Technology, Rapid City, South Dakota, September, 1977.

10. P. J. Smith, and E. M. Agee, Empirical Equations for Mechanical Draft Cooling Tower Plumes, prepared for Indianapolis Power and Light Company, Indianapolis, Indiana, 1969.

11. J. Taft, Numerical Model for the Investigation of Moist Buoyant Cooling Tower Plumes, Cooling Tower Environment - 1974, CONF-740302, 1975.

12. J. H. Meyer, T. W. Eagles, L. C. Kohlenstein, J. A. Kagan, and W. D. Stanbro, Mechanical Draft Cooling Tower Visible Plume Behavior: Measurements, Models, Predictions, Cooling Tower Environment - 1974, CONF-740302, 1975.

13. P. R. Westlin, A Field Study and Analysis of Cooling Tower Plumes, M. S. Thesis, Purdue University, 1972.

TABLE 1. MODEL PERFORMANCE STATISTICS FOR THE BENNING ROAD PLANT

	Parm	δ_{min}	δ_{max}	γ	percent			
					f_2	f_5	f_0	f_F
Hanna-Briggs/S*	H	0.18	2.5	2.4	42	96	10	0
Hanna-Briggs/S	L	0.17	6.5	2.7	22	96	4	0
Hanna-Briggs/SL	L	0.10	1.8	4.5	2	100	0	0
Hanna-Briggs/M	H	0.45	0.8	1.7	84	48	56	0
Hanna-Briggs/M	L	0.28	3.0	1.8	74	100	18	0
Hanna-Briggs/ML	L	0.17	1.3	2.6	22	94	4	0
Eagles-Kohlenstein	H	0.35	4.4	1.6	90	100	42	0
Eagles-Kohlenstein	L	0.46	3.6	1.4	94	100	36	0
Smith-Agee	H	0.03	0.6	7.6	8	40	0	4
Smith-Agee	L	0.08	0.9	4.1	8	68	0	4
May, et al.	H	0.54	2.9	1.5	86	100	74	0
May, et al.	L	0.40	10.	1.6	88	98	46	0
McVehil	H	0.36	4.0	1.6	70	100	30	0
McVehil	L	0.32	3.2	1.5	88	100	24	0
Commonwealth	H	0.20	4.2	2.0	50	100	46	0
Commonwealth	L	0.23	9.3	1.8	84	96	46	0

*S = single cell; M = multiple cell plumes merged instantly; L = latent heat added to buoyancy flux

458

TABLE 2. MODEL PERFORMANCE STATISTICS FOR THE PURDUE PLANT

	Parm	δ_{min}	δ_{max}	γ	percent f_2	f_5	f_0	f_F
Hanna-Briggs/S*	H	2.0	24.	6.6	0	50	100	0
Hanna-Briggs/S	L	0.32	34.	2.8	44	88	88	0
Hanna-Briggs/SL	L	0.19	19.	2.4	63	81	44	0
Hanna-Briggs/M	H	3.5	42.	11.5	0	13	100	0
Hanna-Briggs/M	L	0.42	44.	3.4	38	81	88	0
Hanna-Briggs/ML	L	0.24	26.	2.4	63	88	63	0
Eagles-Kohlenstein	H	1.5	14.	5.4	6	44	100	0
Eagles-Kohlenstein	L	0.35	24.	2.2	63	81	50	0
Smith-Agee	H	0.03	2.2	2.5	63	81	44	0
Smith-Agee	L	0.16	5.8	2.5	50	88	31	0
May, et al.	H	0.98	2.4	1.8	38	69	63	31
May, et al.	L	0.59	2.4	1.6	50	69	56	31
McVehil	H	3.5	34.	10.0	0	13	100	0
McVehil	L	0.53	65.	4.8	25	63	88	0
Commonwealth	H	4.3	16.	8.4	0	13	100	0
Commonwealth	L	1.1	8.6	2.7	44	75	100	0

*S = single cell; M = multiple cell plumes merged instantly; L = latent heat added to buoyancy flux

	Parm	δ_{min}	δ_{max}	γ	percent			
					f_2	f_5	f_0	f_F
Hanna-Briggs/S*	H	0.18	24.	3.1	32	85	32	0
Hanna-Briggs/S	L	0.17	34.	2.7	27	94	24	0
Hanna-Briggs/SL	L	0.10	19.	3.9	17	95	11	0
Hanna-Briggs/M	H	0.45	42.	2.7	64	40	67	0
Hanna-Briggs/M	L	0.28	44.	2.1	65	95	35	0
Hanna-Briggs/ML	L	0.17	26.	2.6	32	93	18	0
Eagles-Kohlenstein	H	0.35	14.	2.1	70	86	56	0
Eagles-Kohlenstein	L	0.46	24.	1.6	86	95	39	0
Smith-Agee	H	0.03	2.2	5.8	21	50	11	3
Smith-Agee	L	0.08	5.8	3.6	18	73	8	3
May, et al.	H	0.98	2.9	1.6	74	92	71	10
May, et al.	L	0.40	10.	1.6	79	91	48	10
McVehil	H	0.36	34.	2.5	53	79	47	0
McVehil	L	0.32	65.	2.0	73	91	40	0
Commonwealth	H	0.20	16.	2.8	38	79	59	0
Commonwealth	L	0.23	9.3	2.0	74	91	59	0

*S = single cell; M = multiple cell plumes merged instantly; L = latent
heat added to buoyancy flux

ENVIRONMENTAL COST OF POWER PLANT WASTE HEAT
AND CHEMICALS DISCHARGE IN TROPICAL MARINE WATERS

J.M. López
Center for Energy and Environment Research
Mayaguez, Puerto Rico

ABSTRACT

A 1125 MW, oil-fired power plant has been discharging once-through cooling water in Guayanilla Bay, Puerto Rico for several years. The heated effluent enters an enclosed cove connected to the eastern portion of the bay by a narrow mouth. This Thermal Cove and surrounding area once supported luxuriant growth of mangroves, seagrasses and the associated plant and animal life of these ecosystems. In this study, a critical review was made of previous investigations concerned with various aspects of the intake and discharge area environments. An assessment of environmental degradation due to the power plant activity is offered which considers losses in the major ecosystem components and the accumulation of hazardous chemicals in the receiving system.

INTRODUCTION

The South Coast electric power plant complex, located in Guayanilla, Puerto Rico is comprised at present of six oil-fired generating units with a total generating capacity of 1125 MW. Once-through cooling water is withdrawn from Guayanilla Bay at a rate of 1,597,882 lpm (604,800 gpm). A 10°C temperature rise is imposed on the cooling water which is discharged through a 100 m canal into a nearly enclosed lagoon 900 m long by 200 m wide. The heated lagoon, referred to as Thermal Cove, in turn discharges into Guayanilla Bay through its 30 m wide mouth. In addition to heated seawater, the power plant effluent contains chemical contaminants such as petroleum hydrocarbons, trace metals (Cu, Cr, Hg, Zn and Ni) and chlorine emanating either from the power plant or from other industries that discharge wastewaters in Guayanilla Bay. The ecosystem in the area affected by this heated effluent is composed of seagrasses, mangroves and soft bottom communities. Seagrasses, predominantly Thalassia testudimum communities, occur in shallow flats (1 m) immediately outside of the mouth of the Thermal Cove. Red mangroves, Rhizophora mangle are the dominant trees in the community that fringes the entire eastern shore of the Thermal Cove. Similar communities are found in the cooling water intake region in Guayanilla Bay. Several investigations have been conducted at this laboratory into the nature and extent of the ecosystem response to this heated effluent. For these, comparative ecological studies were performed using the cooling water intake region as a comparison site. The configuration of the receiving area, being nearly enclosed, is such that most of the impact of the heated effluent on the environment is localized (Fig 1).

This allows for an assessment of ecological losses and consequences to the environment within distinct physical bounds. In this paper I review the existing information on losses in the biota of the Thermal Cove and present recent data on the levels of hazardous chemicals accumulated there as a result of the plant's operation over the years. The ecological losses or changes and the accumulation of chemicals and their significance represent an estimate of the environmental cost of discharging waste heat and chemicals associated with the generation of electricity in tropical marine waters.

ECOLOGICAL STUDIES

Kolehmäinen et al. (1) summarized results of studies performed by Puerto Rico Nuclear Center scientists in the Guayanilla Bay Thermal Cove. About 95% of zooplankters entering the cooling system were killed in the condensers and in the discharge canal. Within 100 m of the end of the discharge canal (8°C above ambient) further zoopankton mortality was observed. However, in areas at 4°C and 6°C above ambient, species diversity and biomass were higher than in areas at ambient temperature. Most of the mortality apparently occurred in the long exposure (14 min.) to high temperatures in the discharge canal with only 10% of the mortality occuring in condensers and pumps.

Benthic macroanimals were absent from the area within the Thermal Cove (1). This can be the combined effect of erosion by the strong effluent stream, high temperature and chemical toxicity. The heated effluent exits the Thermal Cove as a surface layer leaving the benthos unaffected outside of the Thermal Cove. Loss of benthic macroanimal communities extends to the area occupied by this lagoon.

About 19 ha of fringing mangroves (predominantly Rhizophora mangle) line the eastern shore of Guayanilla Bay including the Thermal Cove. Trees nearest the discharge canal and at the mouth of the lagoon were killed by sediment erosion from around their roots caused by strong currents generated by the power plant effluent (1). Seedlings from red mangrove trees in the Thermal Cove are smaller than those from areas not affected by the heated effluent and showed very low probablility for survival and growth (2). Banus and Kolehmainen (2) found no young rooted and growing seedlings in the Thermal Cove. In 1974 they found most trees showing visible signs of stress such as lesser and smaller leaves and few and small seedlings.

Kolehmainen et al. (3) found that mangrove root communities in the Thermal Cove decreased in species diversity as temperatures increased above 34°C. In Thermal Cove mangrove roots a species of barnacle and the tree oyster made up most of the biomass. The lowest biomass occurred near the canal discharge where currents and temperatures are greatest.

462

Fish fauna within the heated lagoon (28 species) was less diverse than in the intake area (53 species). The dominant species in the Thermal Cove were the mojarras and the sea bream (1). Recent fishing efforts by gill nets and trawling has yielded little or no fish while some success is obtained at the mouth of the lagoon. No significant fishery appears to exist in the Thermal Cove as a result of the power plant discharge.

Schroeder (4) determined that seagrass (Thalassia) beds occuring near the mouth of the Thermal Cove and receiving the heated effluent contained less plant material (leaves and root biomass) per unit area than comparison areas within Guayanilla Bay.

CONTAMINATION BY CHEMICALS

Chemical contaminants moving through the power plant cooling system may be augmented by corrosion losses of trace metals and petroleum spills or oil and grease discharges. Chlorine may react with organic substances at the increased temperature of this effluent to form substances that are more hazardous. The potential toxicity of this discharge, however, has not been determined. It is conceivable that synergism may exist in the combined effects of chemicals and heat. Bottom sediments of natural water systems are the repository of substances occurring in the overlying waters and their composition reflect the longterm chemical regime of the said waters. The chemicals discharged by the power plant accumulate in the sediments of the Thermal Cove.

Surface sediment samples were obtained from the Thermal Cove and intake areas. Portions were dried and ground and wet digested with modified aqua regia and hydrogen peroxide prior to atomic absorption analysis for Cd, Cu, Ni, and Zn and Cr. Mercury determinations were performed by flameless atomic absorption. The sediments were also soxhlet-extracted with a benzene-methanol mixture and content of petroleum hydrocarbons was determined gravimetrically after saponification.

Results (shown in Table I) demonstrate that the Thermal Cove sediments have accumulated significant amounts of Cd, Cu, Ni, Zn, and petroleum hydrocarbons containing increased levels relative to the intake and adjacent areas. The Thermal Cove sediments in fact, showed the highest conentration of Zn, Cu, Cd, Ni and petroleum hydrocarbons of any other area in Guayanilla Bay. These data imply an enrichment by the power plant of the load in the waters of Guayanilla Bay. The Thermal Cove acts as a catchment basin and sink of pollution. The increase from intake to discharge area in ug/g is from 1.6 to 2.3 for Cd, from 47 to 117 for Cu, from 20 to 47 for Ni and from 0.19 to 0.34%. No appreciable enrichment was observed for Cd, Cr and Hg although it is evident that at least translocation of chemicals freely occurs. The actual chemical form of these substances or whether the power plant chemically changes them is not known.

The accumulated chemicals are likely partially responsible for the lack of benthic organisms. In addition, this pool of hazardous substances can be potentially available for assimilation in the biospere. These can become biologically available when associated to organic matter such as detrital particles of mangroves or zooplankton which abound in the area. Through that route the hazardous substances may become magnified in the marine food web that eventually reaches the human consumer. In effect, other research at this laboratory (5) has shown that trace metals become available to turtle grass and mangrove tissue in Guayanilla Bay. In particular, mercury accumulation and cycling by mangroves can be substantial compared to known sources to the bay. Mercury is actually permeating the biospere and levels in some top predators, consumed by humans, show biomagnification to unacceptable levels.

CONCLUSIONS

The environmental costs of producing electricity using coastal tropical waters for cooling can be approximated by considering losses to the biota of the Thermal Cove in Guayanilla Bay. Studies have shown that the area of the Thermal Cove (900 m X 200 m) is essentially denuded of life or severely impaired as a habitat. That area is lost for shelter, feeding or breeding grounds of most animals. It is lost for fishing also. Several hectares of mangrove forests are destroyed or severely deteriorated. Losses in the overall efficiency of the Thalassia ecosystem outside of the cove are also in evidence where lower biomass of these important plants occur in the affected areas. These effects on the aquatic environment do not consider possible environmental cost due to possible air pollution resulting from combustion of petroleum by the power plant.

One important impact of the heated effluent discharge that is often overlooked is the addition of chemical contaminants such as trace metals and petroleum hydrocarbons to the receiving system. The data presented, demonstrate a net accumulation of these hazardous substances in the sediments confined to the Thermal Cove area. This is a cost to the environment since the area is rendered virtually a biological desert partially due to chemicals and heat . The chemical accumulation can have far reaching consequences as it may provide a long lasting pool of biologically available hazardous substances. This can lead to widespread bioaccumulation that can affect human health and also impair commercial fisheries through fish-flesh tainting by hydrocarbons, toxicity and biomagnification to unacceptable levels of substances such as mercury, as has been shown to be the case in Guayanilla Bay. The environmental cost of the Costa Sur plant waste heat and chemical discharge includes the area of the Thermal Cove and the ecosystems it represents. This cost, however, goes beyond that because of the remote, long-lived effects of the accumulated chemicals.

ACKNOWLEDGMENTS

REFERENCES

1. Kolehmainen,S.E., F.D. Martin and P.B. Schroeder "Thermal Studies on Tropical Marine Ecosystems in Puerto Rico" In:"Environmental Effects of Cooling Systems at Nuclear Power Plants" IAEC, Vienna (1975)

2. Banus, M.D. and S.E. Kolehmainen "Rooting and Growth of Red Mangrove Seedlings from Thermally Stressed Trees" In: Thermal Ecology II, Esch, G.D. and McFarlane, R.W. (eds.) ERDA (1976)

3. Kolehmainen, S.E., T. Morgan and R. Castro "Mangrove Root Communities in a Thermally Altered Area in Guayanilla Bay, Puerto Rico" In: Thermal Ecology, Gibbons, J.W. and Sharitz, R.R. (eds.), USAEC, (1974)

4. Schroeder, P.B. "Thermal Stress in Thalassia Testudinum" Ph. D. Dissertation, The University of Miami (1975)

5. López, J.M. and H.J. Teas "Trace Metals Cycling in Mangroves" Symposium on Trace Metals Cycling in Coastal Plant Ecosystems, American Botanical Society, Virginia Polytechnic Univ. (1978)

TABLE I
RELATIVE CONCENTRATION OF CHEMICALS
IN SEDIMENTS OF INTAKE AND THERMAL COVE

	INTAKE	THERMAL COVE
Cadmium, ug/g	1.6	2.3
Copper, ug/g	47	117
Chromium, ug/g	34	37
Nickel, ug/g	20	47
Mercury, ug/g	0.46	0.50
Zinc, ug/g	57	91
Petroleum hydrocarbons, % dry wt.	0.19	0.34
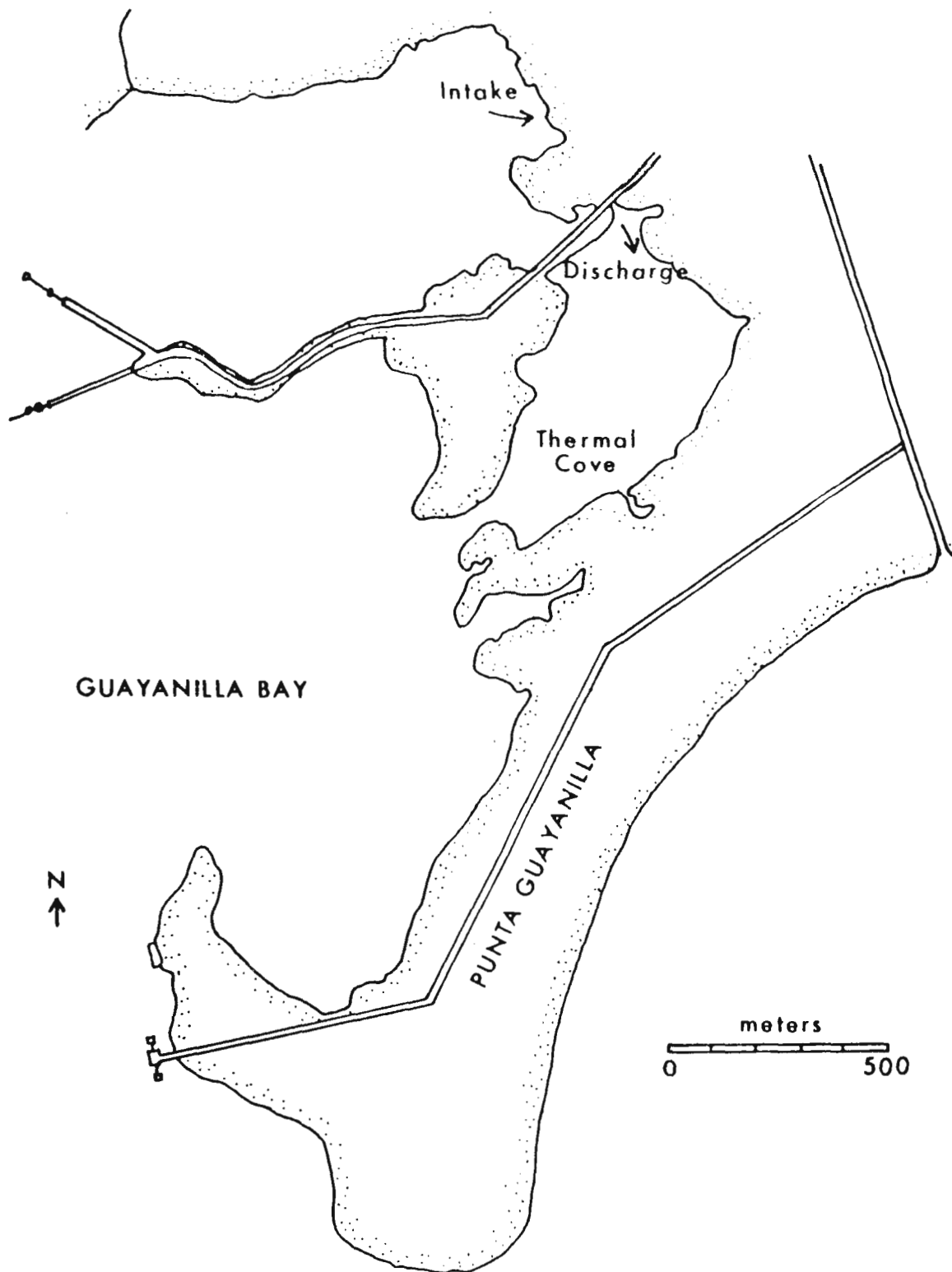
FIGURE I
LOCATION OF STUDY AREA IN GUAYANILLA BAY

Intake

Discharge

Thermal
Cove

GUAYANILLA BAY

PUNTA GUAYANILLA

N

meters

0   500

THEORY AND APPLICATION IN A BIOLOGICAL ASPECT

T. Kuroki
Tokyo University of Fisheries
Minato-ku, Tokyo, JAPAN

ABSTRACT

From a view-point of bio-thermodynamics, the author expounds
the theory of thermal stimulus on aquatics. The strength of
thermal stimulus depends upon temperature change (θ), but not
upon temperature (T) itself in a poikilothermal animal. For
the purpose of good management and utilization of waste heat,
data should be retreated along the understanding of stimulation
(θ) in a short period response of animal and of the stimulation
quantity ($Q=\theta \cdot t$) in a long period response. These interpre-
tation under the relations between responses of aquatics and
$\ln(\theta)$ (or $\ln(Q)$) are shown in several examples. A new plank-
ton collector (MERI-O type) which is to record environmental
factors in real time will be introduced.

INTRODUCTION

For a nice management to protect a marine ecosystem against
waste heat and for an effective utilization of waste heat to
aquaculture, exact informations about a thermo-dynamical phys-
iology and a temperature conditional ecology of aquatics is
essential. In general, the body temperature of poikilother-
mal animal is almost equal to the temperature of surrounding
water under a steady condition for about 20 minutes or more.
So, the water temperature (T°K) itself is only a physiological
condition for fish, it can not be stimulus for fish-body.
The thermal stimuli for fish should be the temperature change
(inceasings or decreasings $\pm \Delta$T°K). Then, the thermal irri-
tability (Weber ratio) of aquatic animal can be expressed as
"$\Delta\theta/\theta$", not as "ΔT/T"; where ΔT or θ is a temperature differ-
ence from the initial state, and $\Delta\theta$ is a differential value of
θ by small space or by short time.
Tamiya(1952)[1] had discussed about the threshold curve(Weiss'
hyperbola) that the susception at the part of longer duration
of stimulus on this curve follows to "Weber's Law" ($\Delta\theta/\theta$;con-
stant) and that, in the part of shorter duration, the suscep-
tion for stimulus follows "Quantity Law" ($\Delta Q/Q$;constant, where
$Q=\theta \cdot t$ and $\Delta Q=\Delta\theta \cdot t$ or $\Delta Q=\theta \cdot \Delta t$). In Tamiya's theory, the order
of length (short or long) of period of stimulus duration should
be determined relatively with the length of period in order to

468

recognize the response of living body change.   Therefore, for
the plans of management and utilization of waste heat, it is
very important to select the scale order of space or time
length best fitted to the biological aspect.   In this paper,
only aquatic animal(fish) is studied; but the theory and its
develop-ment can be applied also to other animals, even to insects
or vegetables.

THERMAL SUSCEPTION OF FISH

Two examples of thermal susception of fish under various water
temperature are shown here.   One of them is an electro-physi-
ological experiment by Kuroki[2] and the other is a study of e-
cological migration by Hanaoka[3].

Physiological aspect

First, electrifying threshold curves(Weiss' hyperbola) of carp
were obtained in various water temperature (5-35°C) as Fig. 1
of example at 15°C.   From these curves, rheobase (q) and
chronaxie (p) at various temperature were determined as Fig. 2.
Here, it should be recognized that the rheobase q is the minimum
strength of stimulus in electrifying threshold; on the other
hand , chronaxie p is the stimulus duration where the quantity
of electric energy in stimulus for threshold is minimum.   The
value of p shows the shortest at 26°C and that the value of q
shows the least at 13°C.   That is, fish selects a zone of
water temperature being nearer to one of the two temperatures
according to physiological needs.

Ecological aspect

Hanaoka (1972)[3] had proposed the "migration triangle" to show
the environmental conditions for fish schools under their mig-
ration in the fishing ground.   In Fig. 3, the relations between
water-temperature and salinity (osmotic pressure) along the
migration course of fish schools are drawn as triangle shapes
ckockwise or anti-clockwise with months elapsed.   There is a
certain range of moderate water temperature for fish, and fish
schools migrate from a higher temperature zone to a lower one
in a stage of their life cycle, and they migrate by otherwise
desposition in the other stage.   It should be noted that fish
does not always select a single optimum temperature, but that
they will select various temperatures in a certain range.

Thermal stimulation on fish

Usual kinds of fish are poikilothermal animals, therefore their
body temperatures are almost equal to the surrounding water
'temperature.   If there would be any difference between two temper-

atures of body and water, it should be only ±0.2°C; + means
body temperature is higher than water temperature, perhaps, in
an exothermal state of fish and - means lower body temperature
in an endothermal state. [4] As a special case, several kinds
of fish (tuna and shark) have a system of keeping warmness, so
called "wonderful net". [5] In case when fish school run into
the water mass where a temperature differs withΔT_0 (= θ_0) from
the other water mass at time t = -t_0, after a delay t_0 of heat
transmission to the sensor of fish, the strength of thermal
stimulation is exponential to t, (cf. Fig. 4).

$$\theta = \theta_0 \cdot e^{-ct} \tag{1},$$

where, θ ; temperature difference at t=t

θ_0; temperature difference at t=-$t_0\sim0$

C ; exponential constant

$$\frac{d\theta}{dt} = \theta_0 \cdot e^{-ct} \cdot (-c) = -c \cdot \theta \tag{2}.$$

Here, several assumptions can be developed as follows: In a
sensitive organ, there is a certain reversible system;

$$P \underset{k'}{\overset{k}{\rightleftarrows}} P' \tag{3},$$

where k and k' in the relation are rate constants in the pro-
cess[es] indicated by arrows.   When the system receives a stimulus
of thermal strength θ , following change of the reaction occurs
with an additional rate constant $K_s\theta$(proportional to θ),

$$P \underset{k'}{\overset{k+k_s\theta}{\rightleftarrows}} P' \tag{4}.$$

Dennoting (P'), the concentration of P' will increase as fol-
lows;

$$\frac{d[P']}{dt} = (k + k_s\theta)[P] - k'[P'] \qquad (5).$$

A certain parameter G may be assumed, which is quantitatively related with the occurrence of response as a sign of irritability. A small definite value of ΔG corresponds to a definite magnitude of response. The significance of this parameter is that it is quantitatively related to the <u>free energy</u> (F) determined by the concentration of P' in the following way;

$$\frac{dG}{dF} = \alpha \qquad (6),$$

$$(\; \alpha \; ; \quad \text{constant} \;).$$

The relation between F and the concentration of P' is given by the Second Law of thermodynamics, thus

$$\frac{dF}{d[P']} = \frac{RT}{[P']} \qquad (7),$$

(R ; gas constant)
(T ; absolute temperature).

From the equations (6) and (7) ,

$$\frac{dG}{d\theta} = \frac{\alpha RT}{[P']} \frac{d[P']}{d\theta} \qquad (8).$$

From the equations (2) and (5),

$$\frac{d[P']}{d\theta} = \frac{(k + k_s\theta)[P] - k'[P']}{-c\theta} \qquad (9).$$

Substituting (9) to (8) ,

$$\frac{dG}{d\theta} = \frac{\alpha RT}{c\theta}\left\{ k' - (k + k_s\theta)\frac{[P]}{[P']} \right\} \qquad (10).$$

For simplicity, let us introduce K,

$$K = \left\{ k' - (k + k_s\theta)\frac{[P]}{[P']} \right\}$$ (11).

Integrating the equation (10) under the condition that T and K are nearly independent of θ,

$$\ln\theta = \frac{cG}{\alpha R T K} + \beta$$ (12),

(β ; constant),

or

$$G = \frac{\alpha R T K}{c}\ln\theta - \gamma$$ (13),

($\gamma = \frac{\alpha R T K}{c}\beta$; constant).

The equations (12) and (13) show that the value of response G has linear relation with logarithmic value of θ. Furthermore , from the equations (10) and (11), the Weber ratio in thermal stimulation follows;

$$\frac{\Delta\theta}{\theta} = \frac{\Delta G \cdot c}{\alpha R T K}$$ (14).

Examples of application

Hirata (1960)[6] exerimented about the feeding activity of gold-fish and the temperature chage in every one hour for several days of every month. He found that there was a positive correlation between the total feeding frequency of a day and the average water temperature of the day, and that most of the maximum feeding frequencies occurred just at the time of the inflection point of water temperature change (cf. Fig. 5).
Kuroki (1967)[4] rearranged these data considering the equations

472

(12) and (13), and obtained Fig. 6.   In this figure, K > 0 or k'[P'] > (k+k$_s$θ)[P], in other words, leftward reaction is stronger than rightward reaction at all time in the equation (4); and k'[P'] is quite higher than (k+k$_s$θ)·[P] in summer (B-line in Fig. 6), and not so higher in winter (D-line).
Thermal motive power for upstream or downstream movements of rainbow trout fry from the data of Northcote (1962)[7] is shown in Fig. 7.   The number of movement is seemed to be proportional to a certain quantity of temperature chage.   This quantity is found to be the sum of two decreases between the maximum temperature of one day(afternoon) and the minimum temperature of the nex day(early morning) in 3 consecutive days.   The results of these examples prove the equations (12) or (13); that is, the magnitude of response G have the proportional relation with the logarithm of temperature change θ.

INVESTIGATION OF THE INFLUENCES OF WASTE HEAT

We can measure the temperature continuously at any point in the mixing area of waste warm water and surrounding cool water, but it is very difficult to measure quantitatively the responses (various changes of behavior or shape) of aquatic animals in the same area.
Generally, it is very difficult to select biological factor to measure, because the relations between the response of aquatic animals and mixing water are complicated and abstruse.   In the physiological or ecological states of poikilothermal animal, "warmness" is essential for the animal life, and "coolness" is also as the same important as "warmness"; but the necessary period of wamness or coolness should be quite different in various stages.   Some proposals about methods to investigate the influences of waste heat on aquatic animals will be descibed in this section:

In case of relatively long duration stimulus

When the response of aquatics G can be measured in the intervals of several seconds, the thermal stimulus θ (or temperature change in mixing zone of waste heat) will be relatively long duration for aquatics, because the θ must be transmitted to sensors of fish-body in scores of seconds.   In this case, the influence of water temperature on aquatics can be considered along the law of animal irritability in the equation (14).   If the minimal quantity of response ΔG is constant, then the equation (14) is equal to Weber's Law (Δθ/θ = constant).   And, it will be proper to measure the water temperature with the Eulerian method in this case; that is, measuring apparatus can be set on fixed points in the mixing zone.

In the case relatively short duration stimulus

The thermal stimulus θ should be transmitted to the fish-body in the time length of several scores seconds just same as the above case, but the stimulus duration is relatively shorter than the period of response in this case.   For example, the response period of aquatics is the time length of hours or days, and the stimulus is transmitted twice or more times, consecutively or interruptedly, during the period.   In this condition, the influence of temperature on aquatic animals should follow the "Quantity Law" of vegetable irritability;

$$\frac{\Delta Q}{Q} = \frac{\Delta G \cdot c'}{\alpha R T}$$

(15).

Tamiya had proved theoretically the equation (15)[1]   If ΔG is set constant, the value of $\Delta Q/Q$ will be constant as of Weber's Low in a broad sense.   To investigate the phenomena of "Quantity Law", it is necessary to apply a Lagrange's method; for example, a telemetry apparatus to measure continuously the position of fish and the surrounding water temperature at the same time.

Practical period and distance to measure in the sea

It takes only a few seconds to recognize the response ΔG of a swimming behavior of fish under a sharp temperature gradient. But it may take several days or months to recognize the response ΔG or G such as vernalization and maturity of aquatics.   When there is a spatial temperature gradient of about 0.02°C per meter in the sea and if fish swim with the speed 0.1 ~ 2.0 m/sec the water temperature should be measured once per 10 seconds ~ twice per one second, because the threshold of fish against temperature change is estimated about ± 0.02°C .   Then measuring apparatus must be set at every one meter distance.   For another example, usually plankton and fish-egg can be drifted with vortices or currents at velocity range 1 ~ 100 cm/sec.   If the threshold of plankton is assumed to be about ± 0.5°C, then the measuring period should be once per 25 sec. in high velocity current (1m/sec) and may be once per 2500 sec. (about 42 minutes) in low velocity (1cm/sec.).

CONCLUSION

One should know the role of thermal stimulus on the sense of aquatic animals.   When treating the data for utilization of waste heat, the strength of thermal stimulation θ and the quantity of stimulation Q (= θ·t) must be understood in the strict sense.   The apparatus to measure the influences of waste heat on the poikilothermal animals should be designed under the full

474

understanding of θ and Q .   In Japan, a special purpose apparatus to collect planktons and fish-eggs in the sea off the nuclear power stations is under design and will be set up at the Marine Ecology Research Institute (Fig. 8).

REFERENCE

1. H. Tamiya (1952): "A New Interpretation of the Weber Law and the Weiss Law"; Cytologia, Vol. 17, No. 3, pp. 243 -269.
2. T. Kuroki (1954): "On the Relation between Water Temperature and the Response for Stimuli"; Mem. Fac. Fish. Kagoshima Univ., Vol. 3, No. 2, pp. 19-24.
3. T. Hanaoka et al. (1972): "Studies on the Osmotic Pressure of Environmental Media and Body Fluid of Marine Fish (I)"; Bull. Jap. Soc. Sci. Fisheries, Vol. 38, pp. 1351-1356.
4. T. Kuroki (1967): "Thermal Stimulation on Fish"; Bull. Jap. Soc. Sci. Fisheries, Vol. 33, pp.264-274.
5. F. G. Carey (1966): "Fishes with Warm Bodies"; Sci. American, Vol. 212, No. 4, pp. 36-44.
6. H. Hirata (1960): "Diural Rhythm of the Feeding Activity of Goldfish with Special Reference to the Inflection point of Temperature change"; Bull. Jap. Soc. Sci. Fish. Vol. 26, pp. 783-791.
7. T. G. Northcote (1962); "Trout Migration at Loon Lake"; Jour. Fish. Res. B. Canada, Vol. 19, No. 2, pp. 201-270.

Fig.1. Example of Weiss-curves at 15 °C
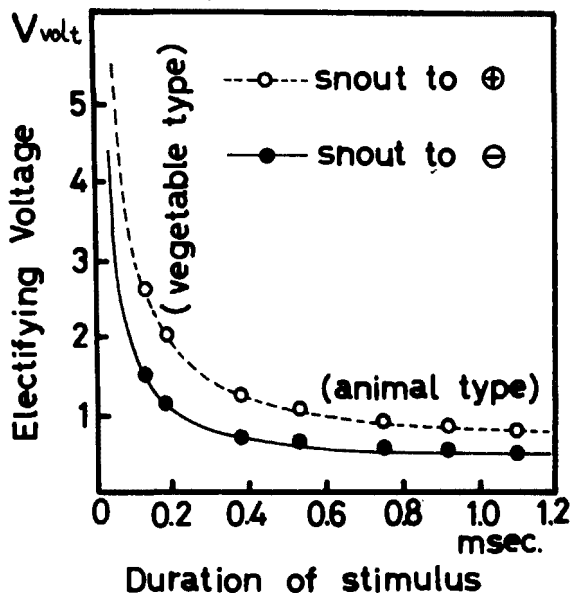
Fig.2. Chronaxie and Rheobase
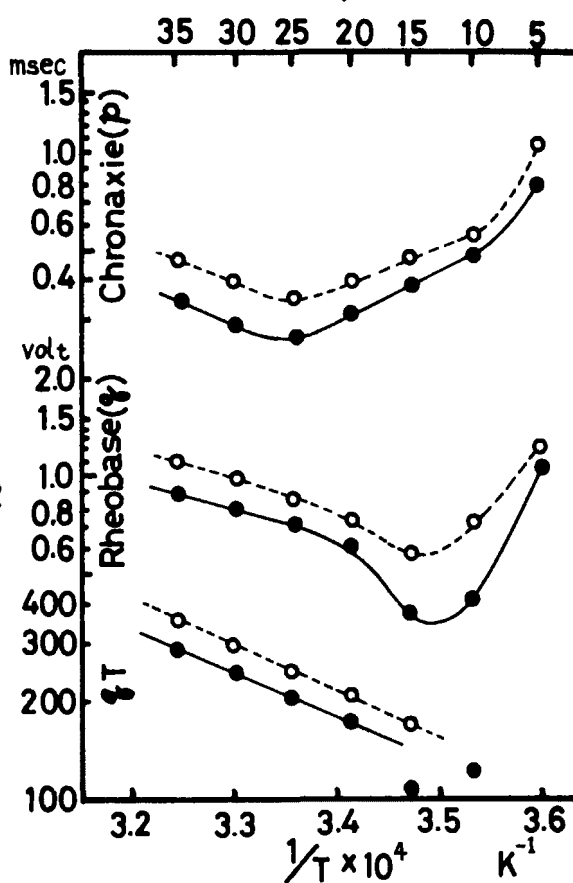
Fig.3. Migration triangle (Hanaoka, 1972)
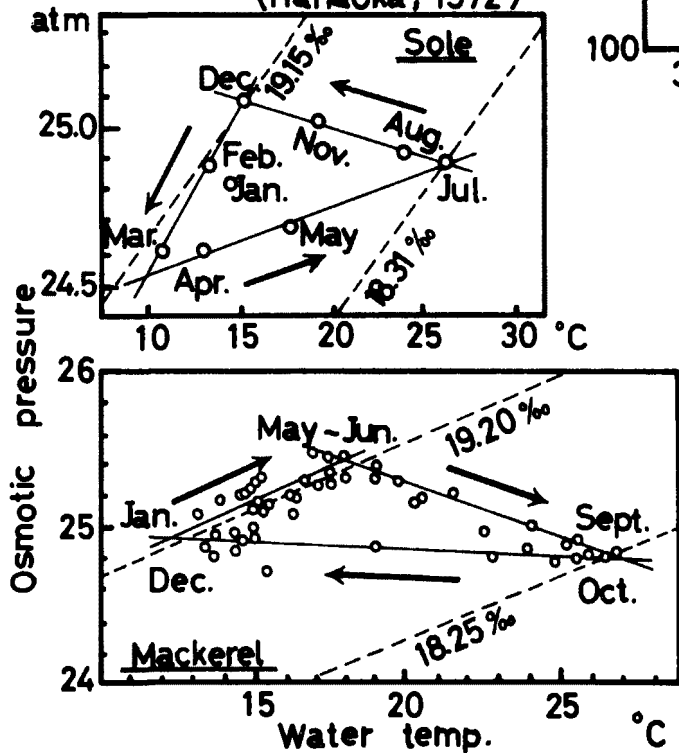
Fig.4.
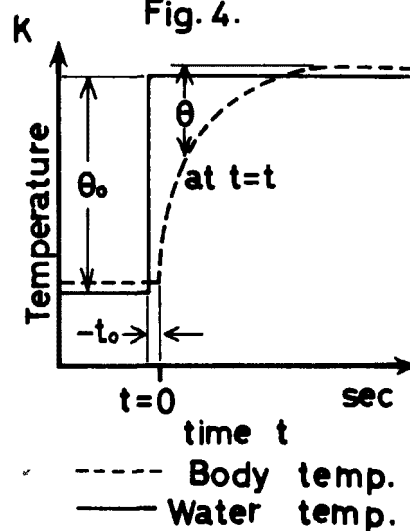
Fig.5. Feeding activity of gold fish. (Hirata, 1960)
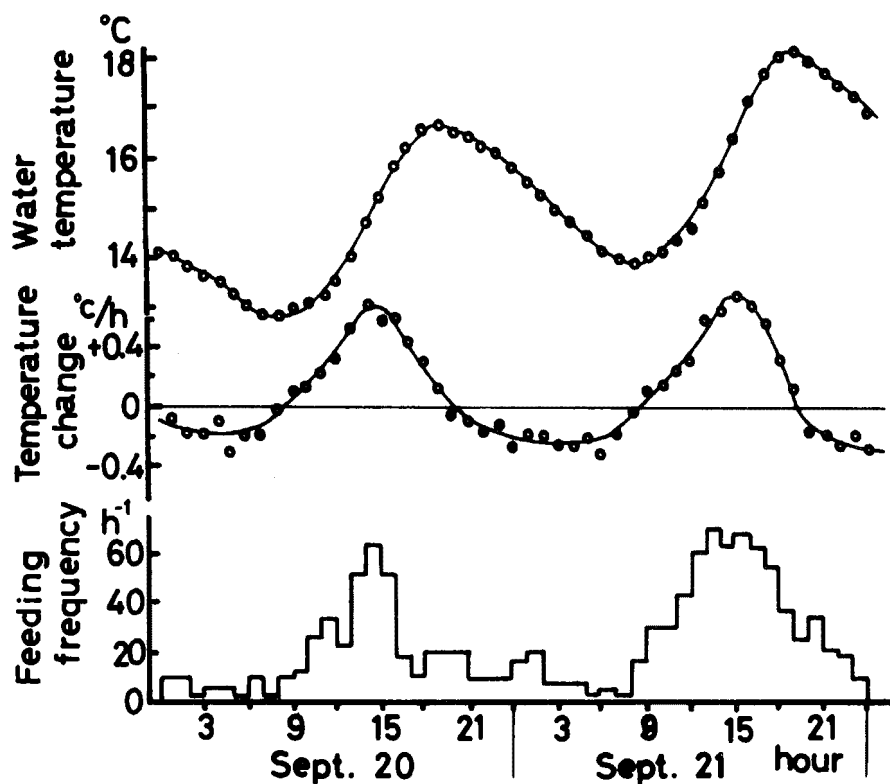
Fig. 6.

Log. relations between temp. increasing and feeding activity.

Range
A ; May (17 ~ 23°c)
B ; Aug.(18 ~ 25°c)
C ; Sep.(13 ~ 18°c)
D ; Nov.(11 ~ 14°c)
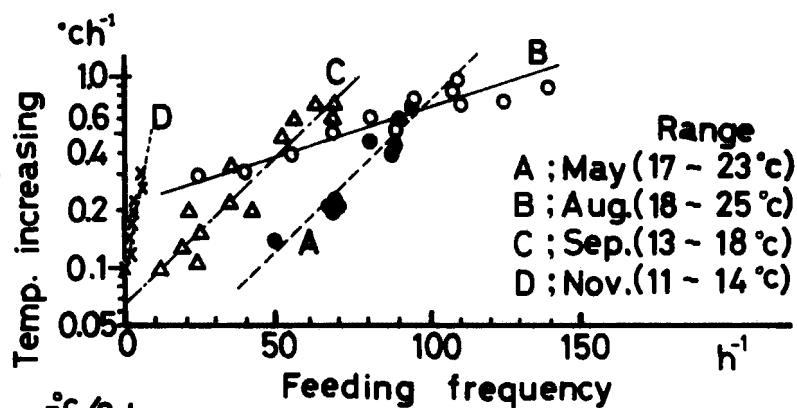
Fig.7.

Downstream and upstream movement of rainbow trout fry
(After Northcote)

Number of fry / trap(4~6 hours)

477
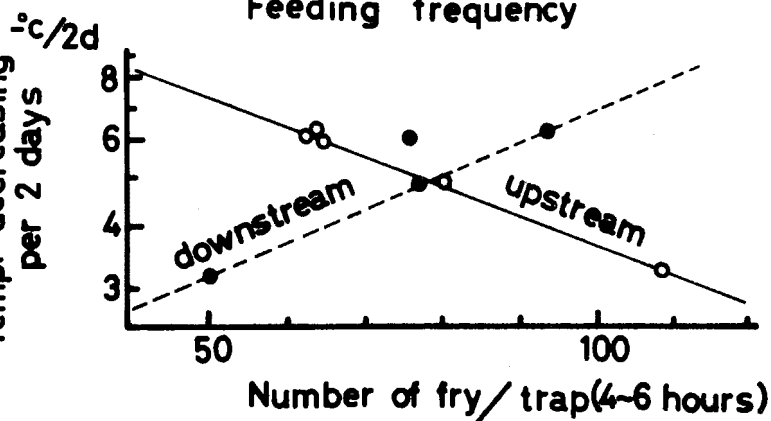
Fig.8. "MERI-O" plankton collector and measuring system.

① General measure
(thermister,
salinometer,
turbidity-meter)

② Screening mesh
(with a mechanism
of back flushing)

③ Rotary main net
and precise counter
of plankton (with
size recorder)

④ Suction pumps

Plan

part ①   part ②   part ③   part ④

Section

Side view
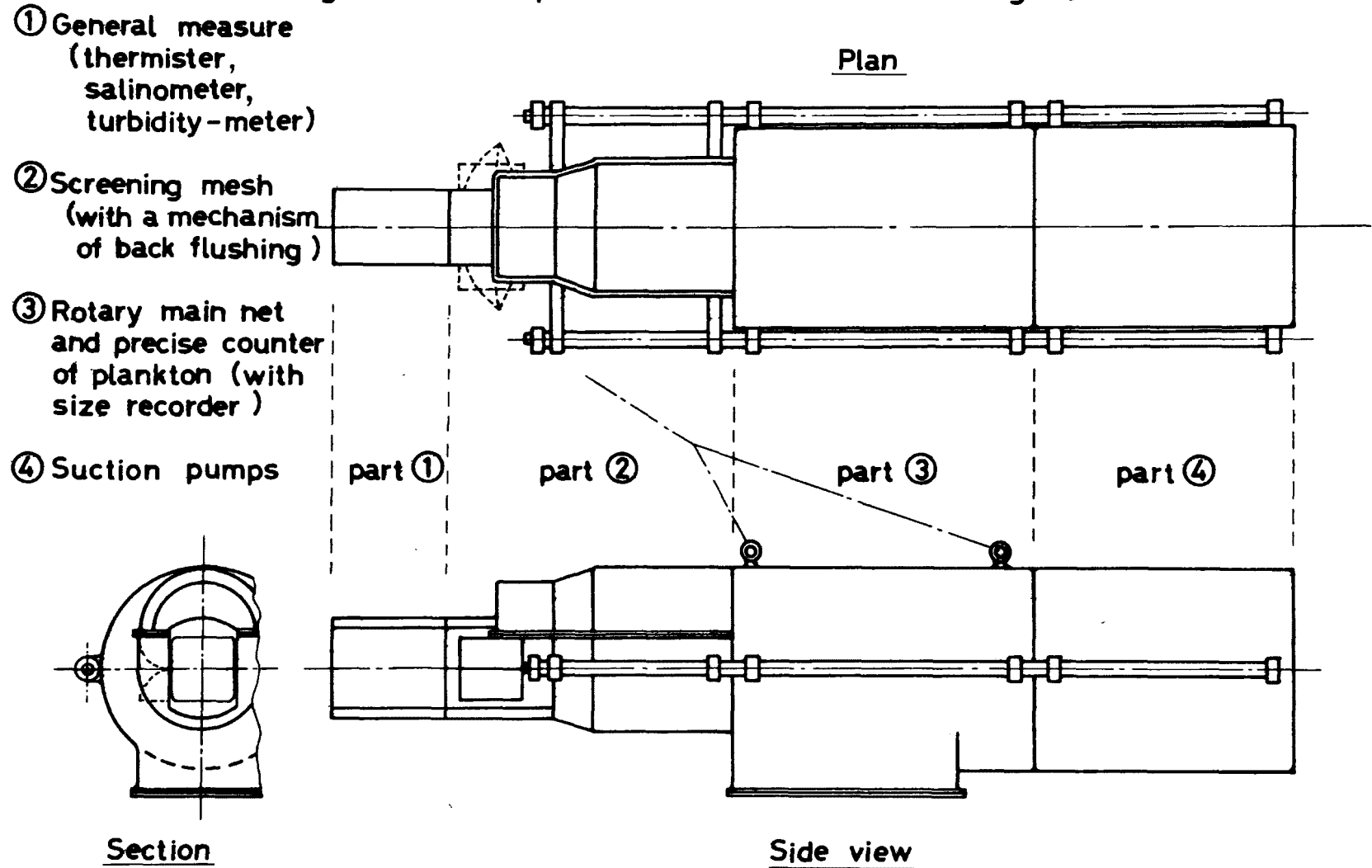
(Depressor and stabilizer, not illustrated)

0   20   40
cm

478

OCCURRENCE OF HIGHLY PATHOGENIC AMOEBAE IN THERMAL DISCHARGES

J. F. De Jonckheere
Laboratorium voor Hygiëne
Katholieke Universiteit Leuven, Belgium

ABSTRACT

Primary amoebic meningoencephalitis and amoebic meningoencephalitis are human diseases caused by free-living amoebae *Naegleria fowleri* and *Acanthamoeba* spp. respectively.

In a region with temperate climate, *N. fowleri* is present in its infective stage in warm discharges of different industries. In control surface waters this pathogen could not be demonstrated. The incidence of high concentrations of pathogenic *N. fowleri* in warm discharges stresses the need of controlling this agent by disinfection of the cooling water or the need to prevent its dispersal in nature by using closed-cycle cooling systems. The use of saltwater would also prevent its growth.

Also the number of pathogenic *Acanthamoeba* spp. can be increased in warm discharges, thereby contributing to the abundance of this pathogen in the environment. Moreover *Acanthamoeba* spp. are very resistant and therefore very difficult to eliminate. The epidemiology of *Acanthamoeba* infections is however still obscur.

INTRODUCTION

Some 20 years ago, free-living amoebae of the genus *Acanthamoebae* were isolated from tissue cultures and recognized for the first time as potentially pathogenic [1]. It was suggested that free-living amoebae might produce disease in man.

The first human cases of infection by free-living amoebae were reported in 1965 in Australia and the disease was thought to be caused by *Acanthamoeba* sp. [2]. In 1966 three cases of infection by free-living amoebae were reported in the USA [3] and the disease was named primary amoebic meningoencephalitis (PAM) to differentiate it from secondary infections of the brain caused by *Entamoeba histolytica*.

Only in 1968 the causative organism of PAM was recognised as *Naegleria* sp. [4, 5]. This pathogenic *Naegleria* was in 1970 identified as different from *N. gruberi*, a common amoeboflagellate found in water and soil, and it was named *N. fowleri* [6] in honor of Dr. Malcolm Fowler, who first recognized the disease. The separate species identity of *N.*

fowleri has since been confirmed by different techniques.
After the first reports in Australia and the USA, cases of PAM were recognized throughout the world ; for a review see Willaert [7].

Pathology

The majority of human infections was caused by *N. fowleri*. To differentiate PAM from infections caused by *Acanthamoeba* spp. the latter was called amoebic meningoencephalitis (AM) [8]. PAM usually affects young, previously healthy people. It has an acute course and the incubation time is probably 3 to 7 days. Diagnosis is usually made postmortem. Almost all known cases had a history of recent swimming or water contact, and the amoeba is entering through the nose.
Infections occurred after swimming in chlorinated swimming pools in Belgium [9] and Czechoslovakia [10], in lakes in Virginia [11] and Florida [3], in hot springs in California [12] and New-Zealand [13], in thermal polluted waters in Belgium [14] and Czechoslovakia [15], and after contact with chlorinated tap water in Australia [16].

AM caused by various species of *Acanthamoeba* occurs in debilitated individuals. It is usually a more chronic disease resulting in death after several weeks or months [8]. The actual site of invasion by *Acanthamoeba* is not known. Strains of *Acanthamoeba* have also been identified in chronic diseases of the human eye in the USA [17] and England [18].

Ecology of the amoebae

Free-living amoebae are widespread in nature, especially strains of *Naegleria* and *Acanthamoeba* can be found in every natural water.

Reports on the isolation of pathogenic *N. fowleri* and pathogenic *Acanthamoeba* spp. from the environment have been very scarce after the discovery of human infections by these amoebae.

Pathogenic *N. fowleri* were reported to be isolated in 1972 in Australia from tap water [16] and in 1973 from soil [19], in India in 1972 [20] and in the USSR in 1973 [21] from sewage sludge samples, and in 1974 in Poland [22] and in 1975 in Belgium [23] from thermal polluted water.

Isolations of pathogenic *N. fowleri* from thermal polluted waters have since been confirmed in Belgium [24], Poland [25], Florida and Texas [26], and from sewage in Korea [27]. Pathogenic *N. fowleri* were also isolated from freshwater lakes in subtropical regions [28] and on one occasion from the nose of a boy who had been swimming previously in a lake [29].

While *Acanthamoeba* spp. can be isolated from almost every environment, pathogenic *Acanthamoeba* strains have been isolated from tissue cultures in the USA [1, 30] and France [31], from sewage sludge in India [20], from hot water springs in New Zealand [32], from swimming pools in

Czechoslovakia [33], Belgium [34] and France [35], from salt water in the USA [36] and from lakes in Poland [25].

SAMPLING OF THERMAL POLLUTED WATERS IN BELGIUM

Because of the importance of water with high temperatures in the infection with *N. fowleri* and the ability of pathogenic *N. fowleri* and pathogenic *Acanthamoeba* spp. to grow at higher temperatures than nonpathogenic strains [37], we have investigated the impact of thermal discharges on the occurrence of pathogenic *Naegleria* and *Acanthamoeba* in a region with temperate climate.

Screening for pathogenic *N. fowleri* (Fig. 1) was started in 1974 while a selective screening for pathogenic *Acanthamoeba* (Fig. 2) in thermal discharges was started beginning of 1978, although pathogenic *Acanthamoeba* had been infrequently identified in swimming pools and aquarium samples previously [38].

N. fowleri investigations

Regular sampling for pathogenic *N. fowleri* were initiated in May 1974 and extended till August 1977. During this period the warm discharges of 39 different factories have been investigated in Belgium (Fig. 3). Part of these were sampled at intervals of 2 to 6 months. In three warm water-bodies the occurrence of pathogenic *N. fowleri* was also determined quantitatively. Isolations were performed during summer as well as during winter. The isolation procedure has been published [39], while the method for quantitation is in Press [40].

In eight of these factory discharges and the surrounding surface water, pathogenic *N. fowleri* were found on several occasions. These pathogenic strains were highly virulent, killing all mice within 5 days when instilled intranasally. That these sites may be dangerous for human health is shown by the occurrence of PAM after swimming in one of these thermal polluted waters [14].

During almost every sampling of these eight factories, nonpathogenic variants of *N. fowleri* [41] were isolated. It was first thought that these are related very closely to the pathogens and that they could become virulent under certain circumstances [41]. Evidence has now accumulated that these isolates are much more different [42] and a new species is being created (in preparation). This nonpathogenic species seems however to have the same ecological preference as the highly pathogenic *N. fowleri* but is more widespread. Apart from being isolated from discharges with pathogenic *N. fowleri*, it was isolated from the warm discharges of 6 other factories. Apart from 2 aquaria we have never isolated in Belgium a nonpathogenic variant from waters others than thermal discharges. Pathogenic *N. fowleri* strains were only found in thermal polluted water.

Of the eight factories with pathogenic *N. fowleri*, four are metallurgical factories, three chemical plants and one an electricity power plant. The 6 with only nonpathogenic variants, were 4 metallurgical factories, one chemical plant and one cooking plant. Since it is believed these variants are indicatororganisms for pathogenic *N. fowleri*, the use of a more selective isolation method [39] may prove the presence of pathogenic strains at these 6 factories.

In all cases of positive factories, be it with pathogenic or nonpathogenic strains, the factories were rather old, indicating that these *Naegleria* spp. need a long time to become established in a favorable warm environment, in a country with a temperate climate where it can normally not survive in nature [43].

The quantitative studies have shown that pathogenic strains can be isolated from samples as small as one ml, thus proving to be very hazardous to human health. Furthermore the dispersal of high concentrations of pathogenic organisms in surfacewater can pose serious problems to recreational waters in the neighbourhood. Also the water distribution works have been very concerned by the presence of highly pathogenic amoebae in this water which is used, after treatment, as drinking water for a large population of our country.

However, it is shown that these amoebae do not withstand low chlorine concentrations [44] and that their cysts are effectively distroyed by chlorine levels commonly used in our country by drinking water distributors [34].

Acanthamoeba spp. investigations

While preparing this text, the ecology of pathogenic *Acanthamoeba* spp. in warm discharges has been investigated only since a short time.

To be able to look for any relation between the results with *Acanthamoeba* and the ecology of *N. fowleri*, investigated previously, the same warm water discharging factories were chosen.
The approach for the isolation of *Acanthamoeba* was different than for *Naegleria* because of the biological differences between these genera and because *Acanthamoeba* strains do grow much slower than other common amoebae. The exact isolation procedure will be published elsewhere [in preparation].

From a total of 9 places sampled, three were control waters and 6 thermal discharges. In all control waters *Acanthamoeba* strains were found while in three thermal discharges this genus was not isolated. In the other 3 discharges there was a definite increase in number of *Acanthamoeba* compared to the controls. The *Acanthamoeba* isolates were tested for cytopathic effect in Vero cell cultures and for virulence in mice. Since these experiments are still being performed and the results therefore incomplete, it is difficult to draw definite conclusions as to the impact of higher water temperature on the prevalence of pathogenic *Acanthamoeba*

strains. It is noted however that part of the *Acanthamoeba* strains in control waters and in thermal waters are pathogenic. As the total number of *Acanthamoeba* is increased in some thermal waters, also the number of pathogenic strains was higher. During this study it became also obvious that a high proportion of the *Acanthamoeba* strains obtained after incubation at 37 °C, are pathogenic for mice. Any local increase in *Acanthamoeba* number should therefore be prevented as it allows the dispersal of pathogenic strains. Although only few human cases of *Acanthamoeba* infections are known [8] and its epidemiology is unknown, any enhancement of *Acanthamoeba* growth and dispersal should be prevented. This in particular as the cysts of this genus are highly resistant against chlorine, even at the highest concentrations used for preparing drinking water [34].

CONCLUSIONS

It has been shown that *Escherichia coli* dies off more quickly at high temperatures than at lower temperatures [45] thereby establishing a beneficial effect of the cooling waters. We would emphasize that *E. coli* is not the only pathogen to man present in water. We have found that the total number of bacteria is raised when the water comes out of the cooling system. These bacteria were isolated at 37 °C, the temperature of the human body.
Most importantly, we showed that amoebae, highly pathogenic to man, have found a favorable habitat in cooling water. Besides the high temperature, which makes it possible for them to compete with other more common protozoa, the higher supply of bacteria, which act as their food, is a factor in their favor.

As *N. fowleri* does not tolerate salt concentrations of 0.5 % [6] and is never demonstrated in sea water, while pathogenic *Acanthamoeba* spp. tolerate high salt concentrations and have been isolated from brackish and salt water environments [36], the use of seawater for cooling purposes could only prevent the spread of *N. fowleri*. As the occurrence of the disease produced by *N. fowleri* is directly related with water contact, this would however already be beneficial.
The only effective measure to prevent dispersal of both pathogens in the environment is the use of closed-cycle cooling systems.

Now that emphasis is given to the efficient use of waste heat as an energy-saving measure, it should be realized that such water should be treated effectively to prevent an increase of fatal human diseases.

AKNOWLEDGEMENT

REFERENCES

1. CULBERTSON, C.G., J.W. SMITH, H.K. COHEN and J.R. MINNER. Experimental infection of mice and monkeys by *Acanthamoeba*. Am. J. Path. 35, 185-197, 1959.

2. FOWLER, M. and F. CARTER. Acute pyogenic meningitis probably due to *Acanthamoeba* sp. : a preliminary report. Brit. Med. J. 2, 740-742, 1965.

3. BUTT, C.G. Primary Amebic Meningoencephalitis. Engl. J. Med. 26, 1473-1476, 1966.

4. CULBERTSON, C.G., P.W. ENSMINGER and W.M. OVERTON. Pathogenic *Naegleria* sp. - Study of a strain isolated from human cerebrospinal fluid. J. Protozool. 15, 353-363, 1968.

5. CARTER, R.F. Primary amoebic meningoencephalitis. Clinical, pathological and epidemiological features of six fatal cases. J. Path. Bact. 96, 1-25, 1968.

6. CARTER, R.F. Description of a *Naegleria* sp. isolated from two cases of primary amoebic meningoencephalitis, and the experimental pathological changes induced by it. J. Path. 100, 217-244, 1970.

7. WILLAERT, E. Primary amoebic meningoencephalitis. A selected bibliography and tabular survey of cases. Ann. Soc. belge Méd. trop. 54, 416-440, 1974.

8. MARTINEZ, A.J., C. SOTELO-AVILA, J. GARCIA-TAMAYO, J. TAKANO MORON, E. WILLAERT and W.P. STAMM. Meningoencephalitis due to *Acanthamoeba* sp. Pathogenesis and Clinico-Pathological study. Acta neuropath. (Berl.) 37, 183-191, 1977.

9. JADIN, J.B., J. HERMANNE, G. ROBYN, E. WILLAERT, Y. VAN MAERCKE and W. STEVENS. Trois cas de meningo-encephalite amibienne primitive observés à Anvers (Belgique). Ann. Soc. belge Méd. trop. 51, 255-266, 1971.

10. CERVA, L. and K. NOVAK. Amoebic meningoencephalitis : sixteen fatalities. Science 160, 92, 1968.

11. DUMA, R.J., W.I. ROSENBLUM, R.F. MCGEHEE, M.M. JONES and E.C. NELSON. Primary amoebic meningoencephalitis caused by *Naegleria*. Two new cases, response to Amphotericin B, and a review. Ann. Intern. Med. 74, 861-869, 1971.

12. HECHT, R.H., A. COHEN, J. STONER and C. IRWIN. Primary amebic meningoencephalitis in California. Calif. Med. 117, 69-73, 1972.

13. CURSONS, R.T.M., T.J. BROWN, B.J. BRUNS and D.E.M. TAYLOR. Primary amoebic meningoencephalitis contracted in a thermal tributary of the Waikato River-Taupo : A case report. N.Z. Med. J. 84, 479-481, 1976.

14. VAN DEN DRIESSCHE, E., J. VANDEPITTE, P.J. VAN DIJCK, J. DE JONCKHEERE and H. VAN DE VOORDE. Primary amoebic meningoencephalitis after swimming in stream water. Lancet ii, 971, 1973.

15. CERVA, L., M. FERDINANDOVA, K. NOVAK, V. PTACKOVA, M. SCHROTTENBAUM and V. ZIMAK. Meningoencephalitis durch Amoebida *Naegleriidae*. Einer weiteren Fall in der Tschechoslowakei. Isolierung des Erregers. Munch. med. Wschr. 111, 2090-2094, 1969.

16. ANDERSON, K. and A. JAMIESON. Primary amoebic meningoencephalitis. Lancet i, 902-903, 1972.

17. NAGINGTON, J., P.G. WATSON, T.J. PLAYFAIR, J. Mc GILL, B.R. JONES and A.D. Mc G. STEELE. Amoebic infection of the Eye. Lancet ii, 1537-1540, 1974.

18. JONES, D.B., G.S. VISVESVARA and N.M. ROBINSON. *Acanthamoeba polyphaga* keratitis and *Acanthamoeba* uveitis associated with fatal meningoencephalitis. Trans. ophthal. Soc. UK. 95, 221-232, 1975.

19. ANDERSON, K. and A. JAMIESON. Primary amoebic meningoencephalitis. Lancet ii, 379, 1972.

20. SINGH, B.N. and S.R. DAS. Occurrence of pathogenic *Naegleria aerobia*, *Hartmannella culbertsoni* and *H. rhysodes* in sewage sludge samples of Lucknow. Curr. Sci. 41, 277-281, 1972.

21. GORDEEVA, L.M. Isolation and cultivation of Limax amoebae capable to grow at 37 °C. Progress in Protozoology, Abstr. IV Congr. Int. Protozool. 159, 1973.

22. KASPRZAK, W. and T. MAZUR. Small free-living amoebae isolated from "warm" lakes : investigations on epidemiology and virulence of the strains. 3rd. Int. Cong. Parasitol. Munich Abs. ICP III, 1, 188-189, 1974.

23. DE JONCKHEERE, J., P. VAN DIJCK and H. VAN DE VOORDE. The effect of thermal pollution on the distribution of *Naegleria fowleri*. J. Hyg. (Camb.) 75, 7-13, 1975.

24. DE JONCKHEERE, J. and H. VAN DE VOORDE. The distribution of *Naegleria fowleri* in man-made thermal waters. Am. J. Trop. Med. Hyg. 26, 10-15, 1977.

25. KASPRZAK, W. and T. MAZUR. Environmental strains of *Naegleria fowleri*. IV Int. Congr. Parasitol. Warsazawa Sect A. 29, 1978.

26. STEVENS, A.R., R.L. TYNDALL, C.C. COUTANT and E. WILLAERT. Isolation of the etiological agent of primary amoebic meningoencephalitis from artificially heated waters. Appl. Environ. Microbiol. 34, 701-705, 1977.

27. SOH, C.T., K.I. IM, B.P. CHANG and H.K. HWANG. Pathogenicity of free-living amoebae isolated from various places in Seoul. V Int. Congr. Protozool. Abst. 412, New York, 1977.

28. WELLINGS, F.M., P.T. AMUSO, S.L. CHANG and A.L. LEWIS. Isolation and identification of pathogenic *Naegleria* from Florida lakes. Appl. Environ. Microbiol. 34, 661-667, 1977.

29. CHANG, S.L., G.R. HEALY, L. Mc CABE, J.B. SHUMAKER and M.G. SCHULTZ. A strain of pathogenic *Naegleria* isolated from a human nasal swab. Hlth. Lab. Sci. 12, 1-7, 1975.

30. TYNDALL, R.L., E. WILLAERT, A. STEVENS and A. NICHOLSON. Isolation of *Acanthamoeba* from cultured tumor cells. J. Cell. Biol. In press.

31. PELOUX, Y., A. NICOLAS, L. PEYRON and J. BEURLET. Problèmes posés au laboratoire par les "amibes libres". A propos d'un cas de contamination de cultures cellulaires par une amibe du genre "*Hartmannella*". Path. Biol. 22, 587-592, 1974.

32. JAMIESON, J.A. Studies of amoebae of the genus *Naegleria*. M.S. Thesis. University of Adelaide, 48 p., 1975.

33. CERVA, L. Studies of Limax Amoebae in a Swimming Pool. Hydrobiologia 38, 141-161, 1971.

34. DE JONCKHEERE, J. and H. VAN DE VOORDE. Differences in destruction of cysts of pathogenic and nonpathogenic *Naegleria* and *Acanthamoeba* by chlorine. Appl. Environ. Microbiol. 31, 294-297, 1976.

35. DERR-HARF, C. Etude des amibes libres dans les eaux de Strasbourg. Doctoral Thesis, Strasbourg, 141 p., 1977.

36. SAWYER, T.K., G.S. VISVESVARA and B.A. HARKE. Pathogenic amoebas from brackish and ocean sediments, with a description of *Acanthamoeba hatchetti*, n.sp. Science 196, 1324-1325, 1977.

37. GRIFFIN, J.L. Temperature tolerance of pathogenic and nonpathogenic free-living amoebas. Science 178, 869-870, 1972.

38. DE JONCKHEERE, J. Identifikatie, ekologie en destruktie van *Naegleria fowleri*, Carter 1970. Doctoral thesis, Leuven, 201 p., 1977.

39. DE JONCKHEERE, J. Use of an axenic medium for differentiation between pathogenic and nonpathogenic *Naegleria fowleri* isolates. Appl. Environ. Microbiol. 33, 751-757, 1977.

40. DE JONCKHEERE, J. Quantitative study of *Naegleria fowleri* in surface water. Protistologica. In press. 1979.

41. DE JONCKHEERE, J. and H. VAN DE VOORDE. Comparative study of six strains of *Naegleria* with special reference to nonpathogenic variants of *N. fowleri*. J. Protozool. 24, 304-309, 1977.

42. STEVENS, A.R., E. GALLUP, J. DE JONCKHEERE and E. WILLAERT. Differences in ultrastructure and lectin sensitivity of pathogenic and nonpathogenic *Naegleria fowleri*. IV Int. Congr. Parasitol. Sect. A, 31-32, 1978.

43. CHANG, S.L. Resistance of pathogenic *Naegleria* to some common physical and chemical agents. Appl. Environ. Microbiol. 35, 368-375, 1978.

44. DERREUMAUX, A.L., J.B. JADIN, E. WILLAERT and R. MORET. Action du chlore sur les amibes de l'eau. Ann. Soc. Belge Med. Trop. 54, 415-428, 1974.

45. BROCK, T.D. High temperature systems. Ann. Rev. Ecol. System. 1, 191-220, 1970.
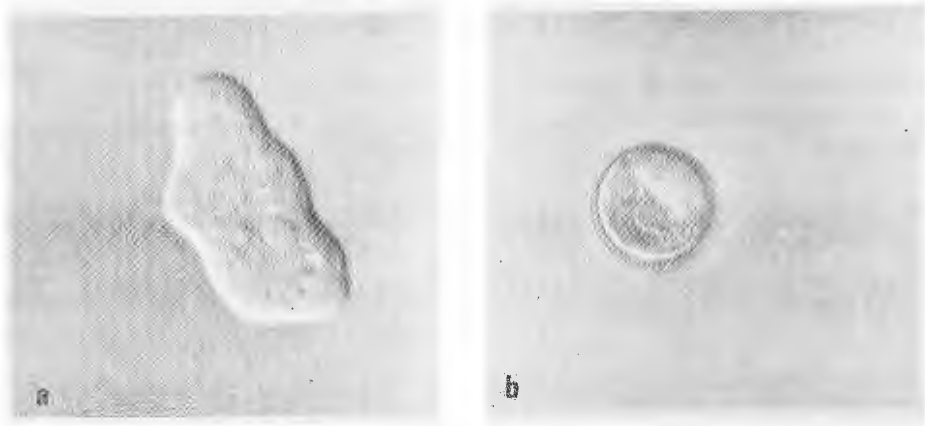
Fig. 1. *Naegleria* sp. with differential interference contrast (1,750 X)
    a. Trophozoite with bulging pseudopodia and prominent karyosome
       in nucleus
    b. Typical round cyst
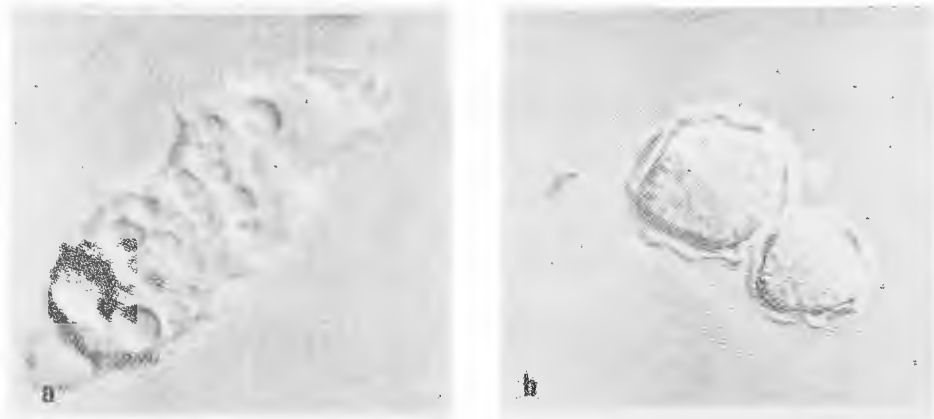
ғig. 2. *Acanthamoeba* sp. with differential interference contrast (1,750 X
    a. Trophozoite with typical filliform pseudopodia and many
      vacuoles
    b. Two typical polyhedral cysts, with outer wall loosely applied
      to the inner cyst wall.
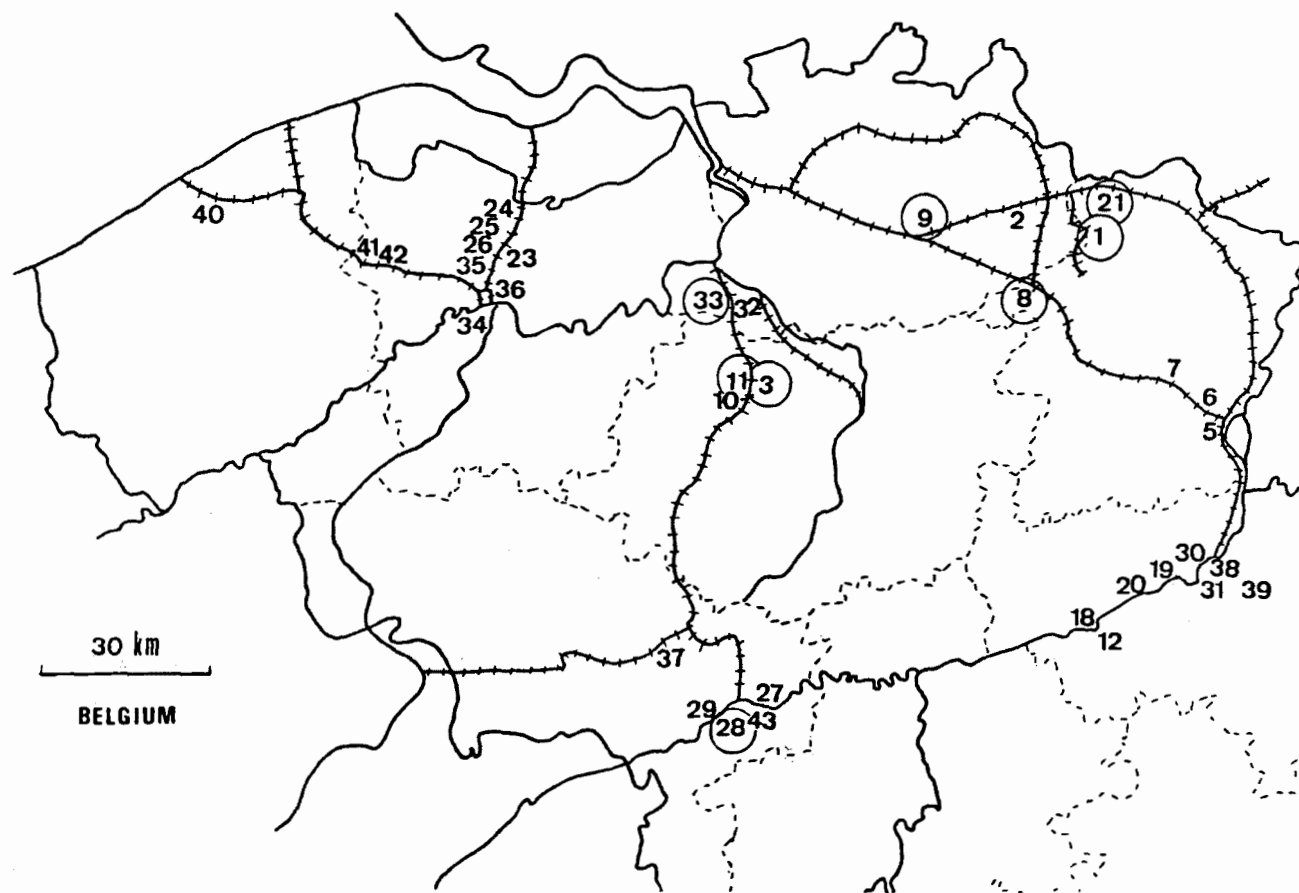
Fig. 3. Map of Belgium with factories sampled. Sites positive for pathogenic *N. fowleri* are circled. The broken lines are limits of the different provinces ; thick lines are rivers ; thick lines with cross-lines are canals.

RELATION BETWEEN ZOOPLANKTON MIGRATION AND
ENTRAINMENT IN A SOUTH CAROLINA COOLING RESERVOIR

P. L. Hudson and S. J. Nichols
U. S. Fish and Wildlife Service
Southeast Reservoir Investigations
Clemson, South Carolina U.S.A.

ABSTRACT

Knowledge of the vertical and areal distribution of zooplankton could be used to influence the siting and design of intake structures for condenser cooling water systems of steam-electric and hydroelectric power stations. We studied the vertical distribution of zooplankton in Keowee Reservoir, South Carolina, a cooling reservoir for a 2580-MW nuclear power plant. The nuclear plant withdraws hypolimnetic water from depths of 20-27 m, beneath a surface skimmer wall for once-through condenser cooling. Diel and seasonal variations in vertical distributions of zooplankton influenced the degree of entrainment at the power plant. For about 9 months, zooplankton was surface oriented, and only relatively small amounts were entrained. During July, August and September, however, most zooplankters were bottom-oriented during the day, and large numbers were entrained whereas at night most moved to or near the surface and few were entrained. The danger of entrainment during these months was thus restricted largely to the 12 to 13 daylight hours.

INTRODUCTION

Entrainment in power plant water intake systems and impingement on intake screens cause substantial losses of plankton and fish [1]. Wide variations in the magnitude and causes of these losses, however, preclude reliable prediction of the effects of planned power plants. Knowledge of zooplankton distributional patterns could facilitate the placement and design of water intake structures to control or reduce entrainment.

Zooplankton, an essential component of the food chain in reservoirs, is readily entrained in the condenser cooling water systems of steam-electric power stations. However, various species are often confined to relatively restricted zones, and their uneven vertical distribution varies diurnally and seasonally. Typically, zooplankton migration is upward at night and downward during the day. Although, the diurnal behavior of zooplankton has been summarized and documented by Hutchinson [2], seasonal variation in migration remains obscure. The ideal zone for withdrawal of cooling water would be that at which plankton population density is lowest over a 24-hour period.

Skimmer walls have been used to a limited extent to enable the withdrawal of cooling water from selected depths. A skimmer wall is a concrete barrier extending from just above full surface water elevation to a depth that allows only hypolimnetic water to pass into the intake structure. Skimmer walls increase generating efficiency by providing a year-round supply of cool water. Skimmer walls may also reduce the entrainment of larval fish [3] and zooplankton [4,5]. The objectives of the present study were to (1) determine the diel and seasonal vertical distribution of zooplankton in Keowee Reservoir, South Carolina; (2) measure the entrainment of zooplankton beneath a skimmer wall; and (3) evaluate the effects of power plant operation on the zooplankton community in the discharge area.

RESERVOIR DESCRIPTION

Keowee Reservoir was filled between 1968 and 1971 to provide cooling water for Duke Power Company's Oconee Nuclear Station. The 7435 ha reservoir has a mean depth of 15.8 m at full pool (243.7 m above mean sea level). The reservoir has two sections (south and north) of nearly equal area (Fig. 1). The 2580-MW Oconee Nuclear Station is located between the two sections; cooling water is withdrawn from the south section and discharged into the north section. Cooling water withdrawn from the south reservoir passes under a skimmer wall (Fig. 2) 19.8–27.4 m below full pool surface level, flows over a submerged weir (the top of which is 9.1 m below the surface), and then travels 1.5 km down a canal to the plant. Water from the plant is discharged into the north section of the reservoir, 9–12 m below the full-pool surface level. Maximum cooling water flow is 134 m3/s, and mean flow is 99 m3/s at 80% generating capacity. Maximum condenser cooling water flow is about four times the average outflow from Keowee Reservoir and could theoretically circulate the entire volume of the reservoir through the station in 4.5 months.

METHODS

Zooplankton abundance was estimated monthly at five sites (A,B,C,D, and X, Fig. 1.) in Keowee Reservoir, from July 1973 to November 1977. Samples were collected at each site by taking four 5-min oblique (15 m to surface) tows with a high speed Miller sampler [6] with a 0.156-mm-mesh net. The data obtained from these monthly samples indicated a need for a study of the vertical distribution and entrainment of zooplankton. Only monthly data from September 1976 through August 1977 are used in this paper.

Vertical distribution and entrainment were measured by sampling for 4-day periods in September 1976 and February, May, and August 1977. On the first day of each period, a series of horizontal tows were taken immediately outside the skimmer wall (Fig. 1, solid arrows) at mid-day (1200–1400) and at night (2400–0200). Duplicate tows were made with the

Miller sampler at 5 m depth intervals from the surface to 20 m (Fig. 2).
On the second and third day, four oblique tows from the bottom of the
intake canal to the surface at two stations (Fig. 1, solid arrows) were
taken at 3-hour intervals for 24 hours. On the 4th day duplicate
oblique tows from the bottom to the surface were taken at eight stations
(1.0 km apart) along a transect extending 8.4 km from the nuclear plant
discharge cove up the north basin of the reservoir (Fig. 1, dashed lines).

Each zooplankton sample was concentrated or diluted to a fixed volume,
depending on the abundance of organisms, and four 1-ml subsamples were
withdrawn and placed in a rotary counting chamber. All organisms in the
subsample were counted and identified to species. This subsampling
procedure was repeated three times. Because of their large size, all
Chaoborus and Leptodora in the entire sample were counted.

RESULTS AND DISCUSSION

Vertical Distribution

Vertical distributions of zooplankton in Keowee Reservoir were similar in
February and May (Fig. 3) and represent the type of distributions that
were typical during periods when water temperatures from the surface to
a depth of 10 m were relatively homothermous and lower than 20 C (mid-
October to June). In February and May, zooplankton was concentrated in
water less than 15 m deep during the day and migrated upward about 5 m
during the night. The vertical patterns shown in Figure 3 reflect the
distribution of the dominant species--Bosmina longirostris, Diaptomus
mississippiensis, and Diaphanosoma branchyurum--which accounted for 96%
(by number) of the zooplankton population in February and 78% in May.
Less abundant species, such as Mesocyclops edax, Cyclops vernalis,and
Tropocyclops prasinus, had vertical distributions similar to the common
species in May, but during the daytime in February, most were 20 m below
the surface. Holopedium amazonicum was not collected in February but
maintained a population maximum at 5 m in May, with no evidence of
diurnal migration. Chaoborus punctipennis was benthic in February but
planktonic in May; peak numbers were at the 15 m depth contour. Most of
the zooplankton was above the top of the skimmer wall opening during
February and May, and thus not subject to entrainment (Fig. 3).

As thermal stratification developed in the summer and surface water
temperatures rose above 20 C, zooplankton populations concentrated at
greater depths during the day but migrated toward the surface at night
as indicated in the August 1977 and September 1976 samples (Fig. 3).
The depth of maximum zooplankton numbers was difficult to assess because
sampling below 20 m was made impractical by bottom obstructions; however,
a daytime sample taken in August at a depth of 23 m indicated that
densities continued to decline with increasing depth. Since no samples
were taken below 20 m in September, day-night comparisons of zooplankton
densities were restricted to 0-to 20-m zone. Since zooplankton moved
upward at night, any sizable population movement into the 0-to 20-m zone

from below 20 m would substantially increase population densities at night. Abundance of most species increased only slightly at night, but the densities of Mesocyclops and the semi-planktonic Chaoborus doubled, indicating that a large proportion of their populations were below 20 m during the day. Woodmansee and Grantham [7] reported similar behavior for these two species in a small Mississippi reservoir. Because dominant species in Keowee Reservoir (Bosmina, Diaptomus, and Diaphanosoma) did not increase in numbers in the 0-to 20-m zone at night in September, we assumed that the maximum population density during the day was in the vicinity of the 20-m depth contour. All species migrated toward the surface at night during August and September except Holopedium, which maintained a maximum density at 5 m, as in May.

The vertical distribution we observed generally paralleled that described by Hutchinson [2]. He described various nocturnal migration patterns, which are slight deviations from the simplest type where the organisms start moving upward before or shortly after sunset and reach the upper layers sometime before midnight. They remain near the surface for several hours and descend at dawn. Since we did not sample at close time intervals for 24-hour periods at the skimmer wall, we could not determine the specific kind of nocturnal migration. However, our samples at noon and midnight should approximate the distribution extremes over a 24-hour period and our 20-m-deep daytime sample should yield a suitable estimate of the maximum zooplankton population subject to power plant entrainment.

Few investigations have been made of daytime vertical distribution of zooplankton through a season or over a year. Plew and Pennak [8] found a slow seasonal drift of the zooplankton population downward in spring and upward in autumn. Langford [9] found that zooplankton populations moved downward during the day as summer progressed, and Hutchinson [2] presumed this to be due to increasing surface temperature. To place temporal bounds on our daytime summer vertical distribution, we determined the mean temperature where the zooplankton population density was greatest in the water column. The maximum densities in May, July, and August were at depths where temperatures ranged from 19 to 23 C. Water of these temperatures were at the depth of the skimmer wall opening from mid-July to late August which was the time period of maximum entrainment.

Entrainment

Migration patterns of zooplankton differ according to species, sex, and age of individuals. However, since the dominant species behaved similarly in Keowee Reservoir, this section deals mainly with total zooplankton.

The 24-hour pattern of zooplankton abundance in the intake canal during February and May (Fig. 4) reflected the differences in day-night densities at the skimmer wall opening. In May, day and night densities at 20 m near the skimmer wall opening (20-m depth contour) were about 1/liter and the densities in the canal fluctuated from 0.8 to 1.1/liter

over the 24-hour period (Fig. 3 and 4). In February, day and night differences at the skimmer wall opening (3.0 vs. 1.5/liter) produced a slight diel periodicity in the canal (Fig. 4). Overall mean population densities in the canal during February and May (3.0 and 1.0/liter, respectively) were low compared with surface populations at the control stations (D and X, Fig. 1) at that time (6.0-13.0/liter).

In August and September the distinct diel fluctuation in zooplankton densities in the canal (Fig. 4) correlated with the day-night population differences at the skimmer wall opening (Fig. 3). Maximum densities of zooplankton occurred at the skimmer wall opening during daylight, but this timing did not correspond with peak densities in the canal (Fig. 3 and 4). The difference in the time of peak abundance was the result of travel time (which is a function of volume of water in the intake canal and pumping rate at the Oconee Station) between the skimmer wall sampling station and stations in the canal, a 6- to 9-hour time lag. Zooplankton entrained at the skimmer wall at midday (1400 hours) reached the canal sampling stations between 2000 and 2300. The different density patterns in the canal in August and September were probably due to different pumping rates and diurnal migration patterns at the skimmer wall. The water level in the canal was lower and pumping rates were higher during August (110 m^3/s) than in September (80.4 m^3/s), which could have produced a 2- to 3-hour difference in zooplankton travel time. Furthermore, the amount of zooplankton and extent of time spent at the skimmer wall opening could vary due to differences in depth distribution (Fig. 3) and migration patterns between August and September, thus shifting the density peaks by as much as 2 to 3 hours. Overall, maximum and minimum densities at the skimmer wall opening were similar to the values in the canal, and entrainment varied diurnally with 12 hours of high values followed by 12 hours of low values.

Reservoir Zooplankton

High zooplankton densities in the discharge cove were followed by declines in densities 1 km from the cove based on transect data (Fig. 5). Zooplankton densities usually were lowest during all sample periods 2-4 km away and either recovered (Fig. 5 A,B,D) or continued to decline (Fig. 5C). The density levels at both ends of the transect had little relation to entrainment levels, whereas those near the middle (2-4 km) of the transect were similar to the mean 24-hour density in the canal (Table 2).

Zooplankton densities in the discharge cove were usually higher than the maximum concentrations observed in the intake canal, except in the August samples. For example in February 1977, the maximum density was 4.5/liter in the canal and based on transect samples nearly 12/liter in the discharge cove. Zooplankton densities from the monthly sampling in the discharge cove (Station C) were sometimes the highest in the reservoir in 1976-77 (Table 1). Since about 9 months of the year these large numbers of zooplankters were not passing through the plant, the high densities in the discharge cove probably resulted from concentrating

currents. Preliminary dye and drogue studies in the cove indicated the presence of counter currents and back eddies. The densities of Bosmina in a surface sample taken in the cove were 12 times those in the canal. Bosmina is a small, weak-swimming cladoceran that tends to air-lock (an air bubble forms under the carapace) easily [10]. Passage through the condenser tubes could cause air-lock, and as the plankters float to the surface, back eddies or counter currents could concentrate sizable populations in the discharge cove. A concentration of zooplankton in a discharge area also occurred in Lake Monona, Wisconsin [11]. However, high concentrations in Keowee Reservoir were localized, since the discharge cove represents less than 1% of the reservoir surface area.

Zooplankton numbers 1 to 4 km from the discharge cove should be similar to densities noted in the intake canal (Table 2). Pumping rates during this study ranged from 88 to 110 m^3/s and only 12 days were required to replace the water in an area 1 to 4 km from the discharge structure. The densities at 1 to 4 km were close to the mean densities in the canal during October and August but were higher in May and lower in February (Table 2).

The reduction in zooplankton abundance 1 to 4 km from the discharge cove may have resulted from latent mortality due to plant passage. Duke Power Company [5] estimated zooplankton mortality of 0 to 33% (annual mean 2%) after passage through Oconee Nuclear Station; maximum mortality was in July. Additional delayed mortality could have occurred further upstream from the discharge cove, but our data did not show this trend. Bosmina numbers in the area 1 to 4 km from the discharge structure were 20 to 63% lower than the mean numbers in the canal, whereas Diaptomus densities were usually higher. Numbers of zooplankters entrained from mid-October to June were substantially lower than the numbers normally found in the water column (Table 1 and 2), resulting in an estimated area of low zooplankton density covering about 15% of the area of the reservoir. Therefore the overall effect of entrainment in this 1 to 4 km area was apparently dilution.

Zooplankton densities in late July (Fig. 5C) showed different horizontal distributions. Low concentrations of organisms were not observed, but there was a steady decrease in numbers upstream from the discharge cove. During these months, maximum concentrations of zooplankton were found at the skimmer wall opening (20 m deep); this high concentration, combined with the long photoperiod (14 hours), resulted in the entrainment of maximum numbers (8/liter). During August intake canal zooplankton densities were at the highest levels (Fig. 4). Consequently, inordinately large numbers of plankton were discharged into the north basin, compared with the average standing crops in other parts of the reservoir.

The zooplankton distribution pattern along the transect, 4.0-8.5 km from the discharge cove, probably varied independently of entrainment. Populations in this area were affected by reproduction and repopulation from other areas of the reservoir. Variation in zooplankton abundance

in this section of the reservoir depended on environmental factors, and possibly on the operational level of the Jocassee Pumped-Storage Station, located 15.7 km upstream from the Oconee Station. On any given date densities in the 4.0-8.5 km area were as high as (Fig 5D), lower than (Fig. 5C), or equal to (Fig. 5A,B) entrainment levels.

CONCLUSIONS

Zooplankton diel migration in Keowee Reservoir during most of the year placed most of the population above the skimmer wall opening during the day and virtually always at night. This behavior resulted in seasonal and diurnal variations in entrainment. Selective withdrawal of water with low zooplankton densities, coupled with latent mortality, created an area of low standing crop covering 15% of the reservoir surface for about 9 months. Maximum numbers of zooplankton during the day in July and August followed the 20 C isotherm downward as the surface waters warmed. During the day, concentrations at the skimmer wall opening were high and large numbers were entrained and discharged into the north basin. Because entrainment was reduced by the presence of the skimmer wall, there was a dilution of zooplankton in most of the outfall area (1 to 4 km up north basin) and a possible scarcity of food for higher aquatic animals.

Entrainment does not appear to be a major factor in determining reservoir-wide zooplankton abundance. The use of a skimmer wall and the withdrawal of hypolimnetic water for steam electric plants' cooling systems appears highly desirable in systems such as the Keowee Reservoir. Oconee Nuclear Station has maintained state water quality temperature standards, the cool water has increased thermal efficiencies for power plant operation, and entrainment of zooplankton is relatively small over most of the year.

Knowledge of zooplankton behavior could be used to predict the zones of influence around steam electric and hydroelectric plant cooling water intakes. Three-dimensional velocity profile models superimposed on 24 hour movement patterns of zooplankton would allow prediction of entrainment levels. At Multi-level inlet-outlet hydroelectric stations, this knowledge could reduce entrainment or facilitate the transport of excess production from a reservoir to a tailwater system.

REFERENCES

1. Boreman, J. 1977. Impacts of power plant intake velocities on fish. Topical Briefs: Fish and Wildlife Resources and Electric Power Generation, No. 1. U. S. Fish and Wildlife Service. Ann Arbor, Michigan. 10 pp.
2. Hutchinson, G. E. 1967. A treatise on limnology. Vol. II. Wiley and Sons, Inc. New York, N. Y. 1115 pp.
3. Ruelle, R., W. Lorenzen, and J. Oliver. 1977. Population dynamics of young-of-the-year fish in a reservoir receiving heated effluent. Pages 46-67 in W. Van Winkle, ed. Proceedings of a Conference on Assessing Effects of Power-Plant-Induced Mortality on Fish Populations. Pergamon Press, N. Y.
4. Davies, R. M., and L. D. Jensen. 1974. Zooplankton entrainment. Pages 162-172 in L. D. Jensen, ed. Environmental responses to thermal discharge from Marshall Steam Station, Lake Norman, North Carolina. Electric Power Research Institute, Research Project RP-49, Pala Alto, Calif.
5. Duke Power Company. 1977. Zooplankton. Pages 271-334 in Oconee Nuclear Station environmental summary report, 1971-1976. Duke Power Company, Charlotte, N. C.
6. Miller, D. 1961. A modification of the small Hardy plankton sampler for simultaneous high-speed plankton hauls. Bull. Mar. Ecol. 5: 165-172.
7. Woodmansee, R. A., and B. J. Grantham. 1961. Diel vertical migrations of two zooplankters (Mesocyclops and Chaoborus) in a Mississippi lake. Ecology 42: 619-628.
8. Plew, W. F., and R. W. Pennak. 1949. A seasonal investigation of the vertical movements of zooplankters in an Indiana lake. Ecology 30: 93-100.
9. Langford, R. R. 1938. Diurnal and seasonal changes in the distribution of limnetic crustacea of Lake Nyssissing, Ontario. Univ. Toronto Stud. Biol. Ser. No. 45 (Publ. Ontario Fish Lab. 56). 42 pp.
10. Martin, D. B., and J. F. Novotny. 1975. Studies to determine methods for culturing three freshwater zooplankton species. Ecological Research Series, U. S. Environmental Protection Agency. Corvallis, Oregon. (EPA-6660/3-75-010). 33 pp.
11. Brauer, G. A., W. H. Neill, and J. J. Magnuson. 1974. Effects of a power plant on zooplankton distribution and abundance near plant's effluent. Water Research 8: 485-489.

TABLE 1. MEAN MONTHLY ZOOPLANKTON DENSITIES (NO./LITER) IN KEOWEE RESERVOIR, SEPTEMBER 1976 TO AUGUST 1977. STATION LOCATIONS ARE SHOWN IN FIGURE 1. (STANDARD ERRORS IN PARENTHESES).

STATIONS	1976				1977							
	SEPT.	OCT.	NOV.	DEC.	JAN.	FEB.	MAR.	APR.	MAY	JUNE	JULY	AUG.
A	5.78	5.57	1.51	2.40	3.98	3.05	4.34	3.85	8.04	5.20	3.86	5.40
	(0.33)	(0.40)	(0.16)	(0.03)	(0.08)	(0.14)	(0.16)	(0.26)	(0.15)	(0.35)	(0.06)	(0.84)
B	3.41	3.08	1.01	1.31	2.25	1.69	1.50	1.76	3.27	4.26	4.08	4.81
	(0.22)	(0.29)	(0.09)	(0.11)	(0.27)	(0.21)	(0.08)	(0.02)	(0.08)	(0.12)	(0.18)	(0.66)
C	11.88	4.00	2.63	4.60	10.55	5.95	4.67	2.64	5.12	5.14	3.15	3.50
	(0.25)	(0.26)	(0.13)	(0.41)	(1.30)	(0.54)	(0.21)	(0.24)	(0.30)	(0.17)	(0.20)	(0.14)
D	4.07	3.88	1.04	1.27	4.84	5.87	11.13	12.27	12.54	5.98	3.04	2.64
	(0.15)	(0.17)	(0.22)	(0.16)	(0.31)	(0.20)	(0.62)	(0.75)	(1.02)	(0.20)	(0.29)	(0.14)
X	7.08	10.38	2.13	2.29	6.32	7.16	28.61	7.78	13.09	6.83	3.10	3.38
	(0.55)	(0.33)	(0.21)	(0.05)	(0.28)	(0.93)	(2.42)	(0.21)	(1.43)	(0.44)	(0.30)	(0.31)

TABLE 2. MEAN ZOOPLANKTON DENSITIES (NO./LITER) AT THE SKIMMER WALL OPENING, IN THE INTAKE CANAL, AND 1-4 KM UP THE NORTH BASIN FROM DISCHARGE COVE, KEOWEE RESERVOIR, SEPTEMBER 1976 to AUGUST 1977.

LOCATION	27 SEPTEMBER- 1 OCTOBER 1976	7-11 FEBRUARY 1977	9-13 MAY 1977	1-5 AUGUST 1977
SKIMMER WALL	6.25	2.21	1.08	3.00
INTAKE CANAL	2.93	3.03	0.96	3.74
NORTH BASIN	3.53	2.06	2.17	3.20
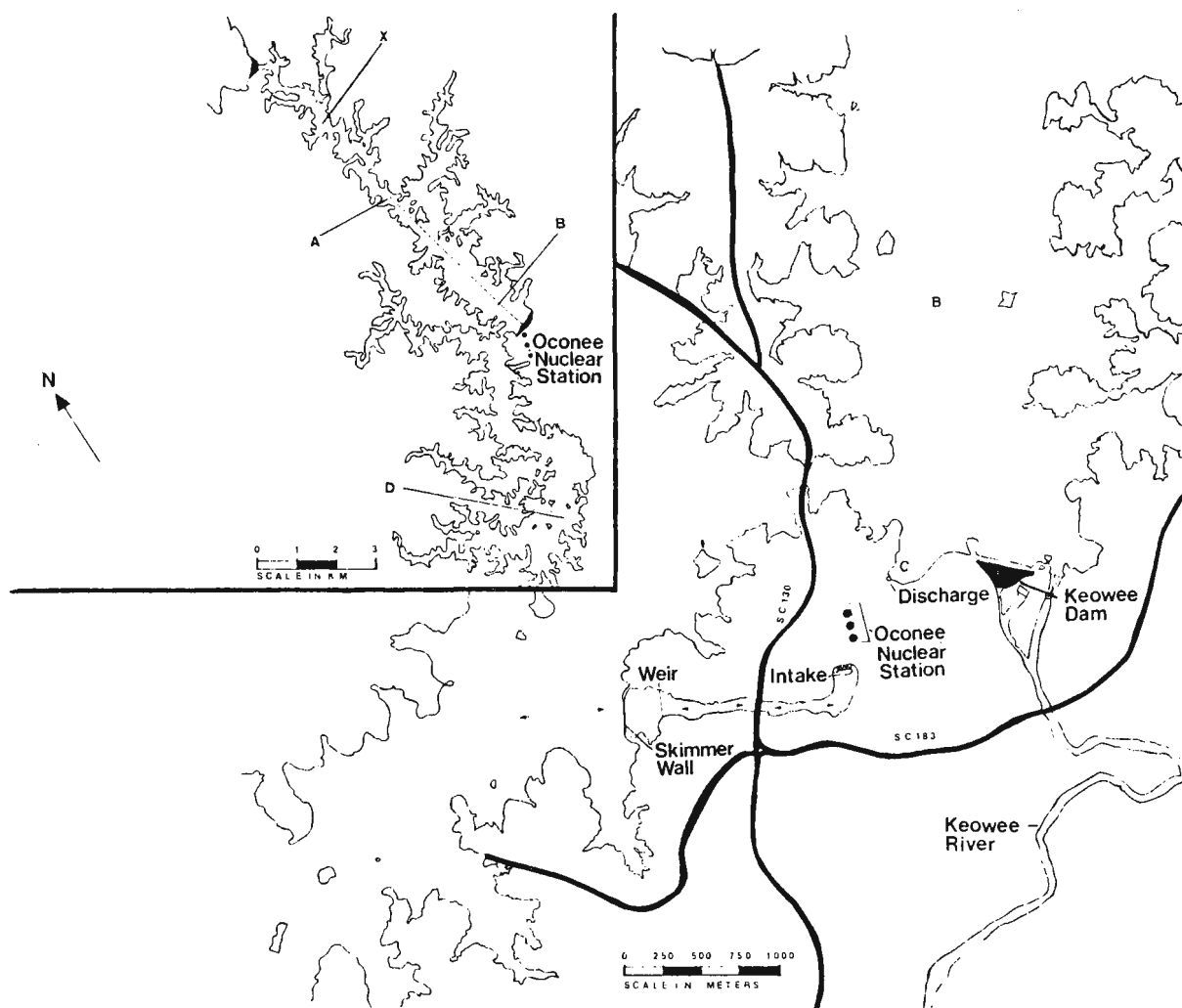
Fig. 1. Zooplankton sampling stations in Keowee Reservoir,
South Carolina. Letters A,B,C,D, and X indicate
regular zooplankton monitoring stations. Solid lines
with arrows indicate sampling stations outside and
inside intake canal. Dashed line indicates location
of transect.

500

full pond el 244 m

Skimmer
wall

submerged
weir

el. 235

flow

el. 224 m

reservoir bottom el. 216 m
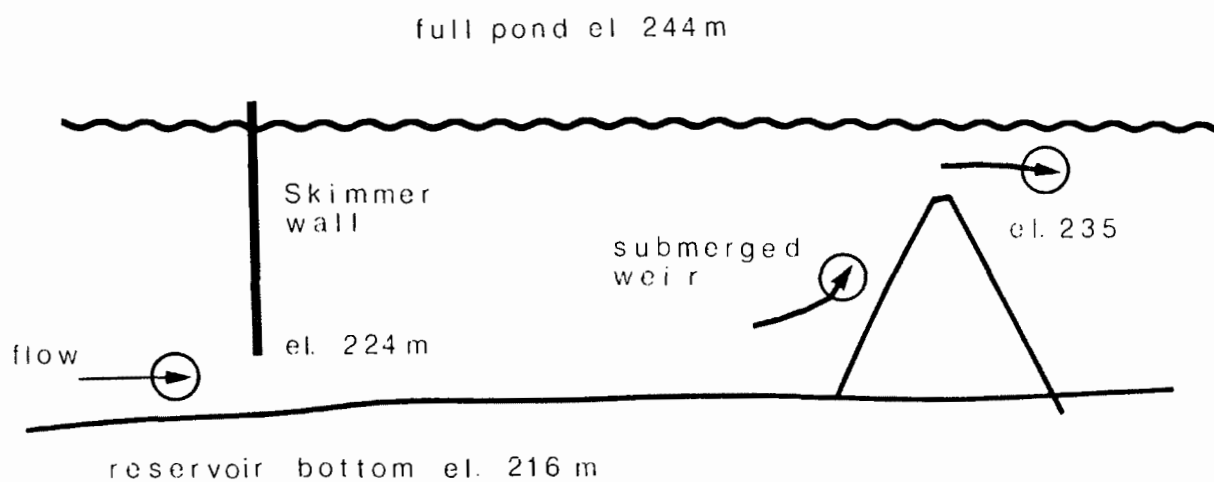
Fig. 2. Schematic Profile of the Intake Skimmer Wall
and Submerged Weir, Oconee Nuclear Station,
Keowee Reservoir, South Carolina.

NUMBER PER LITER
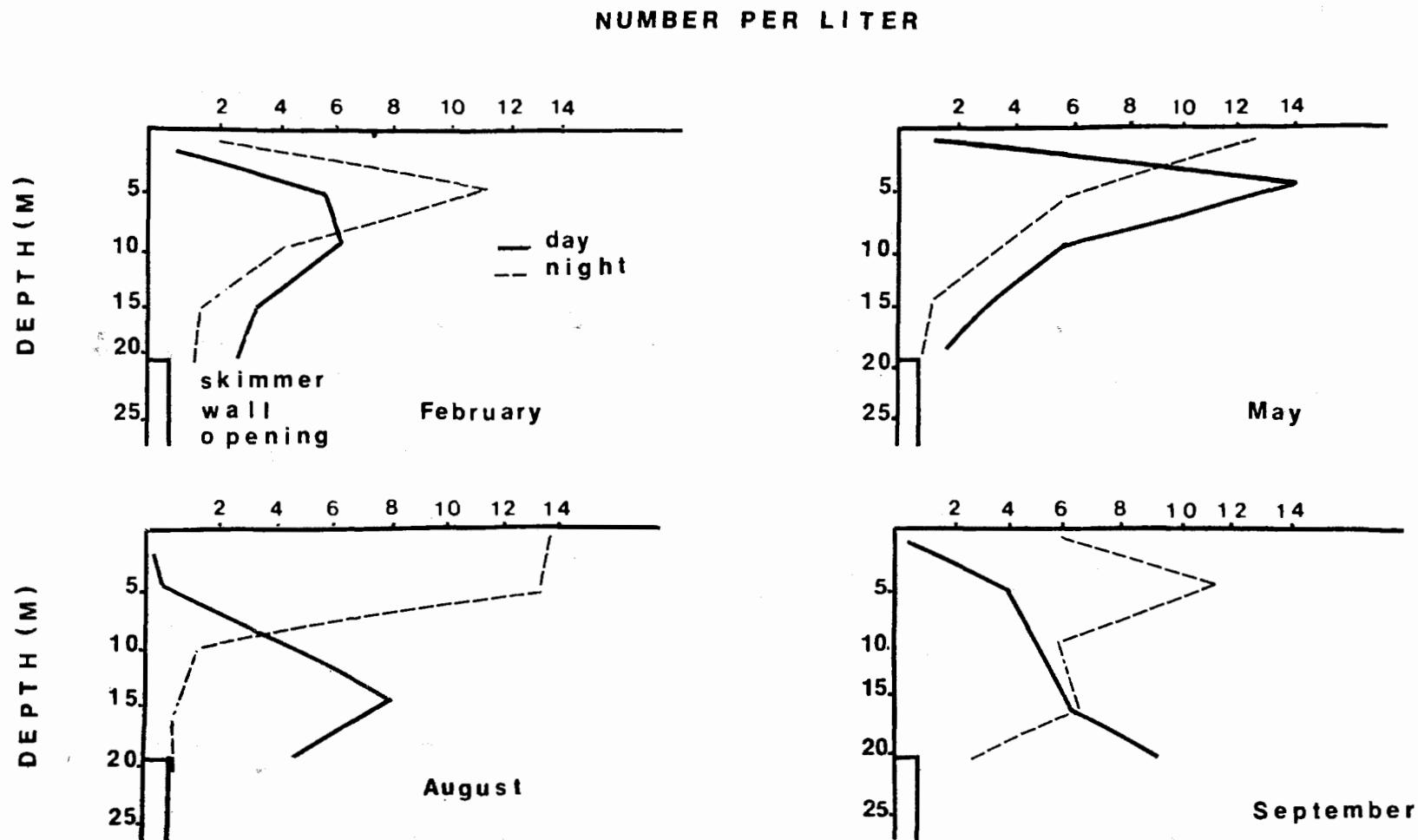
Fig. 3. Vertical Distribution of Total Zooplankton in Front of the
Skimmer Wall (1200 to 1400 hours) and (2400 to 0200 hours)
on February 9, May 11, August 3, 1977 and September 29, 1976.
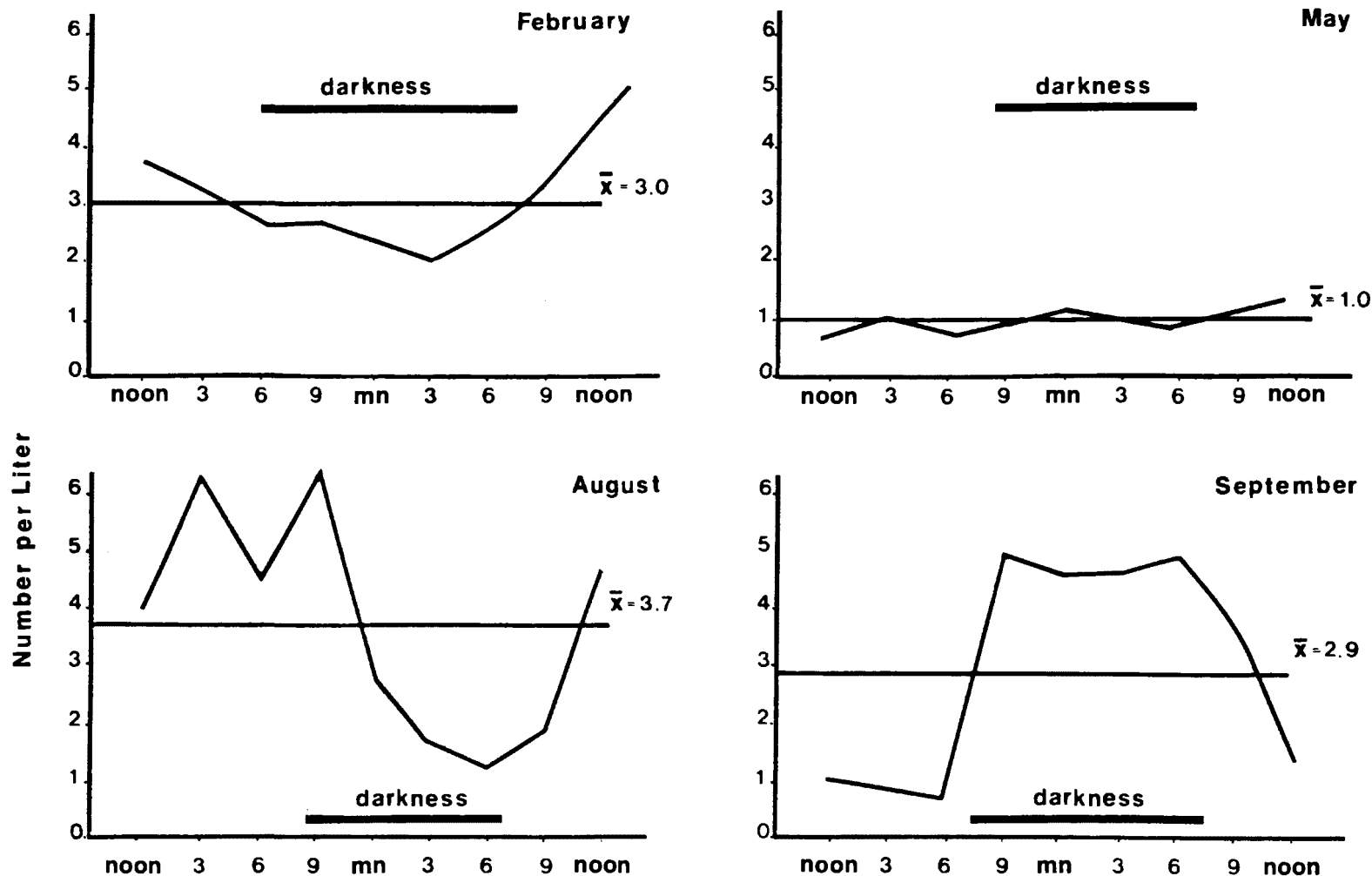
Fig. 4.   Total Zooplankton Densities in the Intake Canal During a
Twenty-four Hour Period on February 7-8, 1977, May 9-10,
1977, August 1-2, 1977 and September 28-29, 1976.
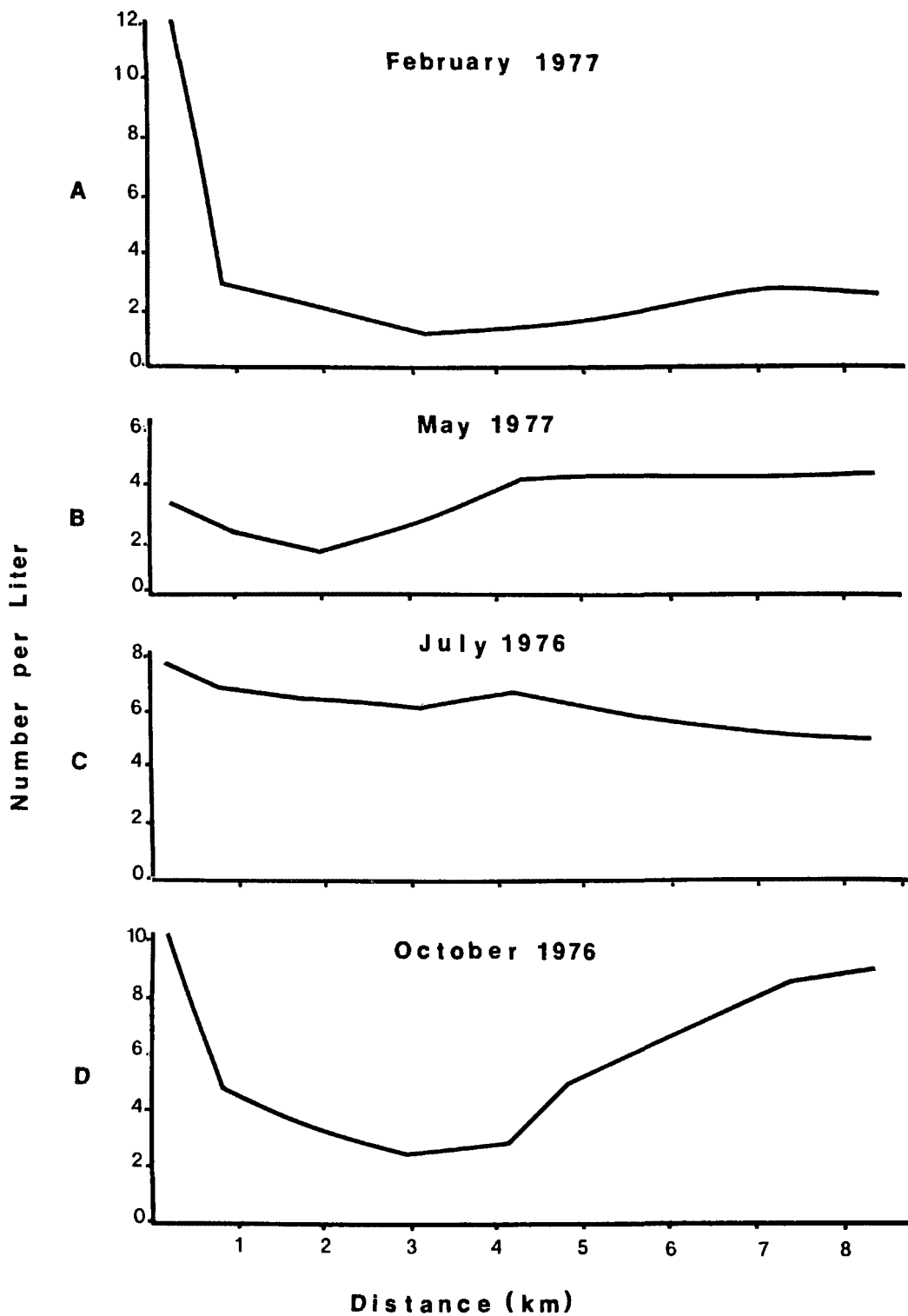
Fig. 5.   Total Zooplankton at Eight Stations 1 km Apart
          Along 8.4 km Transect from Discharge Cove up
          North Basin; February 10, 1977, May 12, 1977,
          July 30, 1976 and October 1, 1976.

504

EFFECTS OF A HOT WATER EFFLUENT
ON POPULATIONS OF MARINE BORING CLAMS IN BARNEGAT BAY, NEW JERSEY

K. E. Hoagland
Lehigh University
Bethlehem, Pennsylvania U.S.A.
and
R. D. Turner
Harvard University
Cambridge, Massachusetts U.S.A.

ABSTRACT

The Oyster Creek Nuclear Generating Station began operation in December 1969. By 1971, damage to wooden structures from marine boring clams was evident in Oyster Creek and adjacent parts of Barnegat Bay. Increased salinity and temperature in Oyster Creek, brought about by the Station's cooling system, allowed shipworms to develop large breeding populations. Actions taken in 1974-1976 to reduce the environmental impact of the cooling system included reduction of the temperature of the effluent and removal of infested wood from Oyster Creek. The shipworm population declined, but primarily because of cold winter and spring temperatures coupled with prolonged winter and spring outages of the Generating Station in 1976 and 1977. No outage occurred in the winter-spring of 1978, and there was an outbreak of shipworms in the summer, 1978. The dominant shipworm in Oyster Creek is now a subtropical species. Population structure of this shipworm differs from that of native species in unaffected portions of Barnegat Bay.

INTRODUCTION

The Oyster Creek Nuclear Generating Station at Forked River, New Jersey (Fig. 1) began operation in December 1969. It is owned by the Jersey Central Power and Light Company (J.C.P.& L.). It uses Forked River as a source of cooling water and Oyster Creek as a discharge canal for its once-through cooling system. When the station is pumping water, Forked River flows from Barnegat Bay upstream into the South Branch of Forked River [1], [2]. Salinity in both creeks is now that of adjacent portions of Barnegat Bay. Characteristics of Barnegat Bay have been reviewed elsewhere [3].

Docking facilities have been in Oyster Creek since 1944, but not until the summer of 1971 did the property owners become aware of large-scale damage to wooden structures caused by marine boring clams, the Teredinidae (often called shipworms). Because the creek formerly had been of low salinity, "...freshwater to about 2,500 feet downstream of US Route 9 ..." [4], it had been thought safe for untreated wood, despite the fact that shipworm attacks have occurred from time to time in Barnegat Bay proper [5]. Under new conditions caused by the Generating Station cooling system, the Oyster

505

Creek marinas were providing massive amounts of wood for shipworm infestation.

We began research into the attack of Teredinidae during the summer of 1971 at the request of three marina owners. Early work by one of us [1] indicated that the Generating Station was responsible for the attack by pulling larvae of the teredinids into Forked River and Oyster Creek, by increasing the salinity of both creeks such that teredinids could breed there, and by substantially increasing the temperature of Oyster Creek.

The study was expanded in Sep, ember, 1976, when the U.S. Nuclear Regulatory Commission (NRC) funded the study. In 1974-1975, the NRC required the J.C.P.& L. Company to buy the Oyster Creek marinas, remove untreated wood from the creek, and reduce the temperature of the effluent by increasing the pumping of unheated "dilution" water from Forked River.

This paper reviews the data on plant operations and species distribution and population growth of Teredinidae in the vicinity of Oyster Creek. The purpose is to see if J.C.P. & L.'s actions reduced the shipworm infestation. We comment on the siting and operation of plants producing waste heat, with regard to potential shipworm attacks.

METHODS

Untreated straight-grain white pine panels, 2 x 9 x 21 cm, are used to collect populations of Teredinidae. The panels are weighed, soaked in artificial sea water for 2 weeks, attached to aluminum racks, and set into the water vertically, resting about 15 cm above the water-sediment interface. All panels are aligned similarly with respect to currents and depth. They are placed along creek or bay shoreline off docks or bulkheads, 0.8 to 2.0 meters deep. There are 19 stations (Figs. 1 & 2). Stations 1, 2, 16, and 17 are inshore bay control stations. Stations 3 and 7 are creek controls; 4 - 6 and 9 record shipworms in the south branch of Forked River; 10 - 13 are in Oyster Creek. Stations 8, 14, and 15 are bay stations having a slight thermal influence. Stations 18 and 19, not figured, are offshore bay controls located on Long Beach Island near Barnegat Light. Due to space constraints, we present data from stations 1,2,3,4,5,8,11,12,1? and 18; the remainder are discussed elsewhere [6].

Data are reported from 2 types of panels. Cumulative panels are deployed in sets of 12 each May, and are removed one each month to record cumulative attack of the shipworms. When removed, a cumulative panel is replaced with a panel that is then left in the water for 12 months --- this is called a yearly panel. The yearly panels provide information on species composition, age structure, size of individuals, and population density.

Temperature and salinity are monitored monthly, except at stations 1,5,11, and 14, where constant-recording instruments are located. In the laboratory the shipworms are removed from the panels, measured, and identified to species. Analysis of reproductive condition of the shipworms is performed,

.but is not reported here. Once dissected, the remaining wood chips are treated with acid to remove calcium carbonate fragments, dried to constant weight, and the weight is recorded. Comparison of the final weight with the pre-submergence weight tells the percentage of wood destroyed by marine boring organisms.

RESULTS

The complete data are available in our reports to the NRC [6]. Salinities in Oyster Creek and Forked River (TABLE I) are the same as in Barnegat Bay and are higher than control creeks (eg, station 3). Power plant actions to reduce the shipworm population have not included reduction in salinity.

In the period October, 1971 to May, 1974, temperatures in Oyster Creek were as high as 12° C above ambient water temperatures and usually ran 4 to 10° C above. Since then, the volume of water pumped has increased (TABLE II), and temperatures have been between 2 and 7° C above ambient (TABLE III). Constant recording thermometers have shown temperatures in Forked River to be 1 to 2° C above ambient [6], suggesting that recirculation of the heated effluent occurs [3].

TABLE IV lists major outages of the Generating Station. In 1974 - 1977, there were lengthy outages in spring and/or winter. In 1978, the annual refueling outage did not occur until September. J.C.P. & L. removed some of the untreated pilings and trash wood from Oyster Creek over the period January - March, 1976. Therefore a part of the shipworm breeding population and its habitat was destroyed. No wood was removed from Forked River.

TABLE V summarizes wood weight loss for the 1977-1978 cumulative panel series. The 1976 series showed significant damage (greater than 30% loss of wood weight) at stations 1, 2, 4, 5, 8, and 11, with more than 70% loss at stations 1, 2, and 8. Damage by type of station was: Northern bay > Oyster Creek and the mouth of Forked River > South Branch of Forked River > Southern bay > Creek controls. The 1978 series, after 3 months, showed significant damage only in Oyster Creek.

TABLE VI reviews the species composition and total number of shipworms found in cumulative and yearly panels, (1) in 1973, after the Generating Station began operating but before corrective action was taken; (2) 1976 and 1977, after water temperature was reduced and wood was removed from Oyster Creek; and (3) in 1978, after the plant remained in operation over one continuous winter and spring period. Panels deployed in Oyster Creek or at the mouth of Forked River before September, 1975, became riddled with shipworms after a few months. Between Fall, 1975, and Winter, 1977-1978, settlement was moderate in Oyster Creek and Forked River (less than 30 animals per panel). However, a new outbreak of shipworms occurred in the summer of 1978.

Teredo navalis has always dominated the Long Beach Island area (station 18), and Bankia gouldi, the inshore bay areas (stations 1 and 2). Between 1971

and 1974, B. gouldi and a few T. navalis occurred in Oyster Creek and
Forked River. In 1974, the semi-tropical Teredo bartschi and Teredo
furcifera were found in Oyster Creek. Soon T. furcifera was found at
other stations (TABLE VI), but we found no T. bartschi in 1976 or 1977,
and assumed that it had been eliminated by the cold waters of the winters
of 1975 and 1976. The outbreak of shipworms in 1978 was especially
interesting in that it was composed entirely of Teredo bartschi. Of the
areas suffering severe attack in 1977-1978, stations 2, 11-12, and 18,
each area is dominated by a different species of shipworm.

DISCUSSION

The heavy attack of shipworms at some bay control stations (#2 and 18) but
not others (#17) may result from local water current patterns; shipworms do
poorly in regions of poor circulation. Pollution from marinas, competition
for space with other fouling organisms such as Limnoria and Hydroides, and
shellfish disease are other factors that we [6] and others [7] have
implicated. Oyster Creek and the South Branch of Forked River should be
compared with creek stations 3 and 7, and these have had only light attack
since our study began. These stations are comparable in water flow, tem-
perature, and salinity to Oyster Creek and the South Branch of Forked
River before the Generating Station began operations. Outbreaks of ship-
worms on Long Beach Island, either before or during our study, are not
relevant to the situation in Oyster Creek, for the outbreaks are of the
non-estuarine species T. navalis, in an oceanic environment.

The change in species composition in Oyster Creek acts to prolong the
breeding season, because Teredo species are capable of producing larvae
later into the Fall than the native estuarine species, B. gouldi. T.
navalis, also native to New Jersey, is normally found offshore, but is more
common in the Generating Station's cooling system creeks than in natural
tidal creeks. The result is that four species of the Teredinidae, 2 native
and 2 introduced, can live in Oyster Creek, increasing the likelihood that
the proper physical conditions will trigger an outbreak of at least one of
them. The subtropical T. bartschi releases its young as pediveligers that
settle in aggregations adjacent to the parent. Our laboratory studies show
that individuals mature in 6 weeks or less, depending on water temperature;
2 to 3 generations can easily occur in one year. This life history pattern
led to the outbreak of shipworms in 1978 in Oyster Creek. So far, only 3
T. bartschi have been found in the mouth of Forked River; spread of this
species must take place by movement of infested wood from one creek to the
other unless currents are swift and distance is short, because the pedi-
veligers remain free-living for only a few hours or days. The fact that
Clapp Laboratories [8] reported a few T. bartschi from Oyster Creek during
1976-1977 when we found none indicates that a localized few surviving
adults are responsible for the Oyster Creek outbreak. The outbreak can be
correlated with the lack of a plant shutdown in 1978 until September,
allowing the proper conditions for the subtropical T. bartschi to breed.
We are now conducting laboratory studies of this species to delineate its
physiological tolerances and preferences.

CONCLUSIONS

The shipworm outbreak in Oyster Creek and the South Branch of Forked River is due to: 1) increased salinity allowing entry of 3 species of <u>Teredo</u>, and more consistent reproduction of the estuarine species <u>B</u>. <u>gouldi</u>; 2) higher temperatures, allowing faster growth and reproduction of native shipworms and survival and breeding of subtropical species; 3) rapid water flow; and 4) the presence of untreated wood. Reduction of temperature and of the amount of wood can reduce the shipworm populations, but if any significant amount of penetrable wood is present, an outbreak can occur, given favorable temperatures and salinities.

At Oyster Creek, control of the cooling system temperature necessitated circulation of saline water into 2 low salinity creeks; this alters the local biota. We believe that siting of a cooling system such that it puts bay water into an estuary is a poor strategy. Given present conditions at Oyster Creek, we recommend that schedulable plant shutdowns occur in the Spring when the bay is undergoing its natural warming cycle. The temperature of receiving waters should remain less than 9° in winter to prevent growth and breeding of shipworms all year around. Any marine vessels coming to the area of thermal addition from sub-tropical or tropical waters should be treated to kill boring and fouling organisms that might otherwise be introduced.

Finally, there is need to study population genetics of the introduced shipworms to see if they are being selected to be more resistent to cold temperatures. If so, they might eventually spread throughout Barnegat Bay.

REFERENCES

1 Turner, R.D., 1974. Bull. Amer. Mal. Union 39:36-41.

2 Young, J.S. & A.B. Frame, 1976. Int. Revue ges. Hydrobiol. 61: 37-61.

3 Kennish, M.J. & R. K. Olsson, 1975. Environ. Geol. 1:41-64.

4 Directorate of Licensing, U.S. A.E.C., 1973. Docket No. 50-219, Chapt. 5, p. 17, ¶5.5.21.

5 Nelson, T.C., 1922. New Jersey Agric. Coll. Exp. Sta. Report. State of New Jersey Publ.

6 Hoagland, K.E., R.D. Turner, M. Rochester, &/or L. Crocket, 1977-1978. Analysis of populations of boring and fouling organisms in the vicinity of the Oyster Creek Nuclear Generating Station. 8 reports to the U.S. Nuclear Regulatory Commission.

7 Hillman, R.E., 1978. Journ. Invert. Pathol. 31:265-266.

8 Richards, B. et al, Annual Report to J.C.P.&L., No. 14819, June 1, 1976 - Nov. 30, 1977.

TABLE I
A SUMMARY OF SALINITY DATA SELECTED SHIPWORM STATIONS

Month: Station	1972 1	8*	1973 1	7	1974 2	8°	1975 1	7	1976 1*	7	1977 1	7*	1978 1	7
1	6.0	18.5	2.5	10.0	20.0	17.0	15.0	14,0	15.8	#	20.4	25.0	14.2	16.5
2	-	-	-	-	-	-	-	-	-	19.8	10.0	28.0	14.8	11.0
3	6.6	17.0	2.0	8.1	10.0	14.0	16.0	11.0	2.8	22.5	18.7	20.0	10.5	8.5
4	-	-	-	-	-	-	-	-	-	29.0	22.3	28.0	17.1	24.0
5	-	-	-	-	-	-	-	18.0	18.4	29.0	25.5	27.5	16.6	22.0
8	-	-	-	-	-	-	21.0	19.0	18.6	28.5	23.9	28.0	20.6	24.5
11	13.0	23.5	19.0	19.0	22.0	20.0	19.5	19.0	16.8	28.5	24.0	27.0	16.2	21.5
12	13.0	25.0	21.0	19.2	22.0	22.0	20.0	19.0	18.4	28.0	24.0	28.0	15.1	23.5
17	-	-	-	-	-	-	-	-	-	32.0	26.7	32.0	18.6	37.0#

TABLE III
A SUMMARY OF TEMPERATURE DATA SELECTED SHIPWORM STATIONS

Month: Station	1972 1	8*	1973 1	7	1974 2	8°	1975 1	7	1976 1*	7	1977 1	7*	1978 1	7
1	2.5	23.5	2.2	27.0	2.8	26.6	4.4	28.0	3.0	27.0	0.2	23.9	1.0	23.3
2	-	-	-	-	-	-	-	-	-	27.0	0.1	24.4	2.5	21.6
3	2.5	25.5	4.4	27.7	3.9	28.3	6.6	30.0	4.5	30.0	0.1	25.5	#	27.2
4	-	-	-	-	-	-	-	-	-	27.5	0.0	25.0	0.0	22.2
5	-	-	-	-	-	-	-	27.0	3.5	28.0	0.3	25.0	1.4	22.8
8	-	-	-	-	-	-	6.6	29.0	3.0	29.0	1.8	26.1	1.8	24.4
11	13.9	26.5	11.1	30.0	10.0	32.2	10.5	30.0	1.5	30.5	3.5	25.8	5.5	25.5
12	14.2	29.0	12.2	31.1	11.1	32.2	11.1	31.0	2.8	30.3	4.9	26.1	6.0	25.0
17	-	-	-	-	-	-	-	-	-	24.5	0.0	25.0	3.4	26.1
ΔT	11.7	5.5	10.0	4.1	8.3	5.6	6.7	3.0	*	3.5	4.7	*	5.0	2.2

*Generating Station not operating
#Missing or suspect data
-No station yet established
°Increased dilution pumping from June onward
Note: Temperatures are in °C; salinities are in °/oo.

TABLE II

VOLUME OF WATER PUMPED, OYSTER CREEK NUCLEAR GENERATING STATION*

YEAR

Mo.	70 D^1	71 D	72 C^2	D	73 C	D	74 C	D	75 C	D	76 C	D	77 C	D	78 C	D
1	0.0	0.0	3.0	0.1	4.0	0.0	3.2	1.1	4.0	2.0	0.0	1.8	3.2	1.0	4.0	1.9
2	0.0	0.0	2.9	1.0	4.0	0.1	3.9	1.0	3.4	1.9	0.0	1.9	3.5	1.4	4.0	1.8
3	0.0	0.0	3.0	1.0	4.0	0.0	3.1	0.9	3.8	1.8	2.8	1.6	4.0	1.8	4.0	1.9
4	0.0	0.0	2.0	1.0	4.0	0.4	1.5	0.6	0.0	1.8	4.0	2.0	3.8	1.6	4.0	1.9
5	0.0	0.0	0.6	0.1	2.4	1.0	0.3	0.7	0.8	1.0	4.0	1.1	0.0	0.9	4.0	1.6
6	0.2	0.3	1.2	0.3	3.8	1.0	4.0	0.0	3.2	1.8	3.9	1.6	0.0	1.0	4.0	1.8
7	0.8	1.0	4.0	1.0	4.0	1.0	4.0	1.4	4.0	2.0	4.0	1.8	1.0	0.7	4.0	1.9
8	1.0	1.0	3.4	0.8	4.0	1.0	4.0	1.9	3.1	1.9	4.0	1.8	4.0	1.8	4.0	1.9
9	0.4	0.4	4.0	1.0	3.0	1.0	4.0	1.3	2.4	1.1	4.0	1.4	4.0	1.4		
10	0.3	0.0	3.9	1.0	3.7	0.9	2.6	1.5	2.7	1.6	3.9	1.5	3.9	1.6		
11	0.0	0.3	3.6	0.3	4.0	0.9	3.3	1.6	2.4	1.9	4.0	1.9	4.0	1.9		
12	0.0	0.5	3.7	0.0	4.0	1.0	3.6	2.0	2.5	1.7	3.8	1.8	4.0	1.9		

*Data courtesy of J. C. P. & L. Co.

[1] Average number of dilution pumps operating per month. 260,000 gal/min per pump.

[2] Average number of circulation pumps operating per month. 115,000 gal/min per pump. No circulation pump data were made available for 1970-1971.

TABLE IV
OYSTER CREEK NUCLEAR GENERATING STATION
OUTAGE DATES*

1970

1/31	-	2/12
#4/19	-	5/21
10/16	-	10/29

1971

1/25	-	1/28
2/12	-	2/19
3/3	-	3/5
#9/18	-	11/11
11/16	-	11/21

1972

1/28	-	2/2
#5/1	-	6/20
8/9	-	8/15
11/11	-	11/13
12/29	-	12/31

1973

1/1	-	1/13
#4/14	-	6/4
7/21	-	7/25
#9/8	-	10/5

1974

1/12	-	1/20
3/7	-	3/11
#4/13	-	7/3
10/8	-	10/15
11/11	-	11/15

1975

2/4	-	2/9
#3/29	-	5/26
6/13	-	6/15
8/27	-	9/3
9/24	-	10/3
10/5	-	10/6
11/25	-	12/1
12/19	-	12/21
#12/27	-	12/31

1976

| #1/1 | - | 3/11 |
| 7/28 | - | 7/31 |

1977

#4/23	-	8/4
10/21	-	10/22
11/14	-	11/15
12/3	-	12/4

1978

| 6/14 | - | 6/16 |

*Courtesy of J.C.P. & L Company.
Load reductions not included.
#Major outage for refueling or repair.

TABLE V
Percent Wood Weight Loss
Cumulative Panels Submerged May 27, 1977

Months Submerged	1	2	3	4	5	6	7	8	9	10	11	12
Station												
1	0	0	5	5	0	4	6	26	*	1	0	7
2	0	0	56	59	60	60	54	53	*	58	49	*
3	0	0	2	1	0	4	2	1	*	0	3	0
4	0	0	1	8	7	6	8	5	12	3	2	21
5	0	1	2	15	7	11	5	5	5	1	15	15
8	0	1	2	0	16	10	13	4	6	19	4	*
11	0	1	4	21	21	36	19	48	32	56	29	45
12	0	0	10	7	15	19	20	17	19	10	9	17
14	0	0	0	0	3	4	0	1	*	10	3	11
18#	0	11	25	70	79	75	75	*	64	70	73	70

*Panel lost, or unretrievable due to ice cover.
#Station new in 1977.

TABLE VI
SPECIES COMPOSITION AND NUMBER OF SHIPWORMS IN CUMULATIVE PANELS
AFTER ONE SUMMER'S EXPOSURE, AND YEARLY PANELS REMOVED IN AUGUST

SERIES BEGUN: Apr. 30, 1976 | May 27, 1977 | May 31, 1978
PANELS REMOVED: Aug. 8, 1976 | Aug. 8, 1977 | Aug. 8, 1978

Station	Bg	Tn	Tf	Tb	Tsp	Total	Bg	Tn	Tf	Tb	Tsp	Total	Bg	Tn	Tf	Tb	Tsp	Total
1	21					21	1					1		1				1
2	92	4			6	102	113					113	6					6#
3						0						0						0
4	51		1		1	53	3				1	4	1	1				2
5	21		2		2	25	4				2	6	3	1				4
8	42	1				43	1					1						0
11	1					1						0	1	2		46	8	57
12	3					3	7					7				80		80
17			3			3						0						0
18						-					4†	4†		5				5

PANEL DEPLOYED: Aug. 18, 1972 | Aug. 8, 1976 | Aug. 8, 1977
PANEL REMOVED: Aug. 8, 1973 | Aug. 8, 1977 | Aug. 8, 1978

Station	Bg	Tn	Tf	Tb	Tsp	Total	Bg	Tn	Tf	Tb	Tsp	Total	Bg	Tn	Tf	Tb	Tsp	Total
1	~30					~30	9					9	3					3
2						-	106	1				107	42					42#
3	~20					~20						0						0
4						-	6	2				8	5	2				7#
5						-	9					9	4	1			1	6
8						-						lost	17	1				18
11						R	13					13		1		417	36	454
12						R	3					3				180	28	208
17						-	2					2						0
18						-						-		100†				100†

R = panel riddled; more than 100 shipworms. Mostly B. gouldi; some T. navalis.
# = July panels; August panels were missing.
† = more than 100; too small and numerous for an exact count.
- = no station yet established.
Key to the species: Bg = B. gouldi; Tn = T. navalis; Tf = T. furcifera; Tb = T. bartschi; Tsp = T. sp. unknown.
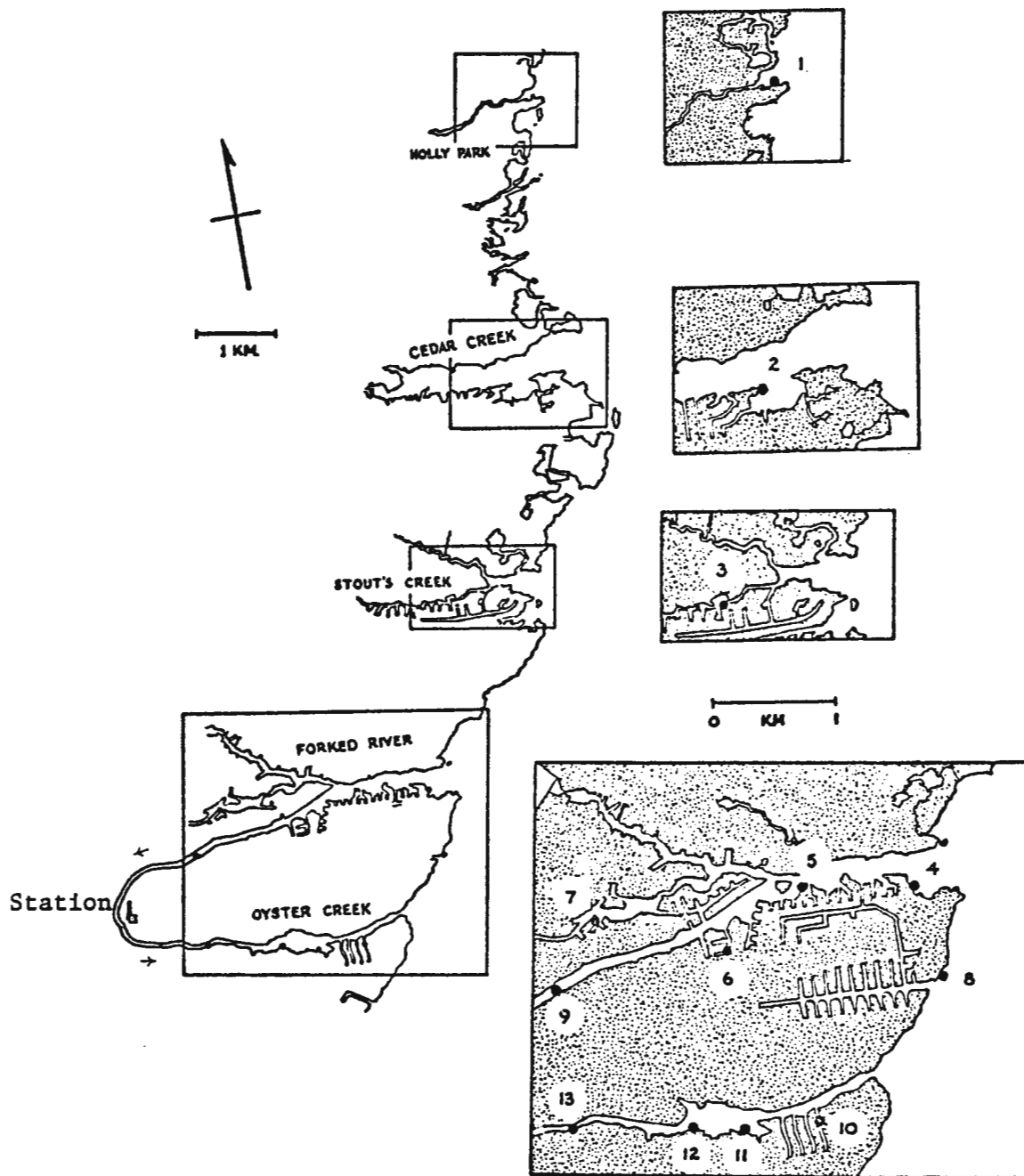
Figure 1: The Relative Locations of Stations 1 - 13, the Oyster Creek
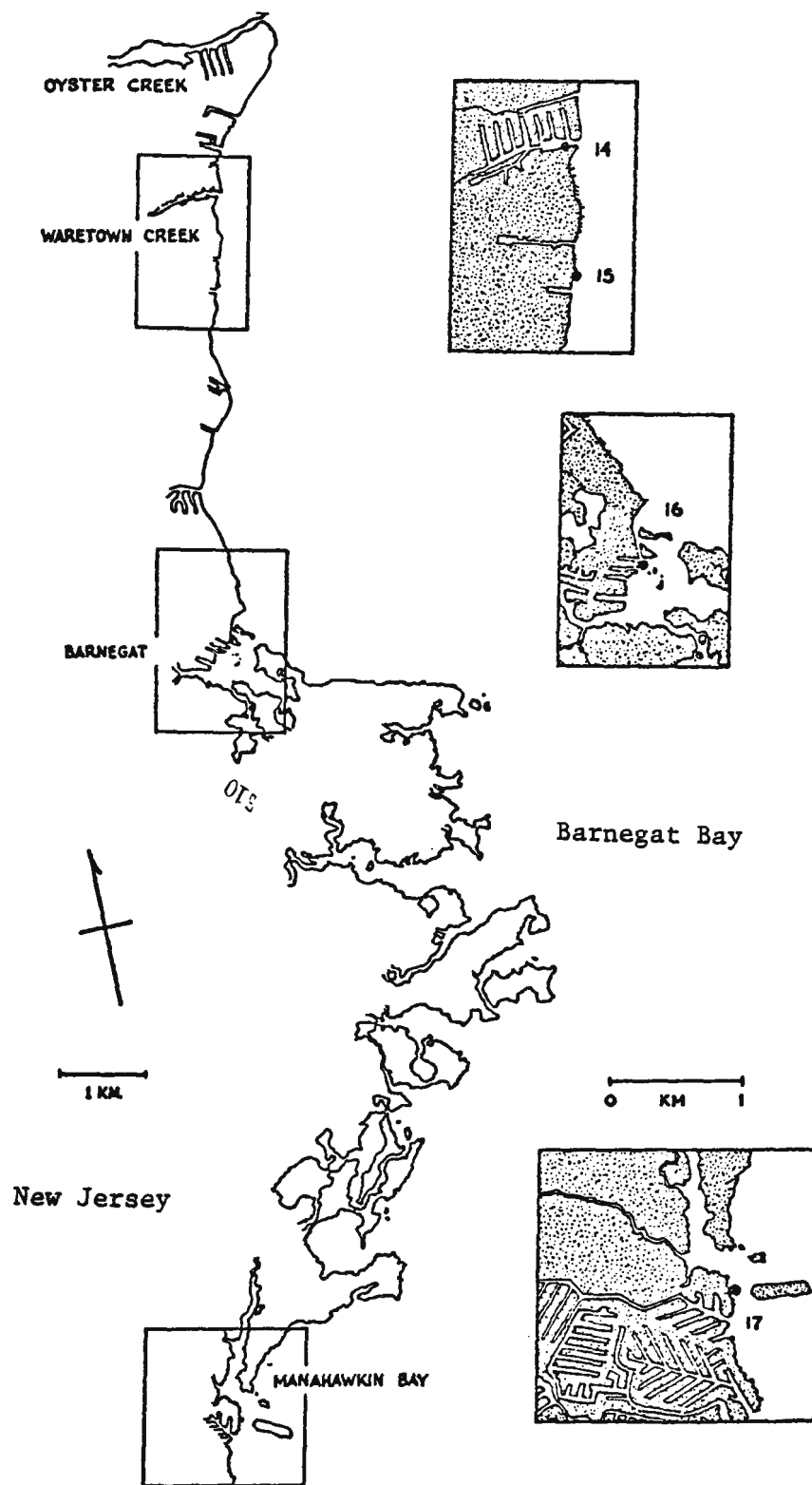Nuclear Generating Station, and its Cooling System

Figure 2: The Relative Locations of Stations 14 - 17.

COLD INFLOW AND ITS IMPLICATIONS FOR DRY TOWER DESIGN

F.K. Moore
Cornell University
Ithaca, New York U.S.A.

ABSTRACT

The phenomenon of cold inflow near the exit of a cooling tower is analyzed in terms of the possibility that the free plume may begin inside the tower at some location determined by compatibility of the plume with the parameters of the tower. It is shown that a dimensionless group which compares the momentum flux of the entrained flow and the buoyancy governs the problem, and critical values of this quantity are found. Results show that conventional natural-draft dry towers should not be greatly affected by cold inflow, but "low" designs may require turbulence generators to enhance entrainment rate at the tower top. In any case, the usual flare near the tower top should be eliminated or reversed. Low towers will also require careful heat-exchanger design to limit sensitivity to wind.

INTRODUCTION

A natural-draft cooling tower contains a mass of slowly-moving air which is slightly buoyant relative to the surrounding ambient air. If it were not for the air's motion, instability would obviously exist, with cold outside air spilling into the tower at its top outer edge. When draft is strong, as in tall chimneys, this cold-inflow tendency is not evident, but it usually occurs in natural-draft evaporative cooling towers, with their lower velocities and wide exits [1], [2]. Under wind, when the plume is laterally displaced, cold inflow can be especially severe at the upwind lip of the tower. In a certain range of wind speeds, inflow may be periodic, in a "puffing" mode [1]. Figure 1 shows a sequence of 3 photos taken about 5 seconds apart of the towers at Didcot, England [3]. The plumes do not always fill the exit area, clearly suggesting a periodic inflow. Experimentally, Jorg and Scorer [4] have studied cold inflow, but in too low a Reynolds number range to be helpful for the study of cooling towers.

Obviously cold inflow, if it occurs, will degrade the performance of a cooling tower by causing a premature separation of the buoyant flow from the tower wall, and an effective narrowing of the exit flow area [5]. Possible plume boundaries of this sort are sketched in Figure 3c. From a design point of view, concern about cold inflow conflicts with a desire to lower the draft height of towers for cost and aesthetic reasons, and the concern must be especially acute for dry natural-draft towers. Not only is the incentive strong to develop low towers, but it is known that dry towers are severely affected by wind [5], and cold inflow may be implicated.

It would be important to understand how premature separation, or cold inflow, is related to tower design parameters. As an obvious extreme case, if a weak flow of buoyant air were introduced over a very wide area, with no side walls, one would expect the same plume development as observed for a large fire [6], namely, an initial buoyant acceleration characterized by a convergent upward flow, this followed by a spreading and dilution of the plume due to turbulent entrainment of ambient air at the plume's boundaries. As we shall see, such a large plume will therefore have the hourglass shape shown in Figure 2. Now, if a low tower wall should be erected around the base of such an outflow, it would have no effect; the converging lower part of the plume will not interact with the wall. Only when the wall is high enough to "catch" the diverging, entrainment-dominated part of the plume can the wall begin to take effect, and begin to cause draft. It would seem that the extreme wide, low tower proposed by Roma [7] would fail for this reason. Figure 3c contains sketches which illustrate these ideas.

In this paper, we will develop quantitative estimates of these effects, beginning with an approximate analysis of a buoyant plume with entrainment, and then matching those results to calculated dry-cooling-tower configurations. For the latter purpose, we will use certain previous calculations [8] which happen to have varied the tower parameters of interest in a systematic way, based on a particular heat-exchanger surface.

We shall be especially interested to know where the plume may start in a tower assuming draft and plume flow rate are properly related. Again, referring to Figure 3c, are any or all of the sketched results possible? The effect of entrainment rate will be explored (presumably, a high entrainment rate will favor the plume being "caught" by the wall), and means of increasing that rate will be discussed.

Finally, we will suggest design parameter limitations for the avoidance of cold inflow, and relate these results to certain new estimates [5] of the sensitivities of tower thermal performance to various loss mechanisms. These results will suggest the proper directions for efforts to develop towers of low draft requirement.

Although our chief concern is with dry, natural-draft towers, most of our results (up through Figure 5) are applicable to wet towers as well.

PLUME ANALYSIS

General Solution

We begin with the classical one-dimensional plume analysis of Morton, Taylor and Turner [9]. Although that theory is generally used to describe plumes emanating from a virtual point source, it is possible to solve their equations for an area source, which reveals the initial convergent behavior of interest here. Morton [10] has made such an extension of [9], but not in a form suitable for our purposes. The basic equations are

$$(b^2 u)' = 2\varepsilon b u \tag{1}$$

$$(b^2 u^2)' = b^2 g\alpha \qquad (\alpha \equiv \Delta\rho/\rho) \tag{2}$$

$$\pi b^2 u\alpha = Q/g \tag{3}$$

which express, respectively, that volume flow in the plume increases with distance by entrainment according to the coefficient ε (α in [9]), that momentum flux increases by buoyancy, and that heat flux is constant along the plume. The sketch illustrates notation. Equations (1-3) assume one-dimensional flow with a "top-hat" velocity profile. The inherent limitations of a one-dimensional flow model near the beginning of the plume (at ①) would not warrant refining the profile assumption.
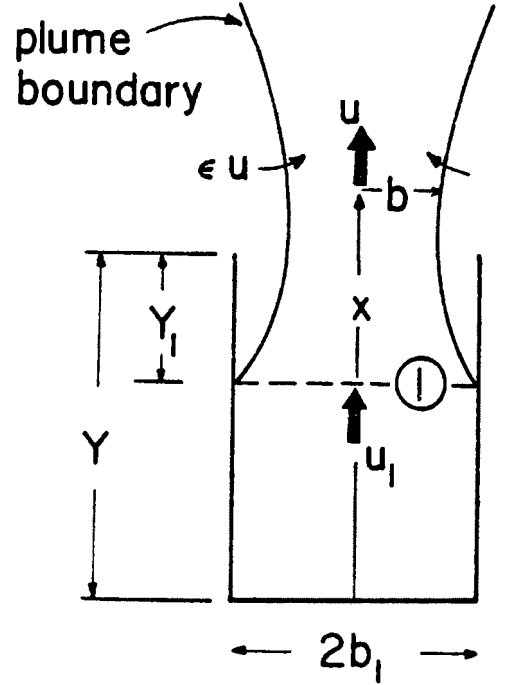
The solution of eqs. (1-3) which envisions a certain flow through level ① (see sketch) is

$$u = 0.8286 \left(\frac{\alpha_1^2 g^2 b_1^2 u_1^2}{\varepsilon^2}\right)^{1/5} C_1^{-1/10} u^*(x^*); \quad C_1 \equiv 1 - \frac{1.6 u_1^2 \varepsilon}{\alpha_1 g b_1} \tag{4}$$

$$b = 1.099 \left(\frac{b_1^4 u_1^2 \varepsilon}{\alpha_1 g}\right)^{1/5} C_1^{3/10} b^*(x^*) \tag{5}$$

where u^* and b^* are dimensionless functions of a dimensionless version of x:

$$x = 0.3433 \left(\frac{b_1^4 u_1^2}{\alpha_1 g \varepsilon^4}\right)^{1/5} C_1^{3/10} x^* \tag{6}$$

The functions u^* and b^* are displayed on Figure 2. The dashed and dot-dashed lines correspond to assumptions of pure entrainment (with a virtual source at $x^* = -2.27$) or pure buoyancy. The plume radius b has a "throat" with $b^* = 1.400$ when $x^* = 0.641$. We note that the coordinate x is not fixed relative to the tower until u and b are specified at ①.

Match to the Tower.

The next step is to match Equations (4) and (5) to tower conditions. The first, and simplest test is to ask whether a plume assumed "anchored" at the tower top would first converge upward, as in Figure 3c or diverge as in Figure 3a. If the former, then we should consider the possibility that it "falls down" into the tower (Figure 3c). If the latter, the plume is secure and no inflow is possible. The dividing condition is a vertical exit (Figure 3b), when the throat of b (Figure 2) is precisely at the tower exit. We may differentiate Equation (5) to find when that happens, and the result is

$$\frac{u_1^2 \varepsilon}{\alpha_1 g 2 b_1} \equiv F = \frac{1}{8} \qquad (7)$$

Where for future reference, we assign the symbol F to the dimensionless group. Divergence (Figure 3a) corresponds to $F > 1/8$. That is, if the momentum of the entrained flow ($u \cdot \varepsilon \rho u$) is large enough compared to buoyancy, cold inflow cannot occur. A typical tower might have $u = 4$ mps, $\Delta\rho/\rho = 0.1$ (air 30°C warmer than ambient), and ε is normally about 0.1 without wind. In such a case, the exit diameter D_E would have to be less than 13m to be entirely proof against inflow. This is about 5 times less than the usual D_E for natural draft, and so we must investigate further to find whether cold inflow should be expected in such cases.

We note that chimneys, with diameters smaller than 13m (and velocities higher than 4 mps) should never experience inflow, and that mechanical-draft towers, which have exit velocities up to 10 mps and quite small diameters (13m is not unreasonable) should also be immune to cold inflow.

We now go the next step and ask, if $F < 1/8$, how far the plume may fall into the tower. Referring to the notation sketch, we should compare the possible Y_1 to Y, the tower height. A simple draft equation would say that

$$\alpha_1 g (Y - Y_1) = \frac{1}{2} u_1^2 C_L \qquad (8)$$

where C_L is the overall pressure-loss coefficient of the tower. Chiefly, it reflects the pressure drop through the bundles, and $C_L = 16$ would be a representative figure. One may introduce Equation (8) into Equations (4) and (5) and find a set of solutions, depending on the choice of ε, for which the plume just grazes the tower exit. Figure 4 shows the results for $\Delta\rho/\rho = 0.1$, $C_L = 16$, $D_E = 61$ m and $Y = 110$ m. In that case, Equation (8) says that if cold inflow does not happen ($Y_1 = 0$), the exit velocity is $u_{1_0} = 3.7$ m/s. These parameters would represent a dry cooling tower. For a wet tower, $\Delta\rho/\rho$ and C_L would both be smaller.

Figure 4 suggests that for this rather ordinary tower, the plume may tend to "fall in" unless ε is greater than about 0.5. If $\varepsilon = 0.2$, the plume could begin about half-way, and the exit flow would be only about 0.72 of the

full-tower value, 3.7 mps, and a corresponding loss of cooling performance would be anticipated. Actually, except under wind, mixing coefficients should not even be as high as 0.2.

Clearly, these results are too pessimistic; cooling towers evidently do not suffer from cold inflow to the degree suggested by Figure 4. In the next section, we shall see how to make more realistic estimates. However, Figure 4 is useful merely to illustrate the idea of a plume "falling in" a cooling tower.

EFFECTIVE ENTRAINMENT RATE

Restricted-Flow Model.

On reflection, one sees that the grazing plumes of Figure 4 are impossible, because there is no way to supply the entrainment flow to the plume boundary. If a plume "falls in", it may go only so far; the sketch shows how the entrainment required by the plume boundary must be supplied through the gap (d) between plume and lip, and it must be supplied in proportion to the penetration depth Y_1.

Let us estimate the cold inflow velocity u_e. First, we note that separation from the lip should be expected, and classical free-surface theory [11] would narrow the gap to $\frac{1}{2}d$, as sketched. We note, too, that the downward velocity u_e might remain constant because pressure tends to be constant along a (dashed) free streamline. Assuming that u inside the plume is nearly constant, the velocity difference across the plume boundary is $u + u_e$. It is this relative velocity which would govern turbulent entrainment. That is, $v_e \approx \varepsilon(u + u_e)$. The entrainment volume flow $\varepsilon(u + u_e)Y_1$ must be provided by that over the lip, $u_e d/2$. Equating these two expressions, one finds that
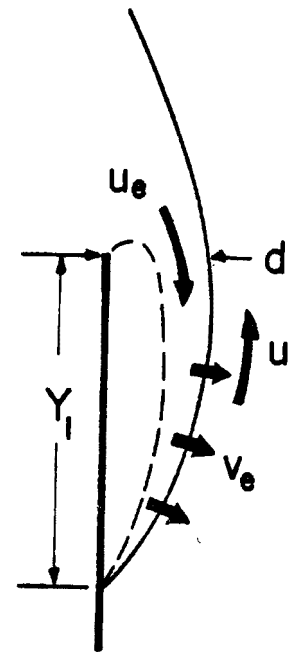
$$\frac{u_e}{u} = (\frac{d/2}{\varepsilon Y_1} - 1)^{-1} \tag{9}$$

For use in calculations which express entrainment as εu, it will be appropriate to define an effective entrainment rate ε_e such that $\varepsilon_e u = \varepsilon(u + u_e)$, which is the true rate. Equation (9) then provides that

$$\frac{\varepsilon_e}{\varepsilon} = (1 - \frac{N\varepsilon Y_1}{d})^{-1} \tag{10}$$

520

where $N = 2$ according to Equation (9), because a free-surface separation was assumed in the model sketched. Actually, the separated zone would probably become fully mixed and u_e would be reduced accordingly. It would be reasonable (and conservative) to take $N = 1$. Obviously, the effective entrainment rate ε_e may be many times the physical rate ε, and we note that penetration depth cannot exceed $(1/N\varepsilon)d$.

Using Equation (10) in the combined tower-internal plume analysis (Equations (4-6, 8), one finds a set of possible solutions for each case. In each set, there is solution with maximum penetration (Y_1). These "worst-inflow" solutions yield Figure 5. Clearly, if the usual value $\varepsilon = 0.1$ applies, effects of cold inflow should be expected for towers less slender in shape than about 1.8, which is typical of current practice [5]. However, if the basic entrainment coefficient ε can be increased to 0.4, very low shapes will "work." Perhaps experiments will show that turbulence generators near the top of the tower (on the inside surface) can substantially increase ε. We should note that, under wind, plumes develop above a tower as if the average ε is about 0.4; however, this effect would perhaps not be felt inside the tower, and no doubt, circumferential variations of ε are important. Thus, one should not rely on wind to provide the ε needed to prevent cold inflow.

It has been proposed by Professor Ernst of Karlsruhe University [3] that cold inflow may be prevented by turning the shell inward slightly at the tower top, causing a local overpressure to oppose inward flow. From the point of view of this paper, such an inward curl of the shell may indeed be helpful if it corresponds to the desired initial plume angle (Figure 3c); the plume which would otherwise "fall in" might thereby be stabilized at the top against small (but not large) disturbances.

In any case, it is obvious that the usual slight flare given to the exit portion of the tower would encourage cold inflow by allowing room for entrainment flow to supply a "fallen-in" plume. Such flares should be eliminated, and replaced by a slight convergence, over the upper third (say) of the tower.

Finally, we may recall the definition of F in Equation 7, and ask how that number compares with the value $1/8$ for vertical exit flow, for the conditions assumed in Figure 5. They were $\alpha_1 = 0.1$ and $C_L = 16$. For no inflow, and $\varepsilon = 0.1$,

$$8F = 14.18 \frac{s\varepsilon}{C_L} = 0.089 \ s \tag{11}$$

Inasmuch as inflow seems not serious if $s > 2$, one concludes that the value of $8F$ should generally be kept greater than about 0.18, or, in round numbers, 0.2. In other words, a substantial degree of initial convergence can occur without significant inflow, for typical cooling-tower parameters.

IMPLICATIONS FOR LOW-TOWER DESIGN

Cold Inflow as a Function of Dry-Tower Design.

Figure 5 has shown how one variable, tower shape(s), can affect prospects for cold inflow. Other variables, such as bundle resistance (C_L), will also be important, presumably. In [5], simple formulas were developed to evaluate the effects of a wide variety of parameter changes for dry towers, and the same approach may be applied here. We will consider F to be a design parameter, in effect, and assume that it should be kept above the value 8F = 0.2 mentioned in the previous section.

Using [5], one may show that

$$8F = 14.18 \frac{s\varepsilon}{\beta\xi^2} \tag{12}$$

In effect, C_L in Equation (11) is replaced by $\beta\xi^2$. Losses outside the heat exchanger are represented by β as a coefficient multiplying exit dynamic head, and the value of β is typically about 1.4. The quantity ξ is the ratio of actual exit area to that which would be needed if there were no heat-exchanger flow resistance [5,8]. It is an optimizing parameter; small ξ means a small tower but a large bundle surface area, and large ξ means the reverse. Thus, ξ would be selected according to the designer's relative weighting of tower and bundle costs. A common choice would be $\xi = 2.5$. Figure 6 illustrates this relationship for a particular type of bundle and tower shape, as calculated in [8].

Equation (12) in conjunction with Figure 6 shows that the designer potentially has the difficulty that the need for a large enough F might compel him to adopt a design with an uneconomically large heat exchanger. With this question in mind, a number of different cases treated in [8] were examined to see how F varies with parameter changes. Figure 7 shows the results.

The left-most pair represent two choices of ξ, within the customary range. Even the larger produced an 8F of 0.28, well above the value expected to be critical for inflow. Next, the effect of changing to a single-pass bundle is considered. Again, $\xi = 2.5$ yields 8F = 0.28, but a larger tower and a smaller heat-exchange area (A_a) are required. Clearly, for a given rela-tion of tower size and A_a, fewer passes tend to help increase F. Doubling heat-rejection rate produces the next example, and a simple economy of scale is evident for both tower size and A_a.

The most interesting case is the last, which considers a low tower shape (s = 1 instead of 1.7). Here, for the same 8F, a smaller ξ (and larger A_a) is needed. Suppose we go to $\xi = 2.5$; then the tower is still low, compared to the first more conventional case, but A_a is now reduced to a reasonable level. However, we must be able to tolerate 8F = 0.16, which Figure 5 suggests is marginal. No doubt, special design features will be needed to make this last case secure against cold inflow, but the requirement seems not to be extreme or discouraging.

Sensitivities to Loss Mechanisms.

Figure 7 also mentions two parameters S_β and S_w. These quantities may be written as follows, for the present purpose:

$$\frac{1}{ITD} \cdot \frac{\partial(ITD)}{\partial\beta} = (\text{const.}) \frac{1}{\xi^2} \equiv (\text{const.})S_\beta \tag{13}$$

$$\frac{1}{ITD} \cdot \frac{\partial(IDT)}{\partial w^2} = (\text{const.}) \left(\frac{D_E}{Q\xi s^2}\right)^{2/3} \equiv (\text{const.})10^{-2}S_w \tag{14}$$

They are derived in [5], and represent the proportional changes of ITD (overall cooling performance) as a loss mechanism other than bundle resistance changes (Equation (13)), and the change as wind-connected loss changes (Equation (14)). The constant is unknown or uncertain in both cases. In both cases, cold inflow might be implicated. In any event, these expressions can describe on a relative basis the susceptibilities of tower performance to aerodynamic losses.

Returning to Figure 7, the two most noticable trends of these susceptibility factors are, first, that large scale reduces the danger of performance loss due to wind, and second, that low shape (small s) greatly increases that danger. Because performance loss due to wind may be traced with some confidence to the behavior of air flow as it enters the bundle face [3,5], great care will be needed in designing heat-exchanger arrangements in the tower.

The Approach to Low Dry-Tower Design.

With the potential siting and cost advantages of a low shape for natural-draft dry cooling, we may recapitulate the results of this discussion, first admitting that the theory of cold inflow advanced here is rough, and requires verification.

1. Cold inflow seems not to be a fundamental bar to the maintenance of draft in towers down to, or even below, $Y/D_E = 1$, provided certain improvements in customary practice are made:
    (a) Instead of the usual outward flare of the upper third of the tower, it should converge slightly, also over the upper third of the tower.
    (b) Care should be taken to promote vigorous flow near the tower wall.
    (c) Introduce turbulence generators just inside the tower exit.
The foregoing suggestions are applicable to wet as well as to dry towers.

2. Low towers will be more sensitive to performance loss due to wind than more slender towers. Although there is no doubt a connection with cold inflow here (a tower precarious in that regard will no doubt be more influenced by wind), here the chief concern must be the heat exchanger and its arrangement in the tower. This matter is discussed in [12].

3. Any developments which reduce the cost of heat-exchange surface (e.g., plastic tubing [7]) will permit lower values of ξ and hence, more security against inflow; however, sensitivity of tower performance to wind losses would be higher (see Figure 7, case s = 1). Whether such a change would be helpful in low-tower design is therefore uncertain.

ACKNOWLEDGEMENT

REFERENCES

1. G. Ernst, "Cooling Towers, Design and Plume Behavior," Seminar of International Centre Heat and Mass Transfer, Dubrovnik, 1975.

2. E. Baer, G. Ernst, and D. Wurz, "Untersuchung zur Schwadenströmung in den Kronen von Naturzugkühltürmen," VDI Kühlturmseminar, Düsseldorf, May 25, 1977. Inst. f. Technische Thermo., U. Karlsruhe.

3. F.K. Moore and K.E. Torrance, "Air Flow in Dry Natural-Draft Cooling Towers Subject to Wind," Report to ERDA, Cornell University, Dec. 8, 1977.

4. O. Jörg and R.S. Scorer, "An Experimental Study of Cold Inflow into Chimneys," Atmos. Environment, v. 1, p 645, 1967.

5. F.K. Moore, "Effects of Aerodyanmic Losses on the Performance of Large Dry Cooling Towers," ASME Publ. 78-WA/HT-18, Winter Annual Meeting, Dec. 10-15, 1978.

6. J.S. Adams, D.W. Williams, and J. Tregellas-Williams, "Air Velocity, Temperature, and Radiant-Heat Measurements within and Around a Large Free-Burning Fire," 14th Symposium (International) on Combustion, p 1045, The Combustion Institute, 1973.

7. C. Roma, "An Advanced Dry Cooling System for Water from Large Power Station Condensers," Proc. Am. Power Conf., v. 35, p 626, 1973.

8. F.K. Moore and C.C. Ndubizu, "Analysis of Large Dry Cooling Towers with Power-Law Heat-Exchanger Performance," Journal of Heat Transfer, Aug. 1976, p. 345.

9. B.R. Morton, G.I. Taylor, and J.S. Turner, "Turbulent Gravitational Convection from Maintained and Instantaneous Sources," Proc. Roy. Soc., Ser. A, No. 234, p. 1.

10. B.R. Morton, "Forced Plumes," Jour. Fluid Mech., v. 5, p. 151, 1959.

11. H. Lamb. "Hydrodynamics," 6th Ed., para. 73, Dover, New York (1945).

12. F.K. Moore, "Aerodynamics of the Heat Exchangers and their Arrangement in Large Dry Cooling Towers," ASME Publ. 78-WA/HT-19, Winter Annual Meeting, Dec. 10-15, 1978.
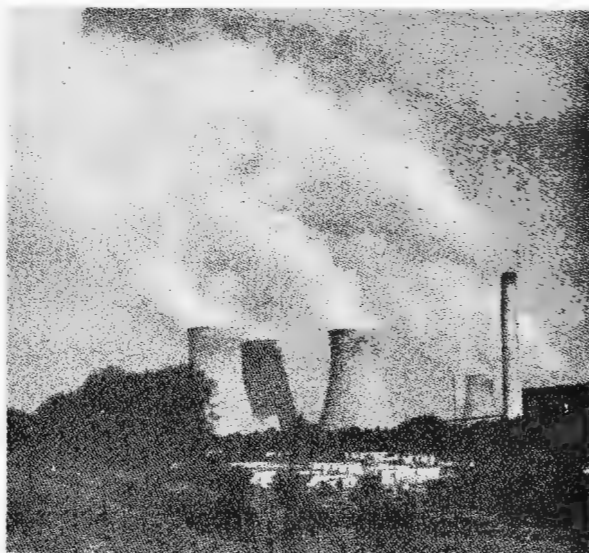
Figure 1. Sequence of photographs, about 5 seconds apart, of the cooling towers at Didcot, England. Flow separation is especially evident in the discharge from the middle tower.
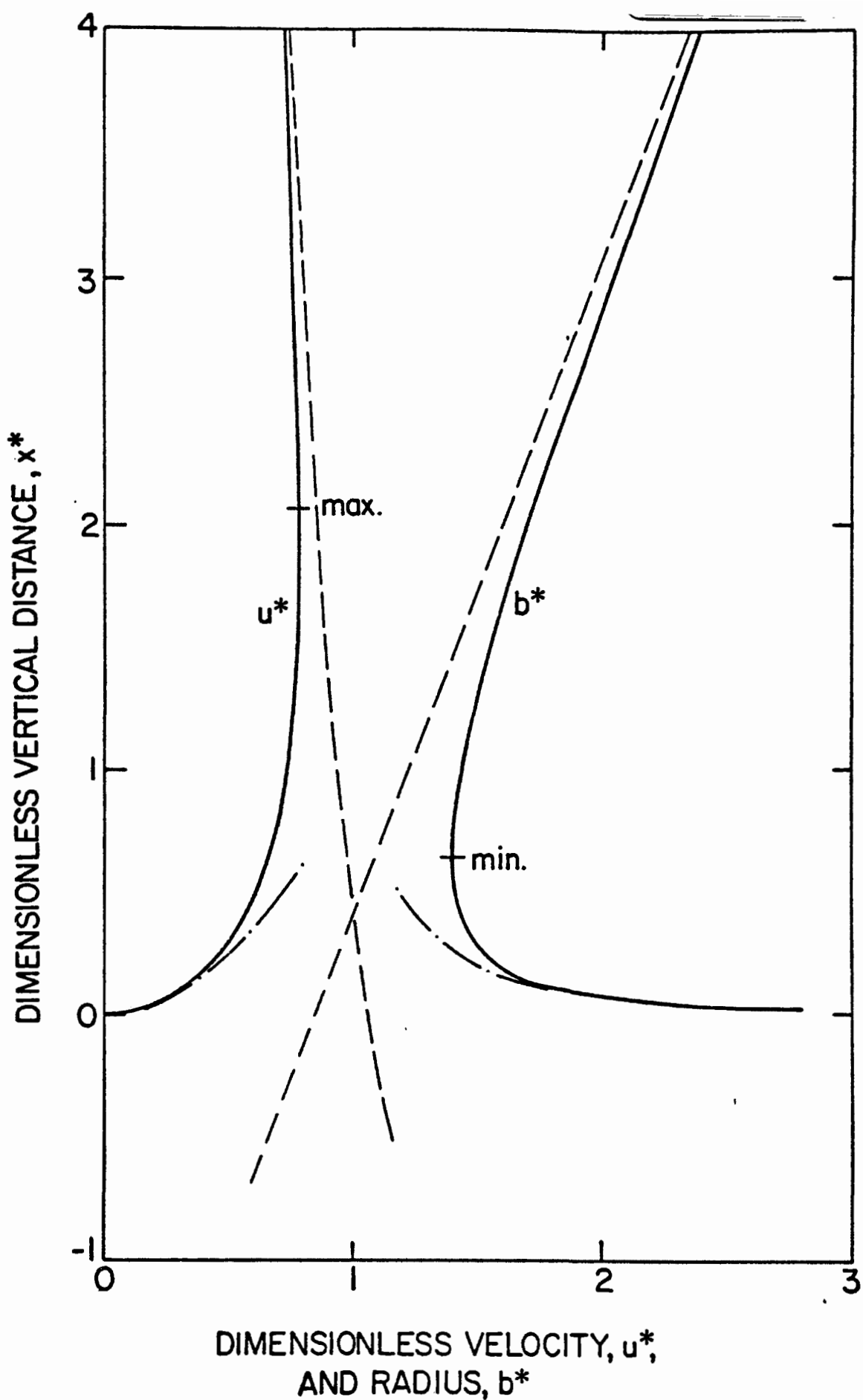
Figure 2. Dimensionless plume velocity (u^*) and radius (b^*) as functions of dimensionless vertical distance (x^*), from Equations (4-6). Dashed lines refer to a pure entrainment or point-source extreme, and the dot-dash lines refer to a buoyant plume with no entrainment.

plume

exit

tower

(a) PLUME DIVERGENT AT EXIT ($\mathcal{F} > 1/8$)

(b) PLUME VERTICAL AT EXIT ($\mathcal{F} = 1/8$)

(c) PLUME CONVERGENT AT EXIT ($\mathcal{F} < 1/8$)
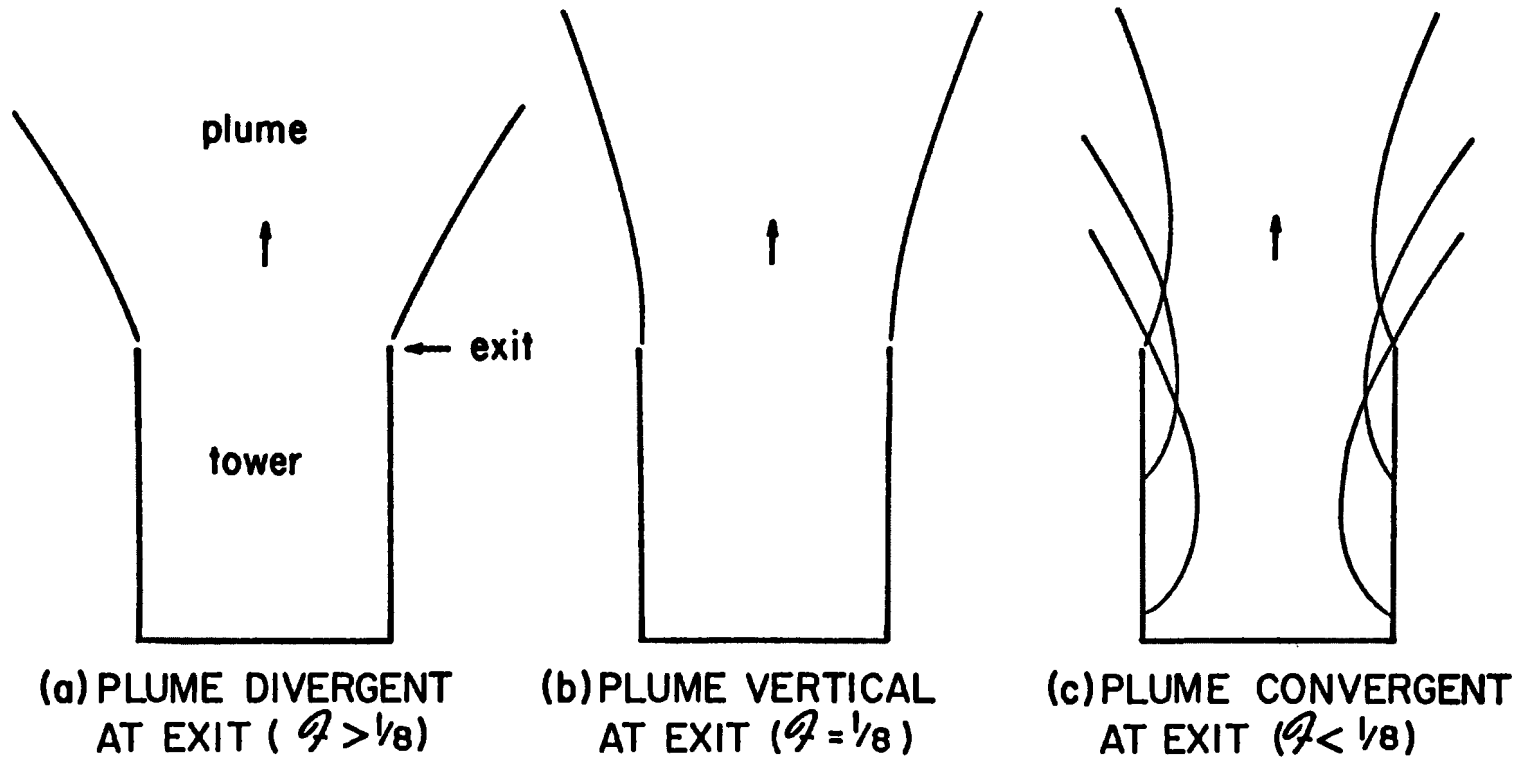
Figure 3. Sketches of possible exit plume shapes, depending on F (Equation (7)). If plume is initially convergent (c), the plume may perhaps originate within the tower; three possibilities are shown.
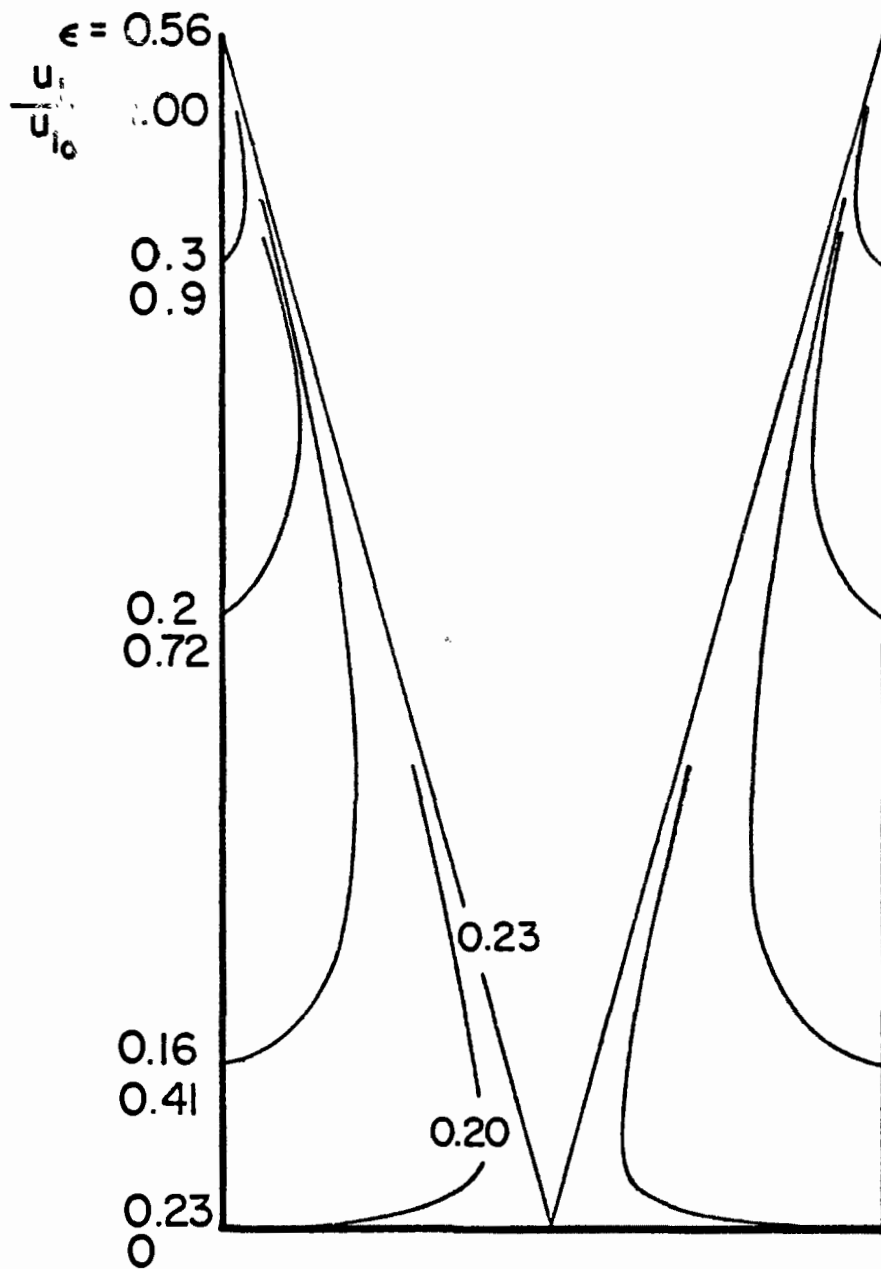
Figure 4. The set of plume boundaries which just graze the tower top, for $\Delta\rho/\rho = 0.1$, $C_L = 16$, $D_E = 61m$, $Y = 110m$, and various entrainment rates ε. Also indicated are the reduced exit flow velocities which result from the "fallen-in" plumes. Solutions are possible only in the range $0.20 < \varepsilon < 0.56$.

528
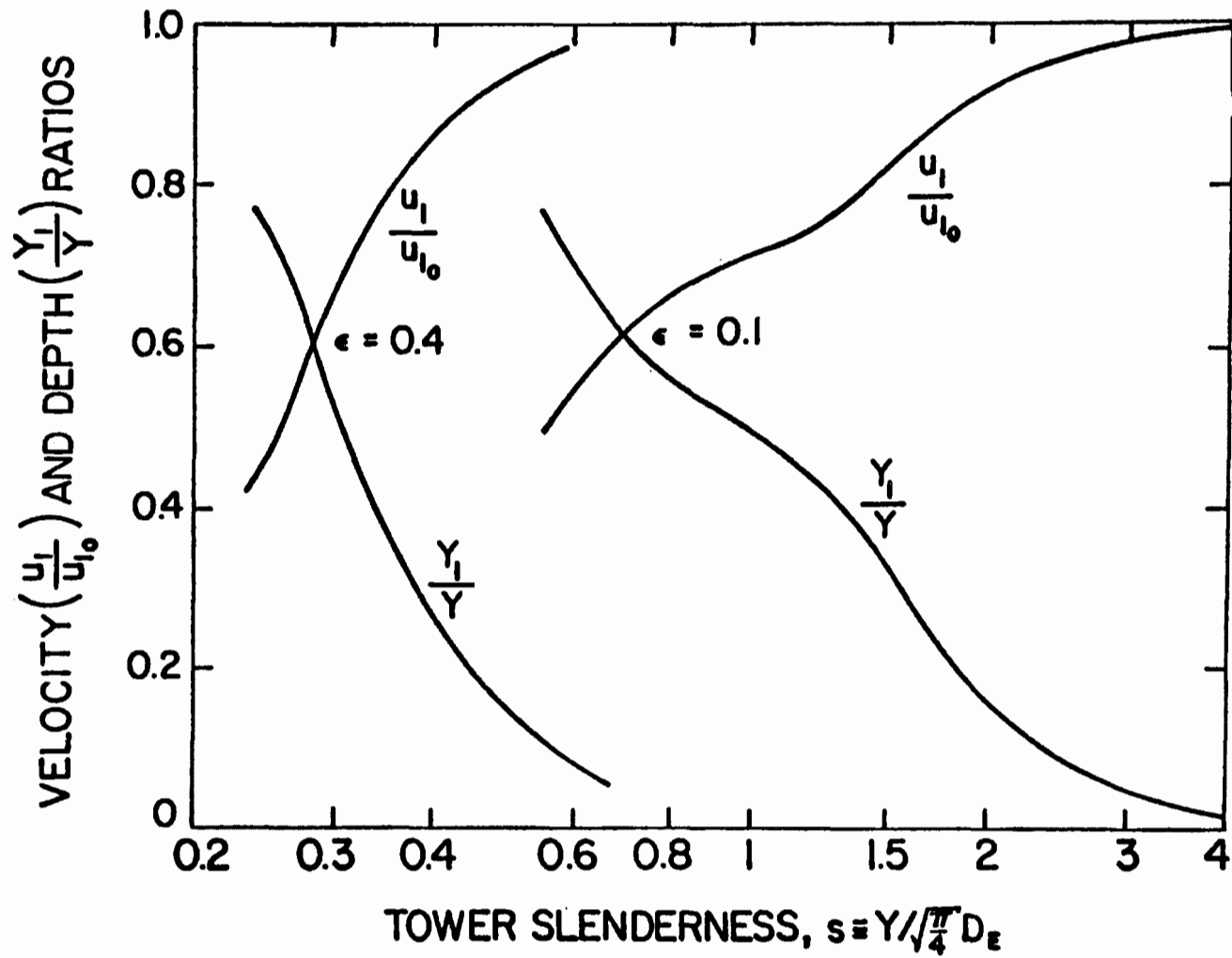
Figure 5. Calculated depths of deepest penetration (Y_1) of plume into the tower, and the corresponding decrease of through-velocity (u_1), for dry towers with $\Delta\rho/\rho = 0.1$, $C_L = 16$, and two values of ϵ, as functions of tower shape. Results are independent of scale.
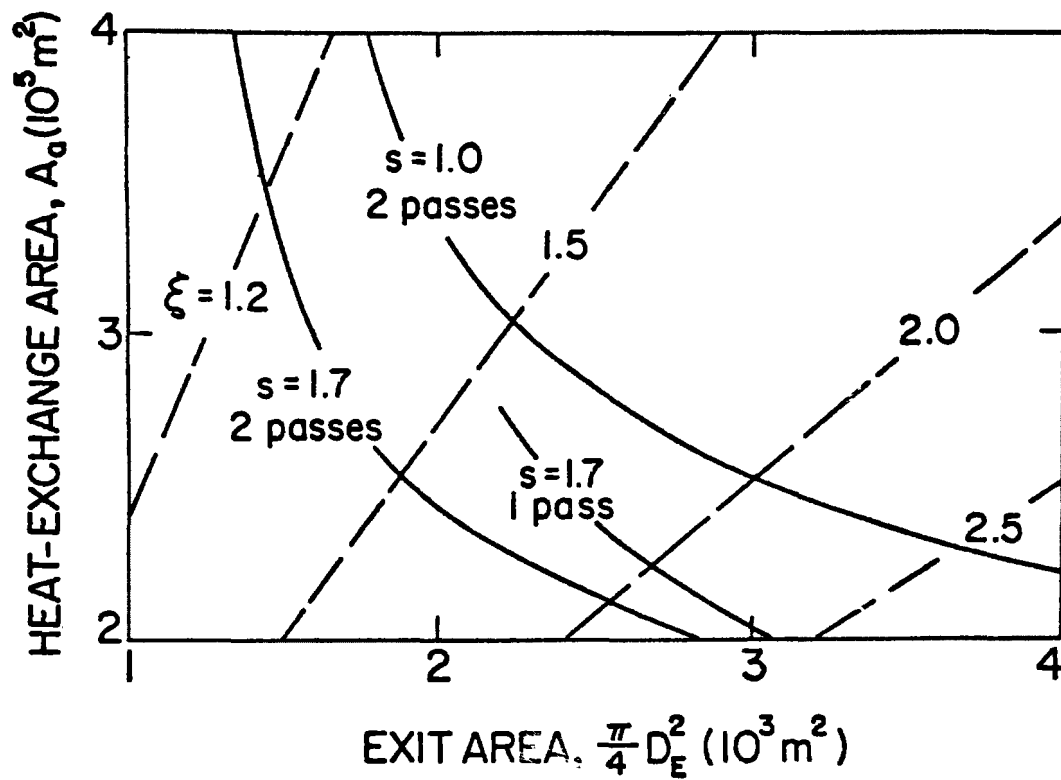
Figure 6. Possible combinations of air-side heat-exchange area (A_a) and tower exit area ($\frac{\pi}{4}D_E^2$), as specified by the parameter ξ. From [8], for spine-fin surface, heat rejection of 608 GJ/hr, and ITD of 22°c.
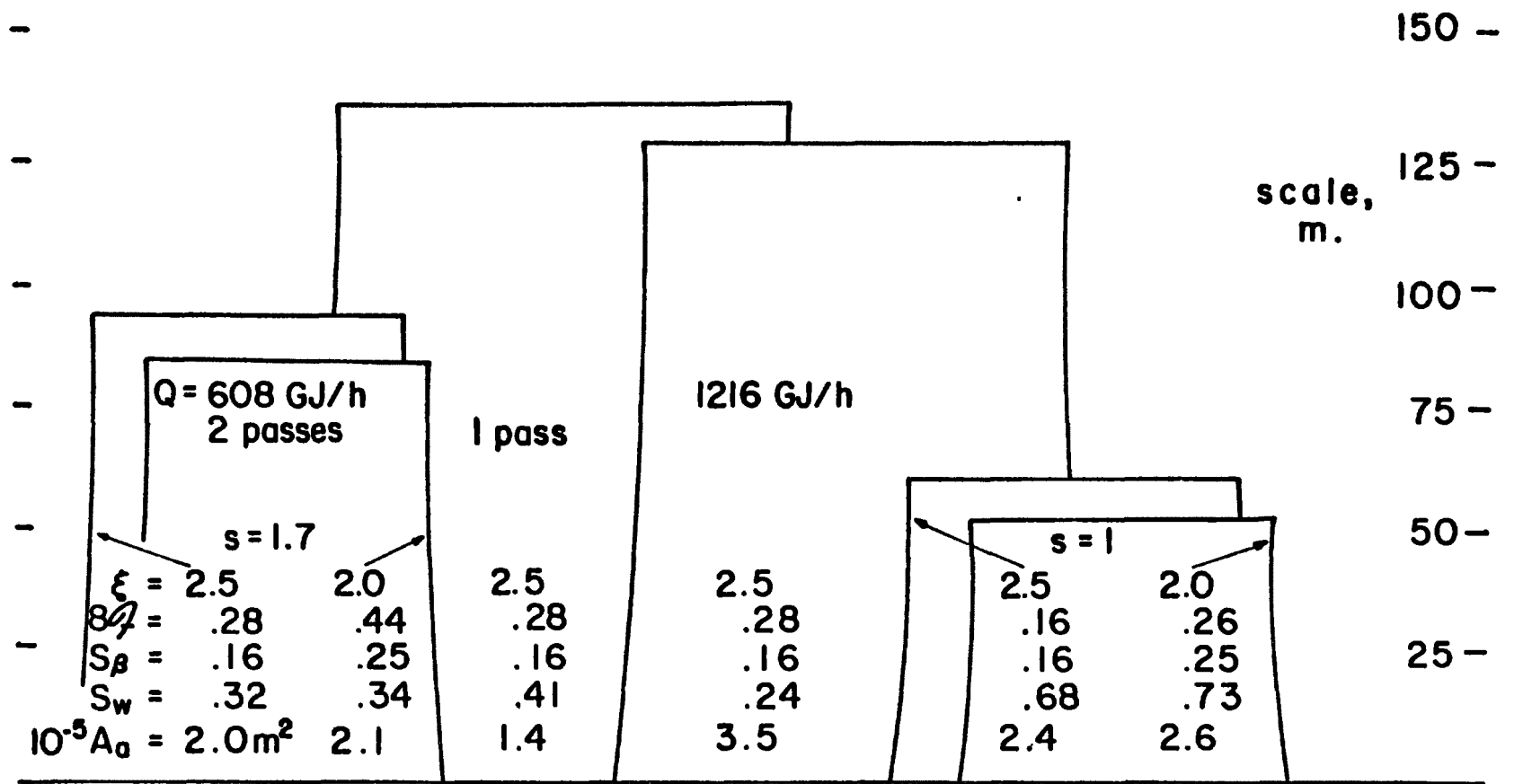
Figure 7. Display of calculations based on [5] and [8] of tower size, inflow parameter (δF), loss sensitivity (S_β), wind sensitivity (S_w), and heat-exchange area, showing effects of (from left) number of passes, tower scale, and low shape, each changed one at a time. Height and exit diameter are measured on the scale given.

AN IMPROVED METHOD FOR EVAPORATIVE, CROSS-FLOW COOLING TOWER PERFORMANCE ANALYSIS

by

Kenneth L. Baker
Thomas E. Eaton
Mechanical Engineering Department
University of Kentucky

The analysis of cross flow cooling towers may use one of several methods. For example, Zivi and Brand [1] or Baker and Mart [2] use enthalpy as the driving force for heat transfer while other analyses use different quantities for calculating heat transfer potentials [3]. This paper presents a more exact method for the analysis of evaporative, cross-flow cooling towers.

A new method of calculating cooling tower performance in a cross-flow tower was developed using the same basic equations as Nahavandi [4] extended to a two-dimensional analysis. The analysis incorporates variations of water and air properties inside the cooling tower fill.

Several tower design and operating parameters are required for the analysis: tower-on water temperature, water loading, air loading, dry bulb temperature, relative humidity, and tower packing hydraulic diameter. The Number of Transfer Units (NTU) is calculated but is not required for this analysis.

A Fortran program, XFCTWET, for analyzing linear (in-line) cross-flow towers has been written. The tower fill is divided into a mesh or grid; the tower analysis proceeds using finite difference techniques. A set of twenty-six (26) equations is iteratively solved for each grid in the tower fill. A typical mesh of 25 X 25 provides accurate results and reasonable computer costs. The variations of all parameters inside the cooling fill

may be output from the program, e.g., local water and air temperatures, relative humidity, and evaporation rates.

References

[1] Zivi, S. M., and Bruce B. Brand, "An Analysis of the Cross-Flow Cooling Tower", Refrigeration Engineering, Vol. 64, No. 8, August, 1956, pp. 31-34, and 90-91.

[2] Baker, Donald R., and Leon T. Mart, "Cooling Tower Characteristics as Determined by the Unit-Volume Coefficient", Refrigeration Engineering, Vol. 60, No. 9, September, 1952, pp. 965-971.

[3] Eaton, T. E., "Evaporative Cooling Tower Performance: A Comprehensive Bibliography", Industrial Heat Rejection Project Report, Mechanical Engineering Department, University of Kentucky, May 1978.

[4] Nahavandi, Amir N., and Johann J. Oellinger, "An Improved Model for the Analysis of Evaporative Counterflow Cooling Towers", Nuclear Engineering and Design, Vol. 40, 1977, pp. 327-336.

INTRODUCTION

Closed cycle evaporative cooling systems are being used extensively at present and are being considered, more than not, for condenser cooling at future sites of steam electric power plants. With the ever increasing emphasis on the efficient use of fuels, it is important that these cooling systems be properly specified, designed, constructed and tested. For the mechanical draft cooling tower, this process carries the burden of another variable to be determined, that of the impact of recirculation on the thermal performance of the cooling equipment and the operating efficiency of the power plant.

Recirculation is defined as the entrainment of the warm exhausted cooling tower plume into the inlet air flow of the tower. The result is an increased inlet air wet-bulb temperature (over the prevailing ambient wet-bulb temperature) and an associated increase in the thermal equilibrium of the cooling tower over that level it would have obtained in the absence of recirculation. If a power plant is already operating near its design thermal equilibrium, the addition of cooling tower plume recirculation may result in inefficient plant operation or in more drastic cases may force a reduction in plant load.

Despite data from field measurements made over twenty years by the Cooling Tower Institute[1] and modeling studies presented to the American Society of Mechanical Engineers in 1972[2,3], neither group has made, until recently, a concerted move to account for recirculation in their codes and associated test practices. In fairness to both groups, it was not clear for some time that instrumentation, sophisticated enough for cost-effective acquisition of multiple-point (including multiple heights) inlet wet-bulb

THE IMPACT OF RECIRCULATION ON THE SITING, DESIGN, SPECIFICATION, AND TESTING OF MECHANICAL DRAFT COOLING TOWERS

K. R. Wilber[1]

R. D. Moore[2]

D. E. Wheeler[3]

A. E. Johnson[4]

ABSTRACT

Significant recirculation of the warm exhausted plume of a mechanical draft cooling tower can occur as a result of wind induced pressure gradients around the cooling tower structure. Despite data and studies (although both somewhat limited) indicating an improved methodology was required for assessment of the contribution of recirculation to thermal performance degradation of these towers, it was only recently that this methodology was developed and demonstrated. This paper presents some of the first field data acquired using this improved assessment methodology. Plume recirculation data from three separate rectangular mechanical draft cooling towers are presented with specific emphasis on entering air wet-bulb temperature profiles and associated performance reductions. For each data set correlations are made with wind speed and the component of wind direction perpendicular to the tower's major axis. Finally, the importance of recirculation on tower specification, operation and design is discussed along with general recommendations for a consistent and repeatable acceptance testing methodology.

1. K. R. Wilber is Assistant Director, Cooling Systems Projects, Environmental Systems Corporation.

2. R. D. Moore is a Project Manager, Cooling Systems Projects, Environmental Systems Corporation.

3. D. E. Wheeler is an Engineer, Cooling Systems Projects, Environmental Systems Corporation.

4. A. E. Johnson is a Mechanical Engineer, Department of Engineering Research, Pacific Gas and Electric Company.

temperatures, was available. Other modeling and dimensional analyses[4] have been conducted since that period, but the need for field data still existed. In 1976, the Electric Power Research Institute funded a study[5] examining specific aspects of cooling tower testing methodology, which addressed, among other areas, instrumentation and instrumentation deployment for reasonable acquisition of inlet air wet-bulb temperature. The approach that evolved proved to be a dramatic improvement over the CTI work which has been criticized for inaccuracy and inconsistency since some heat balance calculations showed errors of 50 percent or more[2]. This work also lacked data on the larger towers characteristic of today's power plants. Finally, resultant correlations of the data could only be made with tower length, while factors such as exhaust velocity, fan stack length, wind speed and direction, intuitively more responsible for exhaust plume dynamics and degree of recirculation were non-correlatable.

With this background, field data acquired on 3 different size rectangular mechanical draft cooling towers under widely varying meteorological conditions are presented. A preliminary correlation (in lieu of more data and more exhaustive data examination) is presented tying increased entering wet-bulb to prevailing wind speed and direction. Further, the impact of recirculation on tower sizing is discussed. Finally, the accuracies and repeatability of the testing methodology are addressed with recommendations for specification and acceptance test approach.

DATA ACQUISITION, PRESENTATION AND ANALYSIS

General Approach to the Data Acquisition

To assess the degree of recirculation on the crossflow mechanical draft cooling towers tested, inlet air wet-bulb temperature measurements were made using a network of nine sensors (three vertically at three positions horizontally along the tower) on each side of the tower within approximately 2 meters of the air inlet. Each sensor was placed at the center point of imaginary equal area segments of inlet air. (More detail regarding the background of this approach is given in References 3 and 5.) Supplementing the inlet wet-bulb sensors were typically 3 wet-bulb sensors located upwind of the tower consistent with the approach specified in ASME PTC-23, 1958, test code for Atmospheric Water Cooling Equipment.

With this requirement for near-simultaneous acquisition of 21 wet-bulb sensors, not to mention system hot and cold water temperature measurements, it was determined that the use of a data acquisition system would provide the most effective measurements approach. Details of the particular system are given in References 5 and 6. Supplementing these temperature measurements, additional performance parameters including waterflow rate, fan horsepower, wind speed and wind direction were acquired and data were analyzed in a fashion generally consistent with existing test code stipulations[7,8]. In two of the campaigns, on-line magnetic tape systems interfaced with the temperature data acquisition system facilitated storage and subsequent analyses of the data.

Data Presentation

Performance data were acquired on three separate cooling towers with design

specifications shown in Table I below.

TABLE I

GENERAL COOLING TOWER DESIGN INFORMATION
FOR THE TOWERS TESTED

	Tower A	Tower B	Tower C
Water Flow Rate (gpm)	192,700	372,000	275,000
Hot Water Temperature (°F)	116.0	100.0	115.7
Cold Water Temperature (°F)	94.0	82.0	84.0
Wet-Bulb Temperature (°F)	79.0	70.0	55.0
Number of Cells	9	13	16
Fan Horsepower	187	189	160
Fill Height (ft)	42	36	40
Fill Length (ft)	324	469	596

A minimum of seven separate tests, conducted under different meteorological conditions on each of the towers listed in Table I, were performed. An example of the type of inlet wet-bulb distribution resulting from the prevailing winds at Tower A, is shown in Figure 1. It is noted that the winds are well within the constraints of the test codes for thermal acceptance testing, yet a difference of nearly five percent results depending on whether one calculates capability based on inlet air wet-bulb temperature or ambient (upwind) wet-bulb temperature.

As a result of the acquisition of inlet wet-bulb temperature profiles on the 3 towers, it was noted that recirculation can be significant and the

FIGURE 1.   EXAMPLE OF INLET MEASURED WET-BULB TEMPERATURE
DISTRIBUTION UNDER A SPECIFIC WIND CONDITION
(TOWER A)
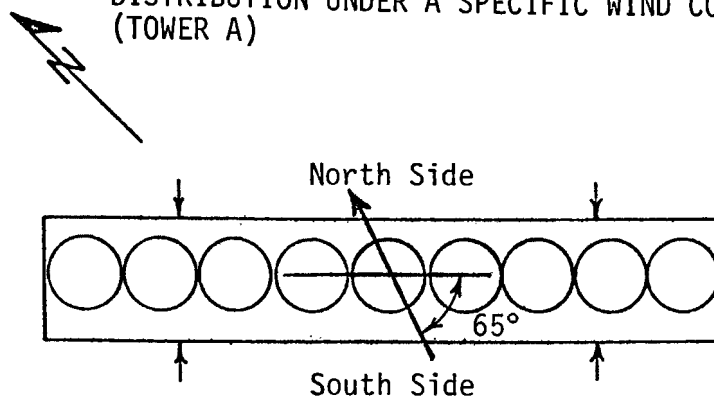
Avg. Wind Speed 1.9 M/Sec   (4.2 mph)

PLAN VIEW

Average Measured Temperatures (°C)

79.3	80.9	79.7
75.9	77.1	76.2
76.5	76.3	75.8

North Side (Facing South)

75.6	74.4	76.5
74.9	74.6	76.6
74.2	76.2	77.1

South Side (Facing North)

Average Hot Water Temperature (°C)   115.9

Average Cold Water Temperature (°C)   94.6

Circulating Water Flow Rate (gpm)   204,670

Average Fan Horsepower   184

Average Ambient Wet-Bulb Temperature (°C)   75.0

Average Inlet Wet-Bulb Temperature (°C)   76.5

Ratio of Tower Capability Based on Ambient Wet-Bulb Temperature
   to Tower Capability Based on Inlet Wet-Bulb Temperature   0.954

539

resultant impact on capability substantial. This fact is shown in Table II, which includes both the increase in the average inlet wet-bulb as well as the associated reduction in tower capability. Recalling that Tower C was the longest of the 3 towers (see Table I), it is not clear, as was suggested by Reference 1, that recirculation is a function of tower length for towers of these proportions; on the contrary, the data seem to indicate that recirculation is inversely proportional to length for winds across the tower, but this conclusion would be premature without additional analyses. The data do suggest that a combination of wind speed and wind direction with respect to the tower's major axis may be more directly responsible for recirculation and degradation of performance. The next section addresses itself to examining the potential for this correlation.

Data Analysis and Discussion

The influence of wind speed and wind direction on increased inlet air wet-bulb temperature was determined using standard correlation techniques. It was found based on 42 cases that individually neither parameter correlated well with increasing wet-bulb ($r = 0.18$ and $r = 0.02$ respectively). It was determined that the component of the wind perpendicular to the tower's major axis was significantly correlated with the increase in wet-bulb over ambient ($r = 0.81$). Using the equation:

$$\Delta = a + b \ (u \ \sin\theta)$$

where Δ = the difference between ambient and inlet air wet-bulb
           temperature (°F)

  a,b = constants

    u = ambient wind speed

    θ = the angle of the prevailing wind with respect to the
          major axis of the cooling tower

TABLE II. REPRESENTATIVE RECIRCULATION DATA AND
THE RELATED IMPACT ON TOWER CAPABILITY

Tower	Test No.	Wind Speed (mph)	Wind Direction (With Respect to the Tower's Major Axis)	Increase in Average Inlet Wet-Bulb Temp (°F)	Decrease in Capability (%)
	1	8	65	4.5	8
	2	6	85	3.9	6
A	3	5	75	2.8	5
	4	2	85	1.6	4
	5	7	35	2.3	6
	1	20	0	-0.1	0
	2	20	30	1.7	5
B	3	20	30	1.4	6
	4	30	75	7.9	15
	5	35	75	8.0	11
	1	9	20	0.3	1
	2	8	40	1.1	2
C	3	9	30	1.6	3
	4	6	60	1.0	1
	5	9	30	0.5	1

Figure 2 shows a "best fit" line plotted using a = 0.13 and b = 0.24 and associated representative data points. Although there is some scatter in the data, it is clear that even relatively light (i.e., less than 10 mph) wind conditions (with θ greater than about 30°) can cause increases in entering wet-bulb in excess of 2°F. Further, it is clear that ground-level measurements made upwind of the tower cannot assess the degree of recirculation existing during a test.

From a design and specification standpoint, if elevated inlet wet-bulb temperatures of over 2°F greater than ambient represents a characteristic situation for a specific tower and site meteorological situation, a reduction in capability on the order of 5-10 percent may be expected. In this situation, the addition of another cell of cooling tower may be required to meet the required cold water return temperatures under demanding meteorological conditions.

Finally, tower capabilities calculated based on multiple tests, using inlet wet-bulb temperature were typically more repeatable under varying meteorological conditions than those using ambient wet-bulb temperatures. As an example for seven tests on Tower B, where substantial recirculation was measured, the standard deviations for capabilities determined using inlet wet-bulb and ambient wet-bulb were 2.76 and 5.77% respectively. Additionally, the average reduction in capability was six percent. The fact that the capabilities are more repeatable using the inlet wet-bulb approach is expected since, the manufacturers performance curves, on which the capabilities are based,
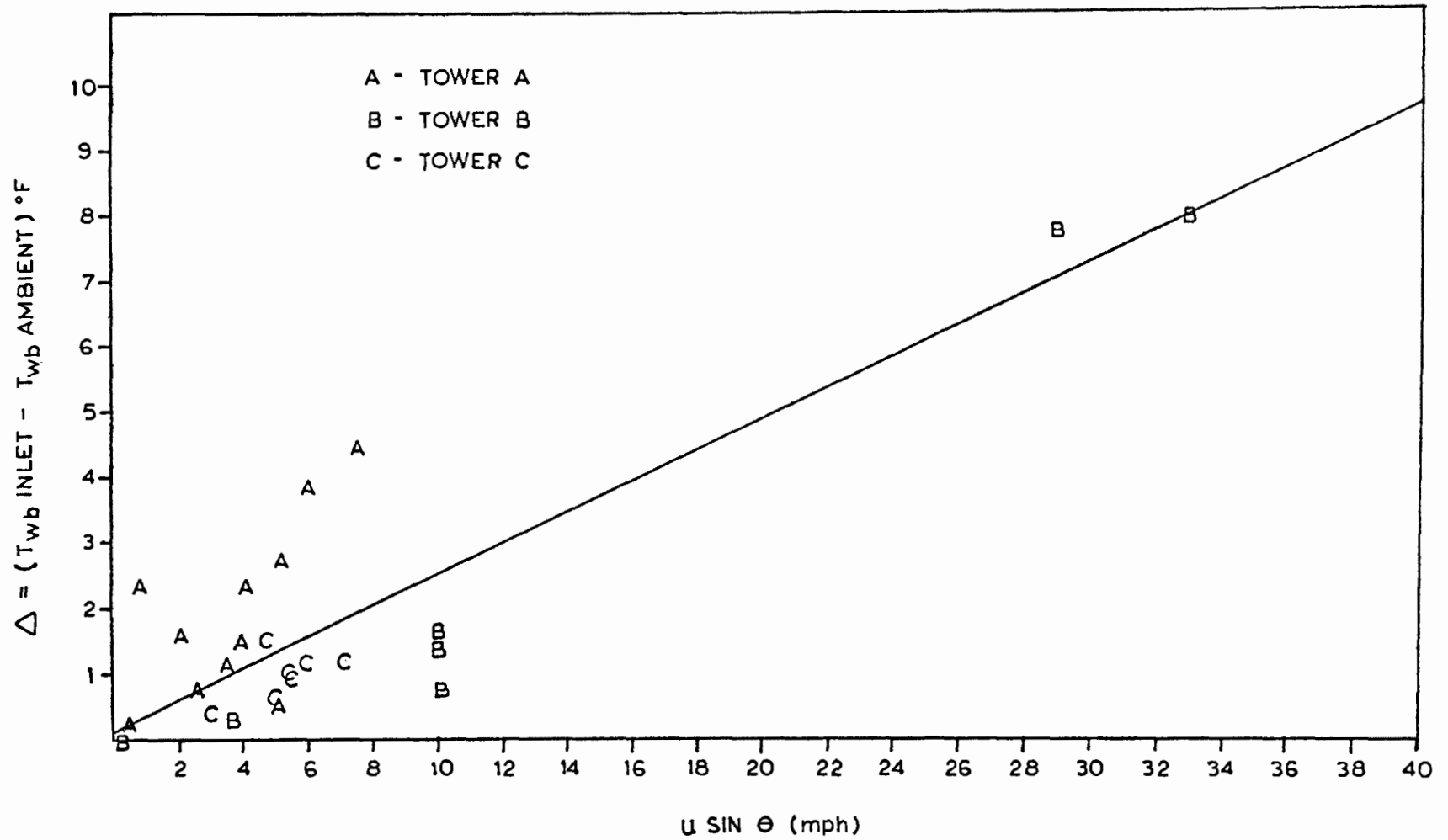
Figure 2: Correlation of Increase in Wet-bulb Temperature with the Component of Wind Perpendicular to the Cooling Tower's Major Axis

543

are constructed using inlet wet-bulb. Despite this, the use of inlet
wet-bulb as the basis for performance and specification has met with
periodic resistance. This resistance is fueled by the false hope that
the manufacturer will assume the responsibility for recirculation or
has some control over the wind-induced eddies on the lee side of the
tower and the resultant rise in inlet wet-bulb temperature. The data
acquired in this study strongly suggest that neither is the case.

CONCLUSIONS

Measurements of plume recirculation were made on three large rectangular crossflow mechanical draft cooling towers. Based on these measurements, the following conclusions are made:

1. Significant wind-induced recirculation can occur if towers are not properly oriented. When proper orientation cannot be effected, consideration in the tower design must be made to increase its capacity to offset expected performance reductions which result from recirculation.

2. A reasonable correlation exists with the component of wind perpendicular to the major axis of the tower and the increase in entering air wet-bulb temperature over the prevailing ambient wet-bulb temperature. It is recognized, however, that more data need to be acquired to refine this correlation.

3. The inlet wet-bulb measurement approach provides a more repeatable result in the determination of cooling tower capability when tests are taken under different wind conditions.

BIBLIOGRAPHY

1. "Technical Sub-Committee #2, Report on Recirculation," Cooling Tower Institute Bulletin PFM-110, July 24, 1958.

2. Reisman, J. I., "A Study of Cooling Tower Recirculation," presented at the American Society of Mechanical Engineers' 93rd Winter Annual Meeting, November 26-30, 1972.

3. Reisman, J. I., and Ovard, J. C., "Accurate Performance Testing of Crossflow Cooling Towers," presented at the American Society of Mechanical Engineers' 93rd Winter Annual Meeting, November 26-30, 1972.

4. Kennedy, J. F. and Fordyce, H., "Plume Recirculation and Interference in Mechanical Draft Cooling Towers," presented at the Cooling Tower Enviroment - 1974, University of Maryland, March 4-6, 1974.

5. Environmental Systems Corporation, "Examination of Specific Aspects of Cooling Tower Testing Methodology, Research Project RP 905-1-2, prepared for the Electric Power Research Institute, August 1978.

6. Wilber, K. R. and Maulbetsch, J. S., "Field Examination of Cooling Tower Testing Methodology," presented at the Cooling Tower Institute Annual Meeting, January 31 - February 2, 1977.

7. The American Society of Mechanical Engineers', "Atmospheric Water Cooling Equipment," Power Test Code No. 23, 1958.

8. The Cooling Tower Institute, "Acceptance Test Code for Water Cooling Towers, ATC-105, February 1975.

An Investigation into the Mineral Concentration of Individual Drift Droplets from a Saltwater Cooling Tower

by

Ronald O. Webb[1]
Richard S. Nietubicz[2]
John W. Nelson[3]

A common assumption in wet cooling device drift studies and drift transport modeling is that the drift droplets carry the same mineral concentration as the circulating water. Using this assumption, cooling device mineral emissions calculated from liquid emission data rarely agree with direct measurements of mineral emission. Ratios of measured to calculated mineral emission values are generally greater than one and sometimes range up to a factor of ten depending on the cooling device and operating conditions. This difference has been attributed to an increase in the bulk concentration of the droplets due to the evaporative cooling process.

This paper presents results of a study to examine residues from individual drift droplets collected near the exit plane of a large natural draft salt water cooling tower located at the Chalk Point steam electric generating plant in southern Maryland. The droplets ranged in size from 10 μm to over 1000 μm in diameter and were collected on a filter paper which yields a stain when a droplet impacts upon it. The stains were individually examined using nuclear analysis techniques to determine the mineral mass residue in each stain. Mineral concentration in the original droplets were then calculated from this data. Results of the measurements are presented together with a description of the examination techniques and sensitivities.

[1]Environmental Systems Corporation
[2]State of Maryland, Department of Natural Resources
[3]Florida State University

COGENERATION TECHNOLOGY AND OUR
TRANSITION FROM CONVENTIONAL FUELS

J. W. Neal
Acting Assistant Director
Heat Engines and Heat Recovery
Division of Fossil Fuel Utilization
Department of Energy
Washington, D.C.

ABSTRACT

Cogeneration -- the simultaneous production of either electricity or mechanical work along with useful thermal energy has long been used to provide industrial and residential/commercial users with on-site energy needs. Also known as total energy systems, integrated energy systems, dual-purpose powerplants, and waste-heat utilization systems, cogeneration provided over 15 percent of the nation's electric energy in 1950. But after 1950, as a result of what appeared to be a limitless supply of cheap energy resources, cogeneration declined. Today, it accounts for only 4 percent of our electric energy.

The oil embargo of 1973-74 and the subsequent quadrupling of oil prices stimulated a new national interest in conservation as an important means of more efficiently using our energy resources. The National Energy Plan submitted by President Carter to the Congress in April of 1977 embodies conservation as its cornerstone. One of the principal strategic components is that industries and the utilities using oil and natural gas should convert to coal and other abundant fuels. Another important element of the plan is that we will endeavor to recover and utilize waste heat to help offset our growing dependence on critical petroleum and natural gas fuels.

This paper deals with the technology for cogeneration, particularly emphasizing the importance of cogeneration power systems being adaptable to a transition from petroleum and natural gas to alternate fuels by the turn of the century. Waste heat is introduced as one of our nearest term alternate fuels where cogeneration has proven to be one of the major applications for its effective use. The technical limitations of representative current technologies for cogeneration are discussed; the need for advanced technology in cogeneration is established. Concluding is the overall strategy for advanced cogeneration technology development as seen by the Department of Energy.

INTRODUCTION

Today, only about one-half of the fossil fuel energy consumed by industry is effectively used and only about one-third of the fuel consumed by utilities is actually converted into electricity. Most of the unused energy is wasted as it escapes through smokestacks or is dumped into rivers. If it was recovered industrial and utility waste heat could be used for further electrical generation, industrial processes, or space heating.

Some of this waste heat can be recovered and re-used by combining presently-independent processes and using the reject heat from one process to provide part of the heat needed for another process, a concept known as thermal cascading. One of the most common methods of recovering and effectively using waste heat in this manner is cogeneration. In cogeneration applications, mechanical work or electricity is simultaneously generated along with useful thermal energy. Since waste heat is recovered and utilized as an alternate fuel, the actual fossil fuels required to produce both the electrical and thermal needs are often no more than required to produce the electrical energy alone.

This cogeneration capability has existed for over 50 years. In 1975 it provided over 15 percent of the nation's electric energy; today however it accounts for only 4 percent. But as the demand grows for heavily used, fast diminishing, and increasing more expensive oil and natural gas, cogeneration can become a valuable energy conserving option. For cogeneration to become a significant form of power generation depends on overcoming barriers due to fuel supply and price uncertainties, technological risks, marginal economics, environmental controls, and fear of regulation on the part of non-utility power generators. Government involvement through DOE's cogeneration program addresses removal of many of these impediments to reverse the decline in cogeneration, along with a strong technology development effort to ultimately permit the substitution of non-critical fuels for oil and gas in cogeneration systems.

One of the more important near term non-critical fuels in this regard is waste heat. In the category of fossil fuels between now and 1985, residual petroleum products can be considered less[1] critical than light distillate and natural gas. For the late 1980's we hope to see coal-derived liquids become commercially available displacing significant quantities of petroleum. And if we accomplish a major shift of the industrial and utility stationary power sector to the direct use of coal, integrated fluidized bed combustion systems and gasification combined cycle systems can both become important options for its environmentally acceptable use in areas previously restricted, for environmental reasons, to oil and gas fired systems.

---

[1]Although not necessarily much cheaper, residuals are projected to be more readily available for power generation than distillate fuels through 1985.

All of these fuels are of importance to cogeneration systems. This paper
attempts to place in perspective the technology requirements for cogeneration
as we see this change in the predominate fuel types between now and the
turn of the century. A major emphasis is placed on the importance of
using waste heat in the near term as an alternate fuel. This can buy
us time for solving the technological and environmental problems associated
with using coal and alternate fossil fuels derived from coal to displace
oil and gas.

COGENERATION PERMITS THE USE OF WASTE HEAT AS FUEL

As previously introduced, cogeneration is one means of using waste heat
as an alternative to additional fossil fuels. This is brought about
by recovering reject heat from a process or from the generation of
electricity and using that in lieu of supplemental fossil fuel to
supply additional energy requirements.

There are two basic applications for cogeneration; industrial cogeneration
which supplies process heat or steam along with the industry electrical
needs, and residential/commerical cogeneration supplying both the
electricity and thermal energy needs of a community.

To further distinguish the two, (Figure 1) cogeneration powerplants
supplying industrial process heat are generally located on the plant
site, or, in the case of clustered industries near the load center to
avoid thermal losses in distributing the high temperature energy to the
process. There are two common arrangements for supplying process heat,
topping systems where electricity is first generated from the combustion
source and the reject heat then supplied to the process; and bottoming
systems where process heat is first supplied by the combustion source
and electricity then generated from the reject heat.

Residential/commercial cogeneration powerplants, on the otherhand, are
predominately central station utilities. Heat rejected as a byproduct
of electrical generation is recovered and distributed to customers
supplying their space heating, hot water, and cooling needs. Heat is
distributed through insulated pipes, usually not over about 25 miles
from the utility.

If we were to embrace cogeneration as a major energy option for both
the industrial and residential/commercial sectors, substantial
energy savings could be achieved between now and the turn of the century
as shown in Table I. By effectively using waste heat as an alternate
fuel in lieu of addition fossil fuel, we could accumulate up to 56
quadrillion BTU's of energy savings by the year 2000. As shown, the
annual savings could amount to over 1.5 quads by 1985 and almost 6.5
quads in 2000. This equates to about three quarters of a million
barrels of oil per day in 1985 and over 3 million barrels per day in
2000. Savings of this magnitude are significant when one considers that
our daily oil import level now in 1978 is around 8 million barrels per
day.

LIMITS OF CURRENT TECHNOLOGY

There are three principal technologies currently available for cogeneration. These are illustrated in Figure 2 and include steam systems for both topping and bottoming, gas turbine topping systems with waste heat boilers, and diesel topping with waste heat recovery.

Because it is externally fired, extraction or non-condensing steam turbines are the only technology available today for cogeneration which has multifuel capability to include coal and a variety of alternate fuels such as industrial wastes. The extraction steam turbine is most commonly configured for the topping of process steam. In this arrangement, a fossil fuel-fired boiler is used to generate high pressure steam which is then expanded through a steam turbine-generator set to produce electricity. Low pressure steam is then extracted at a suitable state point in the expansion step for use in the industrial process.

Considering limitations for steam topping applications, most industrial plants use cheaper, easier installed packaged boilers rather than field installed boilers. Packaged boilers are not ideally suited for steam turbine topping because the generated pressure and temperature are generally too low; they also cannot be economically converted to burn coal.

From the standpoint of heat recovery applications, steam bottoming systems in the power ranges required for cogeneration are also not an optimum means of recovering low temperature heat (400°-1000°F). Steam turbines, below 6000 hp, are generally less advanced than larger multi-megawatt turbines. Their efficiencies are lower and they cost more per kilowatt than the larger steam turbines. Also at these low temperatures steam pressures are low, requiring costly multi-stage turbines to extract work at high efficiency levels. Additionally, because of the large heat of vaporization the phase change of water into steam does not permit a good match with low temperature sensible heat sources, which tends to lower the efficiency of the heat recovery system.

Gas turbine and diesel topping systems offer two distinct advantages over steam turbines-- higher efficiency and greater electrical-to-thermal output. Electrical generation efficiency of the prime mover is very important in achieving maximum energy savings through cogeneration as illustrated in Figure 3. Since basic efficiencies reach approximately 35 percent for diesels and almost 30 percent for gas turbines, overall energy savings can be up to nearly three times greater than those savings for typically 20 percent efficient extraction steam turbines used in cogeneration. In addition, topping of process steam or process heat with more efficient gas turbine or diesel prime movers provides higher electrical-to-steam ratios as shown in Table II. Electrical generation per unit of process heat is four to eight times greater for gas turbines and diesels, respectively, than steam turbines. Moreover, equipment is available in a range of sizes from 100 KW to over 40 MW for diesels and up to 75-100 MW for gas turbines.

The fundamental problem in basing advanced cogeneration systems on a mix of today's higher efficiency diesels and gas turbines is their requirement for high quality distillate petroleum and natural gas fuels. These are in critically short supply, and while encouraging limited diesel and gas turbine based cogeneration will promote more efficient use of these fuels, a more significant shift to such systems could actually aggravate the shortage of these fuels and defeat the national thrust toward utilizing coal and coal-derived fuels.

ROLE OF ADVANCED TECHNOLOGY

It is our future fuels for cogeneration along with environmental considerations which establish a need for advanced technology. Our national program in advanced cogeneration technology must provide us with three important capabilities.

The first is achievable in the early 1980's. That is to shift this critical petroleum based fuel burning capacity in the industrial and utility sector over to the environmentally acceptable use of lower grade, more available, residual petroluem fuels. This will have an immediate effective conservation impact by lessening the competition for higher quality fuels thus making them more available for the transportation and home heating sector where the concept of low grade fuel switching is less feasible. Moreover, since economically competitive future coal-derived fuels will be of a much lower quality than todays distillate, it will be a much easier step for stationary power equipment to adapt from residuals to coal-derived liquids than from clean distillate to coal-derived liquids.

The second important capability is that of being able to convert this low grade oil burning capacity to coal-derived liquid fuels when they become commercialized in the late 1980's.

Thirdly, and a longer term effort, is to develop new environmentally acceptable means of utilizing a maximum range U. S. coal directly in cogeneration applications which would otherwise be restricted to oil and gas fuels due for emissions regulations.

COGENERATION TECHNOLOGY DEVELOPMENT STRATEGY

DOE's cogeneration technology development strategy has been developed around the evolution in fuels as seen between now and the turn of the century. The overall strategy is illustrated in Figure 4.

Two generations of technology are anticipated by then in order to promote a smooth transition from todays predominately oil and gas fueled equipment to future systems using domestic coal fuel resources.

The second generation technologies shown are intended to help us make the transition to alternate fuels with maximum expediency. The importance of the second generation technologies to a smooth evolutionary fuel

552

transition strategy is evident. As shown our nearest term alternate fuel
option is waste heat from various sources including power generation.
This is also the most readily adaptable since environmental impacts
are minimal. The major technical requirements are for cost effective
heat recovery and utilization technology that could be commercialized
by the early 1980's.

More difficulty, and requiring longer time is the adaptation of stationary
heat engines such as diesels and gas turbines to alternate, predominately
lower grade fuels from coal. This transition is seen on Figure 4 via
the development of engine technology for the environmentally acceptable
use of lower grade residual petroleum. Such a step permits definition
of minimum acceptable fuel specifications based on best available new
engine technology. These specifications would be used by the fuel
processing industry to tailor acceptable synthetic liquid coal fuel
products for displacing petroleum fuel in the second generation
stationary powerplants.

It should be emphasized that the second generation engine technologies
are not necessarily optimized for coal-derived fuels. Rather they are
proven on low grade petroleum fuel to the extent that they can be
adapted to coal fuel products that are essentially no worse than
residual petroleum. This is an important first step since it can permit
the use of coal liquids which are minimally processed and thus substantially
more economical than a fully refined coal fuel.

The optimum economical use of coal is dependent on the successful
development of third generation technologies along with the synergistic
benefits of the second generation technologies, and the experience
gained during the initial introduction of coal fuels in that equipment.
That experience can substantially accelerate the commercial availability
of technology for the general use of a wide range of coal in its
most economic forms for a particular applications - either directly,
gasified, or as raw non-processed liquids. The third generation tech-
nologies, designed and developed specifically to use coal and coal-
derived fuels in the most efficient, environmentally acceptable, and
cost effective manner could, with knowledge gained from second generation
technologies begin market entry before 1995.

To evaluate the potential of various technology options shown, the
Department of Energy is identifying opportunities for advanced cogen-
eration in six of the more energy-intensive industries in the United
States (paper and pulp, chemical, petroleum refining, steel, textiles,
and food and kindred products). They currently consume approximately
70 percent of the nation's industrial-thermal energy.

This effort, the Cogeneration Technology Alternatives Study (CTAS)
was initiated in late 1977 and is scheduled for completion in 1979.
During the first year, industrial-process energy requirements are
being defined. Concurrently, the characteristics of advanced
cogeneration powerplants such as those based on open and closed
gas turbines, diesel, Stirling engines, steam turbine, organic
Rankine cycles, and fuel cells will be evaluated along with ancillary

components such as heat pumps, and energy storage to determine optimal configurations. The powerplants operational characteristics will be matched with the industrial energy requirements in future months to assess the technical impact of these advanced systems on industrial cogeneration installations in the 1985 through 2000 time frame.

A similar but smaller effort is underway to define the most appropriate advanced technology options for total energy system applications in the residential/commercial sector. This is known as the Total Energy Technology Assessment Study (TETAS). It was begun in early 1978 and is also scheduled for completion in 1979. Future support by DOE for the development of new power systems designed specifically for cogeneration applications will be strongly influenced by the results of the CTAS and TETAS studies.

SUMMARY

The magnitude of a complete transition to coal-burning capacity in stationary power equipment servicing the residential/commercial and industrial sectors by the year 2000 is staggering, when one considers that it has taken the U. S. an average of 60 years for each of our previous two fuel transitions -- from wood to coal and then from coal to oil and gas. In this regard the early use of waste heat as an alternate fuel source can buy much needed lead time for developing the technologies needed for the transition to alternate fossil fuels derived from coal.

DOE's heat recovery component technology program (Figure 5) is structured to provide that capability. It addresses heat recovery in two categories, low grade heat which is below about 200°F, and high grade heat which is in excess of 200°F. The third area of research is heat exchanger technology. The heat recovery program is discussed in greater detail in a separate paper at this conference. A clarification of its relation to the overall cogeneration technology development effort has been presented here, along with the overall importance of heat recovery in a fuel transition strategy.

Table I
Estimate Cogeneration Energy Savings

| | | Estimated Savings (Quads) | | |
| | | Annual | Annual | Cummulative |
Systems	Market Application	1985	2000	2000
Integrated and total energy	Residential/commercial	0.38	1.52	12.0
Industrial park energy	Industrial/commercial	0.16	0.85	7.0
Industrial process heat	Industrial	0.57	2.64	24.0
General waste heat recovery	All sectors	0.47	1.44	13.0
Total		1.58	6.45	56.0

Table II
Electric-to-Thermal Characteristics of Cogeneration Powerplants

Prime Mover	Electric Power/Process Steam (KWH 10^{10} BTU)
o Steam Turbines	50
o Gas Turbines	200
o Diesels (with recovery of heat from jacket coolant)	300
o Diesels (without recovery of heat from jacket coolant)	400

Figure 1

Typical Cogeneration Powerplant Arrangements

Industrial Cogeneration — Process Heat and Steam

Residential/Commercial Cogeneration — Space Heating and Cooling
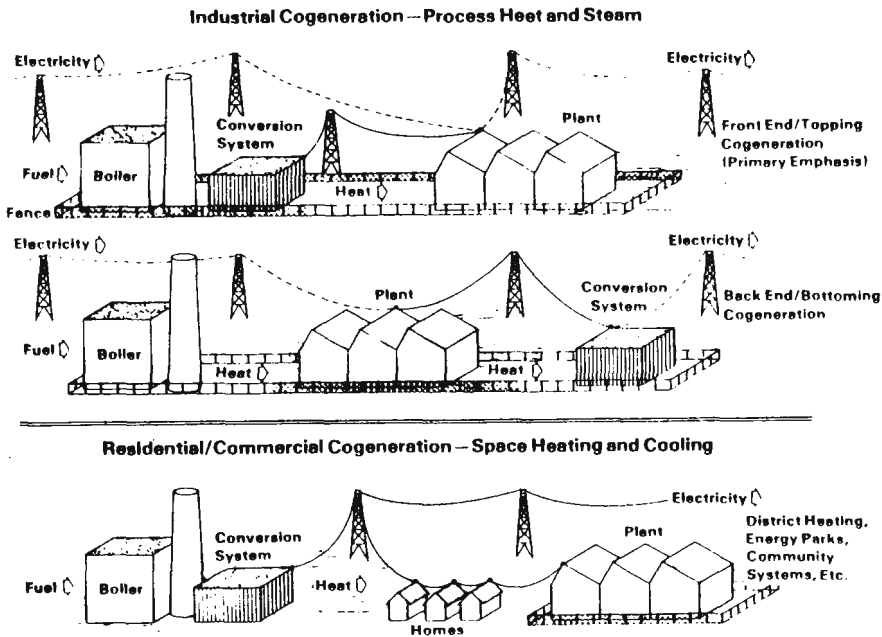
Figure 2

Technologies Currently Available for Cogeneration
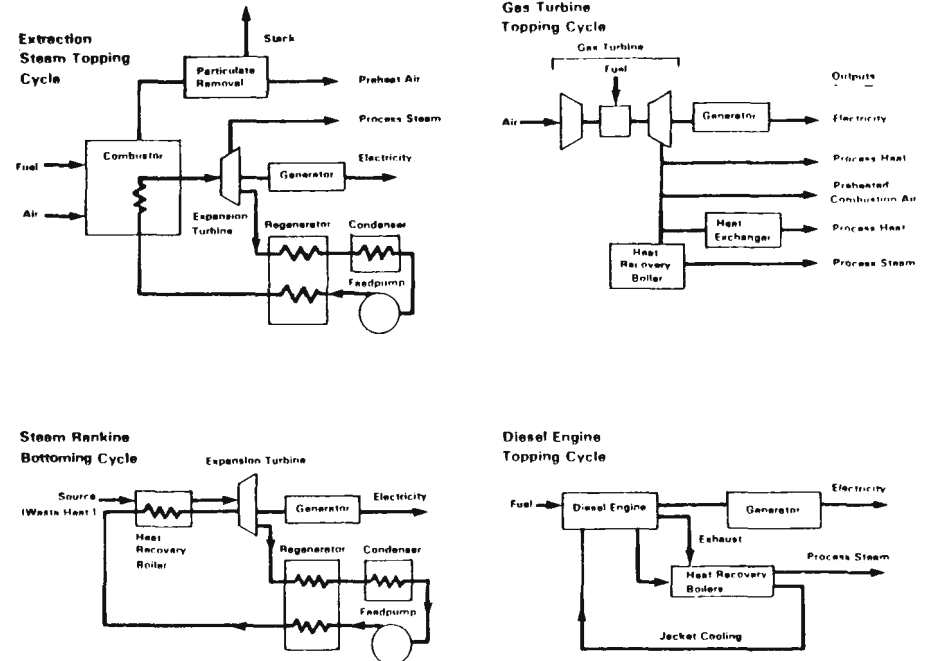
Figure 3

Maximum Fuel Savings in Cogeneration Occurs with High Efficiency Prime Movers

Figure 4

Advanced Cogeneration Technology Development Strategy
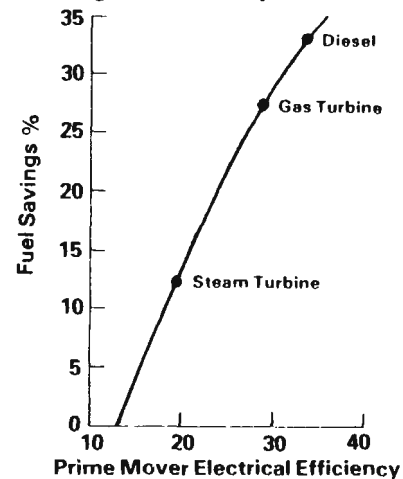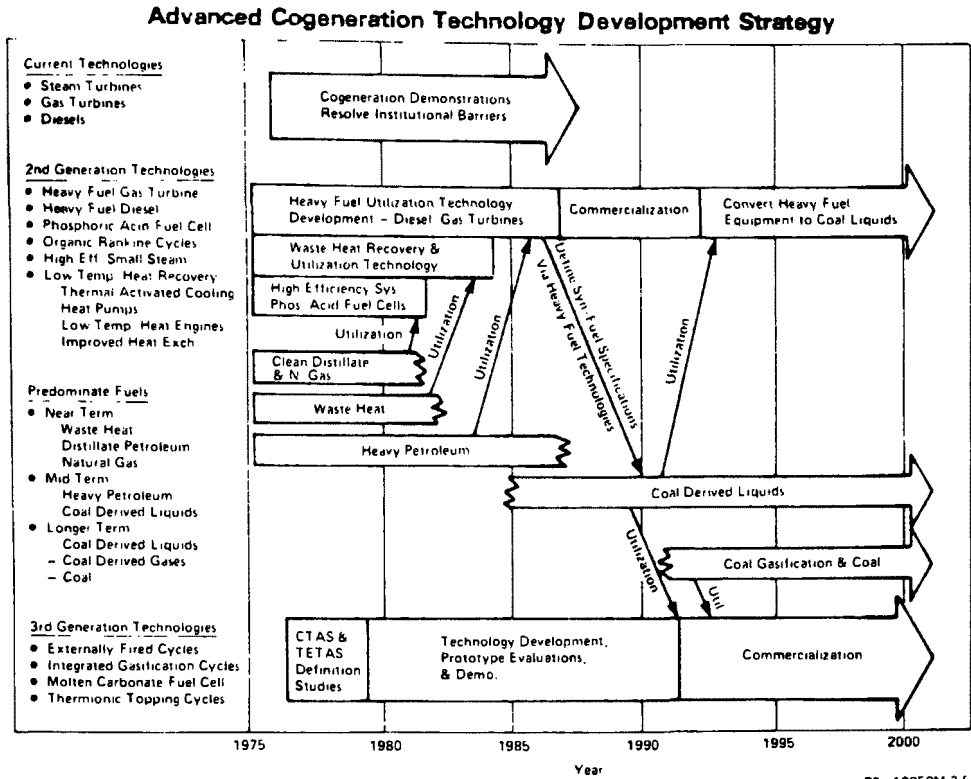
Figure 5

DOE's Heat Recovery Component Technology Program Can Help Buy Time for Transitioning to Coal Derived Fuels

Low Grade Heat (<200°F)

- Recovery from Federal Facilities
- Heat Pumps
- Space Cooling
- Novel Heat Engines

High Grade Heat (>200°F)

- Rankine Bottoming
- Thermionic Converter Topping

Heat Exchanger Technology

- Fouling/Corrosion/Vibration
- Improved Mat'ls/Temp Capability
- Reduced Cost

78 · 10950M 4 5

COGENERATION: THE POTENTIAL AND THE REALITY
IN A MIDWESTERN UTILITY SERVICE AREA

D. M. Stipanuk, Cornell University, Ithaca, NY
W. J. Hellen, Wisconsin Electric Power, Milwaukee, WI

ABSTRACT

A study was performed by Wisconsin Electric Power of the magnitude and location of major boiler fuel users within its service territory. Cost estimates were obtained for coal fired cogeneration units and for steam distribution systems. Steam and electric costs from cogeneration units serving three (3) areas of significant steam load were calculated. The distance between steam loads and the annual steam load factor were shown to significantly affect the cost of steam. Electricity costs were relatively unaffected by the levels of steam sales made in the areas studied.

INTRODUCTION

Wisconsin Electric Power Company (WE) is the largest electric utility in the state of Wisconsin. The WE service territory consists of a band of land approximately 40-50 miles wide along Lake Michigan from the Illinois State Line north about 100 miles which contains the city of Milwaukee. In addition there are small areas served in east central and northern Wisconsin and in the upper penisula of Michigan. The total population served by WE is in excess of 2 million.

The spring of 1977, WE began a study to assess the potential market for steam sales, the cost and operating characteristics of cogeneration units and the costs of steam distribution piping. This report provides a summary of part of this study.

THE EXISTING WISCONSIN ELECTRIC COGENERATION ACTIVITIES

The existing WE cogeneration system provides district heating service for about 600 customers in an area of approximately two square miles in downtown Milwaukee. Historically the system was divided by the Milwaukee River into a Eastside and a Westside system. This division still exists for the low pressure system. The customers served are primarily offices and public buildings. The customers are supplied through a network of high pressure (180 psig) and low pressure (15 psig) steam mains. The largest high pressure steam mains are 30" (O.D.) and the smallest are 4". The smallest low pressure mains consistent with current design philosophies are 6". No condensate is returned from customers.

The primary steam supply point for the district heating system is the Valley Power Plant. The Valley plant is composed of two (2) turbines with two (2) boilers for each turbine. This coal fired cogeneration

558

plant is capable of a continuous steam sendout in excess of 1,000,000 lbs/hr and up to 1,700,000 lbs/hr for limited periods. The continuous sendout at maximum capability is presently limited by the makeup water (demineralizer) capacity.

The two (2) turbines in the Valley plant are controlled extraction units rated at 140 Mw each with no steam extraction. With maximum extraction of 850,000 lbs/hr, each unit drops to 65 Mw resulting in the plant capacity dropping from 280 Mw to 130 Mw.

Additional steam for backup and peaking is available from the East Wells and Commerce Street Plants. The East Wells Plant is coal fired and can continuously supply 132,000 lbs/hr east of the Milwaukee River. Commerce Street is an oil fired unit with a continuous capacity of approximatley 200,000 lbs of steam per hour to the westside. On a first contingency basis the system can supply a peak demand at 1,600,000 lbs/hr.

The existing WE district heating system experiences large variations in steam sales from summer to winter. TABLE 1 shows the monthly variations in steam sendout averaged for the years of 1971 through 1976. Steam sales vary even more significantly than does steam sendout since the system losses represent a large percent of the summer sendout and a much smaller percent of the winter sendout.

In two (2) of the past seven (7) years, the winter electrical peak for Wisconsin Electric and the district heating system peak occurred on the same day. In a third year, a single day separated the two peaks.

COGENERATION UNITS - DESIGN AND COST

WE retained Gilbert Associates, Inc. (Gilbert), a division of Gilbert/ Commonwealth Engineers and Consultants, to supply capital cost estimates and unit heat rate data for coal fired steam cogeneration units in the 600, 300, 200, 100 and 80 Mw sizes. These cogeneration units were to have steam export flows of 250,000 and 500,000 lbs/hr at 250 psig. Capital cost and heat rate data for coal fired steam only units providing 250,000 and 500,000 lbs/hr were also provided.

Unit Design

The unit designs for 600, 300, and 200 Mw units indicated a capability of extracting at most 25% of their cold reheat steam flow. Cold reheat extraction required throttling to achieve the desired supply conditions of 250 psig. The 200 Mw unit cannot supply the full 500,000 lb/hr flow since 25% of its flow is approximately 350,000 lb/hr. All three (3) of these units (600, 300 and 200 Mw) experience a decrease in their electrical capability of approximately 1 Mw for each 10,000 lb/hr of steam extracted.

Gilbert also provided designs for an alternate 200 Mw unit and for 100 and 80 Mw units with controlled extraction turbines. For the 100 and 80 Mw units the electrical output decreased as the amount of steam exported increased. The alternate 200 Mw unit was additionally modified with an oversized high pressure turbine and increased boiler capacity to supply the additional heat input requirements. To improve reliability of steam service the single boiler was changed to two half size boilers. These modifications allowed the 200 Mw unit to maintainits 200 Mw rating at 500,000 lb/hr steam extraction.

UNIT COST ALLOCATIONS

In the development of capital costs and their allocation a two (2) unit site concept was used. This provided for backup steam supply since only one unit was designated to provide steam. Since unit electrical capability declined with increasing steam sendout, a capital cost demand charge was included to provide the required makeup electrical power. The additional cost to maintain fully rated output was approximately equal to the incremental cost per Mw for units from 300 to 600 Mw.

Since a cogeneration unit requires less capital investment than separate steam only and electric only units it was necessary to devise a means of allocating the capital costs of the cogeneration unit. The allocation method used assumed the savings in captial cost for cogeneration construction (including the additional cost to maintain rated output) versus separate steam and electric facilities would be shared equally between steam and electric customers. Costs of the steam only and electric only plants were reduced by the capital savings calculated and these reduced costs were used as the capital costs assigned to steam and electric. The results of these allocations as a function of unit size are shown on TABLE 2.

Energy cost allocations assumed no subsidization of steam cost would be made by the electric customers. For the units studied, this means the amount of fuel charged to electric generation in a cogeneration case will be no more than it would be in an electric only case. The amount of fuel saved in a cogeneration case is allocated equally between the steam and electric units resulting in reduced fuel inputs for each. TABLE 3 illustrates this procedure for the 600 Mw unit.

FIGURE 1 combines the capital and fuel cost allocations discussed previously for the cost of 500,000 lbs/hr of steam exported from cogeneration units, a steam only plant providing 500,000 lbs/hr and for electricity from cogeneration and electric only plants. Annual capacity factors of 70% were assumed for both steam and electric. Significant economies of scale are shown to exist for electric power.

560

STEAM DISTRIBUTION SYSTEMS - DESIGN AND COST

Gilbert provided WE with design and cost data for steam distribution systems with condensate return. Supply lines were of carbon steel and return lines were stainless steel due to the corrosive nature of condensate. Drains, traps, vents, expansion joints and valves were included as needed. From 3" to 4" of insulation was provided on supply lines and 2" on return lines. Assumed supply conditions for the steam are 460° F and 250 psig with returned condensate at 120° F.

Costs were developed for both above and below ground installation. The above ground installation would most likely be used in rural areas or for installations made in industrial parks. Below ground installations would be required in urban areas and for the crossing of roads and other obstacles. Below ground installations were placed in prefabricated, reinforced concrete trench boxes with top slabs of reinforced concrete with manhole access for customer service laterals or for required access to valves etc. Below ground installations with single supply pipe and with dual supply were considered. The reliability required by process steam customers requires the ability to remove a line from service for maintenance and still maintain service. The geographical limitations of many areas do not lend themselves to a loop type of distribution system. The placing of two (2) supply mains in a single trench box provides the required reliability at minimum cost.

Two (2) types of piping runs were assumed for the study: a straight pipe run intended for use as a main supply line or for branch runs of a relatively simple nature; and a complex run was intended for urban areas where obstacles would be present to straight line piping runs and where service laterals to customers were more frequent. TABLE 4 shows installed costs for various sizes of steam distribution piping for the types of piping runs considered.

IDENTIFYING THE POTENTIAL MARKET FOR STEAM

The approach taken by WE to assess the potential market for steam was based on the premise that the potential market consisted of those institutions and industries already established in the WE service territory and presently having a significant demand for process or space heating steam. No considerations were given to speculative situations such as the location of new, large steam using facilities (i.e. refineries or paper mills) within the WE service territory.

To identify institutions and industries currently using steam, data from several sources was used. The Department of Natural Resources (DNR) of the State of Wisconsin annually complies an emmissions survey which lists all major boiler fuel users, their fuel consumption and boiler sizes. The DNR survey does not cover governmental units using boiler fuel. The DNR survey was checked against natural gas

usage data from the two natural gas utilities serving the WE territory.
Data from a period prior to widespread gas curtailments was used.
In this way the report was able to include large governmental boilers
and a check was available to insure the DNR data was accurate and
complete. Several small errors were noted requiring direct contact
with fuel users to verify the correct fuel usage levels.

TABLE 5 contains a summary of the survey data on a county by county
basis for the WE service area. A lower end cut off point of 1×10^{11}
BTU (eq) per year of boiler fuel was used to reduce the task of dealing
with many small users. The lower level fuel cut off chosen corresponds
to an average hourly usage of about 10,000 lbs/hr. Two (2) counties,
Milwaukee and Winnebago, account for almost 70% of the total fuel
consumed in industrial and institutional boilers.

Following the compilation of the data for TABLE 5 a more detailed review
was made of the potential steam users in the following counties.

| Fond du Lac | Milwaukee | Racine | Winnebago |
| Kenosha | Outagamie | Sheboygan | |

This review required the use of county maps on which the location of
major users was plotted. Likely groupings of potential steam customers
were explored to determine if users were in close enough proximity
to one another to warrant a distribution network. No consideration
was given to determining sites for the cogeneration plant itself.

The detailed review using county maps resulted in the selection of
three (3) areas as good potential markets for steam sales. This
selection was primarily based on the proximity of the steam users
to each other, the size of the estimated steam loads and, to a lesser
degree, the nature of the land near the potential users. In one
instance, the area to be served was more rural than others and it was
believed the reduced cost of above ground distribution would justify
the slightly longer pipe runs.

Since the boiler fuel used by the potential steam users was consumed
for both process and space heating needs, a computer program was devised
to estimate the peak steam load for the potential steam users. The
program utilized data gather from operating experience with WE's own
district heating system and degree day data for the WE service
territory.

The peak steam loads were used to estimate pressure drops in piping runs.
Pressure drop calculations were used to size the steam lines used for
the distribution system. The peak load information could also be used
to determine the smallest cogeneration size which could provide the
required steam output. This was beyond the scope of this study.

The three (3) areas selected as providing good potential markets for steam have been designated as WE-S, WE-C and WE-N to maintain the anonymity of the companies included. These areas are shown on TABLES 6, 7, and 8. Information is also contained on these TABLES regarding peak loads, size of pipes and length of pipe runs.

COSTS OF STEAM AND ELECTRICITY FROM COGENERATION UNITS SERVING POTENTIAL MARKET AREAS

Following the selection of potential market areas WE-S, WE-C and WE-N and the selection and costing of pipe runs required, it was necessary to use the previously established allocation method for the capital, fuel and operating expenses of the cogeneration unit.

The cogeneration unit used in the cost calculations for each potential market area was the 600 Mw unit located in pairs on site. Selection of the same unit size allowed WE to analyze only the effect of steam load variations and distribution system differences on costs of delivered steam. The effect of unit size had been analyzed earlier and it was shown that distinct economies of scale existed as unit size increased.

TABLE 9 indicates the annual cost of energy associated with service to the three (3) areas selected. The cost of electricity did not vary significantly between any of the potential steam market areas. The cost of steam varied considerably from area WE-S to areas WE-C and WE-N. WE-S has a steam cost of $14.98 per 100 lbs while WE-C and WE-N were $5.93 and $5.07 per 1000 lbs respectively. The reasons for the large variations in steam cost are found by referring to the cost data of TABLE 9 and to TABLES 6, 7 and 8 where the system peak loads, annual steam usage and distribution system sizes are shown.

Area WE-S has a peak steam load of about 300,000 lbs/hr with an annual steam load factor of only 31%. The loads in area WE-S are predominantly space heating even though the steam is supplied to several large manufacturing plants. In addition, large distances are involved in the distribution system. The identified customers represent the largest steam users in the area. The area near these loads is somewhat rural and land may be available for power plant siting. However, the steam loads do not appear to be favorable for consideration of a cogeneration installation.

Area WE-C has a peak steam load of 494,000 lbs/hr with a relatively high annual load factor of 53%. The loads are a mixture of process and space heating. The identified customers are located in the heart of the down-town Milwaukee area. Distribution distances are relatively small but uncertainly associated with the congested area below urban streets may result in higher than estimated distribution system expenses.

Area WE-N has a peak steam load of 811,000 lbs/hr with an extremely high annual load factor of 67%. The loads are primarily process loads with

a small amount of space heating. The identified customers are located along a river in a fairly dense urban setting. Distribution costs may be higher than those estimated since problems may exist in the area due to below street congestion and additional costs for crossing the river.

The effect of load factor and distribution system costs on the annual cost of steam for the three (3) potential markets is illustrated by the cost information below. Operating costs per 10^3 lb of steam are essentially the same in each area.

	WE-S	WE-C	WE-N
Cogeneration Unit Annual Fixed Charges ($/$10^3$lbs of steam)	7.37	3.59	2.41
Distribution system Annual Fixed Charges ($/$10^3$lbs of steam)	5.82	.56	.94

In summary, steam costs were highly sensitive to the distance between loads due to the expense of distribution systems. Areas with high load factors absorbed the distribution system costs and the cogeneration unit fixed charges in large quantities of steam resulting in lower costs per lb of steam. Dense service areas with high load factors (i.e. process loads) are most likely to result in lower prices for steam relative to areas with poor load factors such as result from space heating loads.

TABLE 1

EXISTING WE DISTRICT HEATING SYSTEM
MONTHLY AVERAGE STEAM SENDOUT
1971 - 1976

	MONTHLY AVG.	STEAM SENDOUT
	10^6LBS	% of Total
Jan.	430	16.3
Feb.	407	15.5
Mar.	362	13.8
Apr.	298	11.3
May.	197	7.5
June	98	3.7
July	56	2.2
Aug.	58	2.2
Sep.	60	2.3
Oct.	111	4.2
Nov.	214	8.2
Dec.	337	12.8
TOTAL	2628	100.00

TABLE 2

COGENERATION UNIT
COMPLETION COSTS [1]

Unit Size (Mw)	1st. Unit	Additional 1st Unit Cost To Maintain Rated MW(2)	2nd Unit
600	355,149	23,814	331,773
300	217,401	23,475	206,264
200	152,062	23,631	140,792
100	92,470	23,631	84,678
80	78,085	23,631	72,457

[1] High Sulphur Coal with SO_2 removal - 10^3 June 1977 dollars.

[2] At 500,000 lbs/hr steam export.

TABLE 3

ENERGY ALLOCATION FOR 600 MW UNIT
EXPORTING 500,000 LB STEAM PER HOUR

No Extraction Heat Rate (BUT/Net KW)	x	Reduced Net Electric Output at 500,000 lb/hr Extraction (Kw)	=	Equivalent No Extraction Heat To Electric MBTU/HR
9891	x	546,904	=	5409

Actual Unit Heat Input MBTU/HR	−	Equivalent No Extraction Heat To Electric MBTU/HR	=	Additional Heat Input Due to Steam BTU/LB Steam
5944	−	5409 [1]	=	1068

Steam Only Unit Heat Rate (BUT/LB Steam)	−	Additional Heat Input Due to Steam (BTU/LB Steam)	=	Heat Savings For Cogeneration (BTU/# Steam)
1404	−	1068 [1]	=	366

Credit To Electric Per LB Steam	=	$\dfrac{366 \text{ BTU/LB}^{[1]}}{2}$	=	168 BTU/LB

Revised Steam Heat Allocation (BTU/LB)	=	$1068 + 168^{[1]}$	=	1236 BTU/LB

[1] See calculation one (1) line above for derivation.

TABLE 4

STEAM DISTRIBUTION SYSTEM COSTS

SINGLE MAIN

Size Steam Supply	Below Grade			Above Grade	
	Rural Straight	Urban Straight	Urban Complex	Rural Straight	Rural Complex
30"	804	889	1129	377	612
20"	591	654	786	275	404
18"	568	632	745	258	367
12"	407	469	539	181	247
10"	351	413	468	149	200
6"	278	334	365	119	146

DUAL MAIN

	Below Ground		
	Rural Straight	Urban Straight	Urban Complex
30"	1562	1629	2108
20"	1148	1222	1486
18"	1089	1171	1397
12"	776	849	989
10"	670	740	850
6"	531	593	655

Excluding: 1) Land and Land Rights
2) Rerouting of Traffic
3) Interruption of Other Services
4) Permits and Fees
5) Drainage from remote locations

Note: All cost $/ft. in June 1977 dollars

TABLE 5

SUMMARY OF
MAJOR BOILER FUEL USERS[1]
BY COUNTY

County	No. of Firms	Total Boiler Capacity (10^6 BTU/hr)	Total Space Heating Fuel in 1975 (10^{12} BTU)	Total Fuel Consumed[2] in 1975 (10^{12} BTU)
Fond du Lac	1	135	.02	2.62
Dodge	1	*	*	.11
Jefferson	1	1.3	-0-	.18
Kenosha	5	1066	1.83	2.44
Milwaukee	48	7155	8.24	20.47
Outagamie	13	3109	1.86	2.44
Ozaukee	1	*	*	.10
Racine	10	1000	2.60	3.87
Sheboygan	3	1127	.12	2.00
Shawano	2	*	*	.55.
Walworth	1	300	.34	.40
Washington	4	70	.05	.37
Waukesha	4	68	.34	.58
Waupaca	2	*	*	.29
Winnebago	14	2020	.64*	10.85
Total	110	16051	16.04*	47.27

(1) All firms using in excess of 1×10^{11} BTU in 1975 excluding electric utilities

(2) Combination of DNR data and information from gas companies

   *Data incomplete due to exclusion of certain firms from DNR data

TABLE 6
STEAM SERVICE AREA WE-S
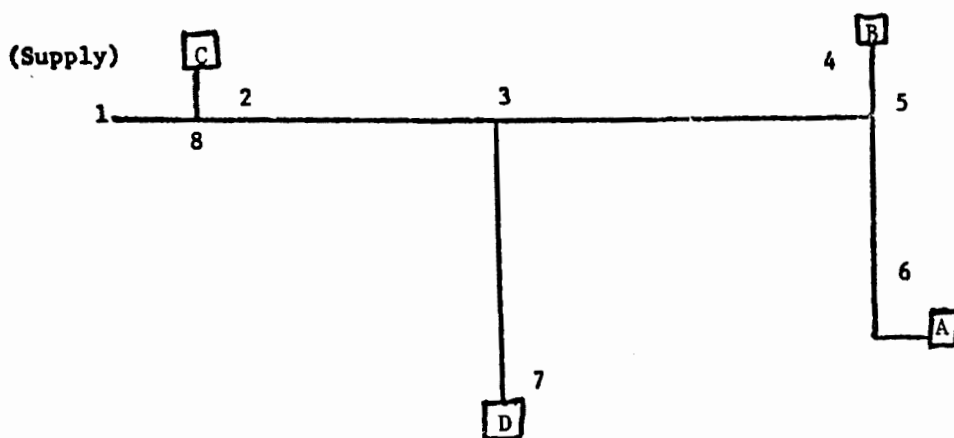
Drawing Not to Scale

		Distribution System			Est. Annual Steam Usage	
		Length	Diameter	Peak Load	$10^6 \#$	
From	To	(Ft.)	(In.)	$(10^3 \ \#/hr)$		
(Supply)						
1	8	0	N/A	307	Customer	Usage
8	2	500	12	109	A	289
8	3	11,600	20	198	B	119
3	7	9,000	10	44	C	325
3	4	10,700	18	154	D	108
4	5	1,780	10	43	Total	841
5	6	6,500	18	111		

TABLE 7
STEAM SERVICE AREA WE-C

Drawing Not To Scale

			Distribution System		Est. Peak Load	Est. Annual Steam Usage	
			Length	Diameter	$(10^3 \ \#/hr)$	$10^6 \#$	
	From	To	(Ft.)	(In.)			
(Supply)	1	2	0	N/A	494	Customer	Usage
	2	3	0	N/A	205	A	1,001
	2	4	5700	18	289	B	1,307
						Total	2,308

569

TABLE 8

STEAM SERVICE AREA WE-N

Drawing Not To Scale

Distribution System

From	To	Length (ft.)	Diameter (in.)	Est. Peak Load (10^3#/hr)
Supply	1	0	N/A	811
1	2	1700	10	102
1	3	3800	30	709
3	4	1900	20	498
4	5	500	6	120
4	6	500	6	
4	7	4400	30	378
7	10	1000	10	72
7	9	1000	18	246
10	11	1000	6	11
9	8	1000	10	110
7	12	4000	10	60

Est. Annual Steam Usage 10^6

Customer	Usage
A	515
B	1406
C	588
D	
E	634
F	869
G	358
H	75
I	367
TOTAL	4,812

FIGURE 1
ANNUAL COST COMPARISON
AT SITE BOUNDARY
SEPARATE VS. COGENERATION FACILITIES
70% ANNUAL CAPACITY FACTOR
HIGH SULFUR COAL WITH SO_2 REMOVAL
JUNE 1977 $

Electric Energy Cost – $/Mwh

Steam Cost – $/1000#

Separate Electric

Cogeneration Electric

Separate Steam

Cogeneration Steam

571
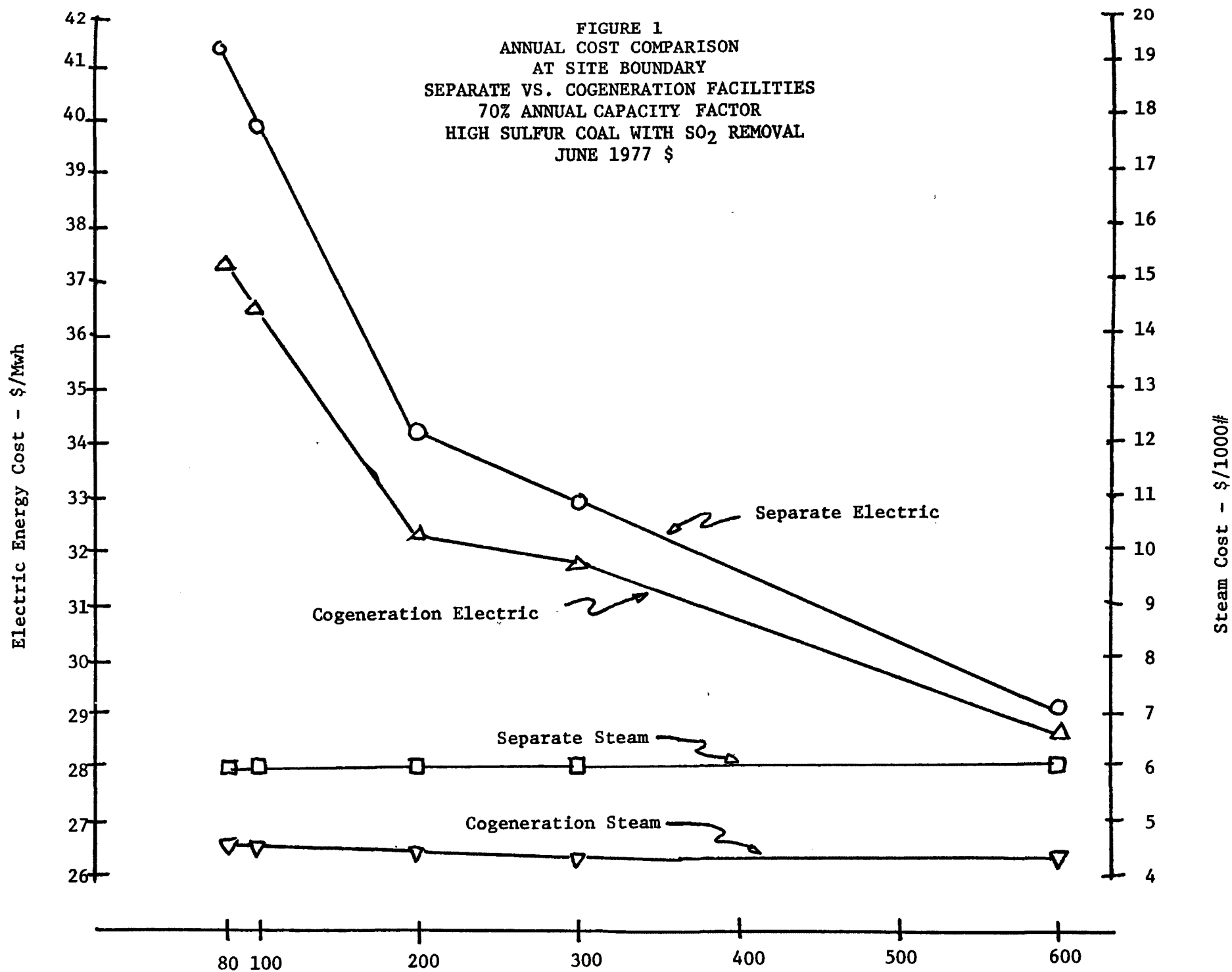
ALTERNATIVE APPROACHES IN INDUSTRIAL COGENERATION SYSTEMS

J. C. Solt
Solar Turbines International
An International Harvester Group
San Diego, California

ABSTRACT

This paper traces the development of cogeneration systems in industry, and discusses some early applications. The effect of changing markets and economic conditions is evaluated and specific examples are presented to illustrate the increasingly favorable climate for cogeneration system applications in today's energy conscious society.

BACKGROUND

In the early 1960's, many people became aware of the fact that it was possible to generate electric power at the site where it was to be used and also to produce process heat from the same system. This allowed generation of electric power less expensively than at a central generating plant, and the savings could be applied against the capital cost of the equipment. The common generic term for this type of system was "total energy."

With few exceptions, early cogeneration or "total energy" systems had no interconnect with electric utilities. Their real challenge was to maintain the appropriate relationship between demand for electricity and heat. But isolation from electric utilities generally meant that equipment was run to meet electrical demand with no regard for heat demand. Excess heat was simply wasted, or any short-fall in heat production was made good by using auxiliary equipment. In either case, economic and thermal efficiency was impaired.

As a result, early cogeneration attempts usually proved disappointing. Industrial process installations were generally more successful than commercial installations because industrial users had higher annual utilization rates for both electricity and heat, and greater maintenance capabilities. Commercial users frequently based economic calculations on ideal conditions which were not present year-round.

Another factor limiting early attempts at cogeneration was that, without a utility tiein, individual users had to come up with their own solutions to peaking and standby problems. A user with a peak electrical use twice that of minimum use would have to buy three units: one to generate minimum load, one to

supply peak power, and a third as a standby. In this example average use rates could be less than 50 percent, substantially diluting any savings offered by onsite cogeneration.

One solution would have been to retain a utility tie and generate only a portion of the electrical demand onsite with the utility supplying the shortfall. The system could then be operated to meet heat demand only. Even with the generator operating at less than 100 percent, more attractive efficiency figures would be obtained because of the more complete exhaust heat utilization. However, in the past, the average electrical utility regarded onsite generation as competition and was unlikely to agree to participation in a "share-the-load" type arrangement.

Concern about fuel availability and cost in the seventies has created new possibilities for successful application of cogeneration. It should be obvious, however, that cooperation between electrical utilities and process heat users is needed if the potential represented by cogeneration is to be realized.

ALTERNATIVES FOR UTILITIES

There are basically two different ways in which an electrical utility and an industrial user can participate in a cogeneration activity. Each alternative has advantages and disadvantages and it is important that both be considered for each individual application to be certain that the utility and the industrial customer take advantage of the appropriate arrangement.

The first alternative is for the electrical utility to own and operate the cogeneration facility. The electrical generation equipment is then tied directly into the utility grid and the equipment can be operated to satisfy the heat requirements of the industrial customer. The industrial customer then continues to buy electrical power in the usual fashion, but he also purchases the process heat (usually in the form of steam) from the utility. The industrial customer typically will be able to purchase this process heat at a lower cost than if he produced it himself, and he does not bear the capital cost of the boilers.

The second alternative is for the electrical utility to furnish an intertie to a system owned and operated by the industrial heat user. As previously stated, this intertie would improve both the capital cost to the industrial user and allow him to operate at an optimum cycle efficiency. The electrical utility benefits by getting additional generating capacity without the problems associated with raising capital, siting the system, and overcoming environmental objections.

573

SOLAR'S EXPERIENCE

Solar Turbines International has been furnishing cogeneration systems to the process industry for more than 17 years. There are over 280 Solar turbines in this type of service and they have accumulated over eight million operating hours. Some of these packages have operated in excess of 100,000 hours. Our largest installation includes 12 turbine generator sets at a single location. Another single-site installation has two generator sets, two natural gas compressor packages, and three mechanical drive refrigeration packages.

HOW A TURBINE WORKS

A gas turbine engine consists of a compressor, a combustor, and an expansion turbine (Fig. 1). Ambient air is drawn in through the compressor and flows steadily into the combustor. Fuel is fired in the combustor and the resulting, high-energy hot gas passes through the expansion turbine. The energy extracted through the turbine section is used to drive the compressor and the load.

Burning is continuous in the combustor, so temperatures in the turbine section are maintained by controlling the fuel-to-air ratio. Most industrial gas turbines use from three to four times as much air as is required to combust the fuel. Consequently, the exhaust stream contains 15 to 20 percent oxygen, so it is possible to burn additional fuel in the exhaust stream to increase the amount of thermal energy available. Since the exhaust is clean and dry it can also be used directly as hot air for drying or curing.

Solar manufactures three industrial turbine engines which can be used in cogeneration topping cycles (Fig. 2). These engines are available in complete generator, compressor or mechanical drive packages capable of driving any type of customer specified equipment.

EXHAUST HEAT UTILIZATION

There are three distinct methods of utilizing gas turbine exhaust heat. Fuel burned in almost any industrial process can be credited totally or partially by one of these methods:

- The most common procedure is to pass the exhaust flow through a heat exchanger (or boiler) and transfer its heat to a process fluid or gas such as H_2O, air, or oil (Fig. 3). Since the exhaust gas contains over 16 percent oxygen, additional fuel can be fired in the exhaust flow to achieve higher initial temperatures or increased energy as required by the particular process. A number of

manufacturers offer these types of heat exchangers and boilers as standard product lines.

- A second common method is to use the exhaust flow, which is relatively clean and dry, as a direct-heating and/or drying medium (Fig. 4). The exhaust flow can be diluted with ambient air to achieve any lower temperature and increased volume flow desired. If the process back pressure is low, this can be done with a simple inductor. At higher back pressures, a fan is required to provide the dilution air. As in the case above, additional fuel can be burned in the exhaust prior to process use to match any temperature/energy requirement.

- A third method, which is frequently utilized in the oil and gas industry, is to use the exhaust flow as highly preheated combustion air in devices such as boilers, space heaters, oil heaters, and hot gas generators (Fig. 5). This is the most efficient method of exhaust utilization since all of the exhaust energy above ambient can be credited to fuel saved in the combustion device.

GENERAL PERFORMANCE

The values shown in all three examples (Figs. 3, 4, and 5) are based on the following assumptions:

Ambient conditions - sea level and $60^{\circ}F$
Fuel   - liquid or gas
Load   - 100 percent

Steam data:

Condensate return - $200^{\circ}F$
Steam conditions   - dry and saturated
Boiler efficiency - 80 percent

For altitudes other than sea level, read the correction factor from the following table, and multiply power output, fuel consumption, and mass flow by the factor. For part-load conditions and other ambient requirements, please contact Solar. The constants shown in these examples can be used to perform a similar preliminary energy balance for other types of systems.

Altitude (ft)		Factor	
	0	Factor	1.000
	2,000		0.930 .
	4,000		0.864
	6,000		0.801
	8,000		0.743
	10,000		0.688

575

EVALUATING THE BENEFITS OF A SOLAR COGENERATION SYSTEM FOR YOUR APPLICATION

Return on investment in a cogeneration system can be determined by considering four primary and two secondary variables. The primary variables are:

- Utility Electrical Rate ($/kWh)

  This should be a composite rate including energy charge, demand charge, and taxes as applicable. If a declining rate structure is in effect, it should be taken into account. This information can be obtained from your utility bill and a rate schedule available from the utility company.

- Annual Utilization (%)

  Like any other capital investment, return improves with higher utilization. Maximum utilization can be achieved by generating the required base load while in parallel with the electrical utility, which would provide peaking and standby power as required.

$$\text{Annual Utilization} = \frac{\text{Annual Hours of Operation}}{8760 \text{ hours/year}}$$

- Fuel Cost - $/Million Btu ($/mm Btu)

  The net cost of onsite generated electricity will be directly proportional to cost of fuel used. Cost is expressed in $/million Btu as a convenient form for the necessary calculations. It can be determined as follows:

Number 2 Diesel

Heating Value = Approximately 130,000 Btu/gal

Cost = 0.363/gal

$$\text{\$/mm Btu} = \frac{1,000,000}{130,000} (0.363) = \$2.79/\text{mm Btu}$$

Natural Gas

One therm = 100,000 Btu

Cost = $0.18/therm

$$\text{\$/mm Btu} = 10 \times 0.18 = \$1.80/\text{mm Btu}$$

• Installed Cost of Cogeneration System ($/kW)

  Precise estimates of system installed cost must be made
  on a case-by-case basis because of variations in such
  factors as site conditions, local labor costs, and heat
  recovery equipment used. However, for purposes of an
  initial economic analysis, the following average values
  of total installed cost can be used.

  Saturn $480/kW
  Centaur $400/kW
  Mars $300/kW

The secondary variables are:

• Net Fuel Rate for Onsite Generated Electricity

  Fuel rate for a generator is expressed in terms of
  Btu/kWh, i.e., the number of Btu's of fuel input required
  to produce one kilowatt for one hour. In order to find
  the incremental fuel required to produce the electricity
  above that fuel required to satisfy the process heat re-
  quirements, we credit the fuel used by the gas turbine
  with the fuel that would have had to be used to satisfy
  the process heat requirements. (In calculating fuel
  credit, one must take into account such factors as boiler
  efficiency so that actual fuel required to satisfy the
  process requirements is determined.) When this value of
  incremental fuel is divided by the number of kilowatts
  produced, the result is a quantity defined as Net Fuel
  Rate (NFR). In equation form:

$$NFR = \frac{\left(\begin{array}{c}\text{turbine}\\\text{fuel}\end{array}\right) - \left(\begin{array}{c}\text{fuel value of}\\\text{heat recovered}\end{array}\right)}{\text{kW output}}$$

  Net fuel rate will vary as a function of the type of heat
  recovery system and average kW output, but typical values
  will range from 4000 to 6000 Btu/kWh, which is less than
  50 percent of the fuel required by the utility. For an
  initial evaluation, an average value of 4500 Btu/kWh is
  satisfactory.

• Maintenance Cost

  Maintenance cost should be considered in calculating net
  cash flow, but has a relatively minor impact. Typical
  maintenance costs vary in the range of 0.18¢/kWh, depend-
  ing primarily on the operating cycle. Frequent starts and
  stops will result in higher maintenance cost while
  continuous operation will result in lower maintenance
  cost.

577

Application and Evaluation

The application and evaluation procedure can be best illustrated with a specific example.

Step

① Select a generator set (or sets) which meets the desired heat load by referring to Fig. 6, which shows the recoverable heat or approximate steam production capacity of Solar's three generator set sizes.

② Check that the kW rating of the unit(s) selected matches favorably with the plant's electrical demand. The system could be sized to provide all or only part of the plant requirements, of either the steam or power, with other equipment or with the utility providing the difference.

③ Assume that a Centaur generator set is selected to provide part of the plant's heat and electrical requirements. List the four primary and two secondary economic variables previously described:

- Utility composite rate + 0.036/kWh

- Annual utilization for three shifts, six days, 50 weeks =

$$\frac{3 \times 8 \times 6 \times 50}{8760} = 82\%$$

- Fuel cost (No. 2 Diesel) = \$2.79/million Btu

- Installed cost = \$400/kW

- Net fuel rate (average value) = 4500 Btu/kWh

- Maintenance cost = \$0.0018/kWh

④ Calculate cost of electricity generated:

Cost = fuel rate x fuel cost + maintenance

Cost = (4500) (2.79)/10^6 + 0.0018 = \$0.0144/kWh

⑤ Calculate saving/kilowatt hour:

= utility rate - cost of electricity generated
= 0.036 - 0.0144 = \$0.021/kWh

⑥ Read annual saving/kilowatt installed from Fig. 7:

Savings = \$150/kW installed

⑦ Calculate simple payback:

$$= \frac{\text{installed cost/kW}}{\text{annual savings/kW}} = 400 \div 150 = 2.7 \text{ years}$$

⑧ Read after-tax discounted cash flow rate of return from Fig. 8:

$$= 21\%$$

Either rate of return or payback can be used to evaluate the investment. This example shows a very attractive return on investment and it is clear that the application with these conditions would be pursued in almost any industry. Your company's financial guidelines should indicate whether the return for your application is practical.

CONCLUSION

Solar has used gas turbine engines to provide site-generated electric power in almost every conceivable application. There are certain industries, however, that present much more favorable economics than others. In general, process industries are excellent candidates for cogeneration type systems because they have a high usage factor (three-shift operation), a high thermal requirement on a 24-hour a day basis, and they normally have a good understanding of the sophisticated mechanical equipment described in this paper. These process industries include:

Natural gas processing
Petrochemical and refining
Paper and pulp
Food processing
Textiles
Clay, cement, and glass
Lumber and wood products
Metals

Solar's equipment can be used for either total or partial electrical power generation, refrigeration, and as direct drive for mechanical equipment in almost any of these applications.
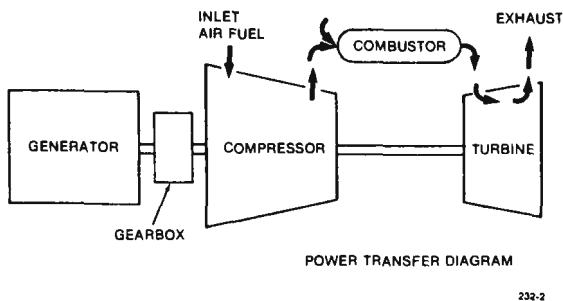
Fig. 1. Basic Simple Cycle Gas Turbine
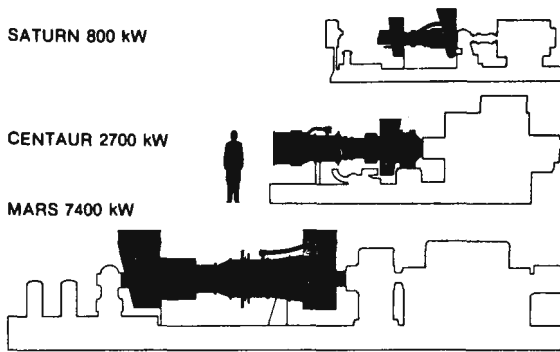
Fig. 2. Solar Gas Turbine Generator Sets

	Saturn	Centaur	Mars
Stack Temperature (°F)	300	300	300
Steam Output (lb/hr)	6425	17,886	33,112
Exhaust Temperature (°F)	848	836	781
Fuel Input (million Btu/hr)	13.22	39.84	80.52
Electrical Output (kW)	800	2628	6865
Air Mass Flow (thousand lb/hr)	49.20	140.0	288.9
Net Fuel Rate (Btu/kWh)	6524	6685	5723
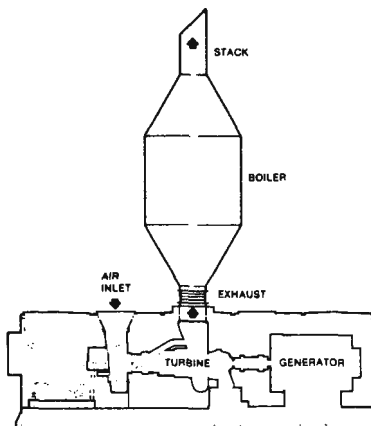
Fig. 3. Unfired Turbine Exhaust Used to Produce 15 psi Steam

	Saturn	Centaur	Mars
Heat Credit (millions Btu/hr)	9.14	27.27	52.28
Exhaust Temperature (°F)	848	836	781
Fuel Input (million Btu/hr)	13.22	39.84	80.52
Electrical Output (kW)	800	2628	6865
Air Mass Flow (thousands lb/hr)	49.20	140.0	288.9
Net Fuel Rate (Btu/kwh)	4361	4783	4113
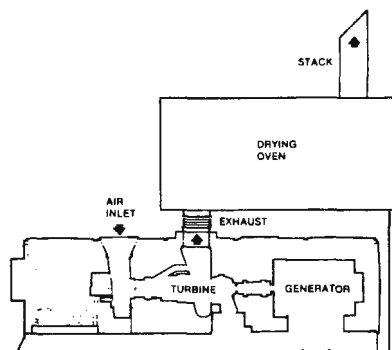
Fig. 4. Turbine Exhaust Used Directly as Hot Air Source

	Saturn	Centaur	Mars
Stack Temperature (°F)	300	300	300
Steam Output (lb/hr)	46,050	135,508	276,359
Additional Fuel (million Btu/hr)	49.2	139	287
Exhaust Temperature (°F)	848	836	781
Fuel Input (million Btu/hr)	13.22	39.84	80.52
Electrical Output (kW)	800	2628	6865
Air Mass Flow (thousand lb/hr)	49.20	140.0	288.9
Net Fuel Rate (Btu/kW)	4361	4783	4113

Fig. 5. Turbine Exhaust Used as Combustion Air in 200 psi Boiler

580

Fig. 6. Cost of Generating Power
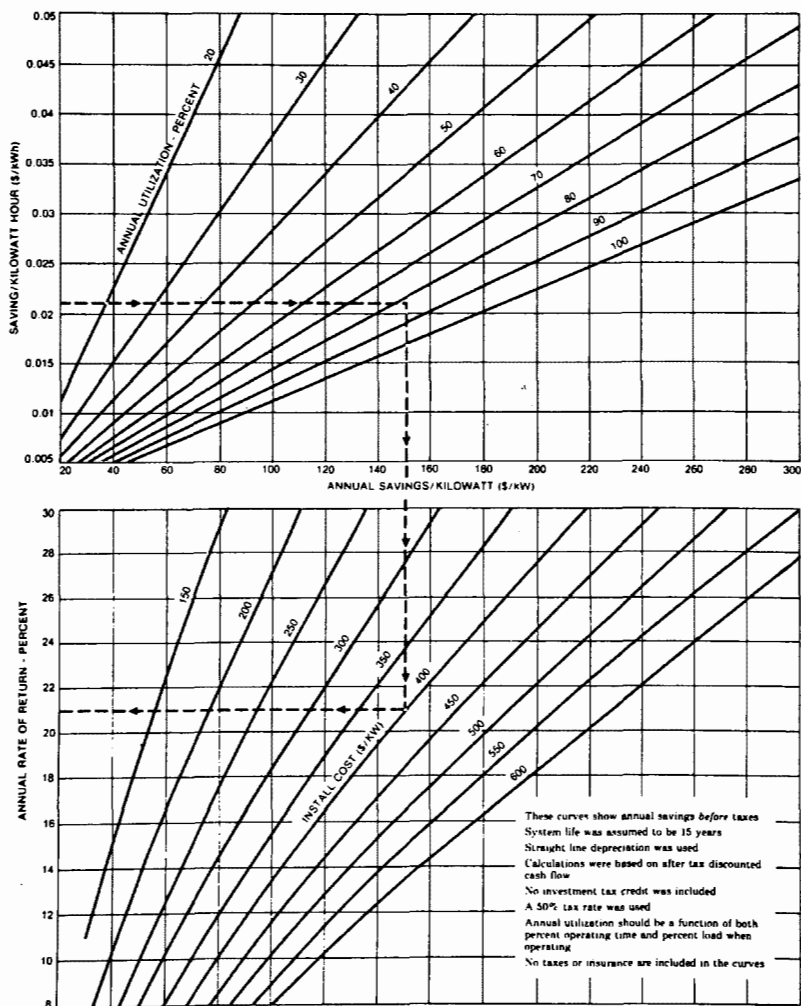
Fig. 7. Economic Evaluation

581

THE ENVIRONMENT FOR COGENERATION IN THE UNITED STATES

ENVIROSPHERE COMPANY

A DIVISION OF EBASCO SERVICES INCORPORATED

B. R. Rossi, J. R. Jackson and E. F. Dul

Presented at

Second Conference on

WASTE HEAT MANAGEMENT AND UTILIZATION

MIAMI BEACH, FLORIDA

DECEMBER, 1978

TABLE OF CONTENTS

A. INTRODUCTION

The national thrust toward energy conservation has directed significant attention toward cogeneration. This attention has taken three primary forms to date:

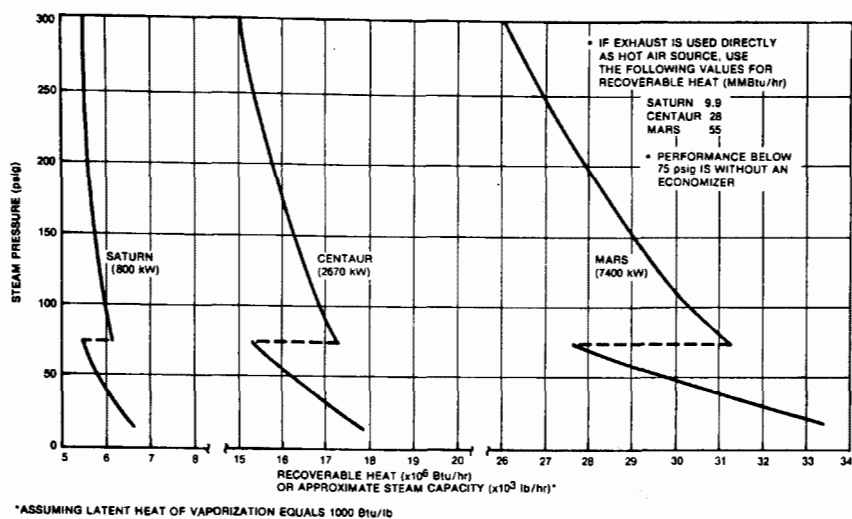- Specific individual utility actions that could be considered to be the vanguard of the "second generation" of cogeneration activities in the nation.

- Legislative and administrative action at the federal and state levels designed to ultimately encourage constructing cogeneration facilities.

- Federal funding of cogeneration research.

Additionally, the electric utility industry, the academic community, and the consulting engineering and industrial sectors have undertaken various degrees of analysis together and separately to evaluate cogeneration opportunities. Based on this, there is little question from the national perspective that in many circumstances cogeneration is an effective conservation method, can be attractive to the utility industry, and will contribute to improving the nation's energy self-sufficiency. It will provide opportunities for:

- More cost-effective and efficient energy use.

- Reduction in national expenditures for energy facility construction and operation.

- Reduction in the degree of environmental effects involved in the current mode of separate development of electric generation facilities and process steam production facilities.

- Movement toward an integrated, total energy economy that focuses on the gross energy cycle rather than the individual sector domains (i.e., oil and gas industry, process steam industry, electric utility industry).

- Assisting utilities to meet future load requirements in view of delays that may be encountered in getting large generating facilities on line.

584

Given the foregoing, the questions which must be raised at this time are: "How is the national effort towards cogeneration supported by the activities of the electric utility industry?" and "What direction should the utility industry assume in this effort?". Related questions are:

- Who is considered as the focal point for implementing cogeneration?

- Are stimuli being provided and in what form?

- What are the formal requirements on the electric utility industry in establishing (or not establishing) cogeneration facilities in the United States?

- What roles are available to the electric utilities in the United States' cogeneration effort?

- What experiences do we have to date and what do they teach us?

In order to answer these questions, this paper is divided into six parts that:

1. Cite the major results of various current studies/ efforts concerning the engineering/economical/ licensing opportunities of cogeneration.

2. Identify the current status of federal legislation fostering cogeneration.

3. Identify the current status of state activities affecting cogeneration.

4. Analyze the targets of the various legislative efforts and the position of the electric industry.

5. Assess the implications to the electric utility industry inherent in the success or failure of the national cogeneration effort.

6. Identify what actions the electric utility industry should take to aggressively and effectively participate in the national thrust toward cogeneration, based on our current experiences.

B. RESULTS OF CURRENT COGENERATION STUDIES/EFFORTS

There have been numerous recent studies performed by all
sectors on the issue of cogeneration and cogeneration
ventures.

Included among the major cogeneration studies performed to
date are:

- Energy Industrial Center Study, performed by
  Dow Chemical Company for the National Science
  Foundation in 1975.

- A Study of Inplant Electric Power Generation in the
  Chemical Petroleum Refining, and Pulp and Paper
  Industries, performed by Thermo-Electron
  Corporation for the Federal Agency Administration
  in 1976.

- The Potential for Cogeneration Development in Six
  Major Industries by 1985, performed by Resources
  Planning Associates, Inc. for the Department of
  Energy in 1977.

- National Coal Policy Project, sponsored by
  Georgetown University and performed this year.

The premier results of these studies include the following:

- Nationwide, current installed cogeneration capacity
  is approximately 4000 MW and represents about four
  percent of the total U.S. electrical power
  generation.

- Without government action, cogeneration capacity
  from process steam can reach 10,000 MW by 1985.

- With government action, cogeneration capacity from
  process steam can reach 12,000-16,000 MW by 1985.

- Widespread application of cogeneration utilizing
  coal could save up to two million barrels of oil
  per day by the year 2000.

- Various mixes of industrial cogeneration activities
  and industry-utility joint ventures can save the
  electric utility industry $2 to $5 billion dollars
  per year in capital investment requirements by
  1985.

- These savings will ease the construction financial burden of the electric utility industry in a period of time when financing remains difficult to obtain.

- The additional fuel required to produce both power and process steam at a common site is about one-half that required for generating electric power only, resulting in a net reduction in air pollutant emissions per unit of energy.

- The maximum potential for cogeneration lies in such process steam industries as: chemical, textile, food processing, pulp and paper, steel, and petroleum refining, with opportunities in cement, beet processing, canning, and minerals processing.

These studies also are very clear in identifying that, without governmental action, these potential benefits could become lost opportunities.

Premier cogeneration projects that currently involve significant utility industry participation should, for logical consideration, be separated into "first" and "second" generation experiences. The first generation experiences, to cite a few, include those by:

- Gulf State Utilities and Exxon Corporation at Gulf States' Louisiana Station Unit No. 1 originated about 1930.

- Houston Lighting & Power Company and Champion Paper Company at HL&P's Deepwater Station initiated about 1928.

- Delmarva Power & Light and Getty Oil's (formerly Tidewater) arrangement at Delaware City, Delaware initiated about 1956.

- Public Service Electric and Gas Company of New Jersey and Exxon Corporation at PSE&G's Linden Station initiated about 1957.

Second generation experiences, or those that have occurred since the total energy hiatus of the 1960's and early 1970's, include:

- Southwestern Public Service Company's activities which were overviewed by its Mr. Cliff Mlinar (Vice President-Marketing) at the 5th Energy Technology Conference and exposition in Washington, D.C. in February, 1978. Its aggressive activities over the past two years have accounted for opportunities that negate the need for about three to four percent of previously planned new plant construction.

- The 50 MW joint venture between the Eugene Water and Electric Board of Oregon and the Weyerheauser Corporation in Springfield, Oregon.

- The current activities of the City of Modesto, California concerning the development of a 65 MW unit to supply process steam to local canneries.

- The recent activities (during part of 1976 and 1977) of Southern California Edison Company which resulted in the identification of 39 projects with a potential of 612 MW of cogeneration.

C. CURRENT FEDERAL STATUS

Federal legislative action affecting cogeneration is incorporated into that part of the National Energy Act entitled, The Public Utility Regulatory Policies Act of 1978. Concerning cogeneration, the principal points are:

- Federal rules will be established to be followed by State PUCs.

- Rates will be "just and reasonable" (no definition supplied) and shall not discriminate against cogenerators and small producers.

- The rate at which utilities will buy power from cogenerators will be at the incremental costs of power produced by the utility.

- All cogenerators and small power producers (under 30 MW or 80 MW for biomass) will be exempt from the Federal Power Act, if FERC decides it is necessary for purposes of the ACT, and will be exempt from state laws and the Public Utility Holding Act. Federal licensing will still be required, but with expressed congressional intent that licensing applications be expedited.

In addition, other points impacting on cogeneration, are as
follows:

Interconnections - A new provision, Subsection G to
Section 202 of the Federal Power Act, will permit FERC
to order the physical connection of transmission
facilities if it will encourage the overall conservation
of energy or capital and promote the efficient use of
facilities and resources.

Wheeling - A new provision to Section 202 of the Federal
Power Act, Subsection H, will permit FERC to order
wheeling of power if it will promote the efficient use
of electric generation and transmission facilities and
conserve a significant amount of energy.

D. LEGISLATIVE STATUS - CALIFORNIA

In order to gain a perspective on the status of state
legislation affecting cogeneration, administrators in
various states were surveyed to determine the extent of
cogeneration activities/regulations within each respective
state. It was found that the states vary widely regarding
cogeneration experience and activities. California, as
discussed below, has progressed the furthest in the area of
cogeneration:

California - Currently there is much activity in the
state regarding cogeneration. Governor Brown has stated
that he supports growth in geothermal, solar and
cogeneration technologies. The Energy Resources
Conservation and Development Commission (Energy
Commission) and the PUC both have taken a lead role
in fostering cogeneration activity in the state. The
"Staff Report on California Cogeneration Activities",
published on January 17, 1978, outlines such actions
as:

. Assembly Bill No. 2046 (Calvo) concerning geo-
thermal power and cogeneration was introduced on
August 8, 1977 and passed the Assembly with no
amendments on January 23, 1978. Although the Calvo
Bill was withdrawn from session, another bill
(SB 1805, Holmdahl) incorporating similar
provisions has been approved by the Governor
(September 20, 1978). The bill concerns the
regulation and review of such facilities as
follows:

a. Revises the existing two-step facility siting
    process before the Siting Board of the Energy
    Commission, which normally requires about 36
    months, for cogeneration applications for
    plants not exceeding 300 MW to complete the
    process in 12 months.

b. Exhaust steam, waste steam, heat, or resultant
    energy produced in connection with cogenera-
    tion technology would be exempted from state
    sales taxes.

E. SUMMARY ANALYSIS OF LEGISLATIVE THRUST AND IMPLICATIONS

It is apparent from the previous discussions that Federal
and State Governments are actively promoting cogeneration
as a means to conserve energy. In addition, the thrust of
the legislation is such that the process industries, as
opposed to the electric utility industry, are the focal
point for implementing cogeneration. However, the utility
industry will likely be faced with having to make decisions
regarding the following activities:

. Providing interconnections with industrial
   cogenerators

. Purchasing excess industrial generated power

. Wheeling industrial generated power

. Developing rate schedules for purchase and standby
   power to encourage cogenerators and small producers

Using the crude "carrot and stick" analogy, significant
effort appears to be directed at offering the "carrot" to
the process industries. However, no "stick" is obvious
or probably even possible. Although this is not a problem
per se, our concern is that, if the "carrot" is not taken
up by the process industries, will the "stick" be brought
down on the utility industry?

To be practical, we believe it is fair to state that a
number of "negative" factors could be expected by the
utility industry, particularly if cogeneration is pursued
without adequate planning. These factors include:

- Loss of major base load demand

- Higher consumer rates in the short term because of fewer customers for existing generating capability

- Maintenance of large bulk capacity standby reserves

- System load management difficulties associated witn the schedule, capacity and reliability of purchased and wheeled industrial power

- System planning difficulties associated with the duration and reliability of industrial cogeneration activities

- Siting and licensing (air quality) concerns associated with industry-utility colocation ventures

The above concerns have been expressed frequently by utility planners and are among the major reasons why cogeneration currently contributes only about four percent of the total U.S.-generated electrical power. Based on the legislative thrust at federal and state levels toward efficient energy use, conservation, and an integrated total energy economy; however, the implications to the electric utility if the process industries do not pursue cogeneration probably are more significant. Potentially, these include:

- Delays in licensing hearings related to determination of the extent of utility-encouraged conservation practices in demonstration of need proceedings. (On this point we would like to note that at a recent rate hearing, a utility was questioned by the state's energy commission representatives about the need for power and site selection process associated with a proposed coal-fired facility. Whereas the utility clearly indicated the factors utilized in establishing the need and the site, the energy agency essentially brought the proceedings to a halt when it was identified that no consideration was given to at least 15 potential cogeneration opportunities within 10 miles of the proposed site which offered substantial opportunity for electrical generation. This may well become a "stock" issue at other hearings in the future.)

. Increasing financial burden caused by continuing
  growth in demand, rising fuel costs, environmental
  controls and inflation.

. Increasing demand for suitable generating sites at a
  time when large land tracts and water resources are
  becoming scarce and more valuable; air quality
  regulations for fossil plants are becoming stricter;
  local opposition to nuclear plants is rising; and the
  licensing process is becoming longer and more
  complicated.

. Risk of further government intervention if cogenera-
  tion opportunities are not pursued by the process
  industries.

F. CONCLUSIONS AND RECOMMENDED ACTIONS

Because the national effort toward energy conservation
initiated by President Carter's National Energy Plan is
directing significant attention towards cogeneration, the
concern of those involved in the electric utility industry
should be as follows:

. Federal and State Governments are looking toward the
  process industries as the focal point for implement-
  ing cogeneration.

. The federal and state thrust toward fostering
  industrial cogeneration is through encouragement
  rather than regulation.

. The role of the utility industry in this national
  effort appears to be considered as one of "accommoda-
  tion" rather than prime responsibility.

. If cogeneration is pursued without adequate planning,
  it will adversely impact the electric utility
  industry.

. If the process industries do not follow through on
  cogeneration activities, the utilities may, by
  default, be held responsible because they will be
  required to demonstrate in rate and environmental
  licensing hearings specific actions taken to promote
  energy conservation, including cogeneration.

In overview then, the electric utility is in the apparent position of being responsible for fostering and accounting for industrial cogeneration activities without any formal means, including federal and state regulatory measures, to influence industrial decisions. The solution to this potential dilemma, as we see it, is for the electric utility industry to take the initiative in the form of positive actions.

The following are typical actions that could be pursued by an electric utility to effectively and aggressively encourage cogeneration activities within its service area. The intent of this section is not to suggest a specific course of action, but rather to outline various actions that reasonably appear positive in nature. Whether a utility employs some or all of these comments or develops its own, the key point to remember is this: <u>it is up to the electric utility industry to define its role in cogeneration before that role is defined by others.</u>

. Identify cogeneration potential within the service area

    a. Institute studies of major industries to determine potential cogeneration opportunities

    b. Enter into discussions with industrial candidates about their planned or proposed cogeneration activities.

    c. Investigate in conjunction with industry on a case-by-case basis the alternative benefits associated with:

        - Industrial byproduct generation
        - Industrial on-site generation with utility management
        - Utility supplied process steam and power
        - Industry-utility joint venture

. Institute provisions for cogeneration activities

    a. Develop costs for standby services, energy purchased from cogeneration and interruptible service

b. Develop rates for standby services, interrupt-
   ible services and price guidelines for the
   purchase of energy that reflect the values to
   the utilities in the rate proposal

c. Assist customers in reviewing projects to
   establish criteria which will expedite cogenera-
   tion efforts

. Document all activities in reports to the Public
  Utilities Commission for subsequent rate, siting
  and licensing hearings.

. Support federal and state cogeneration studies and
  the EEI Task Force on On-Site Generation.

. Actively pursue having the role and responsibility
  of the electric utility industry understood and
  defined in all emerging federal and state
  legislation.

. Ensure federal and state regulatory understanding
  of the implications to the electric utility
  industry if the process industries do not actively
  pursue cogeneration incentives and opportunities.

FUEL COST ALLOCATION FOR THE STEAM IN A COGENERATION PLANT

K. W. Li and P. P. Yang
North Dakota State University
Fargo, North Dakota U.S.A.

ABSTRACT

The paper is intended to propose a method which would allocate the fuel cost to the process steam produced in a cogeneration system. The proposed method is established on the basis of the Second Law of Thermodynamics involving a use of the concept of thermodynamic availability. Several penalty terms are taken into consideration to produce a realistic fuel cost chargeable to the process steam users. An illustrative example is used to show the application of this method to a cogeneration system.

INTRODUCTION

The production of electricity from the fossil fuels is a very inefficient process. The efficiency of the modern power plants ranges from 32% for a simple steam plant to 43% for an advanced, sophisticated steam-gas turbine plants. This means that currently between 57% and 68% of the heating value of the fuel is being discharged as waste heat. Some of this waste heat is unrecoverable, such as radiation and stack loss from the boiler. But much of this heat can be used for the industrial or agricultural applications, or for the heating of building. The use of this waste heat is called waste heat utilization. Through the utilization of waste heat, the overall conversion of the fuel to useable energy can be as high as 80%.

Cogeneration plant is a system which would produce electricity as well as process steam. There are many system arrangements currently in use [1-8]. In one arrangement, steam is first generated and partly expanded in a turbine for production of electricity. Then, the used steam is sent out as the process steam. In another arrangment, steam from the boiler is expanded in a turbine. The process steam is extracted from the turbine at some points. The steam not extracted will continue its expansion process and eventually condense in a condenser. In general, the cogeneration plant has an overall efficiency around 80% [8]. The combined heat and electric power production was often ignored in the past. This was due, in part, to the institutional constraints and the economic distortions it produced. It was also due, in part, to the technical problems. But in recent years there is an increasing awareness that these problems are not unsurmountable. At the time when the energy conservation program is high in the national priorities, the cogeneration system has become increasingly important.

This paper is intended to propose a method which would allocate the fuel cost to the process steam produced in a cogeneration system. This is not a simple matter because steam first serves as a working substance in a turbine and then, serves as the process steam. In the past fuel allocation to these two functions is either arbitrary or based upon BTU content [8]. Because of these, there have been some confusions and distortions in the evaluation of cogeneration systems.

The proposed method has been established on the basis of the Second Law of Thermodynamics. The thermodynamic availability of steam was used to indicate the values of steam. The higher the thermodynamic availability of steam, the more valuable the steam would be. In this paper the availability of steam in a system is first calculated. Then the fuel cost is allocated to the steam according to its availability. The method is straightforward. An illustrative example is used to show its application to a cogeneration system.

THERMODYNAMIC AVAILABILITY OF STEAM

The thermodynamic availability of the working substance including steam is defined by

$$a = (h - h_0) - T_0(s - s_0) \tag{1}$$

Thermodynamic availability is the property which measures the potential of working substance to do work under certain surrounding conditions. The change of the availability in a process means a change in the capacity of a working substance to do work. In a work producing process the decrease of availability is generally larger than the useful work produced. The difference between these two is defined as the irreversibility of the process [10]. In the process where there is no work involved, the irreversibility measures the loss of availability due to the friction or due to the heat transfer through a finite temperature difference.

To measure the process charateristics, the term "process effectiveness" is usually applied. The general definition of the process effectiveness, denoted by ε, is [10].

$$\varepsilon = \frac{\text{Increase in the availability of desired output}}{\text{Decrease in the availability required}} \tag{2}$$

or

$$\varepsilon = \dot{A}_{output} / \dot{A}_{input} \tag{3}$$

For a work producing process the effectiveness defined in Eq. (2) can be easily interpreted as the ratio of the actual useful work obtained to the maximum useful work obtainable. From the thermodynamic viewpoints, all reversible processes between any two given end states are equally effective in producing the useful work, so that the effectiveness of any reversible process is unity. The effectiveness of an actual process, however, is always less than unity. In other words, the term, $1 - \varepsilon$, is a measure of the potential for improvements.

For a heat reception process, the effectivness is the ratio of the increase of availability in the working substance to the decrease of availability in the substance from which the heat is transferred. Similiar interpretations can be given to the processes of heat rejection (cooling) and work absorption (pumping).

To illustrate the calculations of the thermodynamic availability and the process effectiveness, a typical conventional steam turbine system was examined. Fig. 1 shows the turbine system arrangement and its heat balance under full-load conditions. With Eq. (1), the thermodynamic availabilities under various steam conditions were calculated. The results are shown in Fig. 2. It is seen that the steam availability is a function of steam temperature and pressure. The steam with a higher availability is more valuable than that with a lower availability.

Table 1 summarizes the calculated results of the process effectiveness. Also included in Table 1 are the results for $\dot{A}_{output}$, $\dot{A}_{input}$ and $\dot{A}_{loss}$. In this study, the process availability loss per unit time $\dot{A}_{loss}$ is defined as difference between these two terms $\dot{A}_{input}$ and $\dot{A}_{output}$. By the nature of the engineering process, this term must be positive or zero in the limiting case. In this investigation the results of a steam generator analysis (boiler and reheater) and the thermodynamic availability of coal used for plant operation were also obtained. Details of the analysis can be found in the reference [9].

It is interesting to notice from Table 1 that most availability losses takes place in the steam generator (3143 MBtu/hr out of the total loss 3725 MBtu/hr in the plant) and the process effectiveness of this device is only in the neighbourhood of 50%. The condenser is also relatively ineffective. But the availability loss in the condenser is approximately 216 MBtu/hr which is much less than that in the steam generator. These observations are obviously contradictory to those made by the First Law of Thermodynamics. It is believed that the Second Law analysis is very much needed when the real inefficient components are to be identified in the plant system [10].

FUEL COST OF UNIT AVAILABILITY

The cost of steam generated in a conventional power plant or a cogeneration plant mainly consists of two terms: fuel cost and equipment cost. In a cogeneration plant steam is partly used to produce electricity and partly used as process steam. Thus, there arises the question how should the production cost of steam be distributed to these two functions. In this study attention will be focused to the fuel cost allocation.

To determine the fuel cost (C) of steam (or water) under various conditions in a power plant or the process steam in a cogeneration plant, one must know the fuel cost per unit availability (C_1). The relationship between C and C_1 is

$$C = C_1 * a \tag{4}$$

The fuel cost of unit availability, as shown later in this paper, is determined by the method of steam production and the cost of the primary fuel such as coal, oil and nuclear energy. Eq. (4) indicates that for a given C_1, the fuel cost of the steam would increase as the thermodynamic availability of the steam increases. In other words, the steam would be more valuable and costs more if it has a high availability, that is a high potential of producing the useful work. Since the steam is generated continuously in the system under consideration, it is quite convenient to use the term, fuel cost rate, which is defined as below,

$$C_2 = C_1 * a * w \tag{5}$$

or

$$C_2 = C * w \tag{5a}$$

It is seen in Eq. (4) and Eq. (5) that the terms C, C_1, C_2 are interrelated. Once one of them is known, the other two terms can be easily determined. The basic procedures used in this study are first to determine C_2 and C_1 and then, to calculate C by Eq. (4) or Eq. (5).

Fig. 3 indicates three major devices frequently encountered in a power plant or a cogeneration plant. They are the boiler, the turbine and the heat exchanger. Also included in the diagram are their corresponding fuel cost balance equations and the indications of whether or not there is any change in the fuel cost per unit availability (C_1). It is seen that in the operation of each device, the fuel cost is transferable by 100%. It means that the fuel cost of device output is exactly equal to the fuel cost of the device input. For example, the fuel cost of the steam at the boiler outlet must be equal to the sum of fuel costs for the primary fuel, hot air and water.

The fuel cost of unit availability (C_1) may or may not change in the process, depending upon whether or not the substance receives additional useful heat (availability) from an external source. In the steam generator where substance receives additional useful heat (availability) from the combustion, the term C_1 changes as indicated in Fig. 3a. In the turbine process, the term C_1 would remain unchanged because the substance does not receive any additional useful heat (availability). Similarly, in a heat exchanger, the hot fluid would have unchanged fuel cost of unit availability while the cold fluid has changed its fuel cost of unit availability.

Some explanations may be needed for these $C_{2,f}$ and $C_{2,a}$ in Fig. 3a. The term $C_{2,f}$ is the cost of the primary fuel consumed per unit time. Mathematically it is:

$$C_{2,f} = C_{1,f} * a_f * w_f \tag{6}$$

or

$$C_{2,f} = (COST)_f * (HV)_f * w_f \tag{7}$$

Evidently, the terms $C_{1,f}$ and $C_{2,f}$ can be easily calculated if the fuel consumption, price and heating value are known. The term $C_{2,a}$ is the fuel cost associated with the hot air prepared by the extraction steam. In a mathematical form, it is:

$$C_{2,a} = C_{1,a} * a_a * w_a \tag{8}$$

For determination of the fuel cost component of steam (or water), the primary procedures are to set up the cost balance equations for each element in the system and to solve these equations simultaneously. To be more specific, one should first prepare a cost balance for each element (such as the boiler, turbine, and reheater) in terms of the fuel cost of feedwater at the boiler inlet. This feedwater fuel cost is then calculated by taking a cost balance on the control volume which consists of the whole feedwater heater train including the feedwater and condensate pumps. In general, the feedwater fuel cost at the boiler inlet is the sum of the fuel costs of all extracted steam and water entering the feedwater heater train, minus the fuel cost associated with the drain directed back to the condenser.

To illustrate the use of procedures just described, the conventional power plant shown in Fig. 1. will be used. With the following input information, the fuel costs of steam under various conditions were calculated.

coal consumption, w_f = 475,000 (lb/hr)

coal heating value, $(HV)_f$ = 13,297 (Btu/lb)

coal availability, a_f = 13,186 (Btu/lb)

coal price, $(COST)_f$ = 0.8 ($/$10^6$Btu of heating value)

The results are shown in Fig. 2. For simplicity, only the term C is indicated in the diagram. Since the availability (a) and flow rate (w) are indicated at various locations in the diagram, the term C_1 and C_2 can be easily calculated with Eq. (4) and Eq. (5).

It is interesting to note that the fuel cost of steam shown in Fig. 2 varies with the thermodynamic availability of steam. As the availability of steam decreases, the fuel cost of steam would decrease. For instance, the steam has a fuel cost 1.0852 dollars per thousand pounds at the HP turbine inlet conditions. But, the fuel cost of steam would drop to 0.8132 dollars per thousand pounds at the HP turbine exhaust end. Also shown in Fig. 2 are the fuel costs for the boiler feedwater under various conditions. At the condenser outlet where the availability of substance is low (ie. 1.351 Btu/lb), the condensate has a fuel cost a 0.00226 dollars per thousand pounds. But at the boiler inlet, the fuel cost of boiler feedwater would increase to 0.255 dollars per thousand pounds.

In the power plant under consideration, an auxiliary turbine is used to drive the feedwater pump and the extraction steam is used to operate the air preheater. Fig. 2 indicates steam fuel cost, steam flow rate, and other information for these equipments.

FUEL COST CHARGEABLE TO STEAM

In a cogeneration plant electricity and process steam are produced simulataneously. Fig. 4 indicates a typical cogeneration system. In the system the steam of 3515 psia and 1000 F enters the turbine at the rate of 5,492,903 lb/hr. At the extraction point where the pressure and temperature are respectively 153 psia and 634.2 F, the steam is withdrawn for the process use at the rate of 426,539 pounds per hour. A complete heat balance of this cogeneration system is shown in Fig. 4.

To determine the fuel cost of process steam, one must calculate the availability of steam and the steam fuel cost for unit availability such as those shown in Fig. 5. The procedures are identical to those for a conventional power plant. As shown in Fig. 5, the fuel cost of steam at the extraction (153 psia and 634 F) is 0.716 dollars per thousand pounds. With consideration to the value of the return process water, (0.104 dollars per thousand pounds), the fuel cost of the process steam should be 0.612 dollars per thousand pounds. In a general form, the equation is

600

$$\overline{(FCS)} = C_{s,i} - \quad \_ \qquad\qquad (\backsim,$$

To have a more accurate and realistic fuel cost, there are several penalty terms to be included. These penalty terms are related to,

1. condenser loss associated with the process steam F_1.

2. condenser loss associated with the feedwater heater drain F_2.

3. condenser loss associated with the exhaust steam from an auxiliary turbine, F_3.

4. condenser loss associated with the exhaust steam from an air pre-heater, F_4.

The equations used for these penalty calculation are summarized in Table 2. The derivations are straight forward. First, the loss per unit mass of process steam is calculated. Second, the fraction of the loss (DF) shared by the process steam must be determined. In this study the term DF is simply

$$DF_1 = \frac{\dot{A}_{ps}}{\dot{A}_{ps} + \dot{A}_{tl}} \qquad\qquad (10)$$

if the loss is associated with the process steam, or

$$DF_2 = \frac{\dot{A}_{ps}}{\dot{A}_{ps} + \dot{A}_t} \qquad\qquad (11)$$

if the loss is associated with steam from other sources. With all these penalty terms, the equation for the fuel cost chargeable to the process steam would become,

$$FCS = \overline{FCS} + F_1 + F_2 + F_3 + F_4 \qquad\qquad (12)$$

It should be pointed out that the penalty terms are generally small as compared with the term $\overline{FCS}$. Using the numerical information shown in Fig. 4 and Fig. 5, the fuel cost of the process steam (P = 153 psia, T = 634 F) was calculated and found at 0.617 dollars per thousand pounds. Table 3 indicates all calculations involved.

FUEL COST CHARGEABLE TO ELECTRIC POWER

The procedures for the determination of the fuel cost chargeable to the electric power generation are similar to those for process steam. First, the consumption of steam availability for each turbine cylinder is

calculated. Then, this term is multiplied by the unit cost of availability to obtain the fuel cost rate of this particular turbine. In a mathematical form, it is

$$C_{2,t} = C_{1,t} * \left(\sum_i a_i * w_i - \sum_e a_e * w_e \right) \tag{13}$$

To determine the average fuel cost in terms of mills/kwhr, one should calculate the sum of the fuel cost rates for all turbine cylinders and then, divide the resultant expression by the total turbine output. That is

$$\overline{(FCP)} = \frac{(C_{2,HP} + C_{2,IP} + C_{2,LP})}{A_{gen}} * 1000 \tag{14}$$

Like the case of determining the fuel cost chargeable to the process steam, the term $\overline{(FCP)}$ should be modified to reflect the additional costs against the electric power generation. These costs are related to,
1. condenser loss associated with the process steam G_1.
2. condenser loss associated with the feedwater heater drain, G_2.
3. condenser loss associated with the exhaust steam from an auxiliary turbine G_3.
4. condenser loss associated with the exhaust steam from an air pre-heater, G_4.
5. condenser loss associated with the exhaust steam from the LP turbine, G_5.

The equations for the calculation of these terms are summarized in Table 2. It is seen that these terms are generally obtained by multiplying the loss per unit mass of process steam by the distribution factor (DF) and the ratio of the process steam output to the electric power output (R). Evidently, the distribution factor for the calculation of fuel cost chargeable to the power users is either $1.0 - DF_1$ or $1.0 - DF_2$.

In this study, the ratio (R) is not dimensionless, but has a unit of pound per hour per kilowatt. With these corrections, the fuel cost chargeable to the power would become,

$$FCP = \overline{(FCP)} + (G_1 + G_2 + G_3 + G_4 + G_5) * 1000 \tag{15}$$

For illustration, the numerical information in Fig. 4 and Fig. 5 was used and the fuel cost chargeable to the electric power generation was calculated. It was found that the electric power was generated at the fuel cost of 6.832 (mills/kwhr). Table 4 summaries all calculations involved.

602

DISCUSSION

The method proposed here for the prediction of the fuel cost chargeable to the process steam was established on the basis of the Second Law of Thermodynamics. To be more specific, the concept of thermodynamic availability was utilized. This approach is more reasonable and realistic. The value of steam (or water) does not depend upon its energy content but its thermodynamic availability which represents its capability of producing useful work. A process in which the steam is throttled to the atmospheric pressure from a high pressure is an example. In this process, the steam loses little of its energy and its temperature remains almost the same. Experiences indicate that after throttling, the steam loses almost all of its potential of producing useful work. From an energy viewpoint, the process efficiency is high because little energy is lost. However, from the work producing viewpoint, the process efficiency is almost equal to zero. Since the availability is a measure of work-producing potential, a use of this concept becomes necessary in assessing the value of steam (or water).

The proposed method is general is nature. It is applicable to the utility company owned cogeneration plant where the fuel cost chargeable to the process steam is desired. Also, it is equally applicable to the industrial plant where the fuel cost chargeable to the power generation is needed. In this method, the users (power users or steam users) have to pay for their consumption of the steam availability on the same basis. This may be the underlining principle developed in this study. The following case is used as an illustration. The steam acquires a change of availability 100 units at a fuel cost X dollars per pound. In a certain process, 80 units of the availability are consumed for the electric power generation while 20 units of the availability are consumed by the process steam users. By the proposed method, the power and steam users would be required to pay 80% and 20% of the total fuel cost respectively. It is seen that the proposed method gives no preference to either power users or steam users. For some reasons this method may not become acceptable in commercial practice, but it surely provides the fairest means for the distribution of fuel cost at least from the thermodynamic view point.

In practice the BTU method has been frequently adopted for allocating the fuel cost in a cogeneration plant [8]. By this method the steam and power users are charged according to the amount of heat they take. Little attention is given to the thermodynamic steam conditions under which the heat is consumed. Because of these, this BTU method generally charges the steam users much more than that by the availability method proposed in this paper.

Another method of allocating the fuel cost is the adiabatic heat drop method [8]. In this method an arbitrary condenser pressure is first chosen as a reference pressure. The adiabatic heat drop from the initial state to the reference pressure is debited to the electric power

generation. The adiabatic heat drop from the inlet conditions of process steam to the reference pressure is also debited to the heating process and, at the same time, credited to the electric power generation. This adiabatic heat drop method is in some sense similiar to the availability method, because both methods charge the power and steam users in accordance with the consumption of work-producing potentials. However, in the availability method, there is no arbitrary assumption of reference pressure. Also, the assumption of adiabatic heat drop in the real and fictitious turbines would become unnecessary.

In this paper a method has been proposed for the allocation of fuel cost to the process steam and to the electric power generation in a cogeneration plant. No attention was given to the distribution of equipment cost. The systems under consideration are representative of those currently used by utility companies. These are generally more complex than those used in the industrial plant. The proposed method is believed to be equally valid for all these cogeneration systems.

In summary, the study has generated a fair means of allocating fuel cost between the electric power generation and the process steam. The proposed method should provide an additional approach to the problem of steam costs which has had considerable controversies in practice.

REFERENCE

1. Oplatka, G., "Economic Aspects of the Combined Generation of Heat and Electricity". Brown Boveri Review. January 1978.
2. Schwarzinbach, A., "Economic Design of District-Heating Power Plants". Brown Boveri Review. September 1977.
3. Muhlhauser, H., "Steam Turbines in Conventional Combined District Heating and Power Stations". Brown Boveri Review, September 1977
4. Schwarzinbach, A. and Frutschl, H. U., "Gas Turbines for District Heating Power Plants". Brown Boveri Review. September 1977.
5. Hohl, R., "District Heating in Switzerland" Brown Boveri Review. 1973.
6. Kadrnozka, W. and Hanus L., "Optimation of heat and power plants" 8th World Energy Conf. 1970. Div. 4. paper 4.2-34.
7. Schuller, K. H., "Heat extraction for district heating from Nuclear power plant" Brown Boveri Review, 1976.
8. Diamant, R. M. E., Total Energy, Pergamon Press 1970.
9. Yang, Peter, "Computer Simulation of Steam Turbine System and Steam Cost Estimates" M. S. Thesis, Dept. of Mechanical Engineering, North Dakota State University, 1978.
10. Obert, E. F., "Concepts of Thermodynamic" McGraw-Hill Book Co. 1960.
11. Comtois, W. H.,"What is the true Cost of Electric Power and Steam from a Cogeneration Plant" presented in the American Power Conference, Chicago, 1978.

604

NOMENCLATURE AND SYMBOLS

a	=	Availability of a substance (Btu/lb)
$\dot{A}_{gen}$	=	Generator output (kw)
$\dot{A}_{input}$	=	Total availability input to a device or process (Btu/hr)
$\dot{A}_{output}$	=	Total availability gained in a device or process (Btu/hr)
$\dot{A}_{loss}$	=	The difference between $\dot{A}_{input}$ and $\dot{A}_{output}$ of a device or process (Btu/hr)
$\dot{A}_{ps}$	=	Steam availability consumed in the industrial process (Btu/hr)
$\dot{A}_t$	=	Steam availability consumed by the turbine (Btu/hr)
$\dot{A}_{tl}$	=	Total availability of the process steam consumed in the turbine (Btu/hr)
C	=	Fuel cost per unit mass (Dollars/lb)
C_1	=	Fuel cost per unit availability (Dollars/Btu)
C_2	=	Fuel cost rate (Dollars/hr)
$(COST)_f$	=	The cost of fuel (Dollars/10^6 Btu of heating value)
F	=	Cost penalty chargeable to the process steam (Dollars/lb)
FCP	=	Fuel cost chargeable to the electric power (mills/kw-hr)
$\overline{FCP}$	=	Basic fuel cost chargeable to the electric power (mill/kw-hr)
FCS	=	Fuel cost chargeable to the process steam (Dollars/lb)
$\overline{FCS}$	=	Basic fuel cost chargeable to the process steam (Dollars/lb)
G	=	Cost penalty chargeable to the electric power (Dollars/kw-hr)
h	=	Enthalpy of a substance (Btu/lb)
h_o	=	Enthalpy of a substance under ambient conditions (Btu/lb)
$(HV)_f$	=	Heating value of fuel (Btu/lb)
$\dot{m}$	=	Mass flow quantity (lb/hr)
$\dot{m}_{drain}$	=	Heater drain flow quantity that goes to condenser (lb/hr)
R	=	Ratio of the process steam output to the electric power output (lb/kw-hr)
s	=	Entropy of a substance (Btu/lb-R)
s_o	=	Entropy of a substance under ambient conditions (Btu/lb-R)
T_o	=	Ambient temperature (R)
w	=	Flow quantity (lb/hr)
ϵ	=	Device effectiveness (dimensionless)

SUBSCRIPTS:

a	=	air
as	=	Steam for air preheater
at	=	Auxiliary turbine
c	=	Condenser
drain	=	Feedwater heater drain that goes to condenser
e	=	Exit
f	=	Fuel
HP	=	High pressure steam turbine
i	=	inlet
IP	=	Intermediate Pressure steam turbine
o	=	outlet
p	=	Power
ps	=	Process steam
s	=	Steam
t	=	Turbine

TABLE 1   SECOND LAW ANALYSIS OF A MODERN STEAM TURBINE CYCLE

Item Description of component	$\dot{A}_{input}$ $(10^6$ BTU/HR)	$\dot{A}_{output}$ $(10^6$BTU/HR)	$\dot{A}_{loss}$ $(10^6$BTU/HR)	Device Effectiveness (%)
1. Steam turbine cycle	6264.99	2519.3	3725.69	40.2
2. Steam generator	6273.2	3129.4	3143.81	49.93
a. Combustor			1632.77	
b. Heat exchanger			1331.26	
c. Thermal stack gas loss			74.6	
d. Diffusion loss			105.14	
3. HP turbine	806.81	730.84	75.97	90.58
4. IP turbine	817.07	765.87	51.20	93.70
a. Section 1	474.40	451.44	22.96	95.16
b. Section 2	342.67	314.43	28.24	91.76
5. LP turbine	1171.61	1022.59	148.91	87.30
a. Section 1	332.29	309.81	22.48	93.24
b. Section 2	171.08	152.29	18.79	89.02
c. Section 3	151.72	371.84	13.88	90.85
d. Section 4	217.28	192.09	25.19	88.14
e. Section 5	299.24	230.55	68.59	77.05
6. Condenser	216.65		216.65	52.85*
a. Heat transfer loss			102.15	
b. Effulent loss			104.50	

TABLE 1 (continued)

Item Description of component	$\dot{A}_{ipput}$ (10^6BTU/HR)	$\dot{A}_{output}$ (10^6BTU/HR)	$\dot{A}_{loss}$ (10^6BTU/HR)	Device Effectiveness (%)
7. Air preheater	37.87	8.21	29.66	21.7
a. Heat transfer loss				
8. Auxiliary turbine	98.48	79.56	18.92	81.30
9. Feedwater heater train	592.72	537.93	54.79	90.75
a. Heater No. 1	36.64	28.44	8.20	77.65
b. Heater No. 2	42.72	33.70	9.02	78.88
c. Heater No. 3	42.35	37.01	5.35	87.35
d. Heater No. 4	40.08	36.42	3.66	90.85
e. Heater No. 5	107.59	104.46	3.13	97.10
f. Heater No. 6	97.72	82.91	14.82	84.84
g. Heater No. 7	225.62	215.00	10.62	95.30
10. Feedwater pump	79.56	72.72	6.84	91.40
11. Condensate pump	2.17	1.20	0.97	55.30

Note; Calculations were made with the input information, a_f = (BTU/LB of coal),
$\dot{w}_f$ = 475,000 (LB of coal/HR)

* The condenser effectiveness is calculated by treating the effulent loss as the output of the condenser.

TABLE 2   SUMMARY OF EQUATIONS FOR CALCULATION OF COST PENALTY TERMS

Item	Associated condenser loss per unit mass of process steam, CLOSS, ($/lb)	Cost penalty terms for process steam, F, ($/LB)	Cost penalty terms for electric power, G, ($/KW-HR)	Conditions
1. Condenser loss associated with the process steam	$C_{ps,o} - C_{c,o}$	$F_1 = DF_1 * CLOSS$	$G_1 = (1-DF_1) * R * CLOSS$	Process steam returned to condenser directly
	$C_{drain,o} - C_{c,o}$	$F_1 = DF_1 * CLOSS$	$G_1 = (1-DF_1) * R * CLOSS$	Process steam returned to feedwater heater and eventually drained to condenser
	0	$F_1 = 0$	$G_1 = 0$	Process steam not drained to condenser
2. Condenser loss associated with the feedwater heater drain	$(C_{drain,o} - C_{c,o}) * m_{drain} / m_{ps}$	$F_2 = DF_2 * CLOSS$	$G_2 = (1 - DF) * R * CLOSS$	Heater drain directed to condenser
	0	$F_2 = 0$	$G_2 = 0$	No heater drain directed to condenser

TABLE 2 (continued)

Item	Associated condenser loss per unit mass of process steam CLOSS, ($/lb)	Cost penalty terms for process steam, F, ($/lb)	Cost penalty terms for electric power, G, ($/KW-HR)	Conditions
3. Condenser loss associated with the exhaust steam of auxiliary turbine	$(C_{at,o} - C_{c,o})$ $* \dot{m}_{at}/\dot{m}_{ps}$	$F_3 = DF_2 * CLOSS$	$G_3 = (1-DF_2) * R$ $* CLOSS$	Exhaust steam directed to condenser
4. Condenser loss associated with exhaust steam from air preheater	$(C_{drain,o} - C_{c,o}) * \dot{m}_a/\dot{m}_{ps}$	$F_4 = DF_2 * CLOSS$	$G_4 = (1-DF_2) * R$ $* CLOSS$	Exhaust steam or water returned to heater and eventually drained to condenser
	$(C_{a,o} - C_{c,o})$ $* \dot{m}_a/\dot{m}_{ps}$	$F_4 = DF_2 * CLOSS$	$G_4 = (1-DF_2) * R$ $* CLOSS$	Exhausted to condenser directly
	0	$F_4 = 0$	$G_4 = 0$	No exhausted steam or water returned to condenser
5. Condenser loss associated with LP turbine exhaust steam	$(C_{LP,o} - C_{c,o})$ $* \dot{m}_{LP,o}/\dot{m}_{ps}$	$F_5 = 0$	$G_5 = CLOSS * R$	Exhaust steam directed to condenser

TABLE 3   FUEL COST CALCULATION FOR THE PROCESS STEAM

	Availability Consumption Quantity (10^6 BTU/HR)	Flow Quantity (LB/HR)	Cost of Fuel ($\$/10^3$ ln)
$\dot{A}_{ps}$	156.22		
$\dot{A}_{t1}$	149.25		
A_t	2944.36		
$\dot{m}_{as}$		113740.0	
$\dot{m}_{ps}$		426539.0	
$\dot{m}_{at}$		303119.0	
$\dot{m}_{drain}$		660328.0	
$C_{s,i}$			0.716
$C_{s,o}$			0.104
$C_{a,o}$			0.104
$C_{at,o}$			0.119
$C_{drain,o}$			0.005
$C_{c,o}$			0.002
$F_1 \times 10^3$			0.000
$F_2 \times 10^3$			0.001
$F_3 \times 10^3$			0.004
$F_4 \times 10^3$			0.001
$\overline{FCS}$			0.611
FCS			0.617

TABLE 4   FUEL COST CALCULATION FOR THE GENERATOR OUTPUT

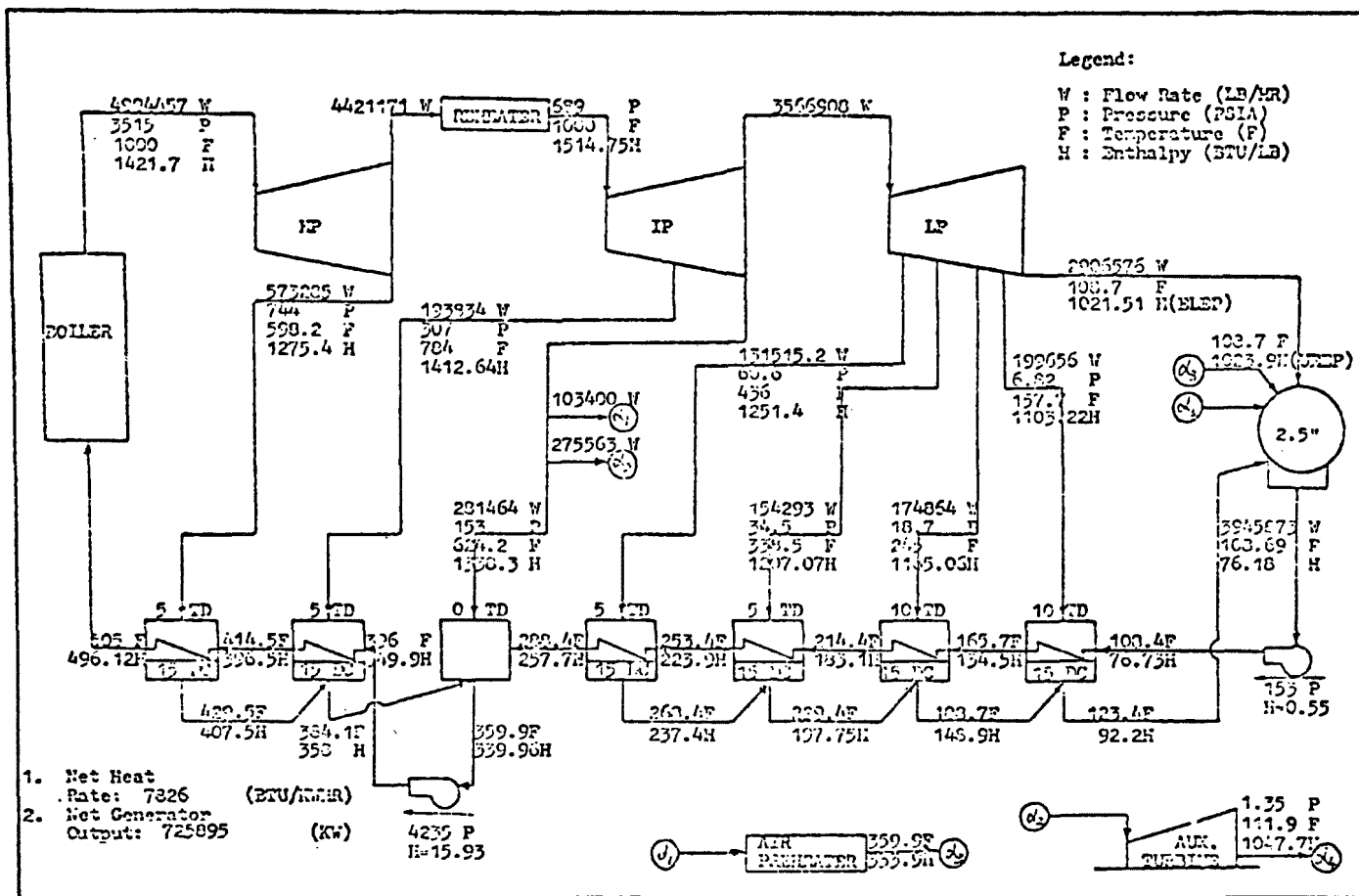|	Availability Consumption Quantity (10^6 BTU/HR)	Flow Quantity (LB/HR)	Cost of Fuel ($/$10^3$ LB)	Generator Output Cost (Mills/ KW-HR)
$\dot{A}_{ps}$	156.22			
A_{tl}	149.25			
$\dot{A}_t$	2944.36			
$\dot{m}_{as}$		113740.0		
$\dot{m}_{ps}$		426539.0		
$\dot{m}_{at}$		303119.0		
$\dot{m}_{drain}$		660328.0		
$\dot{m}_{LP,o}$		2868686.0		
$C_{LP,o}$			0.1113	
$C_{drain,o}$			0.0056	
$C_{a,o}$			0.1043	
$C_{at,o}$			0.1192	
$C_{c,o}$			0.0023	
$G_1 * 10^3$				0.000
$G_2 * 10^3$				0.003
$G_3 * 10^3$				0.043
$G_4 * 10^3$				0.017
$G_5 * 10^3$				0.403
FCP				6.366
FCP				6.832

Fig. 1. Heat Balance Diagram of a Conventional Power Plant
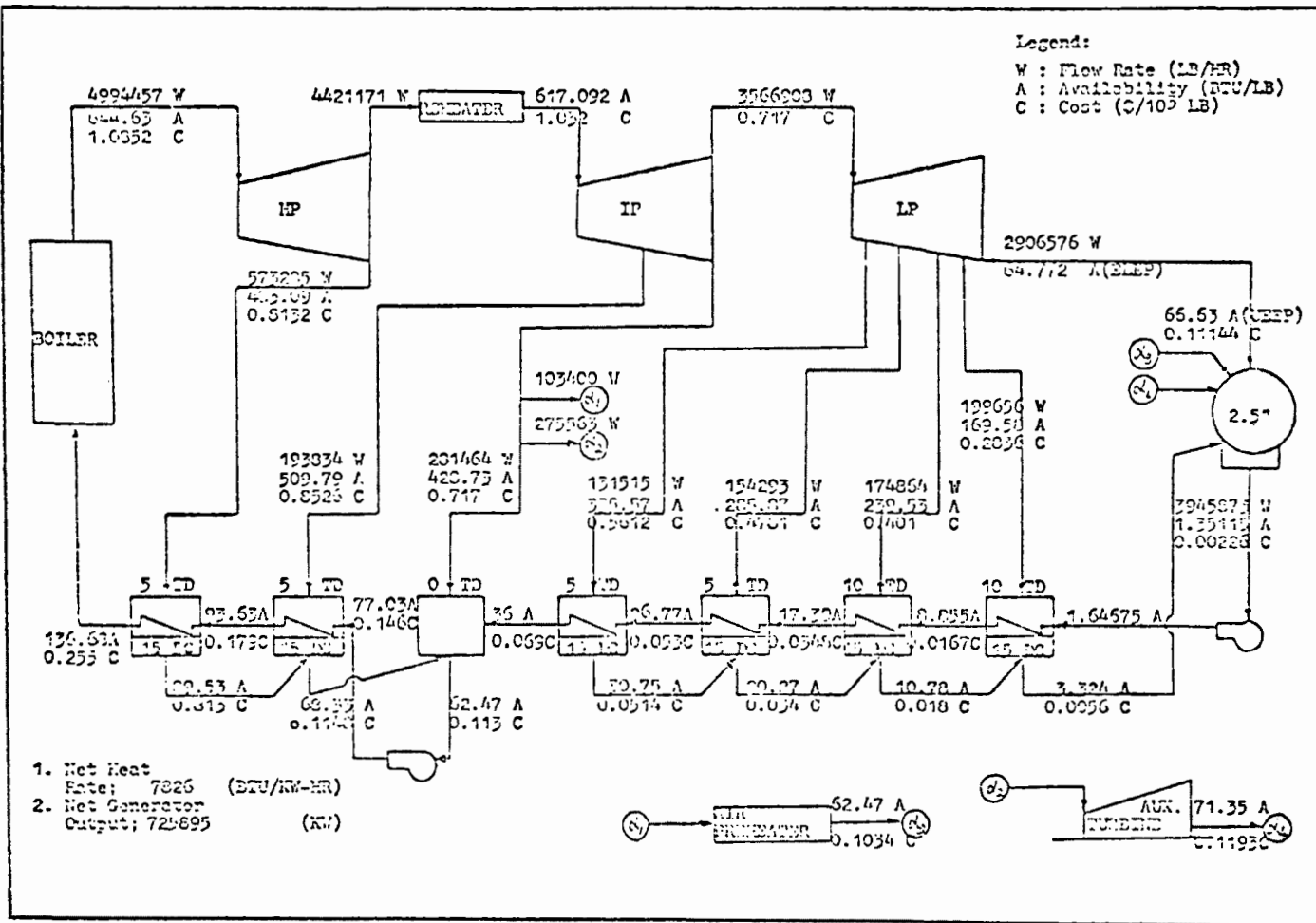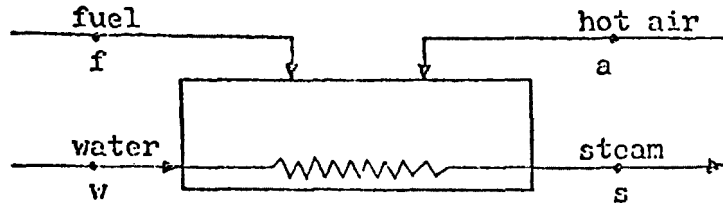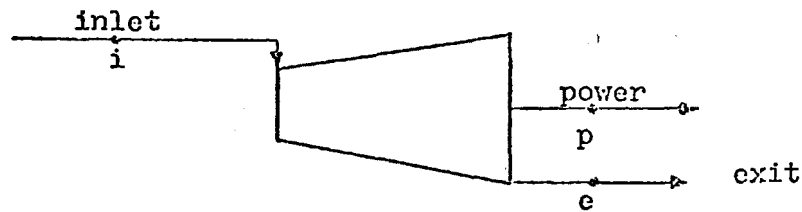
Fig. 2. Steam Availability and Fuel Cost Allocation Diagram of a Conventional Power Plant

Fuel Cost Balance, $C_{2,f} + C_{2,a} = C_{2,s} - C_{2,w}$

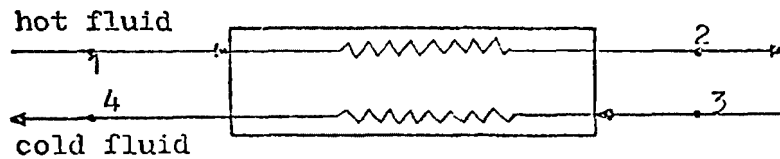Fuel Cost of Unit Availability, $C_{1,s} \neq C_{1,w}$

(a). Boiler (or Reheater)

Fuel Cost Balance, $C_{2,i} - C_{2,e} = C_{2,p}$

Fuel Cost of Unit Availability, $C_{1,i} = C_{1,e}$

(b). Turbine (or Pump)

Fuel Cost Balance, $C_{2,1} - C_{2,2} = C_{2,4} - C_{2,3}$

Fuel Cost of Unit Availability, $C_{1,1} = C_{1,2}$
$C_{1,3} \neq C_{1,4}$

(c). Heat Exchanger (or Condenser)

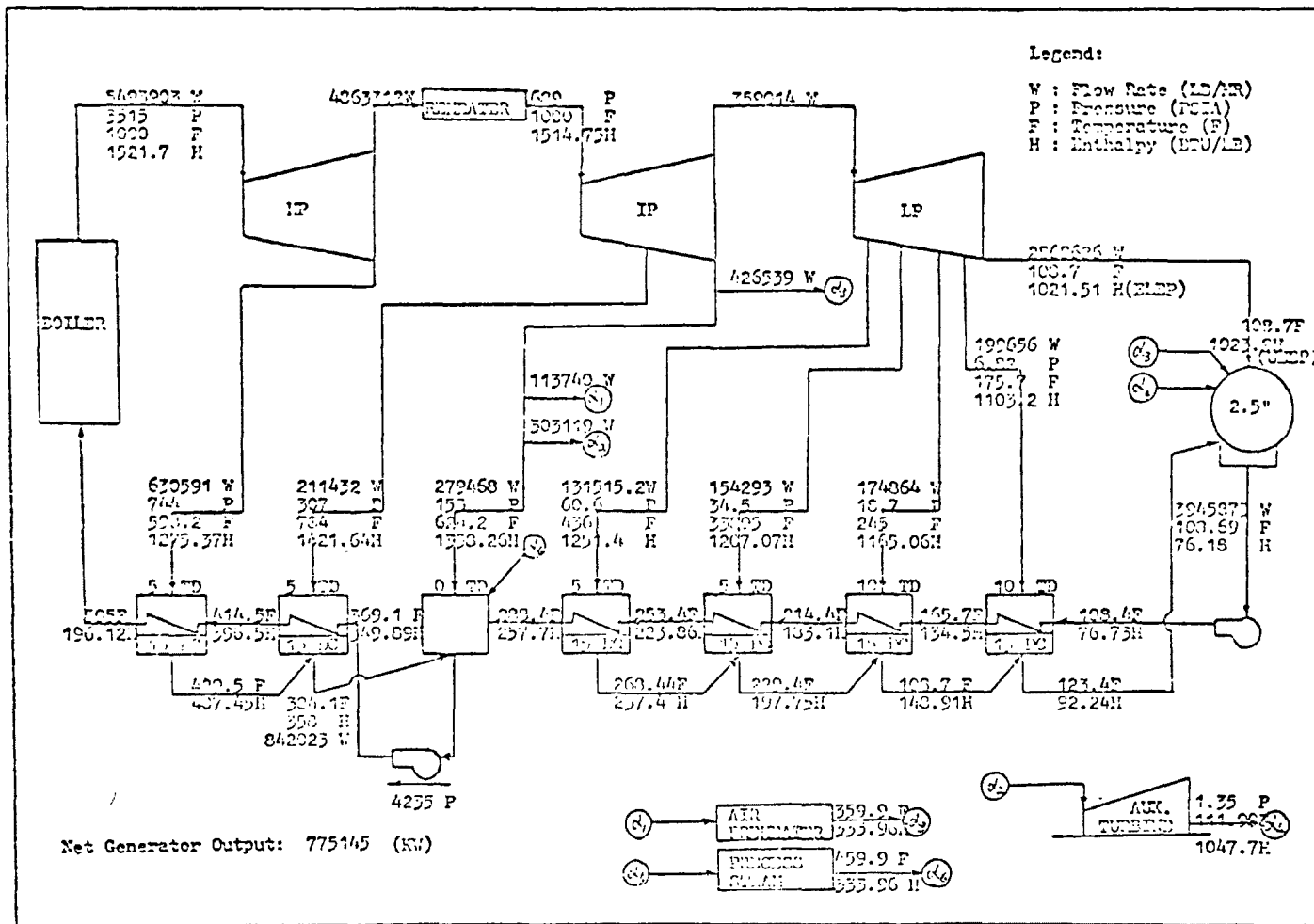Fig. 3. Major Elements and Cost Balance Equations

Fig. 4. Heat Balance Diagram of a Co-generation Power Plant

Fig. 5. Steam Availability and Fuel Cost Allocation Diagram of a Co-generation Power Plant

TECHNICAL REPORT DATA
(Please read Instructions on the reverse before completing)

1. REPORT NO. EPA-600/9-79-031a	2.	3. RECIPIENT'S ACCESSION NO.

4. TITLE AND SUBTITLE Proceedings: Second Conference on Waste Heat Management and Utilization (December 1978, Miami Beach, FL), Volume 1	5. REPORT DATE August 1979
	6. PERFORMING ORGANIZATION CODE

7. AUTHOR(S) S.S. Lee and Subrata Sengupta, Compilers	8. PERFORMING ORGANIZATION REPORT NO.

9. PERFORMING ORGANIZATION NAME AND ADDRESS University of Miami Department of Mechanical Engineering Coral Gables, Florida 33124	10. PROGRAM ELEMENT NO. EHE624A
	11. CONTRACT/GRANT NO. EPA Purchase Order DA86256J

12. SPONSORING AGENCY NAME AND ADDRESS EPA, Office of Research and Development* Industrial Environmental Research Laboratory Research Triangle Park, NC 27711	13. TYPE OF REPORT AND PERIOD COVERED Proceedings; 12/78
	14. SPONSORING AGENCY CODE EPA/600/13

15. SUPPLEMENTARY NOTES IERL-RTP project officer is Theodore G. Brna, MD-61, 919/541-2683. Cosponsors are: EPRI, Florida Power and Light Co., Univ. of Miami, U.S. DoE, U.S. EPA, and U.S. Nuclear Regulatory Commission.

16. ABSTRACT The proceedings document most presentations made during the Second Conference on Waste Heat Management and Utilization, held December 4-6, 1978, at Miami Beach, FL. Presentations were grouped by areas of concern: general, utilization, mathematical modeling, ecological effects, cooling tower plumes, cooling towers, cogeneration, cooling systems, cooling lakes, recovery systems, aquatic thermal discharges, and atmospheric effects. Causes, effects, prediction, monitoring, utilization, and abatement of thermal discharges were represented. Utilization was of prime importance because of increased awareness that waste heat is a valuable resource. Cogeneration and recovery systems were added to reflect this emphasis.

17. KEY WORDS AND DOCUMENT ANALYSIS

a. DESCRIPTORS	b. IDENTIFIERS/OPEN ENDED TERMS	c. COSATI Field/Group
Pollution Cooling Towers Heat Recovery Plumes Management Utilization Mathematical Models Ecology	Pollution Control Stationary Sources Cogeneration Cooling Lakes Thermal Discharges Atmospheric Effects	13B 07A,13I 20M,13A 21B 05A 14B 12A 06F

18. DISTRIBUTION STATEMENT Release to Public	19. SECURITY CLASS *(This Report)* Unclassified	21. NO. OF PAGES 632
	20. SECURITY CLASS *(This page)* Unclassified	22. PRICE

EPA Form 2220-1 (9-73)